ECONOMIC AND ENVIRONMENTAL IMPACTS OF ALTERNATIVE CLOSED-CYCLE COOLING SYSTEMS FOR INDIAN POINT UNIT NO. 3

VOLUME NO. 2

January 1976

RK, INC.

APPENDIX A: Pickard, Lowe and Associates, Inc., "Environmental Effects of Atmospheric Discharges from Two Natural Draft Cooling Towers (Indian Point 2 and 3) at the Indian Point Site," April, 1975.

APPENDIX B: Consolidated Edison Company of New York, Inc., "A Model Study of Cooling Tower Plume Induced Fogging, Icing and Salt Drift Deposits at Indian Point Unit No. 3," December, 1975.

APPENDIX C: Ostergaard Associates, "Sound Emissions Resulting from Construction and Operation of Cooling Towers at Indian Point Unit No. 3 Nuclear Station," May 12, 1975.

APPENDIX A: Pickard, Lowe and Associates, Inc., "Environmental Effects of Atmospheric Discharges from Two Natural Draft Cooling Towers (Indian Point 2 and 3) at the Indian Point Site," April, 1975.

ENVIRONMENTAL EFFECTS OF ATMOSPHERIC DISCHARGES FROM TWO NATURAL DRAFT COOLING TOWERS (INDIAN POINT 2 AND 3) AT THE INDIAN POINT SITE

Keith Woodard Sofia M. Laskowski
Pickard, Lowe and Associates, Inc.
1200 18th Street, N.W., Suite 612
Washington, D.C. 20036

April, 1975

Table of Contents

1.0 Introduction

Potential environmental effects due to operation of two natural draft cooling towers at Indian Point are discussed in this report. Effects considered here are limited to those related to discharges from the cooling tower exits. The report is separated into two parts. The first part (Section 2.0) considers the humid plume, and the second part (Section 3.0) discusses small water droplets (drift) discharged from the towers. Aesthetic effects of large towers, effects of discharges related to the cooling water cycle, and effects of water blown out from the base of the towers are not considered.

The data used in this report are taken from the first year (October, 1973 through September, 1974) of operation of the 400 ft meteorological tower designated as the Indian Point 4 tower. There were a total of 8006 hours when values of speed, direction, ΔT, and two levels of dew point and ambient temperature were recovered for the same hour, representing a minimum of 90% recovery of combined parameters.

2.0 Effects of the Humid Plume

The natural draft cooling towers used to dissipate waste heat to the atmosphere are not expected to have a significant influence on local meteorology. This is due primarily to the height of discharge (approximately 560 ft above plant grade). Under most meteorological conditions the discharge from the towers will condense upon leaving the towers and will be visible (as condensed water vapor) until it is evaporated to invisibility after mixing with the drier (unsaturated) air in the atmosphere.

The length of the visible plume depends on the temperature and humidity of the atmosphere. Colder and more humid weather is conducive to longer plumes. Most of the time the visible plume will extend only a short distance from the towers and will disappear by evaporation. On very humid days, when longer plumes are expected, there would probably be a naturally occurring overcast. On such occasions it is difficult to distinguish cooling tower plumes from the overcast. The following subsections discuss potential effects of the humid plume.

2.1 Visible Plume

To estimate the physical location and frequency of occurrence of the visible plume, a computer model has been developed and applied to the Indian Point site. Meteorological data collected at the site during the 12-month period ending September 30, 1974 were used as input to the model. A model description is included in Appendix A, and summaries of the site data and cooling tower characteristics appear in Appendix C. Using the model to compute plume dimensions for each hour of site data, isopleths of the number of hours of visible (overhead) plume length versus distance downwind have been computed assuming two tower operation, and are shown in Figures 2-1 and 2-2 for distances of 3 and 10 miles, respectively.

These figures show, for example, that in the SSW direction there will be about 400 hours during the 12-month data period when the plume is 2 1/2 miles long, or about 500 hours when plumes are visible for about a mile in that direction. Other directions have a lower frequency. Figure 2-3 is a topographic map of the site region.

The overhead plume is not expected to have any significant deleterious long or short term effect on the plant, terrestrial or aquatic biota, or aircraft operations. The effects of flying an aircraft through the visible portion of a plume have been studied. Both helicopters and fixed wing aircraft have been intentionally flown repeatedly through such plumes and there appear to be no significant adverse effects on the motion of these aircraft. Users of air navigation routes would be informed of the presence of the tower via air navigation charts. Where extended visible plumes are predicted by the model, they would probably occur during periods of high humidity when restricted visibility occurs naturally. The towers would therefore only slightly increase the severity of the condition. Since restricted visibility due to natural causes probably occurs at the same time, little, if any, additional effect on flight operations in the area is expected.

2.2 Ground Fog

Observations of operating natural draft towers have shown that visible portions of the plume rarely extend downward more than half the tower height[1,2]. This has also been found to be the case in wind tunnel tests[3]. On occasion wisps of the visible plume may intersect the ground for a few seconds under high wind conditions, however, sustained ground fog would not occur. Therefore, since the visible portion of the plume is not expected to reach ground level for sustained periods, ground fog due to natural draft tower operation would be rare.

These statements concerning ground fog were confirmed using the computer model with the site data as described in Appendix A. Only three hours of predicted ground fog resulted from the computer runs. Terrain was accounted for in these runs (see Appendix C, Figures 2a through 2p). Thus, it is expected that there would be no safety hazard on highways from fog. Fogging over the river would not occur, therefore, there would be no hazard to boat travel on the river. About 80 hours of natural fog (defined as visibility less than 1/4 mile at the 33 ft level) were measured at the meteorological tower. This represents an annual frequency of about 1.0%.

2.3 Increase in Ground Level Relative Humidity

The computer model (Appendix A) calculates and plots isopleths of long term average off-site increase in relative humidity (RH). Average predicted increases in RH for natural draft tower operation are shown in Figures 2-4, 2-5 and 2-6 for distances of 3, 10 and 50 miles, respectively. The peak offsite average incremental relative humidity increase (in % RH above ambient RH) was found to be .02 to .03% in the north direction between 10 and 50 miles. This is a negligible increase which would have no detrimental effect on the environment.

Incremental increases in relative humidity have also been tabulated as shown in Table 2-1 where the number of hours during which the relative humidity was increased by various amounts for several distances and for various combinations of ambient temperature and relative humidity. The highest incremental increase for any one hour was 9.0% RH which occurred when ambient temperature was about 56 ^{o}F and relative humidity was 36% for this hour. About 98% of all hours had an incremental increase of less than 1.0% RH.

2.4 Ice Formation Due to Condensed Plume

Ice formation on structures is not expected to occur if the structure is lower than half the cooling tower height. The following discussion of icing is applicable to tall structures in the cooling tower vicinity which are higher than half the tower height. Most of the icing potential of a cooling tower is due to the condensate (e.g., condensed plume water droplets) and drift droplets impinging on surfaces at or below freezing. Icing due to drift is discussed in Section 3.2. Ice formation could also result from plume water vapor deposition on surfaces at or below freezing as discussed in Section 2.5.

Condensate droplets are the small water drops (mass mean diameter of about 6 μm) that travel with the humid plume (i.e., stay in the plume). When the plume meets an object, some of the drops will have enough inertia to cross the streamlines and hit the object where they are collected (i.e., aerodynamic capture). The collection efficiency of an object depends, among other parameters, on the size and shape of the object, and on the drop size and drop impingement velocity on the object. Table 2-2 gives the drop collection efficiency of various objects at different impingement velocities. As can be seen from this table the collection efficiency decreases with decreasing drop diameter. For drops of 10 μm (conservatively used as the representative condensate drop diameter) the collection efficiency is small (no greater than 44%).

Ice formation due to condensate droplet impingement on large structures located in the path of the plume will not occur because the collection efficiency for 10 μm diameter drops on large structures is zero. Ice formation on thin objects (e.g., 1/4 inch diameter cylinders) located in the path of the plume will also depend on the plume water concentration, and the plume (or condensate) temperature. When the plume temperature is about 32 ^{o}F and the ambient temperature is $\leq$ 32 ^{o}F, ice formation will depend on the amount of water left on the object after the plume changes direction. That is, when the object is in the path of the plume, water collected on the object will be at approximately the same temperature as the plume and thus no icing will occur. As the plume changes direction, the water remaining on the object will freeze if the ambient air temperature is $\leq 32\,^{\circ}F$. When the plume temperature is $\leq 32\,^{\circ}F$, ice formation will occur upon condensate droplet impingement on the object.

Estimates indicate that ice accumulation on 1/4 inch cylindrical structures will probably not exceed 0.25 inch/hour as illustrated by the calculations shown in Table 2-3 and Figure 2-7.

2.5 Frost Formation Due to the Humid Plume

Formation of frost from the humid plume due to vapor deposition is very slow and insignificant compared to ice accumulated from condensate and drift droplets. Ice accumulation from a humid plume occurs as a result of plume water vapor deposition upon surfaces in the path of the plume.

Vapor deposition takes place when the water vapor pressure in the environment is greater than the vapor pressure exerted by the ice on the surface. Assuming that the surface is already covered with a thin layer of ice, the ice accumulation by vapor deposition is given by

$$\Delta m = 4\pi C F(T)\ \Delta t$$

where

$C = \dfrac{h}{\ln\frac{2h}{d}}$, depends on the geometrical shape of the object upon which water vapor is deposited

h = vertical dimension of the object in contact with the plume

d = horizontal dimension of the object

F(t) = rate of water vapor deposition (M/t-L), a function of temperature, strongly dependent on the vapor pressure gradient between the environment and the collecting surface

Δt = contact time

ΔM = mass of ice accumulated, M

Ice accumulation estimates for the case of a saturated plume (saturated with respect to liquid water) with plume temperature given by $T_{plume} = T_{surface} + 2\ ^{o}F$ in contact with cylindrical and ribbon type bodies of different sizes are given in Table 2-4. Values of F(t) are given in Figure 2-8. As can be seen from Table 2-4, the potential for ice accumulation on structures located in the plume path is negligible.

2.6 Precipitation

During times of naturally occurring snowfall, it is conceivable that snow conditions could be more intense under the cooling tower plume and cause greater accumulation on the surrounding area and roadways. This should not create any greater hazard since normal precautions taken by travelers in such circumstances would be adequate. Such an effect is expected to be very local if it occurs.

During periods of natural rainfall and shower activity, the existence of the humid plume will contribute a small amount of additional rainfall underneath the plume, due to the washout of the condensate droplets by the rain droplets. However, this contribution will be below the level of detection[1, 2] and much below the natural variability of precipitation. Thus, it will not represent a disturbance to the environment.

2.7 Synergistic Effects

No significant synergistic effects of cooling tower operation at the site location are expected. However, there is a potential for some increase in acid mist and sulfate formation if SO_2 plumes in the vicinity mix with the condensed plume. Very little information is available on this subject, thus quantitative estimates are not possible. A considerable effort is underway in the U. S. to more accurately quantify the reaction processes and damage potentials.

3.0 Drift

A very small fraction of the brackish water circulating through the cooling towers will be carried as small droplets in the rising air which leaves the tower top. This drift rate fraction (defined as Kg of salt per second leaving the tower top divided by the Kg of salt per second circulating through the tower heat exchange section) averages about 1 to 2 x 10^{-5} (or .001 to .002 percent) for large natural draft towers with good drift control systems.

The rate at which drift salt deposits on the ground outside the tower (e.g., as Kg/Km^2-month) and the near ground air concentration of such salt (e.g., as $\mu g/m^3$) is a function of distance and direction from the tower and depends on:

a) Tower geometry and operating conditions
b) Mass drift rate (i.e., the drift rate fraction times the circulating rate)
c) Drift drop size distribution
d) Terrain profile
e) Ambient atmospheric conditions including wind direction, wind speed, relative humidity, stability and precipitation rate

These relationships have been characterized in a mathematical model described in Appendix B and in reference 4.

Computer calculations using the model follow the history of representative drift droplets of selected initial size and salinity from the time they leave the drift eliminators in the tower to the place where they deposit on the ground taking account of accretion and evaporation of water from each droplet, of the effect of gravity and air currents on their average motion, and of their statistical distribution in space (around average trajectories) due to turbulent dispersion. The model also accounts for the effect of precipitation (e.g., rainfall), the aerodynamic wake of the tower, and local topography.

3.1 Salt Deposition Due to Drift

The computer model was used to estimate average deposition rates on the ground and near ground air concentration of salt as a function of direction and distance from the Indian Point 3 cooling tower. The combined contribution from the Indian Point 2 and 3 cooling towers was estimated using a computer model that sums and interpolates the contribution of each tower as a function of distance and direction from the Indian Point 3 cooling tower. These estimates are shown in Figure 3-1 through 3-52 for selected time periods: in this case for the annual average and for each of the 12 months from October, 1973 through September, 1974.

The effect of precipitation (e.g., rainfall) on salt deposition rate was not calculated since only daily rainfall measurements were taken and hourly data is needed for the program. For this reason the calculations were made treating each hour of the time period selected as a dry hour.

The highest annual average inland offsite dry deposition rate and airborne concentration of salt estimated in this way is found to be 350 Kg/Km^2-month and 1.5 $\mu g/m^3$, respectively, at 1.2 miles SE from the tower, decreasing to 8 Kg/Km^2-month and 0.04 $\mu g/m^3$, respectively, within 5 miles in the same direction. Analogous results for each of the 12 months investigated are summarized in Table 3-1.

The estimates represented in Figures 3-1 through 3-52 are based on the following:

a) Tower Geometry and Operating Conditions

1. Average air exit speed: 3.8 m/sec
2. Basin water salinity: varies as a function of river water salinity. Monthly values used are given in Table 3-2.

All other conditions as described in Table 2 and Figures 1a and 1b of Appendix C.

b) Terrain Profile

As described by Figures 2a through 2p in Appendix C and classified as shown in Table 3, Appendix C.

c) Mass Drift Rate

Using a drift rate fraction of 0.002% of the circulating water flow rate, the mass drift rate of salt from the tower for each month is varied with river water salinity. Table 3-2 gives the monthly mass drift rate of salt from the tower used in the calculations.

d) Drift Drop Size Distribution

Table 4, Appendix C, represented the assumed drift drop size distribution just downstream of the eliminators

e) Atmospheric Conditions

Data used was that measured for each hour by instruments on the 400 ft meteorological tower at Indian Point 4, for the period of record from October 1, 1973 through September 30, 1974.

The atmospheric conditions for any given hour were classified as to wind direction, wind speed, stability and relative humidity by groups shown in Table 5, Appendix C. The values used to represent each group are given in Table 3, Appendix C.

The joint frequency of occurrence of weather conditions classified by these groups is given in Table 6, Appendix C. Data used were taken from the wind speed and direction instruments at 400 ft above grade. Temperature difference for determining stability was measured between the 400 ft and 33 ft levels. Relative humidity was derived from dew point and dry air measurements at the 400 ft level. Precipitation measurements were available on a daily basis.

3.2 Ice Formation Due to Drift

If the drift is high, ice formation on the ground and on structures may be caused at low ambient temperatures and/or low ground temperatures and low structure temperature.

The accumulation of ice on the ground and on surfaces outside the tower is a function of distance and direction from the tower and depends on the same parameters that influence salt deposition rate by drift. These parameters are described above. In addition, ice accumulation on structures depends on the drift drop collection efficiency of the object. The drift drop collection efficiency of an object depends on the size of the drops and the shape and dimensions of the object and the drop impingement velocity on the object. These relationships have been characterized in the mathematical model described in Appendix B and have been incorporated into a computer model.

The computer model was used to estimate the ice accumulation on the ground and on various structures as a function of time at selected distances from one tower, for each of the 16 discrete sectors used to represent the entire compass (360°) for the winter month of January. These estimates are shown in Figures 3-53 (a through p) and 3-54 (a through p). Figure 3-53 (a through p) gives the estimated ice accumulation on the ground, while Figure 3-54 (a through p) gives the estimated accumulation on various structures. As can be seen from these estimates, ice accumulation resulting from operation of a natural draft cooling tower is not expected to exceed 0.001 cm. To conservatively estimate the ice accumulation resulting from operation of two towers (Indian Point 2 and Indian Point 3) at half the basin salt concentration (i.e., at 7200 ppm instead of 14,400 ppm), the values shown in Figures 3-53 (a through p) and 3-43 (a through p) should be multiplied by 4. In this case (i.e., two towers) the estimated ice accumulation is not expected to exceed 0.004 cm.

References

1. Bōgh, P., Hopkirk, R., Junod H., and Zuend H., "A New Method of Assuming the Environmental Effects of Cooling Towers as First Applied to the Kaiser augst and Leibstadt Nuclear Power Plant," presented at the International Nuclear Industries Fair, October, 1972, Basel, Switzerland.

2. Spurr, G., "The Magnitude of the Problem of Thermal Discharge from Nuclear Power Plants," Central Electricity Generating Board, England, September, 1972.

3. Hoydysh, W., Experimental Work for the General Public Utilities Corporation, Forked River Environmental Report, 1972.

4. Laskowski, S.M., "A Mathematical Transport Model for Salt Distribution from a Salt Water Natural Draft Cooling Tower," presented at the Cooling Tower Symposium, University of Maryland, 1974.

List of Tables

Table 2-1

Incremental Increase in Relative Humidity vs Distance as a Function of Ambient Relative Humidity and Temperature - Hours of Occurrence

FOR ALL AMBIENT RELATIVE HUMIDITY AND AMBIENT TEMPERATURE GROUPS

DISTANCES(METERS) DIRECTION N

PERCENT DELTA RH INCREASE	500.0	1100.0	2000.0	5000.0	10000.0	22000.0	52000.0
.010	599	591	590	587	587	580	567
.050	0	0	0	0	2	6	23
.100	0	0	0	2	4	10	9
.500	0	1	5	10	6	3	0
1.000	0	2	1	0	0	0	0
3.000	0	4	3	0	0	0	0
5.000	0	1	0	0	0	0	0
10.000	0	0	0	0	0	0	0

DISTANCES(METERS) DIRECTION NNE

PERCENT DELTA RH INCREASE	500.0	1100.0	2000.0	5000.0	10000.0	22000.0	52000.0
.010	1070	1056	1045	1039	1031	1002	863
.050	0	0	0	2	3	12	67
.100	0	0	1	1	12	31	74
.500	0	1	14	26	24	25	63
1.000	0	6	6	2	0	0	1
3.000	0	4	4	0	0	0	1
5.000	0	3	0	0	0	0	0
10.000	0	0	0	0	0	0	1

DISTANCES(METERS) DIRECTION NE

PERCENT DELTA RH INCREASE	500.0	1100.0	2000.0	5000.0	10000.0	22000.0	52000.0
.010	504	504	504	503	501	487	320
.050	0	0	0	0	0	2	10
.100	0	0	0	0	0	2	17
.500	0	0	0	1	1	2	145
1.000	0	0	0	0	2	11	11
3.000	0	0	0	0	0	0	1
5.000	0	0	0	0	0	0	0
10.000	0	0	0	0	0	0	0

PERCENT DELTA RH INCREASE	500.0	1100.0	2000.0	5000.0	10000.0	22000.0	52000.0
DISTANCES(METERS) DIRECTION ENE							
.010	187	187	187	185	168	93	88
.050	0	0	0	0	0	0	2
.100	0	0	0	0	0	0	0
.500	0	0	0	0	0	65	61
1.000	0	0	0	2	0	10	15
3.000	0	0	0	0	19	19	20
5.000	0	0	0	0	0	0	0
10.000	0	0	0	0	0	0	1

PERCENT DELTA RH INCREASE	500.0	1100.0	2000.0	5000.0	10000.0	22000.0	52000.0
DISTANCES(METERS) DIRECTION E							
.010	249	246	249	228	161	96	91
.050	0	0	0	0	0	0	3
.100	0	0	0	0	0	2	5
.500	0	3	0	0	44	42	53
1.000	0	0	0	4	27	68	56
3.000	0	0	0	3	5	35	40
5.000	0	0	0	10	11	6	1
10.000	0	0	0	4	1	0	0

PERCENT DELTA RH INCREASE	500.0	1100.0	2000.0	5000.0	10000.0	22000.0	52000.0
DISTANCES(METERS) DIRECTION ESE							
.010	118	117	117	108	58	46	45
.050	0	0	0	0	0	0	1
.100	0	0	0	0	1	0	1
.500	0	0	1	1	15	6	14
1.000	0	1	0	4	37	44	37
3.000	0	0	0	0	3	19	20
5.000	0	0	0	3	3	3	0
10.000	0	0	0	2	1	0	0

PERCENT DELTA RH INCREASE	500.0	1100.0	2000.0	5000.0	10000.0	22000.0	52000.0
DISTANCES(METERS) DIRECTION SE							
.010	160	159	160	160	155	87	68
.050	0	0	0	0	0	0	0
.100	0	0	0	0	0	0	1
.500	0	1	0	0	0	65	68
1.000	0	0	0	0	0	3	20
3.000	0	0	0	0	5	5	3
5.000	0	0	0	0	0	0	0
10.000	0	0	0	0	0	0	0

PERCENT DELTA RH INCREASE	DISTANCES(METERS) 500.0	1100.0	2000.0	DIRECTION SSE 5000.0	10000.0	22000.0	52000.0
.010	189	188	189	188	188	186	85
.050	0	0	0	0	0	1	3
.100	0	0	0	0	1	0	32
.500	0	1	0	1	0	1	68
1.000	0	0	0	0	0	1	1
3.000	0	0	0	0	0	0	0
5.000	0	0	0	0	0	0	0
10.000	0	0	0	0	0	0	0

PERCENT DELTA RH INCREASE	DISTANCES(METERS) 500.0	1100.0	2000.0	DIRECTION S 5000.0	10000.0	22000.0	52000.0
.010	790	774	765	753	659	283	236
.050	0	0	0	1	1	15	66
.100	0	0	0	4	12	30	26
.500	0	1	9	27	75	350	328
1.000	0	4	15	3	9	78	104
3.000	0	11	1	2	34	34	30
5.000	0	0	0	0	0	0	0
10.000	0	0	0	0	0	0	0

PERCENT DELTA RH INCREASE	DISTANCES(METERS) 500.0	1100.0	2000.0	DIRECTION SSW 5000.0	10000.0	22000.0	52000.0
.010	699	697	693	692	685	640	224
.050	0	0	0	0	0	4	19
.100	0	0	0	1	2	19	97
.500	0	0	4	6	7	15	340
1.000	0	0	1	0	4	18	16
3.000	0	2	1	0	1	3	3
5.000	0	0	0	0	0	0	0
10.000	0	0	0	0	0	0	0

PERCENT DELTA RH INCREASE	DISTANCES(METERS) 500.0	1100.0	2000.0	DIRECTION SW 5000.0	10000.0	22000.0	52000.0
.010	830	830	830	830	828	801	296
.050	0	0	0	0	0	1	31
.100	0	0	0	0	1	10	170
.500	0	0	0	0	1	5	311
1.000	0	0	0	0	0	12	20
3.000	0	0	0	0	0	1	2
5.000	0	0	0	0	0	0	0
10.000	0	0	0	0	0	0	0

DISTANCES(METERS) DIRECTION WSW

PERCENT DELTA RH INCREASE	500.0	1100.0	2000.0	5000.0	10000.0	22000.0	52000.0
.010	355	355	355	355	352	313	101
.050	0	0	0	0	0	0	9
.100	0	0	0	0	0	12	51
.500	0	0	0	0	1	11	173
1.000	0	0	0	0	2	18	18
3.000	0	0	0	0	0	1	3
5.000	0	0	0	0	0	0	0
10.000	0	0	0	0	0	0	0

DISTANCES(METERS) DIRECTION W

PERCENT DELTA RH INCREASE	500.0	1100.0	2000.0	5000.0	10000.0	22000.0	52000.0
.010	286	286	286	286	274	233	79
.050	0	0	0	0	0	1	8
.100	0	0	0	0	0	1	3
.500	0	0	0	0	0	22	165
1.000	0	0	0	0	5	16	21
3.000	0	0	0	0	7	13	10
5.000	0	0	0	0	0	0	0
10.000	0	0	0	0	0	0	0

DISTANCES(METERS) DIRECTION WNW

PERCENT DELTA RH INCREASE	500.0	1100.0	2000.0	5000.0	10000.0	22000.0	52000.0
.010	357	356	354	354	333	233	126
.050	0	0	0	0	0	1	26
.100	0	0	0	0	1	13	25
.500	0	0	1	2	4	87	139
1.000	0	0	1	1	5	9	31
3.000	0	1	1	0	14	13	10
5.000	0	0	0	0	0	1	0
10.000	0	0	0	0	0	0	0

DISTANCES(METERS) DIRECTION NW

PERCENT DELTA RH INCREASE	500.0	1100.0	2000.0	5000.0	10000.0	22000.0	52000.0
.010	816	815	810	808	790	728	377
.050	0	0	0	0	1	2	39
.100	0	0	0	0	4	14	69
.500	0	0	3	5	15	56	314
1.000	0	1	1	3	5	11	13
3.000	0	0	2	0	1	5	3
5.000	0	0	0	0	0	0	0
10.000	0	0	0	0	0	0	1

Table 2-1, continued

PERCENT DELTA RH INCREASE	DISTANCES(METERS) 500.0	1100.0	2000.0	DIRECTION NNW 5000.0	10000.0	22000.0	52000.0
.010	638	638	638	637	636	627	597
.050	0	0	0	0	0	3	32
.100	0	0	0	0	1	4	8
.500	0	0	0	1	1	4	1
1.000	0	0	0	0	0	0	0
3.000	0	0	0	0	0	0	0
5.000	0	0	0	0	0	0	0
10.000	0	0	0	0	0	0	0

DELTA RELATIVE HUMIDITY- COUNTS OF OCCURENCES

FOR ALL DIRECTIONS WITH REL. HUM. LESS THAN OR EQUAL TO 60.0 PERCENT
WITH AMB. TEMP. LESS THAN OR EQUAL TO 20.0 DEG.F

DISTANCES(METERS)

PERCENT DELTA RH INCREASE	500.0	1100.0	2000.0	5000.0	10000.0	22000.0	52000.0
.010	88	86	84	83	81	76	72
.050	0	0	0	0	0	0	2
.100	0	0	0	0	0	1	0
.500	0	0	0	3	6	11	14
1.000	0	0	0	2	1	0	0
3.000	0	0	4	0	0	0	0
5.000	0	2	0	0	0	0	0
10.000	0	0	0	0	0	0	0

FOR ALL DIRECTIONS WITH REL. HUM. GREATER THAN 60.0 PERCENT AND LESS THAN OR EQUAL TO 70.0 PERCENT
WITH AMB. TEMP. LESS THAN OR EQUAL TO 20.0 DEG.F

DISTANCES(METERS)

PERCENT DELTA RH INCREASE	500.0	1100.0	2000.0	5000.0	10000.0	22000.0	52000.0
.010	138	138	137	137	136	127	114
.050	0	0	0	0	0	0	0
.100	0	0	0	0	0	0	1
.500	0	0	0	0	1	6	15
1.000	0	0	0	1	0	0	3
3.000	0	0	1	0	1	4	5
5.000	0	0	0	0	0	1	0
10.000	0	0	0	0	0	0	0

Table 2-1, continued

FOR ALL DIRECTIONS WITH REL. HUM. GREATER THAN 70.0 PERCENT AND LESS THAN OR EQUAL TO 80.0 PERCENT
WITH AMB. TEMP. LESS THAN OR EQUAL TO 20.0 DEG.F

DISTANCES(METERS)

PERCENT DELTA RH INCREASE	500.0	1100.0	2000.0	5000.0	10000.0	22000.0	52000.0
.010	69	69	69	68	69	65	55
.050	0	0	0	0	0	0	1
.100	0	0	0	0	0	0	0
.500	0	0	0	1	0	2	6
1.000	0	0	0	0	0	0	5
3.000	0	0	0	0	0	2	2
5.000	0	0	0	0	0	0	0
10.000	0	0	0	0	0	0	0

FOR ALL DIRECTIONS WITH REL. HUM. GREATER THAN 80.0 PERCENT AND LESS THAN OR EQUAL TO 85.0 PERCENT
WITH AMB. TEMP. LESS THAN OR EQUAL TO 20.0 DEG.F

DISTANCES(METERS)

PERCENT DELTA RH INCREASE	500.0	1100.0	2000.0	5000.0	10000.0	22000.0	52000.0
.010	45	45	45	45	45	43	34
.050	0	0	0	0	0	0	0
.100	0	0	0	0	0	0	2
.500	0	0	0	0	0	0	0
1.000	0	0	0	0	0	0	4
3.000	0	0	0	0	0	2	5
5.000	0	0	0	0	0	0	0
10.000	0	0	0	0	0	0	0

FOR ALL DIRECTIONS WITH REL. HUM. GREATER THAN 85.0 PERCENT AND LESS THAN OR EQUAL TO 90.0 PERCENT
WITH AMB. TEMP. LESS THAN OR EQUAL TO 20.0 DEG.F

DISTANCES(METERS)

PERCENT DELTA RH INCREASE	500.0	1100.0	2000.0	5000.0	10000.0	22000.0	52000.0
.010	39	39	39	39	39	39	26
.050	0	0	0	0	0	0	0
.100	0	0	0	0	0	0	9
.500	0	0	0	0	0	0	3
1.000	0	0	0	0	0	0	0
3.000	0	0	0	0	0	0	1
5.000	0	0	0	0	0	0	0
10.000	0	0	0	0	0	0	0

Table 2-1, continued

FOR ALL DIRECTIONS WITH REL. HUM. GREATER THAN 90.0 PERCENT AND LESS THAN OR EQUAL TO 95.0 PERCENT
WITH AMB. TEMP. LESS THAN OR EQUAL TO 20.0 DEG.F

DISTANCES(METERS)

PERCENT DELTA RH INCREASE	500.0	1100.0	2000.0	5000.0	10000.0	22000.0	52000.0
.010	20	20	20	20	19	18	17
.050	0	0	0	0	0	0	0
.100	0	0	0	0	0	0	0
.500	0	0	0	0	0	0	0
1.000	0	0	0	0	0	0	0
3.000	0	0	0	0	1	2	3
5.000	0	0	0	0	0	0	0
10.000	0	0	0	0	0	0	0

FOR ALL DIRECTIONS WITH REL. HUM. GREATER THAN 95.0 PERCENT AND LESS THAN OR EQUAL TO 9999.0 PERCENT
WITH AMB. TEMP. LESS THAN OR EQUAL TO 20.0 DEG.F

DISTANCES(METERS)

PERCENT DELTA RH INCREASE	500.0	1100.0	2000.0	5000.0	10000.0	22000.0	52000.0
.010	18	18	17	17	17	16	12
.050	0	0	0	0	0	0	0
.100	0	0	0	0	0	0	1
.500	0	0	0	0	1	1	0
1.000	0	0	1	1	0	0	0
3.000	0	0	0	0	0	1	5
5.000	0	0	0	0	0	0	0
10.000	0	0	0	0	0	0	0

FOR ALL DIRECTIONS WITH REL. HUM. LESS THAN OR EQUAL TO 60.0 PERCENT
WITH AMB. TEMP. GREATER THAN 20.0 DEG.F AND LESS THAN OR EQUAL TO 30.0 DEG.F

DISTANCES(METERS)

PERCENT DELTA RH INCREASE	500.0	1100.0	2000.0	5000.0	10000.0	22000.0	52000.0
.010	370	368	368	365	365	354	294
.050	0	0	0	0	0	0	5
.100	0	0	0	0	1	7	5
.500	0	0	0	5	4	4	55
1.000	0	0	0	0	0	2	6
3.000	0	0	2	0	0	3	5
5.000	0	2	0	0	0	0	0
10.000	0	0	0	0	0	0	0

Table 2-1, continued

FOR ALL DIRECTIONS WITH REL. HUM. GREATER THAN 60.0 PERCENT AND LESS THAN OR EQUAL TO 70.0 PERCENT
WITH AMB. TEMP. GREATER THAN 20.0 DEG.F AND LESS THAN OR EQUAL TO 30.0 DEG.F

DISTANCES (METERS)

PERCENT DELTA RH INCREASE	500.0	1100.0	2000.0	5000.0	10000.0	22000.0	52000.0
.010	126	124	123	122	123	114	93
.050	0	0	0	0	0	0	2
.100	0	0	0	0	0	1	3
.500	0	0	0	3	3	5	19
1.000	0	0	1	1	0	2	5
3.000	0	2	2	0	0	4	4
5.000	0	0	0	0	0	0	0
10.000	0	0	0	0	0	0	0

FOR ALL DIRECTIONS WITH REL. HUM. GREATER THAN 70.0 PERCENT AND LESS THAN OR EQUAL TO 80.0 PERCENT
WITH AMB. TEMP. GREATER THAN 20.0 DEG.F AND LESS THAN OR EQUAL TO 30.0 DEG.F

DISTANCES (METERS)

PERCENT DELTA RH INCREASE	500.0	1100.0	2000.0	5000.0	10000.0	22000.0	52000.0
.010	97	96	92	90	90	83	60
.050	0	0	0	0	0	0	3
.100	0	0	0	0	0	5	5
.500	0	0	2	6	7	8	26
1.000	0	0	2	1	0	1	3
3.000	0	1	1	0	0	0	0
5.000	0	0	0	0	0	0	0
10.000	0	0	0	0	0	0	0

FOR ALL DIRECTIONS WITH REL. HUM. GREATER THAN 80.0 PERCENT AND LESS THAN OR EQUAL TO 85.0 PERCENT
WITH AMB. TEMP. GREATER THAN 20.0 DEG.F AND LESS THAN OR EQUAL TO 30.0 DEG.F

DISTANCES (METERS)

PERCENT DELTA RH INCREASE	500.0	1100.0	2000.0	5000.0	10000.0	22000.0	52000.0
.010	33	33	33	33	33	30	22
.050	0	0	0	0	0	0	0
.100	0	0	0	0	0	0	0
.500	0	0	0	0	0	1	8
1.000	0	0	0	0	0	2	3
3.000	0	0	0	0	0	0	0
5.000	0	0	0	0	0	0	0
10.000	0	0	0	0	0	0	0

FOR ALL DIRECTIONS WITH REL. HUM. GREATER THAN 85.0 PERCENT AND LESS THAN OR EQUAL TO 90.0 PERCENT
WITH AMB. TEMP. GREATER THAN 20.0 DEG.F AND LESS THAN OR EQUAL TO 30.0 DEG.F

PERCENT DELTA RH INCREASE	DISTANCES(METERS) 500.0	1100.0	2000.0	5000.0	10000.0	22000.0	52000.0
.010	48	48	48	48	46	45	33
.050	0	0	0	0	0	0	2
.100	0	0	0	0	1	0	3
.500	0	0	0	0	1	2	9
1.000	0	0	0	0	0	0	0
3.000	0	0	0	0	0	1	1
5.000	0	0	0	0	0	0	0
10.000	0	0	0	0	0	0	0

FOR ALL DIRECTIONS WITH REL. HUM. GREATER THAN 90.0 PERCENT AND LESS THAN OR EQUAL TO 95.0 PERCENT
WITH AMB. TEMP. GREATER THAN 20.0 DEG.F AND LESS THAN OR EQUAL TO 30.0 DEG.F

PERCENT DELTA RH INCREASE	DISTANCES(METERS) 500.0	1100.0	2000.0	5000.0	10000.0	22000.0	52000.0
.010	23	23	23	23	23	21	18
.050	0	0	0	0	0	0	0
.100	0	0	0	0	0	0	0
.500	0	0	0	0	0	0	1
1.000	0	0	0	0	0	1	3
3.000	0	0	0	0	0	1	1
5.000	0	0	0	0	0	0	0
10.000	0	0	0	0	0	0	0

FOR ALL DIRECTIONS WITH REL. HUM. GREATER THAN 95.0 PERCENT AND LESS THAN OR EQUAL TO 9999.0 PERCENT
WITH AMB. TEMP. GREATER THAN 20.0 DEG.F AND LESS THAN OR EQUAL TO 30.0 DEG.F

PERCENT DELTA RH INCREASE	DISTANCES(METERS) 500.0	1100.0	2000.0	5000.0	10000.0	22000.0	52000.0
.010	17	17	17	17	17	17	15
.050	0	0	0	0	0	0	0
.100	0	0	0	0	0	0	0
.500	0	0	0	0	0	0	1
1.000	0	0	0	0	0	0	1
3.000	0	0	0	0	0	0	0
5.000	0	0	0	0	0	0	0
10.000	0	0	0	0	0	0	0

Table 2-1, continued

FOR ALL DIRECTIONS WITH REL. HUM. LESS THAN OR EQUAL TO 60.0 PERCENT
WITH AMB. TEMP. GREATER THAN 30.0 DEG.F AND LESS THAN OR EQUAL TO 40.0 DEG.F

DISTANCES(METERS)

PERCENT DELTA RH INCREASE	500.0	1100.0	2000.0	5000.0	10000.0	22000.0	52000.0
.010	601	600	597	596	594	561	427
.050	0	0	0	0	0	1	10
.100	0	0	0	0	1	3	29
.500	0	0	1	4	5	24	111
1.000	0	0	2	1	1	7	19
3.000	0	1	1	0	0	5	5
5.000	0	0	0	0	0	0	0
10.000	0	0	0	0	0	0	0

FOR ALL DIRECTIONS WITH REL. HUM. GREATER THAN 60.0 PERCENT AND LESS THAN OR EQUAL TO 70.0 PERCENT
WITH AMB. TEMP. GREATER THAN 30.0 DEG.F AND LESS THAN OR EQUAL TO 40.0 DEG.F

DISTANCES(METERS)

PERCENT DELTA RH INCREASE	500.0	1100.0	2000.0	5000.0	10000.0	22000.0	52000.0
.010	127	127	127	127	127	113	70
.050	0	0	0	0	0	0	2
.100	0	0	0	0	0	2	3
.500	0	0	0	0	0	3	36
1.000	0	0	0	0	0	5	10
3.000	0	0	0	0	0	4	4
5.000	0	0	0	0	0	0	0
10.000	0	0	0	0	0	0	2

FOR ALL DIRECTIONS WITH REL. HUM. GREATER THAN 70.0 PERCENT AND LESS THAN OR EQUAL TO 80.0 PERCENT
WITH AMB. TEMP. GREATER THAN 30.0 DEG.F AND LESS THAN OR EQUAL TO 40.0 DEG.F

DISTANCES(METERS)

PERCENT DELTA RH INCREASE	500.0	1100.0	2000.0	5000.0	10000.0	22000.0	52000.0
.010	162	162	162	162	157	130	74
.050	0	0	0	0	0	0	0
.100	0	0	0	0	0	0	0
.500	0	0	0	0	0	10	51
1.000	0	0	0	0	0	14	29
3.000	0	0	0	0	5	8	8
5.000	0	0	0	0	0	0	0
10.000	0	0	0	0	0	0	0

Table 2-1, continued

FOR ALL DIRECTIONS WITH REL. HUM. GREATER THAN 80.0 PERCENT AND LESS THAN OR EQUAL TO 85.0 PERCENT
WITH AMB. TEMP. GREATER THAN 30.0 DEG.F AND LESS THAN OR EQUAL TO 40.0 DEG.F

PERCENT DELTA RH INCREASE	DISTANCES(METERS) 500.0	1100.0	2000.0	5000.0	10000.0	22000.0	52000.0
.010	48	48	48	48	45	33	14
.050	0	0	0	0	0	0	0
.100	0	0	0	0	0	0	0
.500	0	0	0	0	0	3	18
1.000	0	0	0	0	1	7	10
3.000	0	0	0	0	2	5	5
5.000	0	0	0	0	0	0	0
10.000	0	0	0	0	0	0	1

FOR ALL DIRECTIONS WITH REL. HUM. GREATER THAN 85.0 PERCENT AND LESS THAN OR EQUAL TO 90.0 PERCENT
WITH AMB. TEMP. GREATER THAN 30.0 DEG.F AND LESS THAN OR EQUAL TO 40.0 DEG.F

PERCENT DELTA RH INCREASE	DISTANCES(METERS) 500.0	1100.0	2000.0	5000.0	10000.0	22000.0	52000.0
.010	47	47	47	47	46	39	19
.050	0	0	0	0	0	0	0
.100	0	0	0	0	0	0	1
.500	0	0	0	0	0	4	20
1.000	0	0	0	0	0	1	4
3.000	0	0	0	0	1	3	3
5.000	0	0	0	0	0	0	0
10.000	0	0	0	0	0	0	0

FOR ALL DIRECTIONS WITH REL. HUM. GREATER THAN 90.0 PERCENT AND LESS THAN OR EQUAL TO 95.0 PERCENT
WITH AMB. TEMP. GREATER THAN 30.0 DEG.F AND LESS THAN OR EQUAL TO 40.0 DEG.F

PERCENT DELTA RH INCREASE	DISTANCES(METERS) 500.0	1100.0	2000.0	5000.0	10000.0	22000.0	52000.0
.010	59	59	59	59	55	42	22
.050	0	0	0	0	0	0	1
.100	0	0	0	0	0	0	0
.500	0	0	0	0	0	8	24
1.000	0	0	0	0	1	6	9
3.000	0	0	0	0	3	3	3
5.000	0	0	0	0	0	0	0
10.000	0	0	0	0	0	0	0

Table 2-1, continued

FOR ALL DIRECTIONS WITH REL. HUM. GREATER THAN 95.0 PERCENT AND LESS THAN OR EQUAL TO 9999.0 PERCENT
WITH AMB. TEMP. GREATER THAN 30.0 DEG.F AND LESS THAN OR EQUAL TO 40.0 DEG.F

PERCENT DELTA RH INCREASE	DISTANCES(METERS) 500.0	1100.0	2000.0	5000.0	10000.0	22000.0	52000.0
.010	51	51	51	50	44	29	19
.050	0	0	0	0	0	0	0
.100	0	0	0	0	0	0	0
.500	0	0	0	0	1	10	17
1.000	0	0	0	0	1	7	12
3.000	0	0	0	1	5	5	3
5.000	0	0	0	0	0	0	0
10.000	0	0	0	0	0	0	0

FOR ALL DIRECTIONS WITH REL. HUM. LESS THAN OR EQUAL TO 60.0 PERCENT
WITH AMB. TEMP. GREATER THAN 40.0 DEG.F AND LESS THAN OR EQUAL TO 50.0 DEG.F

PERCENT DELTA RH INCREASE	DISTANCES(METERS) 500.0	1100.0	2000.0	5000.0	10000.0	22000.0	52000.0
.010	552	551	550	550	545	509	364
.050	0	0	0	0	0	2	24
.100	0	0	0	0	1	6	30
.500	0	0	1	2	4	16	111
1.000	0	0	0	0	0	14	18
3.000	0	1	1	0	2	5	5
5.000	0	0	0	0	0	0	0
10.000	0	0	0	0	0	0	0

FOR ALL DIRECTIONS WITH REL. HUM. GREATER THAN 60.0 PERCENT AND LESS THAN OR EQUAL TO 70.0 PERCENT
WITH AMB. TEMP. GREATER THAN 40.0 DEG.F AND LESS THAN OR EQUAL TO 50.0 DEG.F

PERCENT DELTA RH INCREASE	DISTANCES(METERS) 500.0	1100.0	2000.0	5000.0	10000.0	22000.0	52000.0
.010	178	178	178	178	173	154	99
.050	0	0	0	0	0	0	3
.100	0	0	0	0	0	0	2
.500	0	0	0	0	0	6	53
1.000	0	0	0	0	2	10	16
3.000	0	0	0	0	3	8	5
5.000	0	0	0	0	0	0	0
10.000	0	0	0	0	0	0	0

Table 2-1, continued

FOR ALL DIRECTIONS WITH REL. HUM. GREATER THAN 70.0 PERCENT AND LESS THAN OR EQUAL TO 80.0 PERCENT
WITH AMB. TEMP. GREATER THAN 40.0 DEG.F AND LESS THAN OR EQUAL TO 50.0 DEG.F

DISTANCES(METERS)

PERCENT DELTA RH INCREASE	500.0	1100.0	2000.0	5000.0	10000.0	22000.0	52000.0
.010	171	171	171	171	161	131	69
.050	0	0	0	0	0	0	3
.100	0	0	0	0	0	0	1
.500	0	0	0	0	1	20	77
1.000	0	0	0	0	1	10	12
3.000	0	0	0	0	8	10	9
5.000	0	0	0	0	0	0	0
10.000	0	0	0	0	0	0	0

FOR ALL DIRECTIONS WITH REL. HUM. GREATER THAN 80.0 PERCENT AND LESS THAN OR EQUAL TO 85.0 PERCENT
WITH AMB. TEMP. GREATER THAN 40.0 DEG.F AND LESS THAN OR EQUAL TO 50.0 DEG.F

DISTANCES(METERS)

PERCENT DELTA RH INCREASE	500.0	1100.0	2000.0	5000.0	10000.0	22000.0	52000.0
.010	79	79	79	77	72	63	30
.050	0	0	0	0	0	0	2
.100	0	0	0	0	0	2	4
.500	0	0	0	0	0	5	33
1.000	0	0	0	0	1	3	6
3.000	0	0	0	0	4	4	4
5.000	0	0	0	2	2	2	0
10.000	0	0	0	0	0	0	0

FOR ALL DIRECTIONS WITH REL. HUM. GREATER THAN 85.0 PERCENT AND LESS THAN OR EQUAL TO 90.0 PERCENT
WITH AMB. TEMP. GREATER THAN 40.0 DEG.F AND LESS THAN OR EQUAL TO 50.0 DEG.F

DISTANCES(METERS)

PERCENT DELTA RH INCREASE	500.0	1100.0	2000.0	5000.0	10000.0	22000.0	52000.0
.010	71	71	71	68	59	46	26
.050	0	0	0	0	0	0	2
.100	0	0	0	0	0	0	2
.500	0	0	0	0	0	3	20
1.000	0	0	0	0	3	11	13
3.000	0	0	0	0	6	9	8
5.000	0	0	0	1	3	2	0
10.000	0	0	0	2	0	0	0

Table 2-1, continued

FOR ALL DIRECTIONS WITH REL. HUM. GREATER THAN 90.0 PERCENT AND LESS THAN OR EQUAL TO 95.0 PERCENT
WITH AMB. TEMP. GREATER THAN 40.0 DEG.F AND LESS THAN OR EQUAL TO 50.0 DEG.F

	DISTANCES(METERS)						
PERCENT DELTA RH INCREASE	500.0	1100.0	2000.0	5000.0	10000.0	22000.0	52000.0
.010	100	100	100	100	89	66	28
.050	0	0	0	0	0	0	0
.100	0	0	0	0	0	0	7
.500	0	0	0	0	4	19	52
1.000	0	0	0	0	4	12	10
3.000	0	0	0	0	3	3	3
5.000	0	0	0	0	0	0	0
10.000	0	0	0	0	0	0	0

FOR ALL DIRECTIONS WITH REL. HUM. GREATER THAN 95.0 PERCENT AND LESS THAN OR EQUAL TO 9999.0 PERCENT
WITH AMB. TEMP. GREATER THAN 40.0 DEG.F AND LESS THAN OR EQUAL TO 50.0 DEG.F

	DISTANCES(METERS)						
PERCENT DELTA RH INCREASE	500.0	1100.0	2000.0	5000.0	10000.0	22000.0	52000.0
.010	134	134	134	134	123	84	38
.050	0	0	0	0	0	0	2
.100	0	0	0	0	0	1	7
.500	0	0	0	0	5	35	79
1.000	0	0	0	0	5	12	7
3.000	0	0	0	0	1	2	1
5.000	0	0	0	0	0	0	0
10.000	0	0	0	0	0	0	0

FOR ALL DIRECTIONS WITH REL. HUM. LESS THAN OR EQUAL TO 60.0 PERCENT
WITH AMB. TEMP. GREATER THAN 50.0 DEG.F AND LESS THAN OR EQUAL TO 60.0 DEG.F

	DISTANCES(METERS)						
PERCENT DELTA RH INCREASE	500.0	1100.0	2000.0	5000.0	10000.0	22000.0	52000.0
.010	474	470	466	465	450	394	262
.050	0	0	0	0	0	1	37
.100	0	0	0	0	4	17	42
.500	0	0	3	8	13	39	109
1.000	0	0	5	0	6	21	21
3.000	0	4	0	0	0	2	2
5.000	0	0	0	0	0	1	1
10.000	0	0	0	1	1	0	0

FOR ALL DIRECTIONS WITH REL. HUM. GREATER THAN 60.0 PERCENT AND LESS THAN OR EQUAL TO 70.0 PERCENT
WITH AMB. TEMP. GREATER THAN 50.0 DEG.F AND LESS THAN OR EQUAL TO 60.0 DEG.F

PERCENT DELTA RH INCREASE	DISTANCES(METERS) 500.0	1100.0	2000.0	5000.0	10000.0	22000.0	52000.0
.010	123	123	123	123	118	99	60
.050	0	0	0	0	0	0	4
.100	0	0	0	0	0	1	0
.500	0	0	0	0	0	14	30
1.000	0	0	0	0	2	6	7
3.000	0	0	0	0	3	3	2
5.000	0	0	0	0	0	0	0
10.000	0	0	0	0	0	0	0

FOR ALL DIRECTIONS WITH REL. HUM. GREATER THAN 70.0 PERCENT AND LESS THAN OR EQUAL TO 80.0 PERCENT
WITH AMB. TEMP. GREATER THAN 50.0 DEG.F AND LESS THAN OR EQUAL TO 60.0 DEG.F

PERCENT DELTA RH INCREASE	DISTANCES(METERS) 500.0	1100.0	2000.0	5000.0	10000.0	22000.0	52000.0
.010	184	184	184	181	171	139	87
.050	0	0	0	0	0	1	3
.100	0	0	0	1	1	0	7
.500	0	0	0	0	3	27	68
1.000	0	0	0	0	3	11	14
3.000	0	0	0	0	4	4	5
5.000	0	0	0	0	1	2	0
10.000	0	0	0	2	1	0	0

FOR ALL DIRECTIONS WITH REL. HUM. GREATER THAN 80.0 PERCENT AND LESS THAN OR EQUAL TO 85.0 PERCENT
WITH AMB. TEMP. GREATER THAN 50.0 DEG.F AND LESS THAN OR EQUAL TO 60.0 DEG.F

PERCENT DELTA RH INCREASE	DISTANCES(METERS) 500.0	1100.0	2000.0	5000.0	10000.0	22000.0	52000.0
.010	110	110	110	109	95	84	44
.050	0	0	0	0	0	0	2
.100	0	0	0	0	0	0	11
.500	0	0	0	0	7	12	39
1.000	0	0	0	0	5	11	11
3.000	0	0	0	0	2	2	3
5.000	0	0	0	0	1	1	0
10.000	0	0	0	1	0	0	0

Table 2-1, continued

FOR ALL DIRECTIONS WITH REL. HUM. GREATER THAN 85.0 PERCENT AND LESS THAN OR EQUAL TO 90.0 PERCENT
WITH AMB. TEMP. GREATER THAN 50.0 DEG.F AND LESS THAN OR EQUAL TO 60.0 DEG.F

DISTANCES(METERS)

PERCENT DELTA RH INCREASE	500.0	1100.0	2000.0	5000.0	10000.0	22000.0	52000.0
.010	134	134	134	127	114	94	60
.050	0	0	0	0	0	0	1
.100	0	0	0	0	1	0	14
.500	0	0	0	0	2	21	43
1.000	0	0	0	3	9	10	8
3.000	0	0	0	1	5	8	8
5.000	0	0	0	3	3	1	0
10.000	0	0	0	0	0	0	0

FOR ALL DIRECTIONS WITH REL. HUM. GREATER THAN 90.0 PERCENT AND LESS THAN OR EQUAL TO 95.0 PERCENT
WITH AMB. TEMP. GREATER THAN 50.0 DEG.F AND LESS THAN OR EQUAL TO 60.0 DEG.F

DISTANCES(METERS)

PERCENT DELTA RH INCREASE	500.0	1100.0	2000.0	5000.0	10000.0	22000.0	52000.0
.010	153	153	153	152	133	106	56
.050	0	0	0	0	0	0	0
.100	0	0	0	0	0	5	28
.500	0	0	0	0	16	28	58
1.000	0	0	0	0	1	11	8
3.000	0	0	0	0	2	3	3
5.000	0	0	0	1	1	0	0
10.000	0	0	0	0	0	0	0

FOR ALL DIRECTIONS WITH REL. HUM. GREATER THAN 95.0 PERCENT AND LESS THAN OR EQUAL TO 9999.0 PERCENT
WITH AMB. TEMP. GREATER THAN 50.0 DEG.F AND LESS THAN OR EQUAL TO 60.0 DEG.F

DISTANCES(METERS)

PERCENT DELTA RH INCREASE	500.0	1100.0	2000.0	5000.0	10000.0	22000.0	52000.0
.010	135	135	135	133	120	82	31
.050	0	0	0	0	0	0	2
.100	0	0	0	0	0	3	29
.500	0	0	0	0	13	43	69
1.000	0	0	0	1	1	6	3
3.000	0	0	0	0	1	1	1
5.000	0	0	0	1	0	0	0
10.000	0	0	0	0	0	0	0

FOR ALL DIRECTIONS WITH REL. HUM. LESS THAN OR EQUAL TO 60.0 PERCENT
WITH AMB. TEMP. GREATER THAN 60.0 DEG.F AND LESS THAN OR EQUAL TO 70.0 DEG.F

DISTANCES(METERS)

PERCENT DELTA RH INCREASE	500.0	1100.0	2000.0	5000.0	10000.0	22000.0	52000.0
.010	400	390	386	381	367	318	228
.050	0	0	0	0	0	6	37
.100	0	0	0	1	10	24	19
.500	0	0	7	17	18	38	103
1.000	0	2	7	0	4	13	13
3.000	0	8	0	1	1	1	0
5.000	0	0	0	0	0	0	0
10.000	0	0	0	0	0	0	0

FOR ALL DIRECTIONS WITH REL. HUM. GREATER THAN 60.0 PERCENT AND LESS THAN OR EQUAL TO 70.0 PERCENT
WITH AMB. TEMP. GREATER THAN 60.0 DEG.F AND LESS THAN OR EQUAL TO 70.0 DEG.F

DISTANCES(METERS)

PERCENT DELTA RH INCREASE	500.0	1100.0	2000.0	5000.0	10000.0	22000.0	52000.0
.010	189	188	188	188	182	161	97
.050	0	0	0	0	0	2	9
.100	0	0	0	0	1	0	6
.500	0	0	0	1	4	21	69
1.000	0	1	1	0	2	5	8
3.000	0	0	0	0	0	0	0
5.000	0	0	0	0	0	0	0
10.000	0	0	0	0	0	0	0

FOR ALL DIRECTIONS WITH REL. HUM. GREATER THAN 70.0 PERCENT AND LESS THAN OR EQUAL TO 80.0 PERCENT
WITH AMB. TEMP. GREATER THAN 60.0 DEG.F AND LESS THAN OR EQUAL TO 70.0 DEG.F

DISTANCES(METERS)

PERCENT DELTA RH INCREASE	500.0	1100.0	2000.0	5000.0	10000.0	22000.0	52000.0
.010	244	244	243	241	229	199	126
.050	0	0	0	0	0	3	17
.100	0	0	0	0	0	3	17
.500	0	0	1	2	3	23	68
1.000	0	0	0	1	7	11	12
3.000	0	0	0	0	5	5	4
5.000	0	0	0	0	0	0	0
10.000	0	0	0	0	0	0	0

Table 2-1, continued

FOR ALL DIRECTIONS WITH REL. HUM. GREATER THAN 80.0 PERCENT AND LESS THAN OR EQUAL TO 85.0 PERCENT
WITH AMB. TEMP. GREATER THAN 60.0 DEG.F AND LESS THAN OR EQUAL TO 70.0 DEG.F

DISTANCES(METERS)

PERCENT DELTA RH INCREASE	500.0	1100.0	2000.0	5000.0	10000.0	22000.0	52000.0
.010	171	171	171	169	156	130	84
.050	0	0	0	0	0	1	1
.100	0	0	0	0	0	0	9
.500	0	0	0	0	1	23	62
1.000	0	0	0	1	9	12	11
3.000	0	0	0	1	5	5	4
5.000	0	0	0	0	0	0	0
10.000	0	0	0	0	0	0	0

FOR ALL DIRECTIONS WITH REL. HUM. GREATER THAN 85.0 PERCENT AND LESS THAN OR EQUAL TO 90.0 PERCENT
WITH AMB. TEMP. GREATER THAN 60.0 DEG.F AND LESS THAN OR EQUAL TO 70.0 DEG.F

DISTANCES(METERS)

PERCENT DELTA RH INCREASE	500.0	1100.0	2000.0	5000.0	10000.0	22000.0	52000.0
.010	195	193	194	189	181	149	77
.050	0	0	0	1	1	2	4
.100	0	0	0	0	0	1	28
.500	0	1	1	0	2	24	69
1.000	0	1	0	2	3	11	9
3.000	0	0	0	0	5	8	8
5.000	0	0	0	3	3	0	0
10.000	0	0	0	0	0	0	0

FOR ALL DIRECTIONS WITH REL. HUM. GREATER THAN 90.0 PERCENT AND LESS THAN OR EQUAL TO 95.0 PERCENT
WITH AMB. TEMP. GREATER THAN 60.0 DEG.F AND LESS THAN OR EQUAL TO 70.0 DEG.F

DISTANCES(METERS)

PERCENT DELTA RH INCREASE	500.0	1100.0	2000.0	5000.0	10000.0	22000.0	52000.0
.010	206	206	206	204	188	164	93
.050	0	0	0	0	0	0	3
.100	0	0	0	0	0	0	21
.500	0	0	0	0	6	27	95
1.000	0	0	0	1	6	9	9
3.000	0	0	0	0	6	6	5
5.000	0	0	0	1	0	0	0
10.000	0	0	0	0	0	0	0

FOR ALL DIRECTIONS WITH REL. HUM. GREATER THAN 95.0 PERCENT AND LESS THAN OR EQUAL TO 9999.0 PERCENT
WITH AMB. TEMP. GREATER THAN 60.0 DEG.F AND LESS THAN OR EQUAL TO 70.0 DEG.F

DISTANCES(METERS)

PERCENT DELTA RH INCREASE	500.0	1100.0	2000.0	5000.0	10000.0	22000.0	52000.0
.010	225	225	225	222	204	151	51
.050	0	0	0	0	0	0	6
.100	0	0	0	0	0	0	44
.500	0	0	0	0	14	61	117
1.000	0	0	0	1	5	11	5
3.000	0	0	0	1	2	2	2
5.000	0	0	0	1	0	0	0
10.000	0	0	0	0	0	0	0

FOR ALL DIRECTIONS WITH REL. HUM. LESS THAN OR EQUAL TO 60.0 PERCENT
WITH AMB. TEMP. GREATER THAN 70.0 DEG.F AND LESS THAN OR EQUAL TO 9999.0 DEG.F

DISTANCES(METERS)

PERCENT DELTA RH INCREASE	500.0	1100.0	2000.0	5000.0	10000.0	22000.0	52000.0
.010	614	601	589	582	561	478	342
.050	0	0	0	2	6	20	101
.100	0	0	0	5	13	56	40
.500	0	0	19	25	30	54	126
1.000	0	8	6	0	4	6	5
3.000	0	5	0	0	0	0	0
5.000	0	0	0	0	0	0	0
10.000	0	0	0	0	0	0	0

FOR ALL DIRECTIONS WITH REL. HUM. GREATER THAN 60.0 PERCENT AND LESS THAN OR EQUAL TO 70.0 PERCENT
WITH AMB. TEMP. GREATER THAN 70.0 DEG.F AND LESS THAN OR EQUAL TO 9999.0 DEG.F

DISTANCES(METERS)

PERCENT DELTA RH INCREASE	500.0	1100.0	2000.0	5000.0	10000.0	22000.0	52000.0
.010	295	288	292	292	283	243	128
.050	0	0	0	0	0	7	31
.100	0	0	1	1	5	8	33
.500	0	5	2	2	3	33	99
1.000	0	2	0	0	3	2	4
3.000	0	0	0	0	1	2	0
5.000	0	0	0	0	0	0	0
10.000	0	0	0	0	0	0	0

Table 2-1, continued

FOR ALL DIRECTIONS WITH REL. HUM. GREATER THAN 70.0 PERCENT AND LESS THAN OR EQUAL TO 80.0 PERCENT
WITH AMB. TEMP. GREATER THAN 70.0 DEG.F AND LESS THAN OR EQUAL TO 9999.0 DEG.F

DISTANCES(METERS)

PERCENT DELTA RH INCREASE	500.0	1100.0	2000.0	5000.0	10000.0	22000.0	52000.0
.010	209	207	209	206	200	169	102
.050	0	0	0	0	0	2	7
.100	0	0	0	0	0	2	27
.500	0	2	0	1	5	27	65
1.000	0	0	0	2	3	8	4
3.000	0	0	0	0	1	1	1
5.000	0	0	0	0	0	0	0
10.000	0	0	0	0	0	0	0

FOR ALL DIRECTIONS WITH REL. HUM. GREATER THAN 80.0 PERCENT AND LESS THAN OR EQUAL TO 85.0 PERCENT
WITH AMB. TEMP. GREATER THAN 70.0 DEG.F AND LESS THAN OR EQUAL TO 9999.0 DEG.F

DISTANCES(METERS)

PERCENT DELTA RH INCREASE	500.0	1100.0	2000.0	5000.0	10000.0	22000.0	52000.0
.010	98	98	98	98	93	77	33
.050	0	0	0	0	0	0	3
.100	0	0	0	0	0	0	24
.500	0	0	0	0	4	16	36
1.000	0	0	0	0	1	4	2
3.000	0	0	0	0	0	1	0
5.000	0	0	0	0	0	0	0
10.000	0	0	0	0	0	0	0

FOR ALL DIRECTIONS WITH REL. HUM. GREATER THAN 85.0 PERCENT AND LESS THAN OR EQUAL TO 90.0 PERCENT
WITH AMB. TEMP. GREATER THAN 70.0 DEG.F AND LESS THAN OR EQUAL TO 9999.0 DEG.F

DISTANCES(METERS)

PERCENT DELTA RH INCREASE	500.0	1100.0	2000.0	5000.0	10000.0	22000.0	52000.0
.010	66	66	66	66	62	55	25
.050	0	0	0	0	0	0	3
.100	0	0	0	0	0	0	18
.500	0	0	0	0	2	9	18
1.000	0	0	0	0	1	2	2
3.000	0	0	0	0	1	0	0
5.000	0	0	0	0	0	0	0
10.000	0	0	0	0	0	0	0

Table 2-1, continued

FOR ALL DIRECTIONS WITH REL. HUM. GREATER THAN 90.0 PERCENT AND LESS THAN OR EQUAL TO 95.0 PERCENT
WITH AMB. TEMP. GREATER THAN 70.0 DEG.F AND LESS THAN OR EQUAL TO 9999.0 DEG.F

DISTANCES(METERS)

PERCENT DELTA RH INCREASE	500.0	1100.0	2000.0	5000.0	10000.0	22000.0	52000.0
.010	67	67	67	67	63	56	14
.050	0	0	0	0	0	0	2
.100	0	0	0	0	0	0	36
.500	0	0	0	0	4	10	15
1.000	0	0	0	0	0	1	0
3.000	0	0	0	0	0	0	0
5.000	0	0	0	0	0	0	0
10.000	0	0	0	0	0	0	0

FOR ALL DIRECTIONS WITH REL. HUM. GREATER THAN 95.0 PERCENT AND LESS THAN OR EQUAL TO 9999.0 PERCENT
WITH AMB. TEMP. GREATER THAN 70.0 DEG.F AND LESS THAN OR EQUAL TO 9999.0 DEG.F

DISTANCES(METERS)

PERCENT DELTA RH INCREASE	500.0	1100.0	2000.0	5000.0	10000.0	22000.0	52000.0
.010	44	44	44	44	43	39	9
.050	0	0	0	0	0	0	2
.100	0	0	0	0	0	0	20
.500	0	0	0	0	1	4	13
1.000	0	0	0	0	0	1	0
3.000	0	0	0	0	0	0	0
5.000	0	0	0	0	0	0	0
10.000	0	0	0	0	0	0	0

DELTA RELATIVE HUMIDITY- COUNTS OF OCCURENCES

DISTANCES(METERS) ALL DIR, ALL TEMPS, ALL RHS

DRH INCREASE	500.0	1100.0	2000.0	5000.0	10000.0	22000.0	52000.0
.010	7847	7799	7772	7713	7406	6435	4163
.050	0	0	0	3	7	48	339
.100	0	0	1	8	39	148	558
.500	0	8	37	80	194	759	2243
1.000	0	14	25	19	96	299	354
3.000	0	22	12	5	89	148	146
5.000	0	4	0	13	14	10	1
10.000	0	0	0	6	2	0	3

Table 2-2

COLLECTION EFFICIENCY OF CYLINDRICAL AND RIBBON TYPE OBJECTS OF VARIOUS DIMENSIONS FOR DRIFT DROPS AS A FUNCTION OF DRIFT DROP DIAMETER AND WIND SPEED (1)

Wind Speed Group (mph)	Obstacle Dimension (inches)	Collection Efficiency for Drop Diameter (μm) 10	100	150	200	300	500
Type of structure: cylindrical							
0 - 12 mph	1/4	0.07	0.98	0.99	1.0	1.00	1.00
	2	-	0.76	0.86	0.96	0.99	1.0
	120	-	-	0.6	0.12	0.32	0.58
12 - 25 mph	1/4	0.21	1.0	1.0	1.0	1.0	1.0
	2	-	0.89	0.94	0.99	1.0	1.0
	120	-	-	0.16	0.32	0.54	0.74
25 - 32 mph	1/4	0.36	1.0	1.0	1.0	1.0	1.0
	2	0.02	0.85	0.92	0.99	1.0	1.0
	120	-	-	0.22	0.44	0.60	0.84
>32 mph	1/4	0.44	1.0	1.0	1.0	1.0	1.0
	2	0.04	0.9	0.95	1.0	1.0	1.0
	120	-	0.13	0.33	0.52	0.64	0.86
Type of structure: ribbon							
0 - 12 mph	120	-	-	-	-	0.6	0.81
	400	-	-	-	-	-	0.51
	1200	-	-	-	-	-	-
12 - 25 mph	120	-	-	0.31	0.62	0.82	0.9
	400	-	-	-	-	0.4	0.73
	1200	-	-	-	-	-	0.38
25 - 32 mph	120	-	-	0.35	0.7	0.84	0.95
	400	-	-	-	-	0.59	0.84
	1200	-	-	-	-	-	0.51
>32 mph	120	-	-	0.38	0.76	0.88	0.96
	400	-	-	-	-	0.64	0.85
	1200	-	-	-	-	-	0.62

(1) Calculated from Ranz and Wong curves as presented by Mason, Physics of Clouds, 1971.

Table 2-3, continued

Estimated Ice Formation Rates

Cylindrical Object Diameter, inches	Collection Efficiency for 10 μm Droplet	Ice Formation Rate inches/minute
1/4	0.36	0.0111
3/8	0.24	0.0074
1/2	0.15	0.0046
5/8	0.11	0.0034
3/4	0.08	0.0025
7/8	0.05	0.0016
31/32	0.04	0.0012

Table 2-3

Estimated Ice Formation Rates

Caused by Natural Draft Tower Operation

Condensate Droplets Contribution

$$I.F. = \frac{c_w \bar{u} \epsilon}{\rho_{ice}}$$

where

$I.F.$ = ice formation, cm/hour

c_w = plume water concentration, g/m^3

$\bar{u}$ = wind speed, m/sec

ϵ = collection efficiency of object for 10 μm diameter droplet, a function of wind speed and of object shape and dimension (see Table 2-2)

ρ_{ice} = density of ice, 0.917 g/cm^3 (57.15 lb/ft^3)

Ambient conditions:

T = 10 ^oF

u = 12 m/sec (39.4 ft/sec)

RH = 98%

Stability = D

$c_w = 1\ g/m^3\ (6.23 \times 10^{-5}\ lb/ft^3)$

Table 2-4

Estimates of Ice Accumulation
Caused by Plume Water Vapor Deposition on Structures
at Temperatures Below Freezing

Conditions: $T_{ice} = 10\ ^{o}F$

$T_{plume} = 12\ ^{o}F$

$F(T) = 5.8 \times 10^{-8}$ gm/(cm-sec) (see Figure 2-8)

Vertical distance in contact with plume (cm)	Horizontal Dimension (cm)	Ice accumulation rate on structure (cm/hour)
3048.	0.635	1.25×10^{-7}
304.8	0.635	1.82×10^{-7}
3048.	304.8	8.65×10^{-10}
304.8	304.8	3.76×10^{-9}

Table 3-1

Predicted Monthly Average Salt Deposition Rate and Near Ground Airborne Concentration of Salt for Each Month Resulting from Operation of Two Cooling Towers (Indian Point 2 and 3) at the Indian Point 3 Site: Peak Value and at Five Miles Downwind from the Indian Point 3 Tower

Month	Distance (miles) and Direction		Estimated Peak: Deposition Rate, Kg/Km^2-month	Estimated Peak: Near Ground Airborne Concentration, $\mu g/m^3$	Estimates at 5 miles downwind: Deposition Rate, Kg/Km^2-month	Estimates at 5 miles downwind: Near Ground Airborne Concentration, $\mu g/m^3$
October	SSE to SE	1.2	420	2.2	8.0	0.05
November	SE	1.2	1800	8.2	20.0	0.075
December	SE	1.2	320	1.7	6.0	0.02
January	SE	1.2	220	1.0	7.8	0.038
February	SE	1.2	510	3.0	8.0	0.04
March	SE	1.25	15	0.1	0.2	0.001
April	SE	1.25	12	0.06	0.2	0.001
May	SSE to SE	1.2	15	0.08	0.35	0.0015
June	ESE	1.2	150	0.6	5.0	0.03
July	ESE	1.2	420	2.5	20.0	0.07
August	ENE	1.6	250	0.8	30.0	0.1
September	S to SE	1.25	320	1.5	20.0	0.1
Annual Average	SE	1.2	350	1.5	8.0	0.05

Basis: Drift Rate: 0.002% (the corresponding monthly salt drift rate as given in Table 3-2)
Number of towers: two

Table 3-2

Expected Monthly Salt Drift Rate
from the Indian Point Cooling Towers

Month	Basin Salt Concentration ppm(w)	Salt Drift Rate Kg/hour/tower
January	2100	5.7
February	3100	8.4
March	100	0.27
April	100	0.27
May	260	0.71
June	4000	10.9
July	7000	19.1
August	7000	19.1
September	7000	19.1
October	7000	19.1
November	7000	19.1
December	2100	5.7

List of Figures

List of Figures, continued

Figure 2-1

Isopleth of Number of Hours Visible Plume
Extends Distance Downwind in Each Direction
(0 - 3 miles)
(Period of Record-October 1, 1973 through September 30, 1974)

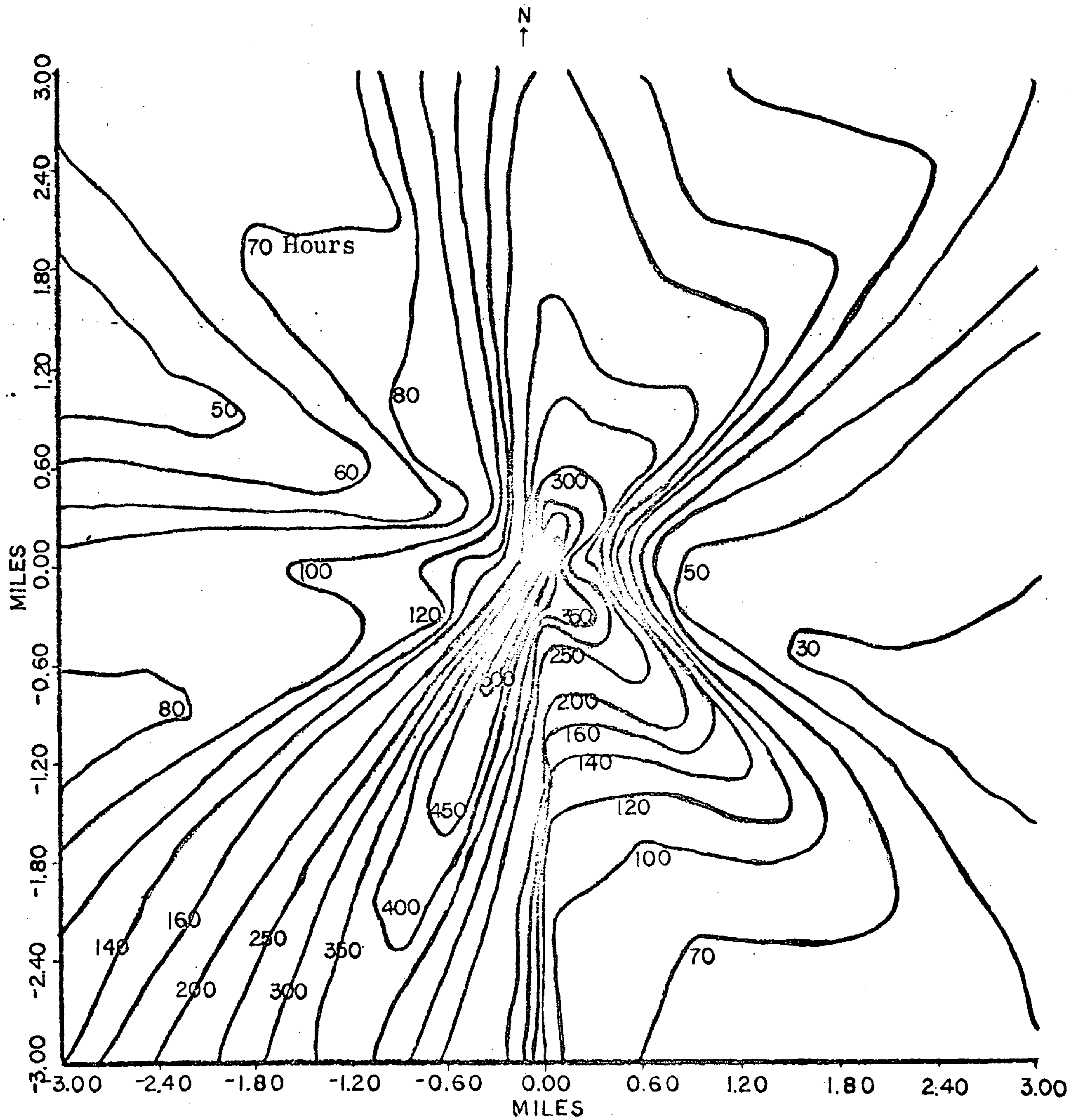

Figure 2-2

Isopleth of Number of Hours Visible Plume Extends Distance Downwind in Each Direction (0 - 10 miles)

(Period of Record-October 1, 1973 through September 30, 1974)

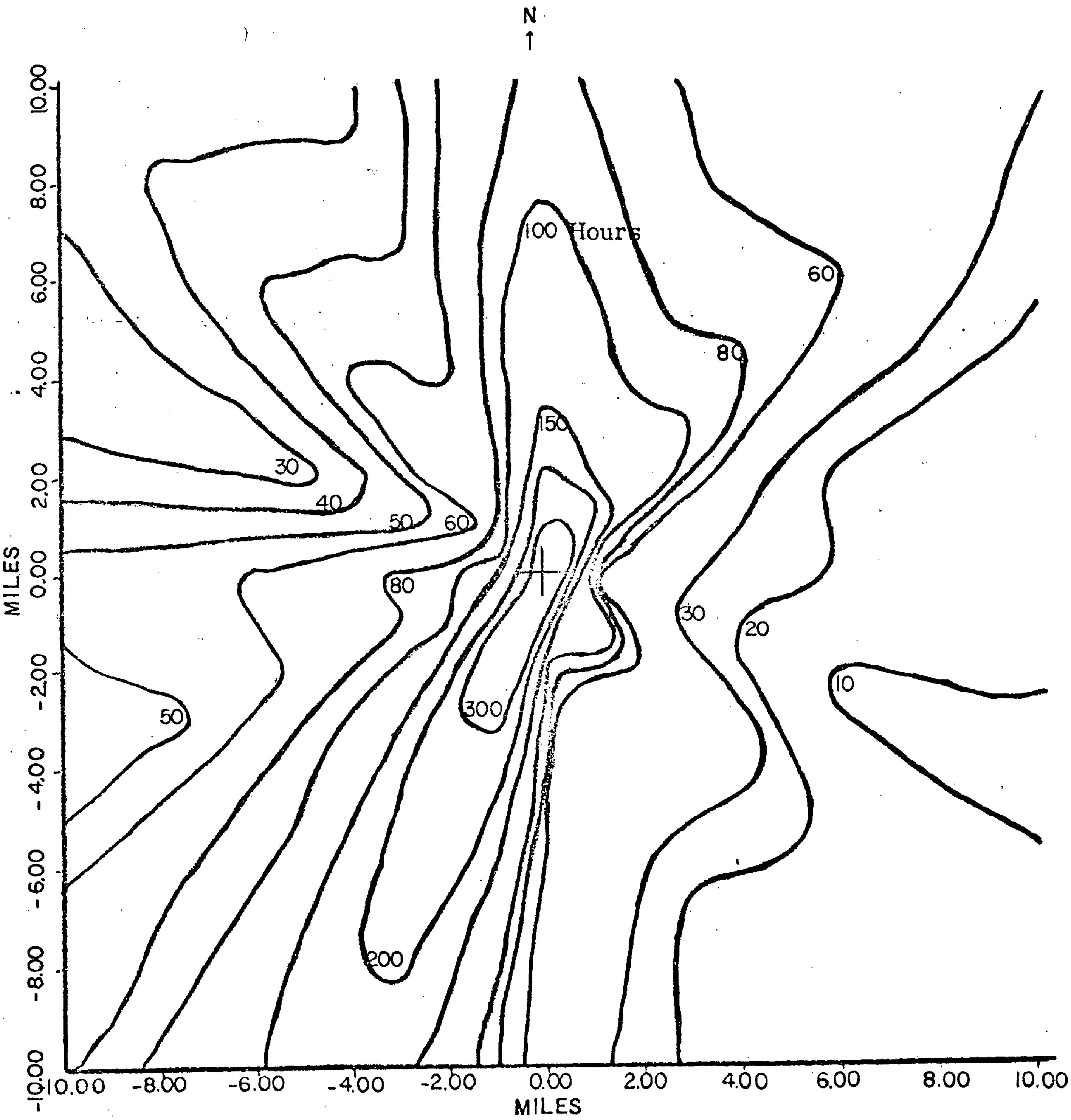

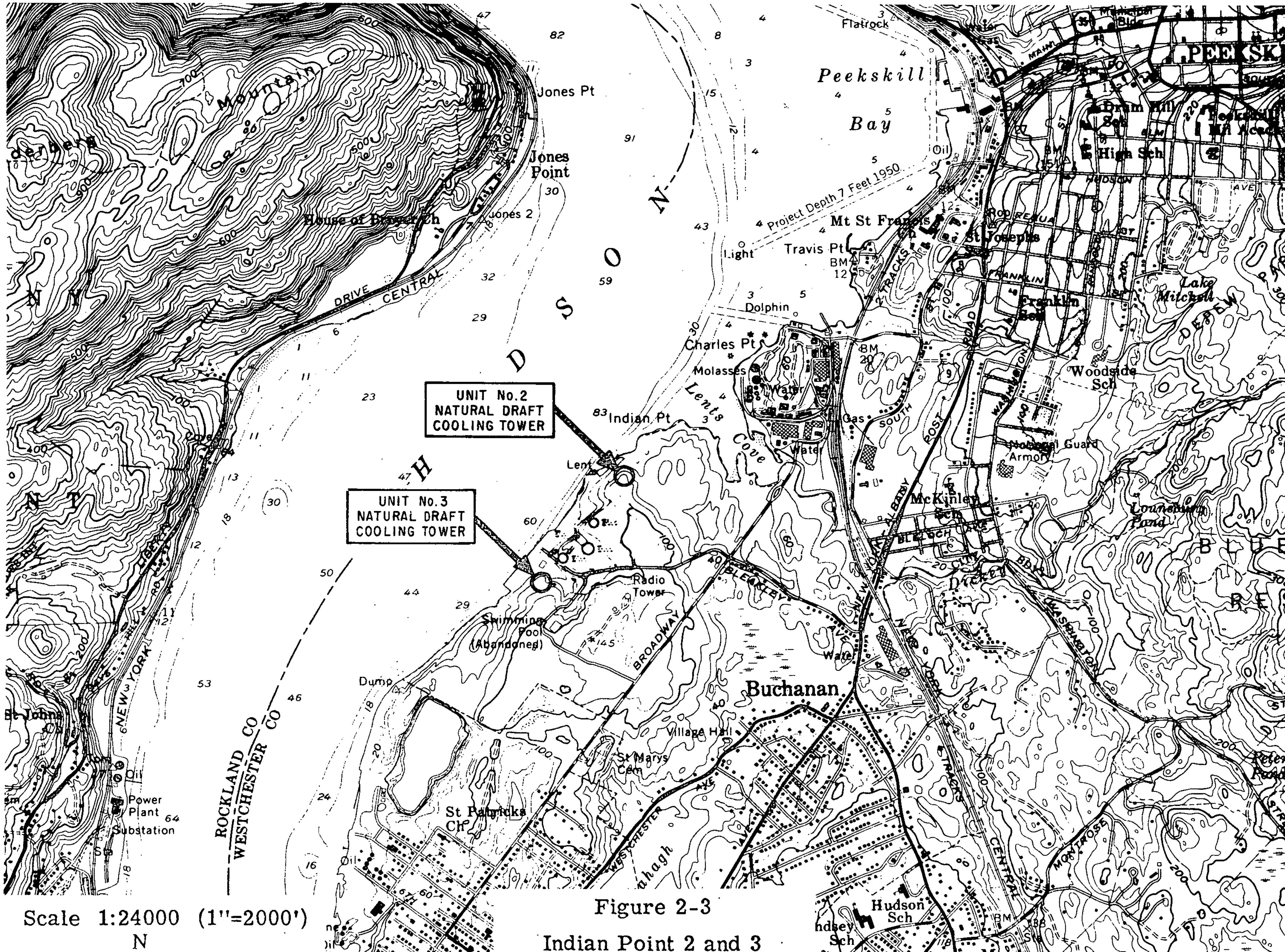

Scale 1:24000 (1"=2000')

N

Figure 2-3

Indian Point 2 and 3
Map of Surrounding Area

Figure 2-4
Isopleth of Average Incremental Increase
in Relative Humidity (RH)
(0 - 3 miles)
(Period of Record-October 1, 1973 through September 30, 1974)

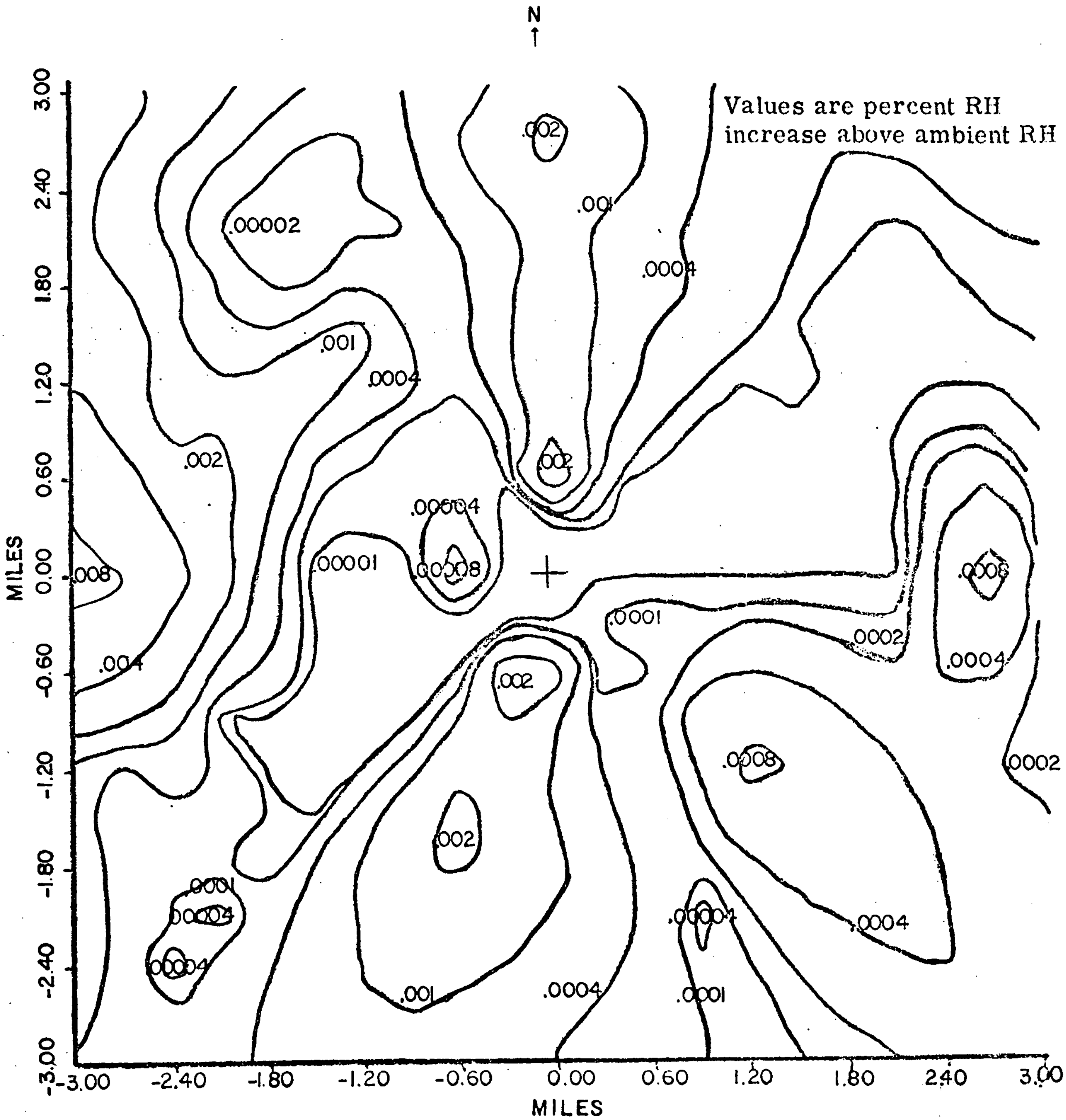

Figure 2-5

Isopleth of Average Incremental Increase

in Relative Humidity (RH)

(0 - 10 miles)

(Period of Record-October 1, 1973 through September 30, 1974)

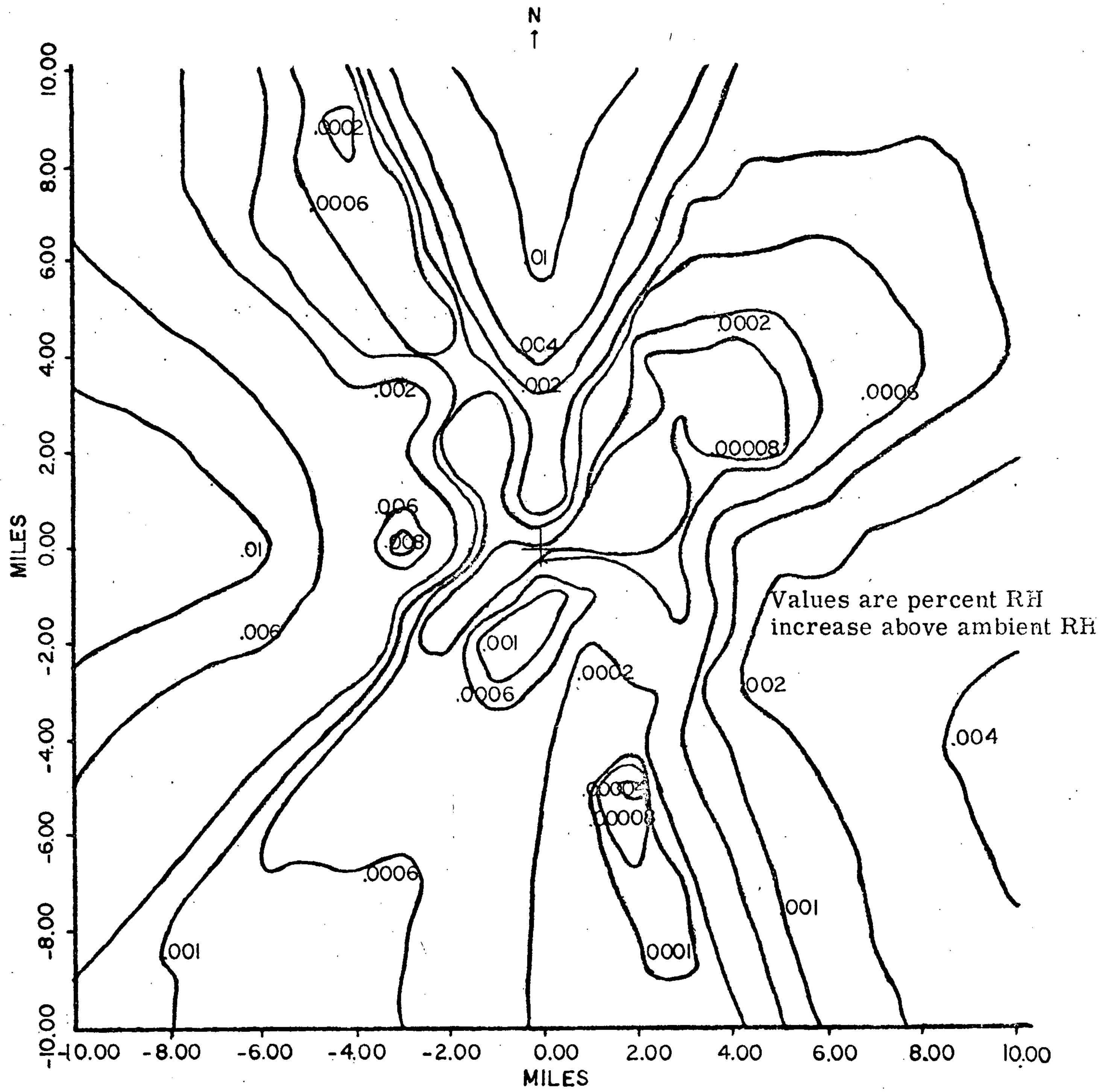

Figure 2-6
Isopleth of Average Incremental Increase
in Relative Humidity (RH)
(0 - 50 miles)
(Period of Record-October 1, 1973 through September 30, 1974)

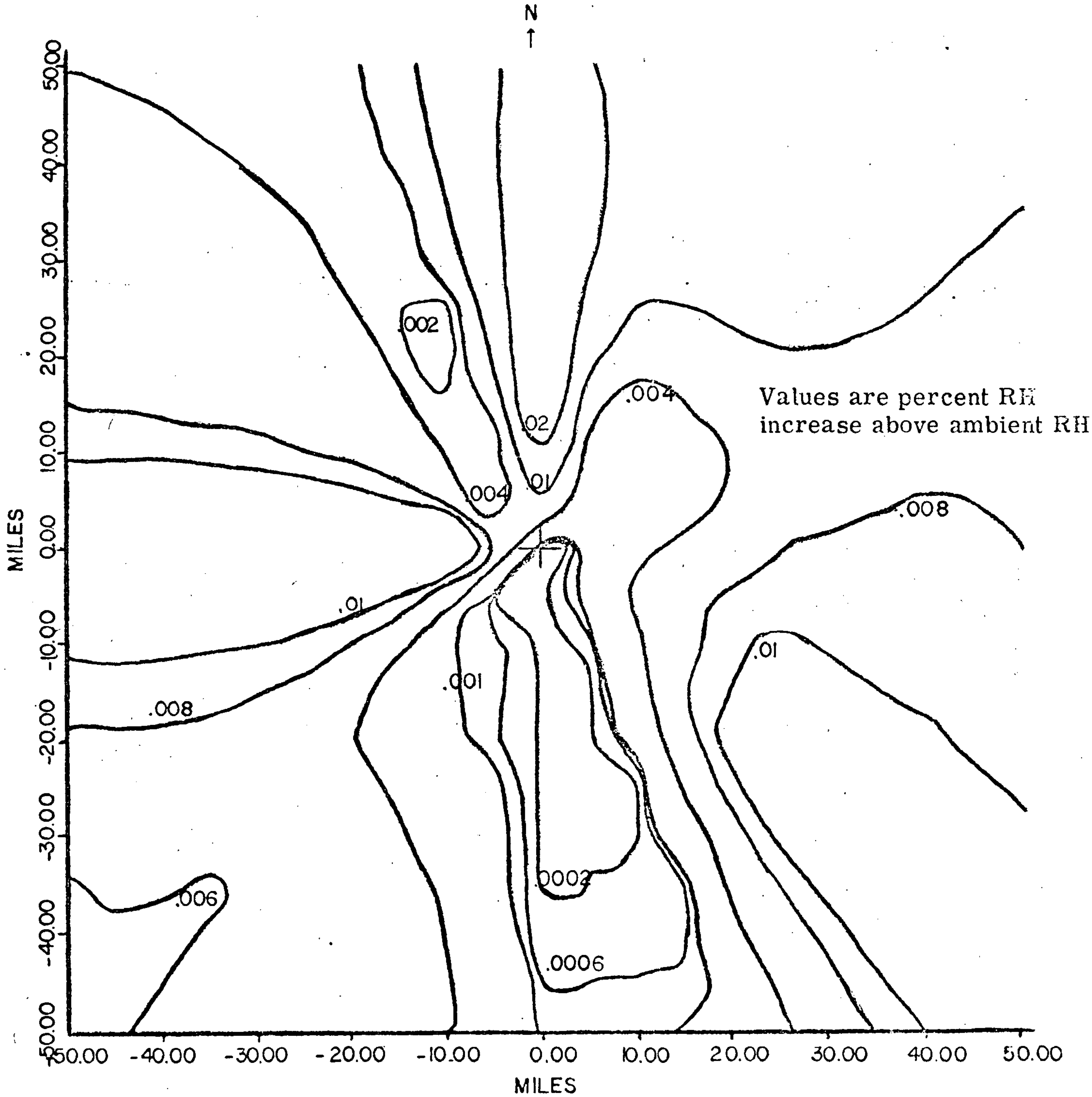

Figure 2-7

Estimated Ice Accumulation on 1/4 Inch Cylindrical Object for Selected Atmospheric Conditions

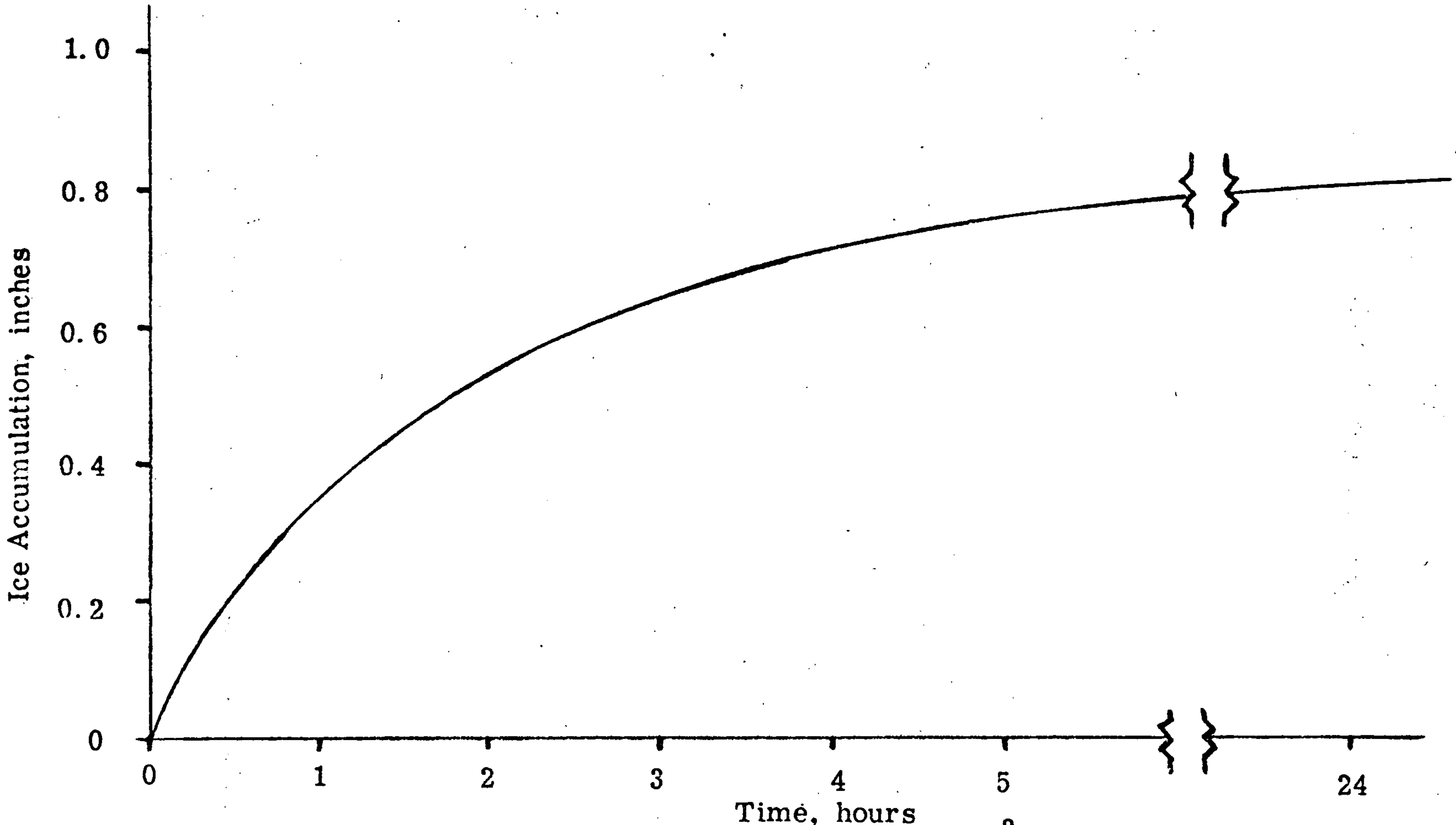

Basis: Assumed plume water concentration as condensate = 1 g/m^3
Downwind distance ~ 100 m
Selected ambient conditions: Wind speed = 12 m/sec
Temperature = 10 °F

Figure 2-8

Vapor Deposition (F[T]) vs Temperature

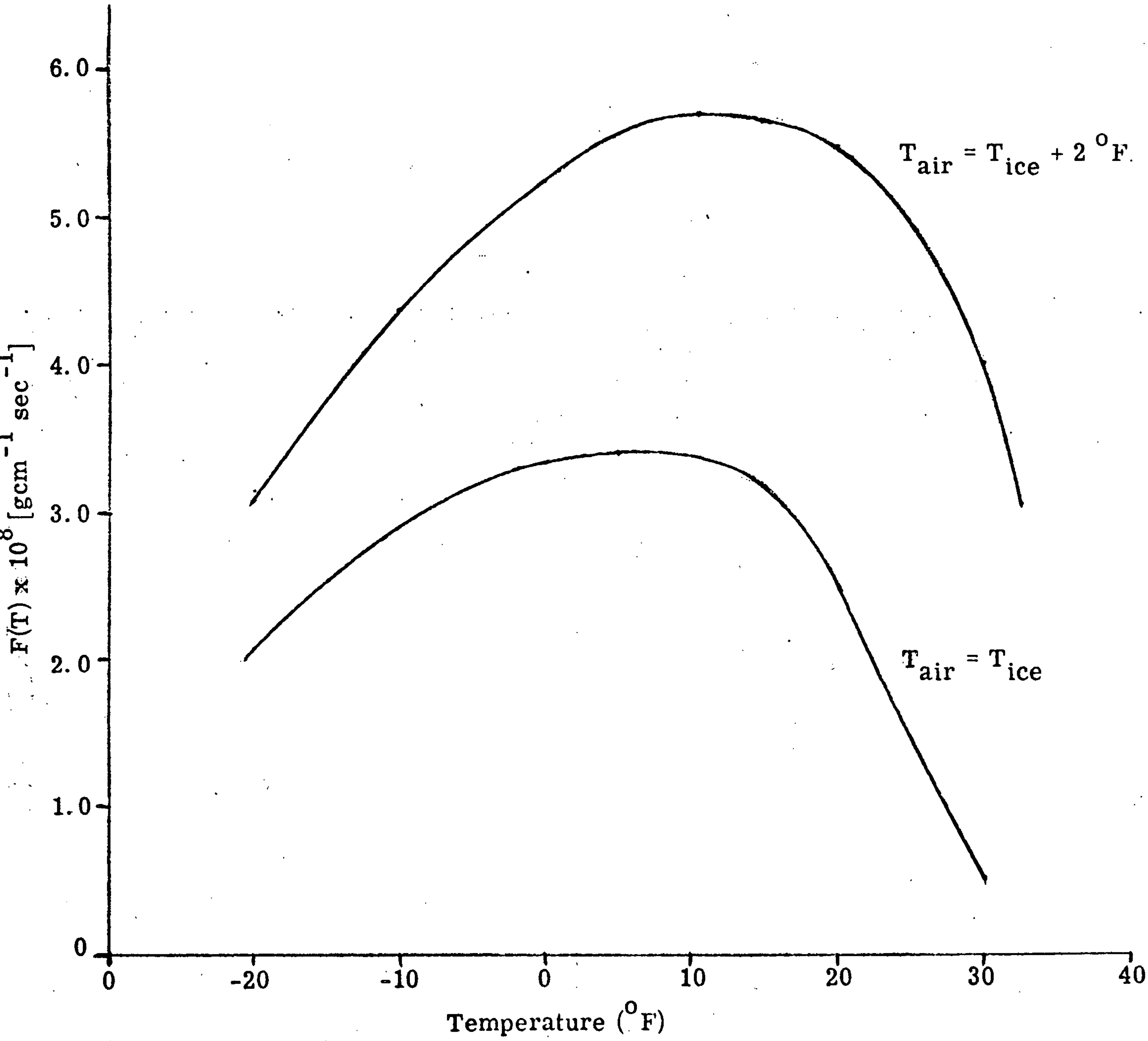

Figure 3-1

Predicted Annual Average Ground Dry Deposition Rates (Kg/Km^2-month) of Salt Resulting from Operation of Two Natural Draft Cooling Towers (Indian Point 2 and 3) as a Function of Distance and Direction from the Indian Point 3 Tower

(0 - 3 miles)

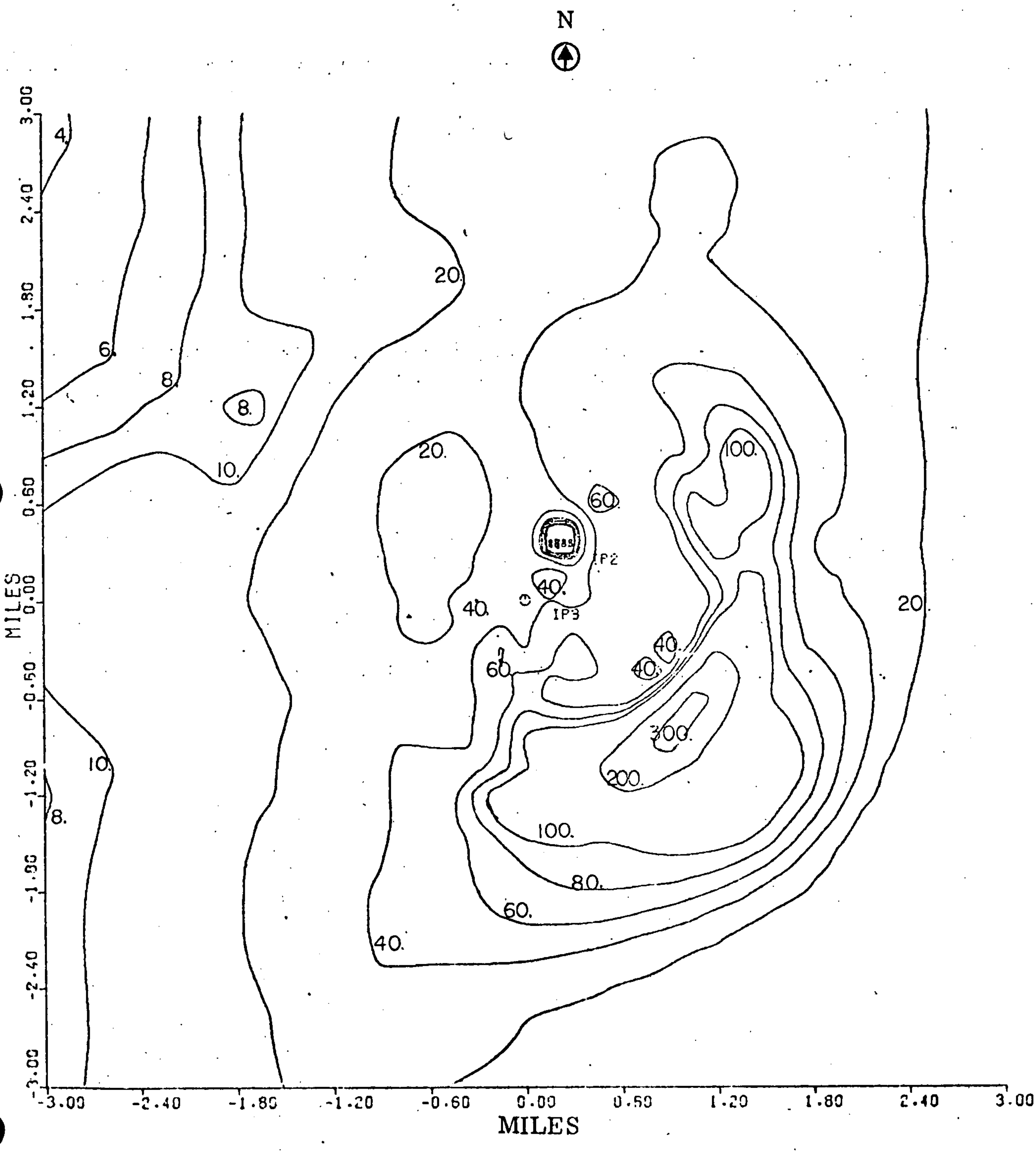

Basis: Drift Rate: 0.002%
Number of towers: two

Figure 3-2

Predicted Annual Average Ground Dry Deposition Rates (Kg/Km^2-month) of Salt Resulting from Operation of Two Natural Draft Cooling Towers (Indian Point 2 and 3) as a Function of Distance and Direction from the Indian Point 3 Tower

(0 - 10 miles)

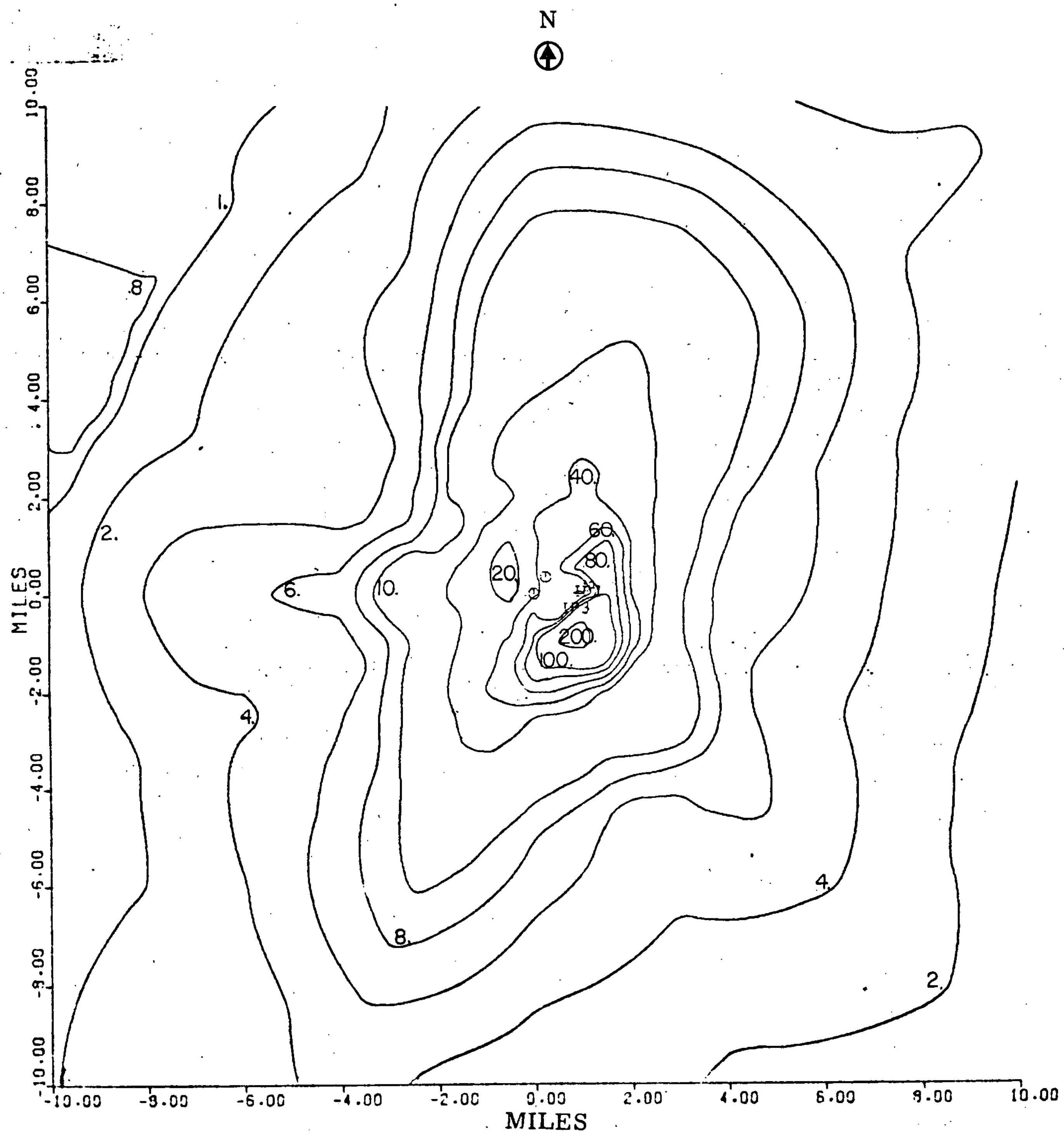

Basis: Drift Rate: 0.002%
Number of towers: two

Figure 3-3

Predicted Annual Average Near Ground Airborne Concentration ($\mu g/m^3$) of Salt Resulting from Operation of Two Natural Draft Cooling Towers (Indian Point 2 and 3) as a Function of Distance and Direction from the Indian Point 3 Tower

(0 - 3 miles)

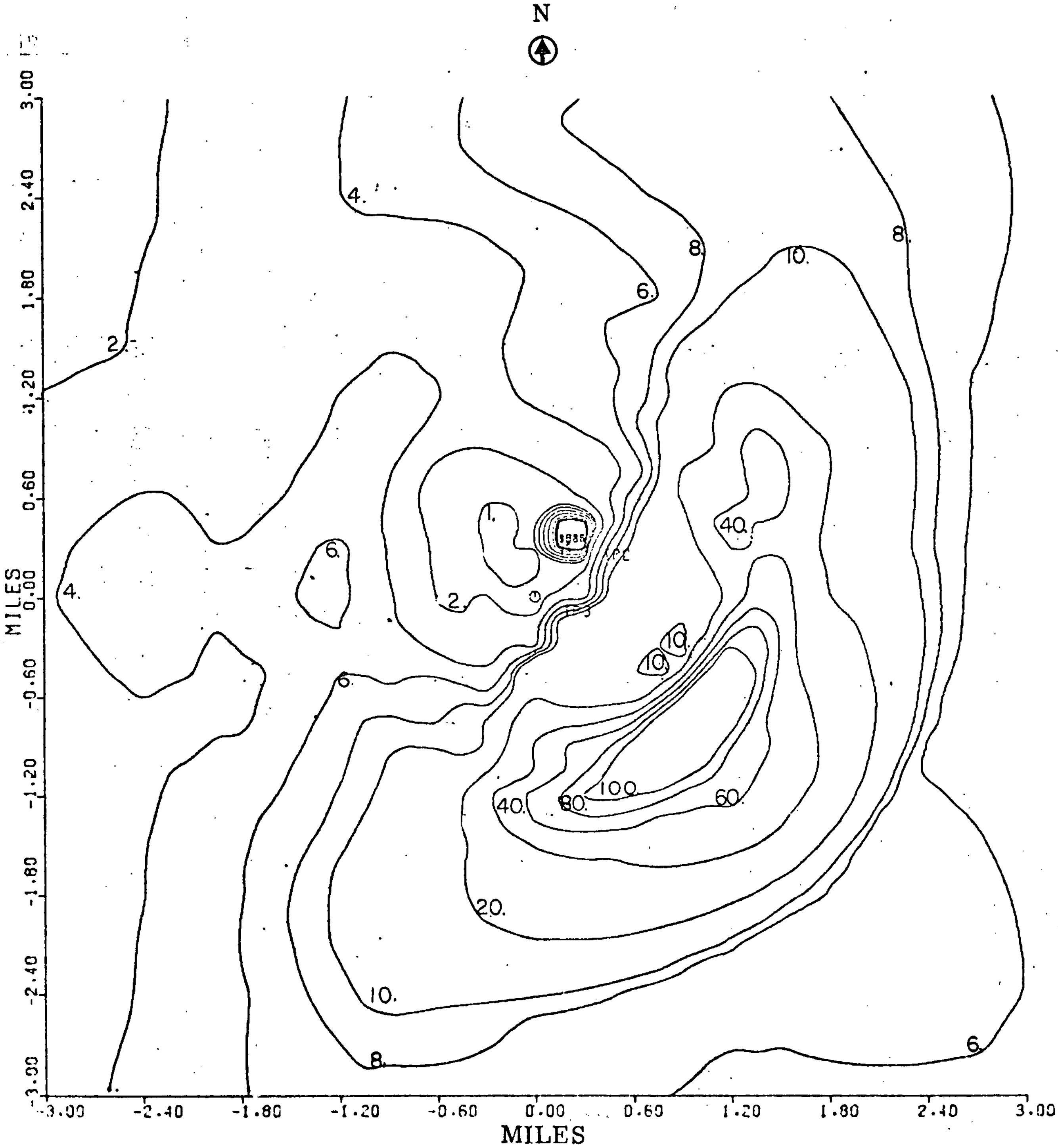

Basis: Drift Rate: 0.002%

Number of towers: two

Note: Divide number on plot by 100 to get $\mu g/m^3$

Figure 3-4

Predicted Annual Average Near Ground Airborne Concentration ($\mu g/m^3$) of Salt Resulting from Operation of Two Natural Draft Cooling Towers (Indian Point 2 and 3) as a Function of Distance and Direction from the Indian Point 3 Tower

(0 - 10 miles)

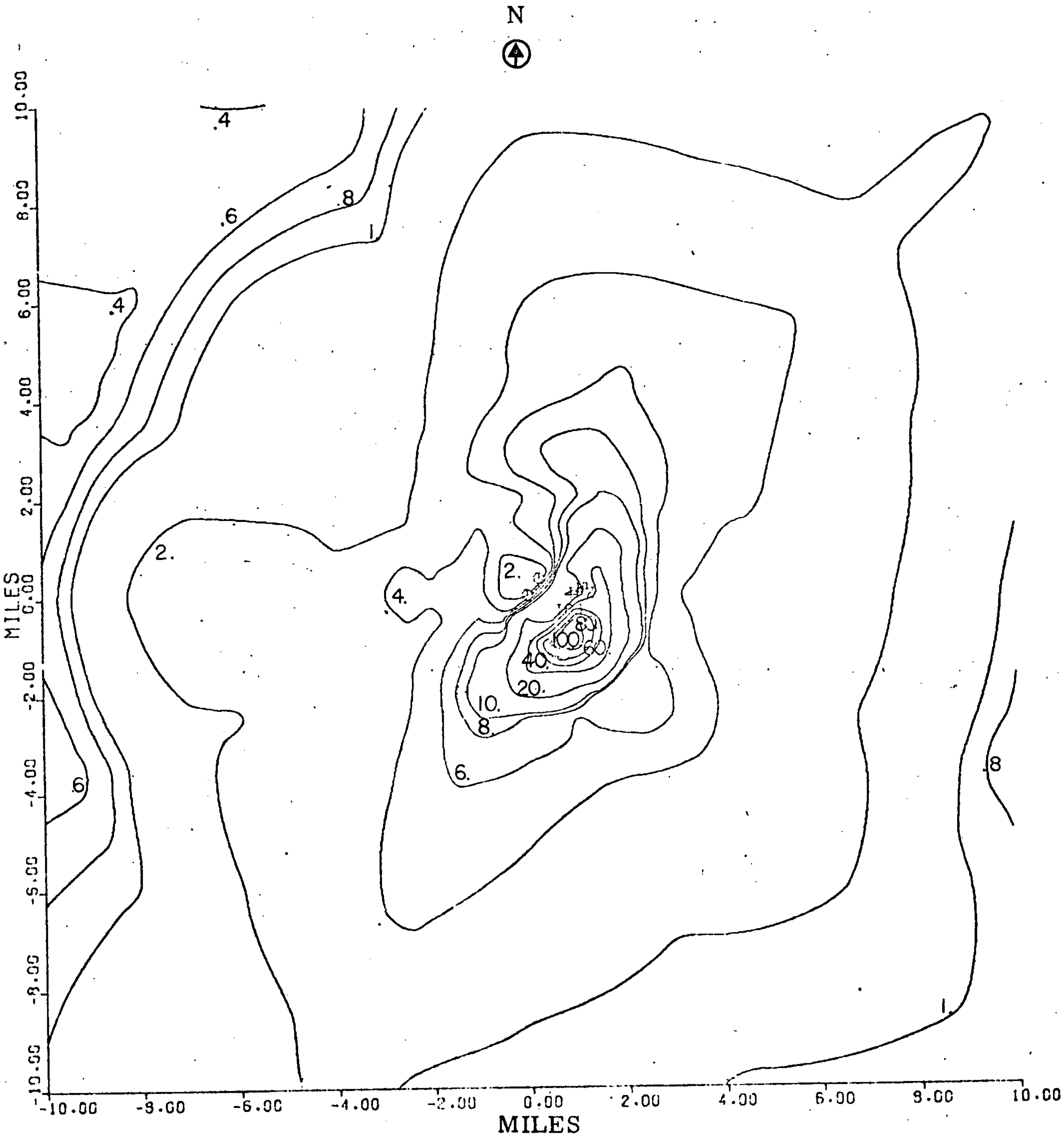

Basis: Drift Rate: 0.002%
Number of towers: two

Note: Divide number on plot by 100 to get $\mu g/m^3$

Figure 3-5

Predicted October Monthly Average Ground Dry Deposition Rates (Kg/Km^2-month) of Salt Resulting from Operation of Two Natural Draft Cooling Towers (Indian Point 2 and 3) as a Function of Distance and Direction from the Indian Point 3 Tower

(0 - 3 miles)

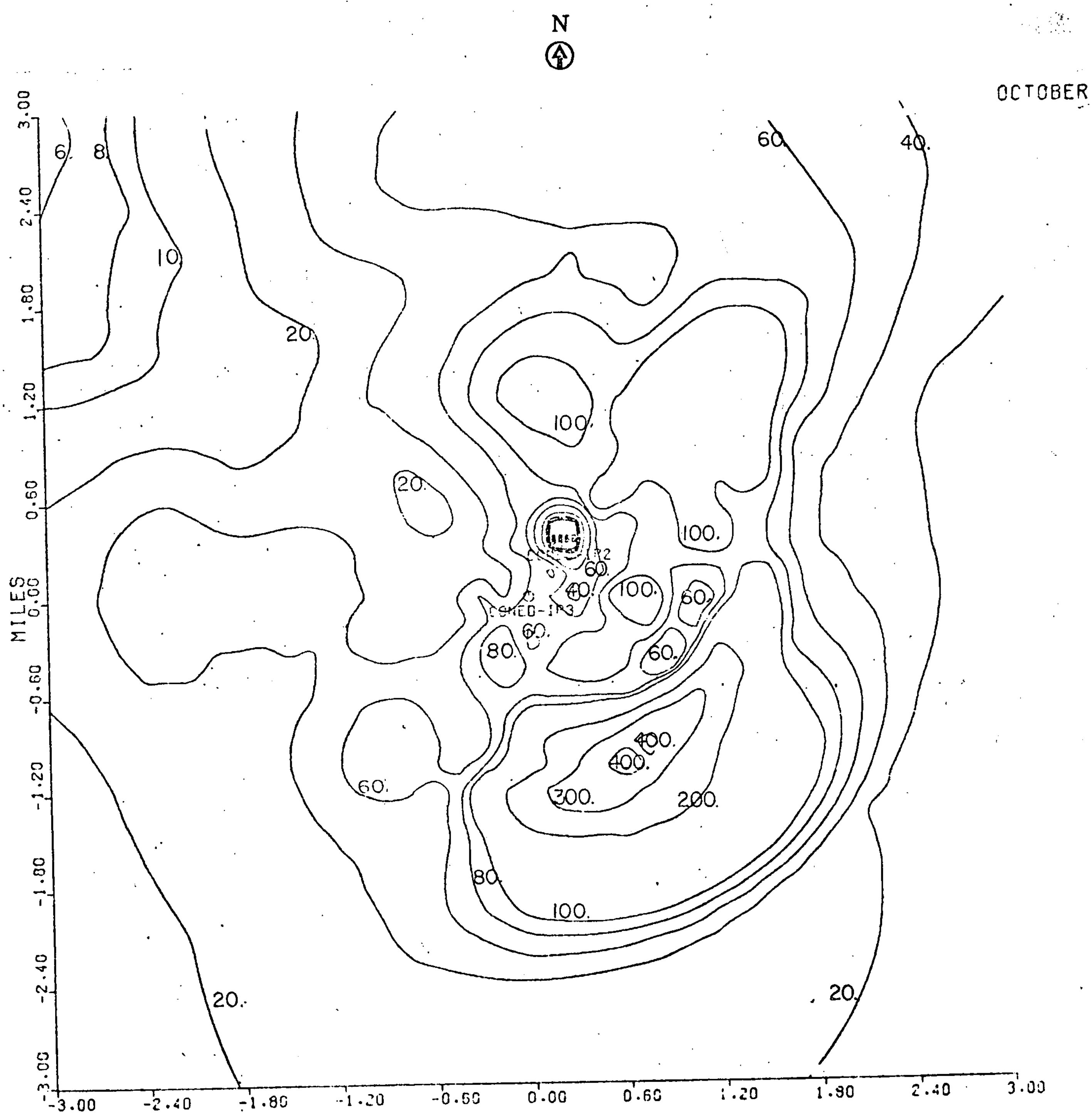

Basis: Drift Rate: 0.002% (19.1 Kg salt/hour/tower)
Number of towers: two

Figure 3-6

Predicted October Monthly Average Ground Dry Deposition Rates (Kg/Km^2-month) of Salt Resulting from Operation of Two Natural Draft Cooling Towers (Indian Point 2 and 3) as a Function of Distance and Direction from the Indian Point 3 Tower

(0 - 10 miles)

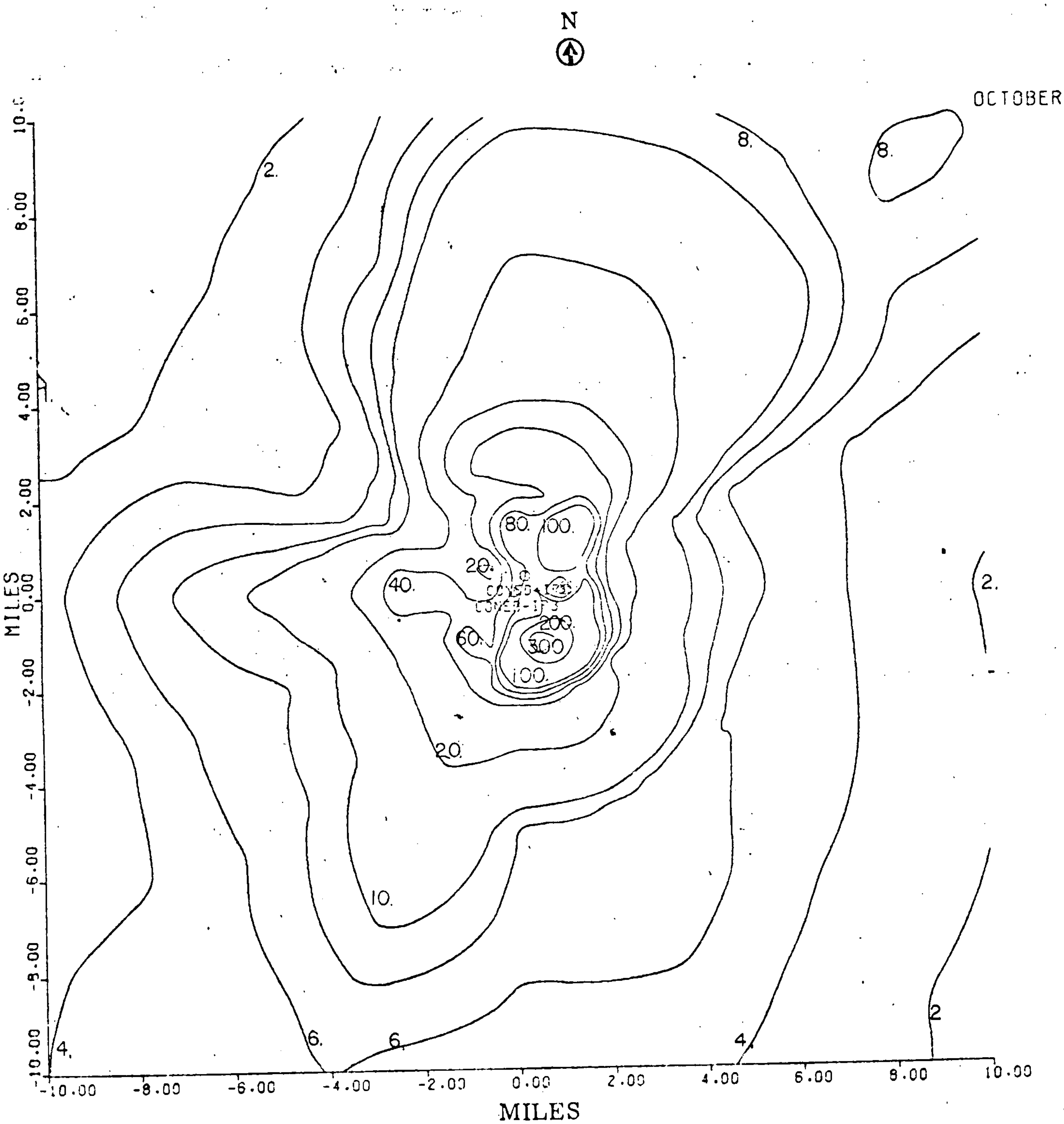

Basis: Drift Rate: 0.002% (19.1 Kg salt/hour/tower)
Number of towers: two

Figure 3-7

Predicted October Monthly Average Near Ground Airborne Concentration ($\mu g/m^3$) of Salt Resulting from Operation of Two Natural Draft Cooling Towers (Indian Point 2 and 3) as a Function of Distance and Direction from the Indian Point 3 Tower

(0 - 3 miles)

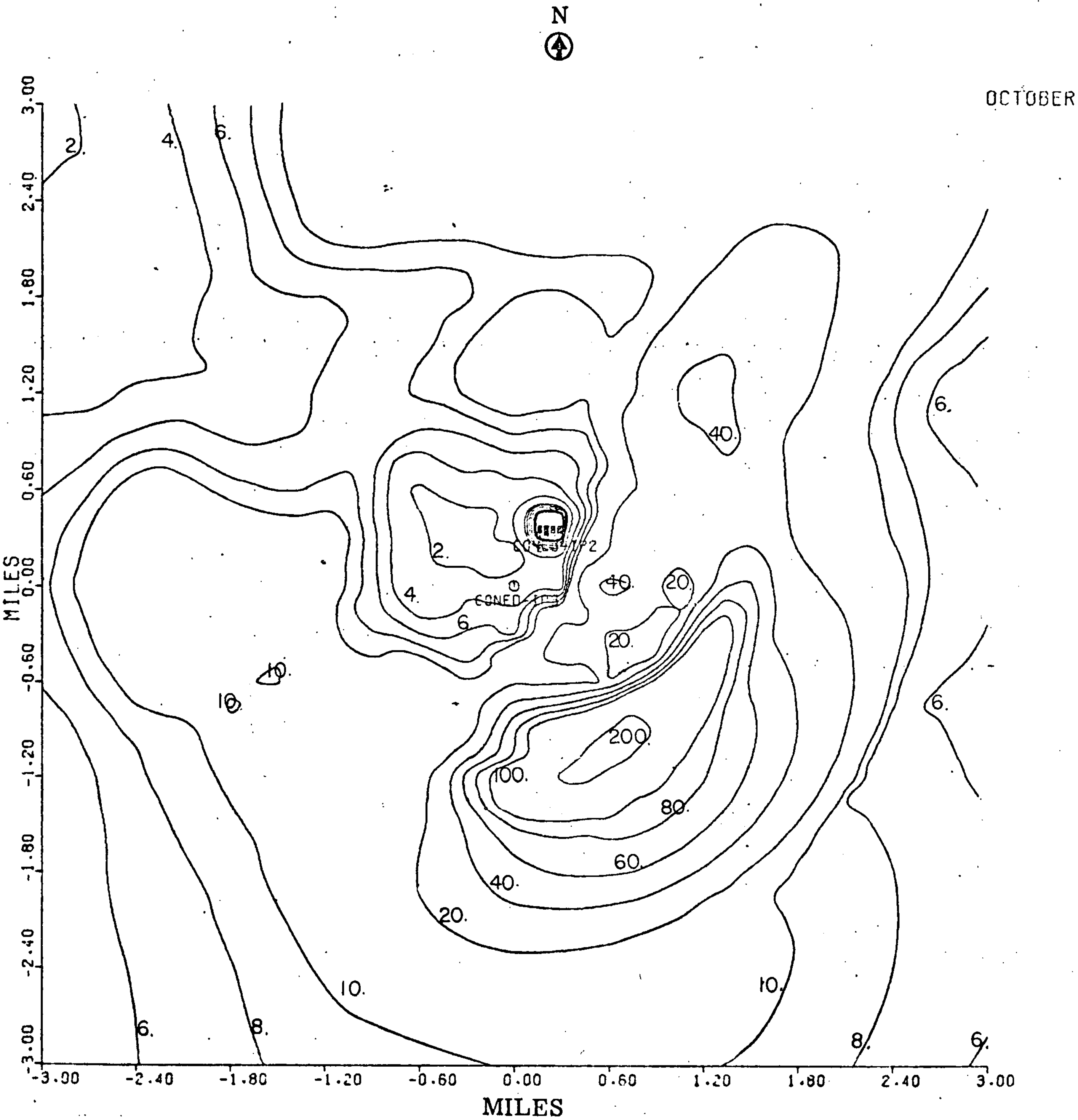

Basis: Drift Rate: 0.002% (19.1 Kg salt/hour/tower)
Number of towers: two

Note: Divide number on plot by 100 to get $\mu g/m^3$

Figure 3-8

Predicted October Monthly Average Near Ground Airborne Concentration ($\mu g/m^3$) of Salt Resulting from Operation of Two Natural Draft Cooling Towers (Indian Point 2 and 3) as a Function of Distance and Direction from the Indian Point 3 Tower

(0 - 10 miles)

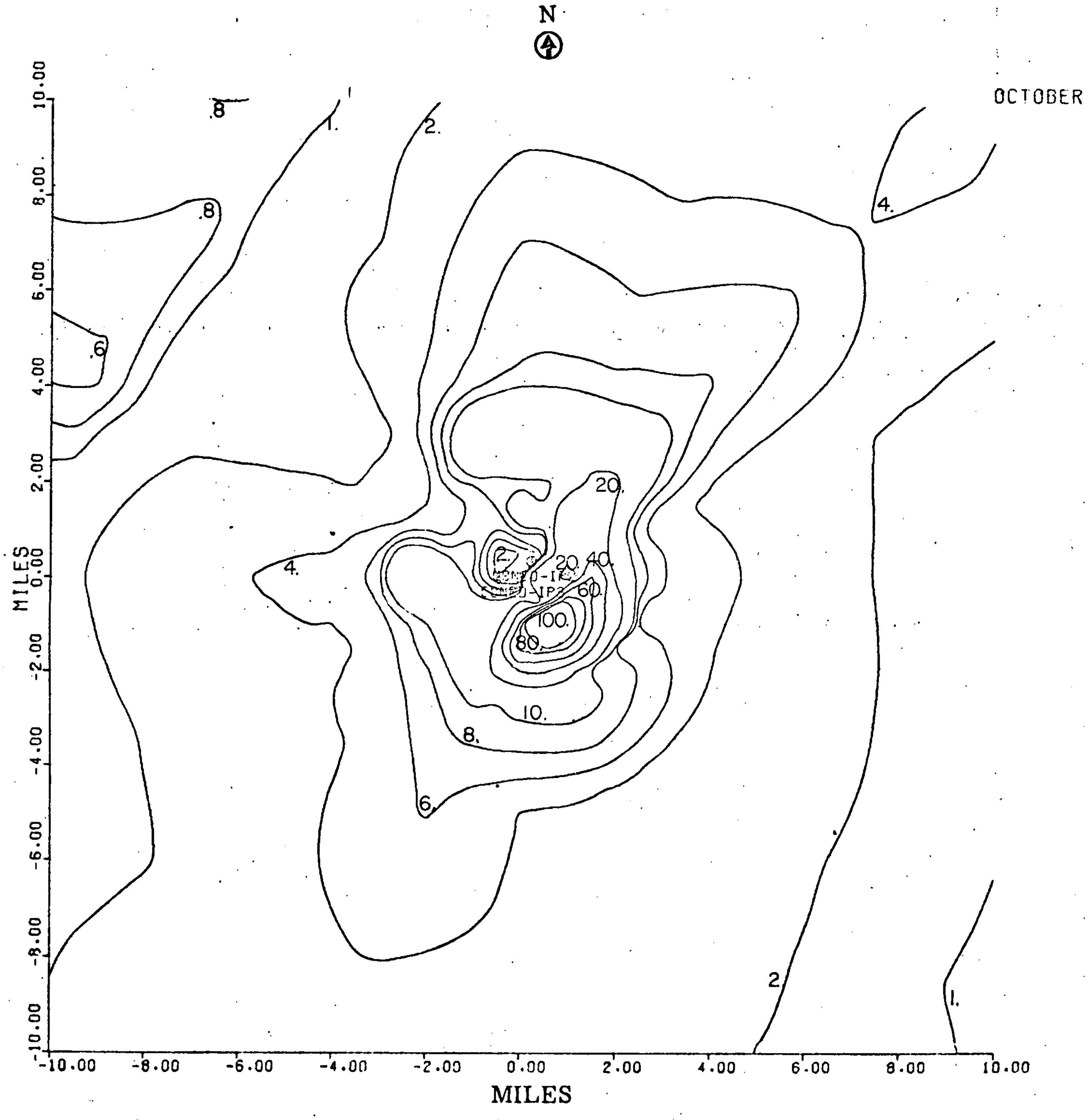

Basis: Drift Rate: 0.002% (19.1 Kg salt/hour/tower)
Number of towers: two

Note: Divide number on plot by 100 to get $\mu g/m^3$

Figure 3-9

Predicted November Monthly Average Ground Dry Deposition Rates (Kg/Km^2-month) of Salt Resulting from Operation of Two Natural Draft Cooling Towers (Indian Point 2 and 3) as a Function of Distance and Direction from the Indian Point 3 Tower

(0 - 3 miles)

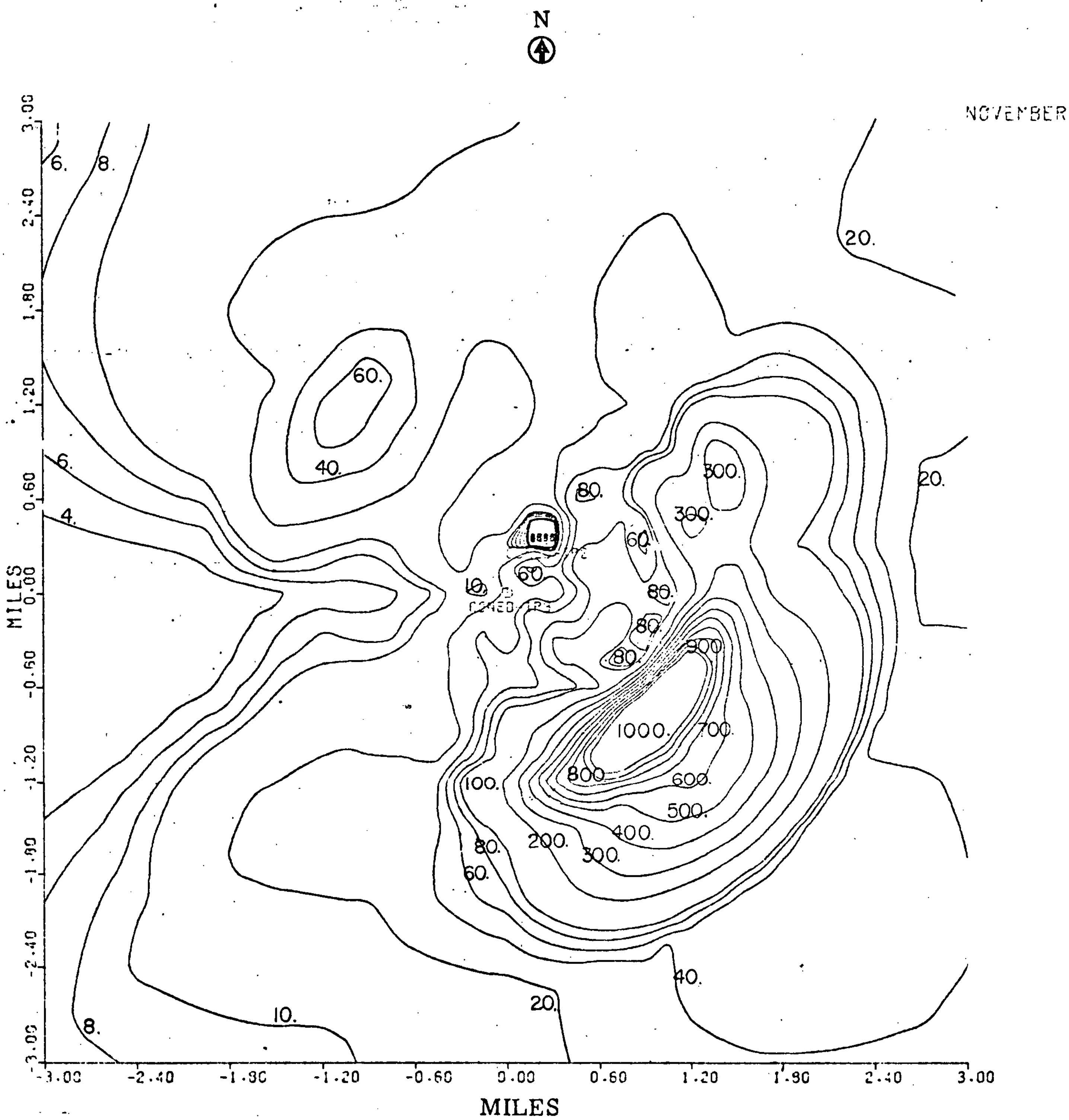

Basis: Drift Rate: 0.002% (19.1 Kg salt/hour/tower)
Number of towers: two

Figure 3-10

Predicted November Monthly Average Ground Dry Deposition Rates (Kg/Km^2-month) of Salt Resulting from Operation of Two Natural Draft Cooling Towers (Indian Point 2 and 3) as a Function of Distance and Direction from the Indian Point 3 Tower

(0 - 10 miles)

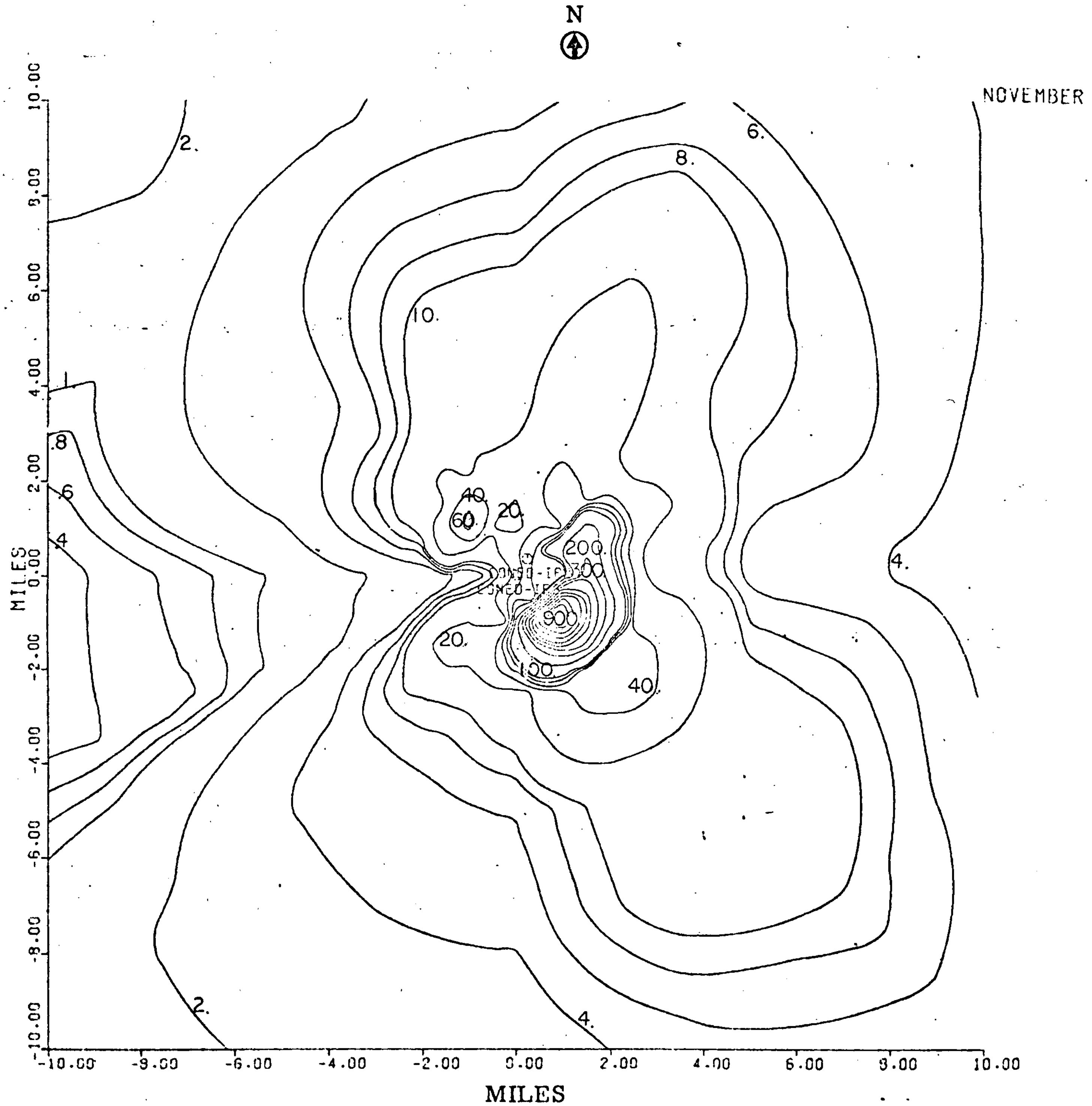

Basis: Drift Rate: 0.002% (19.1 Kg salt/hour/tower)
Number of towers: two

Figure 3-11

Predicted November Monthly Average Near Ground Airborne Concentration ($\mu g/m^3$) of Salt Resulting from Operation of Two Natural Draft Cooling Towers (Indian Point 2 and 3) as a Function of Distance and Direction from the Indian Point 3 Tower

(0 - 3 miles)

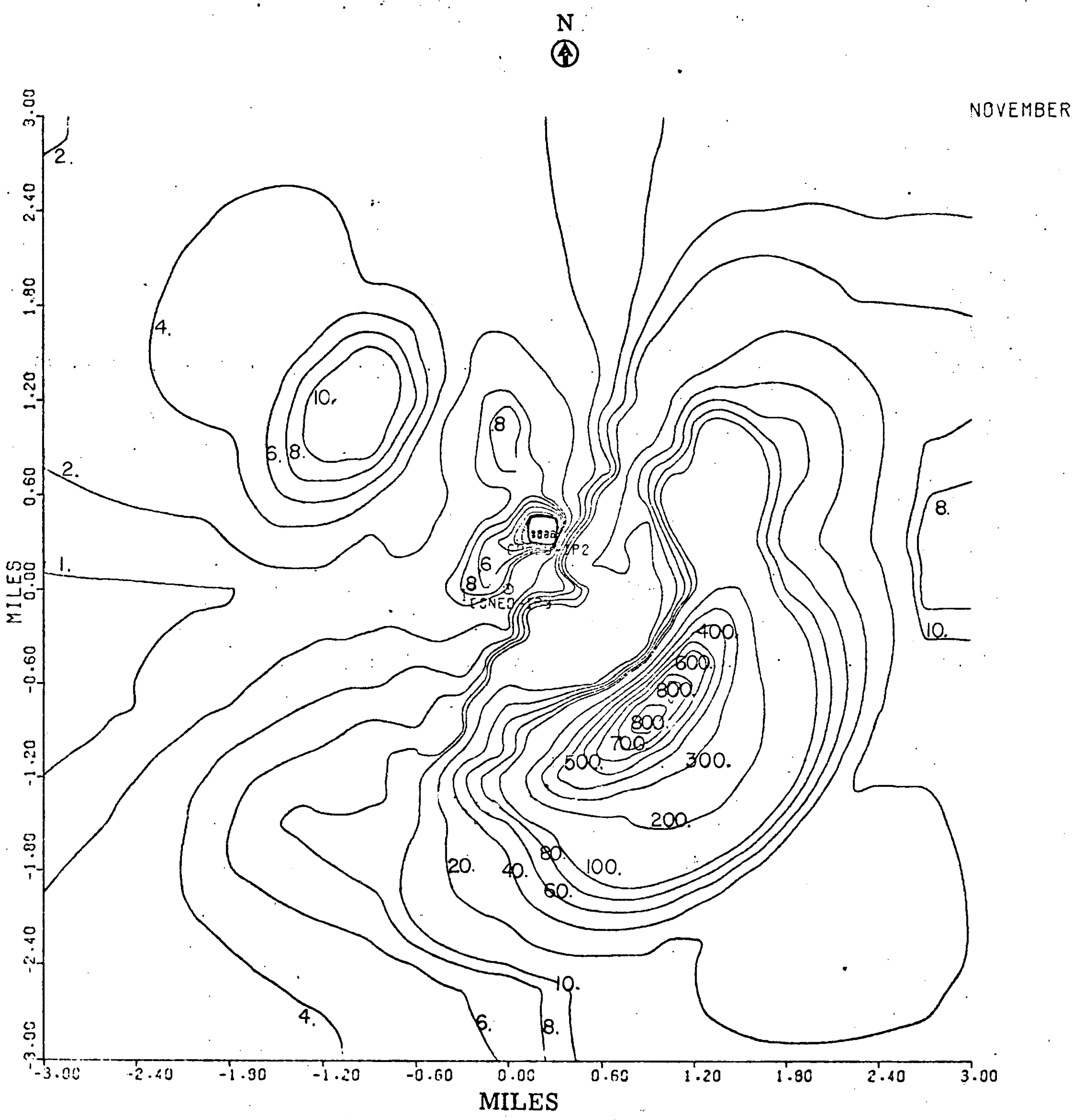

Basis: Drift Rate: 0. 002% (19. 1 Kg salt/hour/tower)
Number of towers: two

Note: Divide number on plot by 100 to get $\mu g/m^3$

Figure 3-12

Predicted November Monthly Average Near Ground Airborne Concentration ($\mu g/m^3$) of Salt Resulting from Operation of Two Natural Draft Cooling Towers (Indian Point 2 and 3) as a Function of Distance and Direction from the Indian Point 3 Tower

(0 - 10 miles)

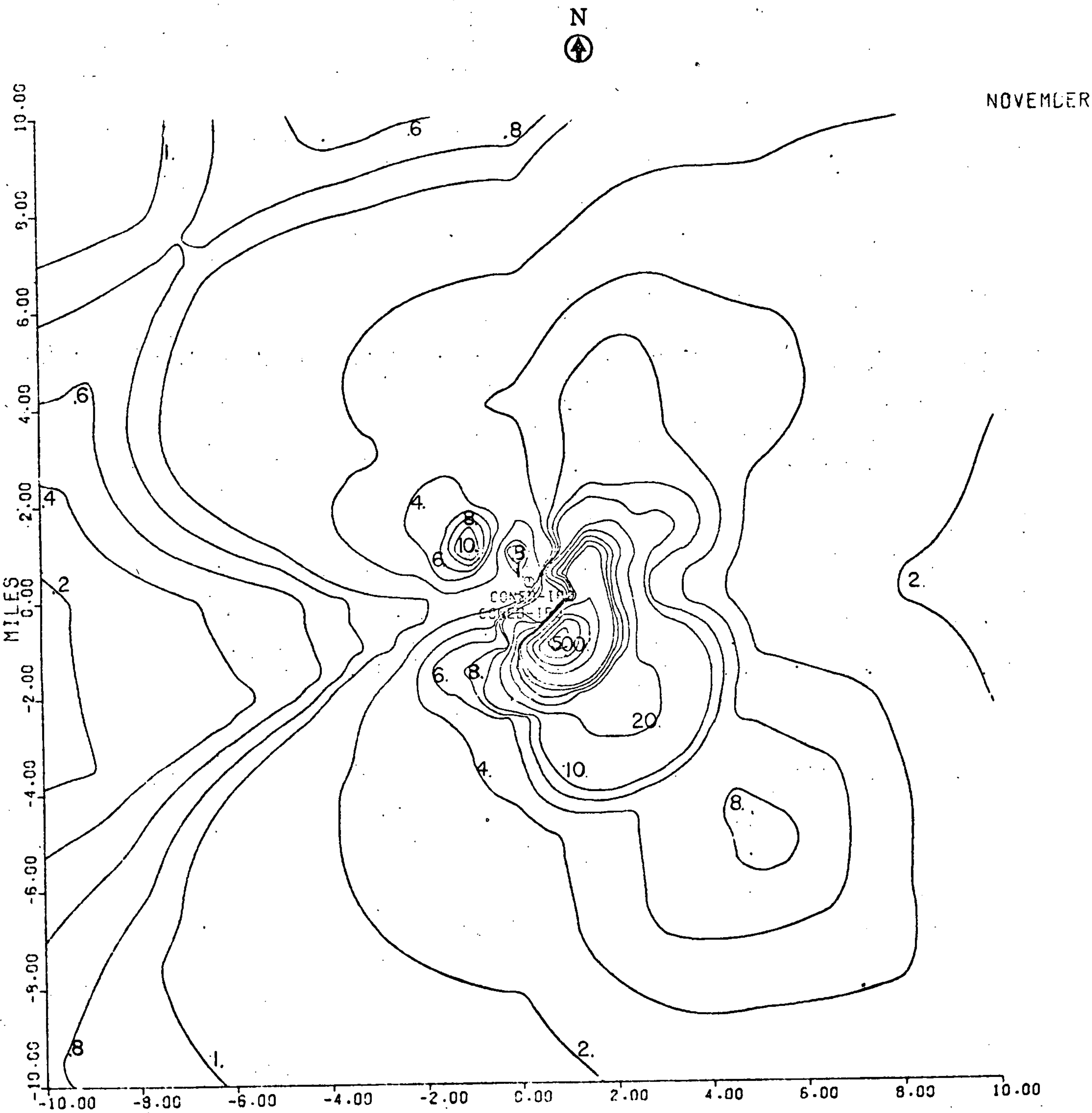

Basis: Drift Rate: 0.002% (19.1 Kg salt/hour/tower)
Number of towers: two

Note: Divide number on plot by 100 to get $\mu g/m^3$

Figure 3-13

Predicted December Monthly Average Ground Dry Deposition Rates (Kg/Km^2-month) of Salt Resulting from Operation of Two Natural Draft Cooling Towers (Indian Point 2 and 3) as a Function of Distance and Direction from the Indian Point 3 Tower

(0 - 3 miles)

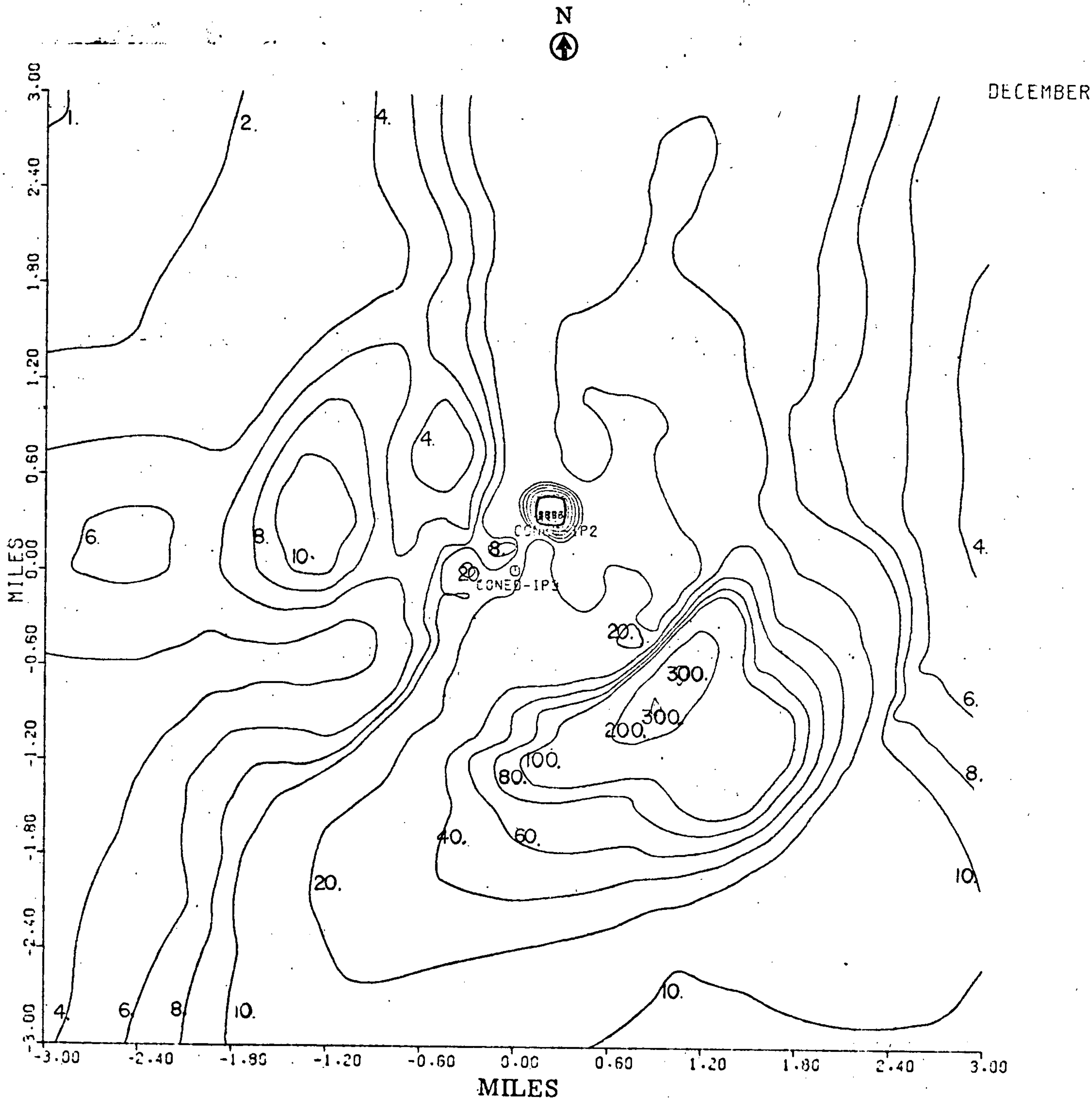

Basis: Drift Rate: 0.002% (5.7 Kg salt/hour/tower)
Number of towers: two

Figure 3-14

Predicted December Monthly Average Ground Dry Deposition Rates (Kg/Km^2-month) of Salt Resulting from Operation of Two Natural Draft Cooling Towers (Indian Point 2 and 3) as a Function of Distance and Direction from the Indian Point 3 Tower

(0 - 10 miles)

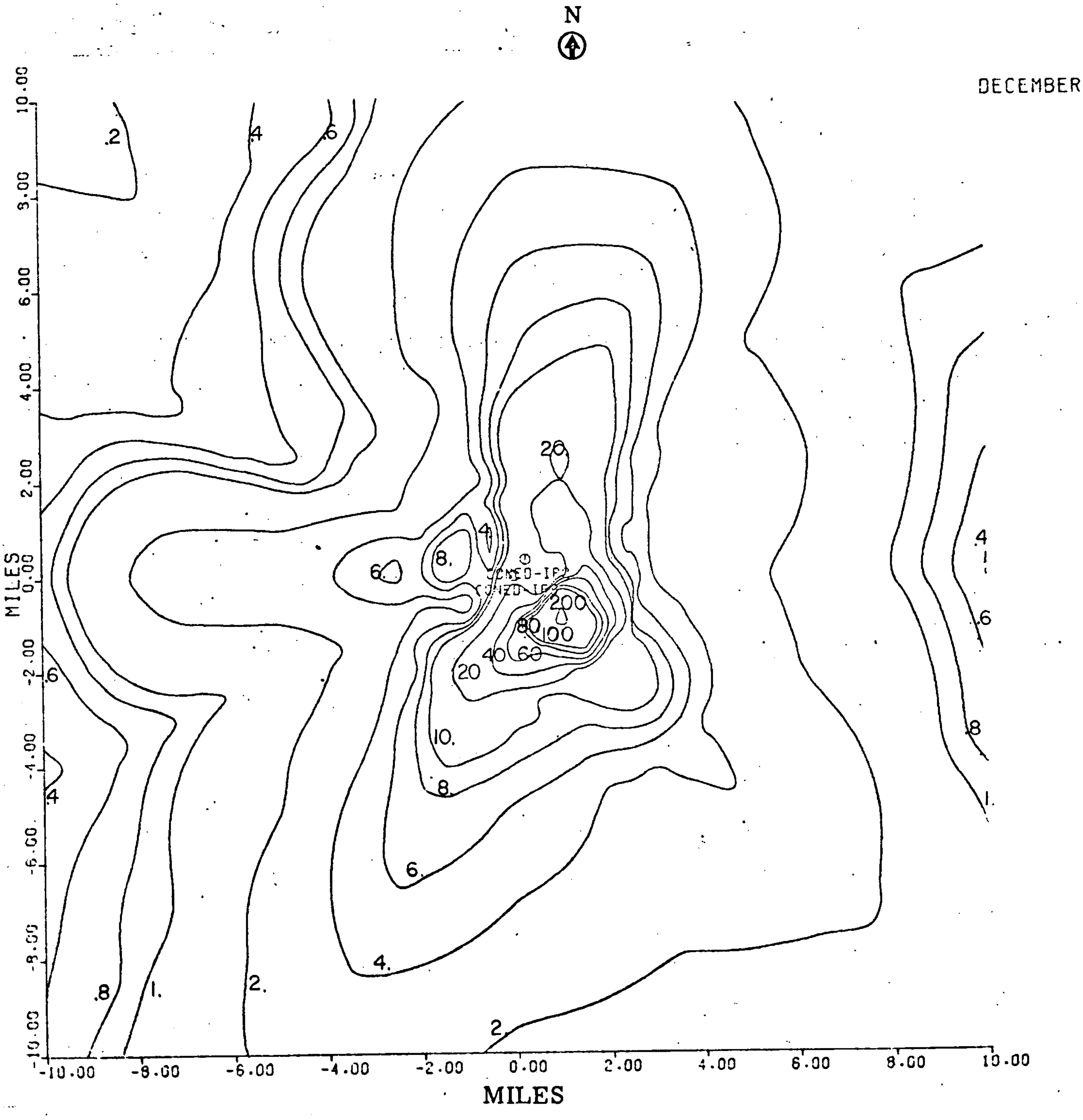

Basis: Drift Rate: 0.002% (5.7 Kg salt/hour/tower)
Number of towers: two

Figure 3-15

Predicted December Monthly Average Near Ground Airborne Concentration ($\mu g/m^3$) of Salt Resulting from Operation of Two Natural Draft Cooling Towers (Indian Point 2 and 3) as a Function of Distance and Direction from the Indian Point 3 Tower

(0 - 3 miles)

N

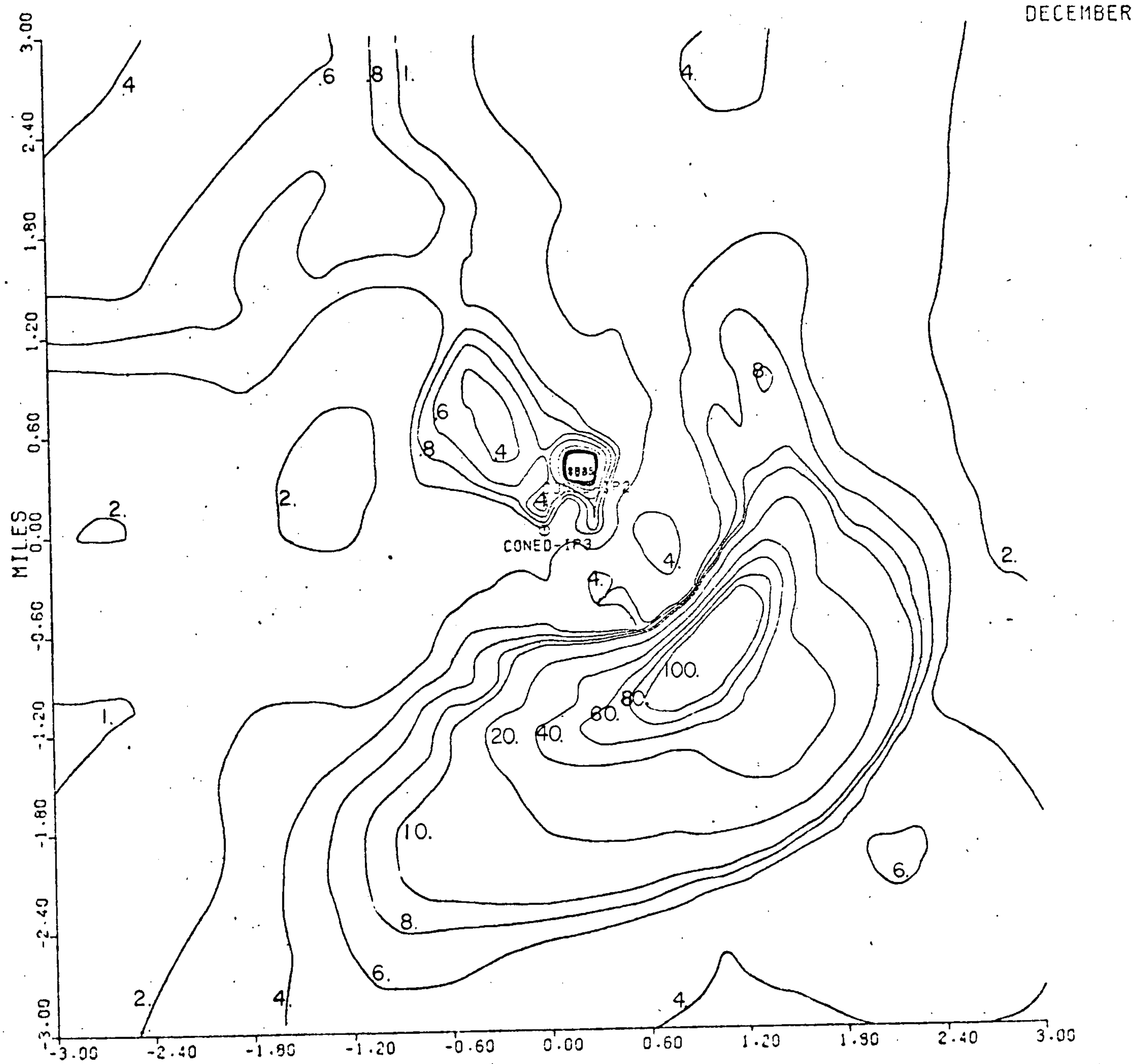

Basis: Drift Rate: 0.002% (5.7 Kg salt/hour/tower)
Number of towers: two

Note: Divide number on plot by 100 to get $\mu g/m^3$

Figure 3-16

Predicted December Monthly Average Near Ground Airborne Concentration ($\mu g/m^3$) of Salt Resulting from Operation of Two Natural Draft Cooling Towers (Indian Point 2 and 3) as a Function of Distance and Direction from the Indian Point 3 Tower

(0 - 10 miles)

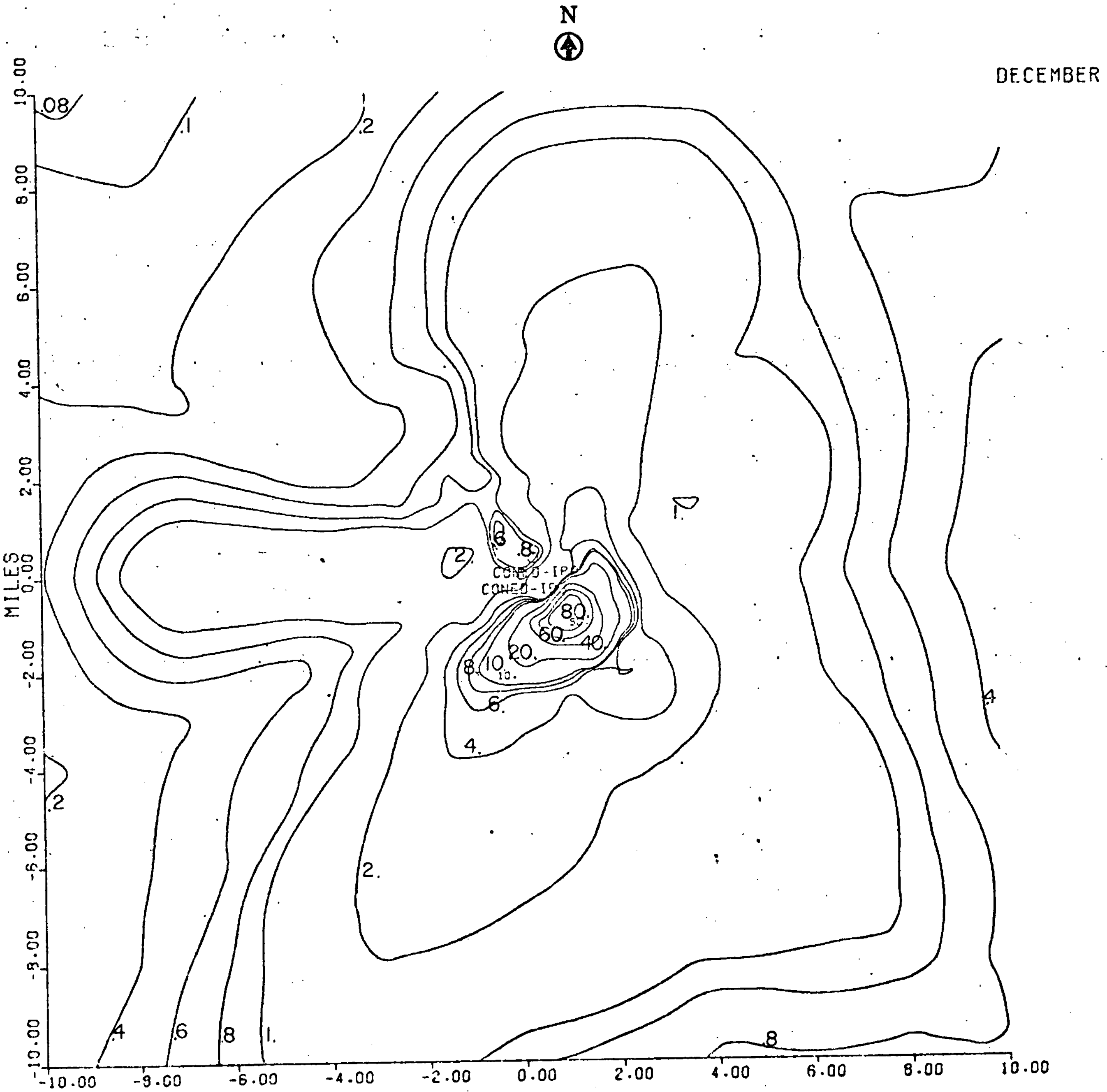

Basis: Drift Rate: 0.002% (5.7 Kg salt/hour/tower)
Number of towers: two

Note: Divide number on plot by 100 to get $\mu g/m^3$

Figure 3-17

Predicted January Monthly Average Ground Dry Deposition Rates (Kg/Km^2-month) of Salt Resulting from Operation of Two Natural Draft Cooling Towers (Indian Point 2 and 3) as a Function of Distance and Direction from the Indian Point 3 Tower

(0 - 3 miles)

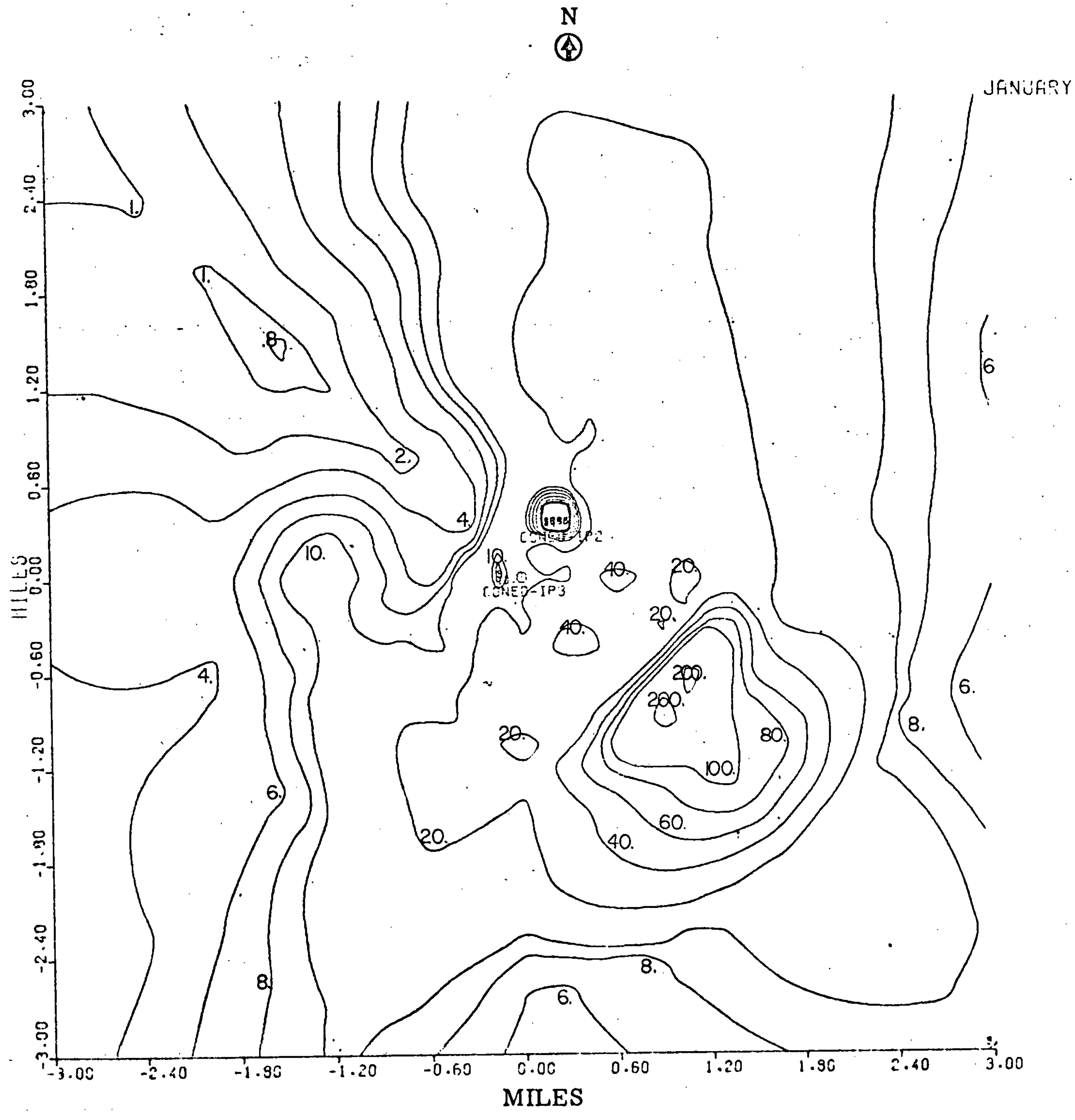

Basis: Drift Rate: 0.002% (5.7 Kg salt/hour/tower)
Number of towers: two

Figure 3-18

Predicted January Monthly Average Ground Dry Deposition Rates (Kg/Km^2-month) of Salt Resulting from Operation of Two Natural Draft Cooling Towers (Indian Point 2 and 3) as a Function of Distance and Direction from the Indian Point 3 Tower

(0 - 10 miles)

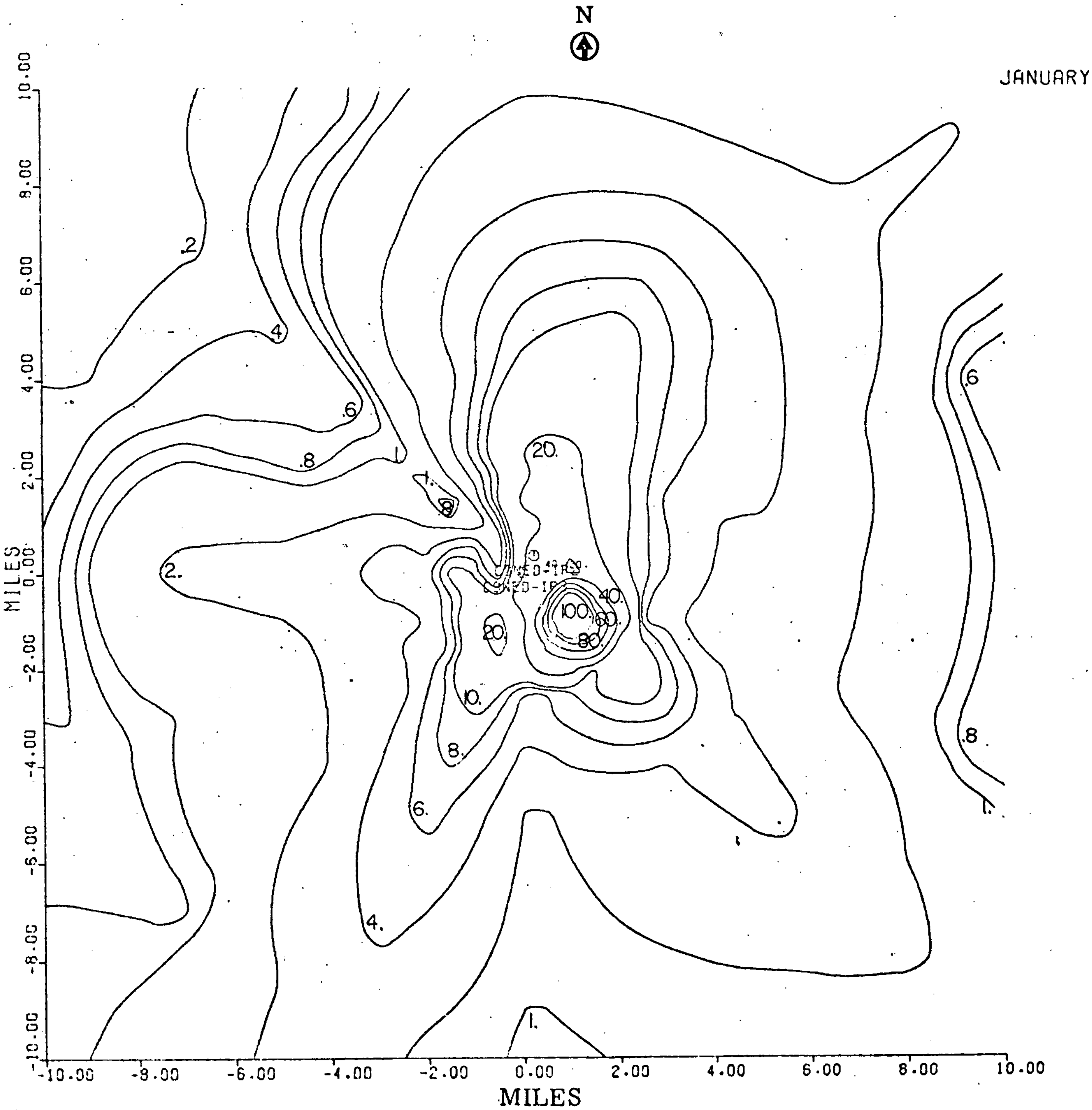

Basis: Drift Rate: 0.002% (5.7 Kg salt/hour/tower)
Number of towers: two

Figure 3-19

Predicted January Monthly Average Near Ground Airborne Concentration ($\mu g/m^3$) of Salt Resulting from Operation of Two Natural Draft Cooling Towers (Indian Point 2 and 3) as a Function of Distance and Direction from the Indian Point 3 Tower

(0 - 3 miles)

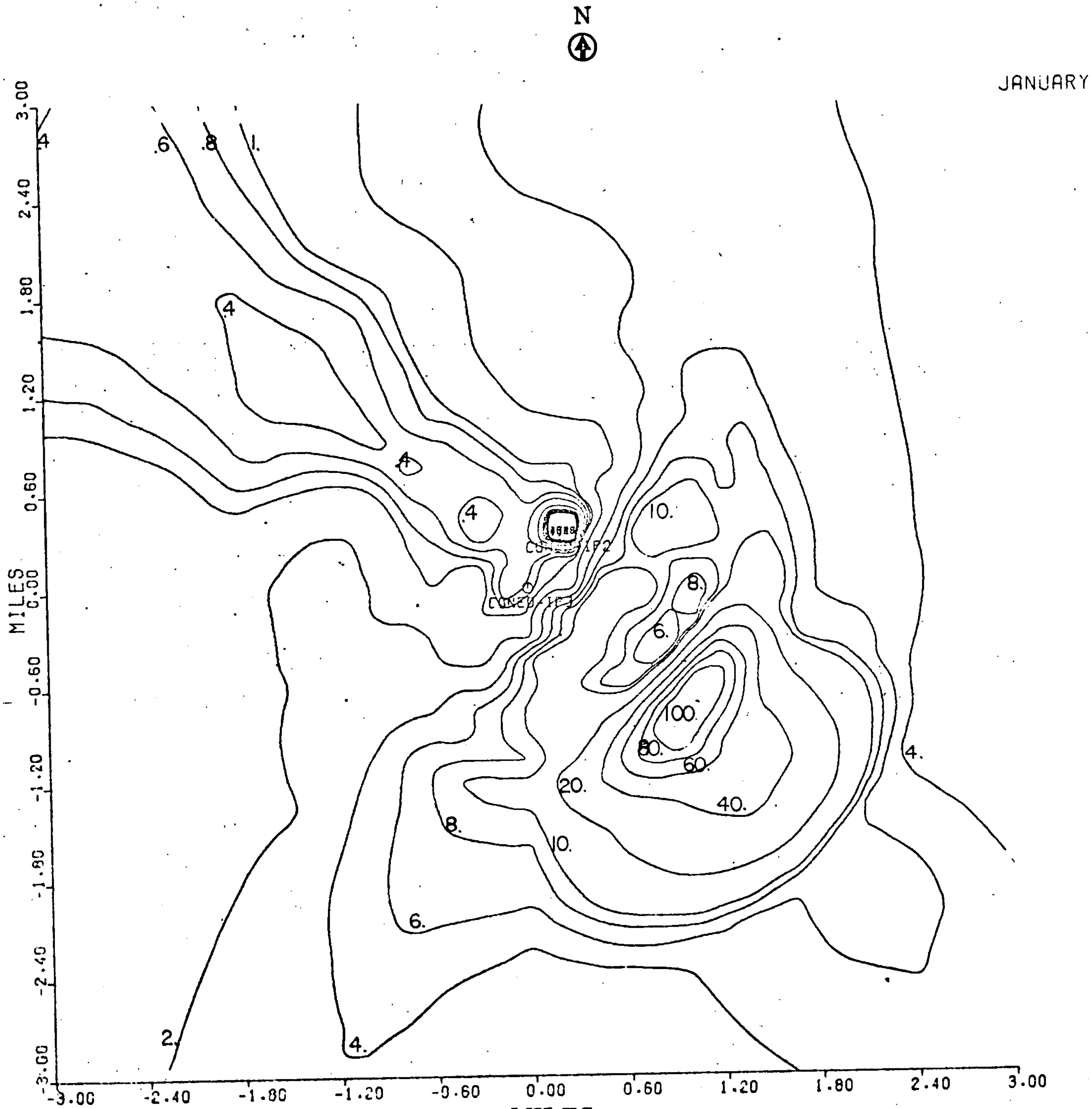

Basis: Drift Rate: 0.002% (5.7 Kg salt/hour/tower)
Number of towers: two

Note: Divide number on plot by 100 to get $\mu g/m^3$

Figure 3-20

Predicted January Monthly Average Near Ground Airborne Concentration ($\mu g/m^3$) of Salt Resulting from Operation of Two Natural Draft Cooling Towers (Indian Point 2 and 3) as a Function of Distance and Direction from the Indian Point 3 Tower

(0 - 10 miles)

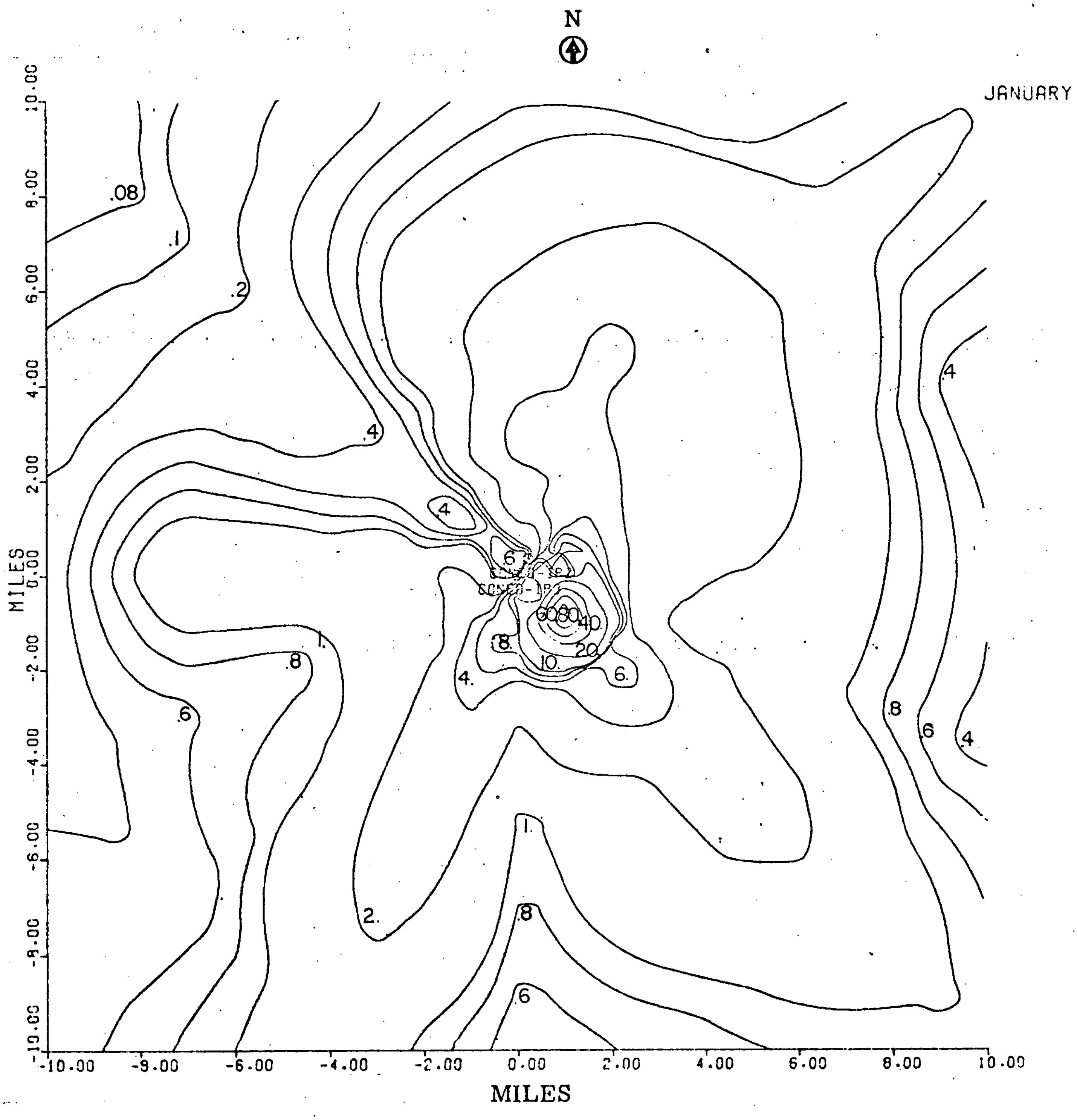

Basis: Drift Rate: 0.002% (5.7 Kg salt/hour/tower)
Number of towers: two

Note: Divide number on plot by 100 to get $\mu g/m^3$

Figure 3-21

Predicted February Monthly Average Ground Dry Deposition Rates (Kg/Km^2-month) of Salt Resulting from Operation of Two Natural Draft Cooling Towers (Indian Point 2 and 3) as a Function of Distance and Direction from the Indian Point 3 Tower

(0 - 3 miles)

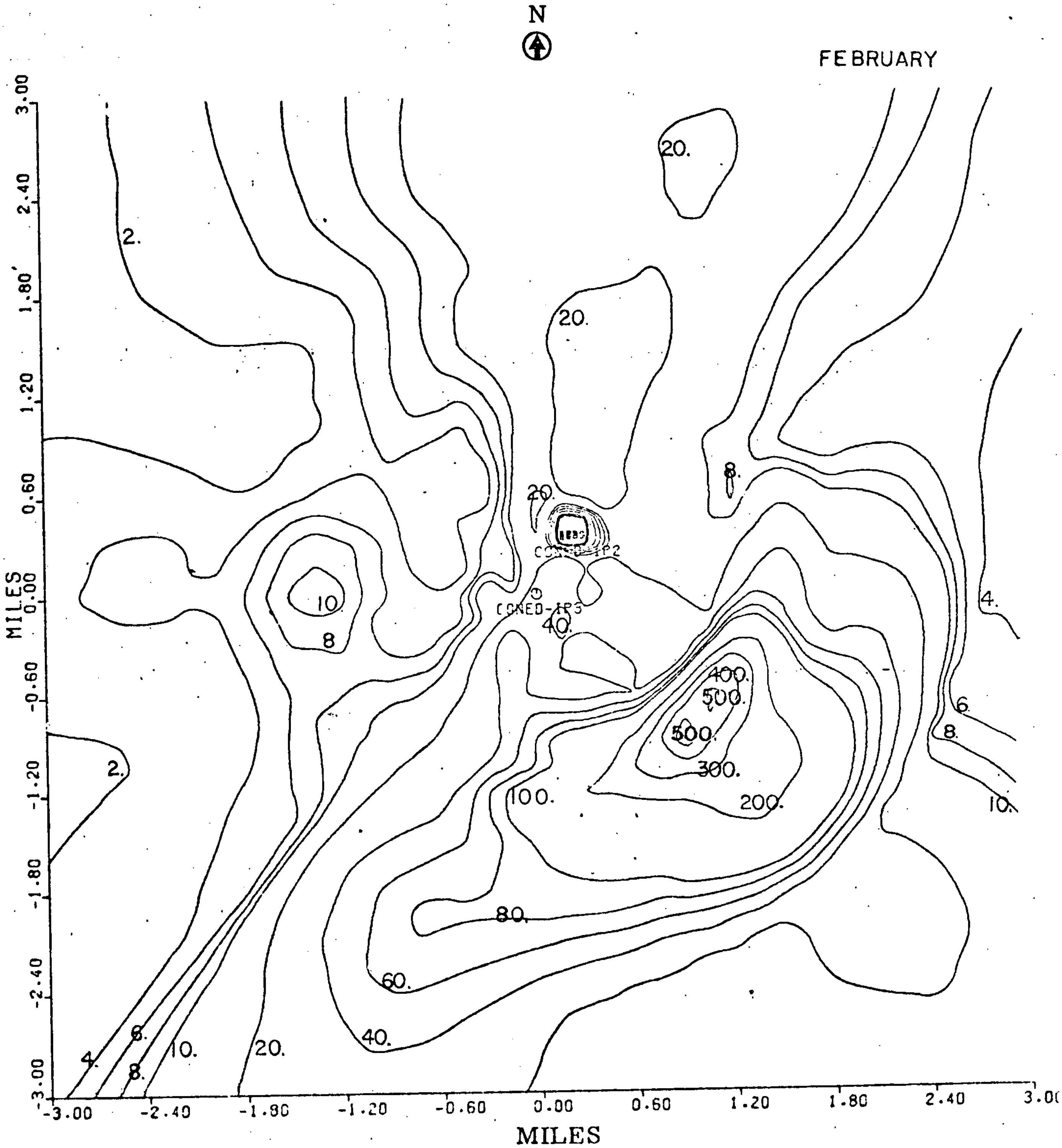

Basis: Drift Rate: 0.002% (8.4 Kg salt/hour/tower)
Number of towers: two

Figure 3-22

Predicted February Monthly Average Ground Dry Deposition Rates (Kg/Km^2-month) of Salt Resulting from Operation of Two Natural Draft Cooling Towers (Indian Point 2 and 3) as a Function of Distance and Direction from the Indian Point 3 Tower

(0 - 10 miles)

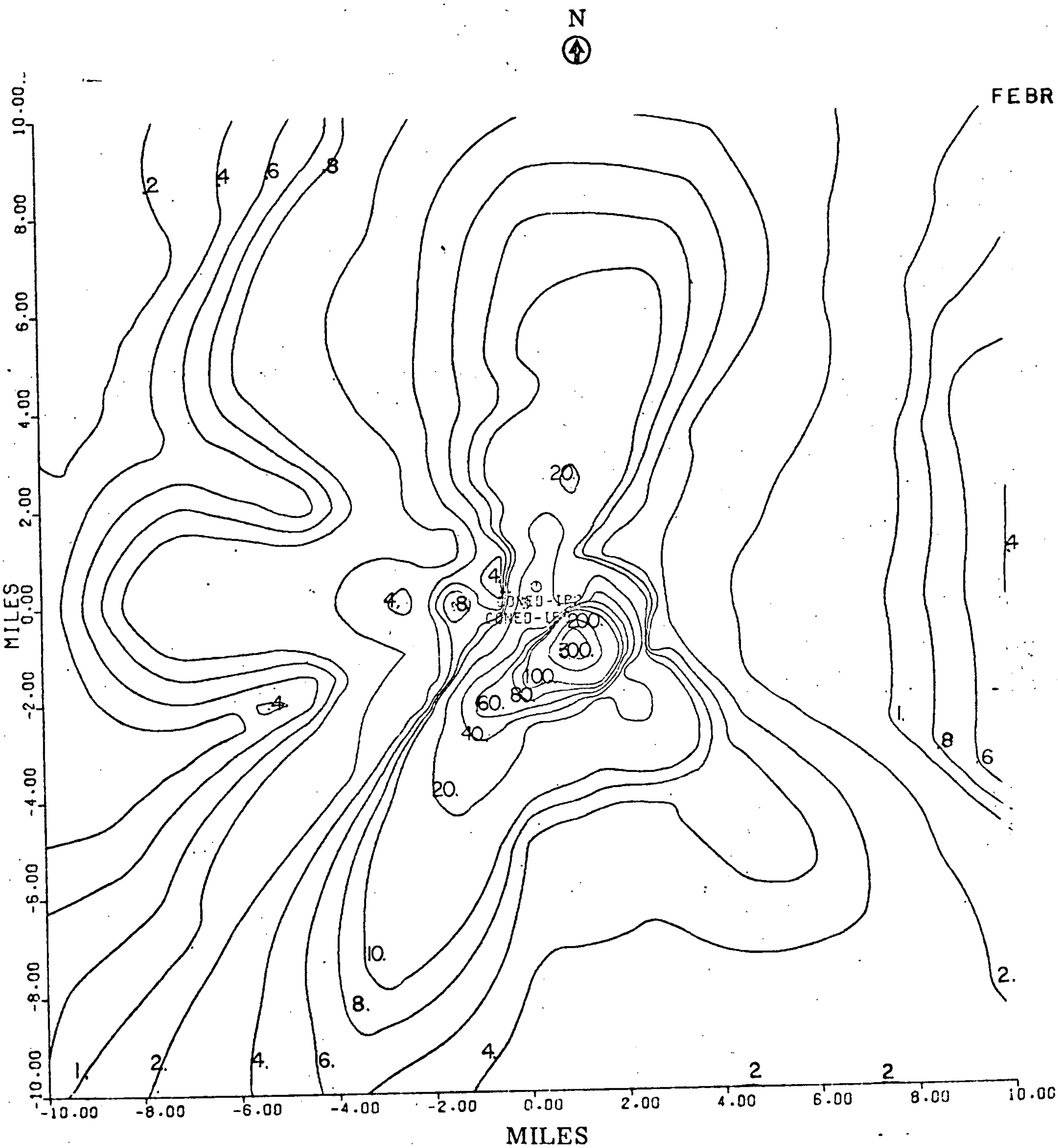

Basis: Drift Rate: 0.002% (8.4 Kg salt/hour/tower)
Number of towers: two

Figure 3-23

Predicted February Monthly Average Near Ground Airborne Concentration ($\mu g/m^3$) of Salt Resulting from Operation of Two Natural Draft Cooling Towers (Indian Point 2 and 3) as a Function of Distance and Direction from the Indian Point 3 Tower

(0 - 3 miles)

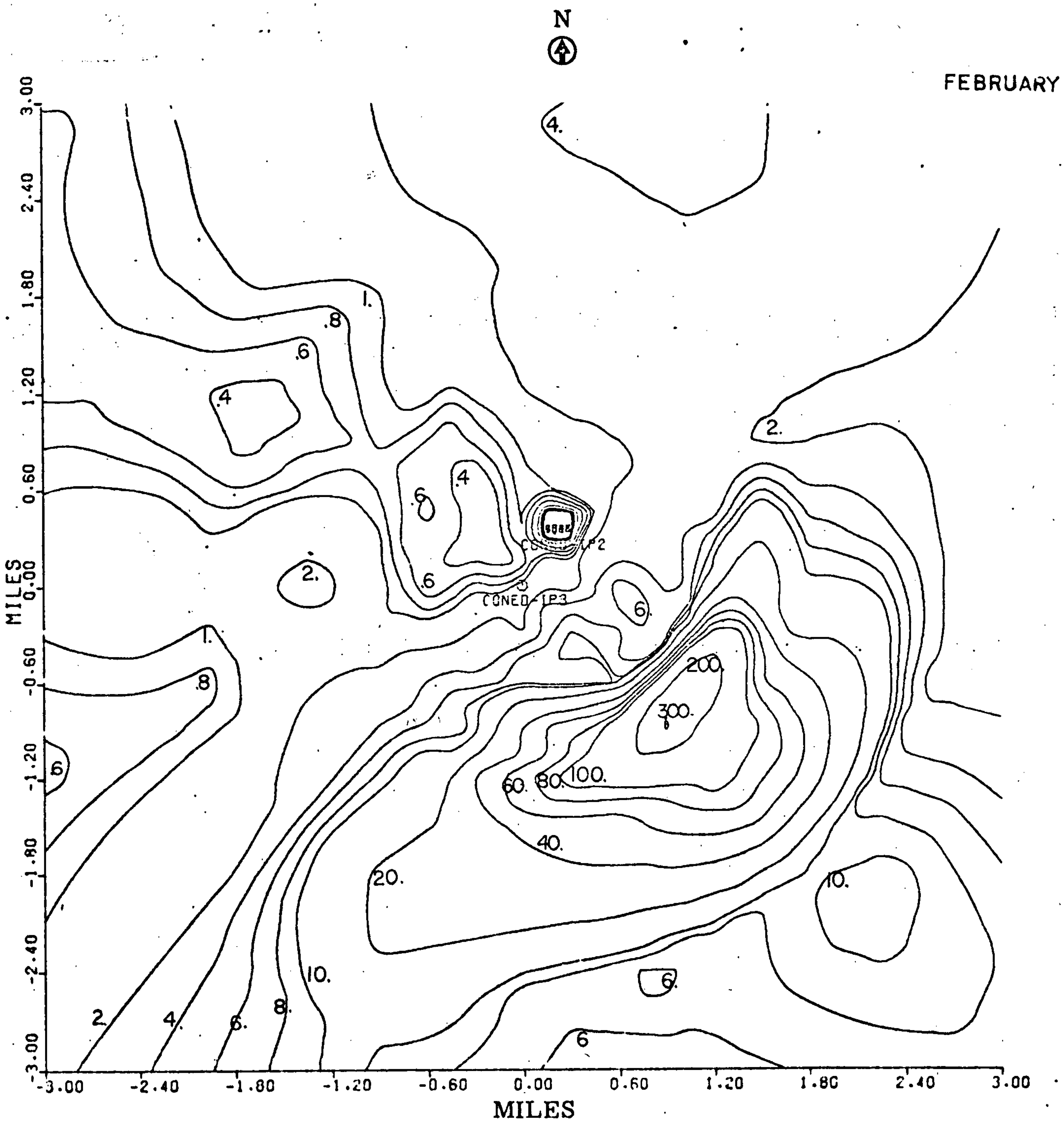

Basis: Drift Rate: 0.002% (8.4 Kg salt/hour/tower)
Number of towers: two

Note: Divide number on plot by 100 to get $\mu g/m^3$

Figure 3-24

Predicted February Monthly Average Near Ground Airborne Concentration ($\mu g/m^3$) of Salt Resulting from Operation of Two Natural Draft Cooling Towers (Indian Point 2 and 3) as a Function of Distance and Direction from the Indian Point 3 Tower

(0 - 10 miles)

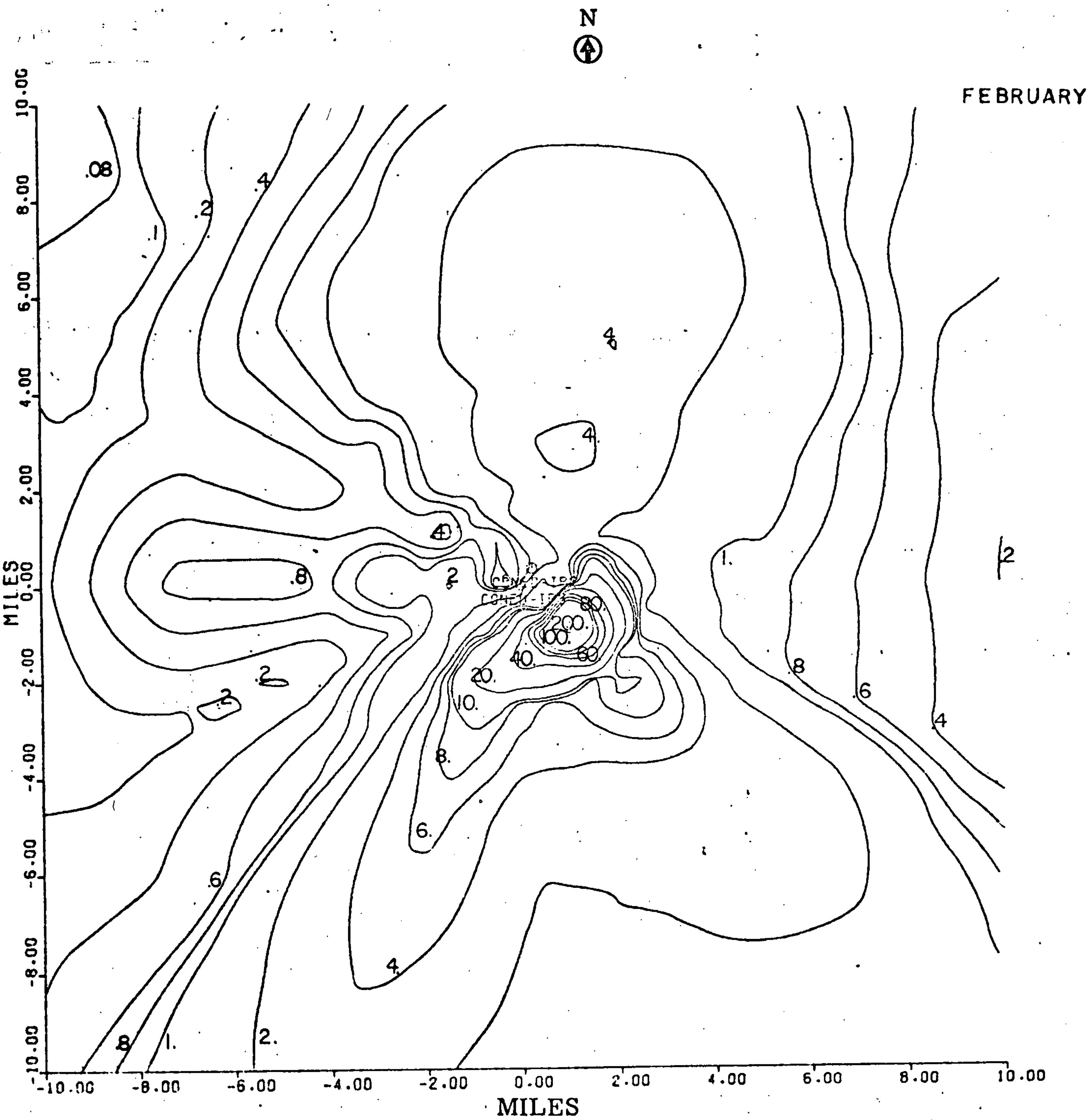

Basis: Drift Rate: 0.002% (8.4 Kg salt/hour/tower)
Number of towers: two

Note: Divide number on plot by 100 to get $\mu g/m^3$

Figure 3-25

Predicted March Monthly Average Ground Dry Deposition Rates (Kg/Km^2-month) of Salt Resulting from Operation of Two Natural Draft Cooling Towers (Indian Point 2 and 3) as a Function of Distance and Direction from the Indian Point 3 Tower

(0 - 3 miles)

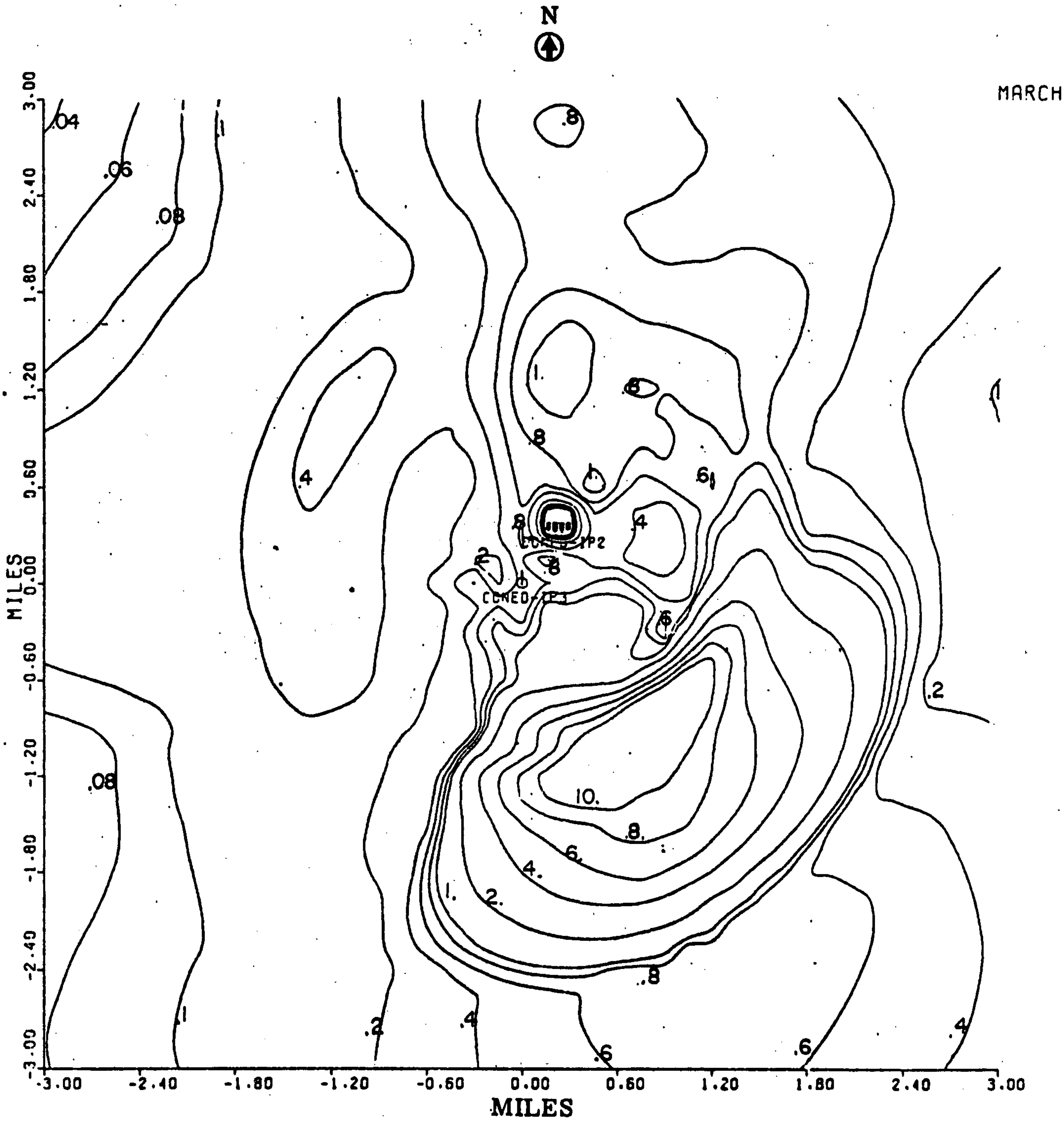

Basis: Drift Rate: 0.002% (0.27 Kg salt/hour/tower)
Number of towers: two

Figure 3-26

Predicted March Monthly Average Ground Dry Deposition Rates (Kg/Km^2-month) of Salt Resulting from Operation of Two Natural Draft Cooling Towers (Indian Point 2 and 3) as a Function of Distance and Direction from the Indian Point 3 Tower

(0 - 10 miles)

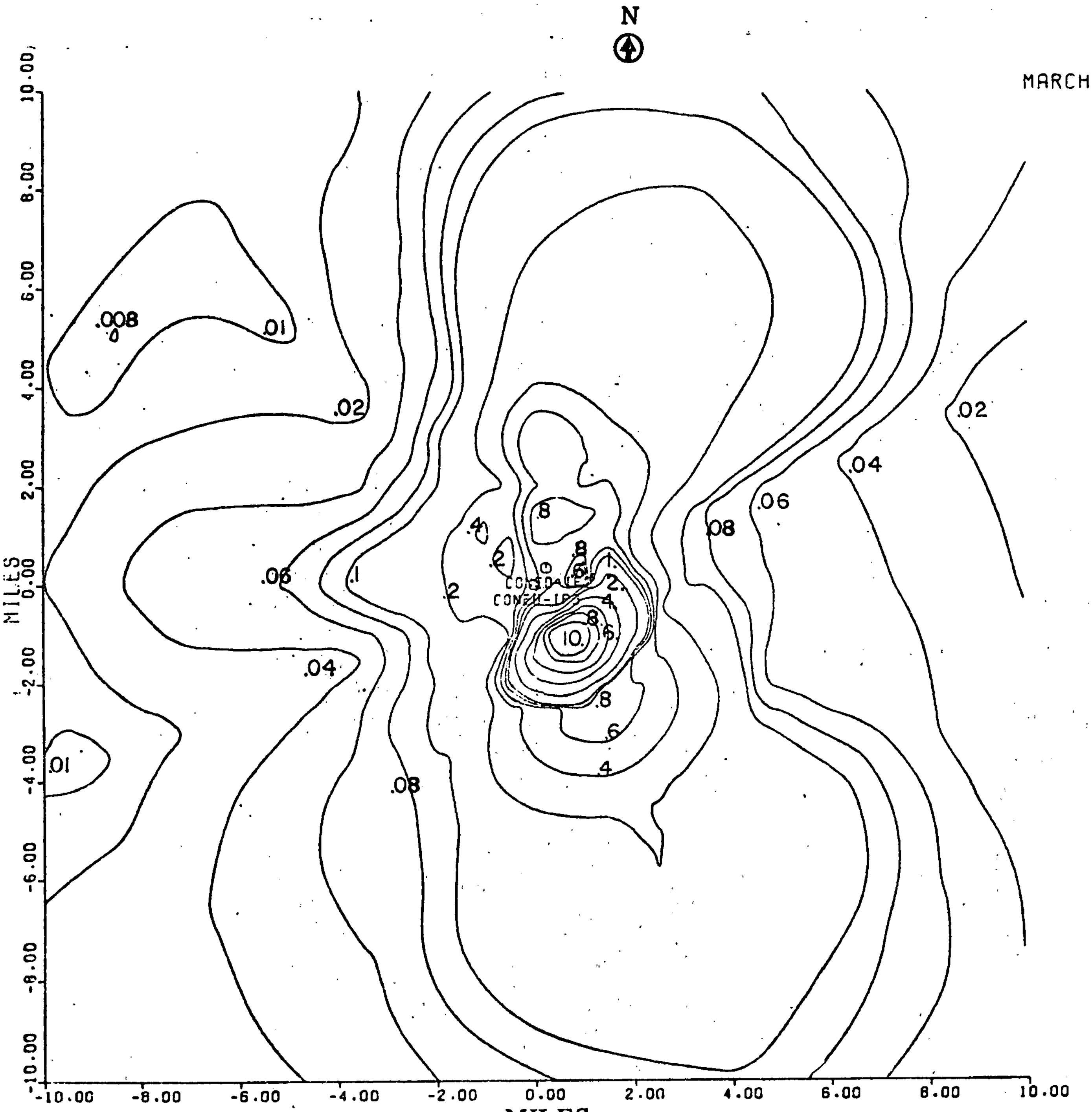

Basis: Drift Rate: 0.002% (0.27 Kg salt/hour/tower)
Number of towers: two

Figure 3-27

Predicted March Monthly Average Near Ground Airborne Concentration ($\mu g/m^3$) of Salt Resulting from Operation of Two Natural Draft Cooling Towers (Indian Point 2 and 3) as a Function of Distance and Direction from the Indian Point 3 Tower

(0 - 3 miles)

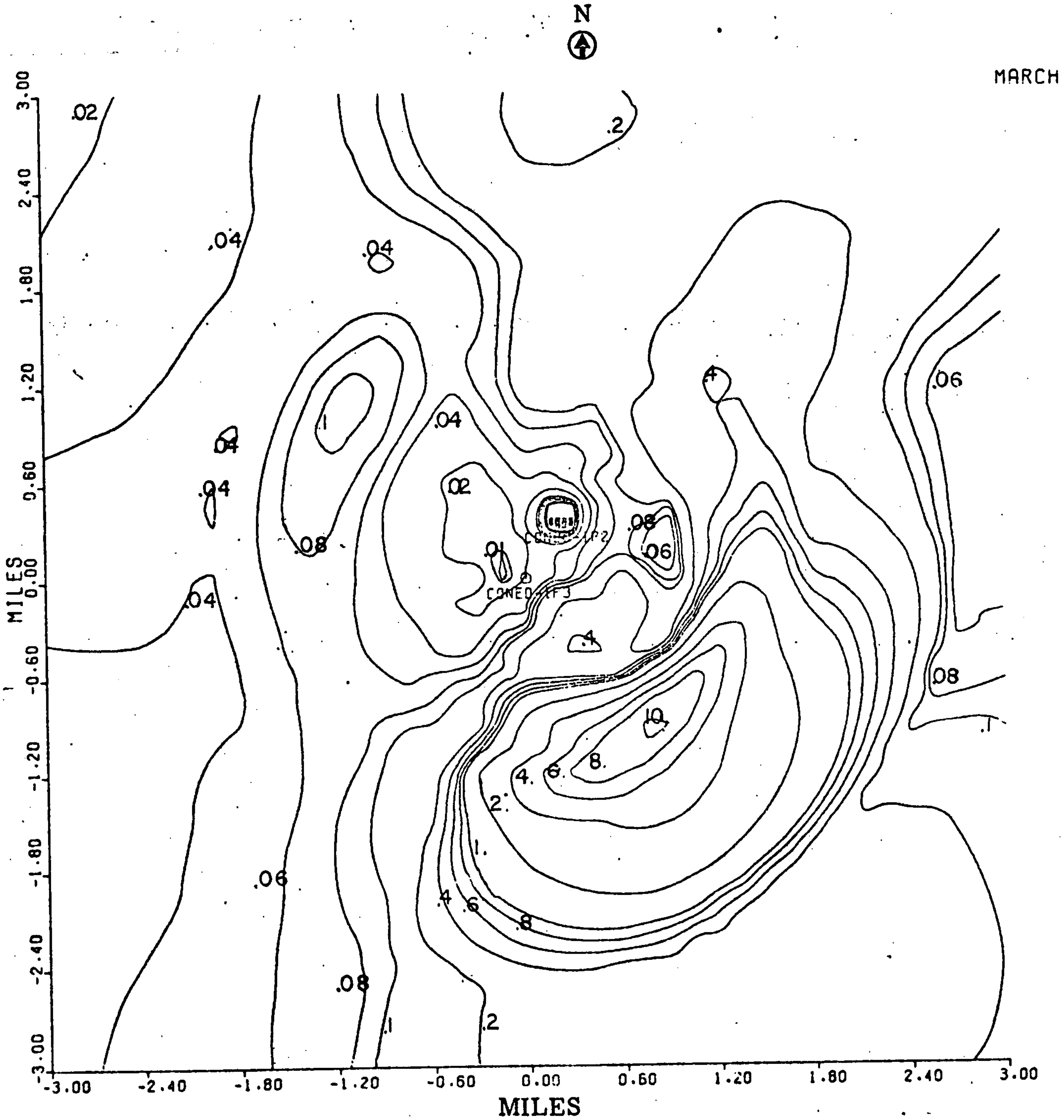

Basis: Drift Rate: 0.002% (0.27 Kg salt/hour/tower)
Number of towers: two

Note: Divide number on plot by 100 to get $\mu g/m^3$

Figure 3-28

Predicted March Monthly Average Near Ground Airborne Concentration ($\mu g/m^3$) of Salt Resulting from Operation of Two Natural Draft Cooling Towers (Indian Point 2 and 3) as a Function of Distance and Direction from the Indian Point 3 Tower

(0 - 10 miles)

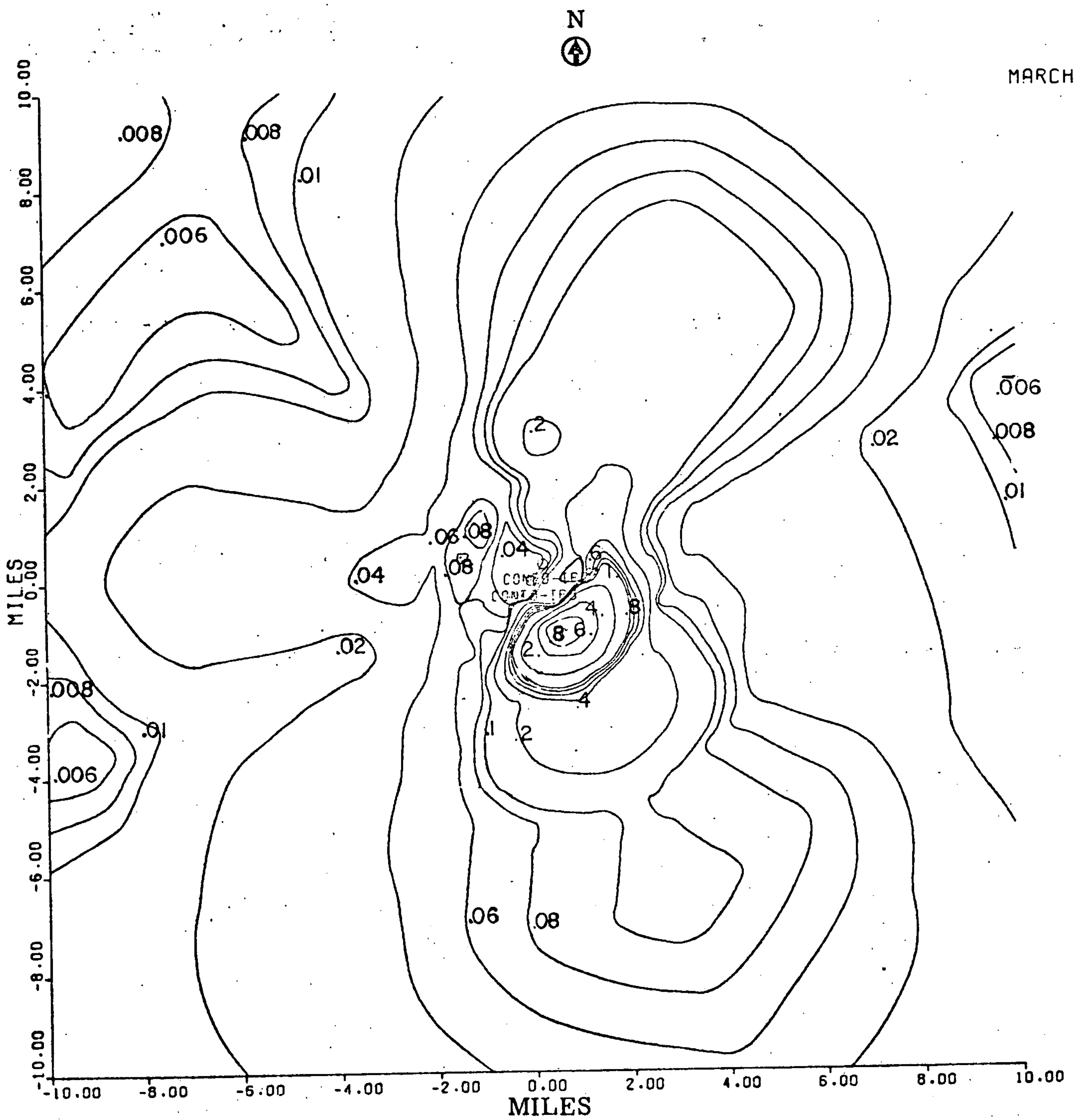

Basis: Drift Rate: 0.002% (0.27 Kg salt/hour/tower)
Number of towers: two

Note: Divide number on plot by 100 to get $\mu g/m^3$

Figure 3-29

Predicted April Monthly Average Ground Dry Deposition Rates (Kg/Km^2-month) of Salt Resulting from Operation of Two Natural Draft Cooling Towers (Indian Point 2 and 3) as a Function of Distance and Direction from the Indian Point 3 Tower

(0 - 3 miles)

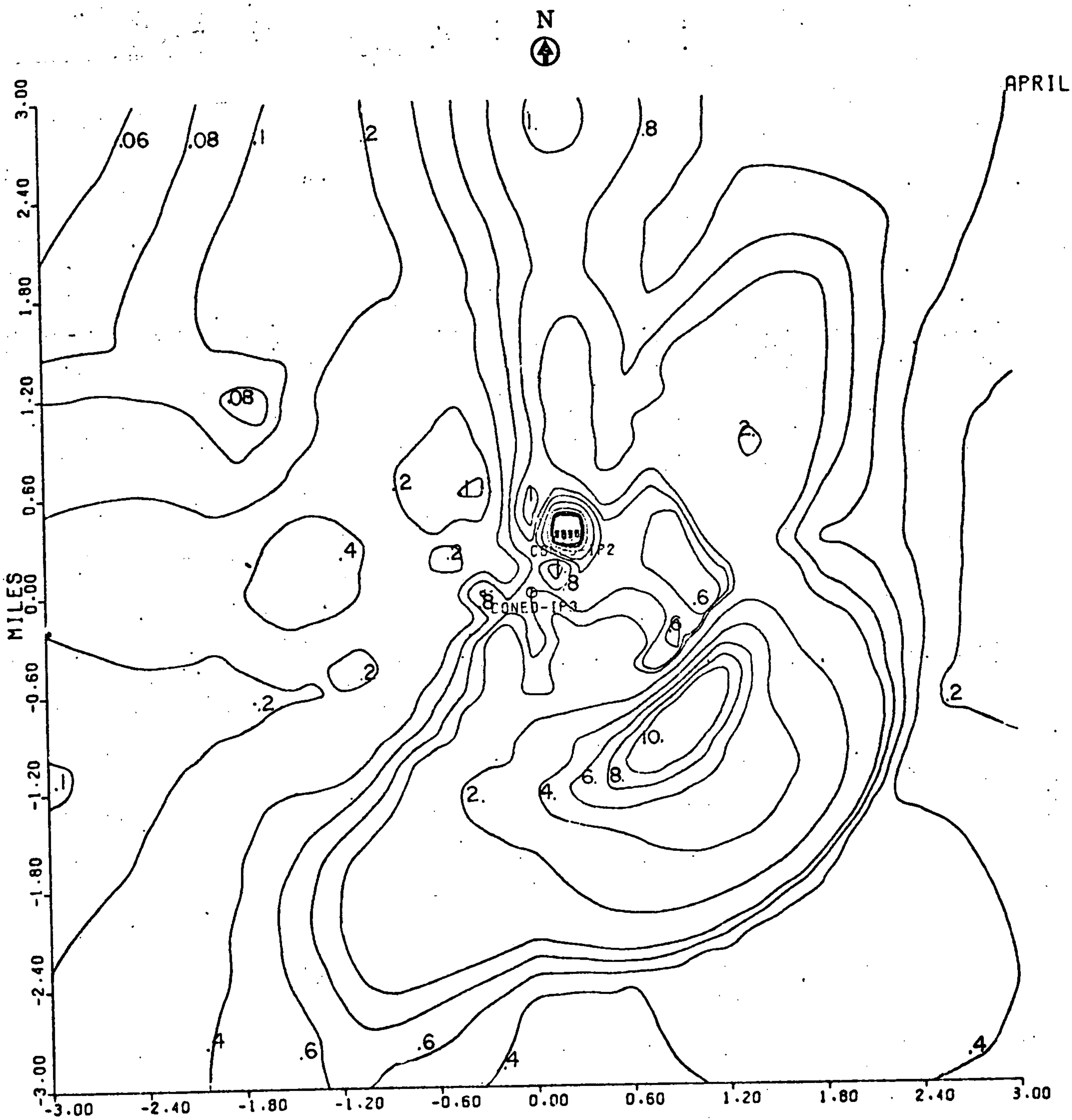

Basis: Drift Rate: 0.002% (0.27 Kg salt/hour/tower)
Number of towers: two

Figure 3-30

Predicted April Monthly Average Ground Dry Deposition Rates (Kg/Km^2-month) of Salt Resulting from Operation of Two Natural Draft Cooling Towers (Indian Point 2 and 3) as a Function of Distance and Direction from the Indian Point 3 Tower

(0 - 10 miles)

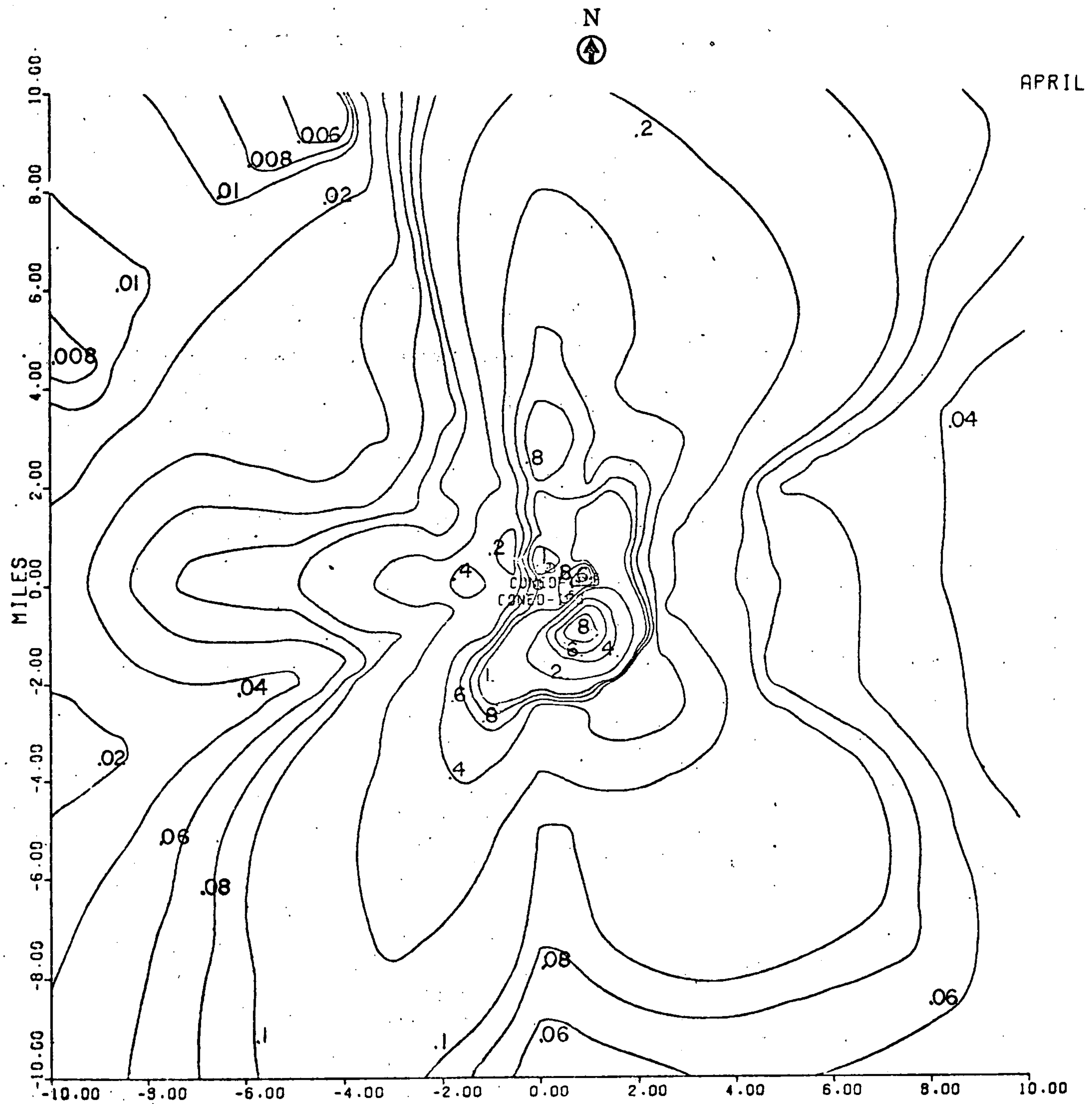

Basis: Drift Rate: 0.002% (0.27 Kg salt/hour/tower)
Number of towers: two

Figure 3-31

Predicted April Monthly Average Near Ground Airborne Concentration ($\mu g/m^3$) of Salt Resulting from Operation of Two Natural Draft Cooling Towers (Indian Point 2 and 3) as a Function of Distance and Direction from the Indian Point 3 Tower

(0 - 3 miles)

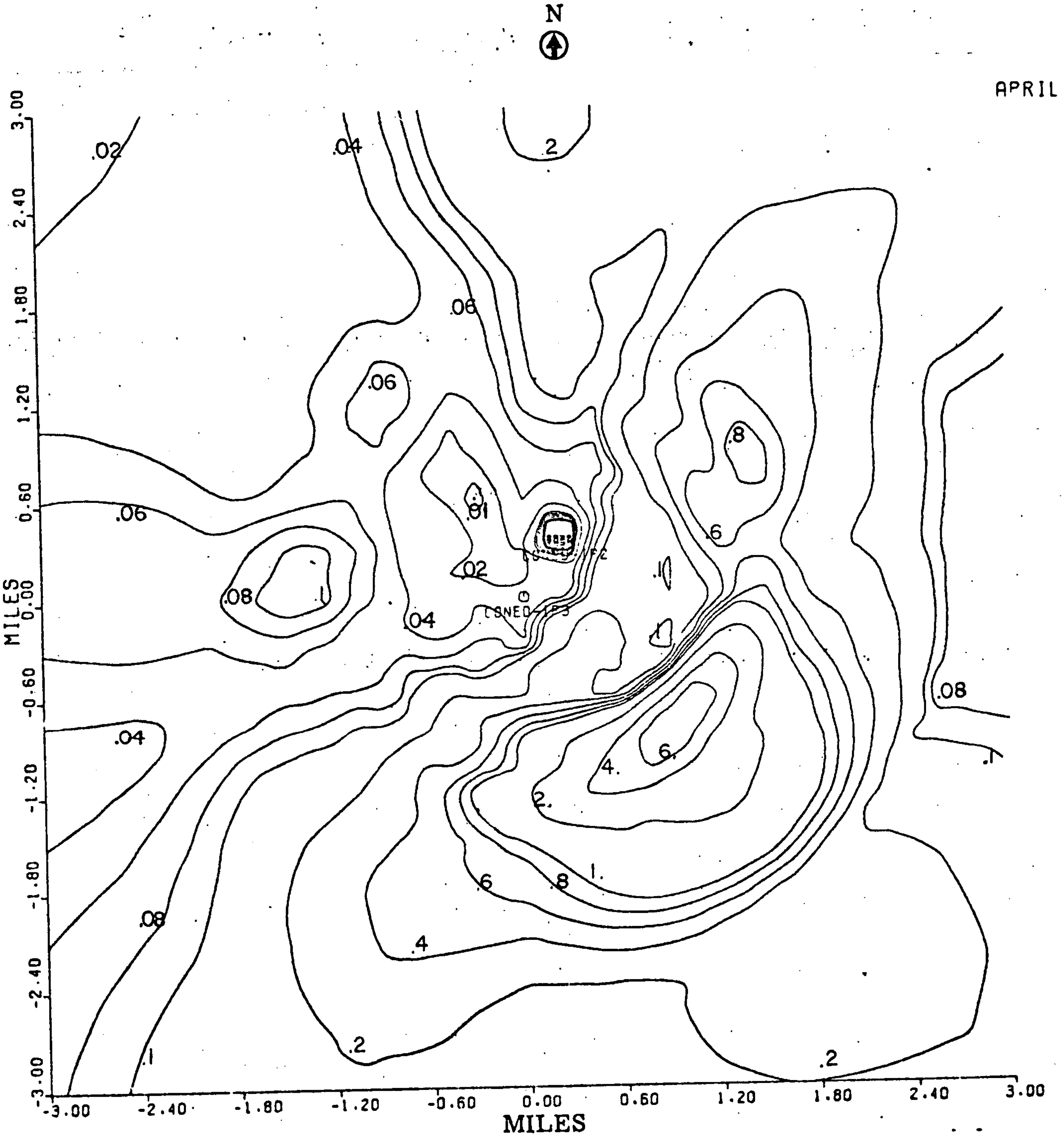

Basis: Drift Rate: 0.002% (0.27 Kg salt/hour/tower)
Number of towers: two

Note: Divide number on plot by 100 to get $\mu g/m^3$

Figure 3-32

Predicted April Monthly Average Near Ground Airborne Concentration ($\mu g/m^3$) of Salt Resulting from Operation of Two Natural Draft Cooling Towers (Indian Point 2 and 3) as a Function of Distance and Direction from the Indian Point 3 Tower

(0 - 10 miles)

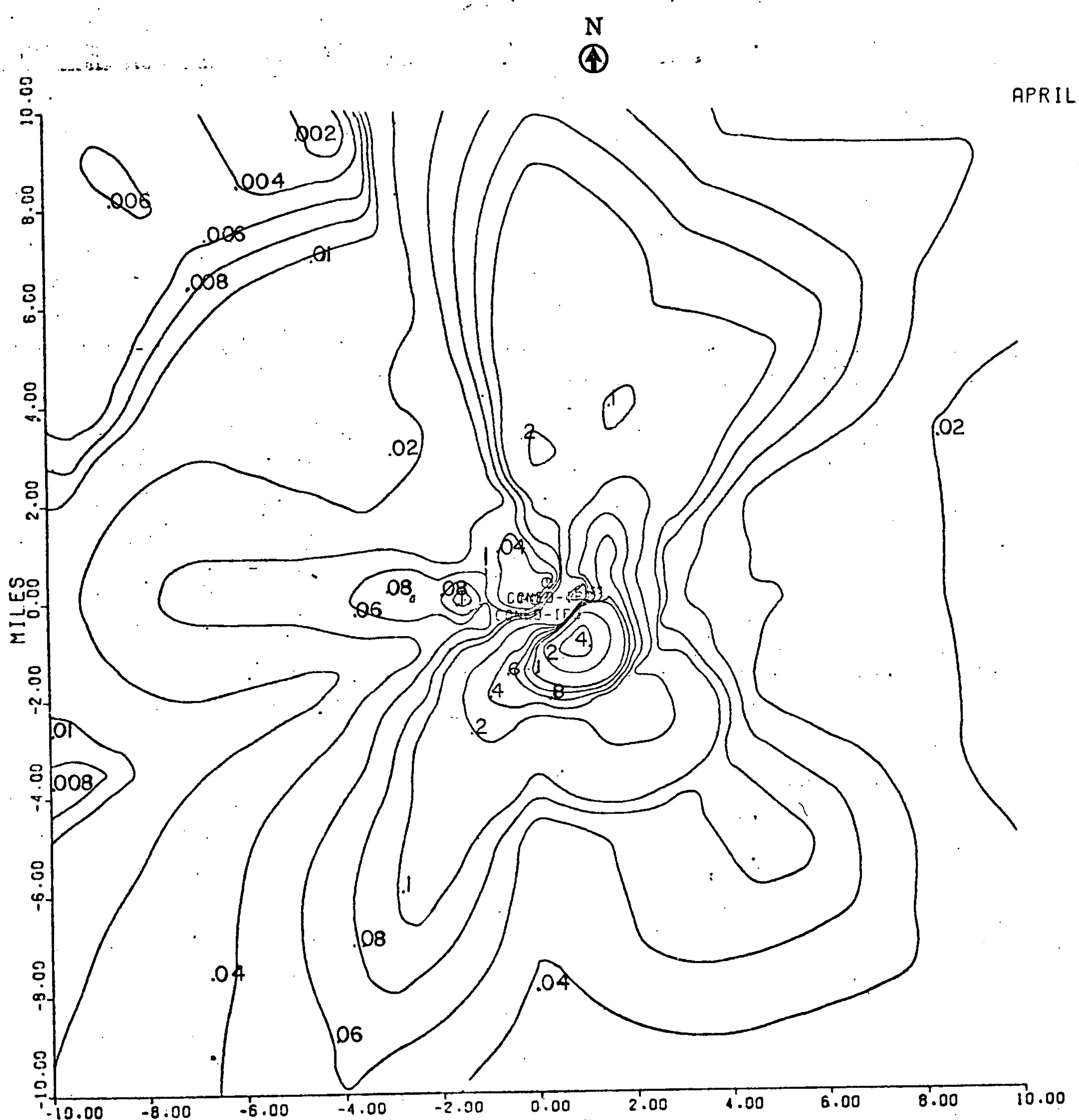

Basis: Drift Rate: 0.002% (0.27 Kg salt/hour/tower)
Number of towers: two

Note: Divide number on plot by 100 to get $\mu g/m^3$

Figure 3-33

Predicted May Monthly Average Ground Dry Deposition Rates (Kg/Km^2-month) of Salt Resulting from Operation of Two Natural Draft Cooling Towers (Indian Point 2 and 3) as a Function of Distance and Direction from the Indian Point 3 Tower

(0 - 3 miles)

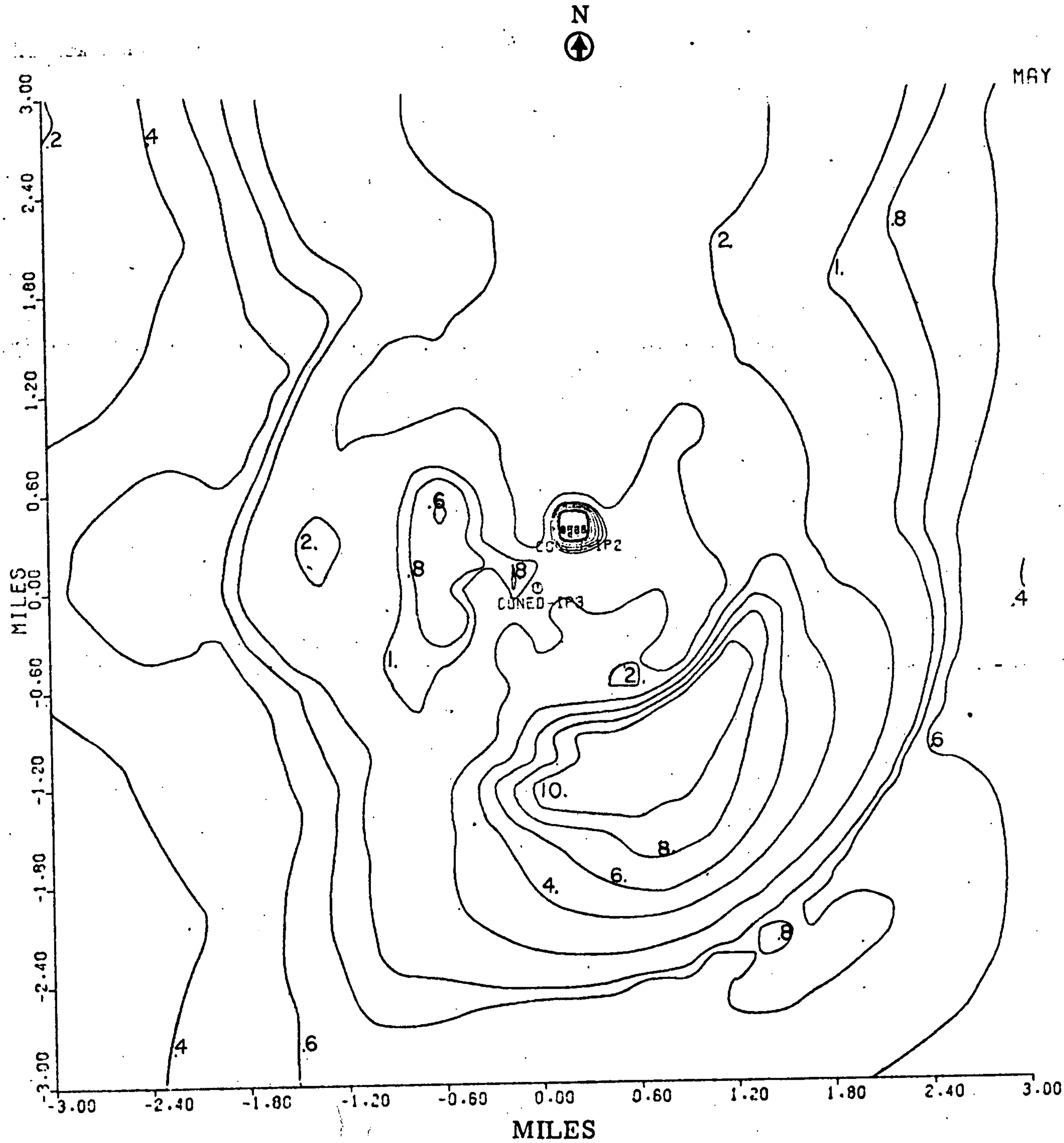

Basis: Drift Rate: 0.002% (0.71 Kg salt/hour/tower)
Number of towers: two

Figure 3-34

Predicted May Monthly Average Ground Dry Deposition Rates (Kg/Km^2-month) of Salt Resulting from Operation of Two Natural Draft Cooling Towers (Indian Point 2 and 3) as a Function of Distance and Direction from the Indian Point 3 Tower

(0 - 10 miles)

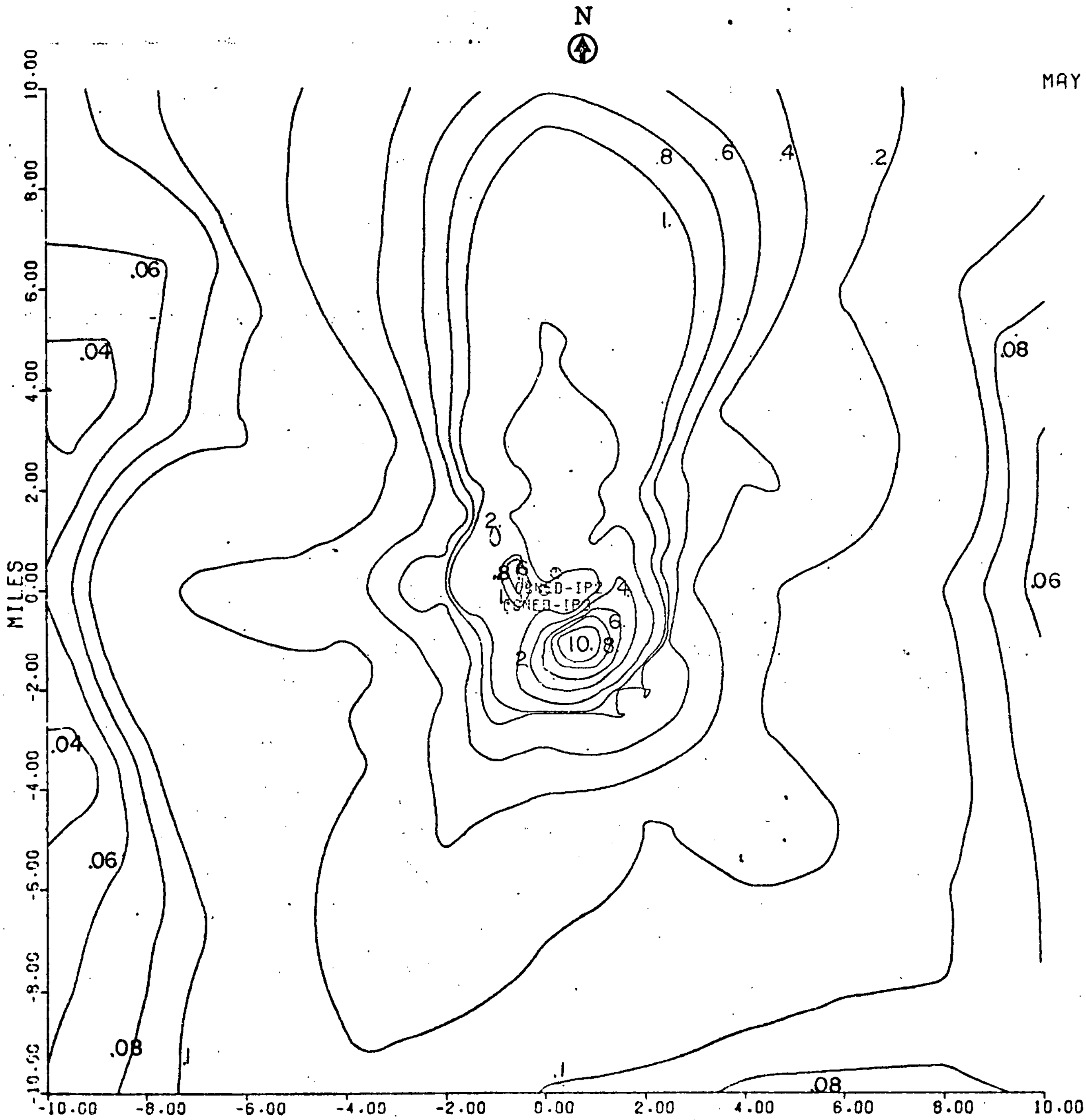

Basis: Drift Rate: 0.002% (0.71 Kg salt/hour/tower)
Number of towers: two

Figure 3-35

Predicted May Monthly Average Near Ground Airborne Concentration ($\mu g/m^3$) of Salt Resulting from Operation of Two Natural Draft Cooling Towers (Indian Point 2 and 3) as a Function of Distance and Direction from the Indian Point 3 Tower

(0 - 3 miles)

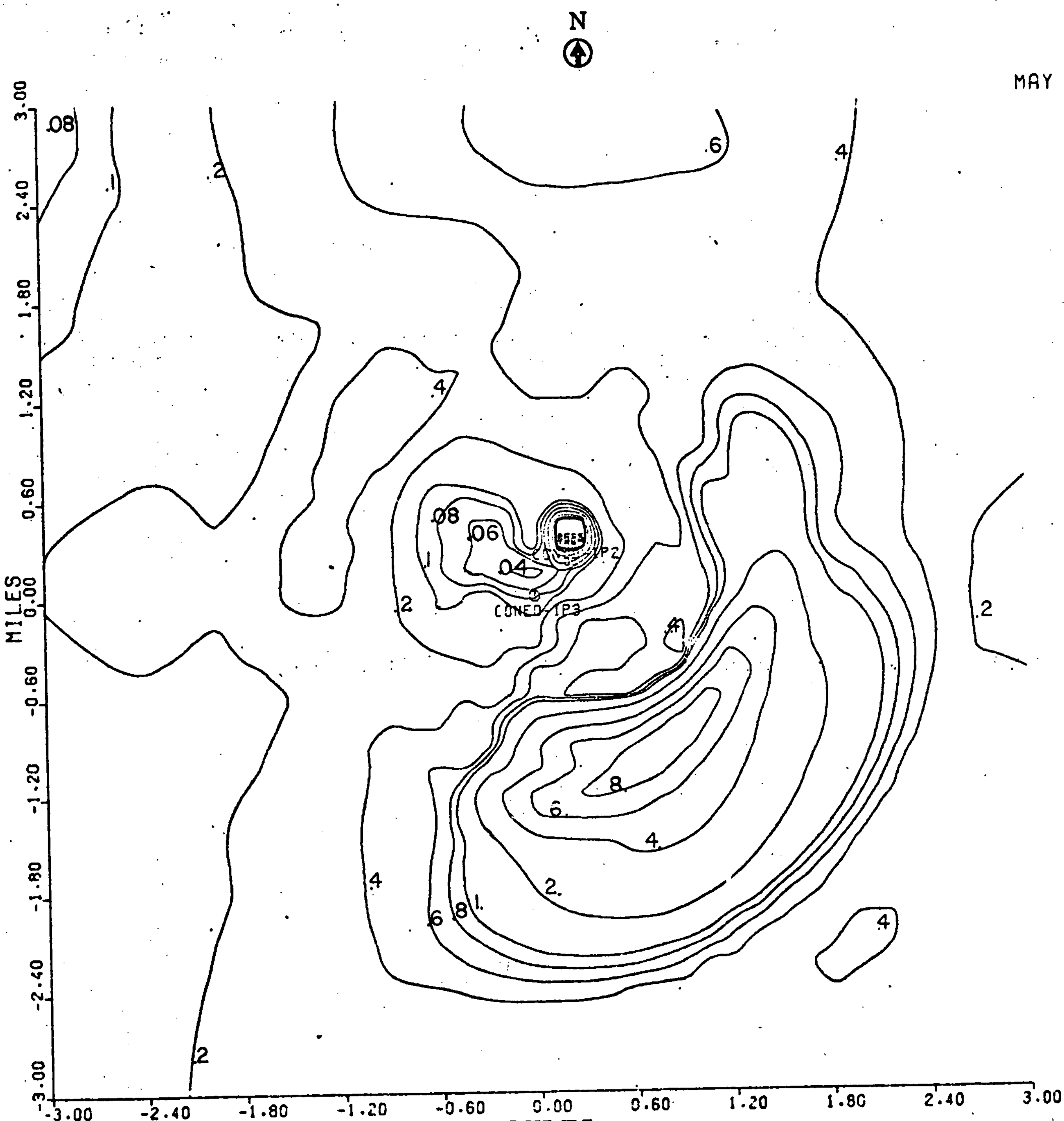

Basis: Drift Rate: 0.002% (0.71 Kg salt/hour/tower)
Number of towers: two

Note: Divide number on plot by 100 to get $\mu g/m^3$

Figure 3-36

Predicted May Monthly Average Near Ground Airborne Concentration ($\mu g/m^3$) of Salt Resulting from Operation of Two Natural Draft Cooling Towers (Indian Point 2 and 3) as a Function of Distance and Direction from the Indian Point 3 Tower

(0 - 10 miles)

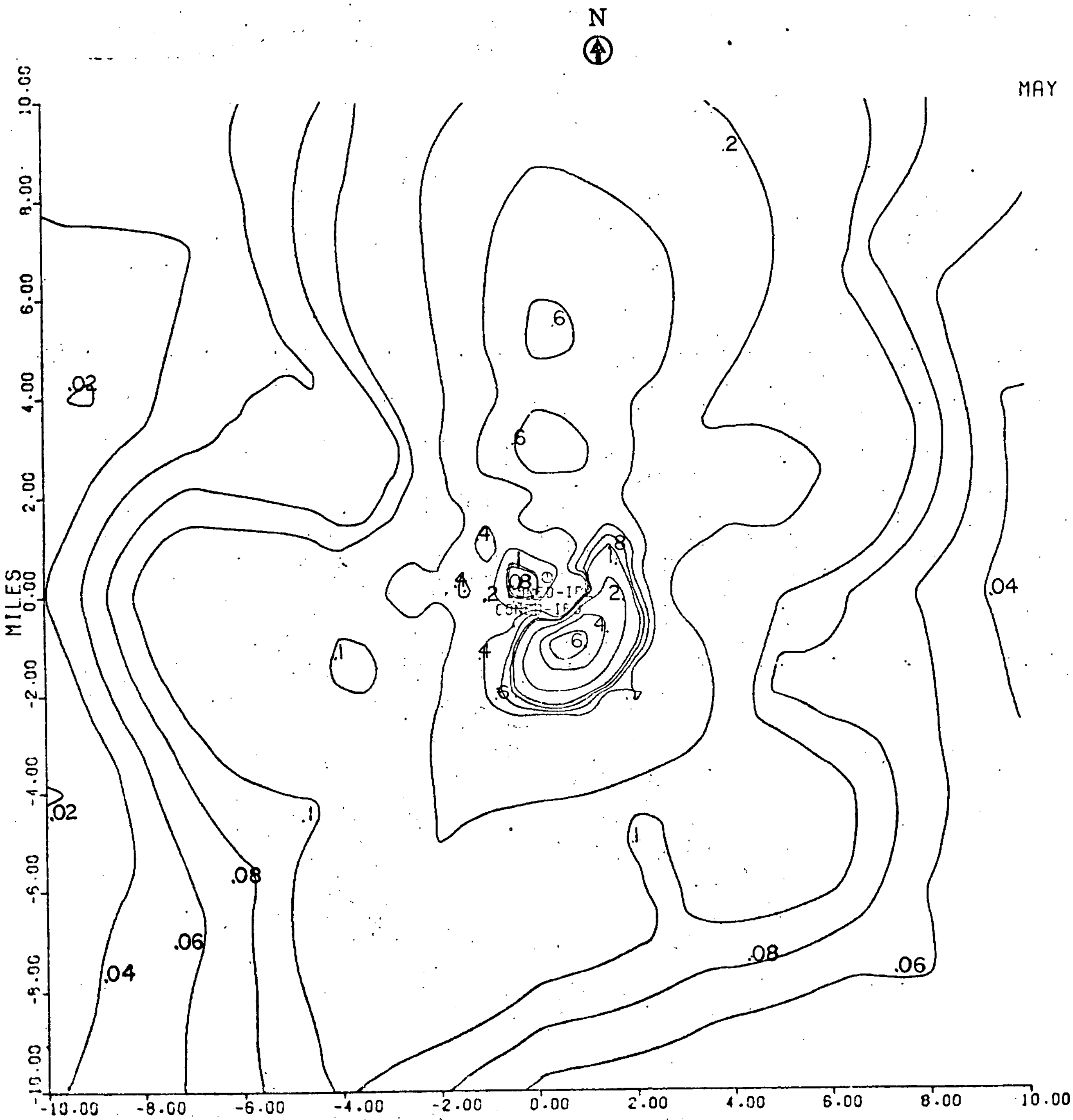

Basis: Drift Rate: 0.002% (0.71 Kg salt/hour/tower)
Number of towers: two

Note: Divide number on plot by 100 to get $\mu g/m^3$

Figure 3-37

Predicted June Monthly Average Ground Dry Deposition Rates (Kg/Km^2-month) of Salt Resulting from Operation of Two Natural Draft Cooling Towers (Indian Point 2 and 3) as a Function of Distance and Direction from the Indian Point 3 Tower

(0 - 3 miles)

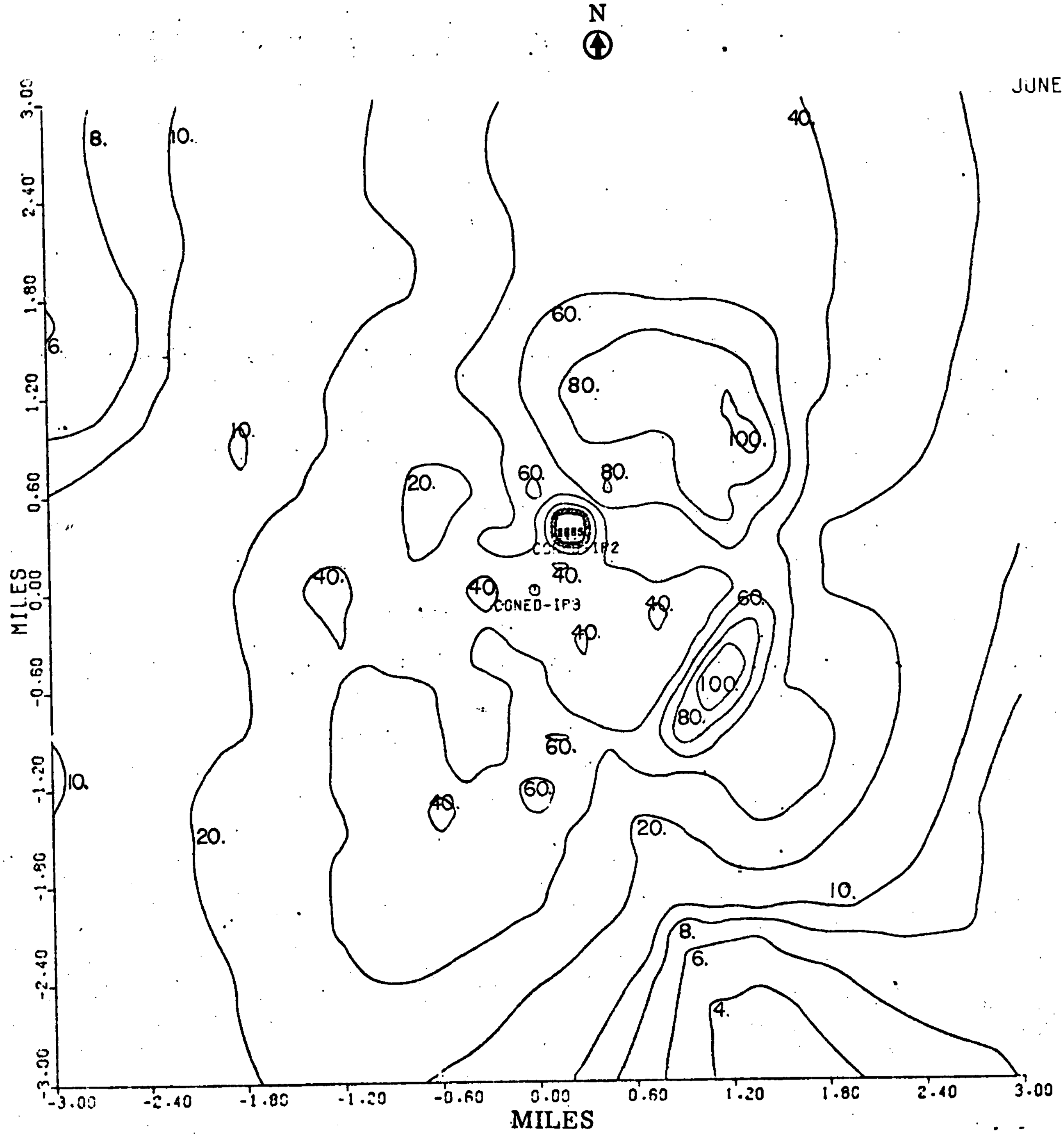

Basis: Drift Rate: 0.002% (10.9 Kg salt/hour/tower)
Number of towers: two

Figure 3-38

Predicted June Monthly Average Ground Dry Deposition Rates (Kg/Km^2-month) of Salt Resulting from Operation of Two Natural Draft Cooling Towers (Indian Point 2 and 3) as a Function of Distance and Direction from the Indian Point 3 Tower

(0 - 10 miles)

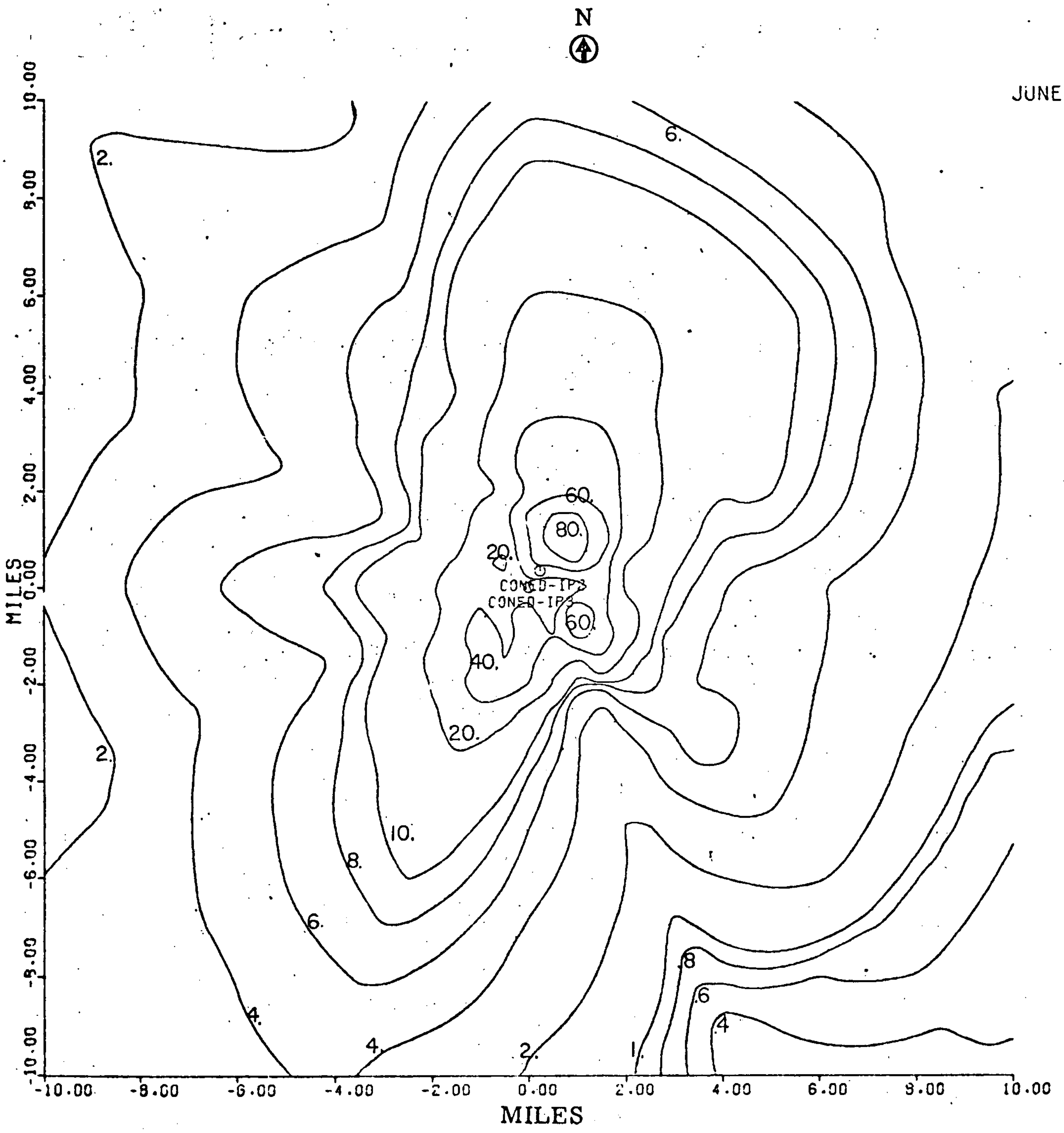

Basis: Drift Rate: 0.002% (10.9 Kg salt/hour/tower)
Number of towers: two

Figure 3-39

Predicted June Monthly Average Near Ground Airborne Concentration ($\mu g/m^3$) of Salt Resulting from Operation of Two Natural Draft Cooling Towers (Indian Point 2 and 3) as a Function of Distance and Direction from the Indian Point 3 Tower

(0 - 3 miles)

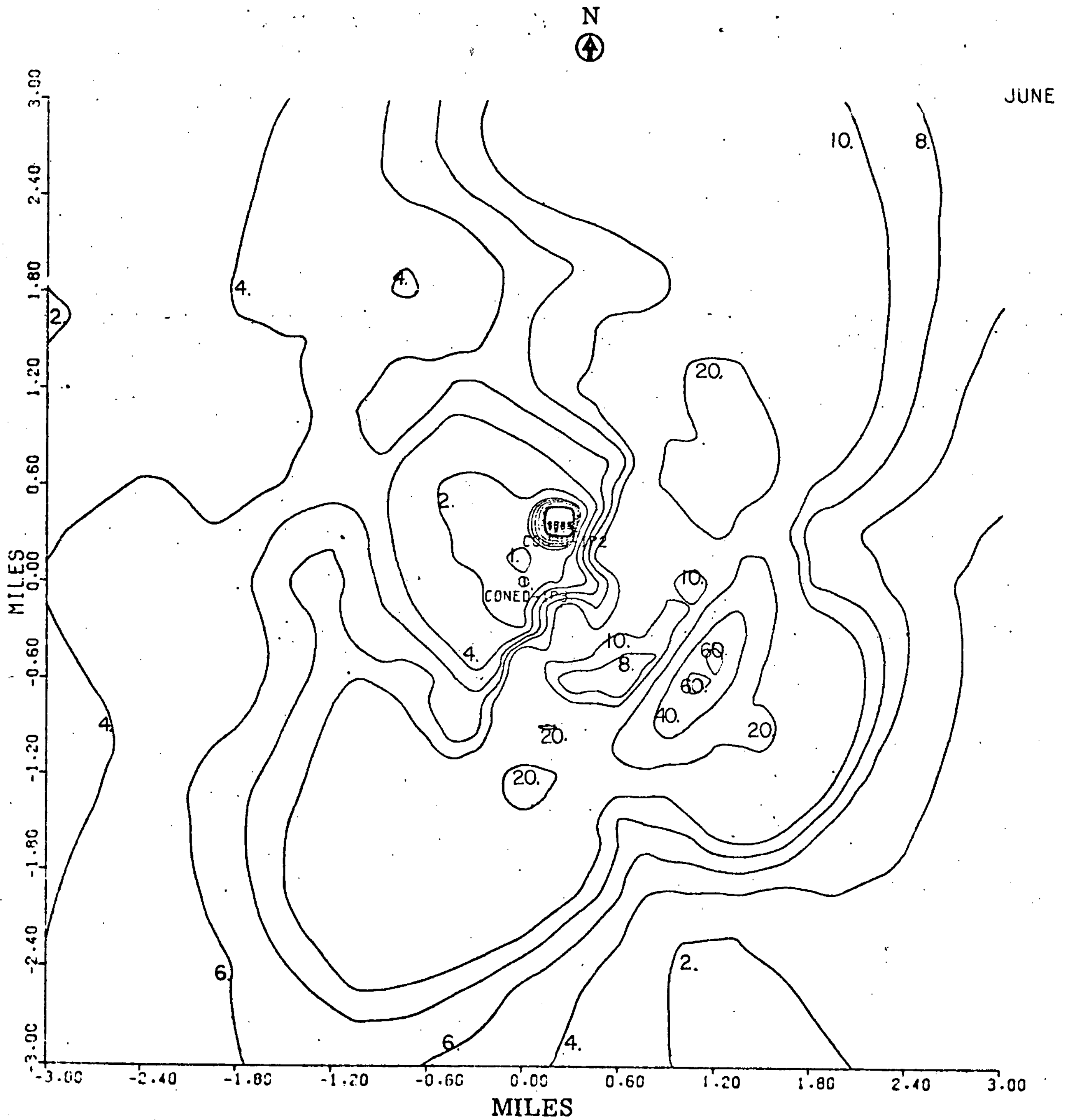

Basis: Drift Rate: 0.002% (10.9 Kg salt/hour/tower)
Number of towers: two

Note: Divide number on plot by 100 to get $\mu g/m^3$

Figure 3-40

Predicted June Monthly Average Near Ground Airborne Concentration ($\mu g/m^3$) of Salt Resulting from Operation of Two Natural Draft Cooling Towers (Indian Point 2 and 3) as a Function of Distance and Direction from the Indian Point 3 Tower

(0 - 10 miles)

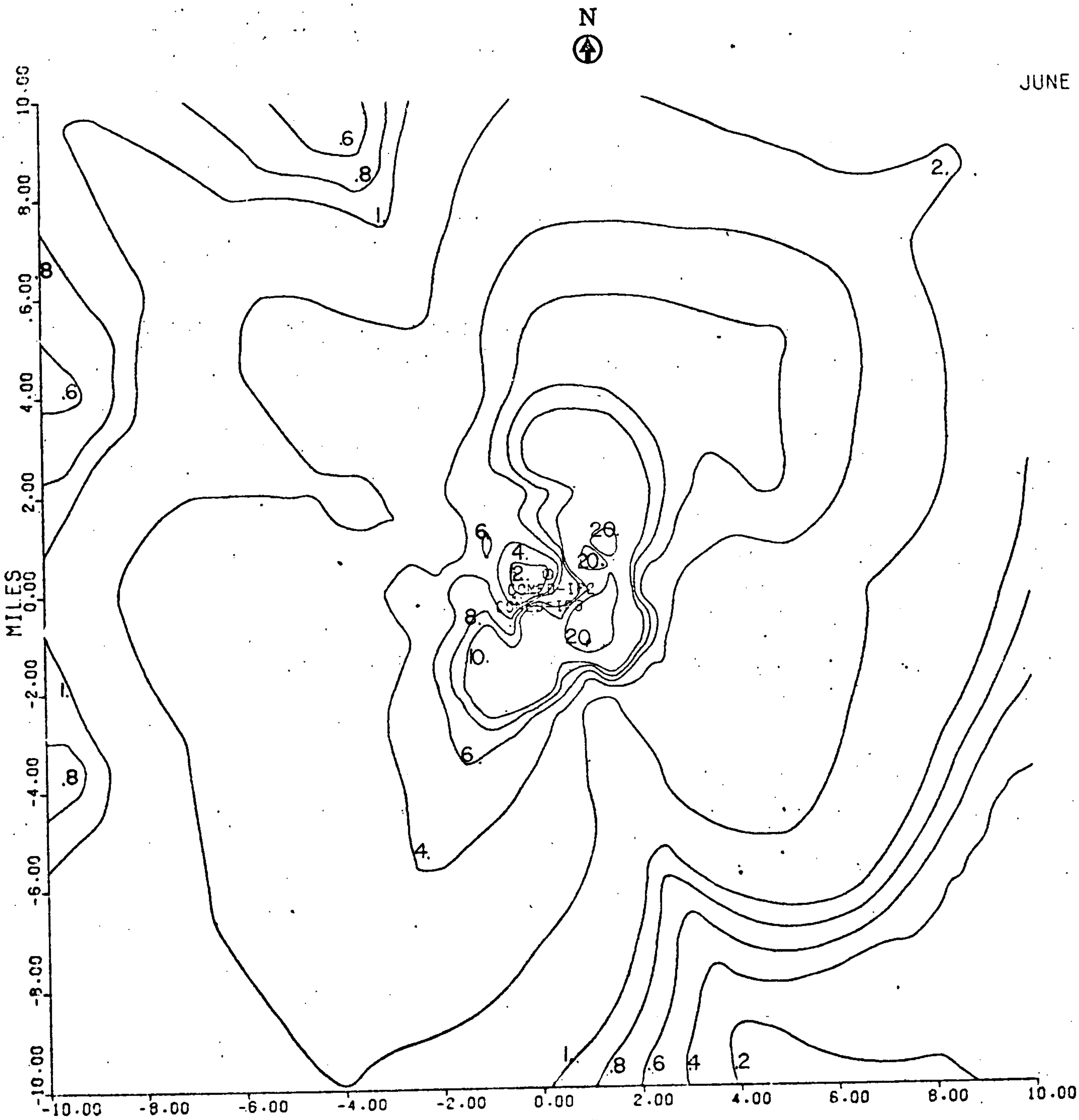

Basis: Drift Rate: 0.002% (10.9 Kg salt/hour/tower)
Number of towers: two

Note: Divide number on plot by 100 to get $\mu g/m^3$

Figure 3-41

Predicted July Monthly Average Ground Dry Deposition Rates (Kg/Km^2-month) of Salt Resulting from Operation of Two Natural Draft Cooling Towers (Indian Point 2 and 3) as a Function of Distance and Direction from the Indian Point 3 Tower

(0 - 3 miles)

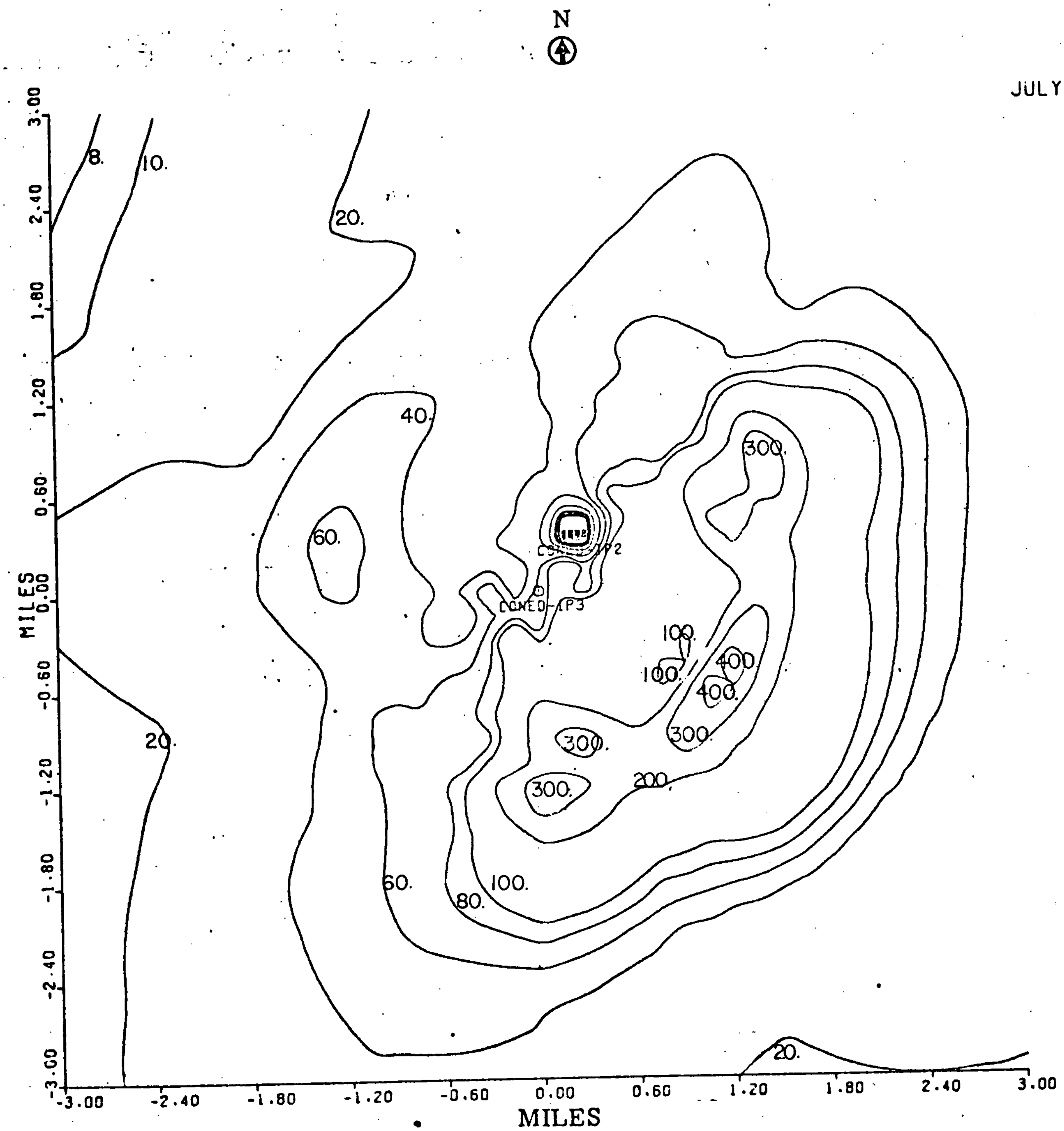

Basis: Drift Rate: 0.002% (19.1 Kg salt/hour/tower)
Number of towers: two

Figure 3-42

Predicted July Monthly Average Ground Dry Deposition Rates (Kg/Km^2-month) of Salt Resulting from Operation of Two Natural Draft Cooling Towers (Indian Point 2 and 3) as a Function of Distance and Direction from the Indian Point 3 Tower

(0 - 10 miles)

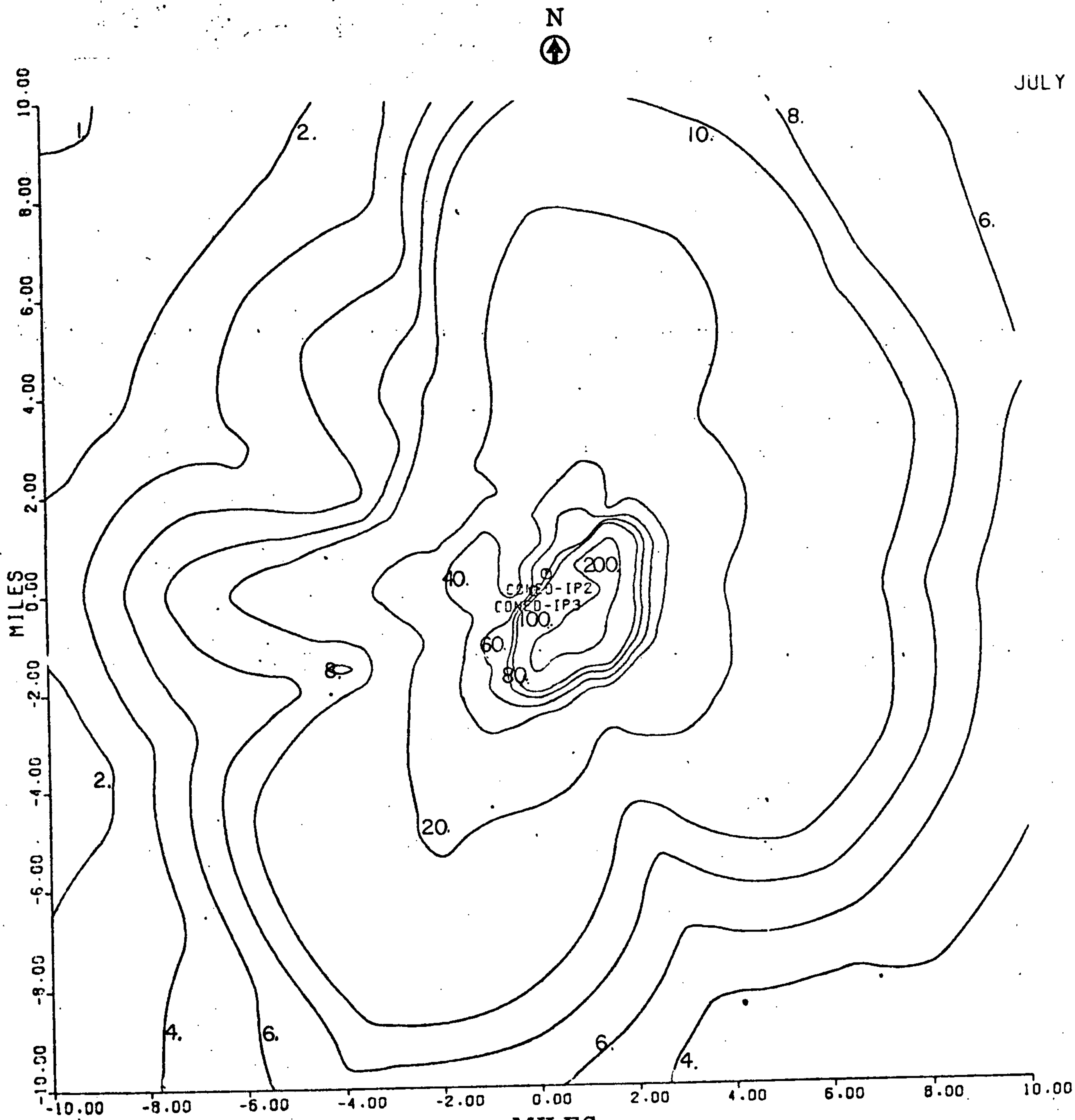

Basis: Drift Rate: 0.002% (19.1 Kg salt/hour/tower)
Number of towers: two

Figure 3-43

Predicted July Monthly Average Near Ground Airborne Concentration ($\mu g/m^3$) of Salt Resulting from Operation of Two Natural Draft Cooling Towers (Indian Point 2 and 3) as a Function of Distance and Direction from the Indian Point 3 Tower

(0 - 3 miles)

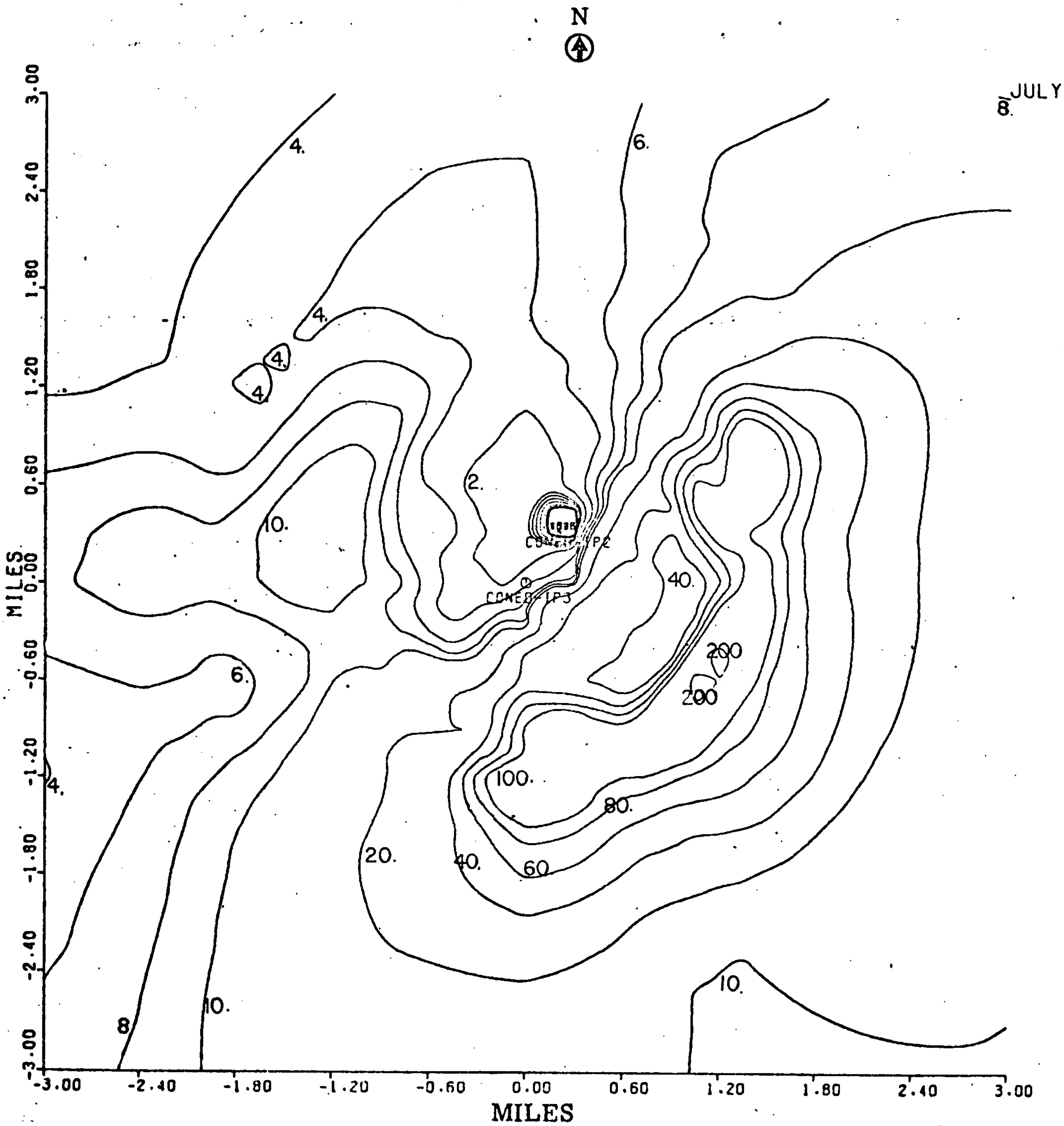

Basis: Drift Rate: 0.002% (19.1 Kg salt/hour/tower)
Number of towers: two

Note: Divide number on plot by 100 to get $\mu g/m^3$

Figure 3-44

Predicted July Monthly Average Near Ground Airborne Concentration ($\mu g/m^3$) of Salt Resulting from Operation of Two Natural Draft Cooling Towers (Indian Point 2 and 3) as a Function of Distance and Direction from the Indian Point 3 Tower

(0 - 10 miles)

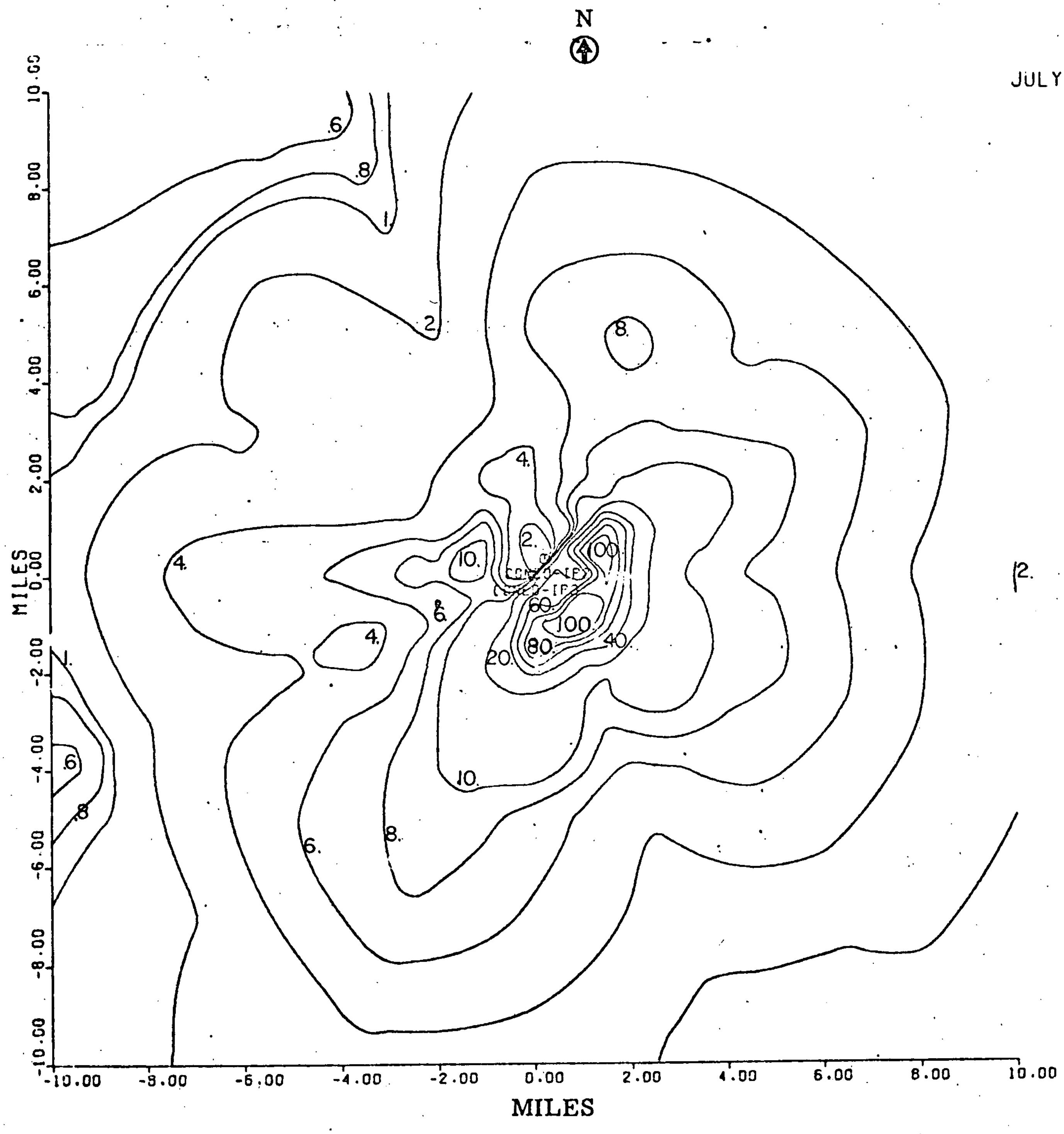

Basis: Drift Rate: 0.002% (19.1 Kg salt/hour/tower)
Number of towers: two

Note: Divide number on plot by 100 to get $\mu g/m^3$

Figure 3-45

Predicted August Monthly Average Ground Dry Deposition Rates (Kg/Km^2-month) of Salt Resulting from Operation of Two Natural Draft Cooling Towers (Indian Point 2 and 3) as a Function of Distance and Direction from the Indian Point 3 Tower

(0 - 3 miles)

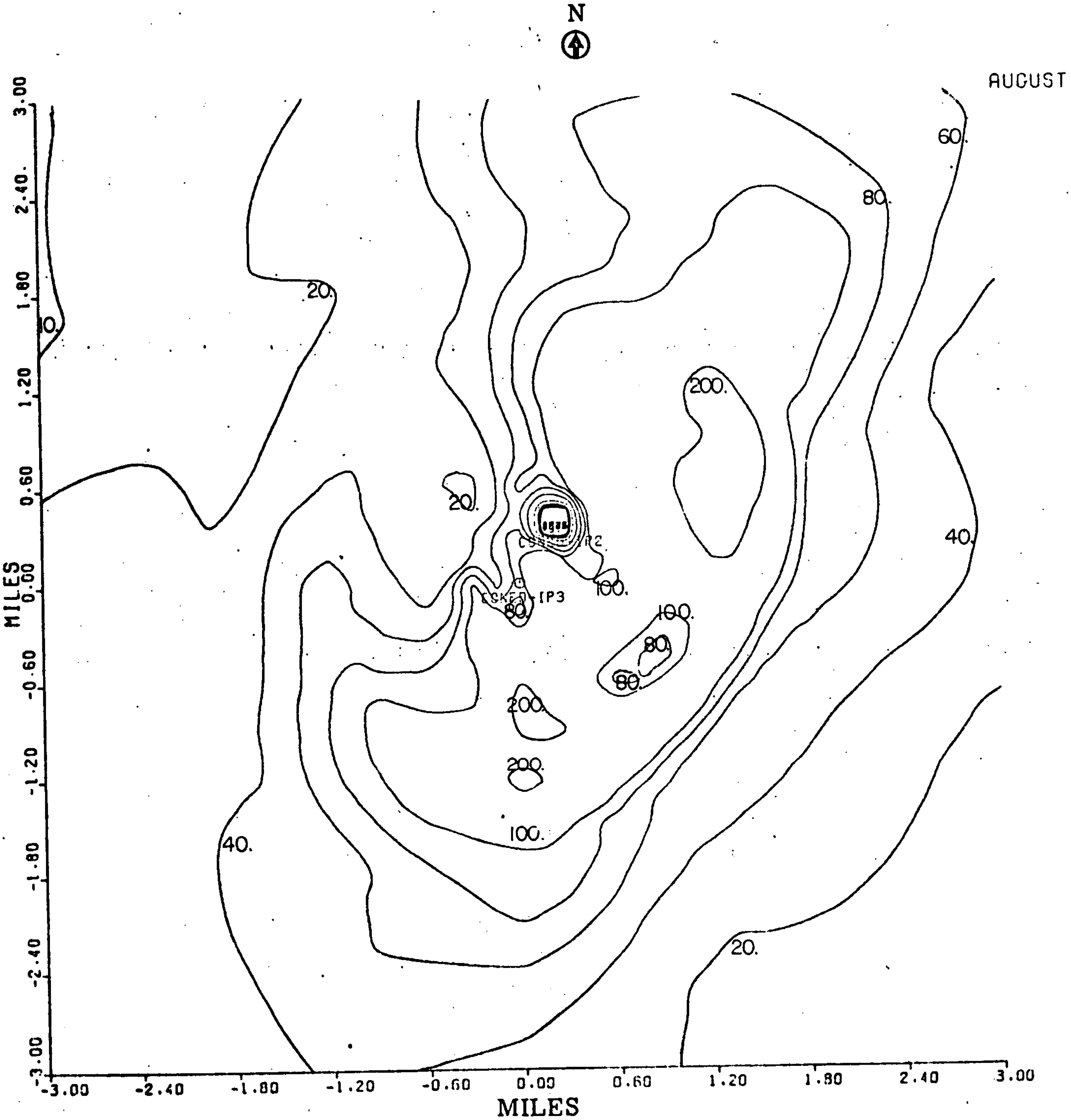

Basis: Drift Rate: 0.002% (19.1 Kg salt/hour/tower)
Number of towers: two

Figure 3-46

Predicted August Monthly Average Ground Dry Deposition Rates (Kg/Km^2-month) of Salt Resulting from Operation of Two Natural Draft Cooling Towers (Indian Point 2 and 3) as a Function of Distance and Direction from the Indian Point 3 Tower

(0 - 10 miles)

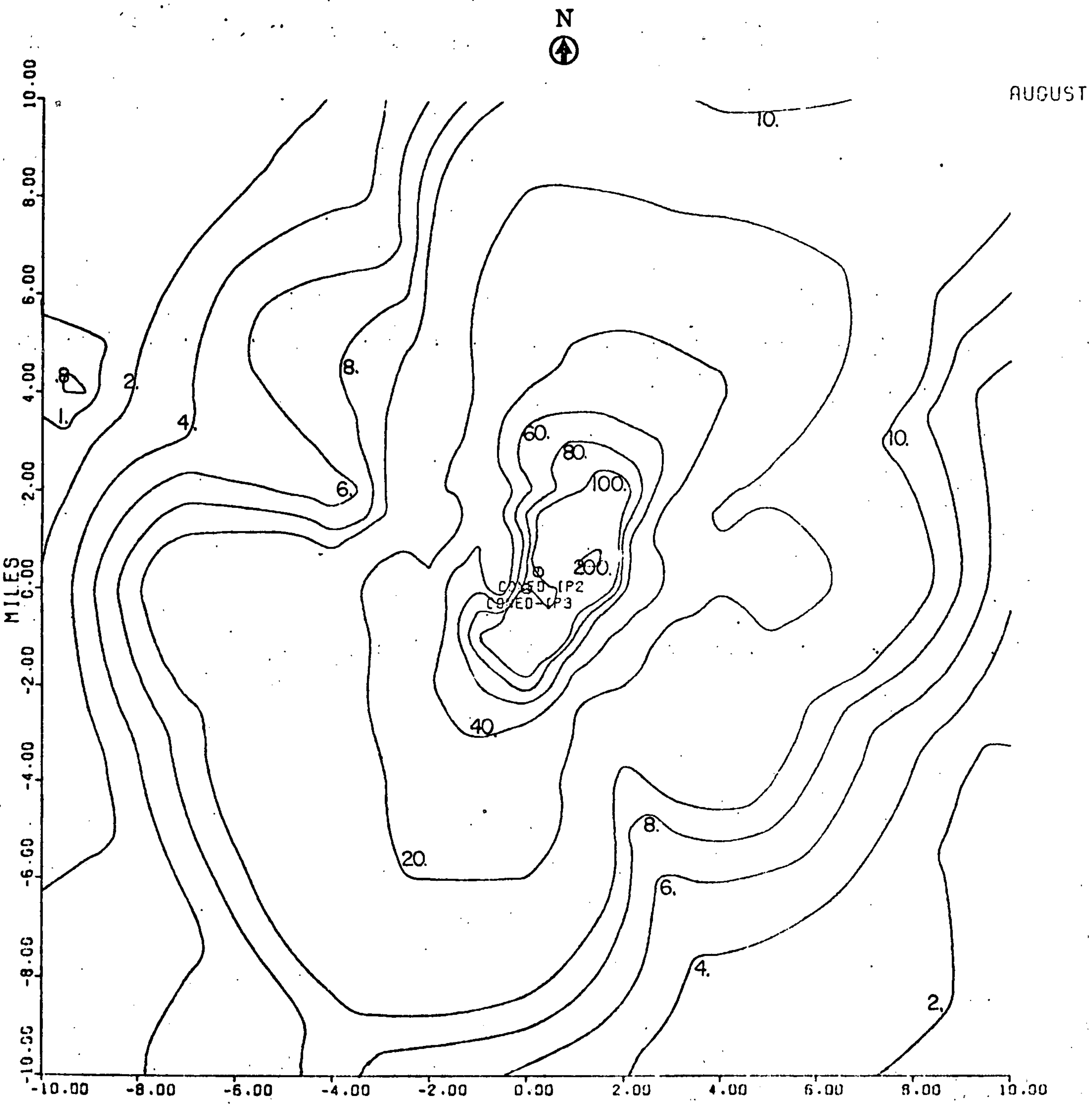

Basis: Drift Rate: 0.002% (19.1 Kg salt/hour/tower)
Number of towers: two

Figure 3-47

Predicted August Monthly Average Near Ground Airborne Concentration ($\mu g/m^3$) of Salt Resulting from Operation of Two Natural Draft Cooling Towers (Indian Point 2 and 3) as a Function of Distance and Direction from the Indian Point 3 Tower

(0 - 3 miles)

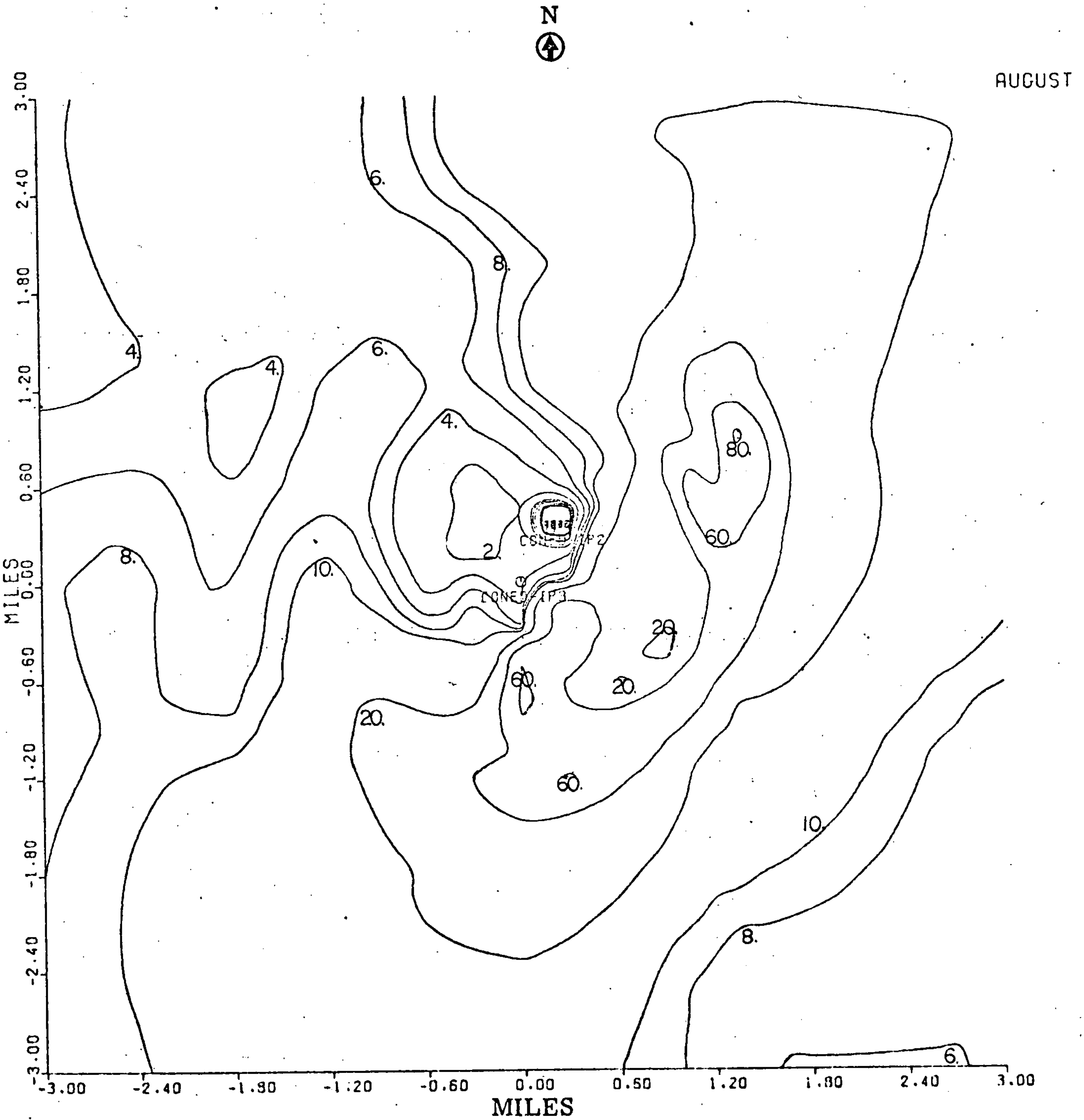

Basis: Drift Rate: 0.002% (19.1 Kg salt/hour/tower)
Number of towers: two

Note: Divide number on plot by 100 to get $\mu g/m^3$

Figure 3-48

Predicted August Monthly Average Near Ground Airborne Concentration ($\mu g/m^3$) of Salt Resulting from Operation of Two Natural Draft Cooling Towers (Indian Point 2 and 3) as a Function of Distance and Direction from the Indian Point 3 Tower

(0 - 10 miles)

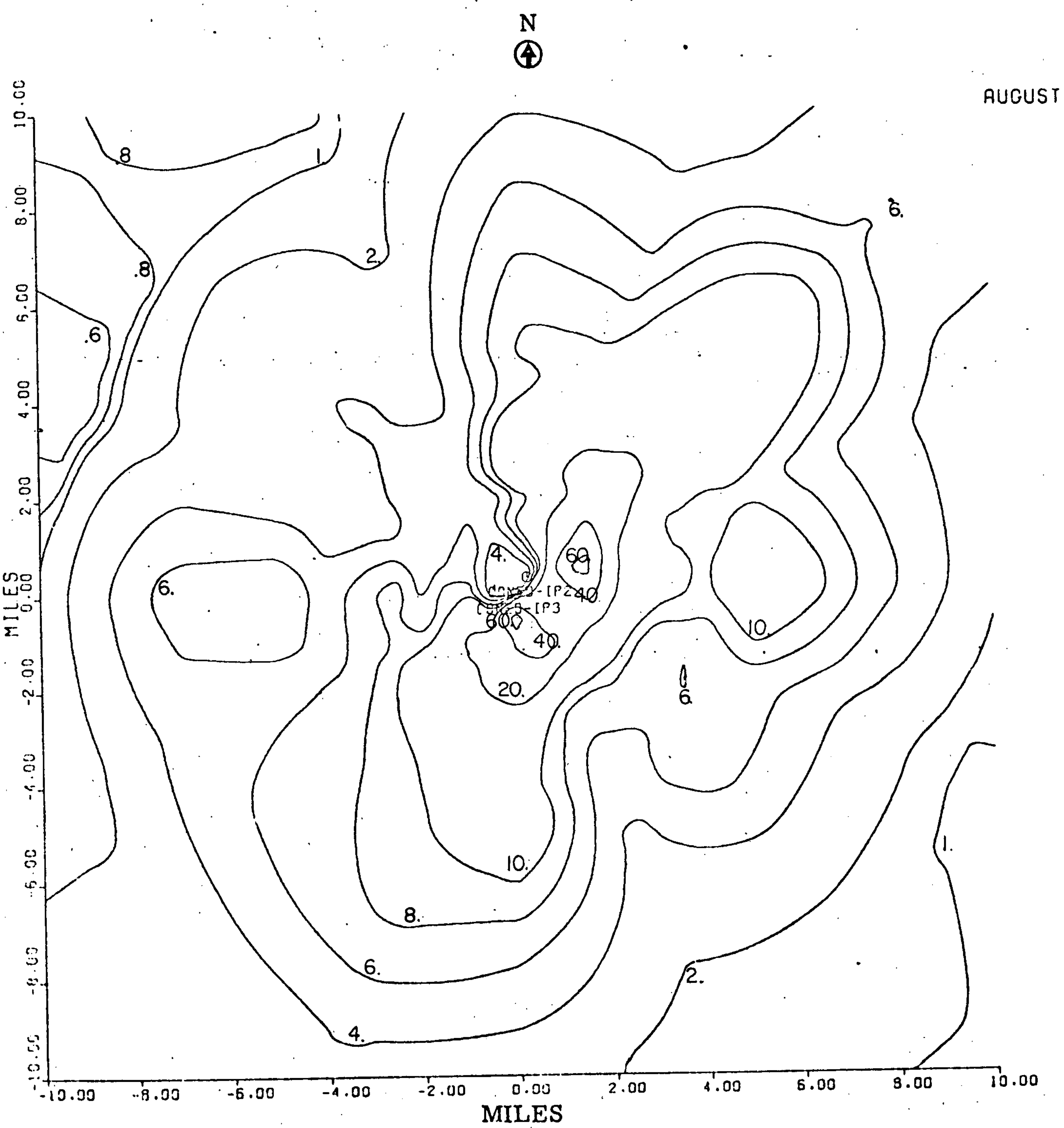

Basis: Drift Rate: 0.002% (19.1 Kg salt/hour/tower)
Number of towers: two

Note: Divide number on plot by 100 to get $\mu g/m^3$

Figure 3-49

Predicted September Monthly Average Ground Dry Deposition Rates (Kg/Km^2-month) of Salt Resulting from Operation of Two Natural Draft Cooling Towers (Indian Point 2 and 3) as a Function of Distance and Direction from the Indian Point 3 Tower

(0 - 3 miles)

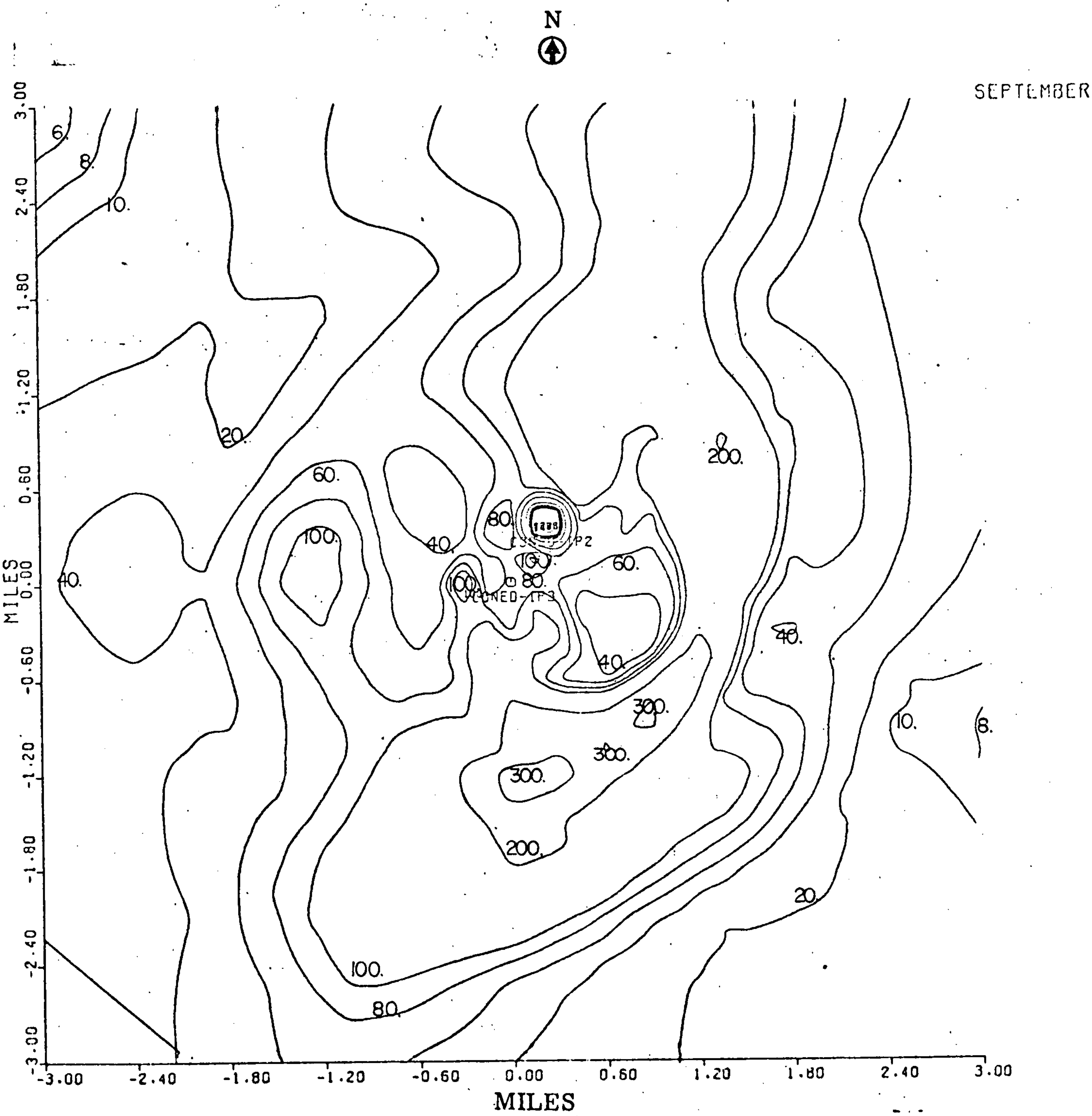

Basis: Drift Rate: 0.002% (19.1 Kg salt/hour/tower)
Number of towers: two

Figure 3-50

Predicted September Monthly Average Ground Dry Deposition Rates (Kg/Km^2-month) of Salt Resulting from Operation of Two Natural Draft Cooling Towers (Indian Point 2 and 3) as a Function of Distance and Direction from the Indian Point 3 Tower

(0 - 10 miles)

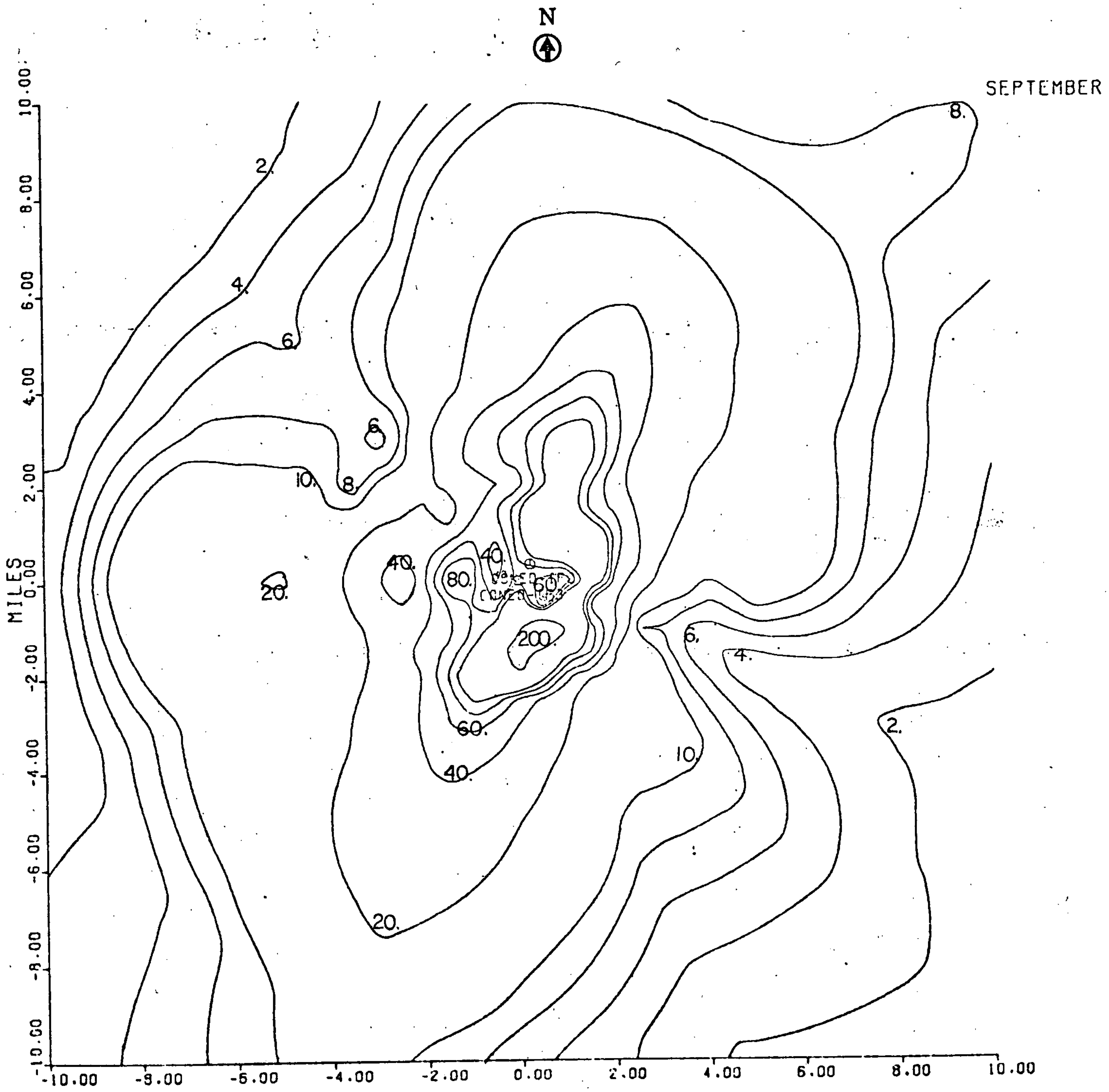

Basis: Drift Rate: 0.002% (19.1 Kg salt/hour/tower)
Number of towers: two

Figure 3-51

Predicted September Monthly Average Near Ground Airborne Concentration ($\mu g/m^3$) of Salt Resulting from Operation of Two Natural Draft Cooling Towers (Indian Point 2 and 3) as a Function of Distance and Direction from the Indian Point 3 Tower

(0 - 3 miles)

N

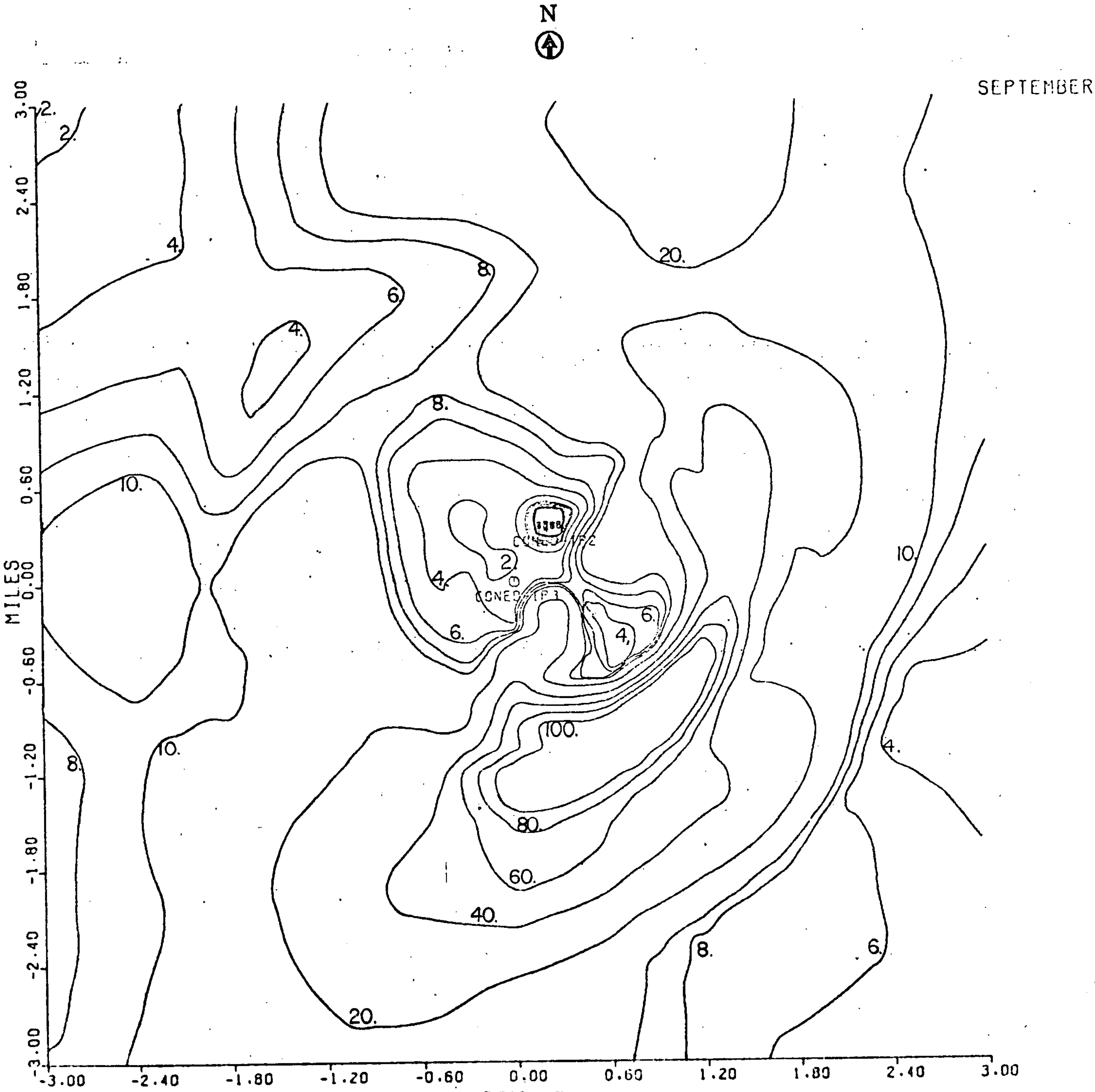

MILES

Basis: Drift Rate: 0.002% (19.1 Kg salt/hour/tower)
Number of towers: two

Note: Divide number on plot by 100 to get $\mu g/m^3$

Figure 3-52

Predicted September Monthly Average Near Ground Airborne Concentration ($\mu g/m^3$) of Salt Resulting from Operation of Two Natural Draft Cooling Towers (Indian Point 2 and 3) as a Function of Distance and Direction from the Indian Point 3 Tower

(0 - 10 miles)

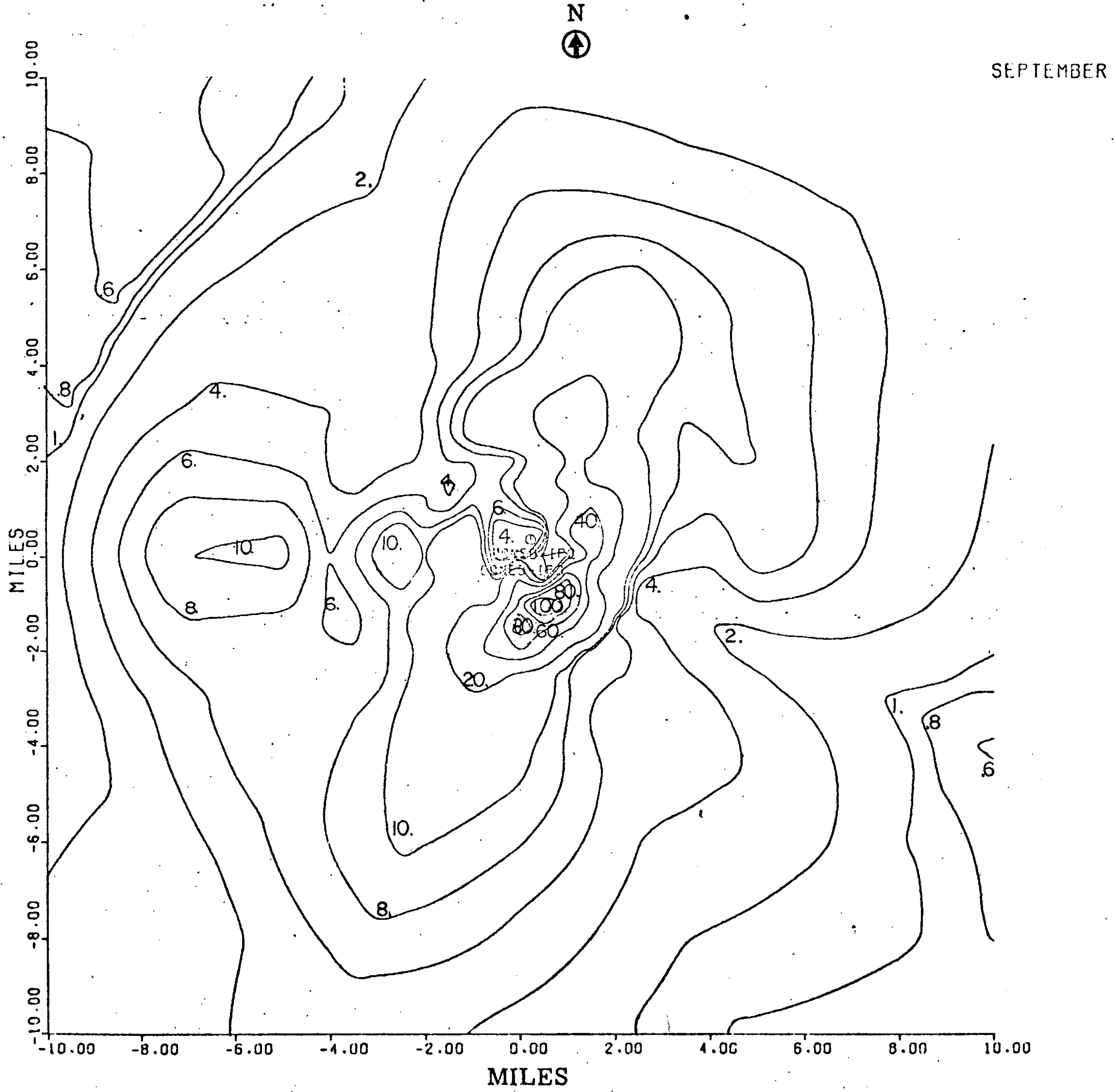

Basis: Drift Rate: 0.002% (19.1 Kg salt/hour/tower)
Number of towers: two

Note: Divide number on plot by 100 to get $\mu g/m^3$

Figure 3-53
(a - p)

Ice Accumulation on the Ground vs Time for the Month of January
Due to Operation of a Natural Draft Tower at the Indian Point Site

Basis: Drift: 0.002% (39.21 Kg salt/hour)
Number of towers: One

Legend

Distance (m) Downwind from Tower	Representation
250	– – – – – – –
800	—— —— —— ——
1600	. . . .
2000	—⊗——⊗—
2500	—⊠——⊠—
3200	—△——△—

Figure 3-53a

Direction N January

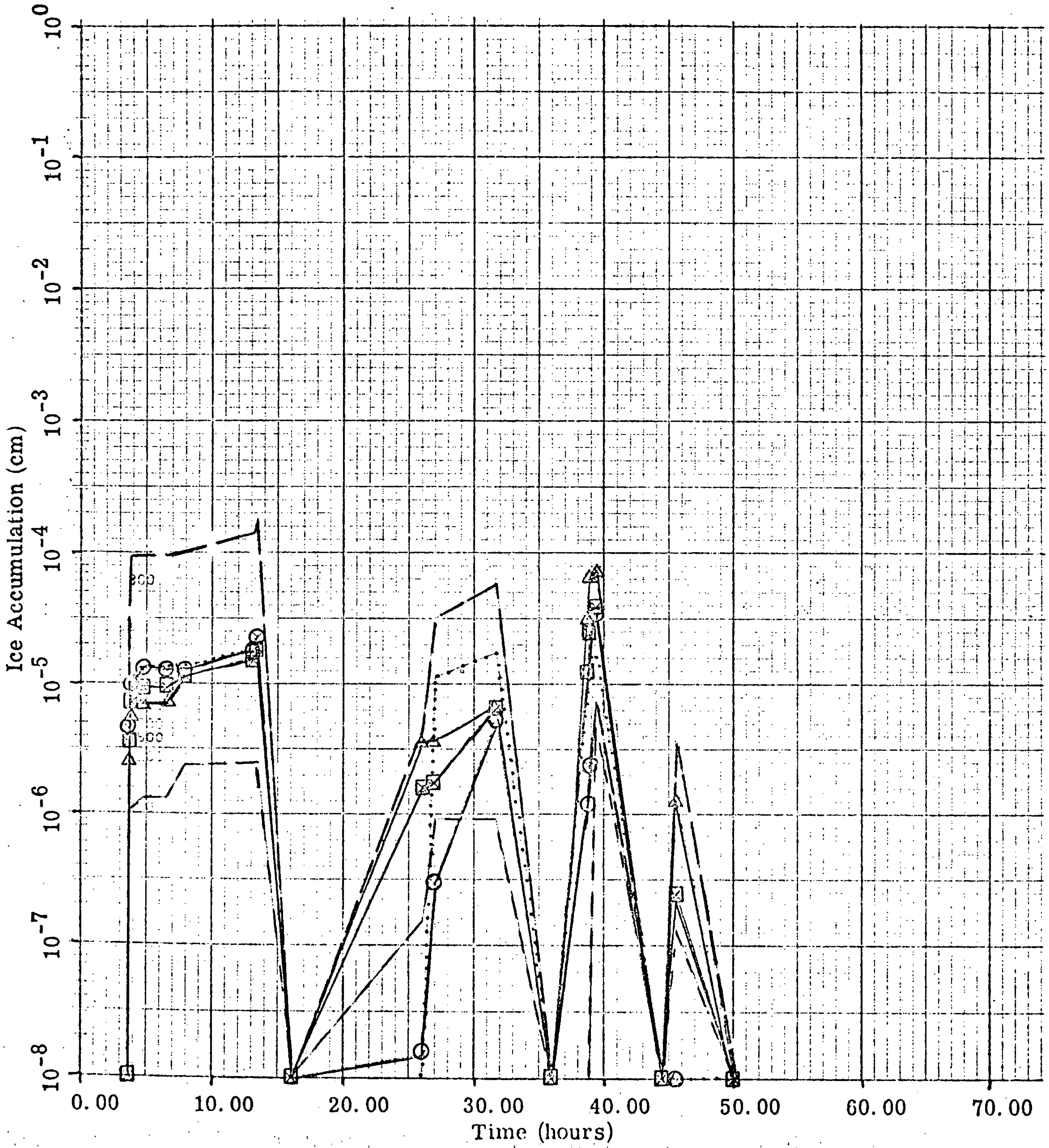

Figure 3-53b

Direction NNE January

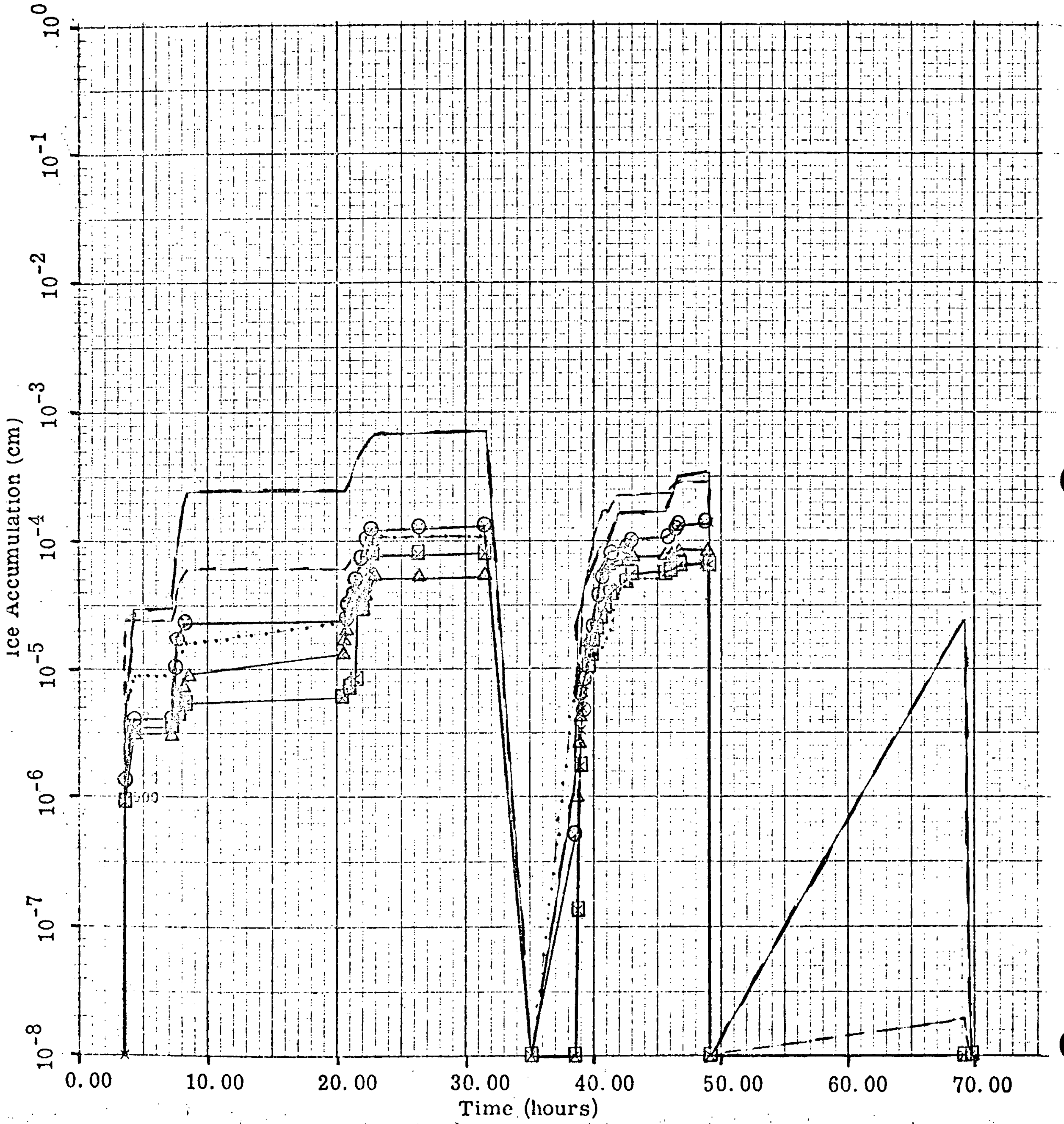

Figure 3-53c

Direction NE January

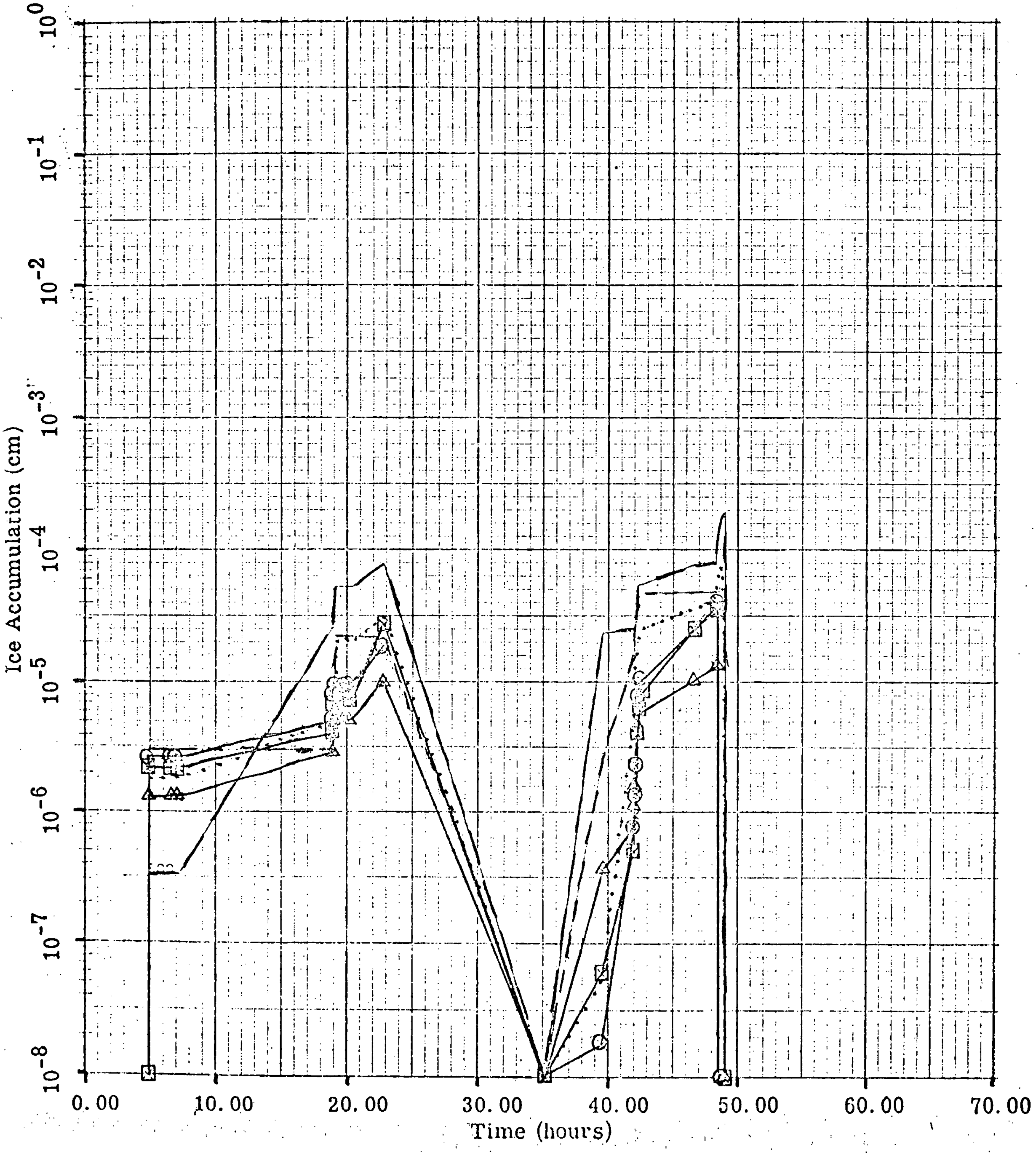

Figure 3-53d

Direction ENE January

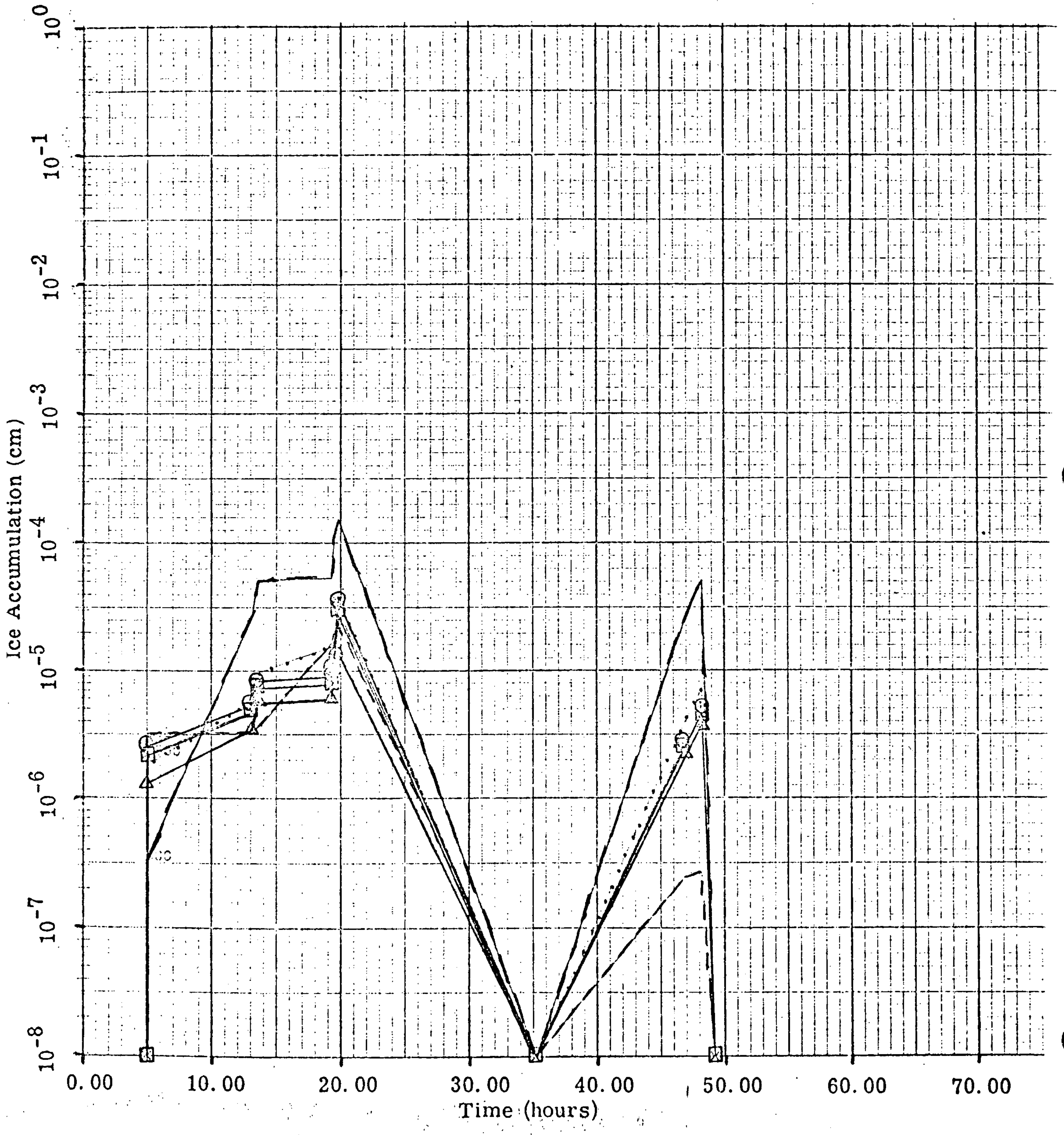

Figure 3-53e

Direction E January

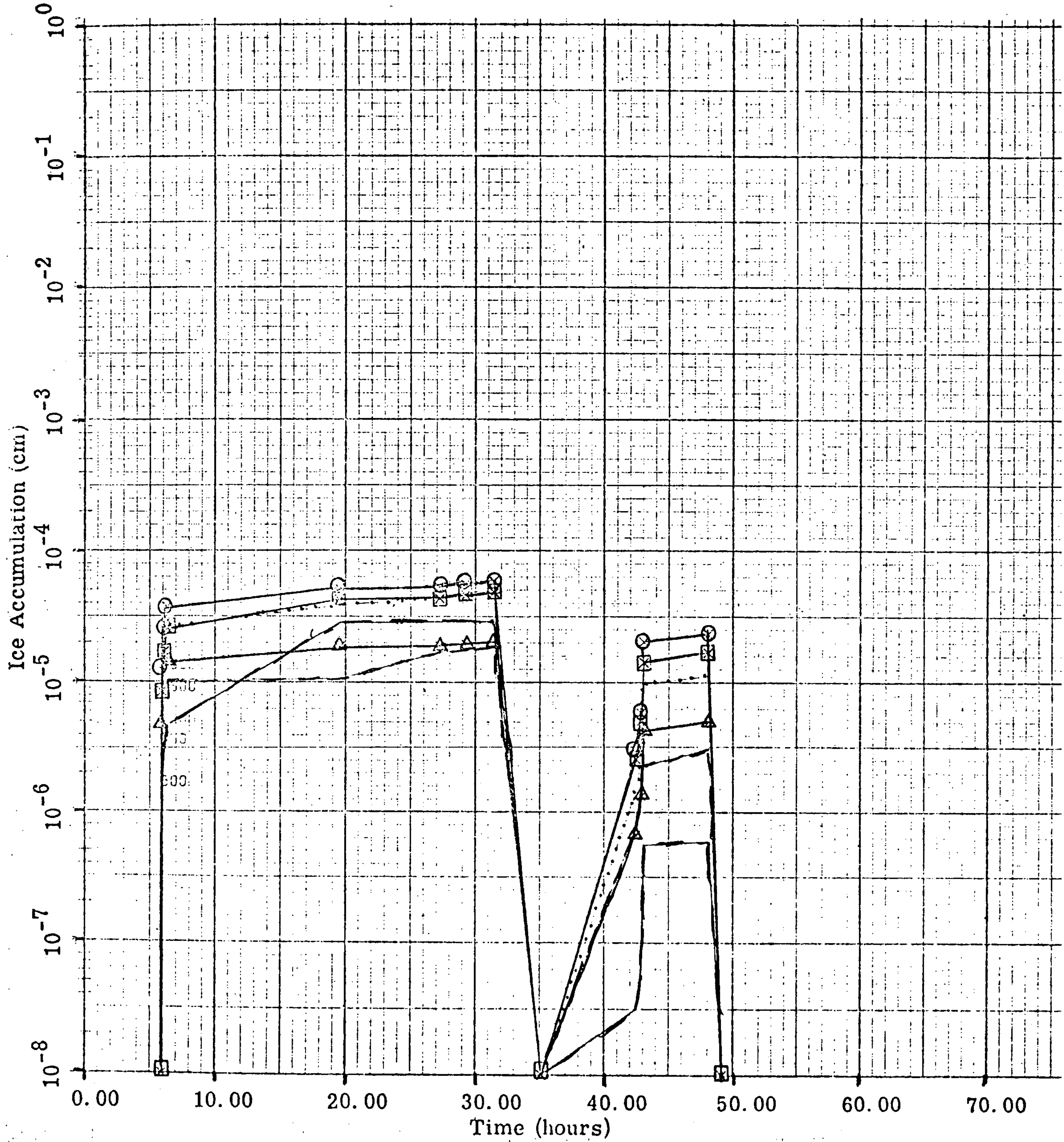

Figure 3-53f

Direction ESE January

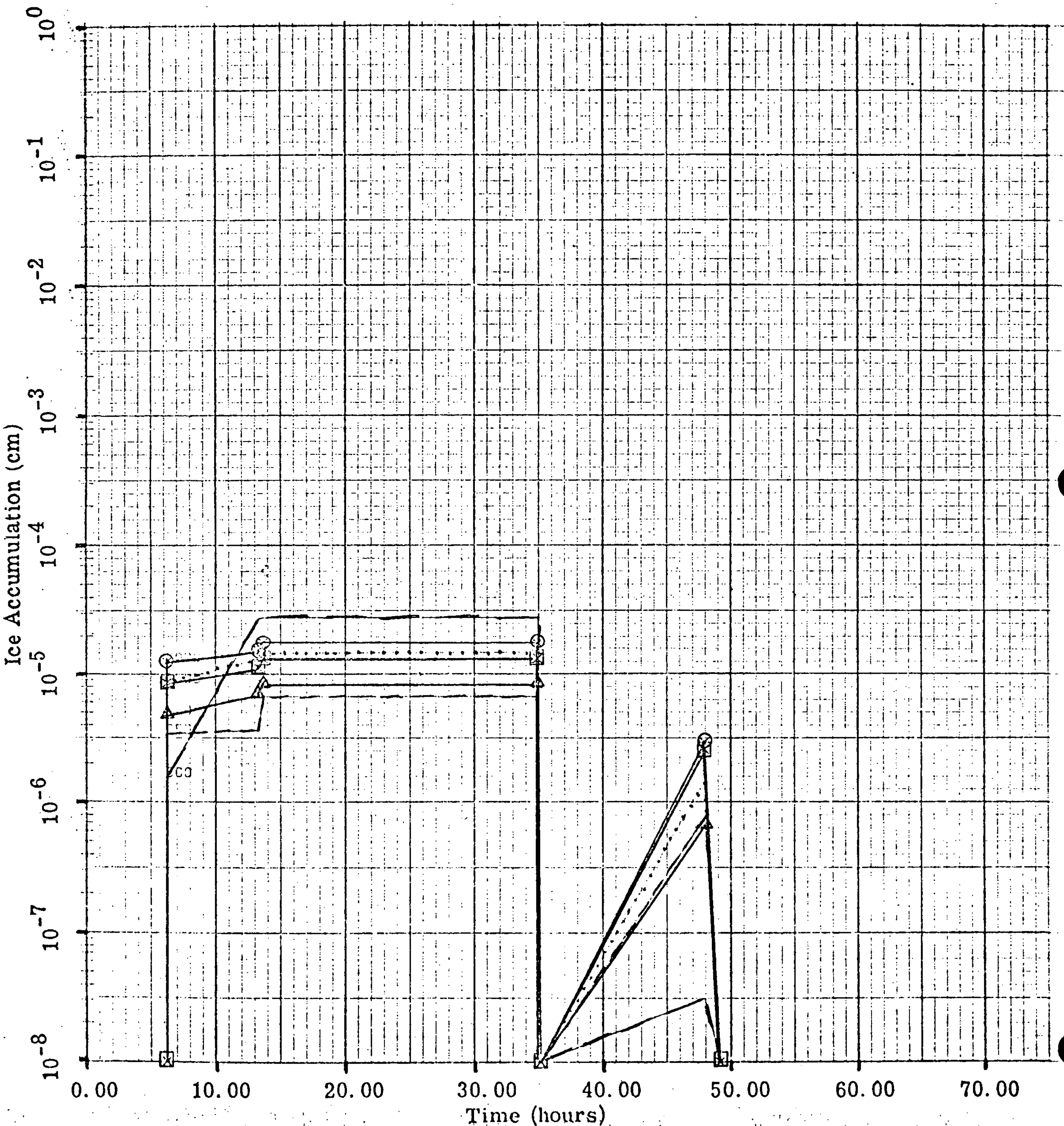

Figure 3-53g

Direction SE January

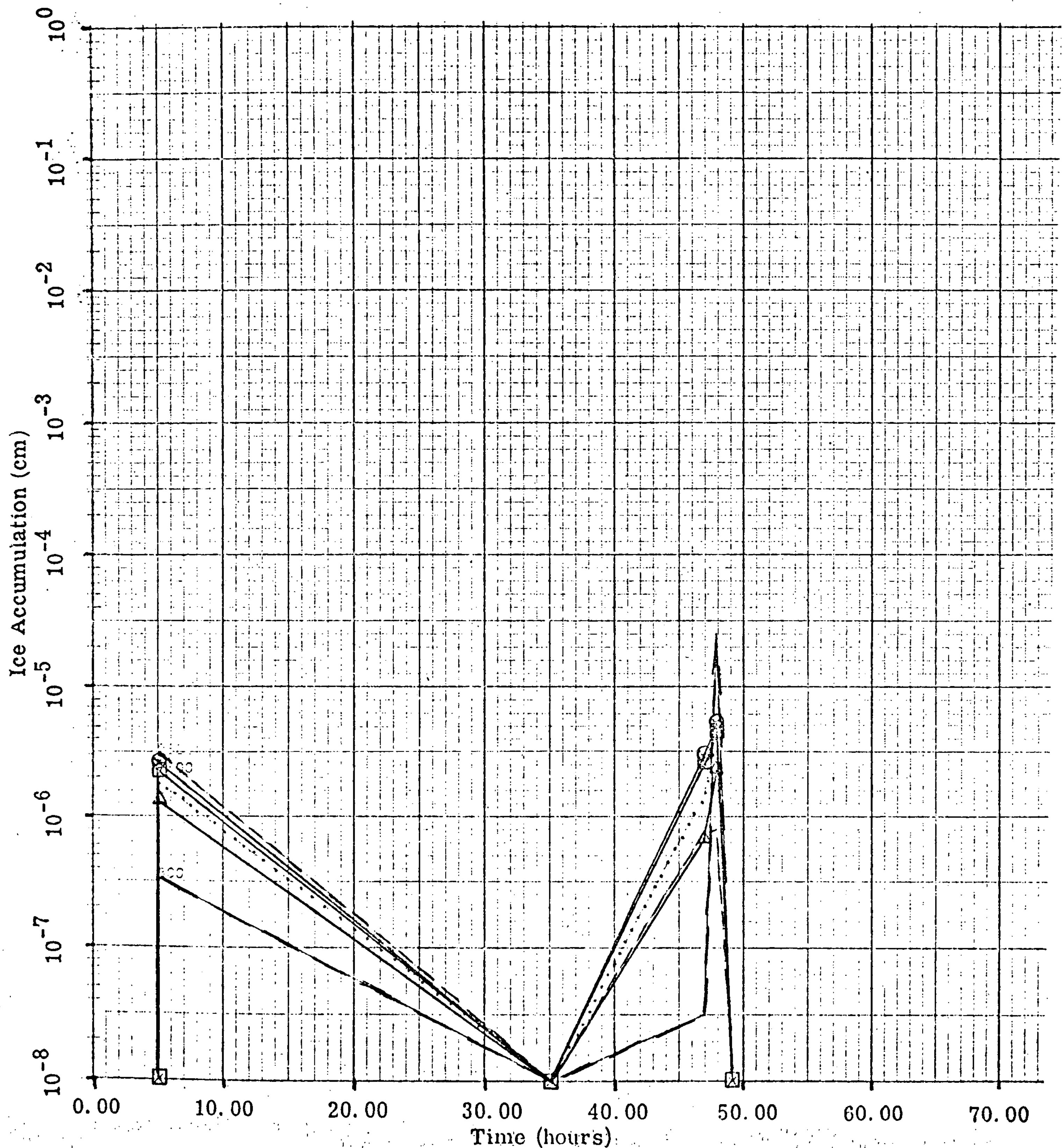

Figure 3-53h

Direction SSE January

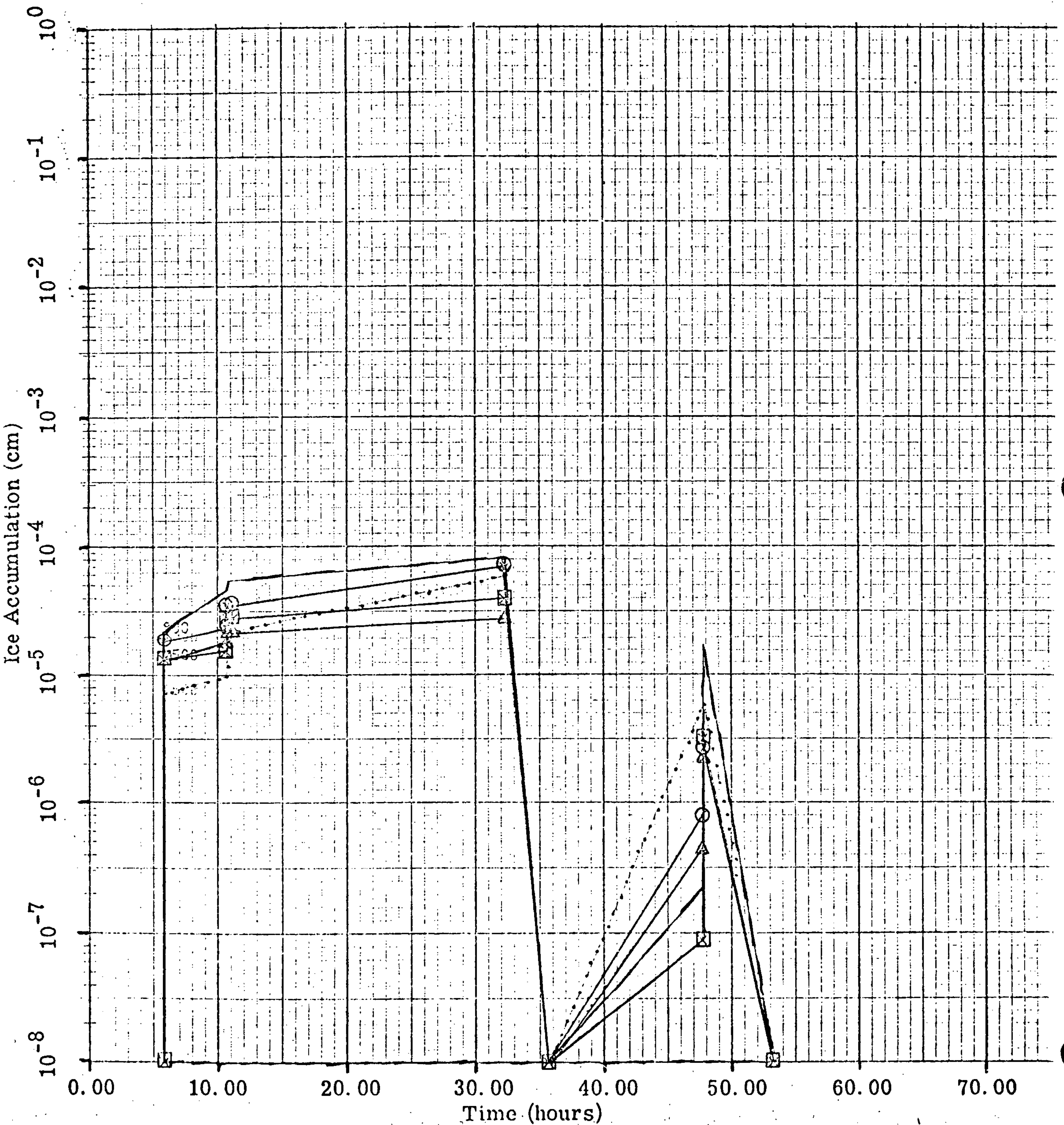

Figure 3-53i

Direction S January

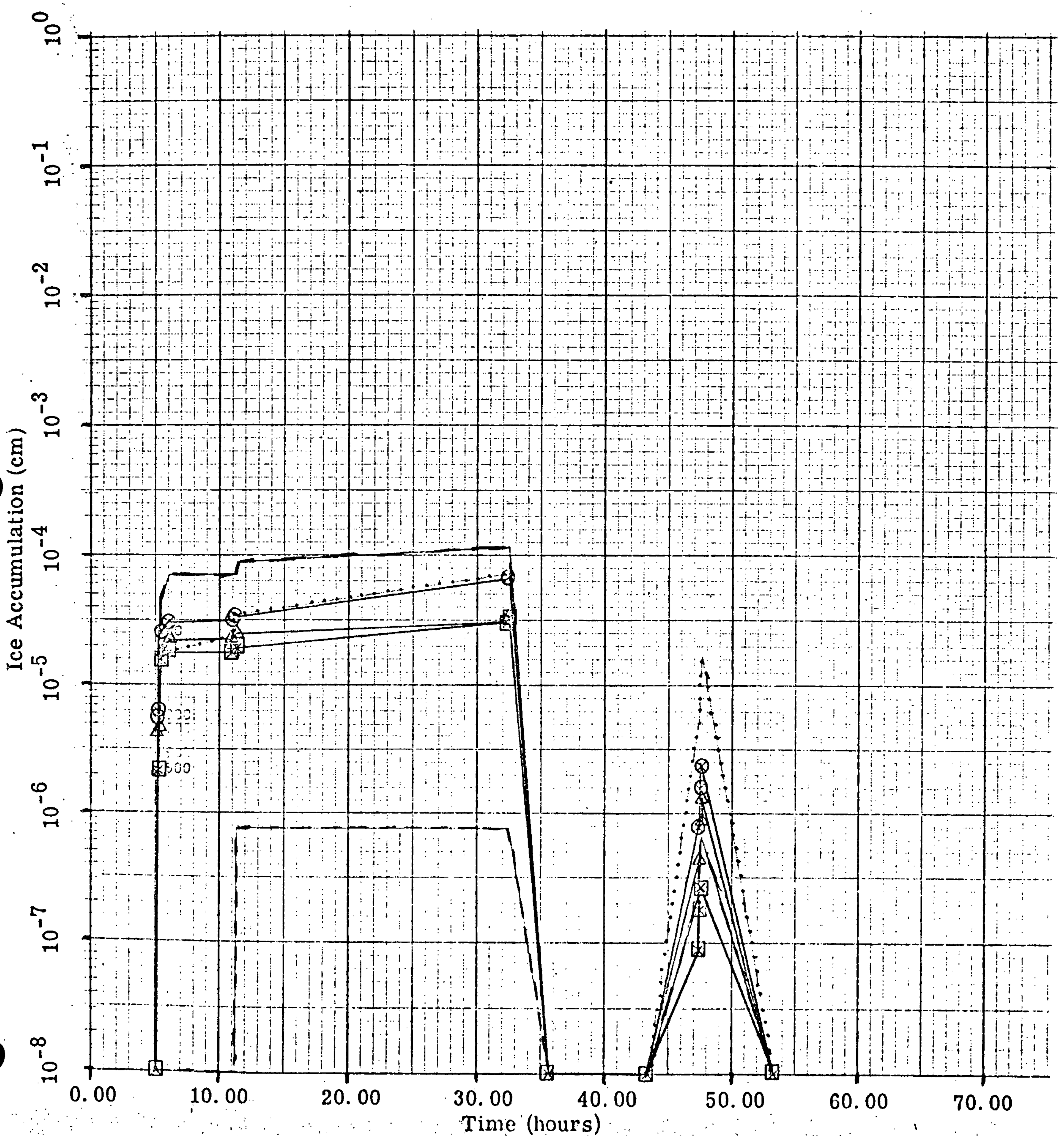

Figure 3-53j

Direction SSW January

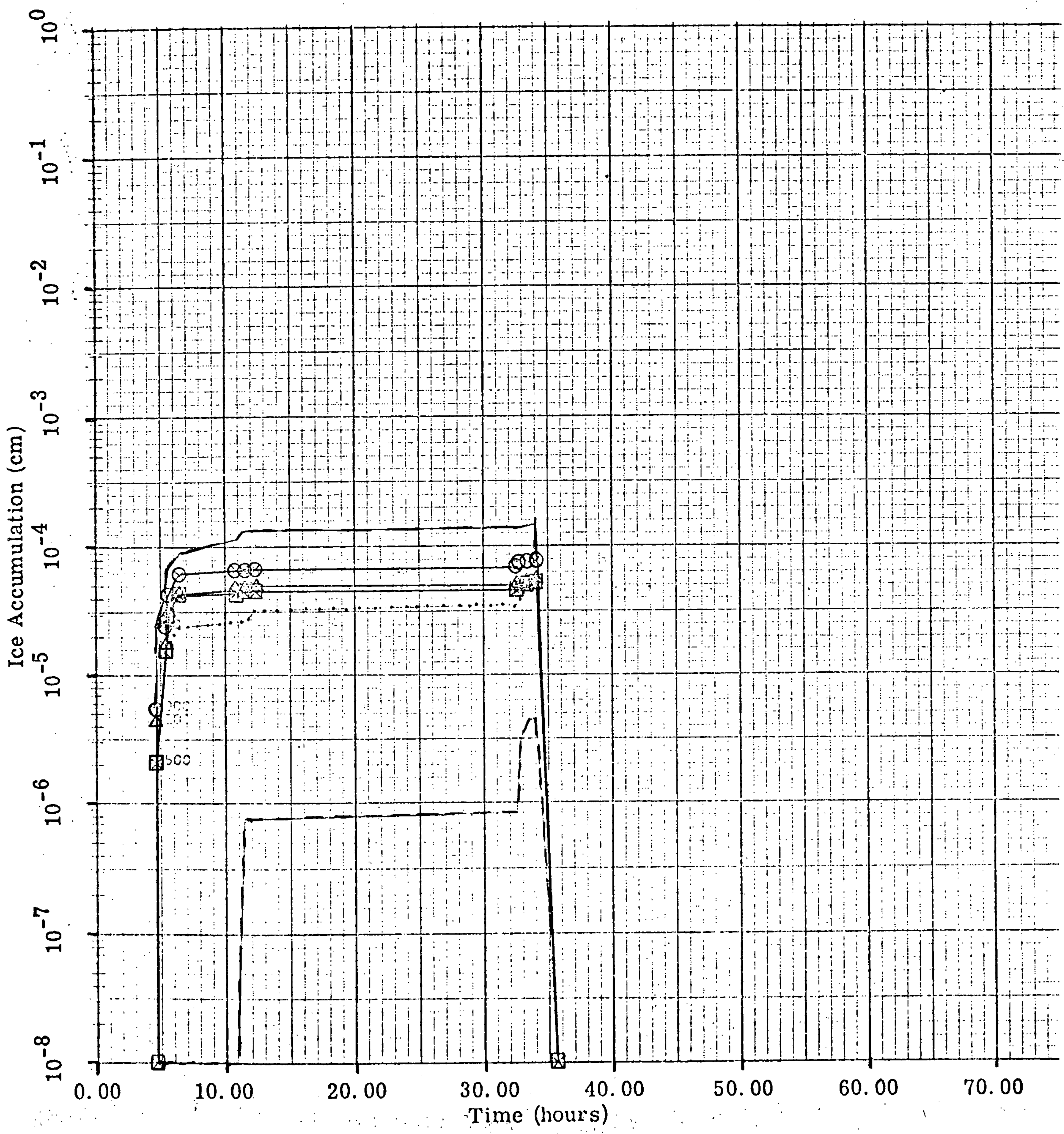

Figure 3-53k

Direction SW January

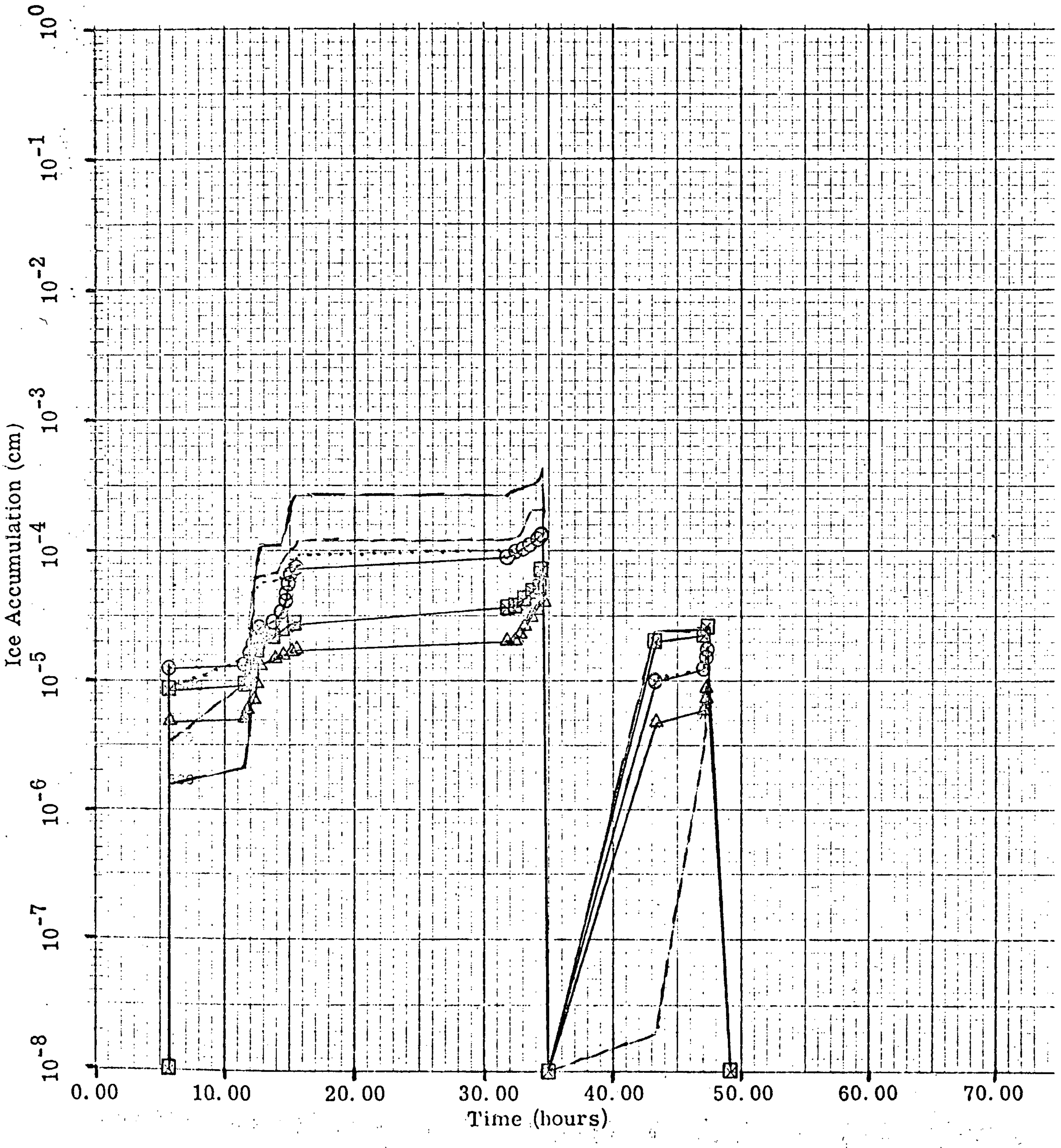

Figure 3-531

Direction WSW January

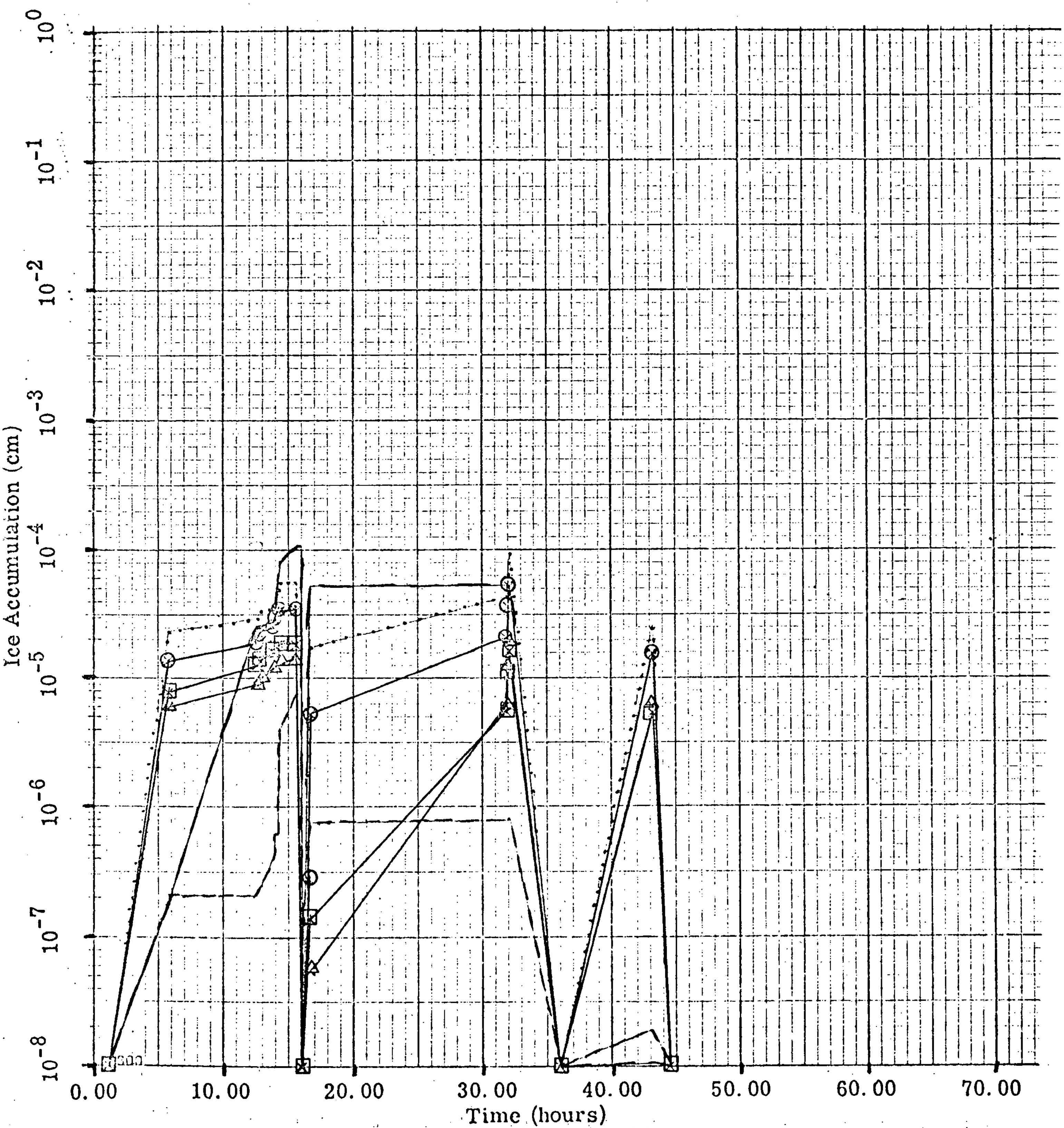

Figure 3-53m

Direction W January

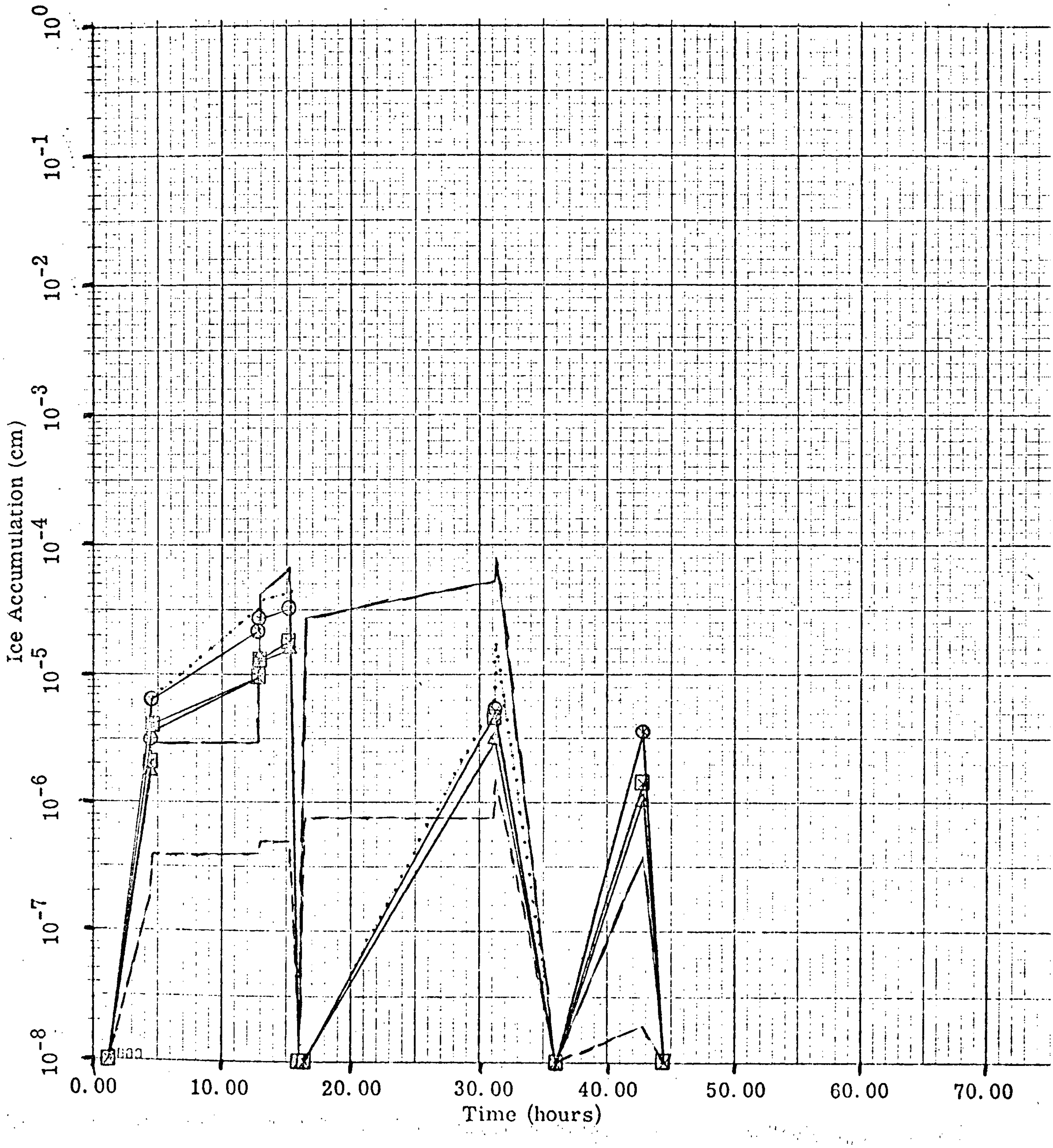

Figure 3-53n

Direction WNW January

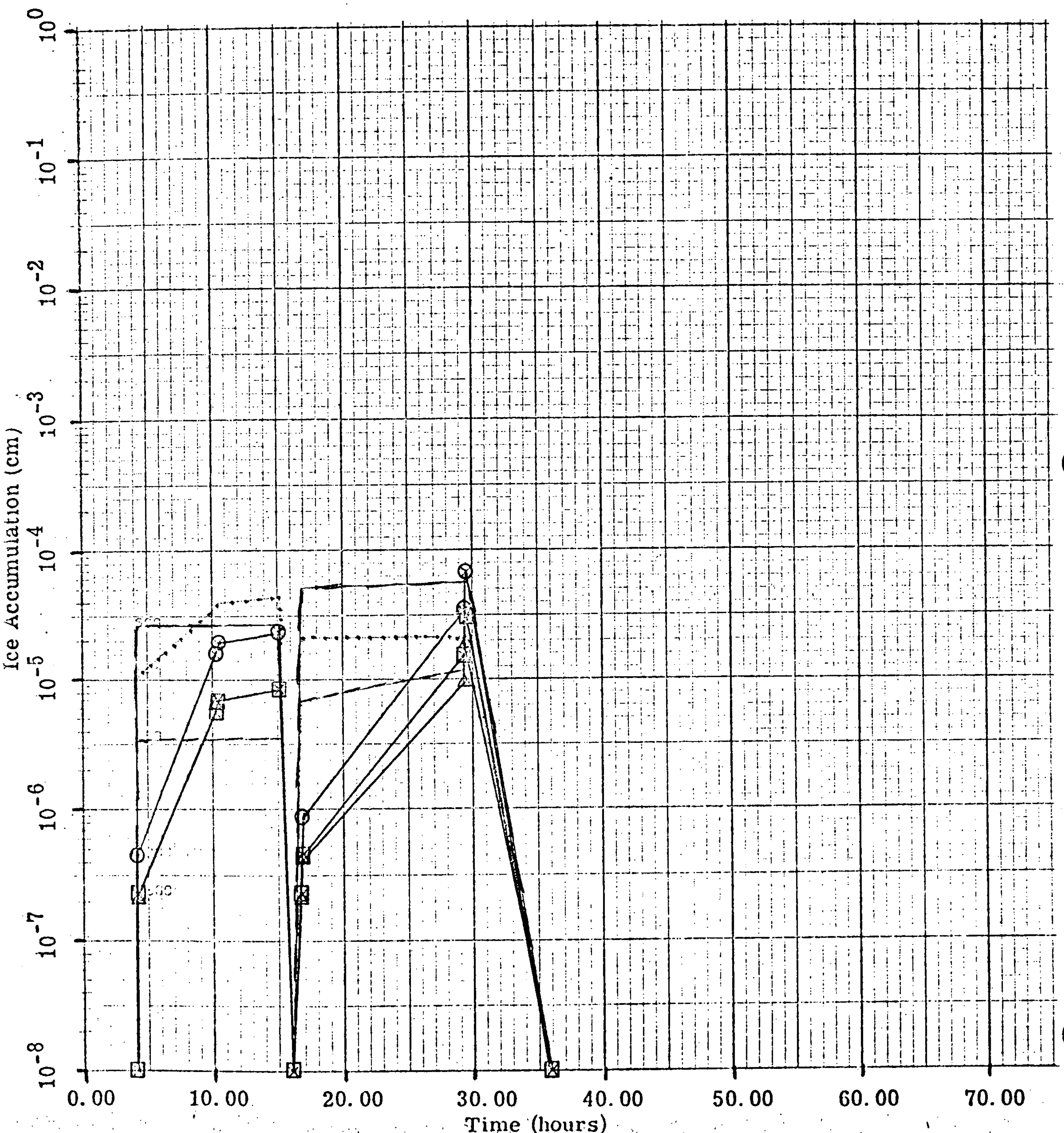

Figure 3-53o

Direction NW January

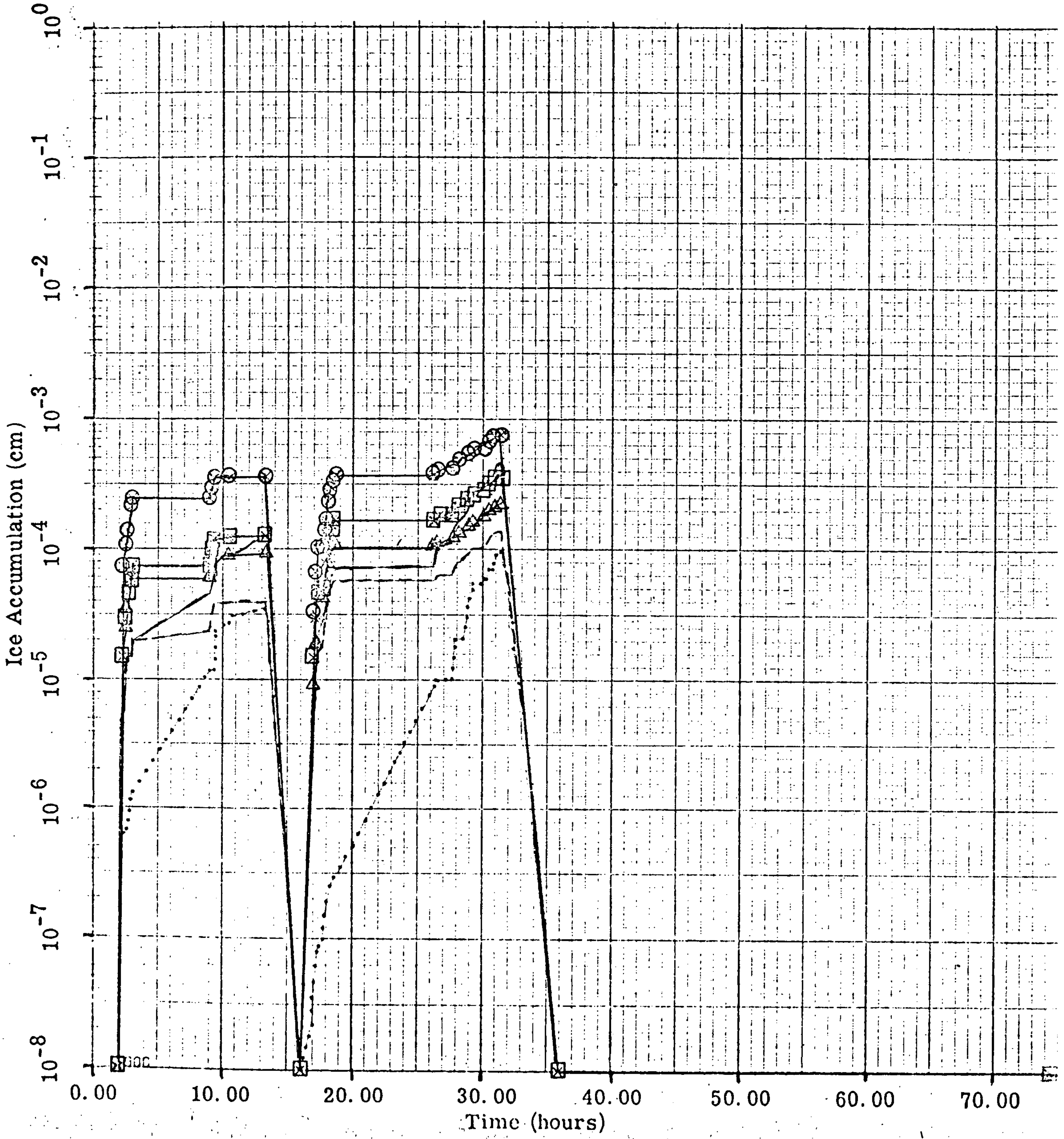

Figure 3-53p

Direction NNW January

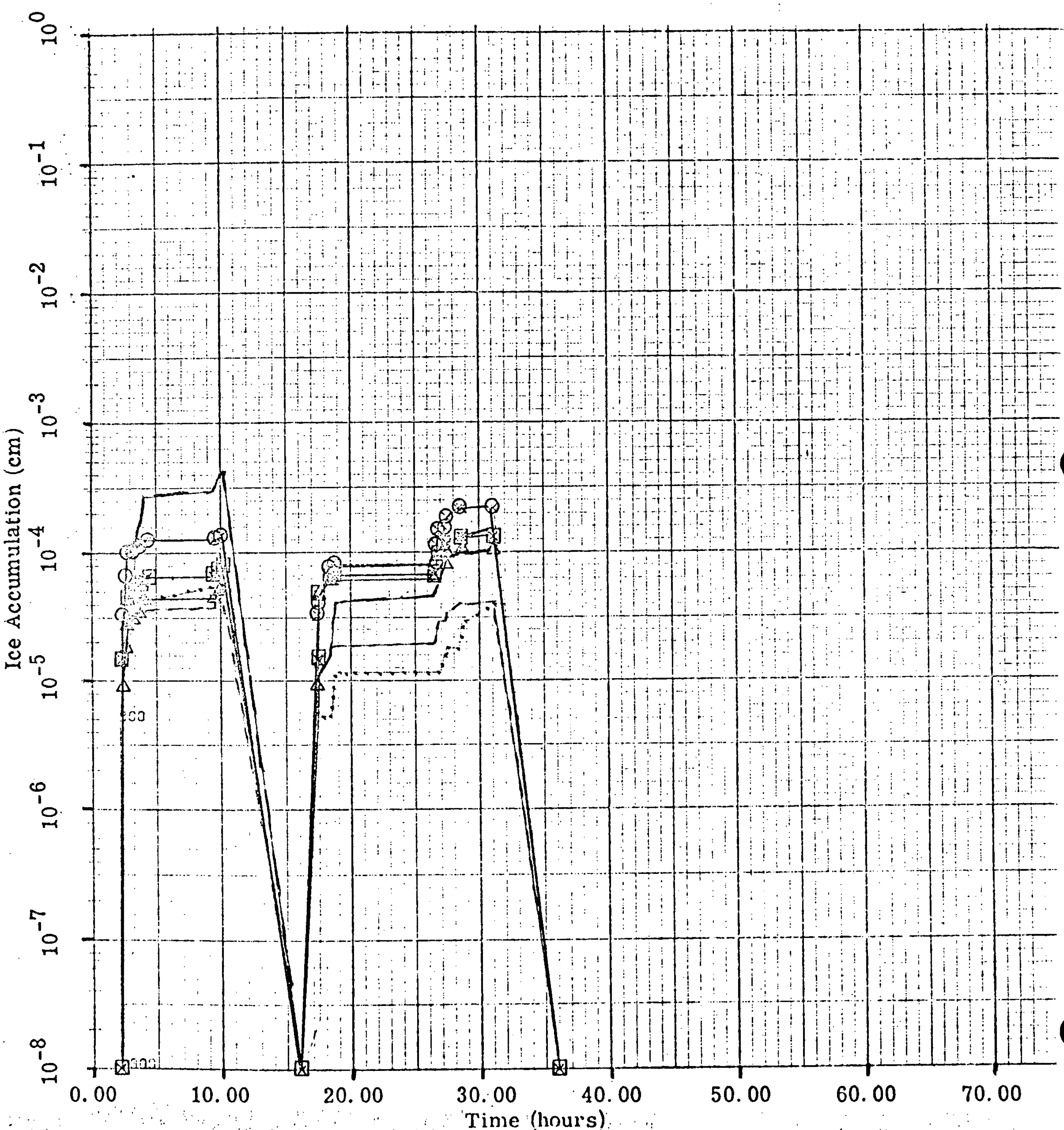

Figure 3-54
(a - p)

Ice Accumulation on Structures vs Time for the Month of January
Due to Operation of a Natural Draft Tower at the Indian Point Site

Basis: Drift: 0.002% (39.21 Kg salt/hour)
Number of towers: One

Note: All values calculated at 250 m downwind from the tower

Legend

The numbers 1 through 6 refer to:

	Object Type	Size, inches	Representation
1	cylindrical	1/4	– – – – – –
2	cylindrical	2	—— —— ——
3	cylindrical	120	. . . .
4	ribbon	120	—⊗——⊗—
5	ribbon	400	—⊠——⊠—
6	ribbon	1200	—▲——▲—

See Table 2-2.

Figure 3-54a

Direction N January

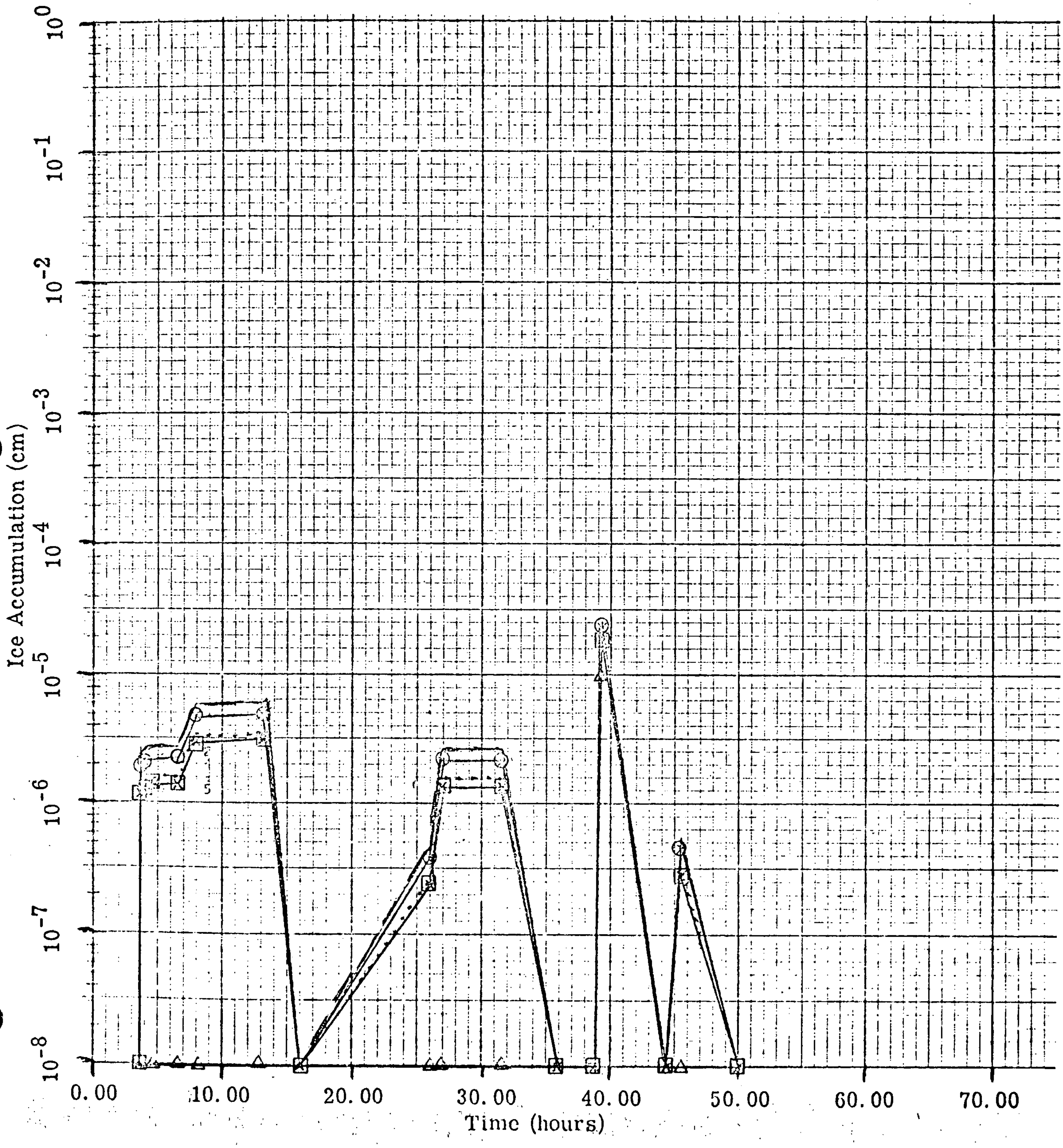

Figure 3-54b

Direction NNE January

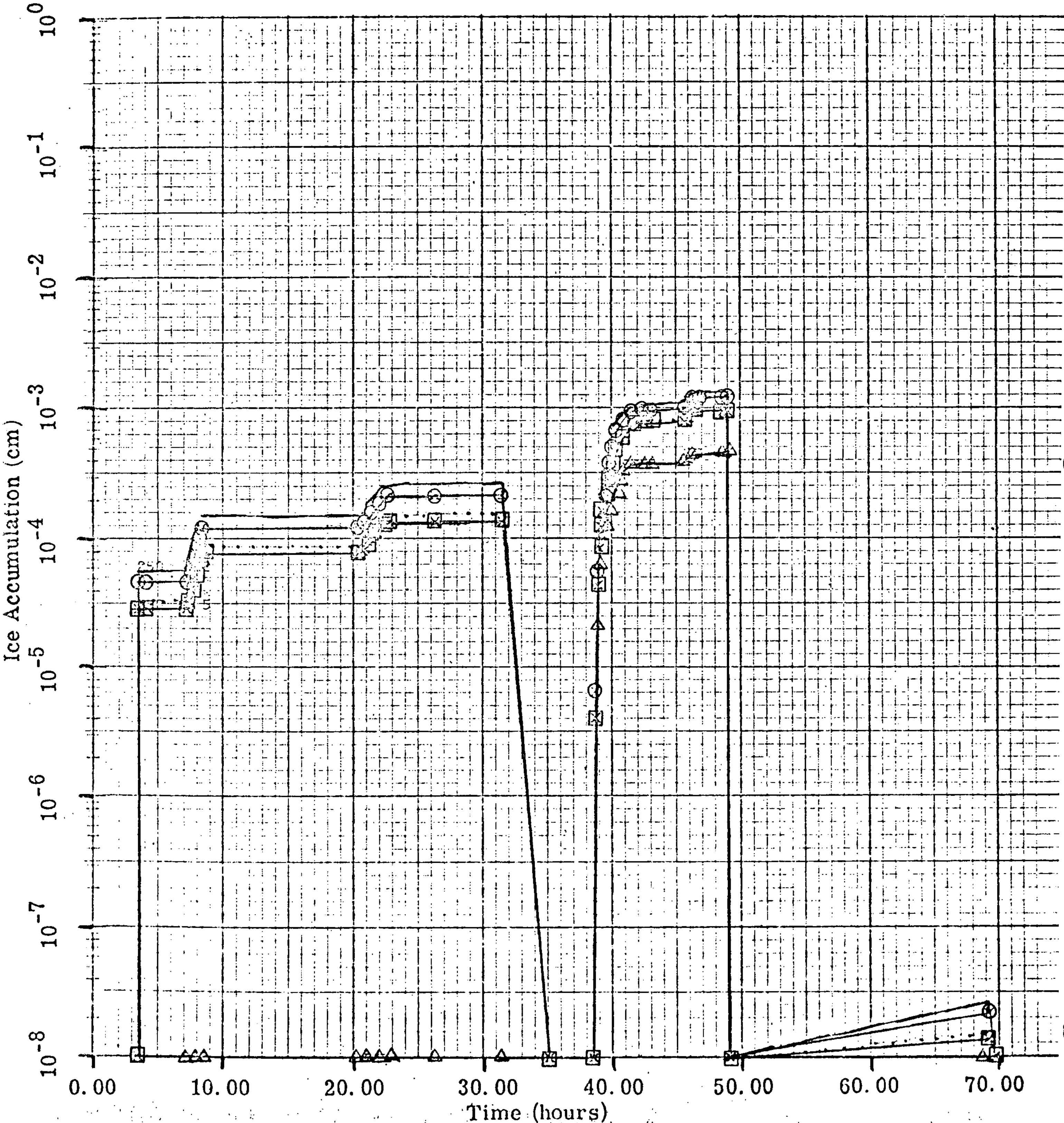

Figure 3-54c

Direction NE January

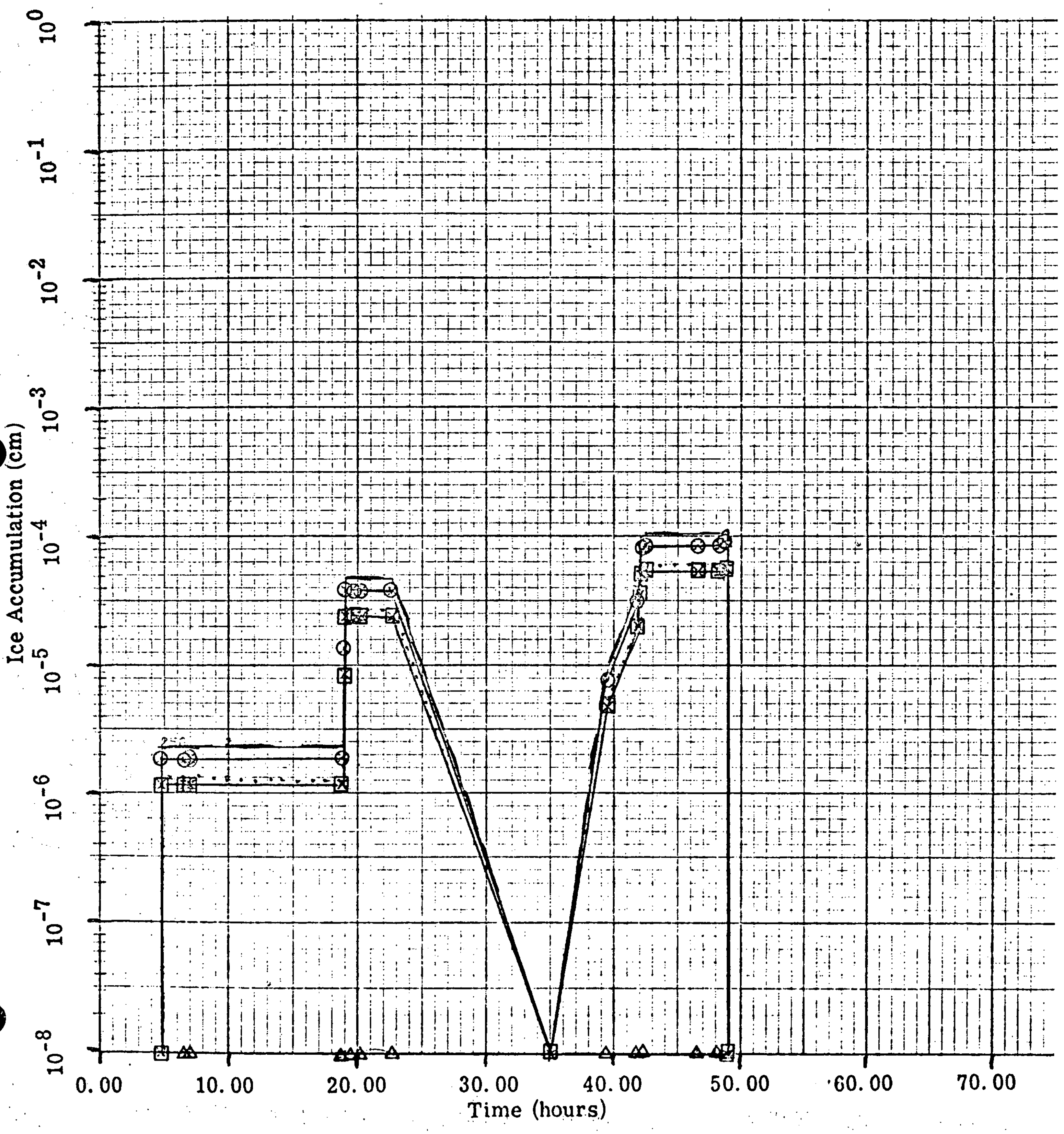

Figure 3-54d

Direction ENE January

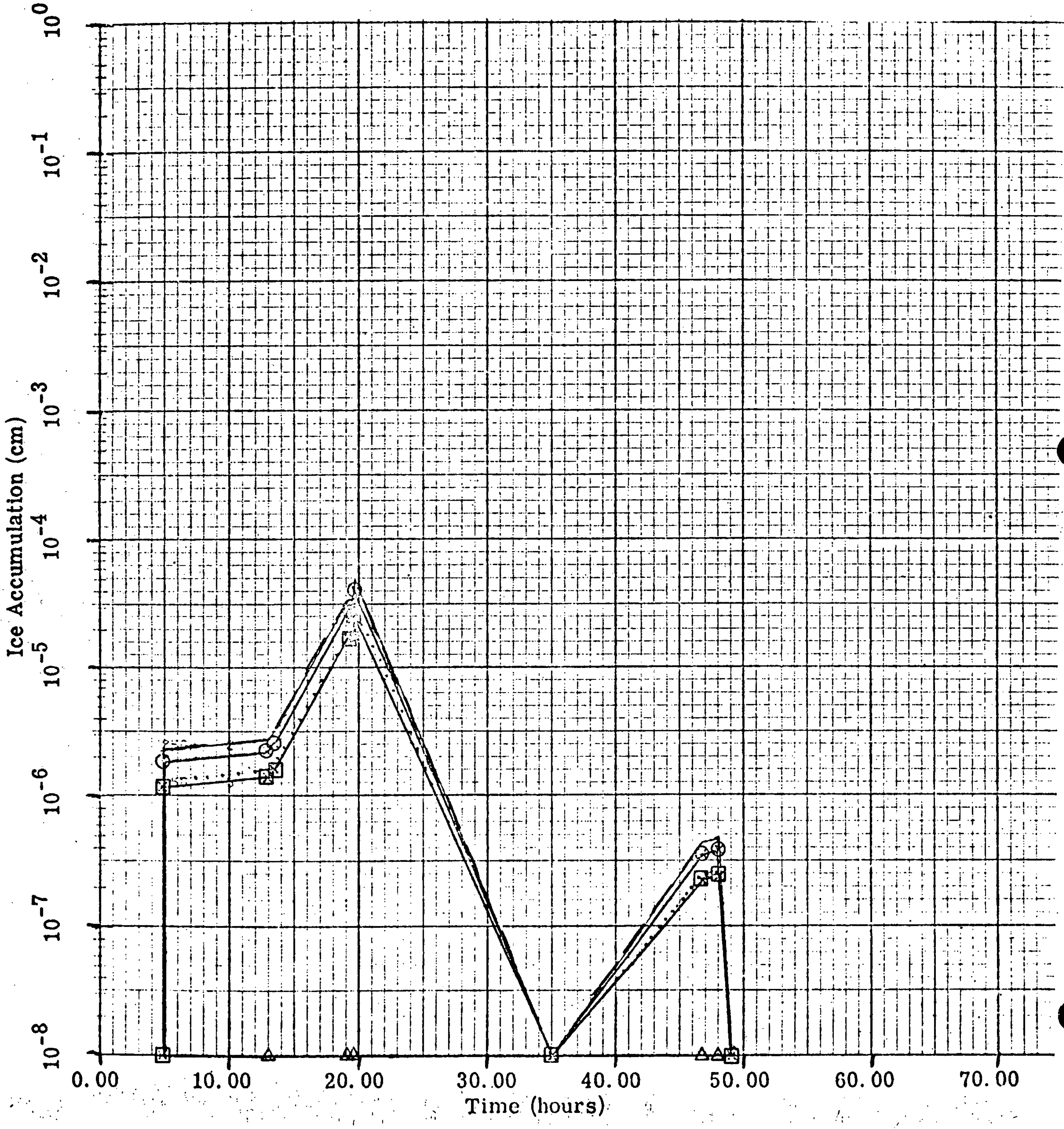

Figure 3-54e

Direction E January

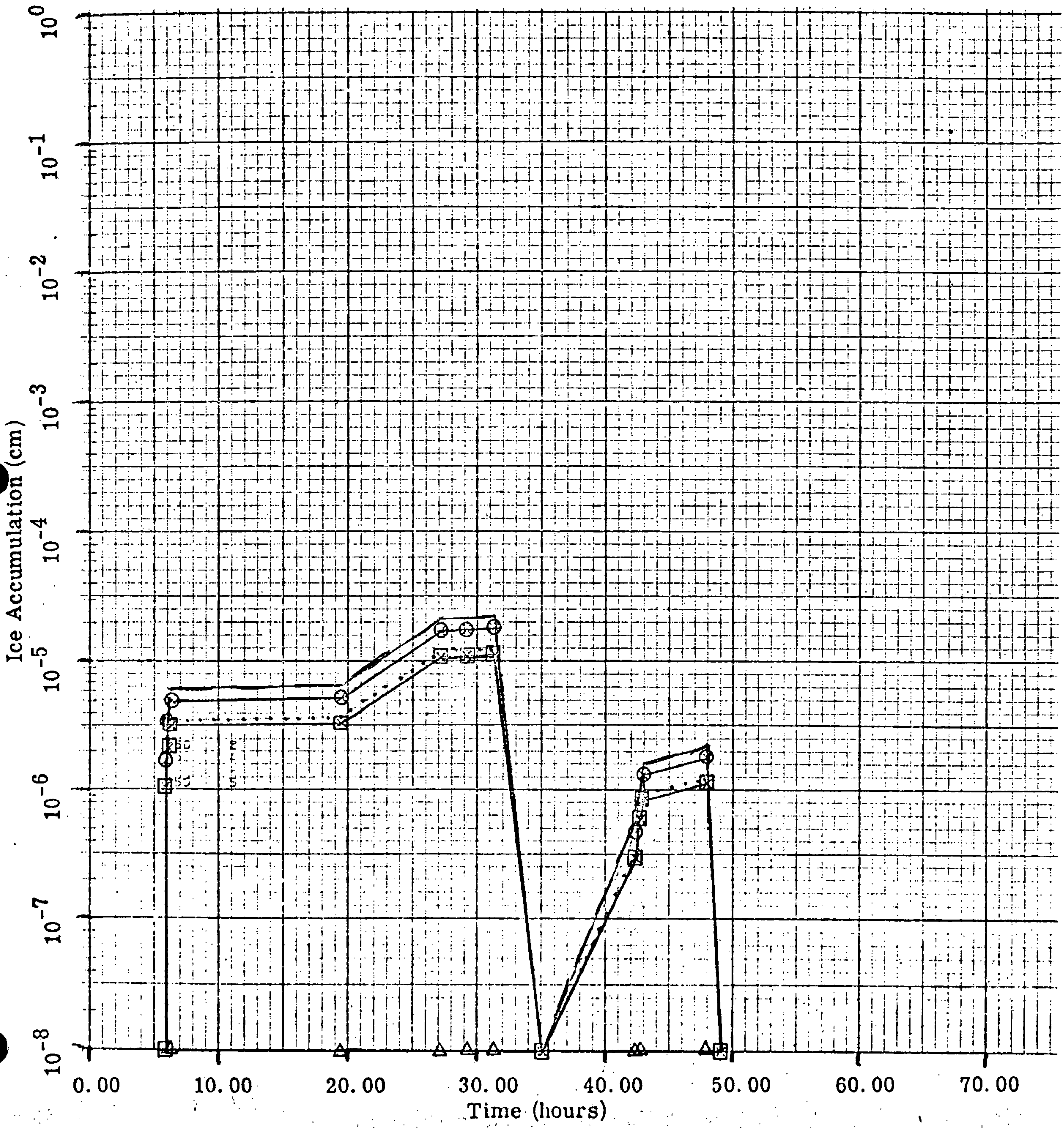

Figure 3-54f

Direction ESE January

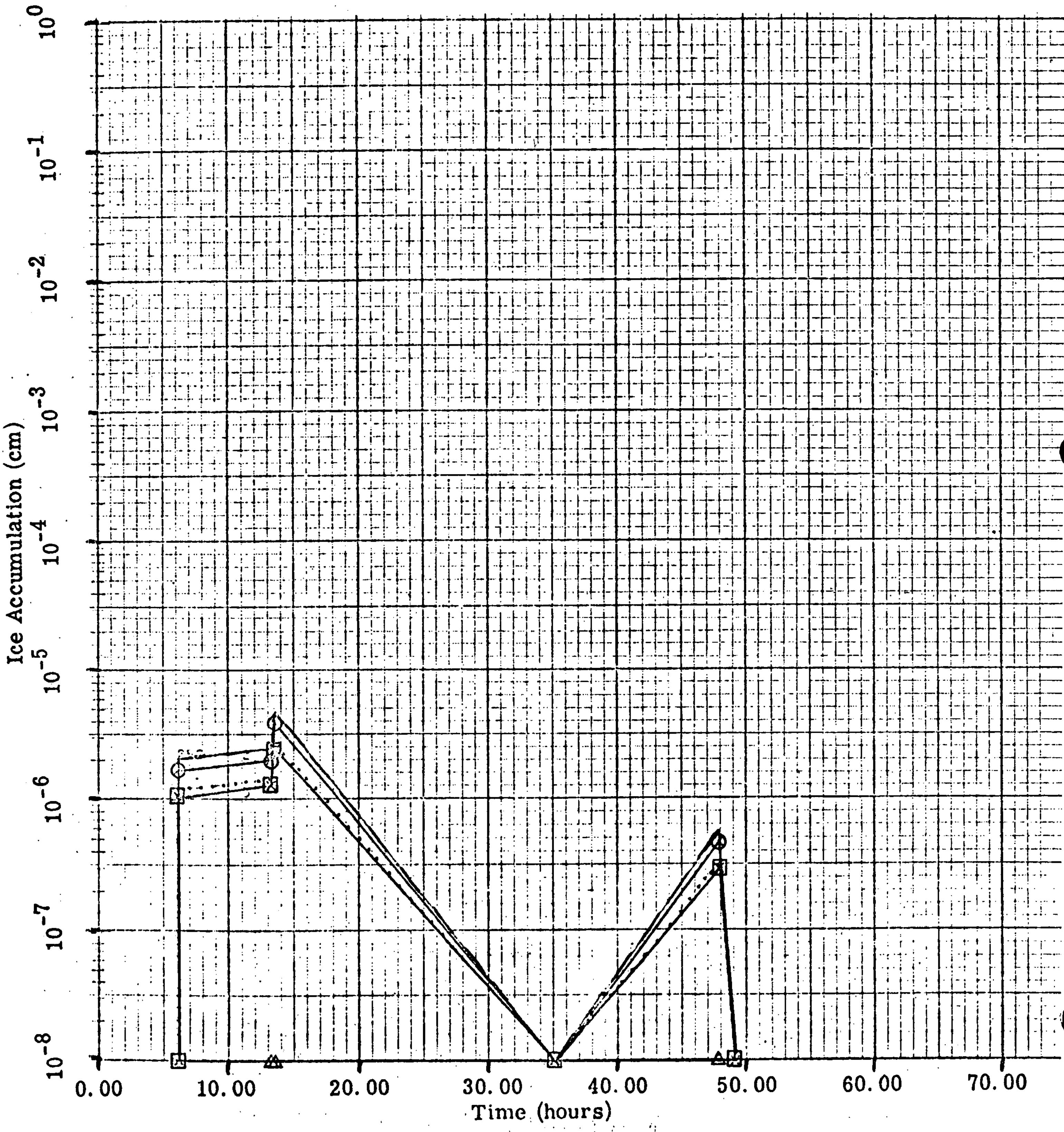

Figure 3-54g

Direction SE January

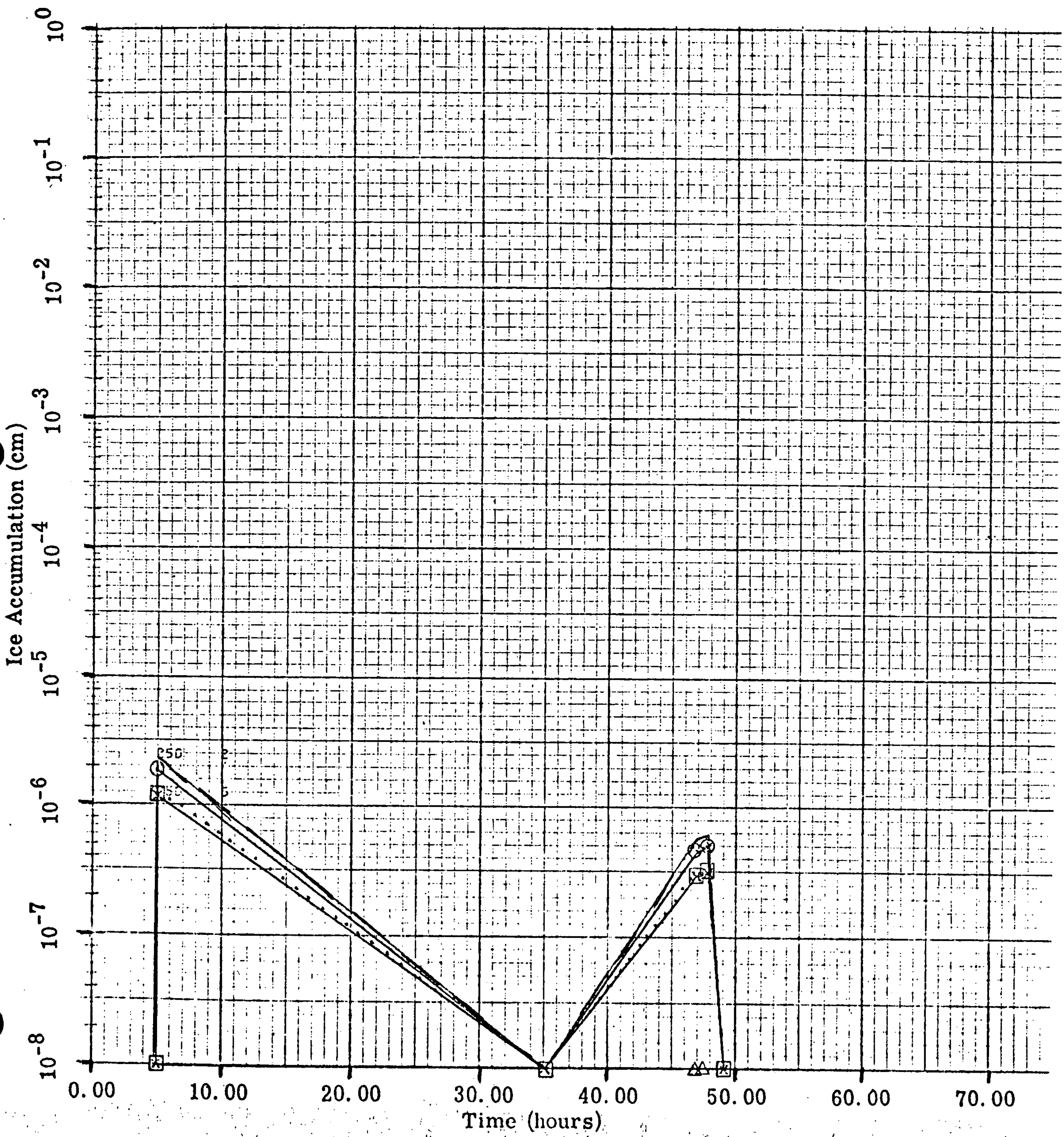

Figure 3-54h

Direction SSE January

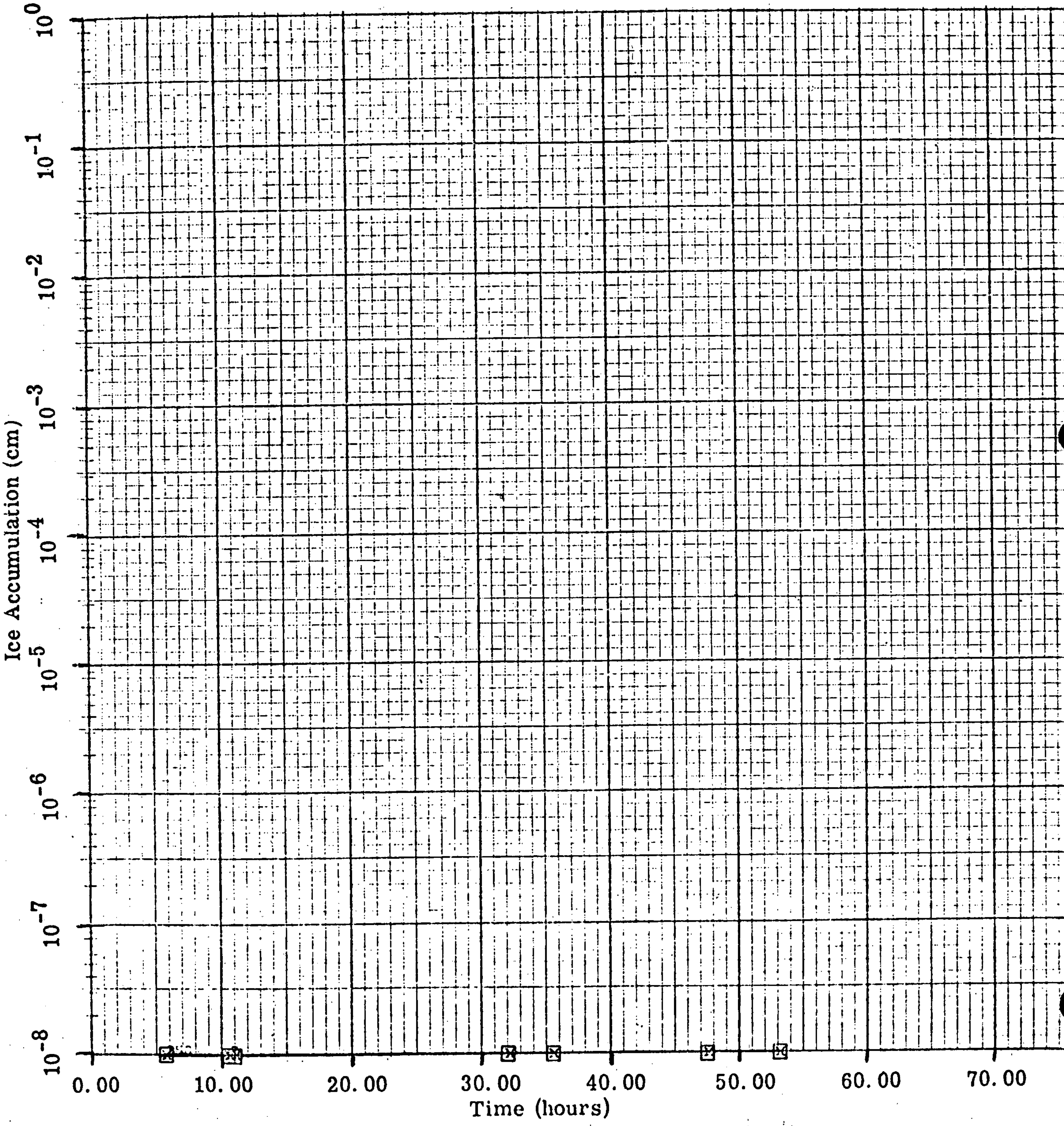

Figure 3-54i

Direction S January

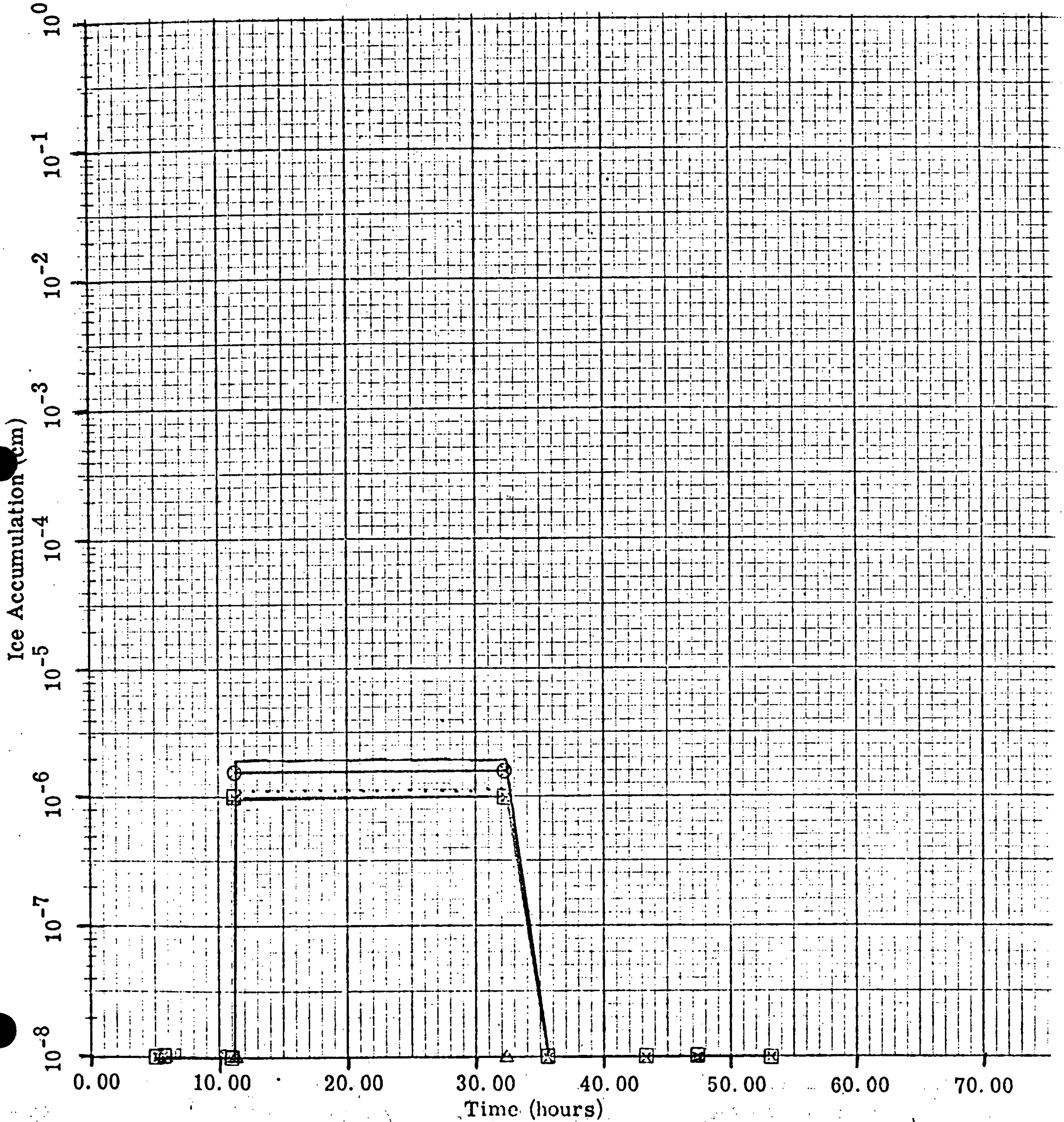

Figure 3-54j

Direction SSW January

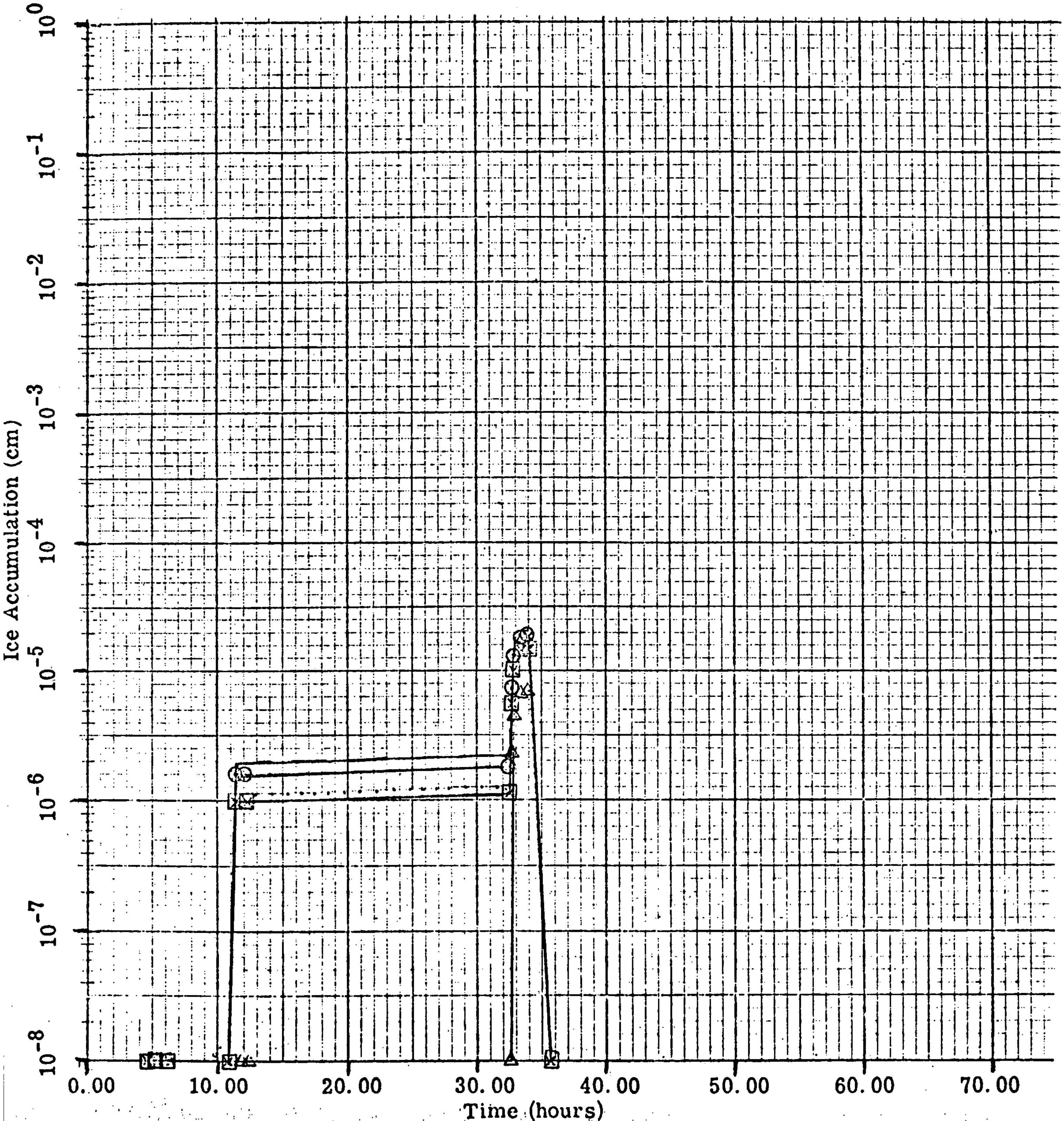

Figure 3-54k

Direction SW January

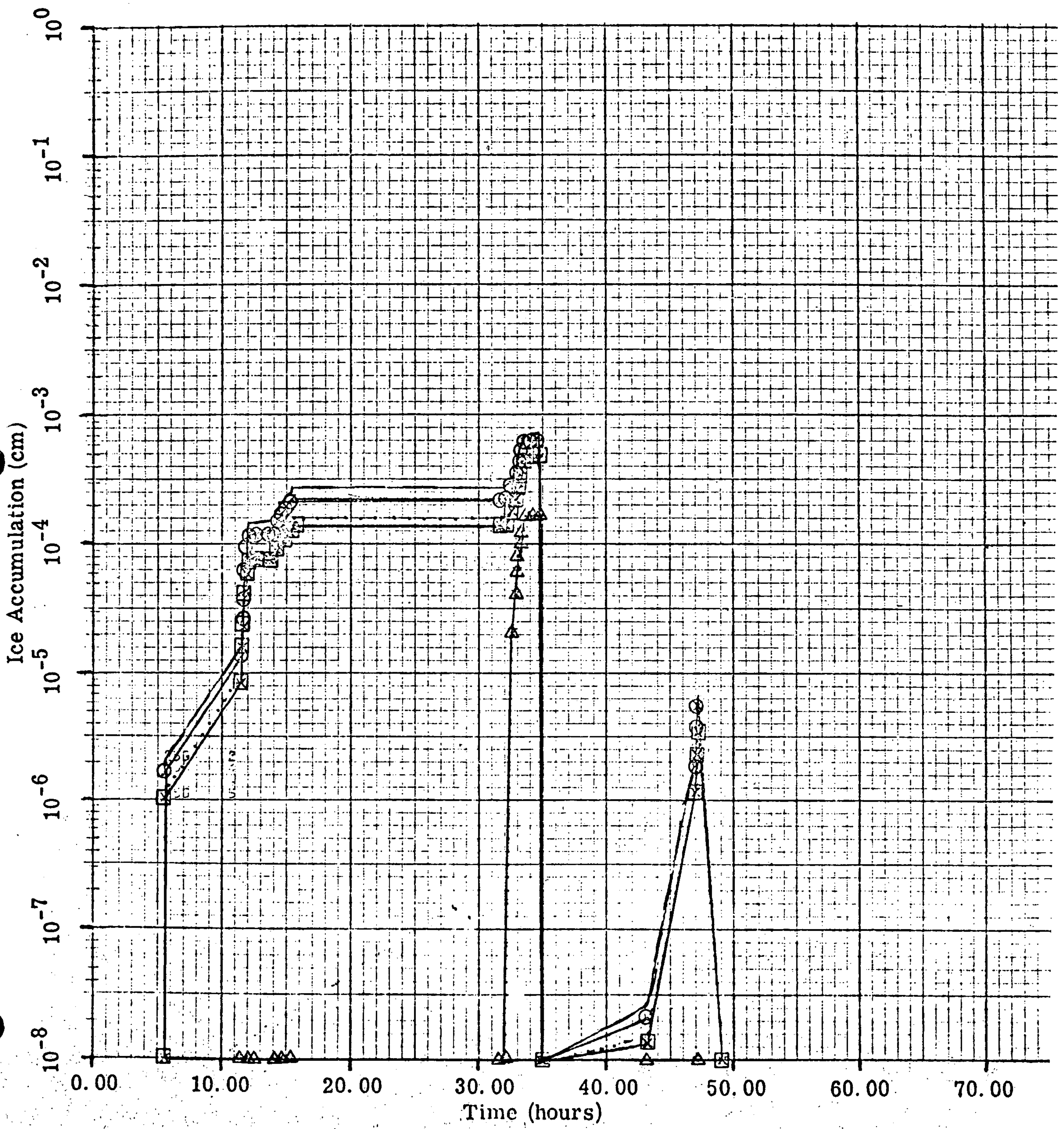

Figure 3-541

Direction WSW January

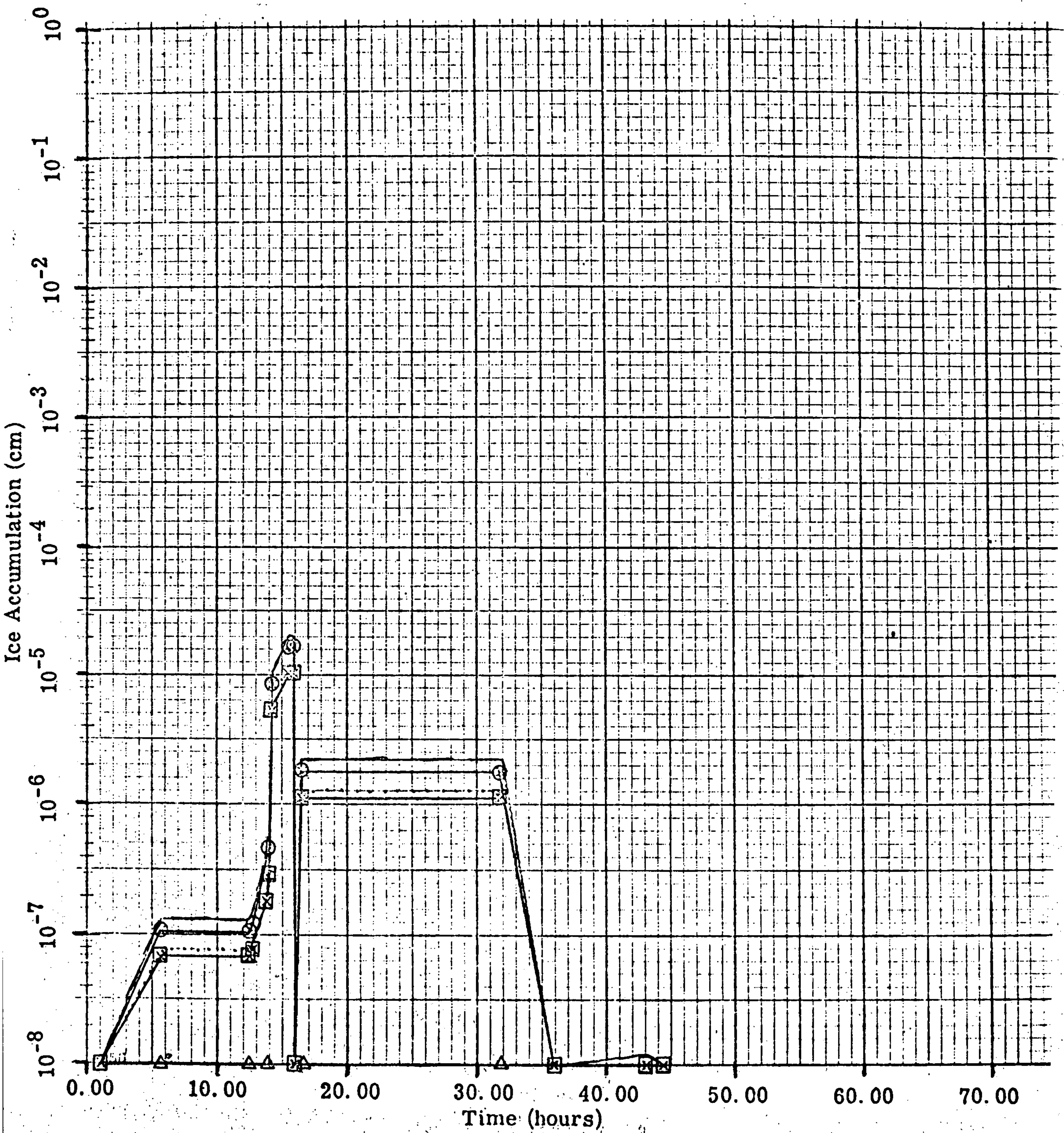

Figure 3-54m

Direction W January

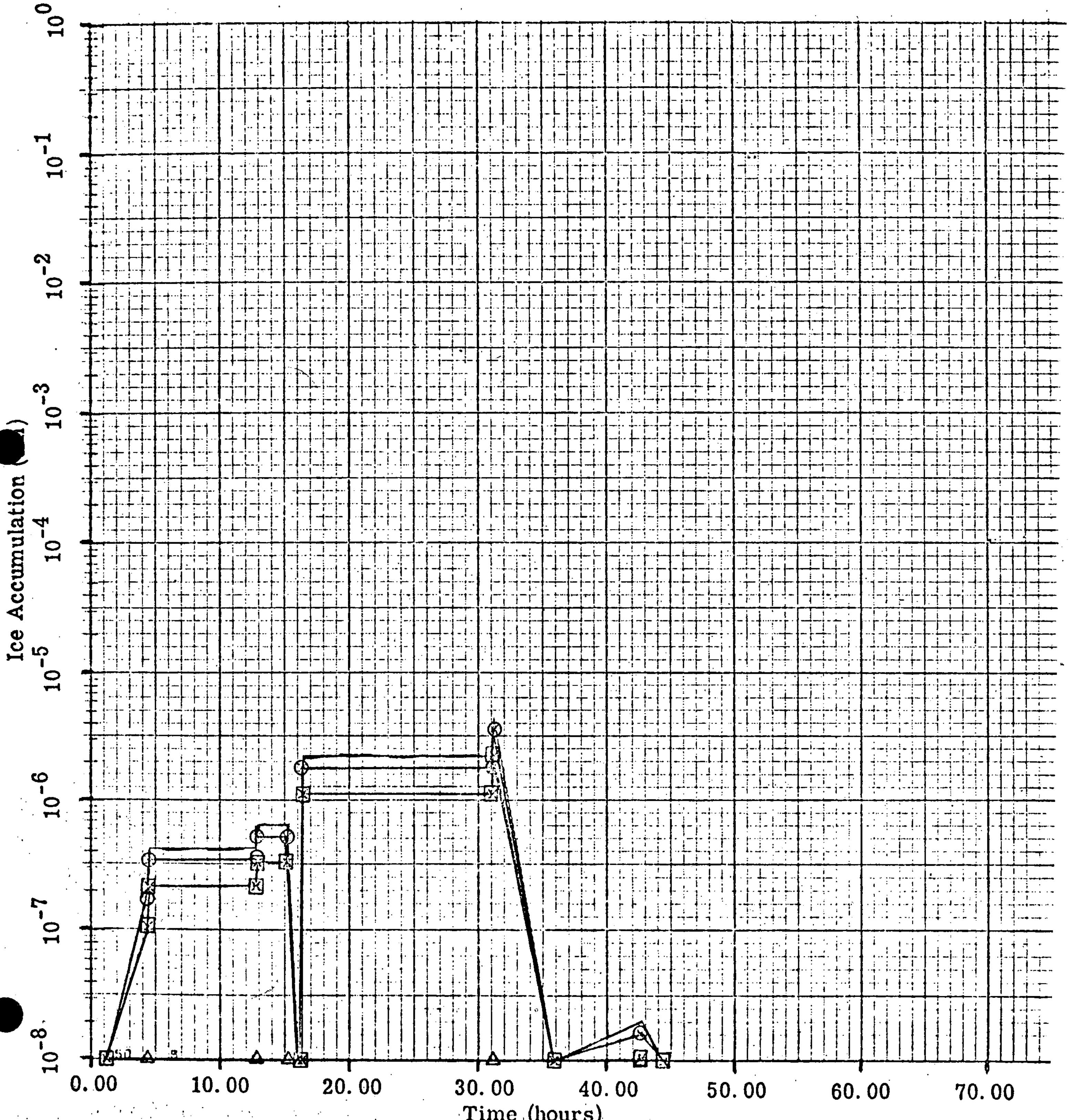

Figure 3-54n

Direction WNW January

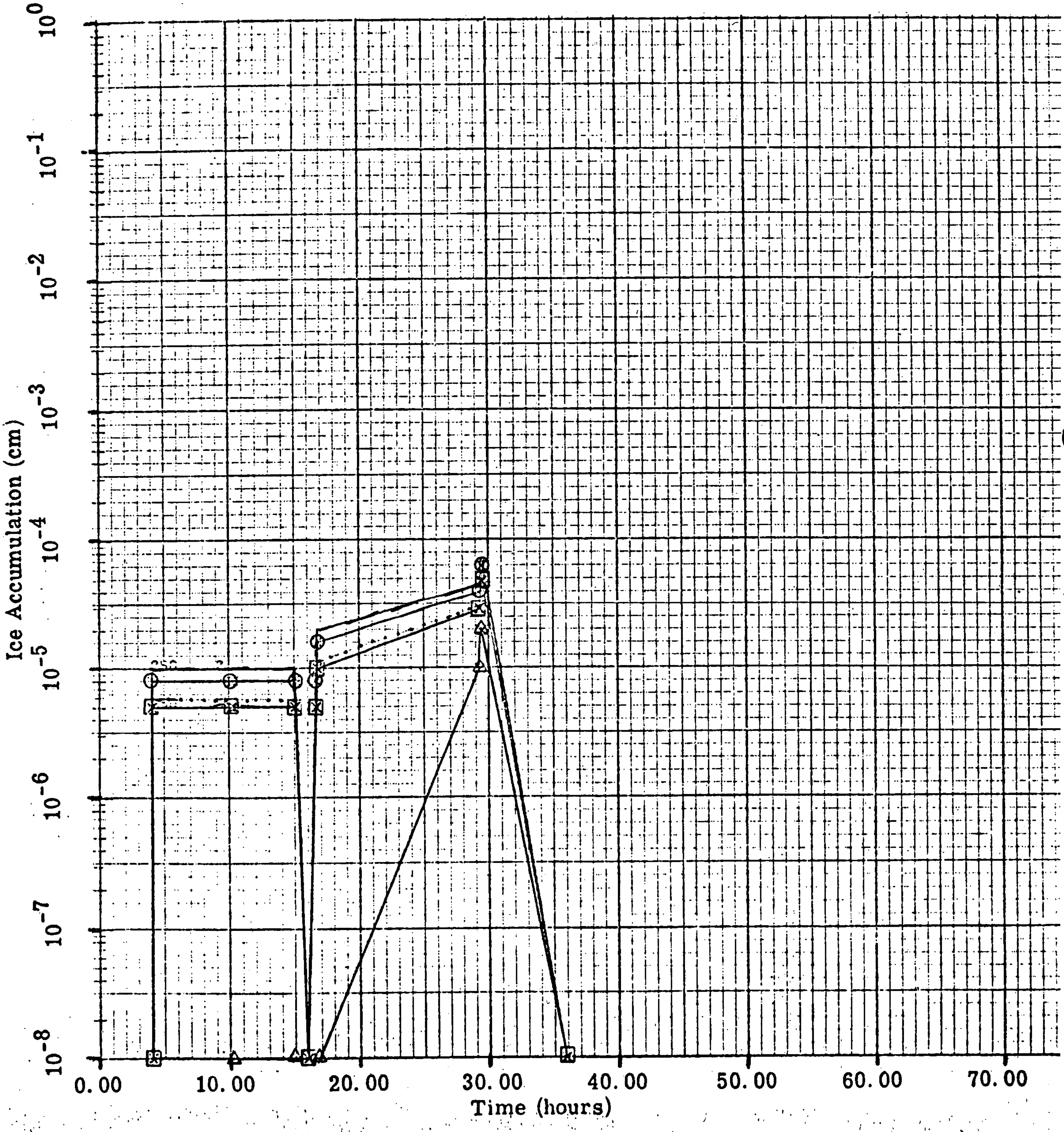

Figure 3-54o

Direction NW January

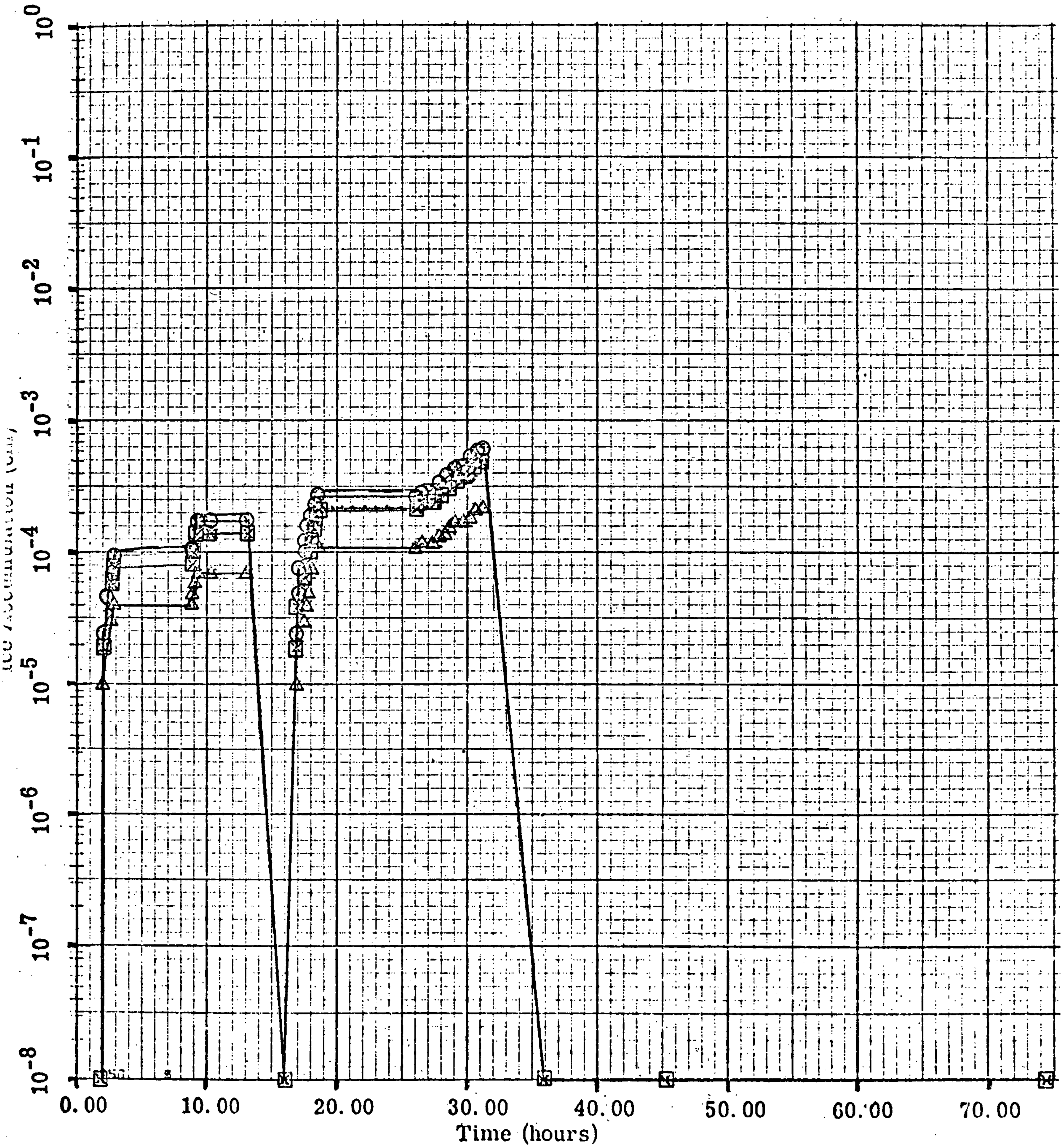

Figure 3-54p

Direction NNW January

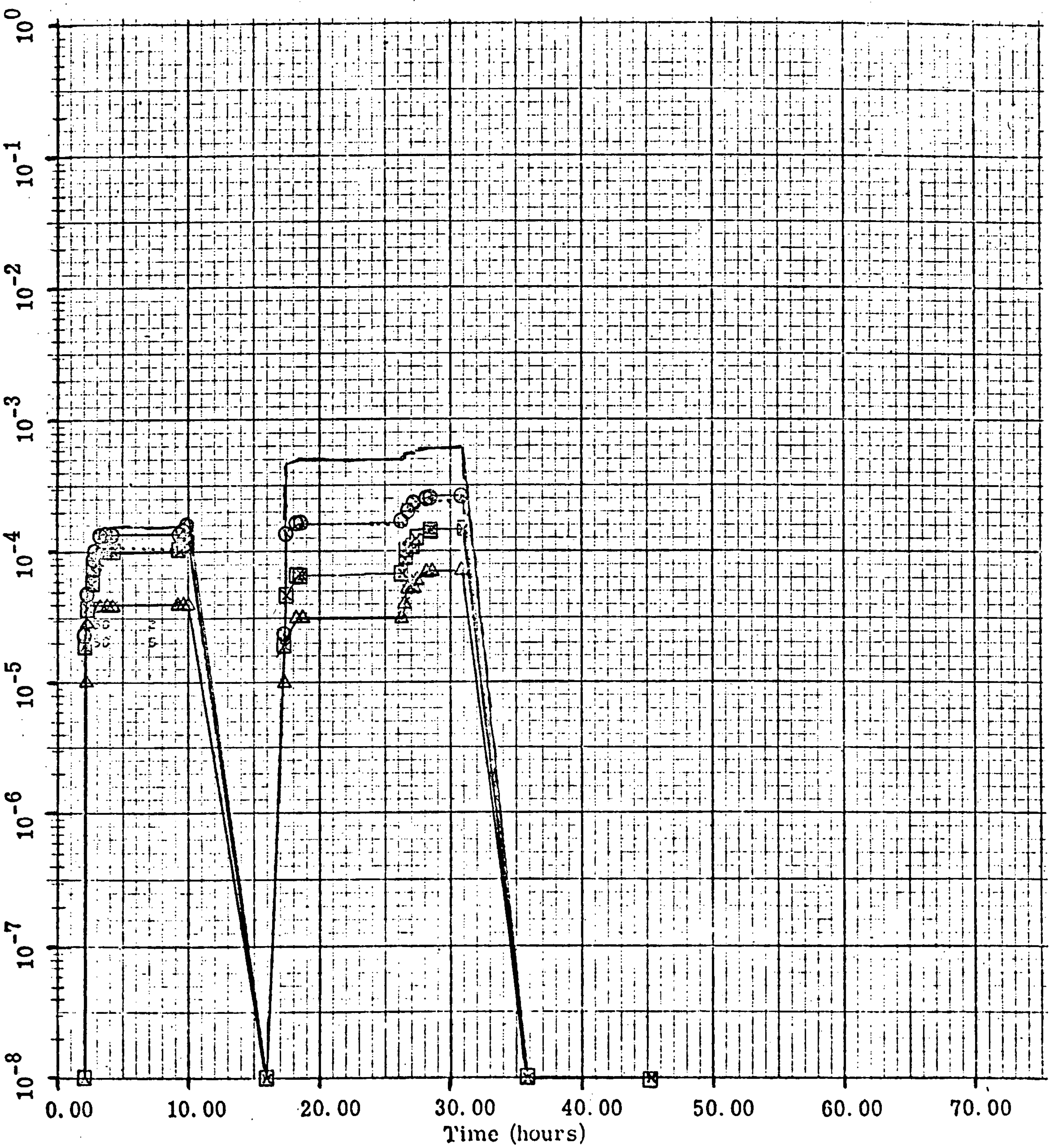

Appendix A

MATHEMATICAL MODEL FOR CALCULATION OF LENGTH OF VISIBLE PLUME, GROUND FOG POTENTIAL, AND INCREASE IN RELATIVE HUMIDITY

A. 1 Introduction

The plume from a cooling tower contains water which has been evaporated in the tower, plus entrained liquid water or drift which has been carried out of the tower in droplet form. As colder ambient air is entrained in the plume, the water vapor may condense and then re-evaporate, and the drops may grow in size, then diminish in size and evaporate as the water is carried away from the tower by the wind. Water in its liquid drop form appears as a visible plume, primarily because the droplets reflect incident light.

The purpose of this appendix is to explain the model used to calculate: (1) the length of the visible plume, (2) the extent of ground fogging, and (3) increases of relative humidity at ground level. Basically, the water (in either vapor or droplet form) is assumed to disperse in the atmosphere in a manner very similar to the dispersion of non-condensable combustion effluents. The essential difference is that the water undergoes phase changes from vapor to liquid and vice-versa, whereas the non-condensable combustion effluents do not. It is also assumed that the enthalpy of the humid tower air disperses similarly.

Any of a number of mathematical models of non-condensing plumes may be adapted to describe the condensation and evaporation behavior. The Halitsky (1966) non-condensing transverse jet plume model has been chosen as the basis for the adaptation. In both the non-condensing model and the adaptation presented in Section A. 3, a simple Gaussian plume is allowed to grow from the end of the jet region.

A. 2 Non-Condensing Plume Model

The condensed plume dispersion model is based upon the Halitsky (1966) transverse jet dispersion model for uncondensed effluents released vertically upward into a horizontal wind stream from a round chimney. Two types of effluents have been considered, mass and heat. The model for dispersion of mass (yielding concentration distributions in the plume) is described by Halitsky (1966). An additional note of clarification is given by Halitsky (1967). The application of the model to dispersion of sensible heat (yielding temperature distributions) is given by Halitsky (1968).

The Halitsky models were developed primarily for the transverse jet region of the plume, i. e., the portion of the plume beginning at the chimney orifice and extending downwind to the station where the jet effect disappears. Beyond this station, dispersion is assumed to proceed as in a conventional simple Gaussian plume, with the sigmas adjusted such that the concentration distribution at the start of the simple plume approximately matches that at the end of the transverse jet.

The principal characteristics of the Halitsky models are:

1) The plume is dispersed symmetrically around a curved centerline whose shape is determined by methods extraneous to the model.
2) The shape of the concentration, the temperature and velocity distributions, the radial dimensions of the finite plume boundary, and the variations of these properties with distance along the plume centerline are derived from experimental data on transverse jets.
3) Excess mass and excess sensible heat flows are conserved through all cross sections of the jet plume normal to its centerline. Excess mass flow is defined as the contaminant mass flow through the chimney orifice less the contaminant mass in a volume flow of ambient atmosphere equal to that leaving the chimney orifice. Excess sensible heat flow is defined

as the sensible heat flow in the total effluent jet less the sensible heat in a volume flow of ambient air equal to that leaving the chimney orifice.

4) Concentrations and temperatures in the plume are derived by adding excess concentrations and temperatures calculated from the assumptions in paragraphs 2 and 3 above to the corresponding ambient values.

5) Jet properties assumed in paragraph 2 were derived from wind tunnel experiments using low turbulence air streams. The equivalent jet properties in a natural atmosphere are not available. The wind tunnel air stream closely resembles a low turbulence atmospheric condition. The behavior of the jet in more turbulent atmospheres is not expected to be radically different close to the orifice, but the rate of growth of the jet should be larger as turbulent energy diffuses radially inward with distance downwind. This would produce more rapid decay of concentration and temperature.

A. 3 Treatment of Condensing Plumes

In applying the Halitsky model to condensed vapor plumes from cooling towers, mass concentration was replaced by water concentration, and sensible heat was replaced by enthalpy of humid air. The term water concentration (gms H_2O /volume of mixture) is used to denote total water, whether in the liquid or vapor phase, as distinguished from specific humidity (gms H_2O vapor/volume of mixture) or mixing ratio (gms H_2O vapor/gm air).

It is assumed that water and enthalpy are independently diffused according to the same dispersion model, and yield independent fields of water and enthalpy concentration in the plume. The local temperature and relative humidity (if condensation does not occur) or the local temperature and quality (percent of water in vapor phase) are then completely determined from thermodynamic considerations, by the local water concentration and enthalpy. It is assumed that condensation occurs when sufficient water is present to achieve or exceed local saturation at the local temperature. For calculating increases in relative humidity where condensation does not occur, the ambient atmospheric humidity is subtracted from the local plume humidity at the point of interest.

A.4 Technical Aspects of the Condensing Plume Model

The Halitsky non-condensing plume model has been developed for emission velocity ratios (emission velocity/wind velocity) equal to or greater than one, for use with combustion effluents. In applying the model to natural draft cooling towers, where the emission velocity is low, it was necessary to apply further theoretical considerations to the jet region in order to allow extrapolation of data to low velocity ratios. This resulted in some modification of the characteristics of the jet region in order to avoid computational discontinuities at the transition from the zone of establishment to the established jet region and at the transition from the established jet region to the simple Gaussian plume. These considerations allowed extrapolation of the data to emission velocity ratios as low as 0.2. At velocity ratios less than this value, it was necessary to arbitrarily assign jet cross section dimensions near the orifice. The effect of these modifications on the length of condensed plume is small since the length of the jet region is very small at low emission velocity ratios.

At the end of the transverse jet region, called Station 2 in the Halitsky (1966) paper, the water concentration and enthalpy distributions used in the jet model (linear decrease from peak at axis to zero at boundary, and rotationally symmetrical) are replaced with Gaussian distributions by the method outlined in Section 4 of the paper. The conversion was effectively made by assigning to the Gaussian plume a rotationally symmetrical $\sigma_r = R_2/\sqrt{6}$ as given by Equation 25 of the paper.

Subsequent growth of the plume was introduced by adding to σ_r the σ_y and σ_z values appropriate to the given stability condition and the downwind distance measured from Station 2.

A complete description of the computer model, including equations, is contained in the reference : Calabrese (1974).

A. 5 Accounting for Terrain

In hilly regions the potential for surface fogging and increases in humidity at higher elevations must be considered. An estimate is obtained by assuming constant wind speed and direction during any given hour, and calculating ground level humidity conditions taking into account the local terrain.

The height of the visible portion of the plume above the local grade is determined for each downwind distance using the Briggs plume rise formulations and the plume dispersion model discussed herein. Both enthalpy and water mass are accounted for in the vertical plane at the downwind positions of interest.

Vertical profiles of ambient temperature and dew point are assumed to be constant with reference to the tower base.

In calculating ground fogging the local grade of the land was followed, and when the visible portion of the plume intersected land, fogging was assumed to occur. It should be noted that if the land slopes significantly upward so that the plume centerline intersects the ground, the calculation is equivalent to that for a ground level release with no plume rise. (The reflection term in the Gaussian plume model would give double the axial concentration at that point.)

A. 6 Application of the Condensing Plume Model

The model is used to calculate the visible length of plume for each hour in a given period of record (usually one year of data) using ambient temperature, dew point temperature and wind data measured at several elevations on a meteorological tower at the site, and typical cooling tower emission characteristics.

For the Indian Point site, the wind speed and direction used were those measured at 400 ft. Temperature measured at 33 ft and 400 ft, and dew point measured at 33 ft and 400 ft were used. No speed gradients or changes in plume direction with increasing plume height were accounted for. Summaries of these data are given in Appendix C, Table 1 . Terrain profiles taken from topographic maps of the Indian Point area were supplied as input for each of the 16 wind direction sectors and are given in Appendix C, Figures 2a through p . Visibility data were taken at the 33 ft level on the site meteorological tower.

Atmospheric stability class for each hour of data was determined from the temperature gradient measured between 33 ft and 400 ft on the Indian Point tower, using the AEC Regulatory Guide 1.23 distribution of Pasquill stability classes according to specified ranges of average temperature gradient.

The hourly vertical profiles of ambient and dew point temperature in the atmosphere were as follows:

	Ambient Temperature	Dew Point Temperature
Value at 33 ft	As Measured	As Measured
Value at 400 ft	As Measured	As Measured
Gradient below 400 ft	Measured gradient between 33 ft and 400 ft	Measured gradient between 33 ft and 400 ft
Gradient between 400 ft and 1500 ft	One-half the above gradient	One-half the above gradient
Gradient above 1500 ft	-0.4 F/100 ft	-0.4 F/100 ft

Plume rise is calculated according to Briggs (1969), assuming no buoyancy effect due to release or recovery of latent heat. Buoyancy flux is based on density difference between the humid tower air and the atmosphere at the height of release. Stability groups are based on the temperature gradient between 33 ft and 400 ft. Hours in which visibility at the 33 ft level was less than 1/4 mile were not used in the analysis on the basis that natural obstructions to visibility or high relative humidity conditions already existed and the tower would have a negligible increase in the severity of such conditions.

A.7 Accounting for Two Tower Operation

For calculating the effect of two tower operation, the effluents from both towers are assumed to be discharged from a single tower with an effective discharge area equal to the total area of both towers. However, for plume rise calculations, only the buoyancy flux for one tower is used. These assumptions tend to overestimate plume length since, in reality, some dilution of each individual plume will take place before the plumes merge.

REFERENCES FOR APPENDIX A

Halitsky, J. (1966), A Method for Estimating Concentrations in Transverse Jet Plumes, Air & Water Pollution Int. J. 10, pp. 821-843.

Halitsky, J. (1967), A Method for Estimating Concentrations in Transverse Jet Plumes, Atmospheric Environment, 1, p. 183.

Halitsky, J. (1968), Temperatures and Concentrations in Heated Plumes, Atmospheric Environment, 2, pp. 419-422.

Briggs, G. A. (1969), "Plume Rise," U.S. Atomic Energy Commission, Division of Technical Information, TID-25075.

Calabrese, R., et al (1974), "Prediction of Temperature and Moisture Distributions in Cooling Tower Plumes," preprints for the American Meteorological Society Symposium on Atmospheric Diffusion and Air Pollution, Santa Barbara, California, 1974. (See Addendum 1.)

Appendix B

1.0 SALT DRIFT MODEL - DESCRIPTION

The salt drift model is based in following the behavior of single particles as they travel from the top of the drift eliminator to the ground (see Figure 2. 1. 1)

Starting at the top of the drift eliminator, in the center of the tower, a typical saline droplet of initial diameter D_{p_o} and concentration c_o will find the following conditions:

1. The air flow through the tower exerts a drag force on the saline drop. As the drag force overcomes gravity force, the saline drop is set in motion. The drop moves through the tower with the air (described by equation of motion).

2. The drop is assumed to experience no horizontal motion because it represents a statistical average.

3. The air temperature inside the tower is greater than the ambient air temperature and remains approximately constant through the tower.

4. The air inside the tower is saturated, i.e., relative humidity of the air inside the tower is 100%.

5. There is a water vapor concentration gradient between the air and the surface of the drop, i.e., the mole fraction of water in air is greater than the mole fraction of water around the drop. Mass transfer (of water vapor) by diffusion will occur from the air to the droplet. Mass transfer by bulk flow exist due to the motion of both air and droplet (see mass transfer equation, section 2.1, pages 5, 6).

6. As the drop is growing by diffusion, the latent heat of vaporization is released to the drop, raising its temperature.

The mole fraction of water in air is given by the partial pressure divided by the total, atmospheric, pressure.

The mole fraction of the water around the drop is given by the vapor pressure that the saline drop exerts divided by the total pressure.

As the drop reaches the top of the tower, it has grown to a diameter $D_p > D_{p_o}$ and has a velocity $\vec{v}z$. At the top of the tower, on the outside, the following conditions exist:

1. A wind speed $\vec{u}x$ in a given horizontal direction, K.
2. The air leaving the tower is buoyant ($T_g > T_{ambient\ air}$, $\rho_g < \rho_{ambient\ air}$.
3. The relative humidity of the air leaving the tower is greater or equal to the ambient air relative humidity.
4. The air as it leaves the tower has a vertical velocity $\vec{u}z$.
5. The air leaves the tower as a plume. The saline drops are within this plume.

The plume, a mixture of hot air-water vapor-saline drops, leaving the tower will be exposed to the above conditions. The plume will rise due to its initial momentum and buoyancy and grow by entrainment of ambient air. It is assumed that plume height predictions by Slawson and Csanady[(1)] for stable low wind speeds and Briggs[(2)] for all other conditions are valid. Plume radius grows after the plume leaves the tower. Plume growth as a function of distance from the tower is given by Slawson and Csanady[(3)] and by the empirical correlation derived from photograph observations at the Paradise plant of TVA (see page 21 of mathematical model). Entrainment of air into the plume changes its relative humidity as a function of distance from the tower and ambient air relative humidity. At a distance equal to ten (10) tower heights it is assumed that the plume is well mixed with the ambient air, i.e., the plume disappears. From 0 to 10 tower heights, the plume height is described by the equation given on page 11 of Section 2.2 of the mathematical model. The vertical velocity of the plume is given by the derivative with respect to time of the plume height equations (see Section 2.2 on page 11 of the mathematical model).

The drop leaving the tower with the air will be within the plume for a certain distance then it leaves the plume, enters the ambient air and continues to fall until it reaches the ground. While in the plume, the typical drop will find the following conditions:

1. The wind exerts a horizontal drag force on the drop causing the drop to experience a horizontal motion $\vec{v}x$ in the direction K of the wind (see horizontal equation of motion ($d\vec{v}x/dt$) on page 10 and Figure 2.1.2 on page 8.

2. The plume exerts an upward vertical drag force on the drop, while gravity exerts a downward vertical force (see figure 2. 1. 2). The drop will move upward with the plume until the gravity force overcomes the decreasing drag force within plume. At this time, the particle starts falling out of the plume. As the drop leaves the plume, $\vec{u}z = 0$.

3. The plume rises and changes in size as a function of distance from the tower.

4. A water vapor concentration gradient exists between the plume and the surface of the drop. Mass transfer by diffusion will occur from (to) the plume air to (from) the drop surroundings, depending on the relative humidity and temperature of the plume. While the mole fraction of the water vapor in the air is greater than the mole fraction of the water vapor around the drop, mass transfer will occur from the plume to the drop (the particle will continue to grow and its temperature to rise). Otherwise, the drop will start to evaporate while cooling.

It is necessary to check whether the drop is inside the plume or in the ambient air as a function of distance from the tower, in order to correct for relative humidity and temperature changes. This is done by calculating the drop coordinates (height and distance) and the plume height and radius. If (HP - RP) <HZ and/or (HP + RP) >HZ for the same distance XD, the drop is in the plume. Otherwise the drop is in the ambient air. (See page 31 for nomenclature)

The drop outside the plume experiences the following conditions:

1. The wind velocity $\vec{ux}$ continues to exert a horizontal force described above on page 1. 2.

2. Gravity exerts a vertical force downward on the drop. The drop is assumed to fall at terminal velocity 10 seconds after it leaves the plume. The terminal velocity of the falling drop varies with changes in the drop size and concentration (density) until steady state (equilibrium) is reached between drop and environment.

3. Ambient air relative humidity is RHA.

4. Ambient air temperature is T_a.

5. Water vapor mass transfer by diffusion will occur between the ambient air and the drop depending on the relative humidity of the air.

The salt model follows the trajectory of single statistically average droplets of diameter D_{p_o}. In order to find the statistical distribution in space of all the droplets represented by the droplet of diameter D_{p_o}, it is necessary to take into account the effect of atmospheric diffusion in the plume and in the ambient air. It is assumed that a normal distribution of drop concentration exists around the trajectory of the representative salt droplet as is illustrated in Figures 2.3.1 and 2.3.2 and as outlined on page 12. The ordinate of the unit normal curve is given by HZ, the height of the droplet at distance XD divided by the diffusion coefficient, σ_z, corresponding to the particular stability condition under consideration. At each selected distance XD, the HZ/σ_z is calculated and the corresponding area under the curve obtained. This area is subtracted from one-half the area of the normal curve. The resultant value corresponds to the fraction of salt deposited between two consecutive distances.

It should be noted that HZ corresponds to the height of the drop above grade at each distance XD. That is, in hilly regions, the effect of the terrain upon the drop trajectory is considered. This is done by following the local grade of the land while following the drop trajectory and adjusting HZ to account for the local grade XD. Since the topography is a function of distance and direction the land is characterized by terrain profile sectors. The number of sectors to be used depends on the site characteristics. As many as 16 sectors can be used to characterize the terrain. The drops trajectory calculations are done for each of the selected sectors.

2.0 MATHEMATICAL MODEL*

2.1 General Equations

Motion of a single drop in a gas flow field is given by:

$$\underbrace{\rho_L \left(\frac{\pi D_p^3}{6 g_c}\right) \frac{d\vec{v}}{dt}}_{\substack{\text{change in motion of drop caused by}\\ \text{all the forces acting on it,}\\ \text{Newton's Law}}} = \underbrace{\rho_L \left(\frac{\pi D_p^3}{6}\right) \frac{\vec{g}_L}{g_c}}_{\text{gravity force on drop}} - \underbrace{\frac{|\vec{u} - \vec{v}|(\vec{u} - \vec{v})}{2 g_c} \rho_g \left(\frac{\pi D_p^2}{4}\right) C_D}_{\substack{\text{fluid resistance opposing relative}\\ \text{movement of drop through the gas}}} + \underbrace{\vec{F}_e}_{\text{any other force}}$$

Mass transfer to the gas phase around the drop (i.e., around the drop surface) is given by:

$$\underbrace{\frac{dm_A}{dt}}_{\substack{\text{rate of mass transfer of A to the stream}\\ \text{over the entire surface}}} = \underbrace{k_{xm} \left(\pi D_p^2\right)\left(x_{Ao} - x_{A\infty}\right)}_{\text{rate of mass transfer by diffusion}} + \underbrace{x_{Ao} \left(\frac{dm_A}{dt} + \frac{dm_B}{dt}\right)}_{\text{rate of mass transfer due to bulk flow}}$$

where:

C_D = drag coefficient

	For:
$= \dfrac{24}{N_{Re}}$	$N_{Re} \leq 2$
$= \dfrac{18}{(N_{Re})^{.6}}$	$2 \leq N_{Re} \leq 1000$
$= 0.44$	$1000 \leq N_{Re} \leq 200,000$

*See Page 31 for Nomenclature.

k_{xm} = mass transfer coefficient for drops[4]

$$= \left(\frac{2 \rho_g \mathscr{D}_{AB}}{D_p} \right) \left[1 + 0.3 \; N_{Re}^{1/2} \cdot N_{Sc}^{1/3} \right]$$

N_{Re} = Reynold's number

$$= \frac{D_p \left| u_{air} - v_{drop} \right| \rho_g}{\mu_{air}}$$

N_{Sc} = Schmidt number

$$= \left(\frac{\mu}{\rho \mathscr{D}_{AB}} \right)_g$$

A heat balance around the drop gives:

$$\underbrace{T - T_{drop}}_{\substack{\text{net heat}\\ \text{transfer by}\\ \text{conduction}}} = \underbrace{\frac{\mathscr{D}_{AB} \, \mathscr{H}_\Delta \, x_A}{k_{air}}}_{\substack{\text{net heat transfer by}\\ \text{diffusion}}} \cdot \rho_{air}$$

And from continuity:

$$\frac{dm}{dt} = - \frac{m_o}{c^2} \frac{dc}{dt}$$

where:

D_p = drop diameter

$$= \left(\frac{6 \, m_o}{\pi \rho_L c} \right)^{1/3}$$

m_o = mass of salt in drop

m = mass of water in drop

Figure 2. 1. 1
Behavior of Salt Particles
in the Operation of a Salt Water Cooling Tower

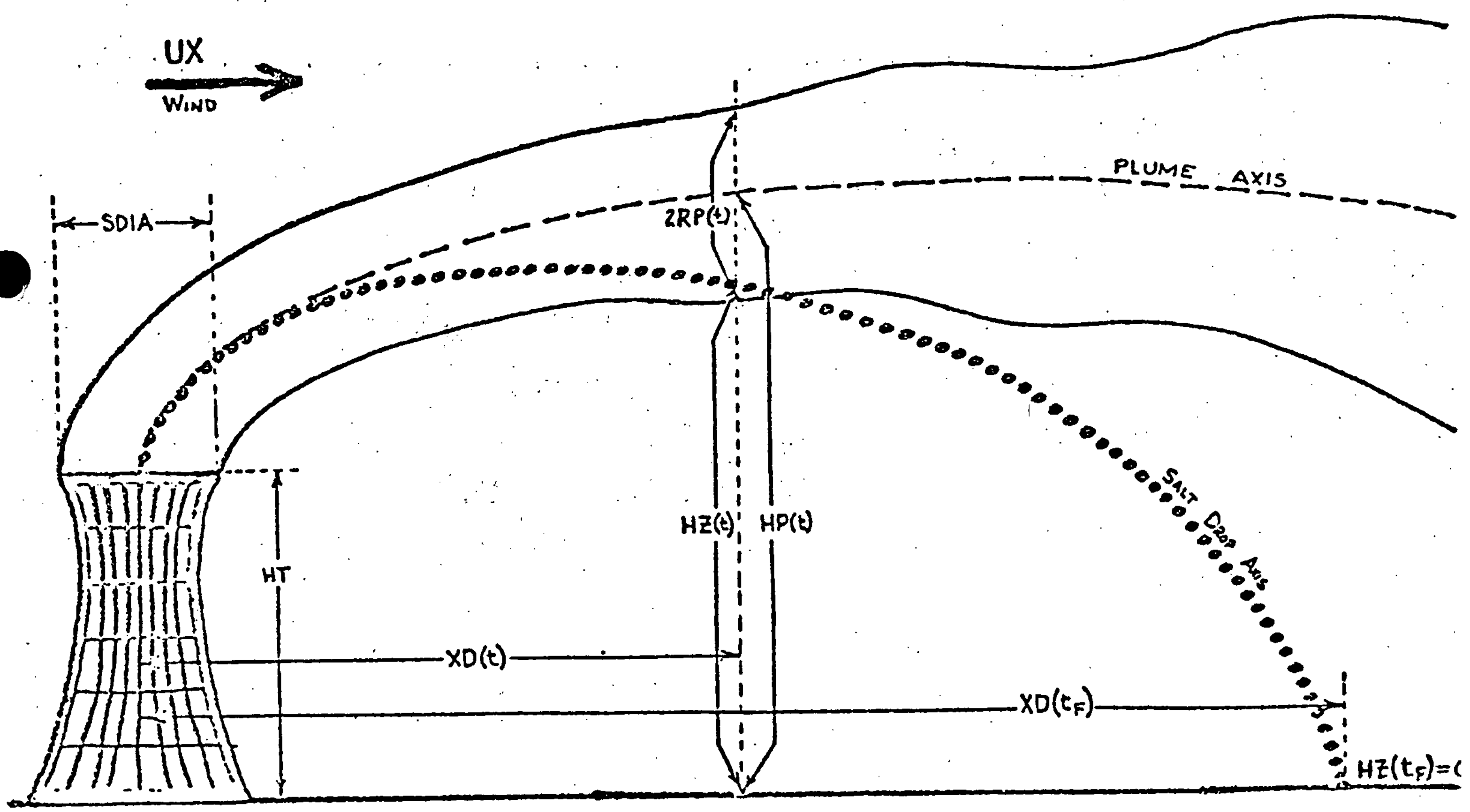

Figure 2.1.2

Forces Acting on a Droplet

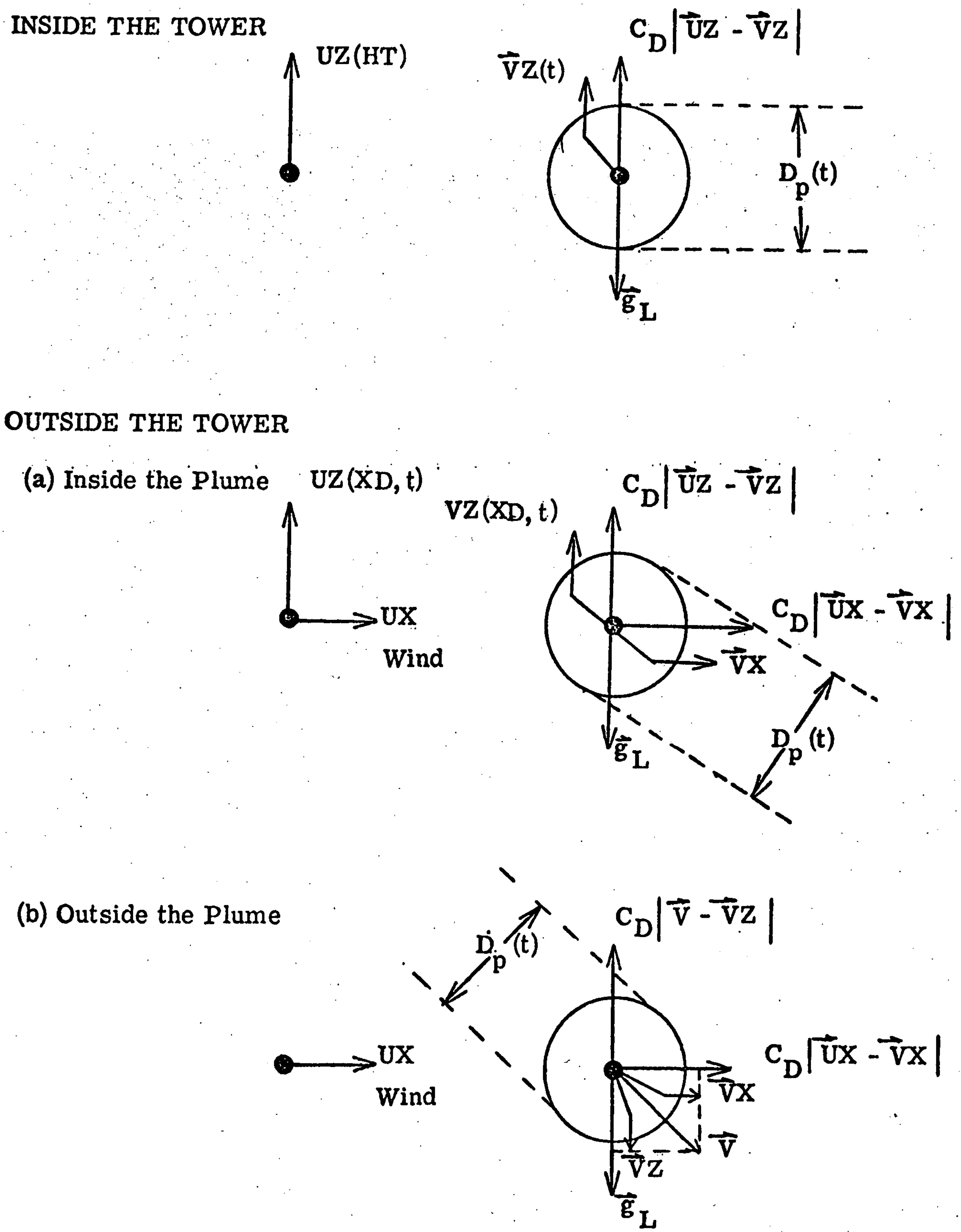

2.2 Application of the General Equations

(1) Inside the tower:

From top of drift eliminator to top of the tower.

Motion of a single drop in the gas flow fluid inside a cooling tower is given by:

$$\frac{d\vec{vz}}{dt} = -\left[g_c - \frac{3}{4} \frac{\rho_g}{\rho_L D_p} \cdot C_D \left| \vec{uz} - \vec{vz} \right| (\vec{uz} - \vec{vz}) \right]$$

Rate of growth and mass transfer to the drop surface is given by:

$$-\frac{dc}{dt} = \frac{3.0}{m_o^{1/3}} \cdot k_{xm} \cdot \frac{c^{4/3}}{\rho_L^{2/3}} \left(\frac{x_{Ai} - x_{A\infty}}{1 - x_{Ai}} \right)$$

where:

$$N_{Re} = \frac{D_p \left| \vec{uz} - \vec{vz} \right| \rho_g}{\mu g}$$

$$N_{Sc} = \left(\frac{\mu}{\rho \mathscr{D}_{AB}} \right)_g$$

$$k_{xm} = \frac{2 \cdot \rho_g \cdot \mathscr{D}_{AB}}{D_p} \left[1 + 0.3\, N_{Re}^{1/2}\, N_{Sc}^{1/3} \right]$$

and:

$$T_g - T_{drop} = \frac{\mathscr{D}_{AB} \cdot \mathscr{H}}{k_g} \cdot \Delta x_A \cdot \rho_g$$

$$HZ = \sum vz \cdot \Delta t$$

$$D_p = \left(\frac{6\, m_o}{\pi \rho_L \cdot c} \right)^{1/3}$$

(2) Outside the Tower

From top of the tower to the ground.

Motion of a single particle in the gas flow field inside the plume and/or in the ambient air:

$$\frac{d\vec{v}z}{dt} = -\left[\vec{g}_c - \frac{3}{4}\,\frac{\rho_g}{\rho_L D_p}\,C_D\,|\vec{u}z - \vec{v}z|\,(\vec{u}z - \vec{v}z)\right]$$

$$\frac{d\vec{v}x}{dt} = \frac{3}{4}\,\frac{\rho_g}{\rho_L D_p}\,C_{D_x}\,|\vec{u}x - \vec{v}x|\,(\vec{u}x - \vec{v}x)$$

Growth/ evaporation and mass transfer to/from the drop surface:

$$\frac{dc}{dt} = \frac{3.0}{m_o^{1/3}}\cdot k_{xm}\,\frac{c^{4/3}}{\rho_L^{2/3}}\left(\frac{x_{Ai} - x_{A\infty}}{1 - x_{Ai}}\right)$$

where:

$$N_{Rex} = \frac{D_p\,|\vec{u}x - \vec{v}x|\cdot\rho_g}{\mu_g}$$

$$N_{Rez} = \frac{D_p\,|\vec{u}z - \vec{v}z|\cdot\rho_g}{\mu_g}$$

$$N_{Sc} = \left(\frac{\mu}{\rho\mathscr{D}_{AB}}\right)_g$$

$$k_{xm} = \frac{2\,\rho_g\,\mathscr{D}_{AB}}{D_p}\left[1 + 0.3\,N_{Re}^{1/2}\cdot N_{Sc}^{1/3}\right]$$

and:

$$T - T_{drop} = \frac{\mathscr{D}_{AB}\mathscr{H}}{k_g}\cdot\Delta x_A\,\rho_g$$

$$HZ = \sum \vec{v}z \cdot \Delta t + HT$$

$$XD = \sum \vec{v}x \cdot \Delta t$$

$$\vec{u}x = \left(\frac{HZ}{HM}\right)^{SNZ} \cdot ux$$

$$D_p = \left(\frac{6\, m_o}{\pi \rho_L c}\right)^{1/3}$$

$$RP = 0.4\,(HP - HT) + SDIA/2$$

For Stable Low Wind Speeds ($\leq$ 6.0 mph)

$$HP = \left\{ C_n + (-1)^{n+1} \left[\frac{3\,(ux)^2}{\alpha^2 \cdot L^2 N^2} \left[(2n-1) + (-1)^n \cos \frac{N \cdot XD}{ux} \right] \right]^{1/3} \right\} \cdot L + HT, \quad (n = 1., 2., \ldots)$$

$$F = g_c Q_h / \pi \rho_a c_p T_a$$
$$\alpha \doteq .\ 0.4$$
$$L = F/ux = 6550./ux$$

$$N^2 = \frac{g_c}{T_a} \frac{d\theta_a}{dz} = 3.32 \times 10^{-4}$$

$$C_n = \left(\frac{24\,(ux)^2}{N^2 \alpha^2 L^2}\right)^{1/3} \sum_{p=1}^{n} (-1)^p (2p-2)^{1/3}, \quad n = 1, 2, \ldots$$

$$\vec{u}z = \frac{F}{RP^2 \cdot ux \cdot N} \cdot \sin\left(\frac{Nx}{ux}\right)$$

For all other wind speeds:

$$HP = \frac{26.7(XD)^{2/3}}{ux} + HT$$

$$\vec{u}z = 17.8\,XD^{-1/3}$$

2.3 Salt Deposition - Calculation Procedure

For each initial set of conditions (i.e., drop diameter, salt concentration, wind speed and stability group), the drop diameter, concentration, velocity (horizontal and vertical) and trajectory (HZ and XD, i.e., particle coordinates) are calculated as a function of time as the droplet travels from the top of the drift eliminators to the ground. The calculations consist in solving above set of simultaneous ordinary differential equations as a function of time. The solution is obtained by finite differences using the advancing technique (Runge-Kutta method).

The salt deposition at the ground versus distance from the tower for each set of parameters is obtained as follows:

1. At each selected distancee calculate $HZ/\sigma_z \Big|_{XD(N)}$
2. Look up area in normal probability distribution table.
3. Total salt deposition up to XD(N) = Pb(N) = 0.5 $\mp$ Area
   - upstream of salt drop axis on ground
   + downstream of salt drop axis on ground
4. Fraction of salt deposition between XD(N + 1) and XD(N) = Prob (N + 1, N) =
   = [Pb(N + 1) - Pb(N)] · PDIA
   where PDIA = mass fraction of drift drop D_p at top of tower.
5. Air concentration = VM = Prob (N + 1, N)/vz

The method is illustrated in Figures 2.3.1 and 2.3.2.

Figure 2.3.1

Method for Calculating Drift Droplet Deposition

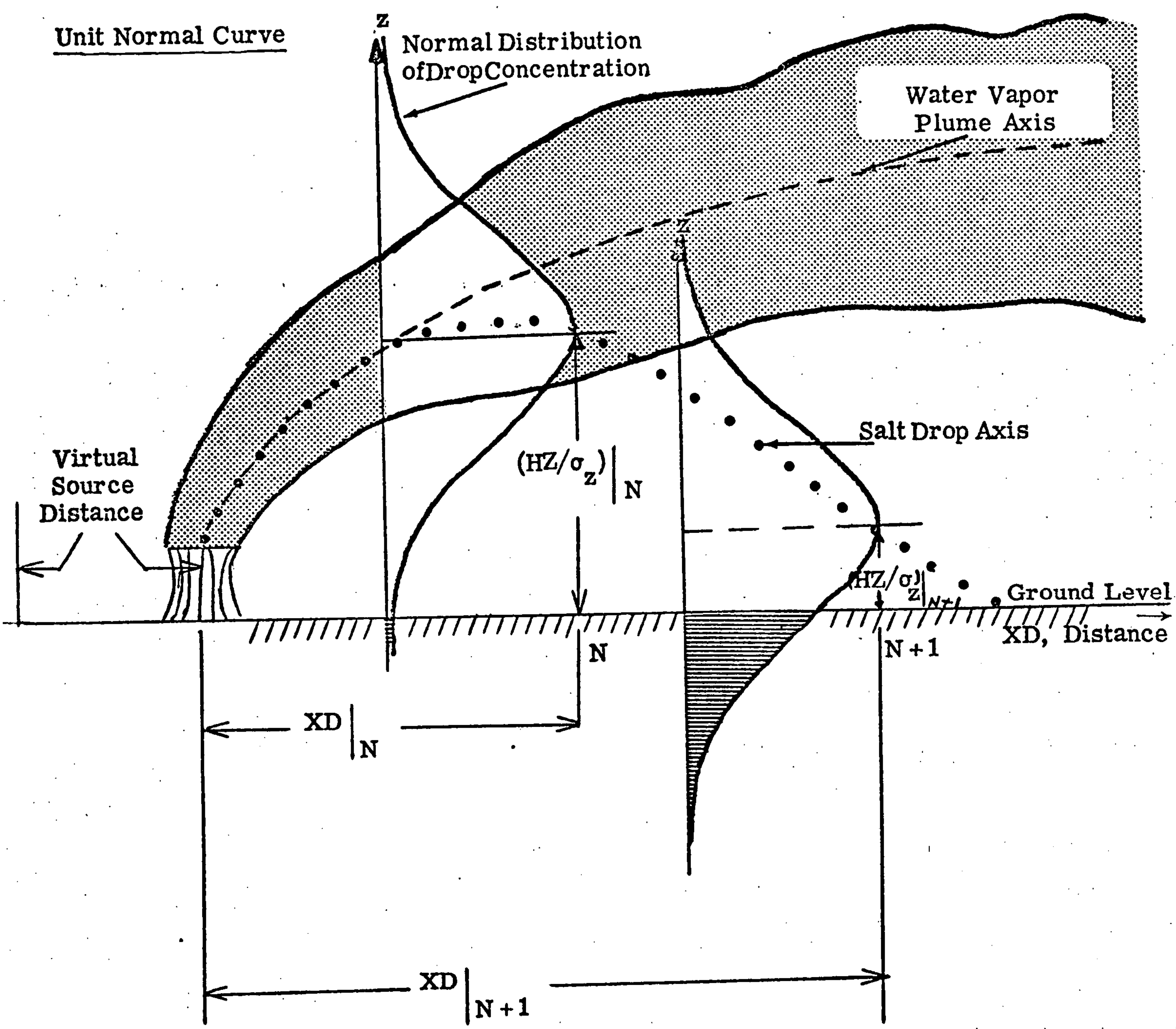

Figure 2. 3. 2

Cross Section of Concentration in the Vertical

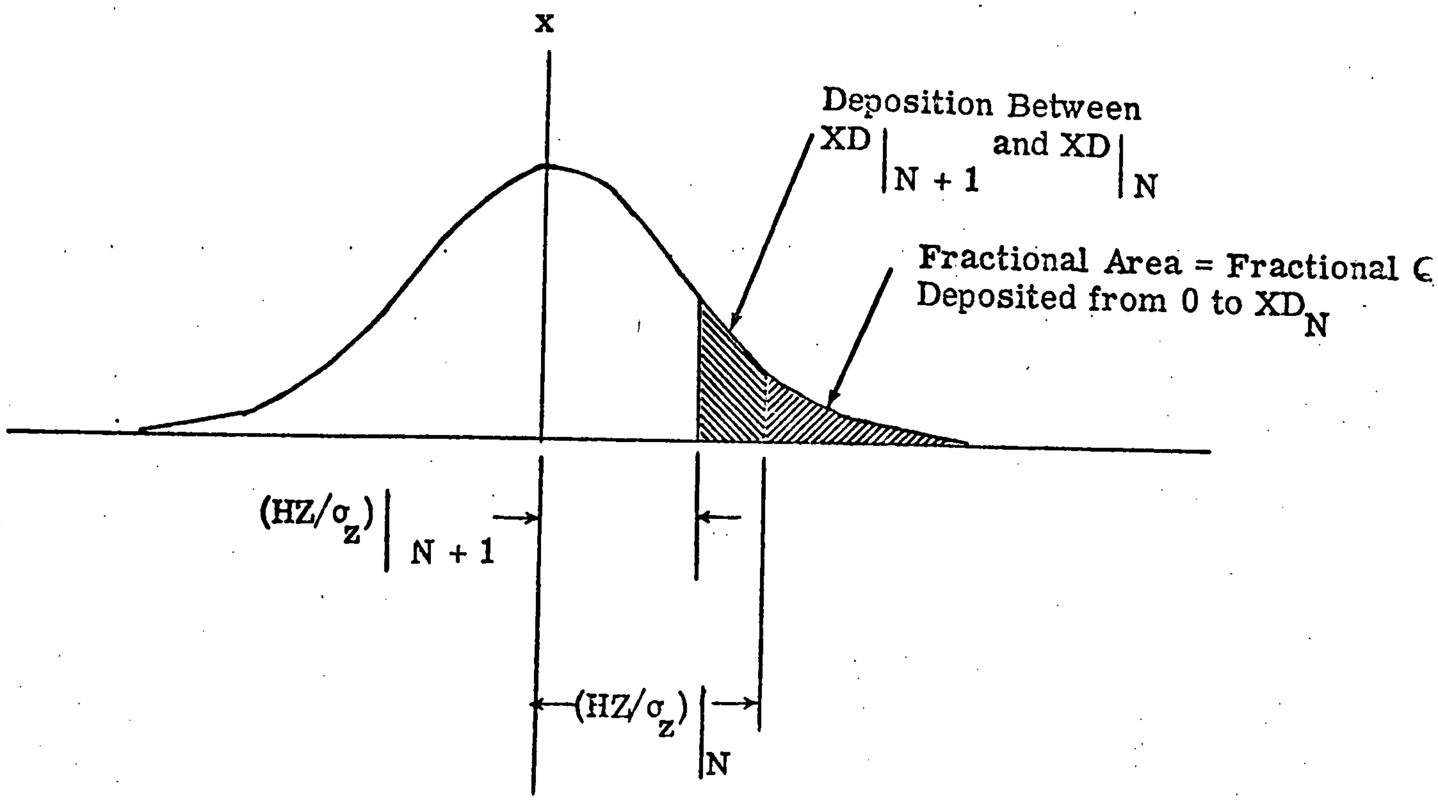

2.4 Assumptions

1. Relative humidity of air inside the tower is 100%.

2. Temperature of air inside tower (from top of drift eliminator to top of tower) remains constant.

3. No drop breakup or coalescence.

4. Inside the tower, horizontal component of velocity is zero.

5. Plume relative humidity varies as a function of ambient air relative humidity and downstream distance from tower.

6. Plume height is described by Slawson and Csanady's equation for stable low wind speeds (wind speeds $\leqq$ 6 mph) and by Brigg's equation for all other conditions.

7. Plume rise estimates assumed no buoyancy effect due to the release or recovery of latent heat (i.e., only sensible heat has been assumed).

8. Plume velocity is described by the derivative with respect to time, of the plume height equation. It applies between $\frac{dHP}{dt}$ = exit velocity to XD = 10 HT.

9. Viscosity, thermal conductivity, diffusion coefficient and Schmidt number remain constant.

2.5 Variables

Independent Variables

Tower height	=	HT
Tower diameter (top)	=	SDIA
Air flow rate through tower	=	Q
Salt concentration in basin	=	c_o
Ambient air temperature	=	T_{air}
Initial drop diameter	=	D_{po}
Ambient air relative humidity	=	RHA
Atmospheric pressure	=	PA
Horizontal wind speed	=	ux
Height of wind instrument	=	HM
Mass fraction of drift drop at tower top	=	FM
Diffusion Group		

Dependent Variables

Vapor pressure of drop solution = VPD

$$= 4.579\ (1 - 0.537c)\ \exp\left\{19.46 - \frac{5310}{273 + T_{drop}}\right\}$$

Mole fraction of drop solution in air $= \dfrac{VPD}{PA}$

Density of drop = ρ_L = f(c) = table of ρ_L versus c

Plume height = f (ux, XD, stability class) - given in section 5.B.2.2, page

Plume radius: for XD: $0 \rightarrow 10\,HT$, RP $= 0.4\ (HP - HT) + SDIA/2.$

$\geq 10\,HT$, $= 0$

Correction factor for wind speed = SNZ = f (stability group)

Dependent Variables (continued)

	Inside Tower	Plume	Ambient
Air vertical velocity $\overline{uz}$	f (Q, SDIA, HT)	$17.8\ ux^{-1/3}$	0
Air horizontal velocity	0	$\overline{ux}$ (HP, HM)	$\overline{ux}$ (HP, HM)
Air temperature	$T_g = f(T_{air}, RHA)$	$T_{gp} = f(T_a, RHA, XD)$	T_a (input)
Relative humidity	RHG (assumed = 100%)	RHP = f (RHA, XD)	RHA (input)
Partial pressure of water in air = $= \frac{RH}{100} \cdot 4.579 \exp\left\{19.46 - \frac{5310}{273 + T}\right\}$	P.P.G.	P.P.P.	P.P.A.
Density of air = $= 1/\left[(T + 273)\left(2.8311 + \frac{4.561 \cdot 18pp}{29(760 - PP)}\right)\right]$	ρ_g	ρ_{gp}	ρ_a
Mole fraction of water in air	PPG/PA	PPP/PA	PPA/PA
Diffusion coefficient of water in air = f(T)	$\mathscr{D}_{AB}$	$\mathscr{D}_{AB}$	$\mathscr{D}_{AB}$
Thermal conductivity of air	k	k	k
Viscocity of air = f(T)	μ	μ	μ
Latent heat of vaporization of drop solution = $f(T_{drop})$	$\mathscr{H}$	$\mathscr{H}$	$\mathscr{H}$
Temperature of drop	$T_g - T_{drop} = \frac{\mathscr{D}_{AB}\mathscr{H}}{k} \Delta x\ \rho_g$	$T_{gp} - T_{drop} = \frac{\mathscr{D}_{AB}\mathscr{H}}{k} \Delta x\ \rho_{gp}$	$T_a - T_{drop} = \frac{\mathscr{D}_{AB}\mathscr{H}}{k} \Delta x\ \rho_a$

2.6 Wind Interaction with Tower Wake

2.6.1 Physical Process Modeled

Wind tunnel test results[5] indicate that at wind speeds greater than 25 mph, tower effluents (plume) wake interactions would occur. These wake interactions were included by combining the wind tunnel experimental results with the model described in the previous section.

The wind tunnel ground concentration results apply to a vapor plume. In a salt laden plume, the saline droplets centerline (axis) are, at all distances, below the center of the vapor plume. In order to use the test results, it is necessary to adjust the ground concentration (obtained in ([5])) by calculating what the value would be if the plume were HZ meters above ground. The correction is based on a normal curve distribution with its axis at the indicated plume height obtained from the vertical profile in the wind tunnel tests. This was done for each drop diameter at two different group speeds and two different ambient relative humidities. The figure 2.6.1 illustrates the method. The calculational procedure is described below.

2.6.2 Calculational Procedure

1. Select a distance XD downwind from the tower.
2. Obtain the height of the plume centerline (axis), HZ, the concentration at the axis and ground concentration from the wind tunnel test results.
3. Normalize the values in 2, above, to a normal probability curve with its axis at the plume centerline (i.e., divide c_{axis} by a number such that $c_{axis,\ normalized} = 0.4$, divide c_{ground} by the same number to obtain $c_{ground,\ normalized}$ = ordinate).
4. In a normal probability table, look up the abscisa, HZ/σ, corresponding to the ground ordinate.
5. Calculate $\sigma = HZ/\text{abscissa}$.

6. Calculate HZ for each drop for the same ambient parameters (X, VX, stability group) using the method described in previous sections.
7. Calculate HZ/σ and look up in the normal probability table the ordinate corresponding to this abscisa. Call this ordinate $c_{g,d,n}$.
8. The ground concentration corresponding to a drop D_p at a distance XD, is:

$$c_{\text{ground, drop } D_p}\Big|_{XD} = \frac{c_{g,d,n}}{c_{g,n}} \cdot \frac{c}{c_o} \cdot \text{PDIA} \cdot c_o$$

where:

$\frac{c}{c_o}$ = experimental ground concentration fraction at XD for the ambient parameters

c_o = initial salt concentration in tower

PDIA = (mass) fraction of drift drop of size D_p at top of tower

Figure 2. 6. 1

Method for Calculating Ground Concentration Due to Tower Wake

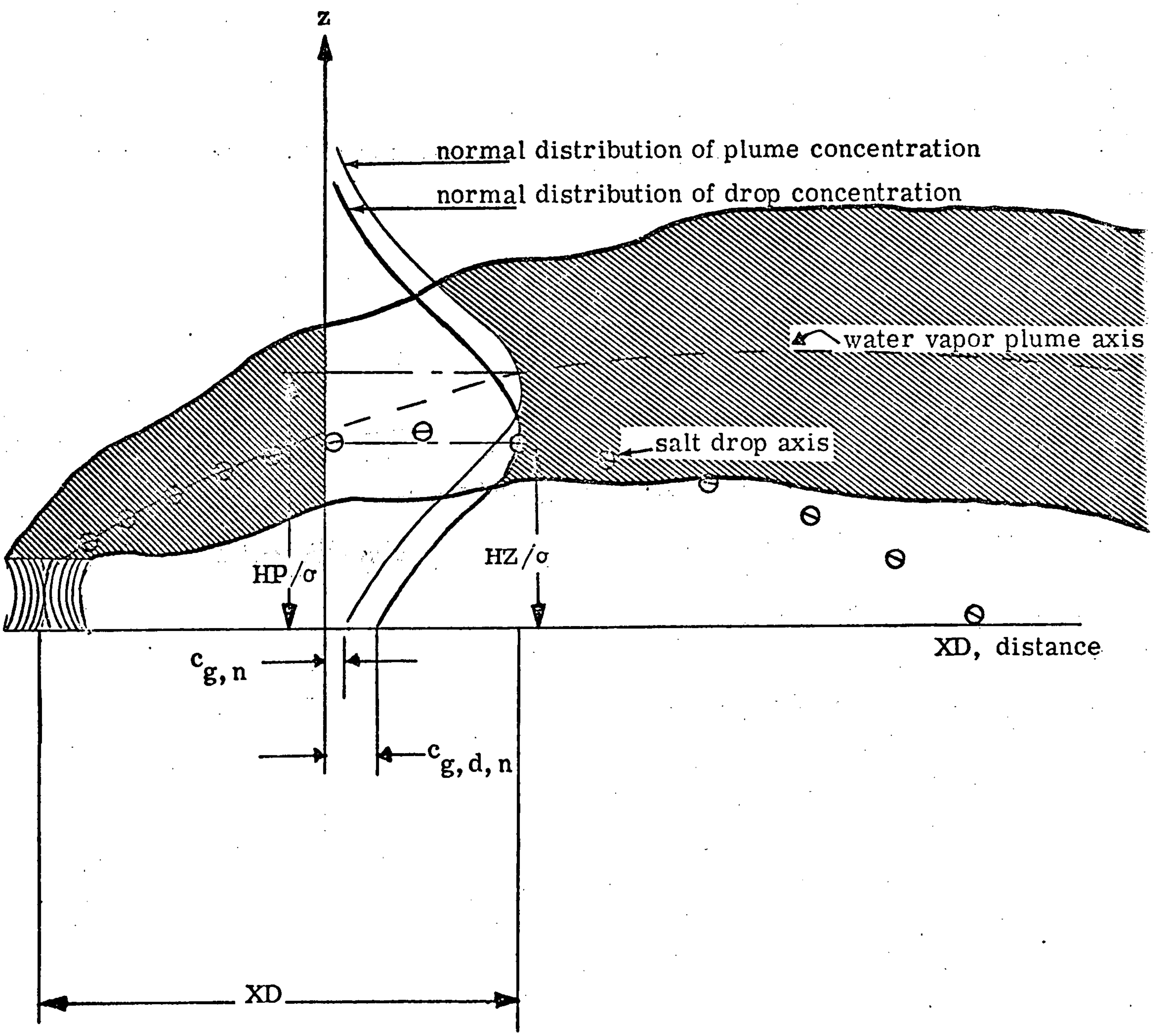

2.7 Salt Deposition - Virtual Source

The diffusion equation is for a point source. Since the cooling tower is not a point source, it is necessary to take horizontal distances (XD) from a virtual point source distance when determining values of σ_y and σ_z. The empirical correlation described below was derived from photograph observations of plume growth at the Paradise plant of TVA.

Salt Deposition-Virtual Source

Virtual source estimate for σ_z:

At 10 HT meters; $\pi(8\ RP_o)^2 = \pi ab$

where:

Stability class C	,	$a = 2b$
D	,	$a = 3b$
E	,	$a = 4b$

and:

$$\sigma_y = a/2 \quad , \quad \sigma_z = b/2$$

For example, for HT = 150 meters, and RP_o = 42 meters

	Virtual Source	Stability Class
XD =	-0.7 km	C
	-3.7 km	D
	-7.0 km	E

2.8 Washout by Rain

2.8.1 Mathematical Model

Definition of:

Washout: Scavenging of the salt drift droplet below the cloud level by falling rain, snowflakes, etc.

Collection Efficiency: Ratio of collision to geometric cross section. For drift drops, the collision efficiency of raindrops is unity.

Washout Coefficient: Fraction of horizontal area swept by rain in a unit time = $= \Lambda = \pi \sum nvr^2$

where: n = number of raindrops of radius r in a unit volume of air

v = fall speed of drops of radius r

Λ = f(RR), RR = rainfall rate

Removal of the drift drops is accomplished by collisions between rain drops and drift particles. The salt drift is then carried to the ground with the rain.

Total fraction drift in plume at any time t is given by:

$$\frac{Q}{Q_o} = \exp(-\Lambda t) = \exp\left(-\frac{\Lambda}{ux} \cdot XD\right)$$

Total fraction of drift deposited in ground, in annulus between $XD\Big|_N$ and $XD\Big|_{N+1}$:

$$FQ = \frac{TMR \cdot THR}{THM} \sum UFREQ \cdot$$

$$\cdot \sum FRR \cdot FHR \cdot \left[\exp\left[\frac{-\Lambda}{ux}(XD(N) - XD_o)\right] - \exp\left[\frac{-\Lambda}{ux}(XD(N+1) - XD_o\right]\right]$$

and:

$$XD_o = \frac{Hux}{w}$$

(Washout begins at the top of tower and does not reach the ground for some distance XD_o; i.e., XD_o represents displacement of horizontal scale)

where:

FQ = fraction of salt deposited in annulus between XD(N) and XD(N + 1)

H = initial height of plume centerline

ux = horizontal wind speed

w	=	fall velocity of rain $\simeq$ 6 m/sec
FRR	=	fraction of rainfall at the given rainfall rate
FHR	=	fraction of time that rain falls at the given rainfall rate
UFREQ	=	fraction frequency of occurrance of wind speed
TMR	=	total monthly rainfall
THR	=	total hours of rainfall per month
THM	=	total hours per month

$$SFQ = \sum_{RR} FRR \cdot FHR \left[\exp\left[-\frac{\Lambda}{ux} (XD(N)-XD_o) \right] - \exp\left[-\frac{\Lambda}{ux} (XD(N+1)-XD_o) \right] \right]$$

The total salt deposition in a given sector K is given by:

$$Q_{sector} = \frac{Q_o \cdot SFQ \cdot FRSEC(K)}{A}$$

where:

FRSEC(K)	=	fraction monthly rainfall in K sector
Q_o	=	salt drift rate
A	=	area of annulus between XD(N) and XD(N + 1)
Q_{sector}	=	salt deposition in sector K at a distance XD(N + 1) - XD(N) from center of tower

2.8.2 Calculational Procedure

Calculate SFQ for each of the different wind speeds as a function of distance from tower. Store as matrix SFQ versus ux versus distance.

Data Internal to Program

- Table .... RR vs Λ
- Table .... RR vs FRR
- Table .... RR vs FHR
- XD (Distance from tower)

2.9 Ice Formation

Ice accumulation may be caused by drift droplets impinging on surfaces at or below freezing. The rate at which ice accumulates on a surface depends on the drop diameter, the drift drop collection efficiency of the surface, the surface shape and dimension, and the meteorological conditions (i.e., wind speed and direction, relative humidity, stability, etc.).

Estimates of ice buildup vs time as a function of distance and direction from the tower are obtained using COOLER output with site hourly weather data, and is calculated as follows:

a) Ice accumulation on the ground ICYCLE 1

1. At each selected distance, the fraction of water deposited on the ground is obtained from COOLER, and is a function of drop diameter and meteorological conditions (wind speed, relative humidity, stability).
2. For each hour of weather data, and for ambient air ground level temperature $\leq 32\ ^{o}F$, the amount of salt and the water deposited are calculated at each distance and in the direction of the wind.
3. The freezing point depression is calculated at each distance. If $T_{ambient} \leq (32\ ^{o}F - \Delta T_f)$, the water deposited in the ground is assumed to freeze. That is, it is assumed that ground temperature is equal to ambient air ground level temperature.
4. Once freezing has occurred, the ice will be melted if during two consecutive hours the ambient air ground level temperature is $\geq 33\ ^{o}F$.
5. Output from the program are plots of ice accumulation vs time for selected distances for each of the 16 discrete sectors used to represent the compass.

b) Ice accumulation on structures ICYCLE 2

1. At each selected distance, the water air concentration fraction at ground level is obtained from COOLER, and is a function of drop diameter and meteorological conditions.
2. The mass of water deposited in an object of a given shape and dimension is calculated at each selected distance.

$m = \bar{u}x * \Sigma Q_d \alpha_{dD}$

where

$\bar{u}x$ = wind speed

Q_d = water air concentration due to a drop of diameter d at the distance under consideration, as a function of weather condition.

α_{dD} = collection efficiency of object of (cylindrical, ribbon) shape and dimension d for drop of diameter D_p.

3. The freezing point depression is calculated at each distance. If $T_{ambient} \leqq (32\ ^oF - \Delta T_f)$, the water deposited on the structure is assumed to freeze. That is, it is assumed that the structure temperature is equal to the ambient air ground level temperature.

4. Once freezing has occurred, the ice will be melted if for two consecutive hours the ambient air ground level temperature is $\geqq 33\ ^oF$.

5. Output from the program are plots of ice accumulation versus time for two different object shapes and three different object dimensions, at selected distances for each of the 16 discrete sectors used to represent the compass (360 ^{o}).

3.0 Outline of Computer Programs

In order to predict average salt deposition rates as a function of distance and direction from a cooling tower, three computer programs were developed:

COOLER: determines salt deposition rates and air concentration fractions versus distance from the cooling tower for each drop size as a function of weather conditions, i. e., wind speed, relative humidity, stability class and tower characteristics.

RAINDEP: estimates the washout by rain; gives salt fraction versus distance as a function of wind speed and rainfall. Described in Section 5. B. 2. 8. 2.

XQCOOL: uses COOLER and RAINDEP output with site hourly weather data in order to determine salt deposition rates and air salt concentrations as a function of distance and direction from the cooling tower.

SUMCOL: uses XQCOOL output to estimate salt deposition rates and airborne concentration of salt resulting from operation of several cooling towers.

In order to predict ice formation rate as a function of distance and direction from a natural draft cooling tower, two computer programs were developed.

ICYCLE 1: uses COOLER output with site hourly weather data in order to determine ice accumulation on the ground vs time at each of the 16 discrete sectors used to represent the compass at at selected distances from the cooling tower.

ICYCLE 2: uses COOLER output with site hourly weather data in order to determine ice accumulation on surfaces of cylindrical and ribbon type shapes and various dimensions versus time for each of the 16 discrete sectors used to represent the compass at selected distances from the cooling tower.

3.1 Outline of Computer Program - COOLER

Mode of Operation

1. Top of the drift eliminator to ground
2. Top of the drift eliminator to top of tower
3. Top of tower to ground
4. Outside plume to ground

Input Data Required

- PA
- c_o
- SDIA
- TA
- HT
- RHA
- DP
- Diffusion Group
- ux
- PDIA
- Terrain profile

Data Internal to Program

- Table .... ρ_L vs c
- Table .... uz vs HT
    - μA
    - kA
    - $\mathscr{D}_{AB}$
- Table .... T_g vs T_a
- Table .... RHP vs RHA vs XD
- Table .... (HZ/σ_z) vs Area (Normal Probability Distribution)

3.2 Outline of Computer Program - XQCOOL

Mode of Operation

Monthly Average: dry, wet, dry plus wet
Seasonal average: dry, wet, dry plus wet
Annual average: dry, wet, dry plus wet

Input Data Required

COOLER output: Drop size, distance from the tower, wind speed, relative humidity, stability group, salt deposition fraction, air salt concentration fraction.

RAINDEP output: salt fraction, distance from the tower, wind speed.

Q_O: salt drift from tower.

Site Meteorology at specified height: hourly data for wind speed, wind direction, relative humidity, temperature (dry bulb and dew point), rainfall, hours of rainfall.

Tower characteristics

Selection of: Pasquill stability class definition, stability group with wind speed, treatment of calms, type of output desired.

Data Internal to Program

- Table.......... Pasquill Stability Class vs. Ambient Temperature vs. Wind Speed
- Table.......... Calm Selector (Selection on treatment of Calm Hours)
- Table........... Site Boundary
- Calculation Procedure for Generation of Isopleths
- Selector switches for type and form of output desired.

Output

- Isopleths of salt deposition rates and air salt concentrations versus distance at desired distances from the tower for the selected time period (month, season, annual) and conditions (wet, dry, wet plus dry).
- Tables of joint frequency of occurrence of weather data.

3.2..1. Calculational Procedure - Dry Deposition

1. For each characteristic drop diameter, wind speed, ambient relative humidity and diffusion group, salt deposition rate and air salt concentration fractions are estimated by COOLER and RAINDEP (described in previous sections).

2. Summation over drop diameter, gives total deposition versus distance from the tower as a function of wind speed, relative humidity and stability group.

3. Each hour of the year relates to one of the groups in (2) with addition of wind direction, i.e, each hour of the year specifies the direction [i.e., rector annulus] in which salt will be deposited.

4. For each of the 16 sectors considered, the monthly, seasonal and yearly deposition rate (as M/L^2 - month) and air salt concentration (M/L^3) is obtained by the summation over the various wind speeds, relative humidity and diffusion groups, multiplied by Q_o/(annulus area - number of months) as a function of distance from the tower.

For each sector:

$$\frac{Q_o}{\text{Annulus Area}} \sum_{\substack{\vec{u}x,\,RHA\\ \text{month}}} \sum_{D_p} \text{Prob}(N) = \begin{array}{l}\text{Monthly Average Deposition rate}\\ \text{in sector, } k_g/(\text{km}^2 \text{ - month})\end{array}$$

$$\begin{array}{l}\text{Season Ave.}\\ \text{Deposition}\\ \text{Rate}\end{array} = \frac{\sum \text{monthly deposition}}{\text{months in season}} \;,\; k_g/(\text{km}^2 \text{ - month})$$

$$\begin{array}{l}\text{Yearly Ave.}\\ \text{Deposition}\\ \text{Rate}\end{array} = \frac{\sum \text{monthly deposition}}{12} \;,\; k_g/(\text{km}^2 \text{ - month})$$

Similarly, for ground air concentration:

$$\frac{Qo}{\text{Annulus Area}} \sum_{\substack{ux,\ RHA \\ month}} \sum_{D_{p_o}} \frac{V\ \text{Prob}\ (N)}{\text{Total hours of month}} = \begin{array}{l}\text{monthly average} \\ \text{air concentration,} \\ \mu g/m^3\end{array}$$

$$\begin{array}{l}\text{Seasonal Average Air} \\ \text{Concentration, } \mu g/m^3\end{array} = \frac{\sum \text{Monthly Air Concentration}}{\text{No. Months in Season}}$$

$$\begin{array}{l}\text{Annual Average Air} \\ \text{Concentration, } \mu g/m^3\end{array} = \frac{\sum \text{Monthly Air Concentration}}{12}$$

3.2.2 Wet Deposition - Calculational Procedure

1. Calculate SFQ for each of the different wind speeds as a function of distance from tower. Store as matrix SFQ versus ux versus distance.
2. For each hour of rain, relate to corresponding wind speed in SFQ matrix, and introduce wind direction.
3. Multiply SFQ by the hourly rainfall and divide by total hours of the month.
4. Summation of step 3 for each month period, in each direction, gives salt deposition in each sector.

<u>Output</u>

Isopleths of salt deposition as a function of distance from the tower.

3.3 Computer Simulations

3.3.1 Parametric Study

$$D_p = f\,(T_a\,,\ \text{RHA, Stability Group, ux, HZ})$$

3.3.2 Correlate Drop Size (Salt Concentration) with Weather Data

Wind Speed (mph)	Representative Wind	Stability Classes	Direction	Temperature	Relative Humidity
0-3	ux = 1.0 m/sec	C, D, E	16 S	72°F	>75, 90% ≦75, 65%
4-6	ux = 2.3 m/sec	C, D, E	16 S	72°F	>75, 90% ≦75, 65%
7-9	ux = 3.5 m/sec	C, D, E	16 S	72°F	>75, 90% ≦75, 65%
10-12	ux = 5.0 m/sec	C, D, E	16 S	72°F	>75, 90% ≦75, 65%
13-18	ux = 7.0 m/sec	D	16 S	72°F	>75, 90% ≤75, 65%
19-25	ux =10.0 m/sec	D	16S	72°F	>75, 90% ≤75, 65%
26-32[1]	ux=13.0 m/sec	D	16S	72°F	>75, 90% ≤75, 65%
≥33[1]	ux-16.0 m/sec	D	16S	72°F	>75, 90% ≤75, 65%

[1] Wake condition also included.

3.3.3 Sensitivity Studies

3.3.3.1 Effect of Drop Size and Mass Drop Size Distribution

3.3.3.2 Effect of Wind Speed Grouping for Low Wind Speeds

3.3.3.3 Effect of Stability Group Definition

3.3.3.4 Effect of Relative Humidity

3.3.3.5 Effect of Tower Height

3.3.3.6 Effect of Basin Salt Concentration

3.3.3.7 Effect of Reference Location for Drop Size Measurements

3.3.3.8 Effect of Plume Rise

3.3.3.9 Effect of Temperature

These studies have been summarized in Reference 6.

NOMENCLATURE

c	=	salt concentration in drop, dimensionless
c_p	=	specific heat H/M-T
C_D	=	drag coefficient, dimensionless
D_p	=	drop diameter, L
$\mathscr{D}_{AB}$	=	diffusion coefficient of water vapor-air, L^2/t
F	=	flux of buoyancy, L^4/t
g_c	=	gravitational conversion factor, M-L/(mass force - t^2)
g_L	=	gravity force, L/t^2
HT	=	tower height, L
HP	=	plume height, L
HZ	=	vertical distance of drop (i.e., drop height), L
$\mathscr{H}$	=	latent heat, H/M
k_{xm}	=	mass transfer coefficient, M/L^2t
k	=	thermal conductivity, H/LtT
L	=	buoyancy length scale, L
m_o	=	mass of salt in drop, M
m	=	mass of water in drop, M
N_{RE}	=	Reynold's number, dimensionless
N_{sc}	=	Schmidt number, dimensionless
PDIA	=	(mass) fraction of drift drop of size D_p at top of tower dimensionless, n
PA	=	atmospheric pressure, p
PP( )	=	partial pressure of water in air; ( ) = g = inside tower gp = inside plume a = ambient air
Q_o	=	salt rate from tower, M/t
Q_H	=	sensible heat flux at the tower, H/t
RP	=	radius of the plume, L
SDIA	=	tower diameter, L
$T_{( )}$	=	temperature, ( ) = g = air inside tower p = air inside plume a = ambient air drop = drop = absolute

VPD	=	vapor pressure of drop solution, P
x_{Ao}, x_{Ai}	=	mole fraction of drop solution in air = VPD/PA, dimensionless
$x_{A\infty}$	=	mole fraction of water in air = PP( )/PA, dimensionless
ΔXA	=	$(x_{Ai} - x_{A\infty})/(1 - x_{Ai})$, dimensionless
α	=	entrainment constant
Θ	=	sector

REFERENCES

1. Slawson, P. R. and Csanady, G. T., Journal of Fluid Mechanics, 47, Part 1, pp. 33-44, (1971)

2. Briggs, G. A., "Plume Rise", U. S. Atomic Energy Commission, Division of Technical Information, TID-25075, (1969)

3. Slawson, P. R. and Csanady, G. T., Journal of Fluid Mechanics, 47, p. 37.

4. Ranz, W. E., and Marshall, W. R., Jr., Chemical Engineering Progress, 48, No. 3, 4, pp. 141-152 and pp. 173-180 respectively, (1952)

5. Forked River Nuclear Station, Unit 1, Jersey Central Power & Light Company, Applicant's Environmental Report (1972)

6. Laskowski, S.M., "A Mathematical Transport Model for Salt Distribution from a Salt Water-Natural Draft Cooling Tower, Part II," presented at the Symposium on Atmospheric Diffusion and Air Pollution, sponsored by the American Meteorological Society, Santa Barbara, California, September, 1974.

Appendix C

SITE SPECIFIC INFORMATION FOR COOLING TOWER ANALYSES

This appendix contains information relative to the specific site and cooling tower configuration being evaluated. The contents are listed below.

Tables

Figures

Table 1

Joint Frequency of Occurrence of 400 ft and 33 ft Wind Speed, Wind Direction, Relative Humidity, Ambient Temperature and Stability
Based on Indian Point 4 Tower Data from October, 1973 through September, 1974

ALL DELTA TEMPERATURE GROUPS (400 ft)

RELATIVE HUMIDITY GREATER THAN 0.0 AND LESS THAN OR EQUAL TO 60.0
AMBIENT TEMPERATURE GREATER THAN 0.0 AND LESS THAN OR EQUAL TO 30.0

SPEED	N	NNE	NE	ENE	E	ESE	SE	SSE	S	SSW	SW	WSW	W	WNW	NW	NNW	TOTAL
0	0	0	0	0	0	0	0	0	0	0	0	0	0	0	0	0	0
1-3	17	5	7	8	4	1	1	4	11	7	9	3	4	2	9	3	95
4-7	30	39	27	6	2	0	1	0	0	13	9	0	2	8	37	44	218
8-12	18	14	7	0	0	0	0	0	0	0	0	0	0	4	40	38	121
13-18	0	0	0	0	0	0	0	0	0	0	0	0	0	0	7	2	9
19-24	0	0	0	0	0	0	0	0	0	0	0	0	0	0	0	0	0
25-32	0	0	0	0	0	0	0	0	0	0	0	0	0	0	0	0	0
32+	0	0	0	0	0	0	0	0	0	0	0	0	0	0	0	0	0
TOTAL	65	58	41	14	6	1	2	4	11	20	18	3	6	14	93	87	443

RELATIVE HUMIDITY GREATER THAN 0.0 AND LESS THAN OR EQUAL TO 60.0
AMBIENT TEMPERATURE GREATER THAN 30.0 AND LESS THAN OR EQUAL TO 45.0

SPEED	N	NNE	NE	ENE	E	ESE	SE	SSE	S	SSW	SW	WSW	W	WNW	NW	NNW	TOTAL
0	0	0	0	0	0	0	0	0	0	0	0	0	0	0	0	0	0
1-3	40	1	12	7	3	1	3	4	10	14	16	9	13	13	6	8	160
4-7	51	51	26	1	1	0	0	1	16	21	21	9	14	39	63	41	355
8-12	33	22	6	0	0	0	0	0	1	6	2	3	8	41	108	89	319
13-18	5	0	1	0	0	0	0	0	0	0	0	0	0	5	30	19	60
19-24	1	0	0	0	0	0	0	0	0	0	0	0	0	0	1	0	2
25-32	0	0	0	0	0	0	0	0	0	0	0	0	0	0	0	0	0
32+	0	0	0	0	0	0	0	0	0	0	0	0	0	0	0	0	0
TOTAL	130	74	45	8	4	1	3	5	27	41	39	21	35	98	208	157	896

RELATIVE HUMIDITY GREATER THAN 0.0 AND LESS THAN OR EQUAL TO 60.0
AMBIENT TEMPERATURE GREATER THAN 45.0 AND LESS THAN OR EQUAL TO 60.0

SPEED	N	NNE	NE	ENE	E	ESE	SE	SSE	S	SSW	SW	WSW	W	WNW	NW	NNW	TOTAL
0	0	0	0	0	0	0	0	0	0	1	0	0	0	0	0	0	1
1-3	34	6	14	5	3	4	4	0	40	15	17	6	11	12	13	7	191
4-7	44	37	32	6	5	1	1	4	30	30	21	10	18	32	39	37	347
8-12	9	20	2	0	0	0	0	0	1	14	16	6	11	18	48	47	192
13-18	0	0	0	0	0	0	0	0	0	1	1	0	1	3	16	7	29
19-24	0	0	0	0	0	0	0	0	0	0	0	0	0	0	1	0	1
25-32	0	0	0	0	0	0	0	0	0	0	0	0	0	0	0	0	0
32+	0	0	0	0	0	0	0	0	0	0	0	0	0	0	0	0	0
TOTAL	87	63	48	11	8	5	5	4	71	61	55	22	41	65	117	98	761

RELATIVE HUMIDITY GREATER THAN 0.0 AND LESS THAN OR EQUAL TO 60.0
AMBIENT TEMPERATURE GREATER THAN 60.0 AND LESS THAN OR EQUAL TO999.0

SPEED	N	NNE	NE	ENE	E	ESE	SE	SSE	S	SSW	SW	WSW	W	WNW	NW	NNW	TOTAL
0	0	0	0	0	0	0	0	0	0	0	0	0	0	0	0	0	0
1-3	41	34	10	6	4	5	5	11	46	41	28	19	33	16	19	12	330
4-7	43	76	32	15	7	2	0	6	59	79	82	30	34	36	37	28	566
8-12	1	10	9	1	0	0	0	0	1	18	24	11	3	2	17	11	108
13-18	1	0	0	0	0	0	0	0	0	0	3	0	0	1	3	1	9
19-24	0	0	0	0	0	0	0	0	0	0	0	0	0	0	0	0	0
25-32	0	0	0	0	0	0	0	0	0	0	0	0	0	0	0	0	0
32+	0	0	0	0	0	0	0	0	0	0	0	0	0	0	0	0	0
TOTAL	86	120	51	22	11	7	5	17	106	138	137	60	70	55	76	52	1013

Table 1, continued

ALL DELTA TEMPERATURE GROUPS (400 ft)

RELATIVE HUMIDITY GREATER THAN 60.0 AND LESS THAN OR EQUAL TO 85.0
AMBIENT TEMPERATURE GREATER THAN 0.0 AND LESS THAN OR EQUAL TO 30.0

SPEED	N	NNE	NE	ENE	E	ESE	SE	SSE	S	SSW	SW	WSW	W	WNW	NW	NNW	TOTAL
0	1	0	0	0	0	0	0	0	0	0	0	0	0	0	0	0	1
1-3	21	19	27	9	9	6	4	3	8	18	23	7	4	6	2	4	170
4-7	18	73	65	12	0	0	0	0	0	10	6	0	0	7	22	9	222
8-12	4	62	9	0	0	0	0	0	0	0	0	0	0	2	11	6	94
13-18	0	3	0	0	0	0	0	0	0	0	0	0	0	0	1	3	7
19-24	0	0	0	0	0	0	0	0	0	0	0	0	0	0	0	0	0
25-32	0	0	0	0	0	0	0	0	0	0	0	0	0	0	0	0	0
32+	0	0	0	0	0	0	0	0	0	0	0	0	0	0	0	0	0
TOTAL	44	157	101	21	9	6	4	3	8	28	29	7	4	15	36	22	494

RELATIVE HUMIDITY GREATER THAN 60.0 AND LESS THAN OR EQUAL TO 85.0
AMBIENT TEMPERATURE GREATER THAN 30.0 AND LESS THAN OR EQUAL TO 45.0

SPEED	N	NNE	NE	ENE	E	ESE	SE	SSE	S	SSW	SW	WSW	W	WNW	NW	NNW	TOTAL
0	1	0	0	0	0	0	0	0	1	0	1	0	0	0	0	0	3
1-3	54	26	36	17	11	3	7	16	18	20	24	11	20	8	3	5	279
4-7	20	31	48	23	6	3	5	3	5	10	5	4	1	9	16	17	206
8-12	6	26	20	4	0	0	0	0	0	0	0	3	2	2	26	9	98
13-18	0	0	3	0	0	0	0	0	0	0	0	0	0	0	6	3	12
19-24	0	0	0	0	0	0	0	0	0	0	0	0	0	0	0	0	0
25-32	0	0	0	0	0	0	0	0	0	0	0	0	0	0	0	0	0
32+	0	0	0	0	0	0	0	0	0	0	0	0	0	0	0	0	0
TOTAL	81	83	107	44	17	6	12	19	24	30	30	18	23	19	51	34	598

RELATIVE HUMIDITY GREATER THAN 60.0 AND LESS THAN OR EQUAL TO 85.0
AMBIENT TEMPERATURE GREATER THAN 45.0 AND LESS THAN OR EQUAL TO 60.0

SPEED	N	NNE	NE	ENE	E	ESE	SE	SSE	S	SSW	SW	WSW	W	WNW	NW	NNW	TOTAL
0	0	0	0	0	0	1	0	0	0	0	0	1	0	0	0	0	2
1-3	32	19	50	34	15	11	8	17	37	19	29	17	14	7	4	5	318
4-7	16	45	87	41	13	5	2	3	9	18	12	3	3	10	12	11	290
8-12	2	8	15	3	1	0	0	0	1	4	6	1	1	4	4	4	54
13-18	0	0	0	0	0	0	0	0	0	0	0	0	0	0	2	1	3
19-24	0	0	0	0	0	0	0	0	0	0	0	0	0	0	0	0	0
25-32	0	0	0	0	0	0	0	0	0	0	0	0	0	0	0	0	0
32+	0	0	0	0	0	0	0	0	0	0	0	0	0	0	0	0	0
TOTAL	50	72	152	78	29	17	10	20	47	41	47	22	18	21	22	21	667

RELATIVE HUMIDITY GREATER THAN 60.0 AND LESS THAN OR EQUAL TO 85.0
AMBIENT TEMPERATURE GREATER THAN 60.0 AND LESS THAN OR EQUAL TO999.0

SPEED	N	NNE	NE	ENE	E	ESE	SE	SSE	S	SSW	SW	WSW	W	WNW	NW	NNW	TOTAL
0	0	1	1	0	0	0	0	0	0	0	0	0	0	0	0	0	2
1-3	78	47	54	34	22	14	21	27	80	115	112	41	23	9	6	5	688
4-7	14	62	88	22	7	6	1	2	28	82	77	10	10	10	2	0	421
8-12	1	7	12	0	0	0	0	0	0	4	34	0	1	0	2	0	61
13-18	0	0	0	0	0	0	0	0	0	0	0	0	0	0	0	0	0
19-24	0	0	0	0	0	0	0	0	0	0	0	0	0	0	0	0	0
25-32	0	0	0	0	0	0	0	0	0	0	0	0	0	0	0	0	0
32+	0	0	0	0	0	0	0	0	0	0	0	0	0	0	0	0	0
TOTAL	93	117	155	56	29	20	22	29	108	201	223	51	34	19	10	5	1172

Table 1, continued

ALL DELTA TEMPERATURE GROUPS (400 ft)

RELATIVE HUMIDITY GREATER THAN 85.0 AND LESS THAN OR EQUAL TO 95.0
AMBIENT TEMPERATURE GREATER THAN 0.0 AND LESS THAN OR EQUAL TO 30.0

SPEED	N	NNE	NE	ENE	E	ESE	SE	SSE	S	SSW	SW	WSW	W	WNW	NW	NNW	TOTAL
0	1	0	0	0	0	0	0	0	0	0	0	0	0	0	0	0	1
1-3	10	13	10	3	2	1	1	1	2	0	4	0	1	0	1	0	49
4-7	4	30	27	0	0	0	0	0	0	0	0	0	0	0	0	0	61
8-12	0	26	4	0	0	0	0	0	0	0	0	0	0	0	1	0	31
13-18	0	13	2	0	0	0	0	0	0	0	0	0	0	0	0	0	15
19-24	0	2	1	0	0	0	0	0	0	0	0	0	0	0	0	0	3
25-32	0	0	0	0	0	0	0	0	0	0	0	0	0	0	0	0	0
32+	0	0	0	0	0	0	0	0	0	0	0	0	0	0	0	0	0
TOTAL	15	84	44	3	2	1	1	1	2	0	4	0	1	0	2	0	160

RELATIVE HUMIDITY GREATER THAN 85.0 AND LESS THAN OR EQUAL TO 95.0
AMBIENT TEMPERATURE GREATER THAN 30.0 AND LESS THAN OR EQUAL TO 45.0

SPEED	N	NNE	NE	ENE	E	ESE	SE	SSE	S	SSW	SW	WSW	W	WNW	NW	NNW	TOTAL
0	4	0	0	0	0	0	0	0	0	0	0	0	0	0	0	0	4
1-3	32	16	30	2	3	3	1	8	4	1	4	0	0	0	3	1	108
4-7	9	28	34	16	0	0	1	0	0	1	0	0	0	0	1	1	91
8-12	5	11	19	3	0	0	0	0	0	0	0	0	0	0	1	0	39
13-18	0	0	0	0	0	0	0	0	0	0	0	0	0	0	0	0	0
19-24	0	0	0	0	0	0	0	0	0	0	0	0	0	0	0	0	0
25-32	0	0	0	0	0	0	0	0	0	0	0	0	0	0	0	0	0
32+	0	0	0	0	0	0	0	0	0	0	0	0	0	0	0	0	0
TOTAL	50	55	83	21	3	3	2	8	4	2	4	0	0	0	5	2	242

RELATIVE HUMIDITY GREATER THAN 85.0 AND LESS THAN OR EQUAL TO 95.0
AMBIENT TEMPERATURE GREATER THAN 45.0 AND LESS THAN OR EQUAL TO 60.0

SPEED	N	NNE	NE	ENE	E	ESE	SE	SSE	S	SSW	SW	WSW	W	WNW	NW	NNW	TOTAL
0	0	0	0	0	0	0	0	0	0	0	0	0	0	0	0	0	0
1-3	37	21	53	28	13	6	7	14	25	17	15	2	0	5	4	2	249
4-7	2	17	71	24	1	1	1	2	12	9	3	3	1	0	0	0	147
8-12	0	5	6	5	1	0	0	0	2	4	0	0	0	0	0	0	23
13-18	0	0	0	2	0	0	0	0	0	1	0	0	0	0	0	0	3
19-24	0	0	0	0	0	0	0	0	0	0	0	0	0	0	1	0	1
25-32	0	0	0	0	0	0	0	0	0	0	0	0	0	0	0	0	0
32+	0	0	0	0	0	0	0	0	0	0	0	0	0	0	0	0	0
TOTAL	39	43	130	59	15	7	8	16	39	31	18	5	1	5	5	2	423

RELATIVE HUMIDITY GREATER THAN 85.0 AND LESS THAN OR EQUAL TO 95.0
AMBIENT TEMPERATURE GREATER THAN 60.0 AND LESS THAN OR EQUAL TO999.0

SPEED	N	NNE	NE	ENE	E	ESE	SE	SSE	S	SSW	SW	WSW	W	WNW	NW	NNW	TOTAL
0	1	0	0	0	0	0	0	0	0	0	0	0	0	0	0	0	1
1-3	42	17	49	32	17	9	13	16	37	51	42	14	9	5	4	2	359
4-7	2	10	64	20	1	0	1	0	3	24	18	1	0	1	0	2	147
8-12	0	6	8	0	0	0	0	0	0	1	0	0	0	0	0	0	15
13-18	0	0	0	0	0	0	0	0	0	0	0	0	0	0	0	0	0
19-24	0	0	0	0	0	0	0	0	0	0	0	0	0	0	0	0	0
25-32	0	0	0	0	0	0	0	0	0	0	0	0	0	0	0	0	0
32+	0	0	0	0	0	0	0	0	0	0	0	0	0	0	0	0	0
TOTAL	45	33	121	52	18	9	14	16	40	76	60	15	9	6	4	4	522

Table 1, continued

ALL DELTA TEMPERATURE GROUPS (400 ft)

RELATIVE HUMIDITY GREATER THAN 95.0 AND LESS THAN OR EQUAL TO 999.0
AMBIENT TEMPERATURE GREATER THAN 0.0 AND LESS THAN OR EQUAL TO 30.0

SPEED	N	NNE	NE	ENE	E	ESE	SE	SSE	S	SSW	SW	WSW	W	WNW	NW	NNW	TOTAL
0	0	0	0	0	0	0	0	0	0	0	0	0	0	0	0	0	0
1-3	1	9	9	2	4	2	0	0	0	1	1	0	1	0	1	0	31
4-7	0	7	15	1	0	0	0	0	0	1	0	0	0	0	0	0	24
8-12	0	2	0	0	0	0	0	0	0	0	0	0	0	0	1	0	3
13-18	0	0	0	0	0	0	0	0	0	0	0	0	0	0	0	0	0
19-24	0	0	0	0	0	0	0	0	0	0	0	0	0	0	0	0	0
25-32	0	0	0	0	0	0	0	0	0	0	0	0	0	0	0	0	0
32+	0	0	0	0	0	0	0	0	0	0	0	0	0	0	0	0	0
TOTAL	1	18	24	3	4	2	0	0	0	2	1	0	1	0	2	0	58

RELATIVE HUMIDITY GREATER THAN 95.0 AND LESS THAN OR EQUAL TO 999.0
AMBIENT TEMPERATURE GREATER THAN 30.0 AND LESS THAN OR EQUAL TO 45.0

SPEED	N	NNE	NE	ENE	E	ESE	SE	SSE	S	SSW	SW	WSW	W	WNW	NW	NNW	TOTAL
0	0	0	0	0	0	0	0	0	0	0	0	0	0	0	1	0	1
1-3	39	13	20	8	7	3	7	12	9	10	10	12	8	4	2	5	169
4-7	3	9	7	6	0	1	0	1	0	0	0	1	1	0	0	0	29
8-12	1	1	1	0	0	0	0	0	0	0	0	0	1	0	0	0	4
13-18	1	0	0	0	0	0	0	0	0	0	0	0	0	0	1	0	2
19-24	0	0	0	0	0	0	0	0	0	0	0	0	0	0	0	0	0
25-32	0	0	0	0	0	0	0	0	0	0	0	0	0	0	0	0	0
32+	0	0	0	0	0	0	0	0	0	0	0	0	0	0	0	0	0
TOTAL	44	23	28	14	7	4	7	13	9	10	10	13	10	4	4	5	205

RELATIVE HUMIDITY GREATER THAN 95.0 AND LESS THAN OR EQUAL TO 999.0
AMBIENT TEMPERATURE GREATER THAN 45.0 AND LESS THAN OR EQUAL TO 60.0

SPEED	N	NNE	NE	ENE	E	ESE	SE	SSE	S	SSW	SW	WSW	W	WNW	NW	NNW	TOTAL
0	0	0	0	0	0	0	0	0	0	0	0	0	0	0	0	0	0
1-3	38	21	18	12	3	6	9	11	39	11	11	6	4	3	2	2	196
4-7	3	2	7	5	0	2	0	1	7	10	1	1	1	0	0	1	41
8-12	0	0	1	1	0	1	0	0	1	9	0	0	0	0	0	0	13
13-18	0	0	0	0	0	0	0	0	0	0	0	0	0	0	0	0	0
19-24	0	0	0	0	0	0	0	0	0	0	0	0	0	0	0	0	0
25-32	0	0	0	0	0	0	0	0	0	0	0	0	0	0	0	0	0
32+	0	0	0	0	0	0	0	0	0	0	0	0	0	0	0	0	0
TOTAL	41	23	26	18	3	9	9	12	47	30	12	7	5	3	2	3	250

RELATIVE HUMIDITY GREATER THAN 95.0 AND LESS THAN OR EQUAL TO 999.0
AMBIENT TEMPERATURE GREATER THAN 60.0 AND LESS THAN OR EQUAL TO999.0

SPEED	N	NNE	NE	ENE	E	ESE	SE	SSE	S	SSW	SW	WSW	W	WNW	NW	NNW	TOTAL
0	0	0	0	0	0	0	0	0	0	0	0	0	0	0	0	0	0
1-3	29	7	28	24	15	7	16	11	25	30	18	8	2	1	2	4	227
4-7	1	4	10	2	1	0	0	0	1	11	7	0	0	0	0	0	37
8-12	0	1	0	0	0	0	0	0	2	1	0	0	0	0	0	0	4
13-18	0	0	0	0	0	0	0	0	0	0	0	0	0	0	0	0	0
19-24	0	0	0	0	0	0	0	0	0	0	0	0	0	0	0	0	0
25-32	0	0	0	0	0	0	0	0	0	0	0	0	0	0	0	0	0
32+	0	0	0	0	0	0	0	0	0	0	0	0	0	0	0	0	0
TOTAL	30	12	38	26	16	7	16	11	28	42	25	8	2	1	2	4	268

Table 1, continued

ALL DELTA TEMPERATURE GROUPS (33 ft)

RELATIVE HUMIDITY GREATER THAN 0.0 AND LESS THAN OR EQUAL TO 60.0
AMBIENT TEMPERATURE GREATER THAN 0.0 AND LESS THAN OR EQUAL TO 30.0

SPEED	N	NNE	NE	ENE	E	ESE	SE	SSE	S	SSW	SW	WSW	W	WNW	NW	NNW	TOTAL
0	0	0	0	0	0	0	0	0	0	0	0	0	0	0	0	0	0
1-3	5	2	3	2	1	3	1	0	4	6	4	2	3	1	2	1	40
4-7	8	12	8	6	2	3	0	1	11	2	3	4	2	2	5	11	80
8-12	7	19	10	0	1	0	0	0	0	4	3	1	0	3	24	32	104
13-18	29	32	8	0	0	0	0	0	0	4	6	0	0	3	57	37	176
19-24	10	0	1	0	0	0	0	0	0	0	0	0	0	3	20	18	52
25-32	3	0	0	0	0	0	0	0	0	0	0	0	0	0	9	1	13
32+	0	0	0	0	0	0	0	0	0	0	0	0	0	0	0	1	1
TOTAL	62	65	30	8	4	6	1	1	15	16	16	7	5	12	117	101	466

RELATIVE HUMIDITY GREATER THAN 0.0 AND LESS THAN OR EQUAL TO 60.0
AMBIENT TEMPERATURE GREATER THAN 30.0 AND LESS THAN OR EQUAL TO 45.0

SPEED	N	NNE	NE	ENE	E	ESE	SE	SSE	S	SSW	SW	WSW	W	WNW	NW	NNW	TOTAL
0	0	0	0	0	0	0	0	0	0	0	0	0	0	0	0	0	0
1-3	4	1	2	2	0	1	1	0	3	8	5	2	4	0	1	0	34
4-7	11	12	11	0	3	2	1	4	11	13	18	7	6	7	11	10	127
8-12	27	36	21	0	1	1	0	1	12	19	17	3	12	21	55	41	267
13-18	29	20	5	1	0	0	0	0	5	10	4	3	8	26	85	74	270
19-24	19	6	0	0	0	0	0	0	0	1	3	0	1	12	52	55	149
25-32	8	1	0	0	0	0	0	0	0	0	0	0	1	8	29	13	60
32+	1	0	0	0	0	0	0	0	0	0	0	0	0	5	4	3	13
TOTAL	99	76	39	3	4	4	2	5	31	51	47	15	32	79	237	196	920

RELATIVE HUMIDITY GREATER THAN 0.0 AND LESS THAN OR EQUAL TO 60.0
AMBIENT TEMPERATURE GREATER THAN 45.0 AND LESS THAN OR EQUAL TO 60.0

SPEED	N	NNE	NE	ENE	E	ESE	SE	SSE	S	SSW	SW	WSW	W	WNW	NW	NNW	TOTAL
0	0	0	0	0	0	0	0	0	0	0	0	0	0	0	0	0	0
1-3	12	0	2	0	0	0	1	2	5	4	6	4	5	2	4	3	50
4-7	15	11	12	3	2	0	0	3	17	20	22	12	9	9	10	9	154
8-12	17	42	11	1	4	0	3	4	23	25	14	6	8	9	15	22	204
13-18	24	27	13	0	1	0	0	1	19	16	18	18	9	22	44	36	248
19-24	16	6	1	0	0	0	0	0	10	1	15	6	6	15	20	34	130
25-32	2	0	0	0	0	0	0	0	0	0	6	0	0	15	10	11	44
32+	0	0	0	0	0	0	0	0	0	0	0	0	0	0	1	2	3
TOTAL	86	86	39	4	7	0	4	10	74	66	81	46	37	72	104	117	833

RELATIVE HUMIDITY GREATER THAN 0.0 AND LESS THAN OR EQUAL TO 60.0
AMBIENT TEMPERATURE GREATER THAN 60.0 AND LESS THAN OR EQUAL TO999.0

SPEED	N	NNE	NE	ENE	E	ESE	SE	SSE	S	SSW	SW	WSW	W	WNW	NW	NNW	TOTAL
0	0	0	0	0	0	0	0	0	0	0	0	0	0	0	0	0	0
1-3	10	5	7	5	3	2	2	0	7	6	13	8	12	4	7	3	94
4-7	40	36	9	6	0	5	2	5	37	35	28	18	22	17	17	15	292
8-12	36	35	12	5	5	4	4	4	45	22	30	25	26	27	39	22	341
13-18	29	30	4	0	2	1	2	0	35	19	43	33	14	34	34	31	311
19-24	8	6	2	0	1	0	1	0	22	5	15	9	3	9	14	7	102
25-32	1	0	0	0	0	0	0	0	2	0	7	2	0	0	5	5	22
32+	0	0	0	0	0	0	0	0	0	0	0	0	0	0	0	0	0
TOTAL	124	112	34	16	11	12	11	9	148	87	136	95	77	91	116	83	1162

ALL DELTA TEMPERATURE GROUPS (33 ft)

RELATIVE HUMIDITY GREATER THAN 60.0 AND LESS THAN OR EQUAL TO 85.0
AMBIENT TEMPERATURE GREATER THAN 0.0 AND LESS THAN OR EQUAL TO 30.0

SPEED	N	NNE	NE	ENE	E	ESE	SE	SSE	S	SSW	SW	WSW	W	WNW	NW	NNW	TOTAL
0	1	0	0	0	0	0	0	0	0	0	0	0	0	0	0	0	1
1-3	10	2	3	0	2	3	2	3	5	5	8	6	4	4	4	5	66
4-7	9	21	13	11	4	1	3	2	8	7	16	6	6	0	7	4	118
8-12	16	56	4	0	0	0	0	0	2	12	23	1	3	3	18	11	149
13-18	15	62	0	0	0	0	0	0	0	1	9	0	0	4	21	15	127
19-24	5	23	0	0	0	0	0	0	0	0	0	0	0	0	24	1	53
25-32	0	3	0	0	0	0	0	0	0	0	0	0	0	0	3	1	7
32+	0	0	0	0	0	0	0	0	0	0	0	0	0	0	5	1	6
TOTAL	56	167	20	11	6	4	5	5	15	25	56	13	13	11	82	38	527

RELATIVE HUMIDITY GREATER THAN 60.0 AND LESS THAN OR EQUAL TO 85.0
AMBIENT TEMPERATURE GREATER THAN 30.0 AND LESS THAN OR EQUAL TO 45.0

SPEED	N	NNE	NE	ENE	E	ESE	SE	SSE	S	SSW	SW	WSW	W	WNW	NW	NNW	TOTAL
0	0	0	0	0	0	0	0	0	0	0	0	0	0	0	0	0	0
1-3	6	1	2	1	1	3	0	4	5	6	4	2	4	3	4	2	48
4-7	7	8	8	3	5	7	9	9	30	27	32	10	10	5	7	3	180
8-12	15	26	16	5	0	0	1	2	12	16	17	6	3	11	8	10	148
13-18	13	26	14	4	3	0	0	2	0	0	1	0	0	7	29	20	119
19-24	2	9	2	1	0	0	0	0	0	0	0	0	0	5	22	7	48
25-32	1	5	1	0	0	0	0	0	0	0	0	0	0	1	8	0	16
32+	0	0	0	0	0	0	0	0	0	0	0	0	0	0	0	0	0
TOTAL	44	75	43	14	9	10	10	17	47	49	54	18	17	32	78	42	559

RELATIVE HUMIDITY GREATER THAN 60.0 AND LESS THAN OR EQUAL TO 85.0
AMBIENT TEMPERATURE GREATER THAN 45.0 AND LESS THAN OR EQUAL TO 60.0

SPEED	N	NNE	NE	ENE	E	ESE	SE	SSE	S	SSW	SW	WSW	W	WNW	NW	NNW	TOTAL
0	1	0	0	0	0	0	0	0	0	0	0	0	0	0	0	0	1
1-3	12	3	5	11	7	2	6	5	11	8	7	8	1	3	5	1	95
4-7	15	24	14	8	5	4	5	10	26	22	25	7	4	4	6	3	182
8-12	15	26	34	4	4	6	4	3	33	25	18	9	6	5	6	6	204
13-18	7	29	19	8	4	3	2	2	20	10	8	1	0	4	7	7	131
19-24	1	4	1	0	1	1	0	0	2	2	2	1	1	2	1	1	20
25-32	0	2	0	0	0	0	0	0	2	1	0	0	0	2	1	2	10
32+	0	2	0	0	1	0	0	0	1	0	0	0	0	0	0	1	5
TOTAL	51	90	73	31	22	16	17	20	95	68	60	26	12	20	26	21	648

RELATIVE HUMIDITY GREATER THAN 60.0 AND LESS THAN OR EQUAL TO 85.0
AMBIENT TEMPERATURE GREATER THAN 60.0 AND LESS THAN OR EQUAL TO999.0

SPEED	N	NNE	NE	ENE	E	ESE	SE	SSE	S	SSW	SW	WSW	W	WNW	NW	NNW	TOTAL
0	5	0	0	0	0	0	0	0	0	0	0	0	0	0	0	0	5
1-3	25	16	12	15	9	12	15	8	22	21	21	16	9	9	8	4	222
4-7	31	30	40	19	8	9	9	12	50	51	45	29	24	10	13	12	392
8-12	20	48	19	4	7	7	10	15	57	44	73	23	17	12	11	7	375
13-18	17	31	11	0	0	0	1	1	35	22	49	11	9	4	6	6	203
19-24	0	8	3	0	0	0	0	0	8	0	15	2	2	2	5	0	45
25-32	0	2	0	0	0	0	0	0	0	0	1	0	1	0	1	2	7
32+	0	0	0	0	0	0	0	0	0	0	0	0	0	0	0	0	0
TOTAL	98	135	85	38	24	28	35	37	172	138	204	81	62	37	44	31	1249

Table 1, continued

ALL DELTA TEMPERATURE GROUPS (33 ft)

RELATIVE HUMIDITY GREATER THAN 85.0 AND LESS THAN OR EQUAL TO 95.0
AMBIENT TEMPERATURE GREATER THAN 0.0 AND LESS THAN OR EQUAL TO 30.0

SPEED	N	NNE	NE	ENE	E	ESE	SE	SSE	S	SSW	SW	WSW	W	WNW	NW	NNW	TOTAL
0	0	0	0	0	0	0	0	0	0	0	0	0	0	0	0	0	0
1-3	0	0	0	0	1	0	1	1	1	0	0	4	0	0	0	0	8
4-7	0	9	4	0	2	0	0	0	0	2	3	0	0	0	0	0	20
8-12	10	20	4	0	0	0	0	0	0	2	0	0	0	1	0	0	37
13-18	5	23	0	0	0	0	0	0	0	2	0	0	0	0	2	0	32
19-24	0	16	0	0	0	0	0	0	0	0	0	0	0	0	1	0	17
25-32	0	3	0	0	0	0	0	0	0	0	0	0	0	0	0	0	3
32+	0	1	0	0	0	0	0	0	0	0	0	0	0	0	0	0	1
TOTAL	15	72	8	0	3	0	1	1	1	6	3	4	0	1	3	0	118

RELATIVE HUMIDITY GREATER THAN 85.0 AND LESS THAN OR EQUAL TO 95.0
AMBIENT TEMPERATURE GREATER THAN 30.0 AND LESS THAN OR EQUAL TO 45.0

SPEED	N	NNE	NE	ENE	E	ESE	SE	SSE	S	SSW	SW	WSW	W	WNW	NW	NNW	TOTAL
0	0	0	0	0	0	0	0	0	0	0	0	0	0	0	0	0	0
1-3	4	1	0	1	1	1	1	0	1	0	1	1	1	1	0	0	14
4-7	5	3	2	1	0	2	3	6	8	5	3	0	1	0	0	4	43
8-12	3	2	2	2	2	0	0	0	3	2	0	1	1	0	1	1	20
13-18	0	4	7	0	0	0	1	1	0	0	0	0	0	0	1	0	14
19-24	0	3	5	1	2	0	0	0	0	0	0	0	0	0	0	0	11
25-32	0	0	0	0	0	0	0	0	0	0	0	0	0	0	0	0	0
32+	0	0	0	0	0	0	0	0	0	0	0	0	0	0	0	0	0
TOTAL	12	13	16	5	5	3	5	7	12	7	4	2	3	1	2	5	102

RELATIVE HUMIDITY GREATER THAN 85.0 AND LESS THAN OR EQUAL TO 95.0
AMBIENT TEMPERATURE GREATER THAN 45.0 AND LESS THAN OR EQUAL TO 60.0

SPEED	N	NNE	NE	ENE	E	ESE	SE	SSE	S	SSW	SW	WSW	W	WNW	NW	NNW	TOTAL
0	1	0	0	0	0	0	0	0	0	0	0	0	0	0	0	0	1
1-3	8	0	0	4	5	4	2	2	6	7	3	2	4	0	1	1	49
4-7	4	9	9	6	10	2	8	14	7	20	11	4	2	0	2	1	109
8-12	1	6	14	1	0	1	3	3	11	9	6	1	0	0	0	0	56
13-18	5	29	8	0	0	0	1	0	3	6	2	1	0	0	0	1	56
19-24	0	6	1	1	3	0	1	0	1	3	0	0	0	0	0	1	17
25-32	0	0	0	0	5	0	0	0	2	4	1	0	0	0	0	0	12
32+	0	0	0	0	0	0	0	0	1	2	0	0	0	0	1	0	4
TOTAL	19	50	32	12	23	7	15	19	31	51	23	8	6	0	4	4	304

RELATIVE HUMIDITY GREATER THAN 85.0 AND LESS THAN OR EQUAL TO 95.0
AMBIENT TEMPERATURE GREATER THAN 60.0 AND LESS THAN OR EQUAL T0999.0

SPEED	N	NNE	NE	ENE	E	ESE	SE	SSE	S	SSW	SW	WSW	W	WNW	NW	NNW	TOTAL
0	1	0	0	0	0	0	0	0	0	0	0	0	0	0	0	0	1
1-3	13	2	8	9	1	4	4	10	9	13	13	10	10	5	3	3	117
4-7	10	9	11	4	1	2	8	10	19	24	28	10	1	1	1	0	139
8-12	3	11	7	2	2	1	3	2	11	27	41	7	4	1	3	1	126
13-18	2	11	4	0	0	0	0	0	3	9	13	0	0	0	1	0	43
19-24	0	6	1	0	0	0	0	0	1	3	3	0	0	0	0	0	14
25-32	1	0	0	0	0	0	0	0	0	0	1	0	0	0	1	0	3
32+	1	0	0	0	0	0	0	0	0	0	0	0	0	0	0	0	1
TOTAL	31	39	31	15	4	7	15	22	43	76	99	27	15	7	9	4	444

Table 1, continued

ALL DELTA TEMPERATURE GROUPS (33 ft)

RELATIVE HUMIDITY GREATER THAN 95.0 AND LESS THAN OR EQUAL TO 999.0
AMBIENT TEMPERATURE GREATER THAN 0.0 AND LESS THAN OR EQUAL TO 30.0

SPEED	N	NNE	NE	ENE	E	ESE	SE	SSE	S	SSW	SW	WSW	W	WNW	NW	NNW	TOTAL
0	0	0	0	0	0	0	0	0	0	0	0	0	0	0	0	0	0
1-3	2	2	0	0	0	0	0	1	1	2	1	1	0	0	0	0	10
4-7	0	4	9	2	2	0	0	0	0	0	1	0	0	0	0	0	18
8-12	1	9	7	0	0	0	0	0	0	0	1	0	0	0	0	0	18
13-18	0	28	2	0	0	0	0	0	0	0	0	0	0	0	2	0	32
19-24	0	2	0	0	0	0	0	0	0	0	0	0	0	0	1	0	3
25-32	0	5	0	0	0	0	0	0	0	0	0	0	0	0	0	0	5
32+	0	15	0	0	0	0	0	0	0	0	0	0	0	0	1	0	16
TOTAL	3	65	18	2	2	0	0	1	1	2	3	1	0	0	4	0	102

RELATIVE HUMIDITY GREATER THAN 95.0 AND LESS THAN OR EQUAL TO 999.0
AMBIENT TEMPERATURE GREATER THAN 30.0 AND LESS THAN OR EQUAL TO 45.0

SPEED	N	NNE	NE	ENE	E	ESE	SE	SSE	S	SSW	SW	WSW	W	WNW	NW	NNW	TOTAL
0	0	0	0	0	0	0	0	0	0	0	0	0	0	0	0	0	0
1-3	4	0	0	0	0	1	1	1	4	1	1	1	2	2	0	0	18
4-7	0	2	6	3	2	4	5	2	13	8	4	3	2	0	3	1	58
8-12	0	1	4	8	1	1	1	1	9	3	1	1	0	0	0	1	32
13-18	2	2	6	4	1	0	0	1	4	0	0	0	0	0	0	0	20
19-24	2	0	1	0	0	0	0	0	0	0	0	0	1	0	0	0	4
25-32	0	1	0	0	0	0	0	0	0	0	0	0	0	0	0	0	1
32+	0	0	0	0	0	0	0	0	0	0	0	0	0	0	0	0	0
TOTAL	8	6	17	15	4	6	7	5	30	12	6	5	5	2	3	2	133

RELATIVE HUMIDITY GREATER THAN 95.0 AND LESS THAN OR EQUAL TO 999.0
AMBIENT TEMPERATURE GREATER THAN 45.0 AND LESS THAN OR EQUAL TO 60.0

SPEED	N	NNE	NE	ENE	E	ESE	SE	SSE	S	SSW	SW	WSW	W	WNW	NW	NNW	TOTAL
0	1	0	0	0	0	0	0	0	0	0	0	0	0	0	0	0	1
1-3	4	1	1	1	0	3	2	2	4	3	3	4	0	1	2	0	31
4-7	0	4	7	5	13	9	15	11	20	15	11	0	0	0	0	0	110
8-12	0	5	5	2	1	1	2	6	26	9	5	0	0	0	0	1	63
13-18	0	4	1	1	0	0	0	1	7	7	2	0	0	0	0	0	23
19-24	0	1	0	0	0	0	0	0	4	5	0	0	0	0	0	0	10
25-32	0	1	0	0	1	0	0	0	6	3	0	0	0	0	0	0	11
32+	0	0	0	0	0	0	0	0	4	1	0	0	0	0	0	0	5
TOTAL	5	16	14	9	15	13	19	20	71	43	21	4	0	1	2	1	254

RELATIVE HUMIDITY GREATER THAN 95.0 AND LESS THAN OR EQUAL TO 999.0
AMBIENT TEMPERATURE GREATER THAN 60.0 AND LESS THAN OR EQUAL TO999.0

SPEED	N	NNE	NE	ENE	E	ESE	SE	SSE	S	SSW	SW	WSW	W	WNW	NW	NNW	TOTAL
0	0	0	0	0	0	0	0	0	0	0	0	0	0	0	0	0	0
1-3	4	0	1	2	3	1	2	1	2	3	4	2	3	2	5	0	35
4-7	1	0	4	3	2	2	2	3	4	9	14	6	2	0	0	0	52
8-12	2	3	0	0	0	0	9	6	13	2	10	1	1	0	0	0	47
13-18	0	1	3	0	0	0	2	1	4	2	2	0	0	0	0	0	15
19-24	0	0	0	0	0	1	0	0	0	0	0	0	0	0	0	0	1
25-32	0	0	0	0	0	0	0	0	0	0	0	0	0	0	0	0	0
32+	0	0	0	0	0	0	0	0	3	0	0	0	0	0	0	0	3
TOTAL	7	4	8	5	5	4	15	11	26	16	30	9	6	2	5	0	153

Sheet 8 of 8

Table 2

COOLING TOWER GEOMETRY AND OPERATING CONDITIONS ASSUMED FOR THE ANALYSIS

Tower Geometry	
Height, meters:	172.0
Top exit diameter, meters:	94.5
Design Conditions	
Water flow rate, gpm:	600,000.0
Heat load, BTU/hr:	7.5×10^{9}
Wet bulb temperature, ^{o}F:	74.0
Relative humidity, %:	55.0
Approach temperature, ^{o}F:	16.0
Range temperature, ^{o}F:	25.0
Drift rate, %:	0.002
Plant factor and power, %:	100.0

Table 3

GROUPS USED TO CLASSIFY EACH HOURLY

MEASURED ATMOSPHERIC CONDITION

Atmospheric Condition	No. of Groups	Group Classification	
Wind Direction	16 Sectors	N, NNE, NE, ENE, E, ESE, SE, SSE, S, SSW, SW, WSW, W, WNW, NW, NNW	
Wind Speed	8	0 - 3.0 mph	
		3.0+ - 6.0	
		6.0+ - 9.0	
		9.0+ - 12.0	
		12.0+ - 18.0	
		18.0+ - 25.0	
		25.0+ - 32.0	
		> 32.0	
		Wake Conditions for Winds 26 mph(1)	
Stability Class	3	Pasquill Category C	
		" D	
		" E	
Relative Humidity	2	> 75%	
		≤ 75%	
Terrain Profile	3	SSE, S, SSW	Represented by SSE
		ENE, NE, NNE, SE, ESE, SW, E	Represented by E
		WNW, NNW, NW, W, WSW, N	Represented by WNW

(1) For hours when wind speeds > 25 mph existed, the effect of the aerodynamic wake of the tower is calculated.

Table 4

ASSUMED MASS DISTRIBUTION IN SELECTED DROP SIZE GROUPS

(Just downstream of eliminators)

Group	Nominal Drop Diameter,(1) microns	Range of Diameter, microns	Fraction of Total Mass in Group
1	50	10 - 70	0.22
2	100	70 - 125	0.42
3	150	125 - 175	0.21
4	200	175 - 260	0.13
5	280	260 - 325	0.012
6	450	> 325	0.008

(1) Calculations described herein were done for each nominal drop diameter with its associated mass fraction except that the 50 and 100 micron diameter groups were combined and treated all as 100 micron diameter droplets. (See Appendix B, reference 6.)

Table 5

REPRESENTATIVE VALUES FOR ATMOSPHERIC GROUPING

Wind Speed (mph)	Representative Wind (m/sec)	Stability Class (2)	Relative Humidity (%)	Representative Relative Humidity (%)
0 - 3(1)	1.0	C, D, E	> 75	90
			≤ 75	65
4 - 6	2.3	C, D, E	> 75	90
			≤ 75	65
7 - 9	3.5	C, D, E	> 75	90
			≤ 75	65
10 - 12	5.0	C, D, E	> 75	90
			≤ 75	65
13 - 18	7.0	D	> 75	90
			≤ 75	65
19 - 25	10.0	D	> 75	90
			≤ 75	65
26 - 32	13.0	D	> 75	90
			≤ 75	65
≥ 33	16.0	D	> 75	90
			≤ 75	65

(1) Calms represented as 0.5 mph with a wind direction of the first subsequent non-calm hour.

(2) Definition of Pasquill Category used:

$$C = \text{Unstable,} \quad \frac{\Delta T\ (^{\circ}F)}{100\ \text{ft}} \leq -0.8$$

$$D = \text{Neutral} \quad -0.8 < \frac{\Delta T\ (^{\circ}F)}{100\ \text{ft}} \leq -0.3$$

$$E = \text{Stable} \quad \frac{\Delta T\ (^{\circ}F)}{100\ \text{ft}} > -0.3$$

Table 6

Joint Frequency of Occurrence of Weather Conditions Obtained from the Indian Point 4 Meteorological Tower (400 ft level) for the Period of Record from October 1, 1973 through September 30, 1974

CONED- INDIAN POINT 3-ANNUAL AVERAGE TOTAL

DIFFUSION GROUP 3

SPEED LE 3.0

RELATIVE HUMIDITY	N	NNE	NE	ENE	E	ESE	SE	SSE	S	SSW	SW	WSW	W	WNW	NW	NNW	PCNT	TOTAL
LE 75.00	0	1	0	0	0	0	0	0	0	0	0	0	0	0	0	0	12.5	1
LE100.00	1	0	0	0	3	0	1	1	1	0	0	0	0	0	0	0	87.5	7
LE100.00	0	0	0	0	0	0	0	0	0	0	0	0	0	0	0	0	0.0	0
PERCENT	12.5	12.5	0.0	0.0	37.5	0.0	12.5	12.5	12.5	0.0	0.0	0.0	0.0	0.0	0.0	0.0		
TOTAL	1	1	0	0	3	0	1	1	1	0	0	0	0	0	0	0		8

SPEED LE 6.0

RELATIVE HUMIDITY	N	NNE	NE	ENE	E	ESE	SE	SSE	S	SSW	SW	WSW	W	WNW	NW	NNW	PCNT	TOTAL
LE 75.00	2	2	2	1	0	0	0	0	1	1	1	0	0	0	0	3	65.0	13
LE100.00	0	2	0	0	0	1	0	0	3	1	0	0	0	0	0	0	35.0	7
LE100.00	0	0	0	0	0	0	0	0	0	0	0	0	0	0	0	0	0.0	0
PERCENT	10.0	20.0	10.0	5.0	0.0	5.0	0.0	0.0	20.0	10.0	5.0	0.0	0.0	0.0	0.0	15.0		
TOTAL	2	4	2	1	0	1	0	0	4	2	1	0	0	0	0	3		20

SPEED LE 9.0

RELATIVE HUMIDITY	N	NNE	NE	ENE	E	ESE	SE	SSE	S	SSW	SW	WSW	W	WNW	NW	NNW	PCNT	TOTAL
LE 75.00	6	12	1	0	1	0	0	1	18	5	1	0	0	0	0	2	79.7	47
LE100.00	2	2	1	0	1	0	0	0	3	2	0	0	0	0	0	1	20.3	12
LE100.00	0	0	0	0	0	0	0	0	0	0	0	0	0	0	0	0	0.0	0
PERCENT	13.6	23.7	3.4	0.0	3.4	0.0	0.0	1.7	35.6	11.9	1.7	0.0	0.0	0.0	0.0	5.1		
TOTAL	8	14	2	0	2	0	0	1	21	7	1	0	0	0	0	3		59

SPEED LE 12.0

RELATIVE HUMIDITY	N	NNE	NE	ENE	E	ESE	SE	SSE	S	SSW	SW	WSW	W	WNW	NW	NNW	PCNT	TOTAL
LE 75.00	4	17	2	0	0	1	0	0	13	4	0	1	1	5	2	3	85.5	53
LE100.00	0	4	1	0	0	0	0	0	3	1	0	0	0	0	0	0	14.5	9
LE100.00	0	0	0	0	0	0	0	0	0	0	0	0	0	0	0	0	0.0	0
PERCENT	6.5	33.9	4.8	0.0	0.0	1.6	0.0	0.0	25.8	8.1	0.0	1.6	1.6	8.1	3.2	4.8		
TOTAL	4	21	3	0	0	1	0	0	16	5	0	1	1	5	2	3		62

SPEED LE 18.0

RELATIVE HUMIDITY	N	NNE	NE	ENE	E	ESE	SE	SSE	S	SSW	SW	WSW	W	WNW	NW	NNW	PCNT	TOTAL
LE 75.00	0	0	0	0	0	0	0	0	0	0	0	0	0	0	0	0	0.0	0
LE100.00	0	0	0	0	0	0	0	0	0	0	0	0	0	0	0	0	0.0	0
LE100.00	0	0	0	0	0	0	0	0	0	0	0	0	0	0	0	0	0.0	0
PERCENT	0.0	0.0	0.0	0.0	0.0	0.0	0.0	0.0	0.0	0.0	0.0	0.0	0.0	0.0	0.0	0.0		
TOTAL	0	0	0	0	0	0	0	0	0	0	0	0	0	0	0	0		0

SPEED LE 25.0

RELATIVE HUMIDITY	N	NNE	NE	ENE	E	ESE	SE	SSE	S	SSW	SW	WSW	W	WNW	NW	NNW	PCNT	TOTAL
LE 75.00	0	0	0	0	0	0	0	0	0	0	0	0	0	0	0	0	0.0	0
LE100.00	0	0	0	0	0	0	0	0	0	0	0	0	0	0	0	0	0.0	0
LE100.00	0	0	0	0	0	0	0	0	0	0	0	0	0	0	0	0	0.0	0
PERCENT	0.0	0.0	0.0	0.0	0.0	0.0	0.0	0.0	0.0	0.0	0.0	0.0	0.0	0.0	0.0	0.0		
TOTAL	0	0	0	0	0	0	0	0	0	0	0	0	0	0	0	0		0

SPEED LE 32.0

RELATIVE HUMIDITY	N	NNE	NE	ENE	E	ESE	SE	SSE	S	SSW	SW	WSW	W	WNW	NW	NNW	PCNT	TOTAL
LE 75.00	0	0	0	0	0	0	0	0	0	0	0	0	0	0	0	0	0.0	0
LE100.00	0	0	0	0	0	0	0	0	0	0	0	0	0	0	0	0	0.0	0
LE100.00	0	0	0	0	0	0	0	0	0	0	0	0	0	0	0	0	0.0	0
PERCENT	0.0	0.0	0.0	0.0	0.0	0.0	0.0	0.0	0.0	0.0	0.0	0.0	0.0	0.0	0.0	0.0		
TOTAL	0	0	0	0	0	0	0	0	0	0	0	0	0	0	0	0		0

SPEED LE 999.0

RELATIVE HUMIDITY	N	NNE	NE	ENE	E	ESE	SE	SSE	S	SSW	SW	WSW	W	WNW	NW	NNW	PCNT	TOTAL
LE 75.00	0	0	0	0	0	0	0	0	0	0	0	0	0	0	0	0	0.0	0
LE100.00	0	0	0	0	0	0	0	0	0	0	0	0	0	0	0	0	0.0	0
LE100.00	0	0	0	0	0	0	0	0	0	0	0	0	0	0	0	0	0.0	0
PERCENT	0.0	0.0	0.0	0.0	0.0	0.0	0.0	0.0	0.0	0.0	0.0	0.0	0.0	0.0	0.0	0.0		
TOTAL	0	0	0	0	0	0	0	0	0	0	0	0	0	0	0	0		0

CONED- INDIAN POINT 3-ANNUAL AVERAGE TOTAL

DIFFUSION GROUP 4

SPEED LE 3.0

RELATIVE HUMIDITY	N	NNE	NE	ENE	E	ESE	SE	SSE	S	SSW	SW	WSW	W	WNW	NW	NNW	PCNT	TOTAL
LE 75.00	8	6	8	3	10	3	3	2	11	13	16	9	7	2	3	6	49.5	110
LE100.00	3	4	7	9	15	7	6	6	9	17	9	10	3	2	2	3	50.5	112
LE100.00	0	0	0	0	0	0	0	0	0	0	0	0	0	0	0	0	0.0	0
PERCENT	5.0	4.5	6.8	5.4	11.3	4.5	4.1	3.6	9.0	13.5	11.3	8.6	4.5	1.8	2.3	4.1		
TOTAL	11	10	15	12	25	10	9	8	20	30	25	19	10	4	5	9		222

SPEED LE 6.0

RELATIVE HUMIDITY	N	NNE	NE	ENE	E	ESE	SE	SSE	S	SSW	SW	WSW	W	WNW	NW	NNW	PCNT	TOTAL
LE 75.00	41	43	26	16	9	4	1	8	49	54	35	18	17	10	14	16	64.0	361
LE100.00	6	13	20	18	15	9	22	15	25	23	26	6	2	0	1	2	36.0	203
LE100.00	0	0	0	0	0	0	0	0	0	0	0	0	0	0	0	0	0.0	0
PERCENT	8.3	9.9	8.2	6.0	4.3	2.3	4.1	4.1	13.1	13.7	10.8	4.3	3.4	1.8	2.7	3.2		
TOTAL	47	56	46	34	24	13	23	23	74	77	61	24	19	10	15	18		564

SPEED LE 9.0

RELATIVE HUMIDITY	N	NNE	NE	ENE	E	ESE	SE	SSE	S	SSW	SW	WSW	W	WNW	NW	NNW	PCNT	TOTAL
LE 75.00	31	52	41	6	13	5	5	6	36	25	28	8	16	27	30	25	62.9	354
LE100.00	9	46	37	9	8	4	12	13	27	19	16	0	4	2	2	1	37.1	209
LE100.00	0	0	0	0	0	0	0	0	0	0	0	0	0	0	0	0	0.0	0
PERCENT	7.1	17.4	13.9	2.7	3.7	1.6	3.0	3.4	11.2	7.8	7.8	1.4	3.6	5.2	5.7	4.6		
TOTAL	40	98	78	15	21	9	17	19	63	44	44	8	20	29	32	26		563

SPEED LE 12.0

RELATIVE HUMIDITY	N	NNE	NE	ENE	E	ESE	SE	SSE	S	SSW	SW	WSW	W	WNW	NW	NNW	PCNT	TOTAL
LE 75.00	36	91	40	8	8	6	5	4	26	24	25	16	11	27	70	56	75.1	453
LE100.00	5	48	29	1	1	2	8	5	19	6	17	1	0	4	1	3	24.9	150
LE100.00	0	0	0	0	0	0	0	0	0	0	0	0	0	0	0	0	0.0	0
PERCENT	6.8	23.1	11.4	1.5	1.5	1.3	2.2	1.5	7.5	5.0	7.0	2.8	1.8	5.1	11.8	9.8		
TOTAL	41	139	69	9	9	8	13	9	45	30	42	17	11	31	71	59		603

SPEED LE 18.0

RELATIVE HUMIDITY	N	NNE	NE	ENE	E	ESE	SE	SSE	S	SSW	SW	WSW	W	WNW	NW	NNW	PCNT	TOTAL
LE 75.00	152	205	58	7	8	4	4	5	97	73	121	64	36	100	273	214	78.1	1421
LE100.00	23	154	47	11	5	0	5	5	38	35	36	3	4	4	16	13	21.9	399
LE100.00	0	0	0	0	0	0	0	0	0	0	0	0	0	0	0	0	0.0	0
PERCENT	9.6	19.7	5.8	1.0	.7	.2	.5	.5	7.4	5.9	8.6	3.7	2.2	5.7	15.9	12.5		
TOTAL	175	359	105	18	13	4	9	10	135	108	157	67	40	104	289	227		1820

SPEED LE 25.0

RELATIVE HUMIDITY	N	NNE	NE	ENE	E	ESE	SE	SSE	S	SSW	SW	WSW	W	WNW	NW	NNW	PCNT	TOTAL
LE 75.00	61	49	8	0	1	1	1	0	41	8	52	19	13	57	166	127	83.3	604
LE100.00	7	55	11	3	6	1	1	0	9	12	3	0	1	0	8	4	16.7	121
LE100.00	0	0	0	0	0	0	0	0	0	0	0	0	0	0	0	0	0.0	0.
PERCENT	9.4	14.3	2.6	.4	1.0	.3	.3	0.0	6.9	2.8	7.6	2.6	1.9	7.9	24.0	18.1		
TOTAL	68	104	19	3	7	2	2	0	50	20	55	19	14	57	174	131		725

SPEED LE 32.0

RELATIVE HUMIDITY	N	NNE	NE	ENE	E	ESE	SE	SSE	S	SSW	SW	WSW	W	WNW	NW	NNW	PCNT	TOTAL
LE 75.00	11	3	0	0	0	0	0	0	1	0	12	1	2	16	53	27	76.4	126
LE100.00	0	12	0	0	6	0	0	0	9	8	2	0	0	1	0	1	23.6	39
LE100.00	0	0	0	0	0	0	0	0	0	0	0	0	0	0	0	0	0.0	0
PERCENT	6.7	9.1	0.0	0.0	3.6	0.0	0.0	0.0	6.1	4.8	8.5	.6	1.2	10.3	32.1	17.0		
TOTAL	11	15	0	0	6	0	0	0	10	8	14	1	2	17	53	28		165

SPEED LE 999.0

RELATIVE HUMIDITY	N	NNE	NE	ENE	E	ESE	SE	SSE	S	SSW	SW	WSW	W	WNW	NW	NNW	PCNT	TOTAL
LE 75.00	1	0	0	0	0	0	0	0	0	0	0	0	0	5	7	8	35.6	21
LE100.00	1	18	0	0	1	0	0	0	9	3	0	0	0	0	5	1	64.4	38
LE100.00	0	0	0	0	0	0	0	0	0	0	0	0	0	0	0	0	0.0	0
PERCENT	3.4	30.5	0.0	0.0	1.7	0.0	0.0	0.0	15.3	5.1	0.0	0.0	0.0	8.5	20.3	15.3		
TOTAL	2	18	0	0	1	0	0	0	9	3	0	0	0	5	12	9		59

CONED- INDIAN POINT 3-ANNUAL AVERAGE TOTAL

DIFFUSION GROUP 5

SPEED LE 3.0

RELATIVE HUMIDITY	N	NNE	NE	ENE	E	ESE	SE	SSE	S	SSW	SW	WSW	W	WNW	NW	NNW	PCNT	TOTAL
LE 75.00	12	12	18	22	45	15	13	11	32	40	38	23	24	16	26	8	49.5	355
LE100.00	19	13	14	19	42	15	18	20	39	33	32	32	28	17	15	6	50.5	362
LE100.00	0	0	0	0	0	0	0	0	0	0	0	0	0	0	0	0	0.0	0
PERCENT	4.3	3.5	4.5	5.7	12.1	4.2	4.3	4.3	9.9	10.2	9.8	7.7	7.3	4.6	5.7	2.0		
TOTAL	31	25	32	41	87	30	31	31	71	73	70	55	52	33	41	14		717

SPEED LE 6.0

RELATIVE HUMIDITY	N	NNE	NE	ENE	E	ESE	SE	SSE	S	SSW	SW	WSW	W	WNW	NW	NNW	PCNT	TOTAL
LE 75.00	42	33	36	18	10	11	12	21	53	59	67	40	39	24	36	28	52.8	529
LE100.00	16	36	34	15	26	21	24	29	57	74	77	35	13	4	7	4	47.2	472
LE100.00	0	0	0	0	0	0	0	0	0	0	0	0	0	0	0	0	0.0	0
PERCENT	5.8	6.9	7.0	3.3	3.6	3.2	3.6	5.0	11.0	13.3	14.4	7.5	5.2	2.8	4.3	3.2		
TOTAL	58	69	70	33	36	32	36	50	110	133	144	75	52	28	43	32		1001

SPEED LE 9.0

RELATIVE HUMIDITY	N	NNE	NE	ENE	E	ESE	SE	SSE	S	SSW	SW	WSW	W	WNW	NW	NNW	PCNT	TOTAL
LE 75.00	40	43	32	6	4	3	5	8	58	52	60	30	32	19	45	41	59.4	478
LE100.00	10	34	16	11	13	7	7	16	51	59	66	14	10	3	3	7	40.6	327
LE100.00	0	0	0	0	0	0	0	0	0	0	0	0	0	0	0	0	0.0	0
PERCENT	6.2	9.6	6.0	2.1	2.1	1.2	1.5	3.0	13.5	13.8	15.7	5.5	5.2	2.7	6.0	6.0		
TOTAL	50	77	48	17	17	10	12	24	109	111	126	44	42	22	48	48		805

SPEED LE 12.0

RELATIVE HUMIDITY	N	NNE	NE	ENE	E	ESE	SE	SSE	S	SSW	SW	WSW	W	WNW	NW	NNW	PCNT	TOTAL
LE 75.00	39	43	12	4	2	0	4	5	28	48	56	26	23	20	45	32	63.1	387
LE100.00	16	19	10	2	2	1	5	9	54	33	50	7	4	4	6	4	36.9	226
LE100.00	0	0	0	0	0	0	0	0	0	0	0	0	0	0	0	0	0.0	0
PERCENT	9.0	10.1	3.6	1.0	.7	.2	1.5	2.3	13.4	13.2	17.3	5.4	4.4	3.9	8.3	5.9		
TOTAL	55	62	22	6	4	1	9	14	82	81	106	33	27	24	51	36		613

SPEED LE 18.0

RELATIVE HUMIDITY	N	NNE	NE	ENE	E	ESE	SE	SSE	S	SSW	SW	WSW	W	WNW	NW	NNW	PCNT	TOTAL
LE 75.00	0	0	0	0	0	0	0	0	0	0	0	0	0	0	0	0	0.0	0
LE100.00	0	0	0	0	0	0	0	0	0	0	0	0	0	0	0	0	0.0	0
LE100.00	0	0	0	0	0	0	0	0	0	0	0	0	0	0	0	0	0.0	0
PERCENT	0.0	0.0	0.0	0.0	0.0	0.0	0.0	0.0	0.0	0.0	0.0	0.0	0.0	0.0	0.0	0.0		
TOTAL	0	0	0	0	0	0	0	0	0	0	0	0	0	0	0	0		0

SPEED LE 25.0

RELATIVE HUMIDITY	N	NNE	NE	ENE	E	ESE	SE	SSE	S	SSW	SW	WSW	W	WNW	NW	NNW	PCNT	TOTAL
LE 75.00	0	0	0	0	0	0	0	0	0	0	0	0	0	0	0	0	0.0	0
LE100.00	0	0	0	0	0	0	0	0	0	0	0	0	0	0	0	0	0.0	0
LE100.00	0	0	0	0	0	0	0	0	0	0	0	0	0	0	0	0	0.0	0
PERCENT	0.0	0.0	0.0	0.0	0.0	0.0	0.0	0.0	0.0	0.0	0.0	0.0	0.0	0.0	0.0	0.0		
TOTAL	0	0	0	0	0	0	0	0	0	0	0	0	0	0	0	0		0

SPEED LE 32.0

RELATIVE HUMIDITY	N	NNE	NE	ENE	E	ESE	SE	SSE	S	SSW	SW	WSW	W	WNW	NW	NNW	PCNT	TOTAL
LE 75.00	0	0	0	0	0	0	0	0	0	0	0	0	0	0	0	0	0.0	0
LE100.00	0	0	0	0	0	0	0	0	0	0	0	0	0	0	0	0	0.0	0
LE100.00	0	0	0	0	0	0	0	0	0	0	0	0	0	0	0	0	0.0	0
PERCENT	0.0	0.0	0.0	0.0	0.0	0.0	0.0	0.0	0.0	0.0	0.0	0.0	0.0	0.0	0.0	0.0		
TOTAL	0	0	0	0	0	0	0	0	0	0	0	0	0	0	0	0		0

SPEED LE 999.0

RELATIVE HUMIDITY	N	NNE	NE	ENE	E	ESE	SE	SSE	S	SSW	SW	WSW	W	WNW	NW	NNW	PCNT	TOTAL
LE 75.00	0	0	0	0	0	0	0	0	0	0	0	0	0	0	0	0	0.0	0
LE100.00	0	0	0	0	0	0	0	0	0	0	0	0	0	0	0	0	0.0	0
LE100.00	0	0	0	0	0	0	0	0	0	0	0	0	0	0	0	0	0.0	0
PERCENT	0.0	0.0	0.0	0.0	0.0	0.0	0.0	0.0	0.0	0.0	0.0	0.0	0.0	0.0	0.0	0.0		
TOTAL	0	0	0	0	0	0	0	0	0	0	0	0	0	0	0	0		0

Sheet 6 of 6

Figure 1a

Cooling Tower Operating Characteristics Assumed for Analysis:
Exit Air Temperature vs Ambient Dry Bulb Temperature
as a Function of Ambient Relative Humidity
(Con. Ed. Indian Point No. 3 Natural Draft Tower)

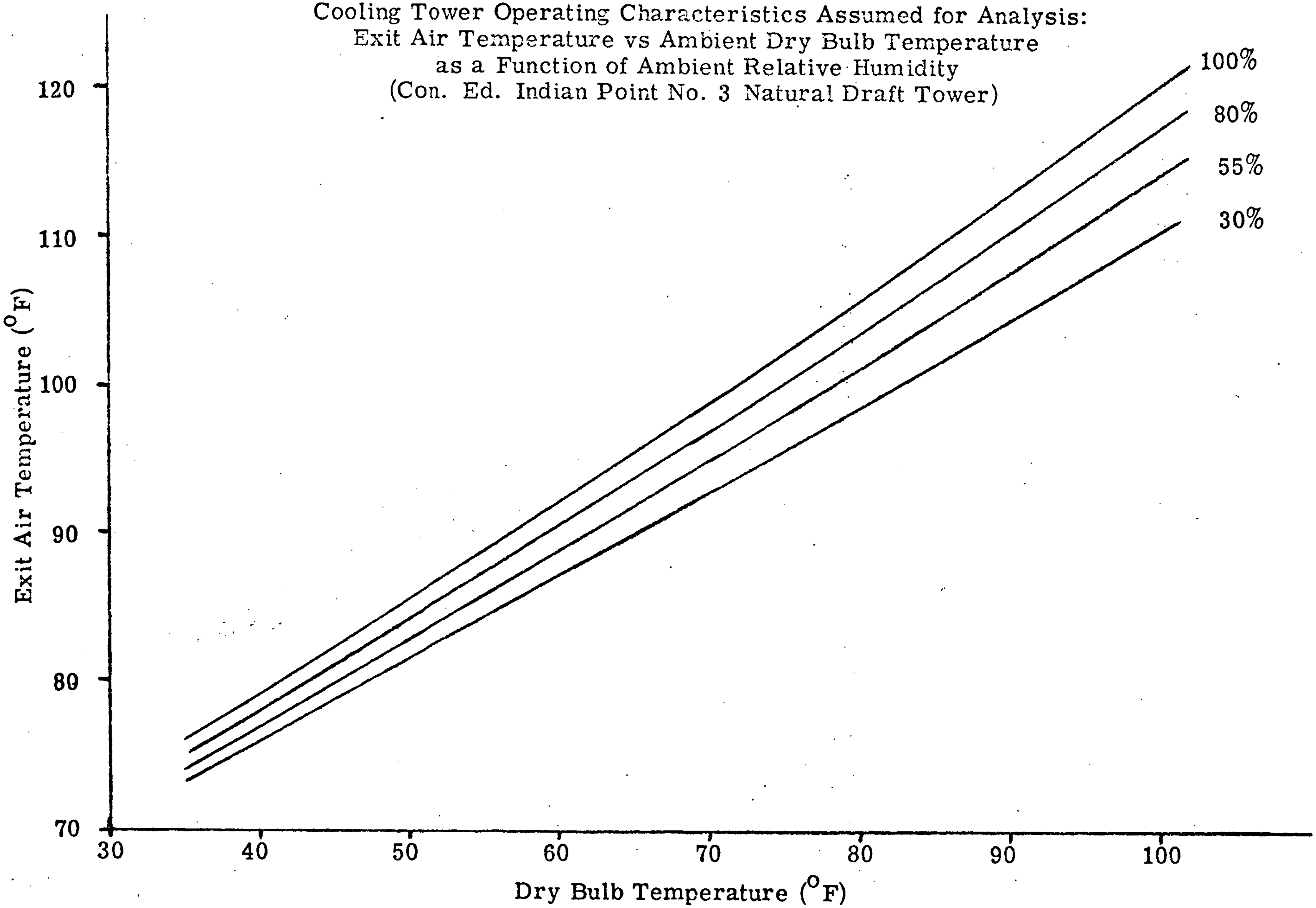

Figure 1b

Cooling Tower Operating Characteristics Assumed for Analysis:
Air Flow Rate and Exit Air Velocity vs Ambient Dry Bulb Temperature
as a Function of Ambient Relative Humidity
(Con. Ed. Indian Point No. 3 Natural Draft Tower)

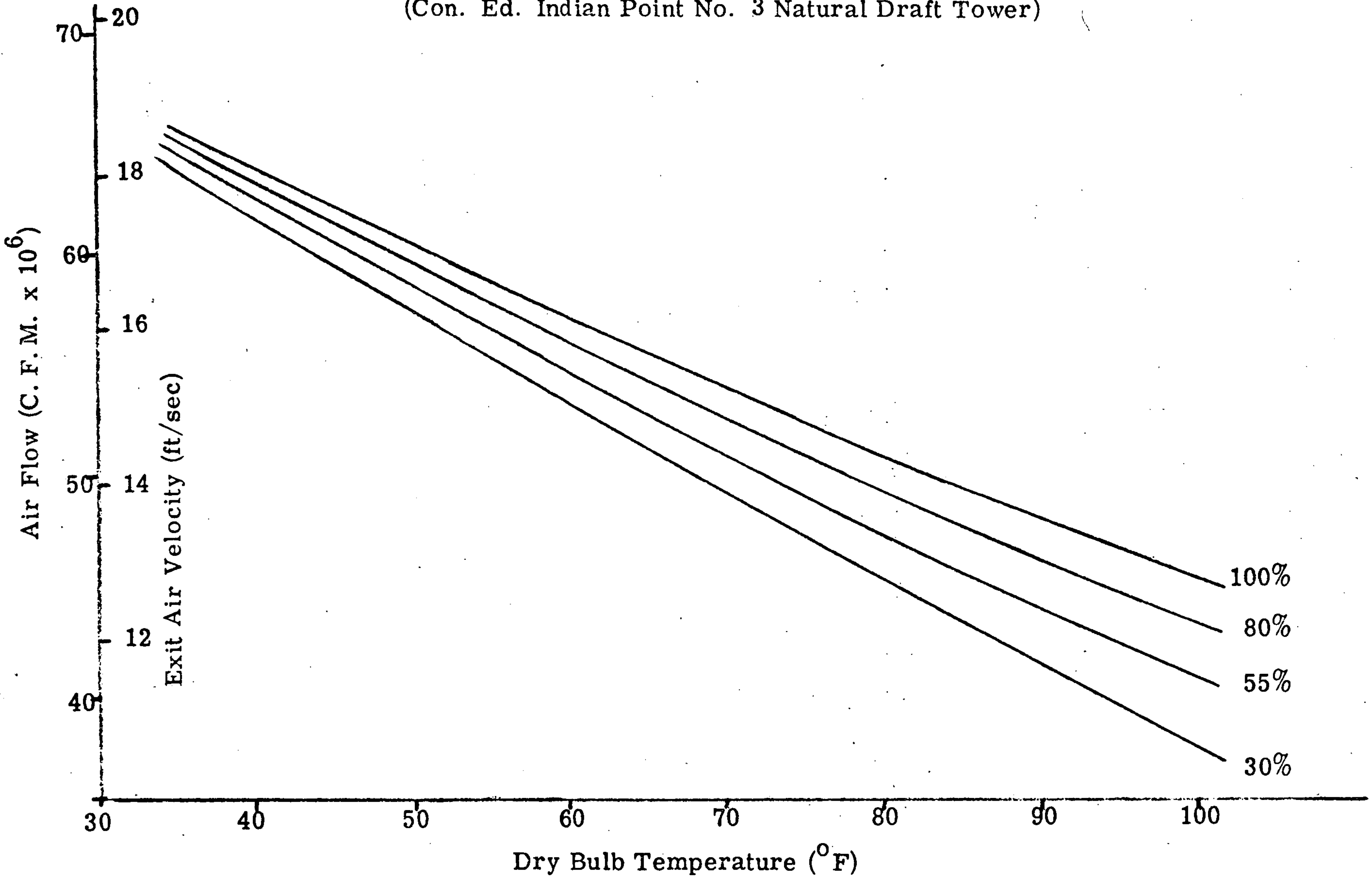

Figure 2

(a - p)

Terrain Profile for 16 direction Sectors
Representing the 0-5 Mile Radius
Surrounding the Indian Point 3 Site

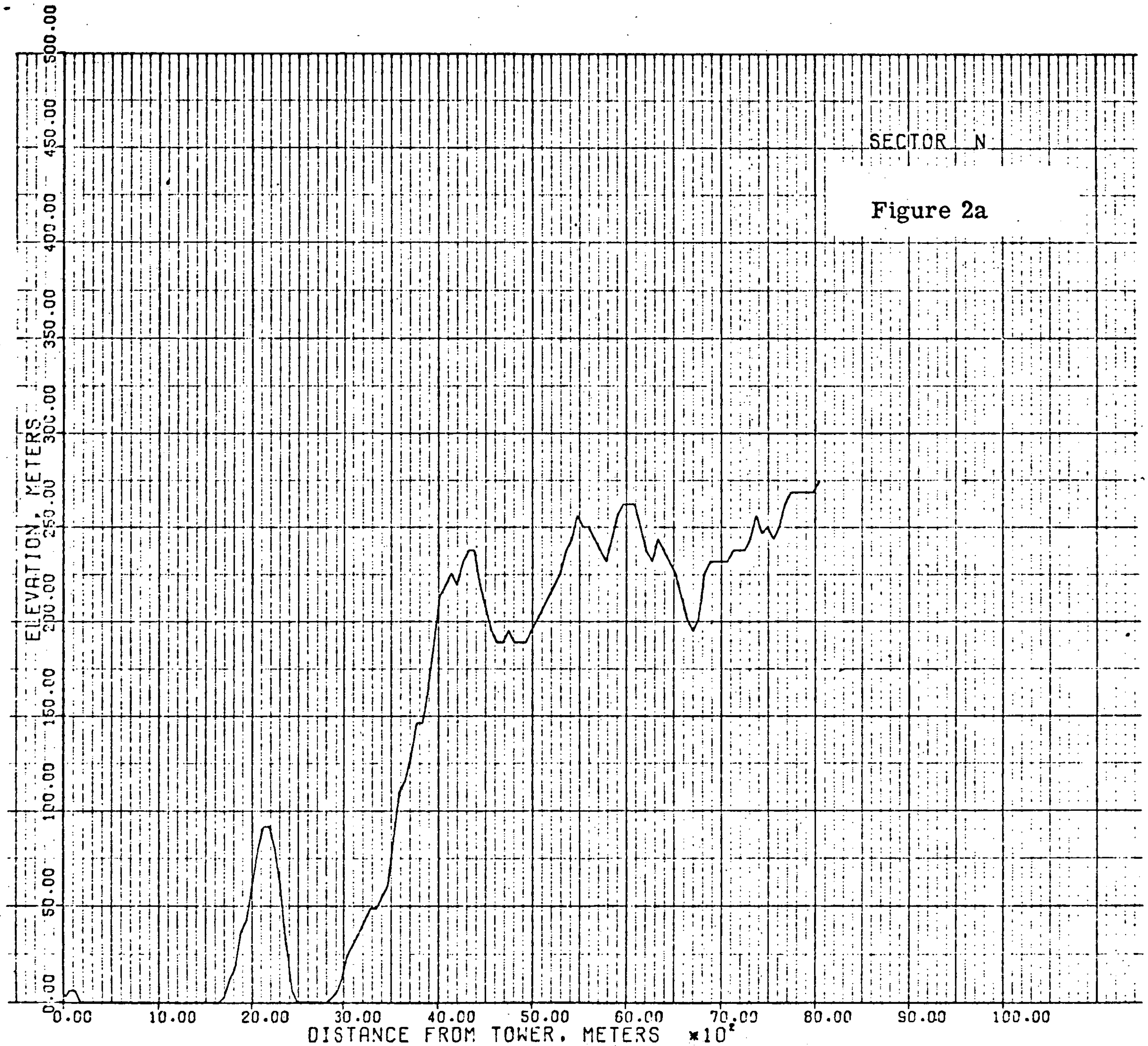
SECTOR N
ELEVATION, METERS
0.00
50.00
100.00
150.00
200.00
250.00
300.00
350.00
400.00
450.00
500.00
0.00
10.00
20.00
30.00
40.00
50.00
60.00
70.00
80.00
90.00
100.00
DISTANCE FROM TOWER, METERS *10²

Figure 2a

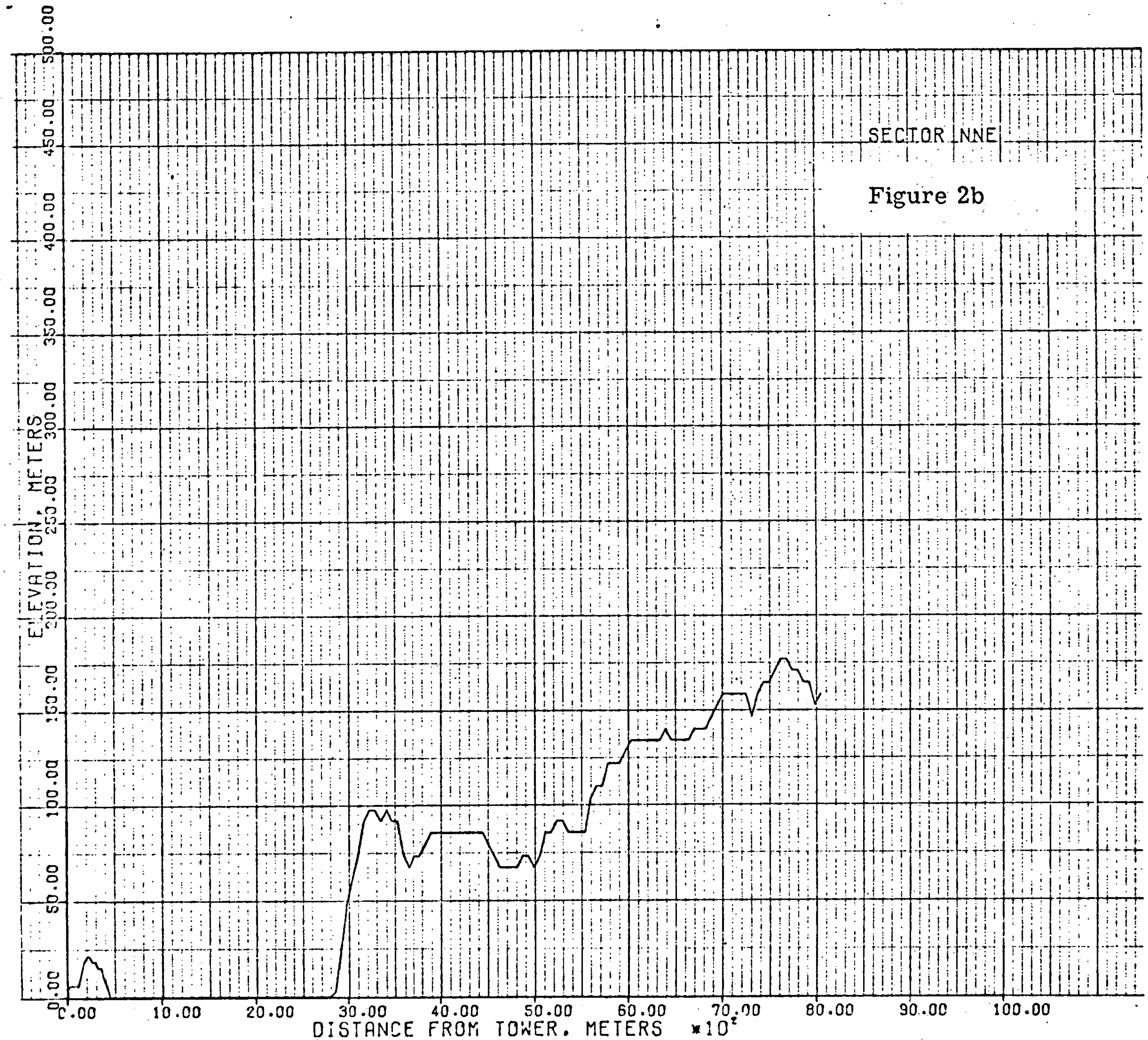
SECTOR NNE
ELEVATION, METERS
500.00
450.00
400.00
350.00
300.00
250.00
200.00
150.00
100.00
50.00
0.00
0.00
10.00
20.00
30.00
40.00
50.00
60.00
70.00
80.00
90.00
100.00
DISTANCE FROM TOWER, METERS *10²

Figure 2b

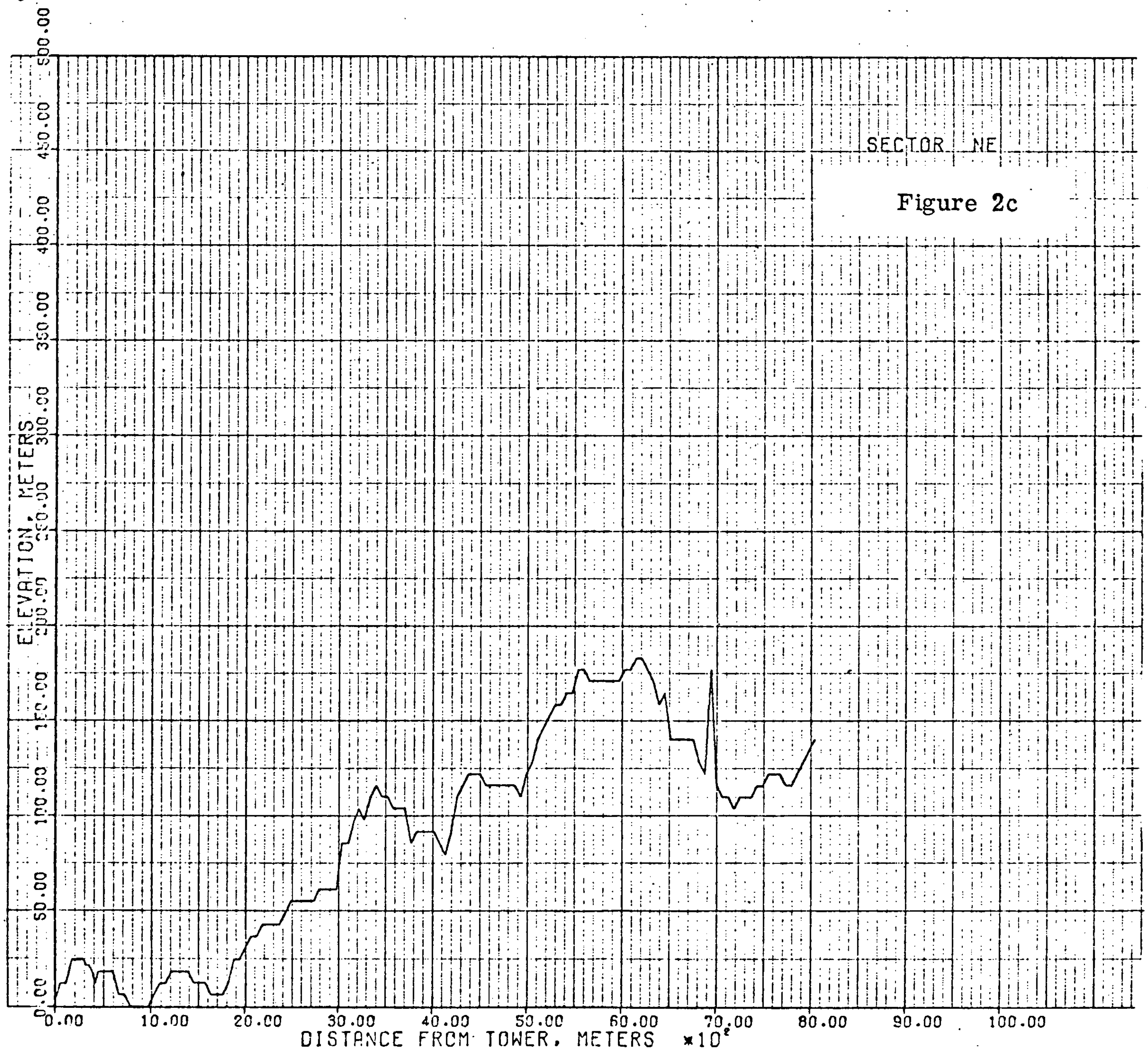
SECTOR NE
ELEVATION, METERS
0.00
50.00
100.00
150.00
200.00
250.00
300.00
350.00
400.00
450.00
500.00
0.00
10.00
20.00
30.00
40.00
50.00
60.00
70.00
80.00
90.00
100.00
DISTANCE FROM TOWER, METERS $\times 10^2$

Figure 2c

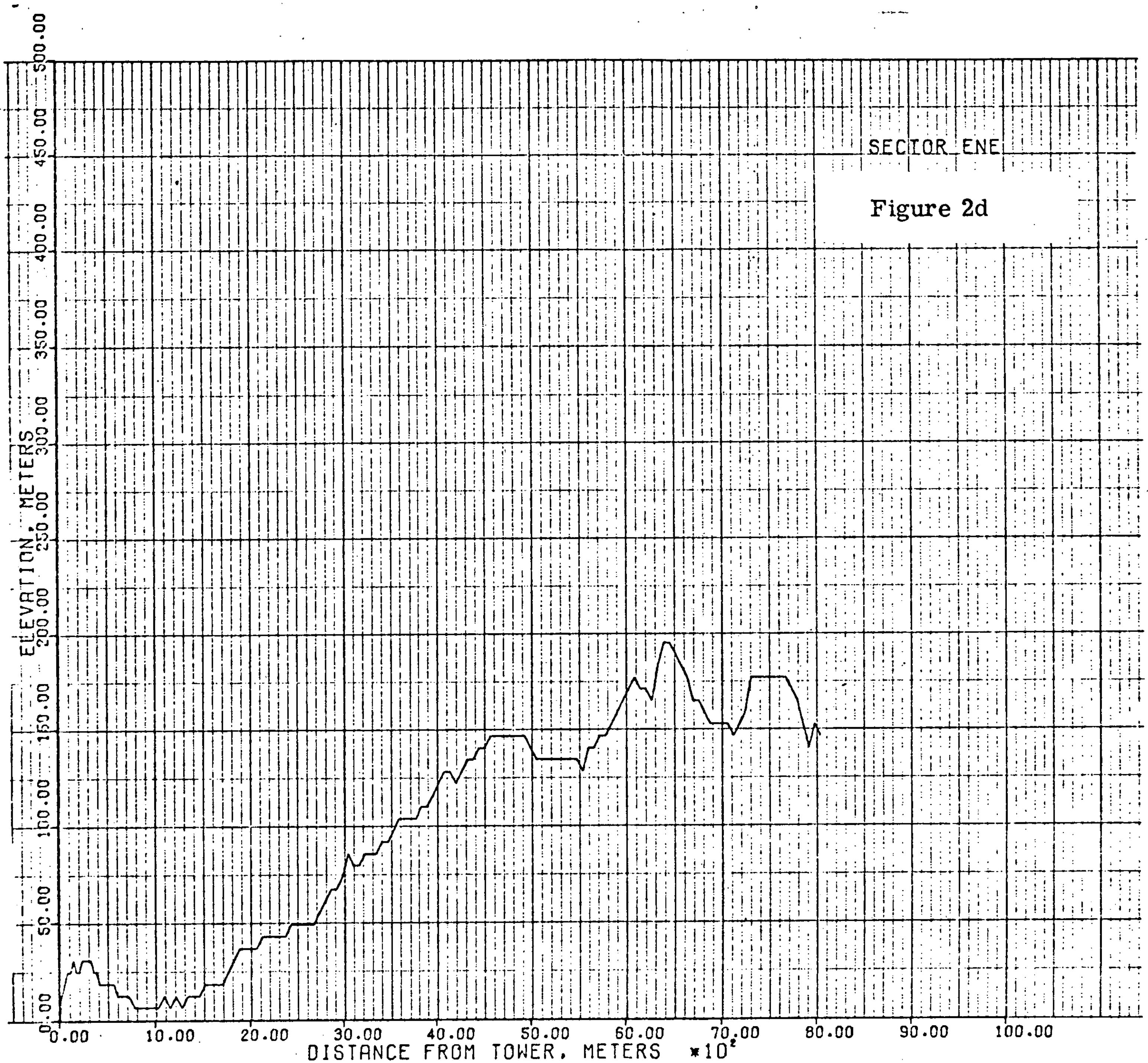
SECTOR ENE
ELEVATION, METERS
0.00
50.00
100.00
150.00
200.00
250.00
300.00
350.00
400.00
450.00
500.00
0.00
10.00
20.00
30.00
40.00
50.00
60.00
70.00
80.00
90.00
100.00
DISTANCE FROM TOWER, METERS *10²

Figure 2d

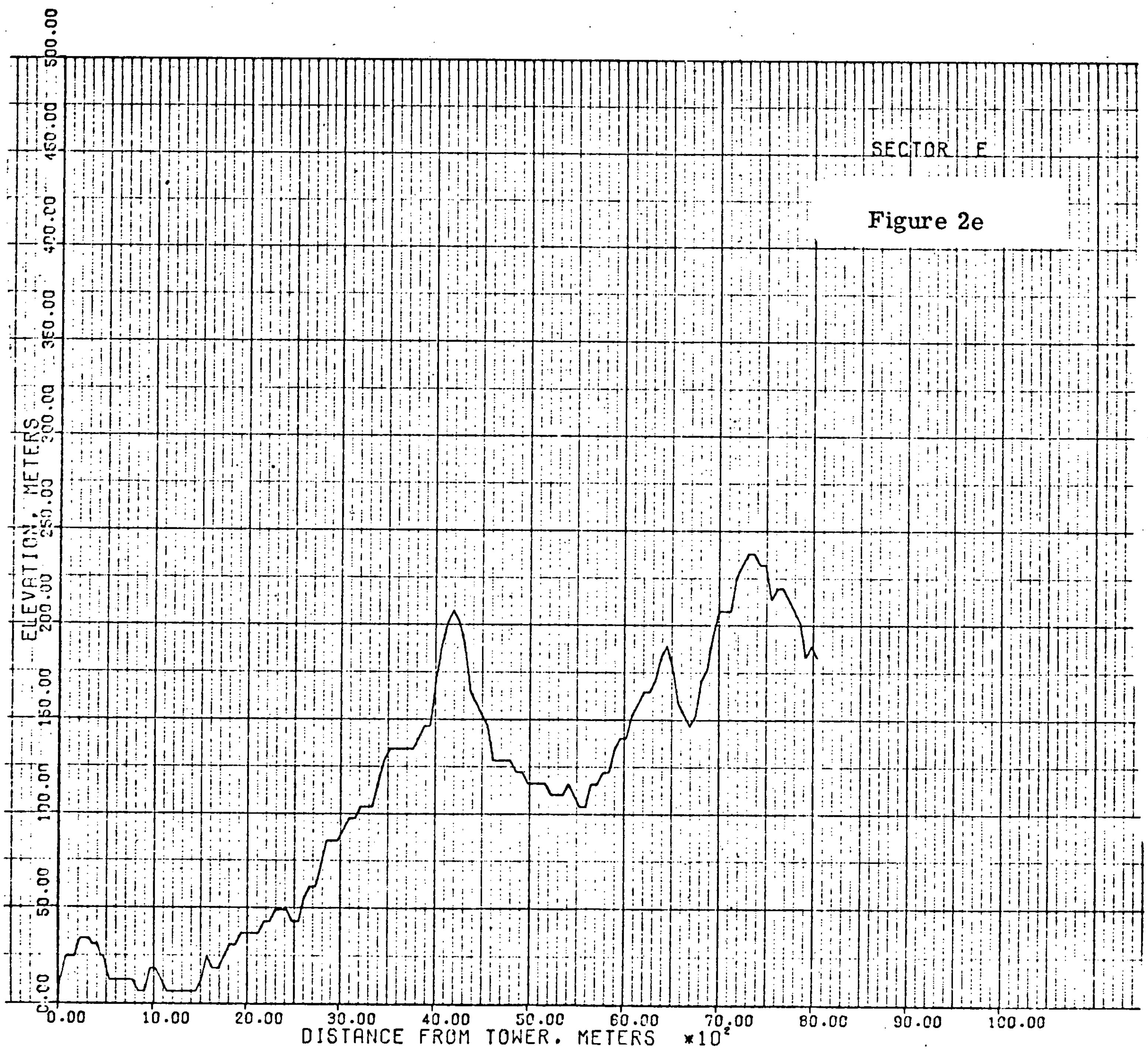
SECTOR E
ELEVATION, METERS
0.00
50.00
100.00
150.00
200.00
250.00
300.00
350.00
400.00
450.00
500.00
0.00
10.00
20.00
30.00
40.00
50.00
60.00
70.00
80.00
90.00
100.00
DISTANCE FROM TOWER, METERS *10²

Figure 2e

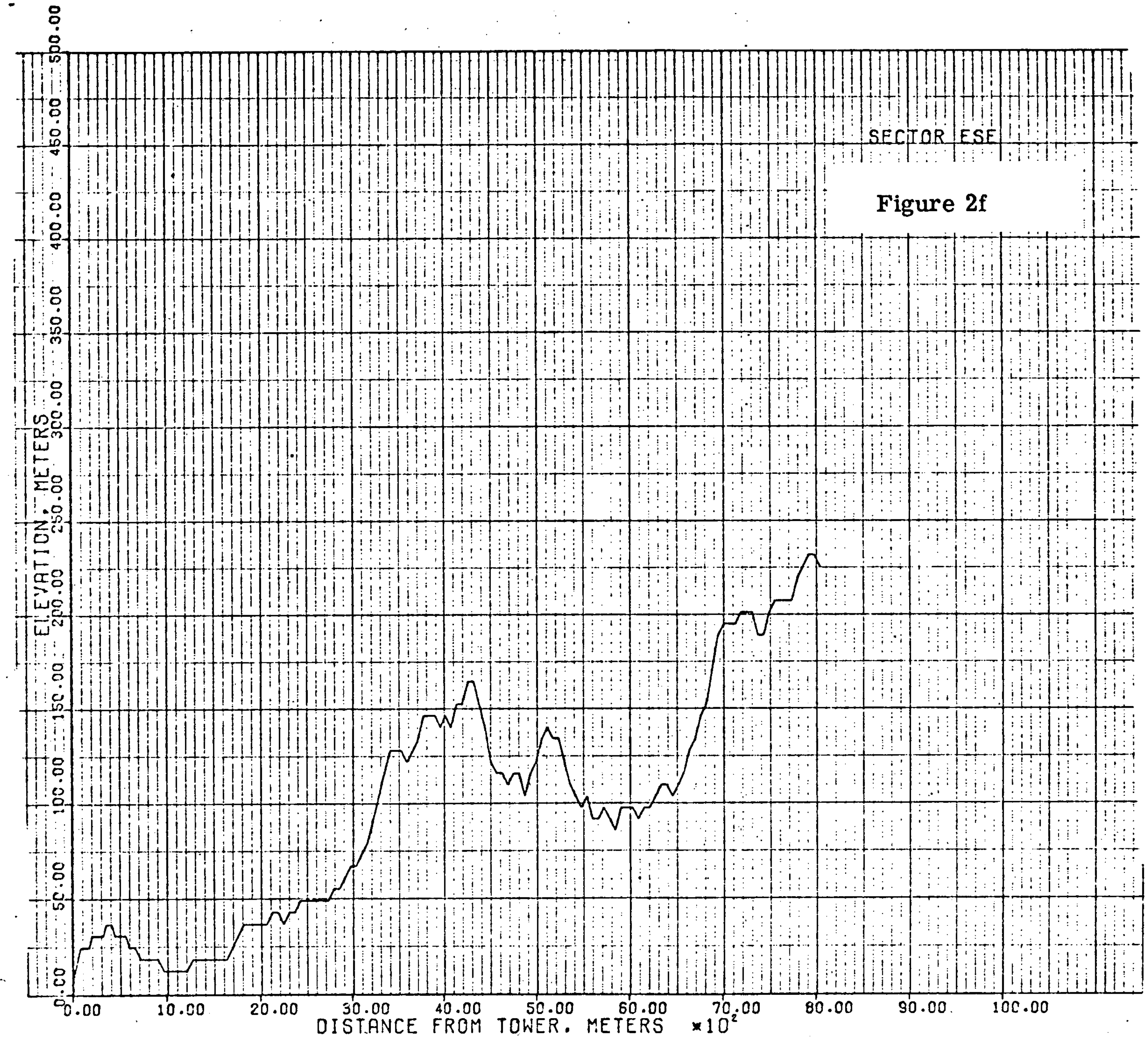

SECTOR ESE
ELEVATION, METERS
0.00
50.00
100.00
150.00
200.00
250.00
300.00
350.00
400.00
450.00
500.00
0.00
10.00
20.00
30.00
40.00
50.00
60.00
70.00
80.00
90.00
100.00
DISTANCE FROM TOWER, METERS $\times 10^2$

Figure 2f

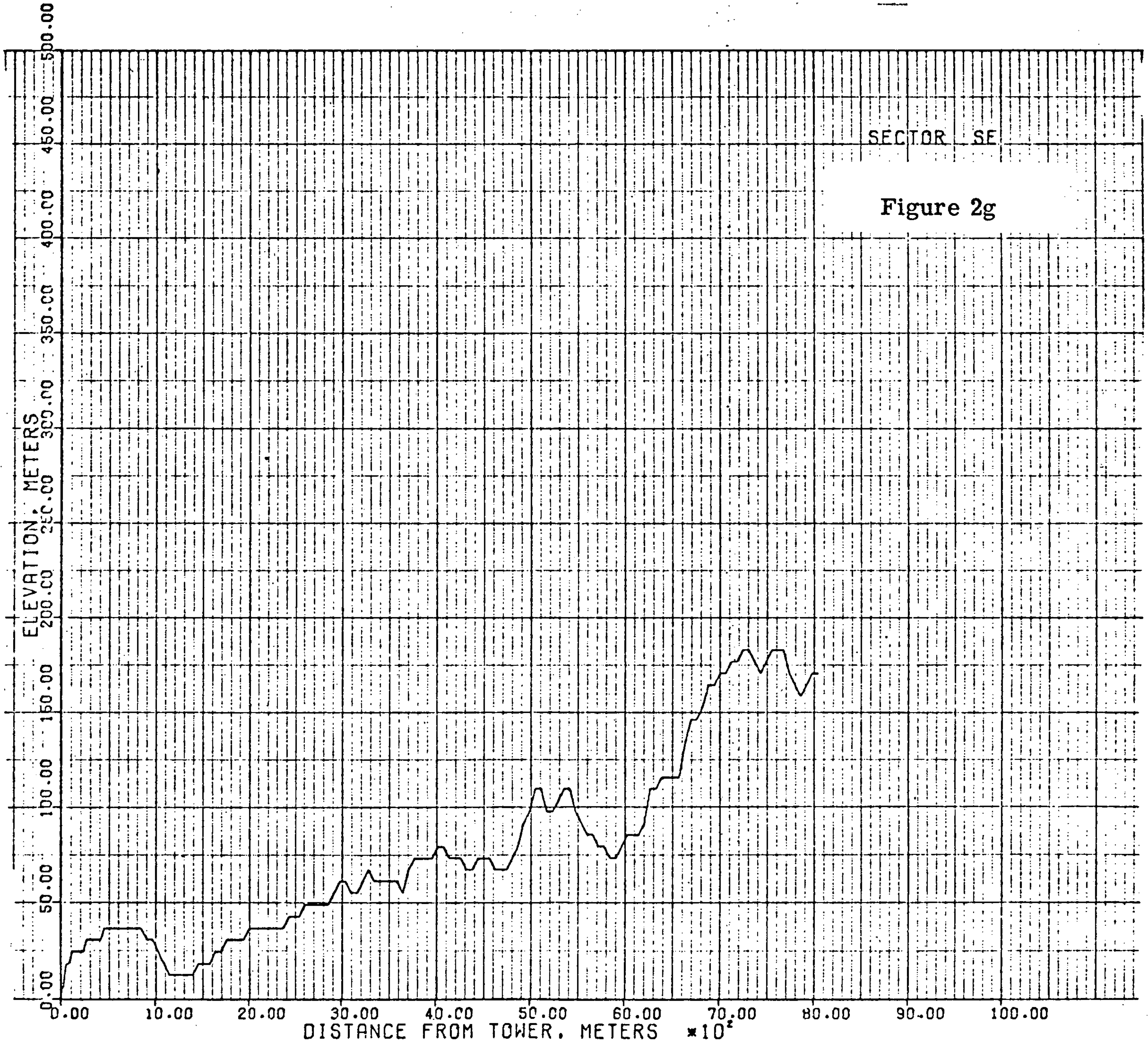
SECTOR SE
ELEVATION, METERS
0.00
50.00
100.00
150.00
200.00
250.00
300.00
350.00
400.00
450.00
500.00
0.00
10.00
20.00
30.00
40.00
50.00
60.00
70.00
80.00
90.00
100.00
DISTANCE FROM TOWER, METERS *10²

Figure 2g

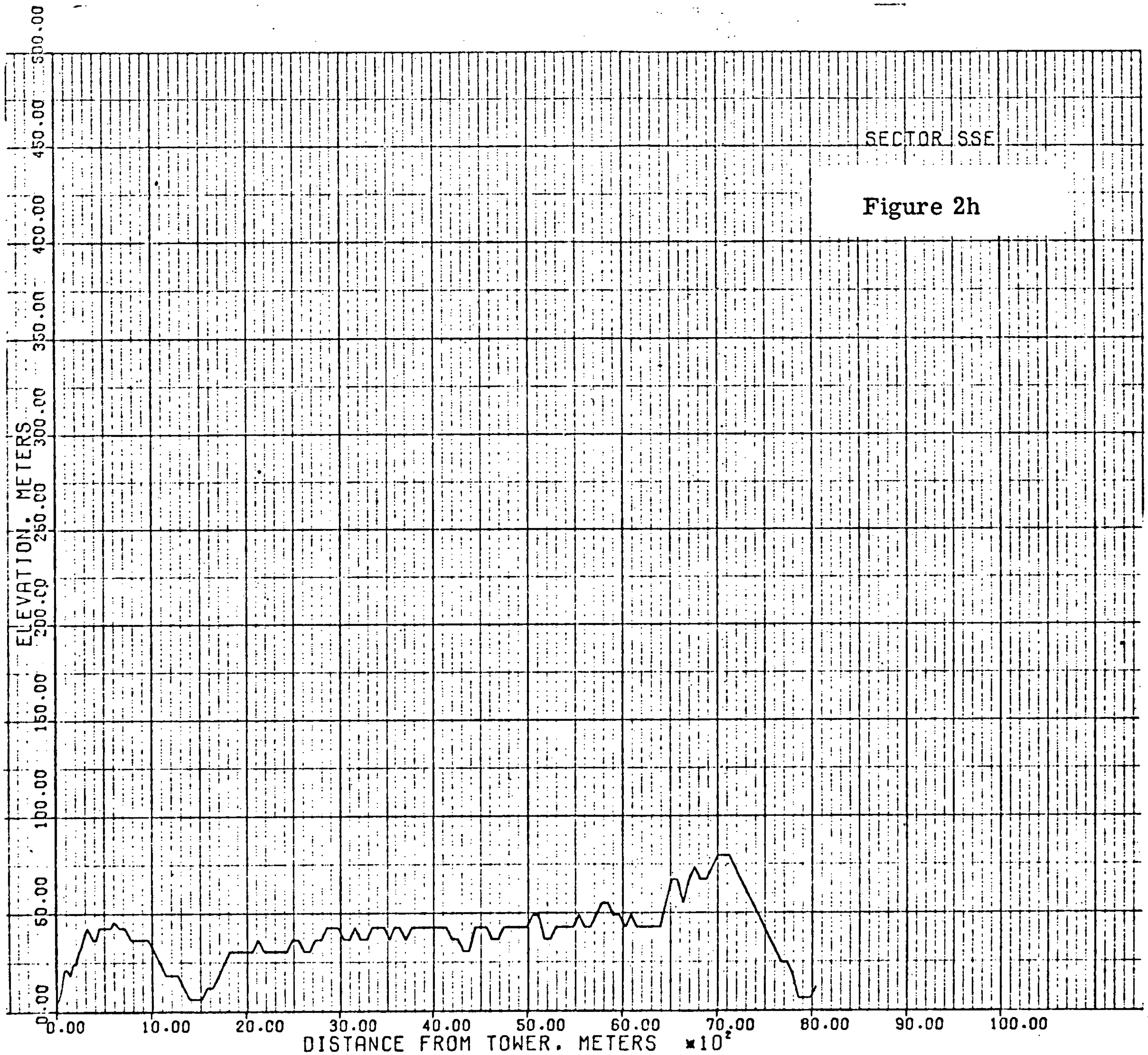
SECTOR SSE
ELEVATION, METERS
0.00
50.00
100.00
150.00
200.00
250.00
300.00
350.00
400.00
450.00
500.00
0.00
10.00
20.00
30.00
40.00
50.00
60.00
70.00
80.00
90.00
100.00
DISTANCE FROM TOWER, METERS $\times 10^2$

Figure 2h

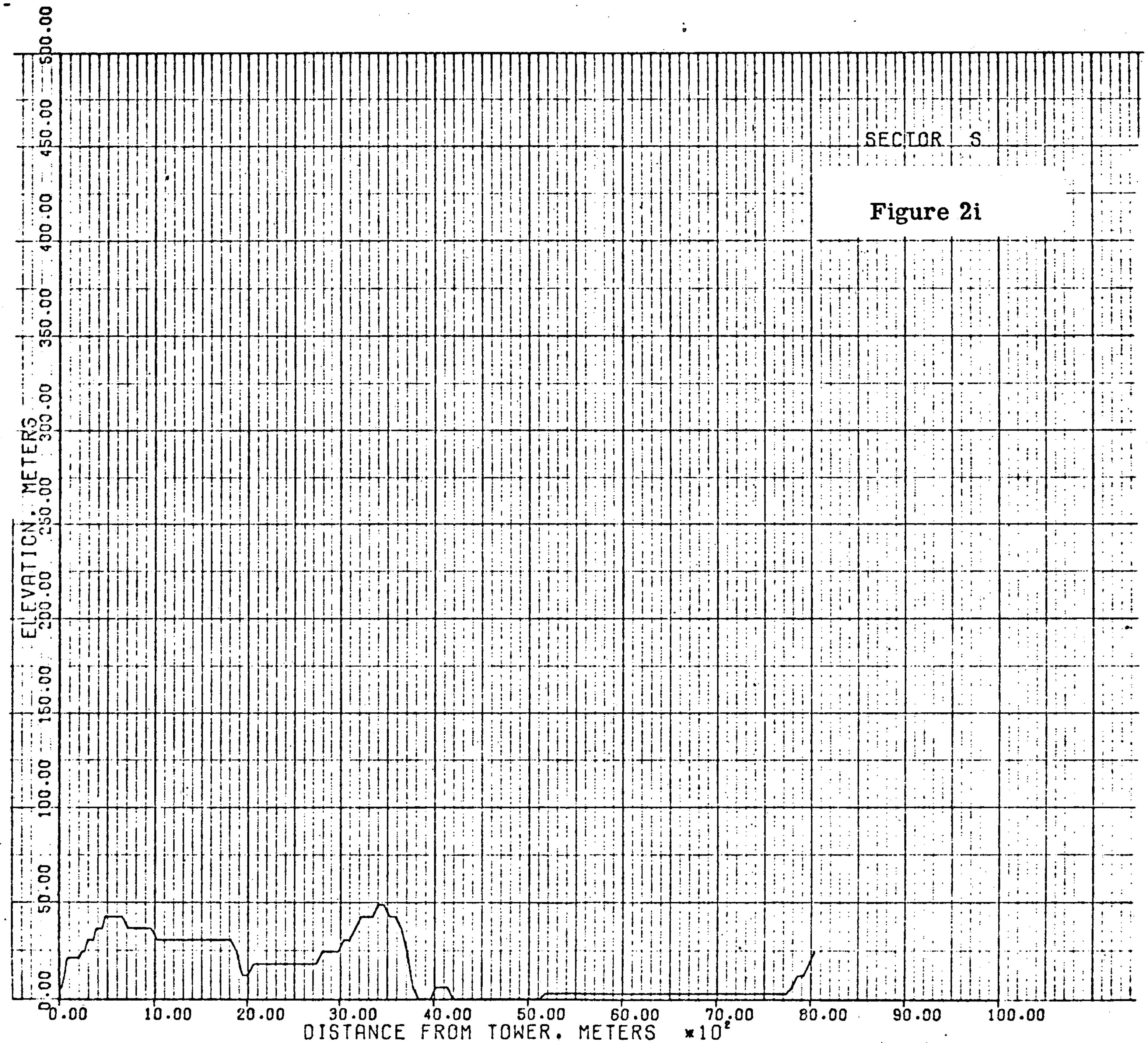
SECTOR S
ELEVATION, METERS
0.00
50.00
100.00
150.00
200.00
250.00
300.00
350.00
400.00
450.00
500.00
0.00
10.00
20.00
30.00
40.00
50.00
60.00
70.00
80.00
90.00
100.00
DISTANCE FROM TOWER, METERS *10²

Figure 2i

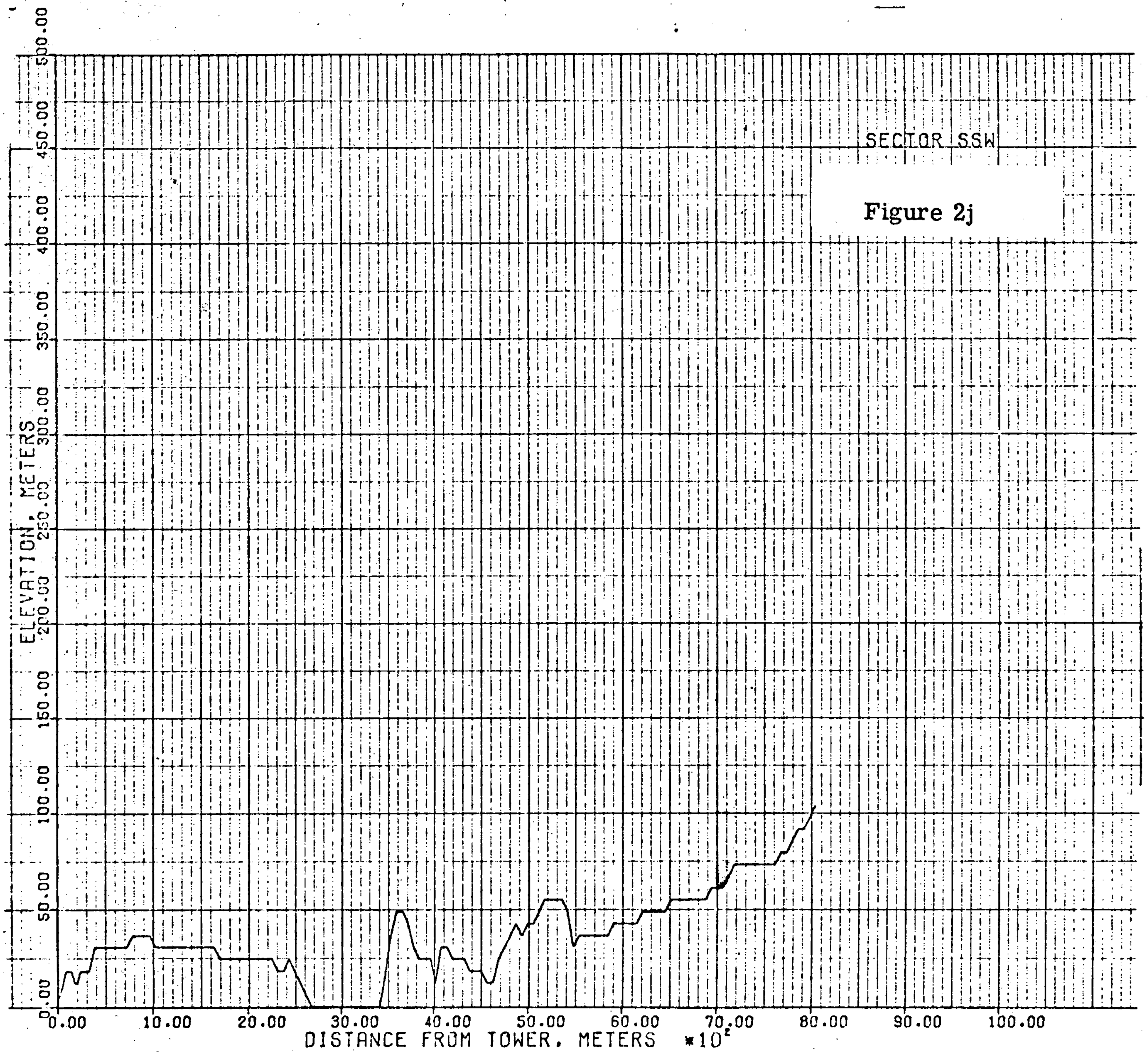
SECTOR SSW
ELEVATION, METERS
500.00
450.00
400.00
350.00
300.00
250.00
200.00
150.00
100.00
50.00
0.00
0.00
10.00
20.00
30.00
40.00
50.00
60.00
70.00
80.00
90.00
100.00
DISTANCE FROM TOWER, METERS *10²

Figure 2j

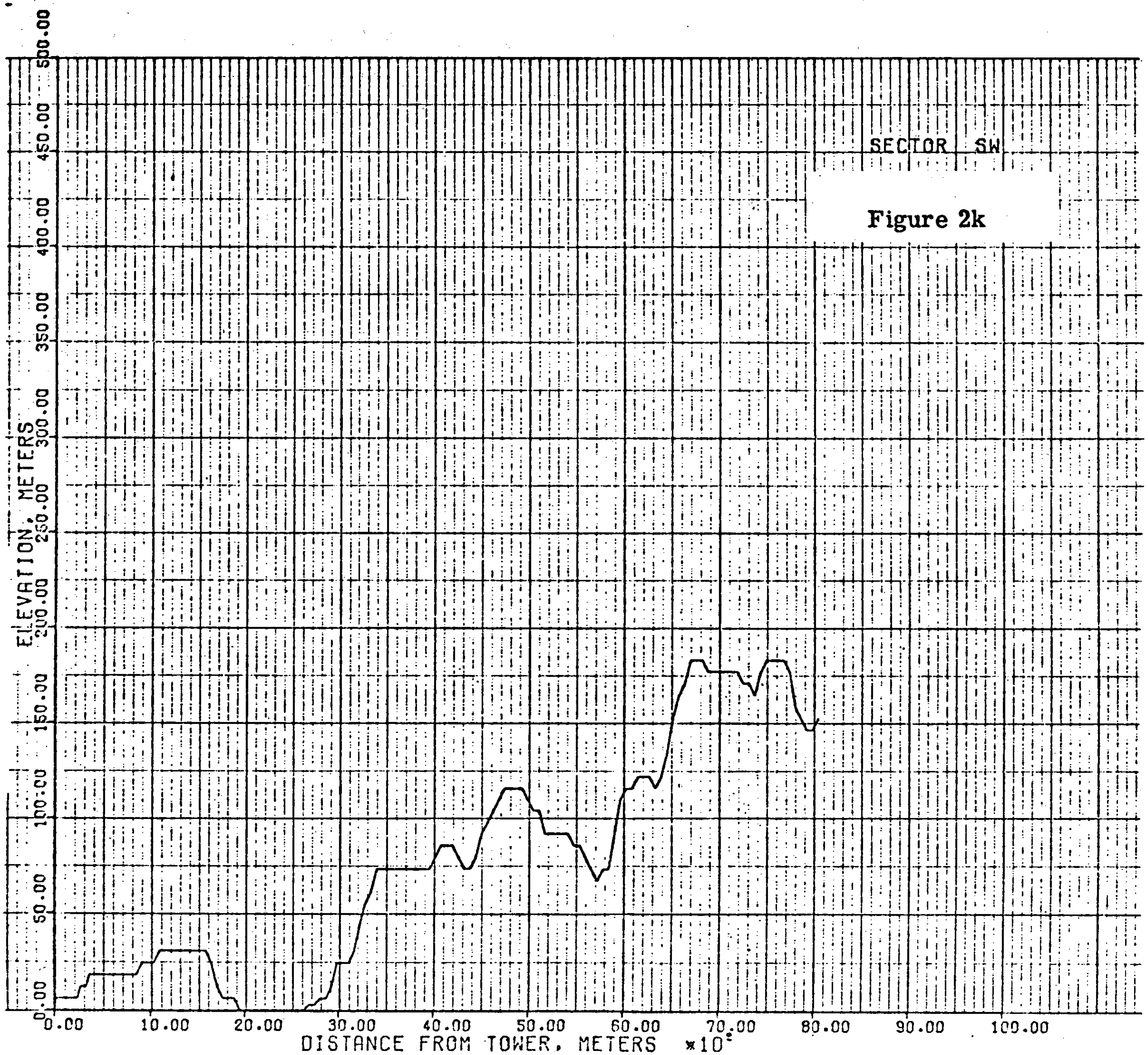
SECTOR SW
ELEVATION, METERS
0.00
50.00
100.00
150.00
200.00
250.00
300.00
350.00
400.00
450.00
500.00
0.00
10.00
20.00
30.00
40.00
50.00
60.00
70.00
80.00
90.00
100.00
DISTANCE FROM TOWER, METERS *10²

Figure 2k

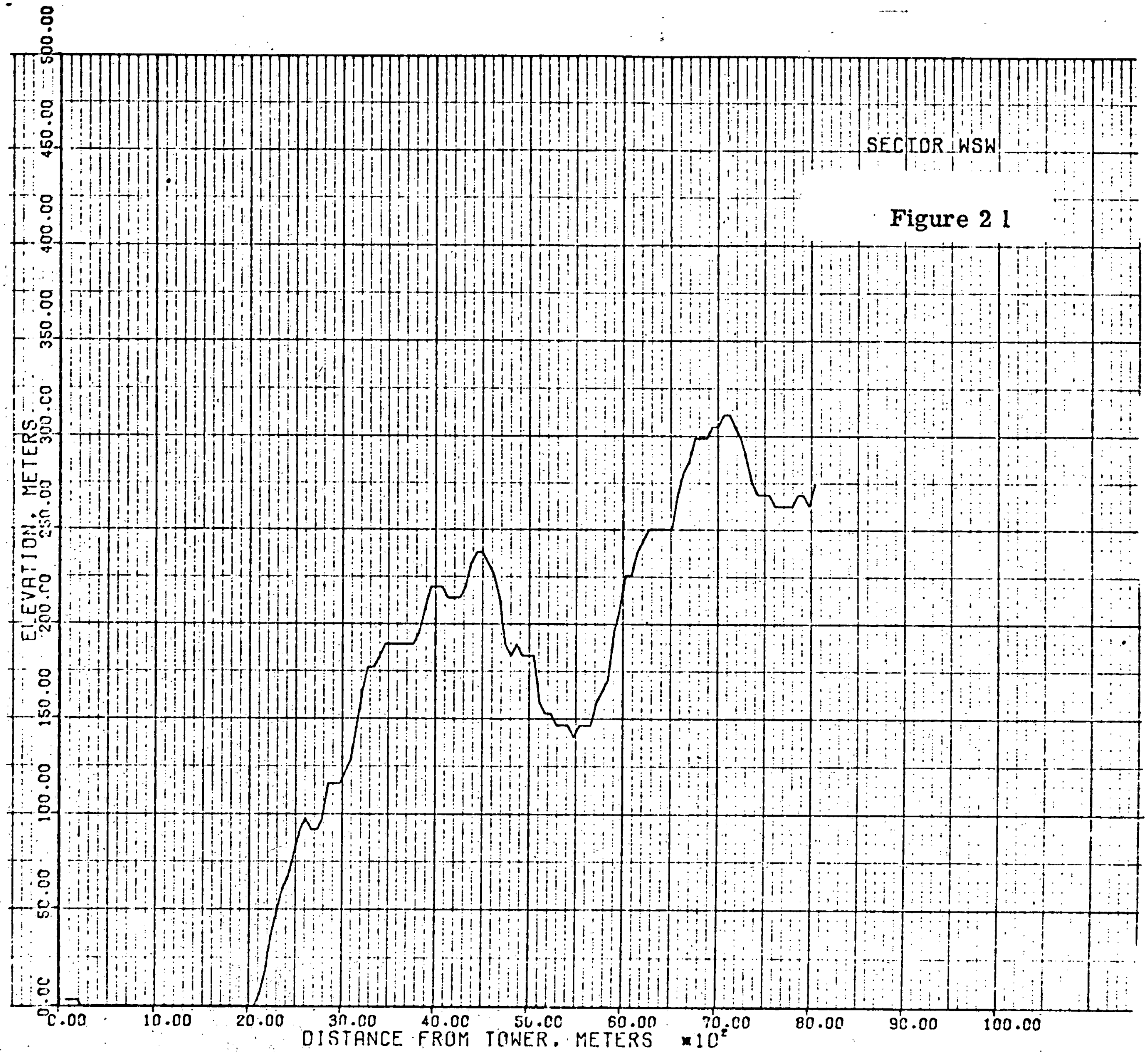
SECTOR WSW
ELEVATION, METERS
0.00
50.00
100.00
150.00
200.00
250.00
300.00
350.00
400.00
450.00
500.00
0.00
10.00
20.00
30.00
40.00
50.00
60.00
70.00
80.00
90.00
100.00
DISTANCE FROM TOWER, METERS *10²

Figure 2 1

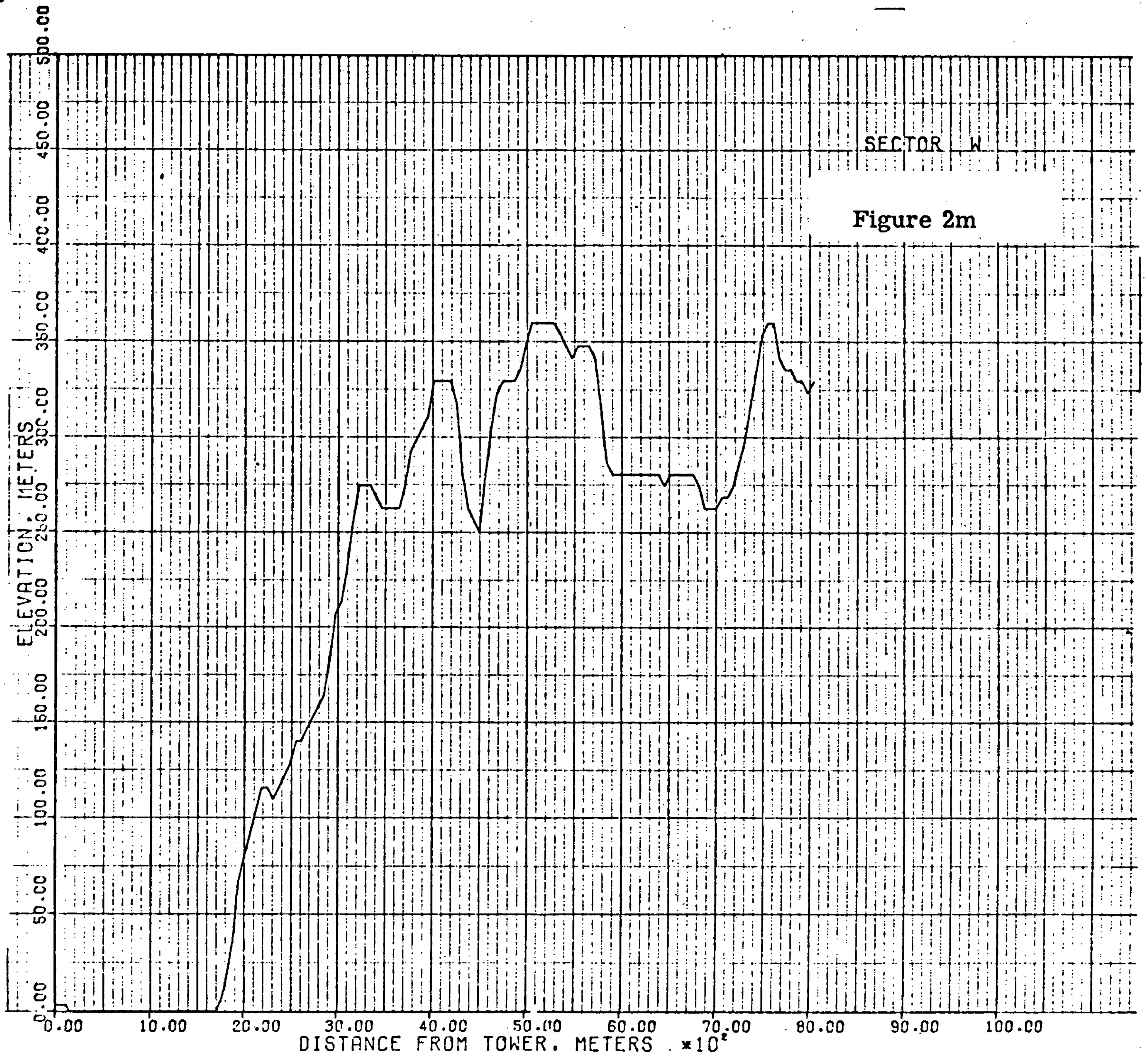
SECTOR W
ELEVATION, METERS
0.00
50.00
100.00
150.00
200.00
250.00
300.00
350.00
400.00
450.00
500.00
0.00
10.00
20.00
30.00
40.00
50.00
60.00
70.00
80.00
90.00
100.00
DISTANCE FROM TOWER, METERS *10²

Figure 2m

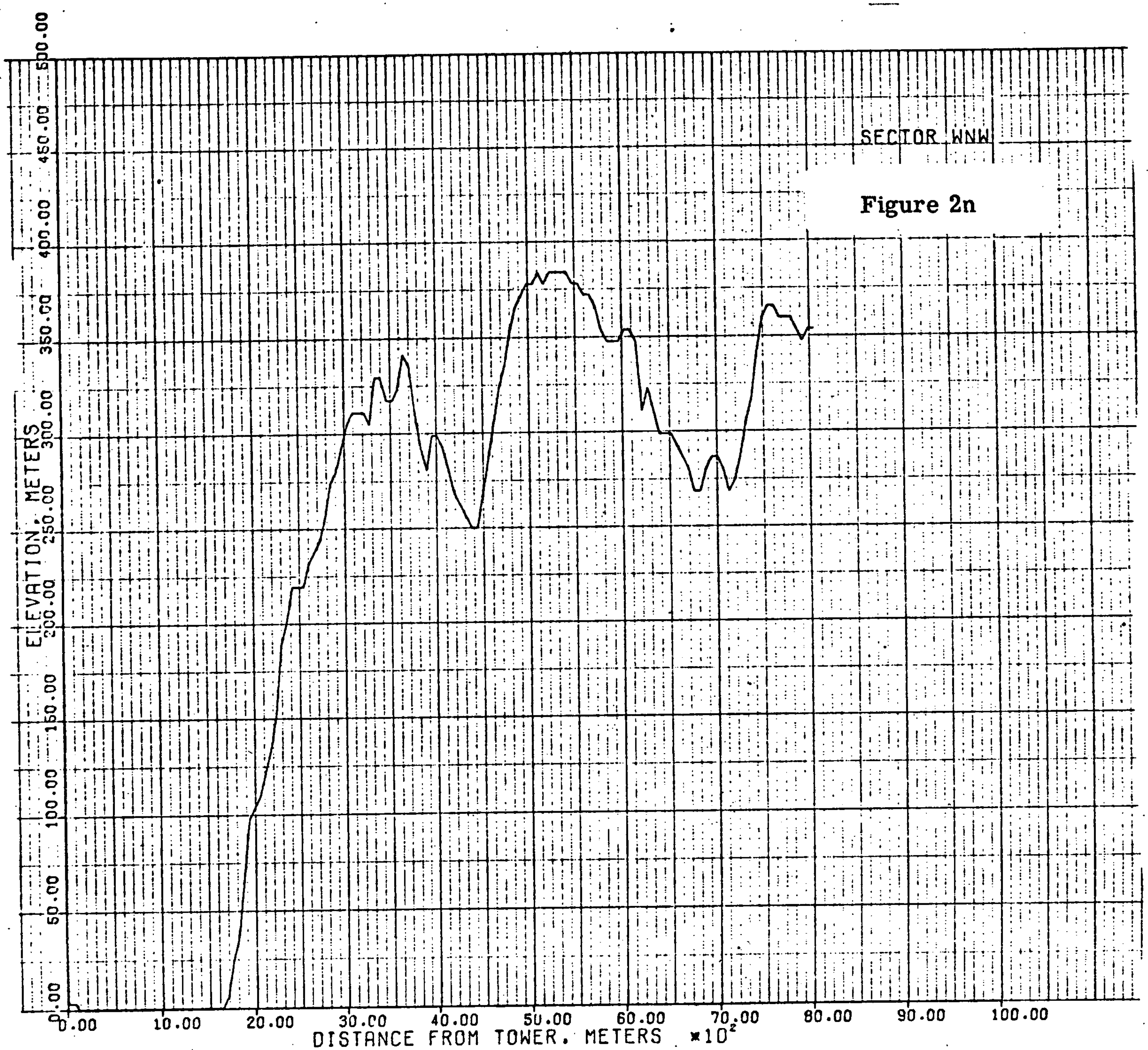
SECTOR WNW
ELEVATION, METERS
0.00
50.00
100.00
150.00
200.00
250.00
300.00
350.00
400.00
450.00
500.00
0.00
10.00
20.00
30.00
40.00
50.00
60.00
70.00
80.00
90.00
100.00
DISTANCE FROM TOWER, METERS $\times 10^2$

Figure 2n

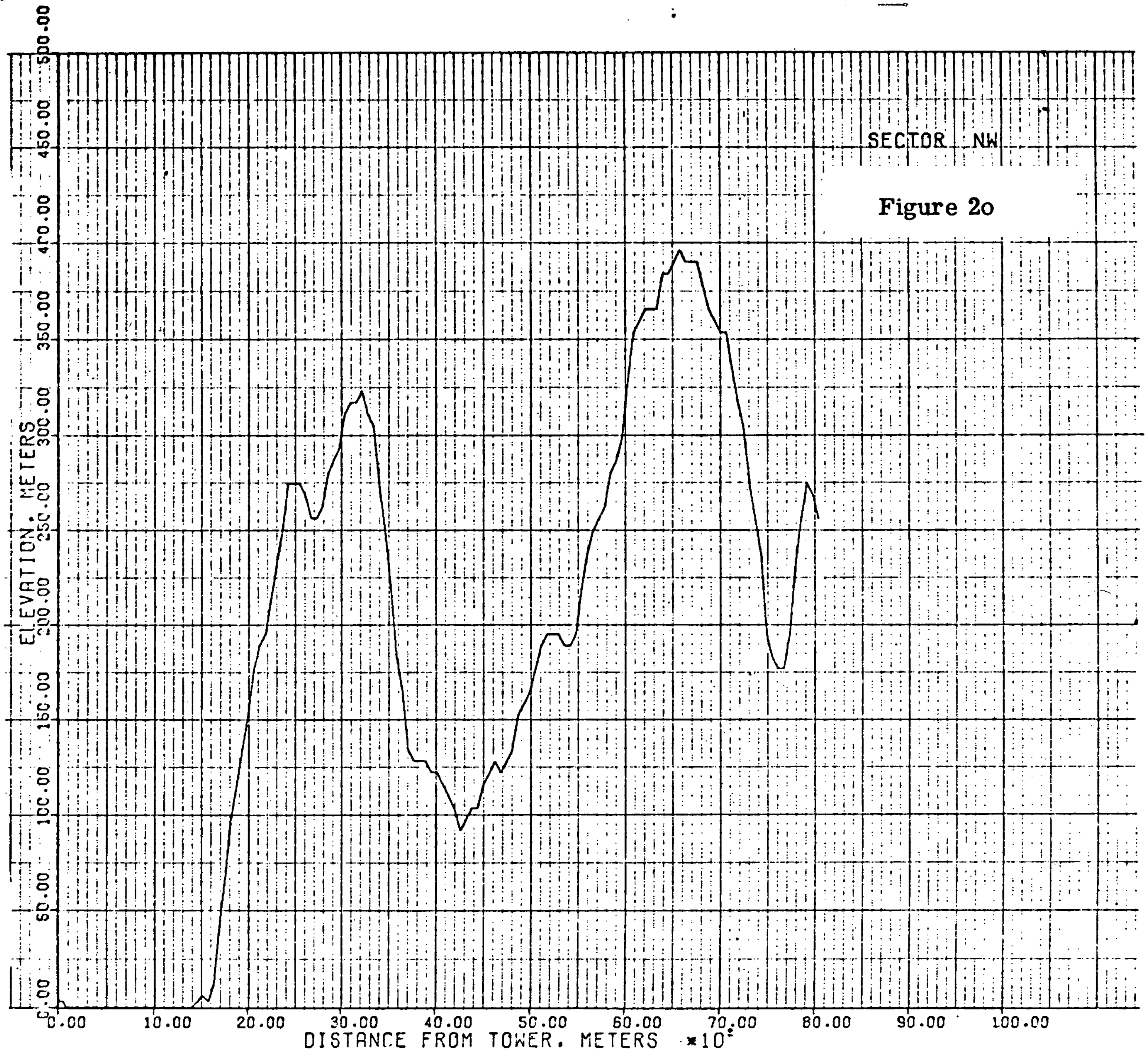
SECTOR NW
ELEVATION, METERS
0.00
50.00
100.00
150.00
200.00
250.00
300.00
350.00
400.00
450.00
500.00
0.00
10.00
20.00
30.00
40.00
50.00
60.00
70.00
80.00
90.00
100.00
DISTANCE FROM TOWER, METERS *10

Figure 2o

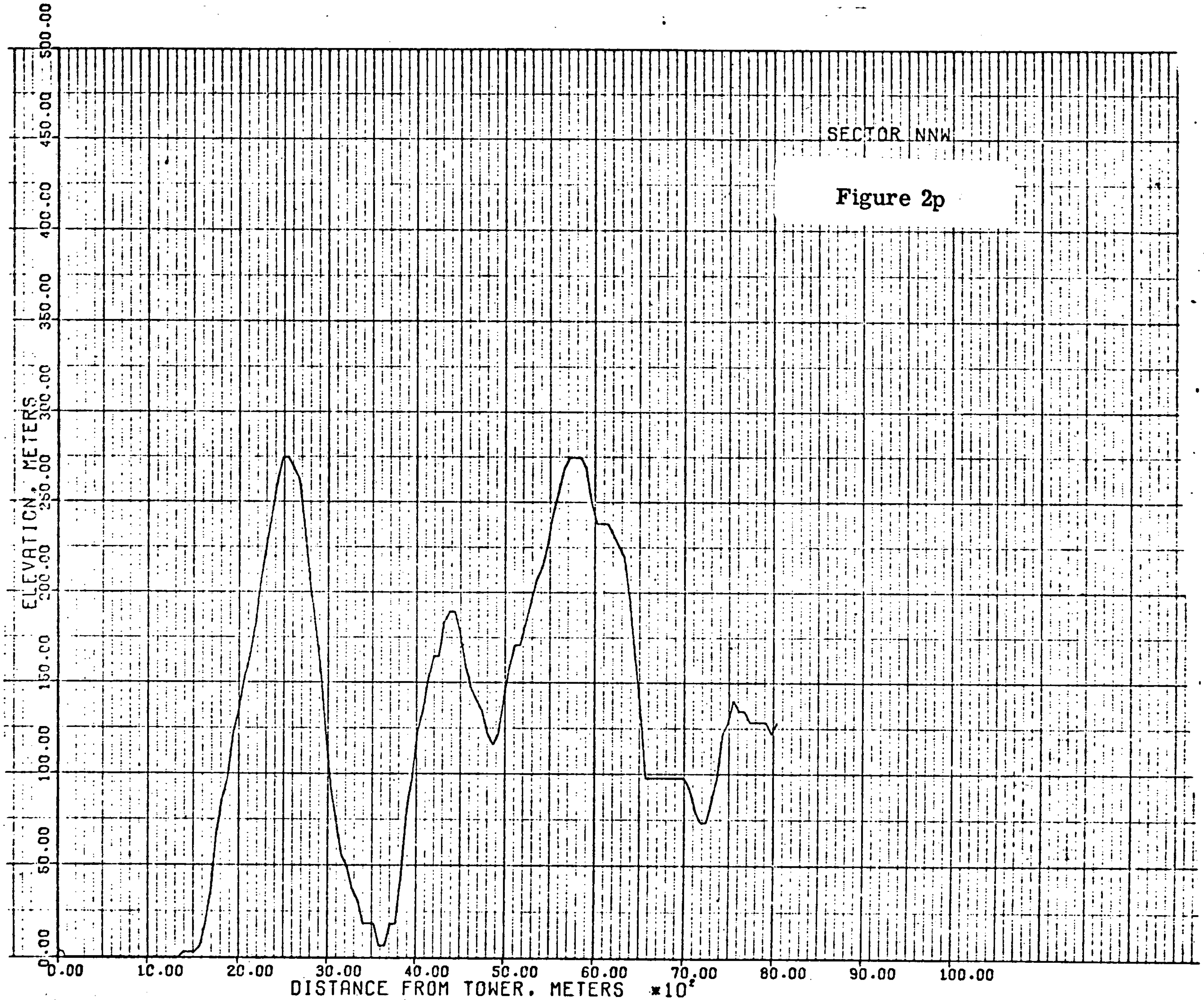
SECTOR NNW
ELEVATION, METERS
0.00
50.00
100.00
150.00
200.00
250.00
300.00
350.00
400.00
450.00
500.00
0.00
10.00
20.00
30.00
40.00
50.00
60.00
70.00
80.00
90.00
100.00
DISTANCE FROM TOWER, METERS *10²

Figure 2p

Addendum 1

Prediction of Temperature and Moisture Distributions in Cooling Tower Plumes

PREDICTION OF TEMPERATURE AND MOISTURE DISTRIBUTIONS IN COOLING TOWER PLUMES

Richard V. Calabrese
University of Massachusetts
Amherst, Mass.

James Halitsky
University of Massachusetts
Amherst, Mass.

Keith Woodard
Pickard, Lowe and Assoc., Inc.
Washington, D. C.

1. INTRODUCTION

Cooling towers remove heat from power plant condenser cooling water primarily by evaporation, and release this heat and moisture into the atmosphere in the form of a warm moist plume. The air-water mixture leaving the top of the tower contains liquid water drops and water vapor. As the mixture rises into the atmosphere and is carried downwind, additional condensation occurs due to entrainment of cooler ambient air. The liquid water drops may subsequently fall to the ground, or may re-evaporate as further dilution occurs. The suspended liquid droplets form the visible part of the cooling tower plume. However, there also exists an invisible plume surrounding the visible plume and extending farther downwind. It may be defined as the region where the air-water vapor mixture has larger mixing ratios and higher temperatures than the ambient air.

The environmental impact of cooling tower plumes may be caused by both visible and invisible plumes. The former contributes directly to visibility reduction, while the latter may lead to other undesirable effects such as increased frequency of fogging, icing of nearby roads and structures, and adverse effects of higher humidity on vegetation. Essentially, the properties of interest are the local mixing ratio and local temperature in the plume. If these are known, psychrometric considerations yield the local liquid water content, a basic parameter for evaluating visibility reduction due to fog. If the ambient temperature and humidity distributions are also known, the potential for fogging due to radiative cooling may be studied.

A moist plume model should provide for the dispersion of enthalpy and moisture in a plume originating in a jet from a finite aperture and expanding along a curved centerline in an atmosphere having arbitrarily specified turbulence and vertical gradients of temperature and humidity.

Several investigators have described the behavior of cooling tower plumes. Csanady (1971), Wigley and Slawson (1971 and 1972) have described the rise of a moist plume. Baker (1967) has presented an empirical formula to calculate the length of the visible plume only. Hanna (1972), Slawson et al (1973), and Stephen and Moroz (1972) have developed theoretical models which, although realistic in their approach, do not account for variation of enthalpy and moisture in the plume cross section and therefore only yield information about the length of the visible plume. Wessels and Wisse (1971) have considered the dispersion of excess plume enthalpy using Gaussian dispersion in plume cross sections. Although such a model allows calculation of ground fogging and considers the invisible plume region, it is only applicable to strong winds where the effects of the initial jet region may be neglected. In addition they have not considered temperature and moisture gradients in the atmosphere. Kaylor et al (1973) have accounted for the effects of the real jet and the variation of diffused quantities in the plume cross section but have not included atmospheric gradients of temperature and moisture.

The model presented here yields information about both the visible plume and the invisible plume, especially with respect to potential for fogging by increase in relative humidity at ground level. The model emphasizes the real characteristics of the plume in the initial jet phase by incorporating a modification of an empirical method by Halitsky (1966) for uncondensed effluents released vertically into a horizontal wind. A Gaussian plume is matched to the jet plume at the end of the jet region and then allowed to expand according to published data on sigma growth (Turner 1969). The shape of the plume centerline is determined from the Briggs (1969) plume rise formula with the buoyancy flux defined in terms of the density difference between the tower effluent and the atmosphere at tower exit. Excess humid air enthalpy and mass of water are conserved in planes normal to the plume centerline, the dispersed quantities being added to the ambient values determined from the profiles of temperature and moisture at the point of interest. Thermodynamic considerations then allow prediction of temperature, liquid water, and water vapor distributions in the plume. Predictions for the combined plume of several towers at one site are achieved by considering an approximate "equivalent jet" having mass, momentum and heat fluxes equal to the sum of the individual tower fluxes. A modification of the model to obtain an estimate of the effect of irregular terrain is also discussed.

2. DISPERSION MODEL

In considering the simultaneous dispersion of enthalpy and moisture, it is assumed that both quantities are dispersed by the same mechanism. Therefore the dispersion model will be developed for an arbitrary quantity, ψ, with the results being related to the quantities of interest later. Halitsky (1966) developed an empirical model for estimating concentrations in isothermal jet plumes by considering published data on jet expansion. He later showed (Halitsky 1967 and 1968) that this method could be extended to heated jets if the path of the plume centerline was described by an appropriate formula.

According to Halitsky (1966), the real jet phase may be divided into two distinct regions, the zone of establishment and the established jet. In Halitsky's Fig. 1, the zone of establishment is characterized by an inner cone whose radius, R_c, diminishes to zero at the end of this region, where axial distance $S = S_1$. The velocity in the inner cone is equal to the tower exit velocity, V_o, and all diffused quantities in the cone retain their initial values. The jet is assumed to be circular in cross section with its outer boundary expanding linearly at rate β_e to radius R_1 at the end of the zone of establishment. The concentration distribution in any cross section is assumed to be trapezoidal.

The established jet region begins at the end of the inner cone and is characterized by decay of both excess velocity and concentration along the plume centerline. The established jet terminates at S_2 with radius R_2 when the excess axial velocity falls to within ten percent of the wind speed. Again the cross section is assumed circular and the plume expands linearly, but at a rate β_j. The concentration distributions in planes normal to the plume centerline are assumed to be triangular.

The values of S_1, R_1, β_e, S_2, R_2, and β_j are functions of the reference emission velocity ratio m $(=V_o/V)$ and are given in Halitsky's Fig. 10. Empirical expressions for these and other quantities are given in Halitsky's Eqs. 4 to 17. Examination of Halitsky's Fig. 10 shows that for low emission ratios $(m < 1.5)$, the jet is not well-defined. This is the case for natural-draft towers where exit velocities are low (about 2.5 m/sec). Therefore it is assumed that for $m < 1.1$ no established jet region exists and that the simple or Gaussian plume begins at the end of the zone of establishment.

If conservation of mass is applied in the zone of establishment, the following expression for R_1 may be derived:

$$R_1/R_o = [6m/(1+m)]^{1/2} \qquad (1)$$

It is recommended that this expression be used instead of Halitsky's Eq. 16 since it fits the data well and allows extrapolation to very low velocity ratios. Eq. 1 shows that at m = 0.2, $R_1 = R_o$. Therefore it is assumed that for $m < 0.2$ no jet plume exists. The application of the conservation equation in this region also allows calculation of the radius of the inner cone from the known value of the plume radius, R, using the following equation:

$$6(R-R_c)^2 R_o^2 = [R^4 - 4RR_c^3 + 3R_c^4] + [R^4 + 2RR_c^3 - 2R^3R_c - R_c^4]/m \qquad (2)$$

Observations of cooling tower plumes reveal that the initial jet region is not circular but ellipsoidal in cross section, the major axis being in the crosswind direction. It is assumed that the degree of flattening is a function of atmospheric stability and can be estimated by the ratio of crosswind to vertical dispersion coefficients as given by the Pasquill charts of sigma growth. If conservation of mass in cross sections normal to the plume axis is considered we may define crosswind and vertical jet radii by

$$R_y = R\sigma_y/\sigma_z \quad ; \quad R_z = R\,\sigma_z/\sigma_y \qquad (3)$$

where R, σ_y, and σ_z are evaluated at the axial distance S. With these definitions, the distance R' from the plume axis to the jet plume boundary along a radius passing through any point of interest (y,z) in a given plume cross section is

$$R' = \left\{\frac{[(z-h)^2 + y^2]R_y^2 R_z^2}{(z-h)^2 R_y^2 + y^2 R_z^2}\right\}^{1/2} \qquad (4)$$

The corresponding radius of the inner cone, R_c', may be described in a similar manner.

With these definitions, the dilution, $D(=\psi_o/\psi_p)$ may be written as follows:

<u>In zone of establishment:</u>

$$\begin{aligned} &D = 1 && b \le R_c' \\ &D = (R'-R_c')/(R'-b) && R_c' < b < R' \\ &D = \infty && b \ge R' \end{aligned} \qquad (5)$$

<u>In established jet region:</u>

$$\begin{aligned} &D = D_a/[1-b/R'] && b < R' \\ &D = \infty && b \ge R' \end{aligned} \qquad (6)$$

where D_a is the axial dilution given by Halitsky's Eq. 4 and $b(=[y^2 + (z-h)^2]^{1/2})$ is the radial distance from the plume axis to the point (y,z) of interest.

The jet plume must now be matched with the simple Gaussian plume at station $S = S_2$ in order for the dispersion model to be complete. Diffusion in the simple plume is described by

$$D = \frac{2\pi\sigma_y\sigma_z V}{\pi R_o^2 V_o} \exp\left[\frac{1}{2}\left(\frac{y}{\sigma_y}\right)^2\right] \cdot \left\{\exp\left[-\frac{1}{2}\left(\frac{z-h}{\sigma_z}\right)^2\right] + \exp\left[-\frac{1}{2}\left(\frac{z+h}{\sigma_z}\right)^2\right]\right\}^{-1} \qquad (7)$$

If the radii of the Gaussian plume are defined as the distance where the concentration falls to five percent of its centerline value, the following expressions result:

$$R_y = \sqrt{6}\,\sigma_y \quad ; \quad R_z = \sqrt{6}\,\sigma_z \qquad (8)$$

If Eqs. 6, 7 and 8 are used to match the axial concentrations at $S = S_2$, the simple plume will expand from station S_2 according to

$$\sigma_y = R_{y2}/\sqrt{6} + \sigma_y' \quad ; \quad \sigma_z = R_{z2}/\sqrt{6} + \sigma_z' \qquad (9)$$

where σ_y' and σ_z' are the Pasquill sigma values taken at the distance $S-S_2$.

3. PLUME RISE

The shape of the plume centerline is described by the generalized Briggs plume rise formulas

$$h = h_s + a\, F^{1/3}\, X^{2/3}\, V^{-1} \qquad (10)$$

and $a = (3/2\gamma^2)^{1/3}$ (11)

where γ is the entrainment coefficient and F is the buoyancy flux. A value of a = 1.6 is suggested by Briggs. The point of maximum rise is taken to be X = 3X* for unstable and neutral conditions, where X* is given by Eq. 4-35 of Briggs (1969). A modification of Eq. 12 for neutral conditions is given by Briggs' Eq. 4-34. The distance to maximum rise for stable conditions is given by

$$X = 2.4V\,(g/T)\,(\partial\theta/\partial z) \qquad (12)$$

where T is the ambient temperature at tower height and $\partial\theta/\partial z$ is the gradient of potential temperature in the atmosphere. The buoyancy flux is defined by

$$F = (1-\rho_o/\rho)gV_oR_o^{\,2} \qquad (13)$$

where ρ is the ambient density at tower exit. It should be noted that even if the tower exit temperature is very close to the ambient temperature the buoyancy flux may be considerable since the saturated tower air is considerably lighter than the ambient air due to its high water vapor content.

Briggs' formulas were developed for dry plumes and may not describe the path of the moist cooling tower plume accurately. However if the two-thirds distance law is assumed to apply, as suggested by Slawson et al (1973), a suitable value of γ may be selected to provide a better fit. A knowledge of both X and h allows calculation of the axial distance, S.

4. CALCULATION OF PLUME PROPERTIES

Before considering the calculation of plume properties from dispersed quantities it is necessary to define a few properties of humid air. The density of humid air is defined from the ideal gas law as

$$\rho = \frac{(1+r+\ell)\rho m_w}{(m_w/m_a + r)R_G T} \qquad (14)$$

where r and ℓ are the vapor and liquid mixing ratios respectively. The moisture concentration is then

$$M = \rho(r+\ell)/(1+r+\ell) \qquad (15)$$

The enthalpy, defined on a wet basis, is, for unsaturated conditions

$$H = [C_{pa}(T-T_R) + r\,C_{p\ell}(T_D-T_R) + r\,\lambda + rC_{pv}(T-T_D)]/(1+r) \qquad (16)$$

where the heat of vaporization, λ, is a function of the dew point temperature, T_D. The reference temperature, T_R, is usually taken as zero degrees F. For saturated conditions, the dry bulb and dew point temperatures are equal. If liquid water is present

$$H = \{[C_{pa} + (r+\ell)C_{p\ell}](T-T_R) + r\lambda\}/(1+r+\ell) \qquad (17)$$

The intial excess concentrations of moisture and enthalpy are then defined by

$$M_e = M_o - M(h_s) \qquad (18)$$

$$H_e = \rho_oH_o - \rho(h_s)\,H(h_s) \qquad (19)$$

where $M(h_s)$, $\rho(h_s)$, $H(h_s)$ are the ambient values of moisture concentration, density, and enthalpy evaluated at the height of the tower. When these excess quantities are dispersed according to the appropriate dilution factors and added to the background concentrations evaluated at the appropriate height above ground, z, we obtain the moisture concentration (M_p) and enthalpy concentration (ρ_pH_p) in the plume

$$M_p = M_e/D + M(z) \qquad (20)$$

$$\rho_pH_p = H_e/D + \rho(z)H(z) \qquad (21)$$

The plume density, moisture concentration, and enthalpy are related to plume temperature, dew point, and mixing ratios by Eqs. 14 to 17. In addition, the vapor mixing ratio is a function of the dew point as described by the molal humidity chart. Therefore simultaneous solution of these equations allows calculation of T_p, T_{Dp}, r_p, and ℓ_p.

The visible plume is characterized by $\ell_p > 0$ and $r_p = r_s$, where r_s is the saturation vapor mixing ratio at the plume temperature, T_p. The invisible plume is described by $\ell_p = 0$ and $r_p \le r_s$. In the invisible plume the relative humidity is

$$RH = \frac{r_p}{(\frac{m_w}{m_a} + r_p)} \Bigg/ \frac{r_s}{(\frac{m_w}{m_a} + r_s)} \;. \qquad (22)$$

5. ADDITIONAL CONSIDERATIONS

In some instances cooling towers may be located where the local grade of the surroundings cannot be ignored. If the nearby hills and valleys are not too steep, a rough estimate of the effect of terrain may be obtained by considering the rise of the plume relative to the local grade. The model is used as previously described but the plume height, h, in Eq. 7 is replaced by the height of the plume centerline above the local grade at the downwind position of interest. Eq. 10 is still used to obtain the plume centerline but the result must be viewed as the height of the plume centerline above the tower base only. The use of this model in hilly areas ignores the fact that the wind may follow the contours of the land. However such an estimate will be conservative in that it does not account for the additional dilution afforded by the interaction of the wind with the local topography.

Very seldom will there be a situation in which only one cooling tower is in operation. Therefore the case where the plumes from several closely spaced towers merge must be considered. Even if only one bank of mechanical towers were present, the combined plume from the individual cells is initially rectangular and not circular as assumed by the model. An equivalent jet of circular cross section may be defined such that the exit area of this jet is greater than or equal to the sum of the areas of the individual cells. It is assumed that this jet originates at an elevation equal to the height of the towers and that entrainment of ambient air from between the towers occurs at this height. This assumption is not realistic as the plumes from the individual towers will not combine until they have risen a considerable distance. However for situations where the length of the visible plume is large compared to the tower spacing, we can obtain an estimate for the properties of the combined plume.

Consider the case of n towers and let subscript E represent the equivalent jet. The radius of the equivalent jet, R_E, must be assumed according to the particular tower configuration. Then the ratio of the equivalent jet area to the combined area of the individual towers is

$$\alpha = A_E / \sum_{i=1}^{n} (A_o)_i \qquad (23)$$

The momentum balance is

$$\sum_{i=1}^{n} [(\rho_o A_o V_o) V_o]_i = (\rho_E A_E V_E) V_E \qquad (24)$$

The mass balance on moisture is

$$\sum_{i=1}^{n} \rho_o A_o V_o \left[\frac{r_o + \ell_o}{1 + r_o + \ell_o}\right]_i + \rho\, Q \left[\frac{r}{1+r}\right] = \rho_E A_E V_E \left[\frac{r_E + \ell_E}{1 + r_E + \ell_E}\right] \qquad (25)$$

where

$$Q = A_E V_E - \sum_{i=1}^{n} (A_o V_o)_i$$

The second term on the left hand side of Eq. 25 accounts for the entrainment of ambient air. All ambient quantities are evaluated at the tower height. The enthalpy balance, which also accounts for entrainment of ambient enthalpy, is

$$\sum_{i=1}^{n} (\rho_o A_o V_o H_o)_i + \rho\, Q\, H = \rho_E A_E V_E H_E \qquad (26)$$

The densities and enthalpies can be related to temperatures and mixing ratios with Eqs. 14 to 17. Therefore Eqs. 24 to 26 can be solved simultaneously for T_E, T_{DE}, r_E, ℓ_E, and V_E. These calculated quantities can be substituted for the single tower values and the equivalent jet can be treated as a single tower for use in the dispersion model.

6. EXAMPLE CALCULATIONS AND DISCUSSION

Calculations were performed for a 270 MW power plant containing one bank of mechanical draft towers of the following specifications: number of cells = 12, cell diameter = 9.45 m, tower height = 17.9m, cell exit velocity = 6.76 m/sec, circulating water flow rate = 183,330 GPM, and heat dissipated in tower = 1.9×10^9 BTU/hr. The tower exit conditions, which are a function of ambient temperature and humidity, were calculated using the method of Leung and Moore (1971). Reference ambient conditions were taken at the elevation of the tower exit. The temperature lapse rate was assumed equal to -0.03, -.01, and +.027 C/m for stabilities B, D, and F respectively. Relative humidity was assumed constant with height. The equivalent jet area was chosen such that $\alpha = 1$.

Fig. 1 shows the length of the visible plume as a function of ambient temperature and relative humidity for stabilities B, D, and F and wind speeds of 2, 5, and 8 m/s. Jogs in some of the curves are due to the approximation to the molal humidity curve used in the computer program.

Visible plume length is seen to be strongly dependent on ambient temperature and humidity, varying inversely with the former and directly with the latter. The dependence on wind speed is not so obvious. For unstable and neutral conditions, light winds allow the plume to rise high to cooler elevations, thereby inhibiting evaporation and producing long plumes, whereas strong winds produce small rise, thereby keeping the plume in warmer regions with greater tendency to evaporate. This latter effect is augmented by the increased dilution resulting from increased wind speed. Therefore the length of the visible plume decreases with increasing wind speed. For stable conditions, plume lengths are insensitive to wind speed. Light winds produce large plume rises to warmer regions where poor axial dispersion due to speed is balanced by increased evaporation due to temperature, whereas strong winds keep the plume low in a cooler environment where the strong dispersion due to speed is again balanced by less evaporation due to temperature. The length of the visible plume increases as the atmosphere becomes more stable. However, the invisible plume will not be as readily detected at ground level as for unstable conditions since the degree of radial dispersion about the plume centerline decreases. The points discussed above show the importance of having accurate knowledge of the ambient profiles of temperature and moisture when calculating visible and invisible plume properties.

Fig. 2 shows the size of the visible plume and the vertical boundary radius ($\sim 2.5\ \sigma_z$) of the invisible plumes for a D stability atmosphere, 40°F ambient temperature, 90 percent relative humidity, and a wind speed of 5 m/sec. The corresponding liquid water concentration

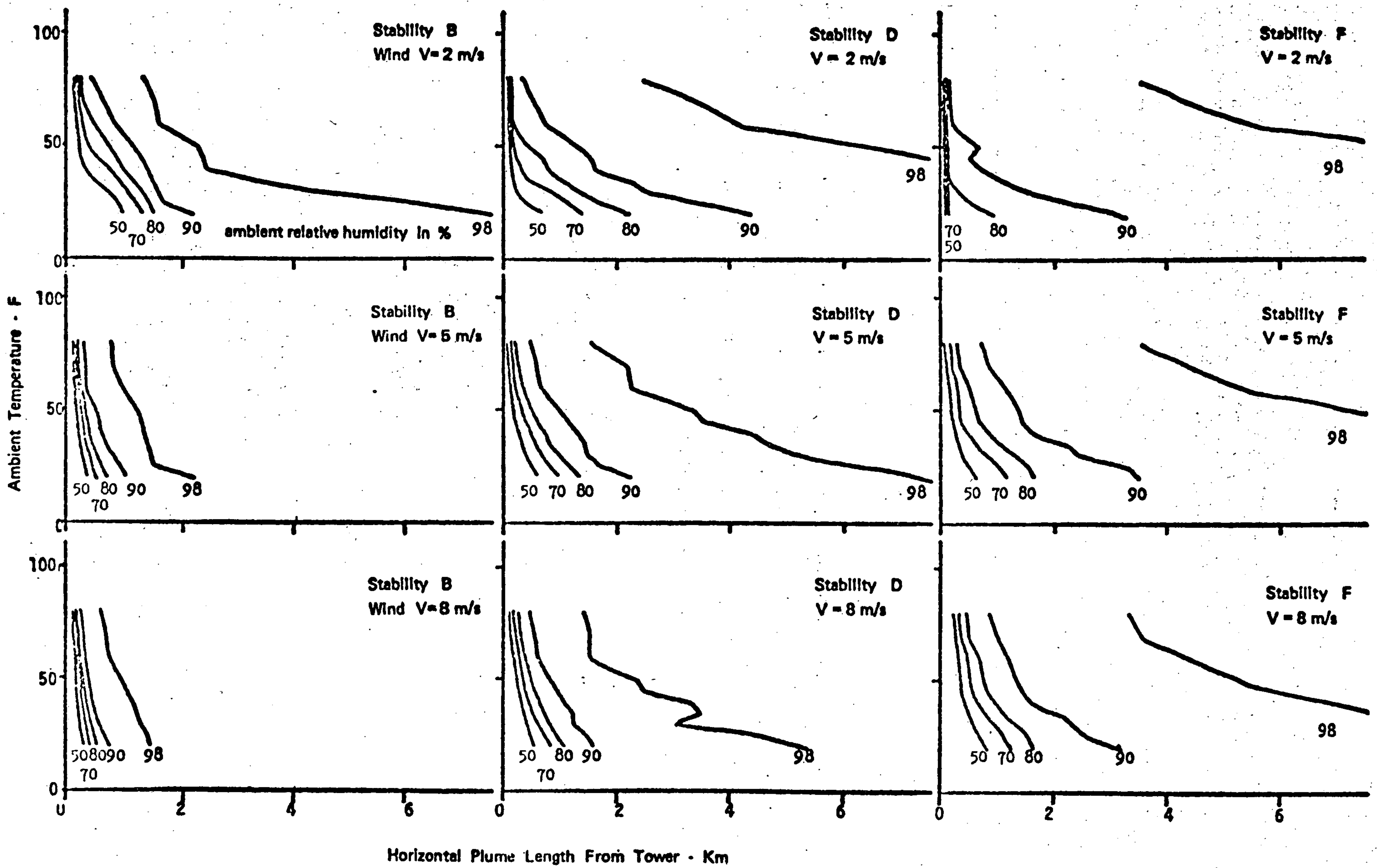

Figure 1. VISIBLE PLUME LENGTHS FOR EXAMPLE CALCULATIONS

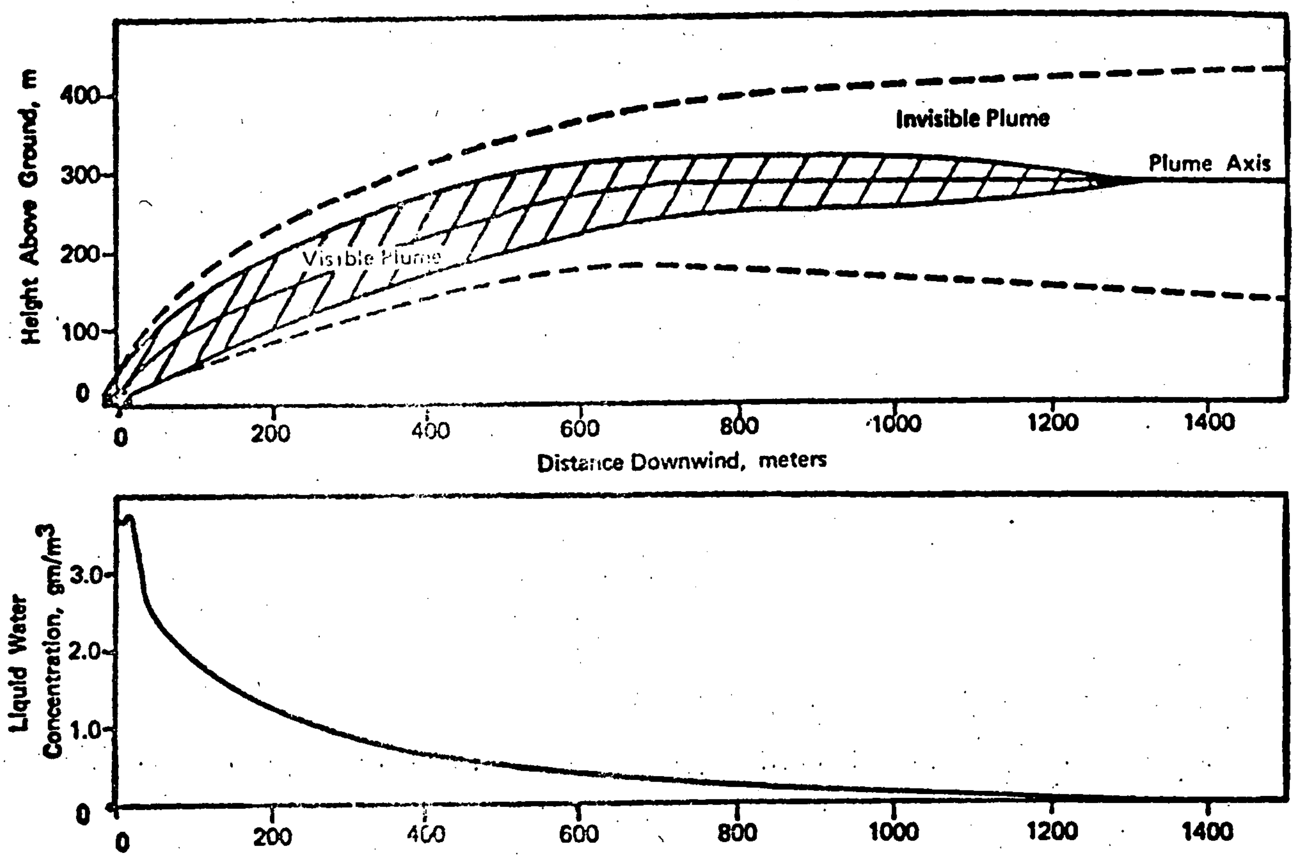

Figure 2. PLUME BOUNDARIES AND AXIAL LIQUID WATER CONCENTRATION

(T=40 F, Relative Humidity = 90%, V=5 m/s, D Stability)

along the axis is also shown. Condensation is seen to occur very close to the tower exit. Although not shown in Fig. 2, the invisible plume extends very far downwind. For the case given, the relative humidity at the plume centerline is still one percent above ambient 8000 meters downwind. For cooling towers located on level topography, the increase in relative humidity at ground level will be of the order of a few percent. It will be highest for unstable atmospheres when the bottom of the plume is brought to the ground close to the tower. Mechanical towers, having lower emission heights, are much more susceptible to ground level fogging than the larger natural-draft towers. If towers are located in hilly areas the increase in ground level relative humidity can be considerable.

7. COMPARISON OF MODEL PREDICTIONS WITH OBSERVATIONS

At present, only limited data on lengths of visible plumes are available in the literature. Most are fragmentary and therefore of little use for model verification. To the authors' knowledge, no data are available for the invisible plume region. Slawson et al (1973) have reported a few observations of the length of the visible plume for strong wind conditions at the Paradise Steam Plant. The results of four of these observations are compared with values predicted by the model in Table I. Ambient profiles of temperature and moisture were not reported so it was necessary to assume atmospheric stability and temperature lapse rates (-.02 and -.01 C/m with C and D stability respectively). Since the reference height for meteorological data was not given, it was assumed to be at the elevation of the top of the tower. The spacing between the three natural draft towers was also not specified; therefore it was necessary to assume several values for α, the equivalent jet area ratio, when more than one tower was in operation (given by n in Table I).

Reference to Table I shows that the model compared favorably with the observations for the first two entries but poorly for the latter two. For the 3/4/71 observation it seems unreasonable that the reported plume length should be so small, given the low ambient temperature and high relative humidity. The 9/7/72 data are also open to question. The plume length observation was made at a different time than for the tower operating conditions and no information is given as to the orientation of the wind to the axis through the base of the three towers. It should be noted that, at the high wind speeds reported, plume downwash may have occurred. The model does not account for this.

TABLE I

COMPARISON OF OBSERVED AND PREDICTED PLUME LENGTHS
DATA OF SLAWSON ET AL (1973)

Date	Time	n	V_o m/sec	$T_o^{(1)}$ F	T F	r gm/kg	RH(2) %	V m/sec	Stab(3)	Observed Length m	Jet Area Ratio α	Predicted Length m
2/10/71	0653 0750	1	2.5	79.0	13.4	0.87	51.0	11.6	D	532-566	1	565
3/2/71	1010 1050	2	2.5	73.6	44.9	4.54	72.4	7.3	D	106-167	1	150
											2	115
3/4/71	0640 0720	1	2.5	72.3	19.1	1.88	85.7	7.0	D	300-465	1	1500
9/7/72	0900 ?	3	3.8	95.9	69.0	13.0	85.3	5.0	C	200 (0815-0942)	1	535
											3	425
											5	365
											10	275

(1) Calculated from reported virtual temperature
(2) Calculated from T and r
(3) Assumed since no data reported - gradients of temperature and moisture also assumed

On the basis of the fragmentary data of Table I, the ability of the model to give realistic predictions of plume properties is encouraging but not conclusive. Meyer et al (1974) have conducted a large number of tests on mechanical draft towers at the PEPCO Benning Road site, but the data were released so recently that sufficient time has not been available to compare observations with our model predictions. It is hoped that this will be done in the near future.

8. CONCLUSIONS

A model has been developed which enables the prediction of the distributions of temperature and moisture in both the visible and invisible portions of a cooling tower plume. The model accounts for the real jet properties of the plume as well as dispersion due to atmospheric turbulence. Ambient profiles of temperature and moisture are considered and an equivalent jet is defined to account for the combined plume from several towers.

The length of the visible plume depends strongly on ambient temperature and relative humidity. Accurate knowledge of the ambient profiles of temperature and moisture is needed to obtain reasonable predictions. The model cannot be fully validated until more accurate data become available for both the visible and invisible plume regions.

NOMENCLATURE

- A = area of emission aperture
- a = coefficient in Briggs plume rise formula
- b = distance from plume axis to a point (y,z) in the plume cross section
- C_{pa} = specific heat of dry air
- $C_{p\ell}$ = specific heat of liquid water
- C_{pv} = specific heat of water vapor
- D = dilution
- F = buoyancy flux
- H = enthalpy of humid air on wet basis
- g = acceleration due to gravity
- h = height of plume centerline
- h_s = height of cooling tower
- ℓ = liquid water mixing ratio
- M = concentration of moisture
- m_a = molecular weight of air
- m_w = molecular weight of water
- n = number of cooling towers
- Q = volumetric flow rate
- R = boundary radius
- R' = boundary radius in flattened jet plume
- R_G = universal gas constant
- RH = relative humidity
- r = water vapor mixing ratio
- S = longitudinal coordinate along curved plume axis
- T = temperature
- T_R = reference temperature for enthalpy
- T_D = dew point temperature
- V = velocity
- X = downwind coordinate
- y = lateral or crosswind coordinate, normal to wind and direction of emission
- z = vertical coordinate, normal to wind in direction of emission
- α = equivalent jet area ratio

β = tangent of angle between jet plume boundary and axis at a given station
γ = plume entrainment coefficient
λ = heat of vaporization of water
ρ = fluid density
σ_y, σ_z = standard deviations of Gaussian concentration distributions
ϕ = concentration of an arbitrary property (amount/volume)

Subscripts

none = in ambient background or atmosphere
a = on plume axis
c = in inner cone
E = in equivalent jet
e = excess quantity or in zone of establishment
j = in established jet
p = in plume
y = in crosswind direction
z = in vertical direction
a = in tower emission aperture
1 = juncture of zone of establishment and established jet
2 = juncture of established jet and simple plume

REFERENCES

Baker, K. G. (1967) Chem. and Process Eng., 56-58
Briggs, G.A. (1969) Plume Rise, U.S. Atomic Energy Commission No. TID-25075.
Csanady, G.T. (1971) J. Appl. Met. 10, 36-42.
Halitsky, J. (1966) Air and Wat. Pollut. Int. J. 10, 821-43.
Halitsky, J. (1967) Atm. Env. 1, 183.
Halitsky, J. (1968) Atm. Env. 2, 419-22.
Hanna, S.R. (1972), J. Appl. Met. 11, 793-99.
Kaylor, F. B., Petrillo, J.L., Tsai, Y.J. (1973) CEP Cooling Tower Symposium Series, pp. 36-42.
Leung, P., Moore, R.E. (1971) J. Power Div. ASCE Proc. 97, 749-66.
Meyer, J. H., Eagles, T.W., Kohlenstein, L.C., Kagan, J.A., Stanbro, W.D. (1974) Mechanical Draft Cooling Tower Visible Plume Behavior: Measurements, Models, Predictions, presented at Cooling Tower Environment-1974, March 4-6, 1974, University of Maryland.
Slawson, P.R., Coleman, J.H., Frey, J.W. (1973) Some Observations of Cooling Tower Plume Behavior at the Paradise Steam Plant, Tennessee Valley Authority, Muscle Shoals, Alabama.
Stephen, D. W., Moroz, W.J. (1972) Eng. Research Bull. B-107, Pennsylvania State University.
Turner, D. B. (1969) Workbook of Atmospheric Dispersion Estimates, Public Health Service Pub. No. 999-AP-26.
Wessels, H.R.A., Wisse, J.A. (1971) Atm. Env. 5, 743-50.
Wigley, T.M.L., Slawson, P.R. (1971) J. Appl, Met. 10, 253-59.
Wigley, T.M.L., Slawson, P.R. (1972) J. Appl. Met. 11, 335-40.

APPENDIX B: Consolidated Edison Company of New York, Inc., "A Model Study of Cooling Tower Plume Induced Fogging, Icing and Salt Drift Deposits at Indian Point Unit No. 3," December, 1975.

A MODEL STUDY OF SALT DRIFT DEPOSITS, INDUCED FOGGING AND ICING BY PLUMES FROM FOUR POSTULATED TYPES OF COOLING TOWERS AT INDIAN POINT UNIT NO.3

January 1976

NUCLEAR AND EMISSIONS CONTROL ENGINEERING DEPARTMENT

CONSOLIDATED EDISON COMPANY OF NEW YORK, INC.

SUMMARY

Environmental effects arising from operations of either of the four postulated types of cooling towers at Indian Point Unit No. 3 have been investigated by means of mathematical modeling techniques. These four types of postulated cooling towers are linear wet, linear wet/dry, round mechanical and fan assisted natural draft cooling towers. The effects are quantized in terms of salt drift deposits, plume induced fogging and icing in an eighteen square mile surrounding area. Maximum salt deposits can reach 6000 $Kg/Km^2/Mo.$ in August. The hours of induced fogging and icing vary from one type of cooling tower to another. The potential fogging and icing abating characteristics of wet/dry mechanical draft cooling towers is demonstrated. The relatively novel design such as fan assisted natural draft cooling tower is found to be environmentally advantageous over the linear and round wet towers based upon results obtained in this study.

ACKNOWLEDGEMENT

The report contained herein is prepared by the Nuclear and Emissions Control Engineering Department. Dr. Peh Sun Ku is the principal investigator. Thanks are due to Mr. Philip Hsiang of the Computer Application Engineering Department for computer technology, Dr. Han C. Moy for his contribution of cooling tower engineering data, Mr. Lester A. Cohen for his contribution in meteorological data, Mr. Dennis Doll for computing and data reduction, Mr. Angelo Combader and Mr. Peter Wemmers for preparing the figures. Thanks are also due to Messrs. David L. Hawkins, Herman Bremer, John Szeligowski and John Drower for their administrative assistance, guidance and encouragement. Assistances from Ms. Linda Burke in typing the manuscript is sincerely appreciated.

TABLE OF CONTENTS

TABLE OF CONTENTS (continued)

LIST OF FIGURES

LIST OF FIGURES (continued)

LIST OF FIGURES (continued)

LIST OF FIGURES (continued)

LIST OF FIGURES (continued)

LIST OF TABLES

1.0 INTRODUCTION

Plumes being investigated here are those from four different types of cooling towers, namely wet, wet/dry, round wet mechanical draft cooling towers and fan assisted natural draft cooling towers. Plumes from the wet mechanical draft cooling towers are saturated with water vapor and laden with entrained liquid drift droplets. Plumes from wet/dry cooling towers are unsaturated and containing less drift droplets. The fogging and icing abatement characteristics of the wet/dry design is particularly noteworthy. When the probability of inducing fog and ice is totally absent, the wet cooling section alone can be operated to take over the full heat load. This versatility is an important feature in view of the derating which would incur to the generators.

Water vapor in cooling tower plumes is a potential source of induced ground fog and a visible cloud at higher elevations. In frigid climates the excess moisture may be precipitated as ice. Both fog and ice are potentially detrimental to transportation and communications by reducing visibility and by causing slippery conditions on roadways and bridges. The plume may block visibility at airport approaches.

The drift droplets in the plume contain high concentrations of salt and minerals. When distributed by some natural dispersion processes some of these droplets tend to fall to the ground as salt deposits. The larger the size the more readily it falls. The smallest droplets may remain in the atmosphere as suspended particulates.

Certain vegetation susceptible to minerals and salts may be damaged by the deposition of salt from drift droplets. Pathogens in the makeup water can be dispersed with the draft droplets.

Interactions of cooling tower and fossil plumes may result in the precipitation of corrosive mists. The hygroscopic dust particles in the fossil plume can initiate the nucleation of fog below saturation.

2.0 THEORETICAL BACKGROUND OF THE MODEL

Theoretical considerations of the model are generally similar to the air quality models which we have been using. Because the actual site is located in a valley with very uneven surrounding terrain, a three dimensional feature must be incorporated. For the same reason, the on-site meteorological data may not be extrapolated to a very large area. Therefore, a fine grid system was incorporated in a smaller area to include the nearby towns, major roads and waterways.

2.1 The Governing Equations

The majority of air quality models which have hitherto been constructed assumed Gaussian dispersion for the species transported by the plume. The concentrations of the species in a three dimensional space are expressed by an equation known as the dispersion equation:

$$c = \frac{Q}{2\pi u \sigma_y \sigma_z} \exp\left(\frac{-y^2}{2\sigma_y^2}\right)\left\{\exp\left[\frac{-(z-H)^2}{2\sigma_z^2}\right] + \exp\left[\frac{-(z+H)^2}{2\sigma_z^2}\right]\right\} \qquad (1)$$

where y is the crosswind dimension and z is the vertical dimension. The standard deviations, σ_y and σ_z, are functions of x, the downwind distance. The concentration of the species is denoted by c, wind speed by u, elevation of the plume center or the effective stack height by H, and the emission rate of the species is Q.

Equation (1) can be transformed into various forms depending on the case under investigation. When the concentration at the ground level is of interest z=o, c is the ground level concentration and is expressed as:

$$c = \frac{Q}{\pi u \sigma_y \sigma_z} \exp\left(\frac{-y^2}{2\sigma_y^2}\right) \exp\left(\frac{-H^2}{2\sigma_z^2}\right) \quad (2)$$

If the maximum concentration at the center-line of the plume is being considered (y=o), the exponential term in the crosswind direction is unity. The plume center-line ground level concentration of the species is:

$$c = \frac{Q}{4\pi \sigma_y \sigma_z} \exp\left(\frac{-H^2}{2\sigma_z^2}\right) \quad (3)$$

The concentrations calculated by Equations (1), (2) and (3) are considered short-term averages. The time scale, however, was not defined in the original derivation.[1] It is open to different interpretations. Turner[2] cited examples to indicate that the results from the last three equations just given, can be regarded as average values of a short period from a few minutes to an hour. The wind data used in this model are hourly averages. Therefore, the concentrations obtained are considered hourly average values.

The long-term average concentrations can be obtained from Equation (1) by integrating in the crosswind direction, averaged over a sector width at downwind distance x from the source, and multiplied by the wind rose frequency to take account of the fraction of time that the wind at a specific speed occurs in that sector.

$$c_a = \frac{fQ}{\sqrt{2\pi}\, u\sigma_z (2\pi x/N)} \left\{ \exp\left[\frac{-(z-H)^2}{2\sigma_z^2}\right] + \exp\left[\frac{-(z+H)^2}{2\sigma_z^2}\right] \right\} \qquad (4)$$

where f is the wind rose frequency, N is the number of sectors in which the wind frequency data are recorded, and $2\pi x/N$ is the sector width. Long-term averages are either monthly or annual depending on the time scale that wind rose data are averaged.

2.2 Salt Drift Droplets Dispersion and Deposit

Equations (1) through (4) were derived for gaseous species. Gas molecules are transported and dispersed as part of the plume.

Solid particles and liquid droplets usually have tendencies to separate from the plume and fall to the ground. Unlike gas molecules, once deposited it would not be reflected. The reflection term, $\exp\left[-(z+H)^2/2\sigma_z^2\right]$ in the dispersion equation (Eq. (1)) does not exist.

If a particle has a falling velocity v_f, and is deposited to the ground having travelled a downwind distance x from the source, the time elapsed is $t=x/u$, where u is the wind speed. This particle falls from a height of $v_f t$ or $v_f x/u$. The average salt dispersion equation is expressed as

$$\chi = \frac{Q}{2\pi u \sigma_y \sigma_z} \exp\left(-y^2/2\sigma_y^2\right) \exp\left[\frac{-(H - z - v_f x/u)^2}{2\sigma_z^2}\right] \qquad (5)$$

where z is the ground elevation, and x is the downwind distance from the tower.

Values of χ represent the salt drift concentrations in the atmosphere. The rate of ground deposition is:

$$w = v_f \chi \tag{6}$$

where w is expressed as mass per unit area per unit time.

Equations (5) and (6) indicate that the falling velocity v_f plays a major role in the salt drift deposition. Its magnitude is proportional to the droplet size. Large droplets fall faster, reach the ground in less time and are closer to the source. The sizes of the drift droplets from cooling towers do not stay constant in flight because they are transported through an environment of changing humidity in the plume. Their sizes are further modified by the humidity of the ambient air after they are separated from the plume.

Falling velocity decreases as the initial size of the droplet is reduced by evaporation. The final falling velocity determines the rate of deposition. At relative humidities near saturation, the initial droplet size may remain constant and falling velocities remain uniform.

Theoretical expression of the rate of droplet size changes as a function of ambient humidity, ambient temperature and salinity in the droplet and is given by Squire.[3]

2.3 Criteria of Fogging and Icing

In determining fogging and icing potentials Equation (2) is used to calculate the hourly plume contributions of moisture and enthalpy to the ambient air at ground level. The local moisture content and enthalpy are the sums of the plume contributed quantities and the ambient values. Based on the state of the moist air (enthalpy and phase) at the local point the fog or no-fog conditions are determined.

If the local plume temperature determined from the enthalpy is above the saturation temperature of the moist air, all moisture is in the vapor phase, and fog does not occur. On the other hand, when the plume temperature is either equal or lower than the saturation temperature corresponding to the moisture content of the plume, fog condition exists. If the local plume temperature is below freezing, icing is assumed to exist.

3.0 MODELING TECHNIQUES

Generally, the heat being rejected to the atmosphere by the plume is a major parameter in formulating the plume rise. For fossil plumes this is manifested by the sensible heat. The exit temperature of the cooling tower plume is low compared to fossil plumes. Therefore the sensible heat is small. Since the large part of the heat carried by the plumes is in the form of latent heat, in terms of the total heat being rejected to the atmosphere, the latent heat in the plume must be considered.

Water vapor in the cooling tower plumes stores the latent heat. As the plume disperses and mixes with the ambient air and cools to the wet bulb temperature, excess moisture is condensed and the latent heat is manifested as a temperature increase. Due to this fact, the temperature in the plume is higher than the ambient. In determining fogging and icing both excess moisture and enthalpy are taken into account.

3.1 Characteristic of the Mechanical Draft Cooling Towers at Indian Point

Mechanical draft cooling towers consists of many cells. The exhaust of each is a stack ventilated by a fan. The cooling water flow rate for Indian Point Unit No. 3 is 630,000 gallons per minute, which requires 26 cooling cells equally divided into two towers. Other parameters of the four postulated types of cooling towers are summarized in Table 3.1.1:

TABLE 3.1.1

SUMMARY OF KNOWN DESIGN PARAMETERS
OF THE POSTULATED COOLING TOWERS AT
INDIAN POINT UNIT NO. 3

	Linear Wet Mechanical Draft Tower	Linear Wet/Dry Mechanical Draft Tower	Round Wet Mech. Draft	Fan Assisted Natural Draft
Number of Towers	3	3	2	2
Cell in each Tower	9,9,8	9,10,9	13	1
Length & Width or Dia. of each (ft.)	520x75	360x75	285ø	200ø
Center to Center Stack Spacing (ft.)	40	40	40	400
Exhaust Fan Stack Diameter	28	28	30	200ø
Height of Tower (ft.)	68	68	67	205
Estimated Drift Rate (% of flow rate)	0.005	0.005	0.005	0.0025
Hot Water Flow Rate (gpm)/cell	24,200	22,500	24,200	315,000

Each individual fan stack is regarded as a source. The finite dimension of each source is identified by considering an equivalent point source of the same strength located upwind at a virtual distance from the actual source. The moisture and enthalpy contributed by the plume to a downwind receptor is the sum of the contributions from each individual source.

3.2 Effective Stack Height

This parameter is needed in both salt drift deposit and fogging and icing models. It is defined as the sum of the height of the cooling tower and the plume rise which is calculated by Briggs' equation:[11]

$$H = h_s + \Delta h = h_s + \frac{1.6\, F^{1/3} x^{2/3}}{u} \qquad (7)$$

where Δh is the height of the plume center above the stack exit, u is the wind speed, F is known as buoyancy factor, x is the downwind distance and h_s is the stack height.

The buoyancy factor, F, of a cooling tower is dependent on both sensible heat and latent heat[4] in the plume which vary with the ambient conditions. An average value of 630 has been used throughout.

In Equation (7) x is replaced by ($10h_s$) when the plume rises to its ultimate height. Because of the mechanical draft cooling tower's low profile the plume rise will reach its ultimate height within 680 feet from the tower. Since the stack and the tower configurations are exactly similar, similar plume heights are assumed for all stacks.

The wind speed (u) in Equation (7) is not specified. Logically, however, it should be the wind speed prevailing at the plume center. A parabolic wind profile has been used to obtain wind speed at higher elevations:

$$u = u_0 \left(H/z_0 \right)^p \tag{8}$$

where u is the wind speed at H, and z_0 is the height where the ground wind speed u_0 is recorded. Values of the exponent "p", depending on stability, are adopted from Smith.[5]

3.3 Mixing Height and Plume Diffusion

A mixing height (approximately 1000 meters) is imposed as a lid. The plume is allowed to approach this lid until the concentration at the edge of the plume ($2.15\sigma_z$)[2] is 1/10 of that at the plume center. The downwind distance at this point is designated as x_I. Beyond this point, the plume is permitted to mix vertically. This mixing process is assumed to continue until the plume reaches a distance equal to $2\ x_I$. At a downwind distance larger than $2\ x_I$, the plume loses its identity and completely merges with the ambient air. By means of this model the entire field traversed by the plume is divided into three regions. In the first region, the plume maintains its undisturbed characteristics. In the second region mixing starts from the plume edge, and finally the plume completely mixes in the the third region. The distance from the source to the end of the Region I is determined by solving the following equations simultaneously:

$$L_m = h_s\,(R+1) + 2.15\,\sigma_z\,(x_I) \qquad (9)$$

and

$$R\,(R+1)^p = R_0\,C^p \qquad (10)$$

where R_o = h_o/h_s

$C = z_o/h_s$

Δh_o calculated from Eq.(7) with $u=u_o$

h_s= stack height

L_m = Depth of the inversion layer

σ_z = vertical diffusion coefficient

x_I = downwind distance of Region I.

The distance x_I in Region I depends on the atmospheric conditions. Under the prevailing stability conditions, the entire area of study at Indian Point (5.0 miles x 3.7 miles) is within Region I.

3.4 Dispersion Coefficients

Horizontal and vertical dispersion coefficients as functions of downwind distances given by Turner [2] are used in this model. The numerical values are correlated empirically for the convenience of computation. General forms of the coefficients in terms of downwind distance x are given below:

Horizontal Coefficient:

$$\sigma_y = a\, x^{b} \qquad (11)$$

Vertical Coefficients:

$$\sigma_z = A\,x^{B} + C\,x^{\alpha - \gamma \log x} \qquad (12)$$

The constants a, b, A, B, C, α and γ are given in Table 3.4.1.

TABLE 3.4.1

CORRELATION CONSTANTS OF HORIZONTAL

& VERTICAL DISPERSION COEFFICIENTS

Atmospheric Stability Class	Horizontal Dispersion Coefficients		Vertical Dispersion Coefficients				
	a	b	A	B	C	α	γ
A	0.470	0.880	0.221×10^{-3}	2.104	0.201×10^{-12}	12.4	2.77
B	0.332	0.885	0.653	1.077	139	-1.0	0
C	0.220	0.890	0.111	0.913	0	0	0
D	0.140	0.896	0.0883	0.858	-0.124×10^{-8}	4.03	0.326
E	0.096	0.902	0.0739	0.838	-0.343×10^{-5}	2.50	0.162
F	0.062	0.912	0.0586	0.797	-0.217×10^{-5}	2.46	0.159

3.5 Downwind and Crosswind Distance

Based on the actual location each cooling tower cell is given a set of coordinates (u_i, v_i) on the UTM coordinate system. The area of study in the vicinity of the cooling tower site is divided into ½ x ½ Km grids. Each grid point has a set of coordinates (U_j, V_j, z_j). U_j, V_j are the UTM (Universal Transverse Mercator) coordinates in kilometers, and z_j is the elevation at the grid point in meters.

The distance and direction between the cells with respect to a grid point are obtained from their respective coordinates. The difference between the wind and source-grid directions, as well as the source-grid distance are used to obtain the crosswind and downwind distances. The downwind distance, x, is then used to compute the dispersion coefficients σ_y and σ_z.

3.6 Topography

The Indian Point vicinity is quite hilly. Ground elevation varies from slightly above sea level to over a thousand feet at Dunderberg Mountain, within two miles of the cooling tower site. Terrain features have been incorporated in the model calculations. The elevation at each grid point throughout the area considered in the model is tabulated as input data to the model.

The elevation at each grid point is given in Table 3.6.1.

TABLE 3.6.1

Ground Elevations (z) In the Vicinity of Indian Point
(x, y = Kilometers; z = meters)

Y=4565.000	X=585.000	Z= 36.58
Y=4565.000	X=585.500	Z= 9.14
Y=4565.000	X=586.000	Z= 0.
Y=4565.000	X=586.500	Z= 0.
Y=4565.000	X=587.000	Z= 0.
Y=4565.000	X=587.500	Z= 0.
Y=4565.000	X=588.000	Z= 0.
Y=4565.000	X=588.500	Z= 3.05
Y=4565.000	X=589.000	Z= 36.58
Y=4565.000	X=589.500	Z= 36.58
Y=4565.000	X=590.000	Z= 54.86
Y=4565.000	X=590.500	Z= 51.82
Y=4565.000	X=591.000	Z= 18.29
Y=4565.500	X=585.000	Z= 30.48
Y=4565.500	X=585.500	Z= 24.38
Y=4565.500	X=586.000	Z= 30.48
Y=4565.500	X=586.500	Z= 0.
Y=4565.500	X=587.000	Z= 0.
Y=4565.500	X=587.500	Z= 0.
Y=4565.500	X=588.000	Z= 36.58
Y=4565.500	X=588.500	Z= 3.05
Y=4565.500	X=589.000	Z= 18.29
Y=4565.500	X=589.500	Z= 33.53
Y=4565.500	X=590.000	Z= 15.24
Y=4565.500	X=590.500	Z= 45.72
Y=4565.500	X=591.000	Z= 45.72
Y=4566.000	X=585.000	Z= 30.48
Y=4566.000	X=585.500	Z= 15.24
Y=4566.000	X=586.000	Z= 30.48
Y=4566.000	X=586.500	Z= 0.
Y=4566.000	X=587.000	Z= 0.
Y=4566.000	X=587.500	Z= 0.
Y=4566.000	X=588.000	Z= 36.58
Y=4566.000	X=588.500	Z= 9.14
Y=4566.000	X=589.000	Z= 21.34
Y=4566.000	X=589.500	Z= 30.48
Y=4566.000	X=590.000	Z= 39.62
Y=4566.000	X=590.500	Z= 45.72
Y=4566.000	X=591.000	Z= 48.77
Y=4566.500	X=585.000	Z= 64.01
Y=4566.500	X=585.500	Z= 60.96
Y=4566.500	X=586.000	Z= 0.
Y=4566.500	X=586.500	Z= 0.
Y=4566.500	X=587.000	Z= 0.
Y=4566.500	X=587.500	Z= 0.
Y=4566.500	X=588.000	Z= 15.24
Y=4566.500	X=588.500	Z= 21.34
Y=4566.500	X=589.000	Z= 18.29
Y=4566.500	X=589.500	Z= 30.48
Y=4566.500	X=590.000	Z= 12.19
Y=4566.500	X=590.500	Z= 18.29
Y=4566.500	X=591.000	Z= 42.67
Y=4567.000	X=585.000	Z= 60.96
Y=4567.000	X=585.500	Z= 3.05
Y=4567.000	X=586.000	Z= 0.

TABLE 3.6.1

Ground Elevations (z) In the Vicinity of Indian Point
(x, y = Kilometers; z = meters)

Y=4567.000	X=586.500	Z= 0.
Y=4567.000	X=587.000	Z= 18.29
Y=4567.000	X=587.500	Z= 6.10
Y=4567.000	X=588.000	Z= 9.14
Y=4567.000	X=588.500	Z= 27.43
Y=4567.000	X=589.000	Z= 30.48
Y=4567.000	X=589.500	Z= 30.48
Y=4567.000	X=590.000	Z= 33.53
Y=4567.000	X=590.500	Z= 54.86
Y=4567.000	X=591.000	Z= 45.72
Y=4567.500	X=585.000	Z= 36.58
Y=4567.500	X=585.500	Z= 3.05
Y=4567.500	X=586.000	Z= 0.
Y=4567.500	X=586.500	Z= 0.
Y=4567.500	X=587.000	Z= 18.29
Y=4567.500	X=587.500	Z= 18.29
Y=4567.500	X=588.000	Z= 9.14
Y=4567.500	X=588.500	Z= 24.38
Y=4567.500	X=589.000	Z= 30.48
Y=4567.500	X=589.500	Z= 36.58
Y=4567.500	X=590.000	Z= 36.58
Y=4567.500	X=590.500	Z= 67.06
Y=4567.500	X=591.000	Z= 60.96
Y=4568.000	X=585.000	Z=103.63
Y=4568.000	X=585.500	Z= 3.05
Y=4568.000	X=586.000	Z= 0.
Y=4568.000	X=586.500	Z= 0.
Y=4568.000	X=587.000	Z= 30.48
Y=4568.000	X=587.500	Z= 30.48
Y=4568.000	X=588.000	Z= 18.29
Y=4568.000	X=588.500	Z= 9.14
Y=4568.000	X=589.000	Z= 18.29
Y=4568.000	X=589.500	Z= 24.38
Y=4568.000	X=590.000	Z= 30.48
Y=4568.000	X=590.500	Z= 45.72
Y=4568.000	X=591.000	Z= 79.25
Y=4568.500	X=585.000	Z= 76.20
Y=4568.500	X=585.500	Z= 30.48
Y=4568.500	X=586.000	Z= 0.
Y=4568.500	X=586.500	Z= 0.
Y=4568.500	X=587.000	Z= 0.
Y=4568.500	X=587.500	Z= 30.48
Y=4568.500	X=588.000	Z= 18.29
Y=4568.500	X=588.500	Z= 9.14
Y=4568.500	X=589.000	Z= 18.29
Y=4568.500	X=589.500	Z= 24.38
Y=4568.500	X=590.000	Z= 27.43
Y=4568.500	X=590.500	Z= 51.82
Y=4568.500	X=591.000	Z=115.82
Y=4569.000	X=585.000	Z=103.63
Y=4569.000	X=585.500	Z= 30.48
Y=4569.000	X=586.000	Z= 0.
Y=4569.000	X=586.500	Z= 0.
Y=4569.000	X=587.000	Z= 0.
Y=4569.000	X=587.500	Z= 0.
Y=4569.000	X=588.000	Z= 30.48

TABLE 3.6.1

Ground Elevations(ẑ) In the Vicinity of Inddan Point
(x, y = Kilometers; z = meters)

Y=4569.000	X=588.500	Z= 18.29
Y=4569.000	X=589.000	Z= 9.14
Y=4569.000	X=589.500	Z= 24.38
Y=4569.000	X=590.000	Z= 24.38
Y=4569.000	X=590.500	Z= 60.96
Y=4569.000	X=591.000	Z= 88.39
Y=4569.500	X=585.000	Z=140.21
Y=4569.500	X=585.500	Z= 97.54
Y=4569.500	X=586.000	Z= 15.24
Y=4569.500	X=586.500	Z= 0.
Y=4569.500	X=587.000	Z= 0.
Y=4569.500	X=587.500	Z= 0.
Y=4569.500	X=588.000	Z= 15.24
Y=4569.500	X=588.500	Z= 0.
Y=4569.500	X=589.000	Z= 9.14
Y=4569.500	X=589.500	Z= 36.58
Y=4569.500	X=590.000	Z= 48.77
Y=4569.500	X=590.500	Z= 42.67
Y=4569.500	X=591.000	Z=128.02
Y=4570.000	X=585.000	Z=274.32
Y=4570.000	X=585.500	Z=152.40
Y=4570.000	X=586.000	Z= 45.72
Y=4570.000	X=586.500	Z= 0.
Y=4570.000	X=587.000	Z= 0.
Y=4570.000	X=587.500	Z= 0.
Y=4570.000	X=588.000	Z= 0.
Y=4570.000	X=588.500	Z= 0.
Y=4570.000	X=589.000	Z= 6.10
Y=4570.000	X=589.500	Z= 27.43
Y=4570.000	X=590.000	Z= 42.67
Y=4570.000	X=590.500	Z= 70.10
Y=4570.000	X=591.000	Z= 76.20
Y=4570.500	X=585.000	Z=268.22
Y=4570.500	X=585.500	Z=237.74
Y=4570.500	X=586.000	Z=201.17
Y=4570.500	X=586.500	Z=100.58
Y=4570.500	X=587.000	Z= 6.10
Y=4570.500	X=587.500	Z= 0.
Y=4570.500	X=588.000	Z= 0.
Y=4570.500	X=588.500	Z= 0.
Y=4570.500	X=589.000	Z= 0.
Y=4570.500	X=589.500	Z= 9.14
Y=4570.500	X=590.000	Z= 51.82
Y=4570.500	X=590.500	Z= 73.15
Y=4570.500	X=591.000	Z= 91.44
Y=4571.000	X=585.000	Z=274.32
Y=4571.000	X=585.500	Z=225.55
Y=4571.000	X=586.000	Z=243.84
Y=4571.000	X=586.500	Z=204.22
Y=4571.000	X=587.000	Z=103.63
Y=4571.000	X=587.500	Z= 0.
Y=4571.000	X=588.000	Z= 0.
Y=4571.000	X=588.500	Z= 0.
Y=4571.000	X=589.000	Z= 0.
Y=4571.000	X=589.500	Z= 6.10
Y=4571.000	X=590.000	Z= 42.67

TABLE 3.6.1

Ground Elevations (z) In the Vicinity of Indian Point
(x, y = Kilometers; z = meters)

Y=4571.000	X=590.500	Z= 97.54
Y=4571.000	X=591.000	Z=128.02
Y=4571.500	X=585.000	Z= 85.34
Y=4571.500	X=585.500	Z=201.17
Y=4571.500	X=586.000	Z= 91.44
Y=4571.500	X=586.500	Z=158.50
Y=4571.500	X=587.000	Z= 91.44
Y=4571.500	X=587.500	Z= 0.
Y=4571.500	X=588.000	Z= 0.
Y=4571.500	X=588.500	Z= 0.
Y=4571.500	X=589.000	Z= 0.
Y=4571.500	X=589.500	Z= 42.67
Y=4571.500	X=590.000	Z= 42.67
Y=4571.500	X=590.500	Z= 45.72
Y=4571.500	X=591.000	Z= 51.82
Y=4572.000	X=585.000	Z= 3.05
Y=4572.000	X=585.500	Z= 3.05
Y=4572.000	X=586.000	Z= 0.
Y=4572.000	X=586.500	Z= 0.
Y=4572.000	X=587.000	Z= 0.
Y=4572.000	X=587.500	Z= 0.
Y=4572.000	X=588.000	Z= 6.10
Y=4572.000	X=588.500	Z= 0.
Y=4572.000	X=589.000	Z= 0.
Y=4572.000	X=589.500	Z= 60.96
Y=4572.000	X=590.000	Z= 82.30
Y=4572.000	X=590.500	Z= 54.86
Y=4572.000	X=591.000	Z=103.63
Y=4572.500	X=585.000	Z= 3.05
Y=4572.500	X=585.500	Z= 3.05
Y=4572.500	X=586.000	Z= 6.10
Y=4572.500	X=586.500	Z= 0.
Y=4572.500	X=587.000	Z= 0.
Y=4572.500	X=587.500	Z= 9.14
Y=4572.500	X=588.000	Z= 57.91
Y=4572.500	X=588.500	Z= 12.19
Y=4572.500	X=589.000	Z= 60.96
Y=4572.500	X=589.500	Z= 0.
Y=4572.500	X=590.000	Z= 73.15
Y=4572.500	X=590.500	Z= 45.72
Y=4572.500	X=591.000	Z= 79.25
Y=4573.000	X=585.000	Z= 0.
Y=4573.000	X=585.500	Z= 12.19
Y=4573.000	X=586.000	Z= 0.
Y=4573.000	X=586.500	Z= 36.58
Y=4573.000	X=587.000	Z=198.12
Y=4573.000	X=587.500	Z=103.63
Y=4573.000	X=588.000	Z=121.92
Y=4573.000	X=588.500	Z= 24.38
Y=4573.000	X=589.000	Z= 76.20
Y=4573.000	X=589.500	Z= 33.53
Y=4573.000	X=590.000	Z= 6.10
Y=4573.000	X=590.500	Z= 30.48
Y=4573.000	X=591.000	Z= 54.86

3.7 Salt Drift in Cooling Tower Plumes

Several sets of entrainment data, droplet sizes and mass fraction distributions were obtained from the literature. They vary in a wide range. The lack of reproducibility may be due to the lack of correlation between different types of drift eliminators used in cooling towers. It is known, however, that the mechanical draft cooling towers have a higher drift rate than the hyperbolic natural draft cooling towers. In this model a uniform rate of 0.005% (5.0×10^{-5}) of the circulating water has been used (0.0025% for fan assisted natural draft cooling towers). It is unclear whether there exist any typical distributions distinctive for natural draft and mechanical draft cooling towers. The data used in this model study are given in Table 3.7.1.[6]

TABLE 3.7.1

SIZE AND MASS DISTRIBUTIONS OF

SALT DRIFT IN COOLING TOWER PLUMES

Droplet Diameter (microns, μ)	Mass Fraction
below 50	0.200
50-100	0.450
100-200	0.320
over 200	0.030

The amount of salt in the drift droplets transported from the tower is directly related to the Hudson River salinity and the blowdown cycle. Assuming blowdown once every two cycles, the salt concentration in the drift will be twice the river salinity, which varies with the fresh water flow rate.[12,13] The river salinity at Indian Point varies from a peak of 3900 ppm in August to a minimum below 100 ppm during spring months. The monthly average values of drift salinity used in the model are given in Table 3.7.2.

TABLE 3.7.2

DRIFT SALINITY USED IN
MODEL CALCULATIONS

Month	Drift Salinity (PPM)
January	2100
February	3100
March	100
April	100
May	260
June	4000
July	7000
August	7000
September	7000
October	7000
November	7000
December	2100

The amount of deposits on the ground depend on the falling velocity (or terminal velocity) which in turn depends on the droplet size. The droplet size is constantly changing when it falls in an unsaturated atmosphere.

To follow the history of each droplet from the tower exit to the ground, correcting for the size and velocity at each step, is quite time consuming.

Results by Hosler et al[7] were adopted for this study. The falling velocity as a function of droplet radius and ambient relative humidity is presented in Figure 3.7.1.

3.8 Moisture and Enthalpy Content in Cooling Tower Plume

A difference in absolute humidity (mass of moisture per unit mass of dry air) between air inlet and exit is the net evaporation in a unit mass of dry air. Similarly, the net enthalpy increase is defined as the difference of enthalpy between the air inlet and exit. The total amount of evaporation and heat being rejected to the atmosphere are obtained by determining the total amount of dry air through the tower utilizing the mass ratio of hot water to dry air, L/G.

The ratio L/G is the slope of the operating line on an enthalpy-temperature diagram. The design L/G ratio is given for a design temperature and humidity. At any other ambient conditions, the design L/G ratio is corrected to a new value by considering the density changes of the ambient air under the design and the given conditions.

The sum of inlet air wet bulb temperature and the approach is the cold water temperature. The hot water temperature is the sum of cold water temperature and the range. The enthalpy of the exit effluent is the sum of the enthalpy of the ambient air and an enthalpy increase due to the product of L/G ratio and range. The effluent enthalpy is a function of the exit temperature between the hot water and air exit temperatures which can be evaluated by iteration utilizing the procedures discussed in the following paragraphs.

To determine the moisture content from the saturation temperature an equation to calculate the water vapor pressure as a function of temperature is necessary. The following equation was selected for this purpose:[8]

$$p(T) = 4.579 \exp(19.46 - 5310.0/T) \qquad (13)$$

where pressure p is in mm Hg and T in degrees Kelvin. This truncated equation for water vapor pressure is reasonably accurate in the temperature range of a cooling tower plume. In a comparison with the experimental data[9] between -10^{o} and $80^{o}C$, the deviation was found to be 5-10%.

An equation representing the heat of evaporation as a function of temperature was obtained from the steam table:[10]

$$\lambda(T) = 752.39 - 0.566\,T \qquad (14)$$

where $\lambda(T)$ is the heat of evaporation in cal/gram and T is in degrees Kelvin.

The mass of moisture per unit mass of dry air is expressed as:

$$m(T) = 0.622\,p(T)/[P_a - p(T)] \qquad (15)$$

where m(T) is the mass of moisture per unit mass of dry air as a function of temperature. P_a is the atmospheric pressure and p(T) is the partial pressure of water at a temperature T calculated from Equation (13).

Equations (13) through (15) are used to calculate the enthalpy content at the inlet and exit. The specific heats of dry air and water vapor are assumed constants. The enthalpy is expressed as:

$$h(T) = 0.24(T-T_o) + m(T_d) \left[0.45(T-T_d) + \lambda(T_d) - (T_d-273)\right] \quad (16)$$

where T is the dry bulb temperature, T_d is the dew point, T_o is a reference temperature taken as 0^oF (or 255^oK) and T_w is the wet bulb temperature. When Equation (16) is applied to the exit condition, the exit temperature T_e replaces T and T_d. At the air inlet, T and T_d are used in Equation (16)to obtain expressions of entnalpy $h_i(T)$ and $h_i(T_w)$ with unknown T_w to be determined. Since $h_i(T) = h_i(T_w)$, the value of T_w can be obtained by iteration from the following equation:

$$\begin{aligned} 0.24(T-T_w) + m(T_d) &\left[0.45(T-T_d) + \lambda(T_d) - (T_d-273)\right] \\ &= m(T_w)\left[\lambda(T_w) - (T_w-273)\right] \end{aligned} \quad (17)$$

3.9 Determination of Fogging and Icing Potentials

At a receptor downwind from the cooling towers the excess moisture and enthalpy transported by the plumes are mixed with the ambient air, increasing the humidity as well as temperature. Therefore, conditions of fogging or icing must be determined by both the moisture content and the enthalpy content of the plume-ambient air mixture at the receptor.

Ambient air temperature is used as a first approximation of the plume temperature to initiate the iterations. Based on the enthalpy content h at a receptor the wet bulb temperature T_w of the plume mixture can be determined. Using this wet bulb temperature and the moisture content at the same receptor, another enthalpy value h' is determined. If $h' < h$ there is no fog. A plume temperature is then determined by Equation (16) with m, h and T_w known.

If h is found to be less than or equal to h', the moisture in the plume air mixture exists in a two phase equilibrium. Fog will occur in both cases.

When the temperatures determined for the fogging cases are below freezing, icing instead of fogging will occur.

The amount of liquid water in the plume is also computed if an estimation of fog visibility is desired.

3.10 Estimation of Visibility

When fog condition exists an estimate of visibility can be made based upon the condensed moisture in the air. Theoretical the visibility can be shown to depend on the radius (r) of the fog droplets and the mass of the condensed moisture in a unit colume of air, (14)

$$V = \frac{2}{3} \frac{r}{m} \ln (1/\epsilon) \qquad (18)$$

where V is the visibility or visual range, r the radius of the droplets, m the mass of liquid water content of air and E is the brightness contrast threshold of the eye.

If $\bar{r}$ represents an average radius of the fog droplets, which remains constant for the same type of fog, Equation (18) can be rewritten as

$$V = K \frac{\bar{r}}{m} \qquad (19)$$

when K being $2/3 \ln (1/\epsilon)$ is considered as a proportionality constant, and $\bar{r}$ is the average radius of the fog droplets.

Based on the data given in one of the physical models of cooling tower induced fog [15] the visibility can be calculated as a function of condensed moisture in the ambient air-plume mixture. The lowest threshold of the condensed moisture content in the modeling calculation is 1×10^{-5} gram water per gram dry air. This threshold corresponds to a visibility of 4000 meter ($2\frac{1}{2}$ miles).

4.0 METEOROLOGICAL INPUT

Meteorological data recorded at the 400 foot tower were used in determining the fogging and icing potentials. Hourly data of atmospheric pressure, temperature, dew point, wind speed and wind direction were the meteorological input of the model.

The temperature differences recorded between 400 and 33 foot levels were used to obtain the temperature gradient, deg. K per 100 m, which is used to determine the atmospheric stability classes based on values given in the AEC Safety Guide 23.

5.0 Results and Discussion of Results

The model discussed in the previous sections was used to evaluate the environmental effect of four types of cooling towers, all rely on mechanical fans to obtain draft necessary for performance. They are:

(1) Linear wet mechanical draft cooling tower

(2) Linear wet/dry mechanical draft cooling tower

(3) Round wet mechanical draft cooling tower

(4) Fan assisted natural draft cooling tower

The physical characteristics of each type has been given in Table 3.1.1.

The environmental effects of the cooling tower plume is two fold: first, the deposition of drift droplets entrained by the effluent containing dissolved minerals, such as chlorides could result in botanical injury. Second, the continuous injection of large amount of water vapor to a small area confined by a valley terrain can upset the natural thermal balance modifying the local micrometeorology and resulting in increased incidences of fogging and icing.

Generally speaking both plume induced fog and ice contain condensed moisture. As fog the condensed moisture is in the form of small droplets, the average size of which depends on the types of fog and the amount of supersaturation. The liquid droplets can continue to exist in a supercooling state to a temperature as low as $-10^{o}C$ [16]. Since supercooling is basically an unstable state, the supercooled droplets are turned to ice particles as soon as they strike a sub-freezing surface or interrupted by the dust nuclei in the atmosphere. Because of this unstable nature of supercooling it is assumed that the freezing point separates the fogging and icing.

Both salt deposits and fogging and icing were calculated based on hourly meteorological data. No precipitation data is available, therefore no allowance was made for raining days. All monthly depositions were accumulated for the entire month with no consideration of wash out by rain.

In the induced fogging and icing calculations all wind data were included to obtain the monthly maximum number of hours of fogging or icing. Under variable conditions a zero degree wind direction was assigned to the data; while a small wind velocity (0.5 mph) was assumed for the calm condition. Plume induced fogging and icing is also included when the ambient air is saturated (relative humidity is 100%). The predicted fog hours are excluded when the visibility meter indicates visibilities less than 1500 feet for these hours. All predicted fog with visibility greater than 2½ miles are excluded. The results presented in the following sections can be regarded as the absolute upper limit of fogging or icing hours.

5.1 Salt Drift Deposits

Instead of computing the salt deposits monthly for the one year period October, 1973 to September, 1974 one representative month for each season was selected:

Spring	-	May
Summer	-	August
Autumn	-	November
Winter	-	February

The river salinity in the three spring months is less than 100 ppm. The value of drift deposits calculated for May which could cause plant damage over a very small area insignificant in comparison with other months. Therefore, May is excluded in the presentation.

Figure 5.1.1 through 5.1.3 are the salt deposits resulted from operating the linear wet mechanical draft cooling towers in the three representative months of summer (August), autumn (November), and winter (February).

A peak of 6000 Kg/Km^2/Month of dry salt (as NaCl) deposits was calculated for August which is the highest value compared to the values obtained for November and February. These are 3000 and 1200 $Kg/Km^2/Mo.$ respectively.

Although the August peak is highest the land area covered is very small where vegetations are scarce. Up to 3000 $Kg/Km^2/mo.$ the drift deposits are limited to the vicinity covering less than half square kilometer. Another peak value of 750 $Kg/Km^2/Mo$ mostly fallen on water, occurs approximately 2 kilometers south of tower site. (Figure 5.1.1)

The twin peak of salt deposits disappeared in November. The peak deposits of 3000 $Kg/Km^2/mo$ as well as the 2000 $Kg/Km^2/mo$ isopleth fall mainly within the boundaries of the plant site. (Figure 5.1.2)

The peak deposits occurring in February is much smaller (1200 $Kg/Km^2/mo$) which falls on the quarry, 1 kilometer southwest of the tower site. (Figure 5.1.3)

Figures 5.1.4 through 5.1.6 are the salt deposits in the three seasonal representative months for the linear wet/dry mechanical draft cooling towers. A wet/dry ratio of 15/85 percent was postulated for the tower operation. With the 15 percent unsaturation the salt deposits were found to have been reduced appreciably be essentially unchanged from the wet tower in the month of August (Figure 5.1.4).

Peak deposits for November and February are reduced to 2700 and 840 $Kg/Km^2/mo.$ respectively, compared to 3000 and 1200 $Kg/Km^2/mo.$ for the linear wet mechanical draft cooling towers in the same months.

Figures 5.1.7 through 5.1.9 present the isopleths of salt drift deposits from the two postulated round mechanical draft cooling towers for Unit No. 3. The pattern of the salt deposits for August was found to be quite different compared to those obtained for the linear mechanical draft cooling towers. A single peak of 8760 $Kg/Km^2/mo.$ located mainly in the river off the west edge of the plant site. Most of the salt deposits isopleths appear to be oriented according to the principal wind vectors in the Indian Point area.

For the round mechanical cooling tower October instead of November was selected to represent the autumn season, as indicated in Figure 5.1.8. A peak of 5000 $Kg/Km^2/mo.$ was calculated which falls in the vicinity of the natural draft cooling tower for Unit No. 2, mainly in the river. Another peak of 3610 $Kg/Km^2/mo.$ is located approximately 1 kilometer southeast of the tower site covering a small area less than 1/10 square kilometer.

A peak deposit of 3090 $Kg/Km^2/mo.$ was calculated for February which falls in the river off the tower site.

Figures 5.1.10 through 5.1.12 present the salt deposits due to operations of the two postulated fan assisted natural draft cooling towers for Unit No. 3.

Due to the higher tower height the patterns of salt deposits are distinctly different from other types of tower. Several peaks appear along the principal wind vector. The maximum for August is 1070 $Kg/Km^2/mo.$ located in the river approximately 1 kilometer west off the site.

Two maxima 1325 and 1488 $Kg/Km^2/mo$ respectively located approximately 1 and 2.5 kilometers south of the tower site. The areas covered by these maxima are less than 1/10 of a square kilometer and the 1488 $Kg/Km^2/mo.$ maximum falls in the water.

The maximum salt deposits for February is 630 $Kg/Km^2/mo$ partly located in the river southwest of the tower site. The 100 $Kg/Km^2/Mo$ isopleth representing the minimum threshold of plant damage covers a net land area approximately ½ square kilometer.

Due to the differences in tower heights and configurations, the hourly maximum salt deposits and atmospheric concentrations are quite different. A comparison is made below:

	Round Mechanical Draft Cooling Tower		Fan Assisted Natural Draft Cooling Tower	
Season	Max. Atm. Salt Conc. ug/m^3	Max. hourly salt Deposition, $Kg/Km^2/Mo$	Max. Atm Salt Conc. ug/m^3	Max. hourly salt Deposition $Kg/Km^2/Mo$
Winter	547	1043	327	624
Spring	53	71	9	16
Summer	1101	2100	147	281
Autumn	1040	1985	234	446

The values for the round mechanical draft cooling towers are of the same order of magnitude for the linear wet and wet/dry mechanical draft cooling towers. Therefore, the tabulated values represent all three types of mechanical draft cooling towers. The values indicate that fan assisted natural draft cooling towers contribute much less ground level salt deposits as well as atmospheric salt concentrations.

5.2 Plume Induced Fog by Linear Wet Mechanical Draft Cooling Tower

Figures 5.2.1 through 5.2.6 present the predicted frequency (Hours/month) of fog occurrences due to plumes from linear wet mechanical draft cooling towers, representing the one year period from winter 1973 to Autumn 1974.

Since fogging (and also icing) is more critical for the winter months no representative month was used. The fogging frequencies were predicted for each of the three winter months. The spring, summer and autumn are represented by April, June and October respectively.

The patterns of the fog occurrences closely correspond to the wind patterns with above freezing temperatures. Figure 5.2.1 indicates that the principal wind pattern were either south or northeast with more frequently southerlies. Due to this wind component a maximum of 11 hours/mo is predicted. This maximum number of hours of fog occurs approximately 4 kilometers north of the tower site. The northeast wind component contributes to a maximum of 7 hours/mo approximately 2 kilometers southwest of the tower site. The 5 hours of fog predicted approximately 3.5 kilometers south of the tower site could have been due to variable winds or calm conditions.

Figure 5.2.2 presents the location and frequency of predicted fog for January (1974). It clearly indicates that the main cause of the plume induced fog in January is due to the wind component from northeast.

As indicated in Figure 5.2.3 only 3 hours of fog is contributed by the cooling tower plumes. It appears to be mainly due to the wind from southwest.

The main contributor of cooling tower induced fog in April (Figure 5.2.4) appears to be the northeast wind which accumulated a maximum frequency of 13 hours/mo. This maximum occurs over the abandoned quarry approximately 1 kilometer southwest of the tower site.

The wind rose pattern in June indicates that low wind speed regime at 1-3 mph is relatively more prominant than spring and winter in all wind directions. This might explain why there are peak frequencies isolated in small areas occurring to the south, north and east of the tower site as indicated in Figure 5.2.5. A maximum frequency of 8 hours/mo. covering a very large area was predicted approximately 1.5 kilometers north of the tower site.

Figure 5.2.6 presents the predicted pattern of fog occurrences in October due to cooling tower plumes. A maximum of 7 hours/mo. can occur. It is located both southeast and southwest of the tower site.

The results are summarized below:

	Predicted Fog (Hours/mo.)
December	11
January	3
February	3
April	13
June	8
October	7

5.3 Plume Induced Fog by Linear Wet/Dry Mechanical Draft Cooling Towers at Three Wet/Dry Proportions

As presented in Figures 5.3.1 through 5.3.10 fog induced by plumes from operations of the postulated wet/dry mechanical draft cooling towers at 100%, 92.5% and 85% wet cooling loads is predicted.

Comparing Figure 5.3.1 and Figure 5.2.2 it clearly indicates that when wet/dry towers are operated as a wet mechanical cooling tower the plume induced fog is essentially identical to that by the wet mechanical tower. Increasing the dry load from 0% to 7.5% (Figure 5.3.2 through 5.3.5) then to 15% (Figure 5.3.6 through 5.3.10) there is an appreciable reduction of induced fog. Comparing Figures 5.3.2, 5.3.6 with Figures 5.2.1 for the hours of induced fog in December a 63% reduction of fog was achieved with dry cooling load of 15%. Despite a large increase to 15% dry load the effect on induced fog in January is negligible. The induced fog in January was eliminated when a 30% dry load was used in the prediction. Comparing Figures 5.3.4 with Figure 5.2.3, a 7.5% dry load would reduce the induced fog by 1/3 at the maximum. Further increase of the dry load to 15% the induced fog in February is completely eliminated.

A maximum of 4 hours of fog was predicted in April for a dry load of 15%, as indicated in Figure 5.3.8. It is a reduction of almost 70% compared to the 13 hours of fog induced by linear wet mechanical towers in the same month. A 50% reduction of induced fog was predicted for June when Figure 5.3.9 is compared with Figure 5.2.5.

Reduction of the induced fog in October is predicted only in the area southwest of the tower site as indicated in Figure 5.3.10 (compared to Figure 5.2.6). However, the area enclosed by the maximum hours of fog to the southeast of the tower site is reduced appreciably.

A summary of the results are tabulated below:

Month	Wet/Dry	Predicted Plume Induced Fog By Wet/Dry Mech. Cooling Tower, Hours/Mo.	
	100/0% Max.	92.5/7.5% Max.	85/15% Max.
December	11	6	5
January	3	3	3
February	3	2	0
April	13	*	4
June	8	*	5
October	7	7	7

* Not predicted

5.4 Plume Induced Fog by Round Mechanical Draft Cooling Tower Plumes

Except for the circular bases the round mechanical cooling tower is fundamentally a multiple cell configuration similar to wet mechanical draft cooling towers. Months of January, April, July and October were taken to represent the four seasons in the one-year study period. The results are summarized below:

Predicted Hours of Induced Fog
(Hours/Mo.)

	Maximum
January	2
April	5
July	1
October	5

The predicted fog for each season was estimated based on the predictions of the representative months.

5.5 Plume Induced Icing by Linear Wet Mechanical Draft Cooling Towers

Icing is more critical in winter. Based on the simple criterion previously discussed icing is assumed when the moisture in the plume is condensed at temperatures below freezing. Supercooled droplets is an unstable state. In a dust and other nuclei contaminated environment supercooling may not prevail and the end results would be ice formation.

As presented in Figures 5.6.1 through 5.6.4 operation of linear wet mechanical draft cooling towers resulted in a number of hours of icing in the winter month and the early spring. The results are summarized below:

Predicted Icing (Hours/Mo.)

Month	Maximum
December	20
January	20
February	30
April	3

5.6 Plume Induced Icing by Linear Wet/Dry Mechanical Draft Cooling Towers

When operated at 100% wet cooling load, the wet/dry cooling tower plumes induced a maximum of 24 hours of icing in January, as shown in Figure 5.7.1. Compared to a maximum of 20 hours of icing in the same month for linear wet mechanical the difference might be attributable to the differences in configuration and the number of cells.

Compared to the wet plumes, the initial 7.5% dry load reduced the induced icing in December from 20 hours/mo to 7 hours/mo. With 15% dry load the hours of icing is further reduced to 4 hours/mo in December.

Reductions of icing hours by plumes from wet/dry towers in January and February are not as effective as in December. In January, the 20 hours/mo icing due to wet tower plumes is reduced to 17 hours/mo at 7.5% dry load. The 30 hours/mo of icing due to wet plumes predicted for February is reduced to 17 hours/mo by 7.5% dry load, and further reduced to 6 hours/mo. when the dry load is increased to 15%.

The 3 hours/mo icing predicted for April was reduced to 1 hour/mo for a dry load of 15%.

The results are summarized as the following:

Wet/Dry	Predicted Icing by Wet/Dry Mech. Cooling Towers (Hours/Mo.)		
Month	100/0% Max.	92.5/7.5% Max.	85/15% Max.
December	(20)	7	4
January	24	17	10
February	(30)	17	6
April	3	*	1

* Prediction not made.
( ) Icing induced by wet cooling towers.

5.7 Plume Induced Icing By Round Mechanical Draft Cooling Towers

The plume induced icing by round mechanical cooling towers was predicted for winter and spring. Winter season is represented by January, 22 hours/mo. of icing was predicted. Spring is represented by April, 2 hours/mo of icing was predicted. The minimum number of hours of icing for these two months are 11 and 1 hour/mo. respectively.

5.8 Plume Induced Fogging and Icing by Fan Assisted Natural Draft Cooling Towers

For the cooling load of Unit No. 3 two fan assisted natural draft cooling towers were postulated. On account of the higher structure (200 feet) , and larger buoyancy factor (approximately 10^4 m^4/sec^3 compared to 700-900 m^4/sec^3 for the mechanical draft cooling towers) the plume should behave resembling the natural draft cooling tower.

The results are summarized below:

Predicted Plume Induced Fog & Ice
(Hours/Mo.)

Month	Fogging	Icing
December	1	3
January	2	3
February	1	2
March	3	0
April	4	0
May	(3)	0
June	(2)	0
July	2	0
August	(1)	0
September	1	0
October	2	0
November	1	0

The number in parenthesis are estimated values. Since the number of hours of fog is small graphic presentations were not prepared.

References

(1) "A Theory of Eddy Diffusion in the Atmosphere", O.G. Sutton, Proc. Roy Soc. (London) A135, 143-165, 1932.

(2) "Work Book of Atmosphere Dispersion Estimates", D. Bruce Turner, U.S. Dept. of H.E.W., 1970.

(3) "The Growth of Cloud Drops by Condensation", Part I & II, P. Squires Aust. J. Sci. Res. A5, 59, 473, 1952.

(4) "Rise and Condensation of Large Cooling Tower Plumes", S.R. Hanna, J. Appl. Meterology 11, 793, 1972.

(5) "Recommended Guide for the Prediction of the Dispersion of Airborne Effluents", Maynard Smith, Ed. ASME, 1968.

(6) "The State of the Art of Saltwater Cooling Towers for Steam Electric Generating Plants", prepared for U.S. Atomic Energy Commission, Westinghouse Electric Corp. Environmental System Dept., Pittsburgh, Pa., 1973.

(7) "Determination of Salt Deposition Rates from Drift from Evaporative Cooling Towers", C. Hosler, J. Pena, and R. Pena, Dept. of Meteorology, Pennsylvania State University, 1972.

(8) "Salt Drift Model - Description", S.M. Laskowski (Pickard, Lowe and Assoc., Inc.), Washington, D.C., Report to Con Edison, July, 1973.

(9) "American Institute of Physics Handbook", Chapter 4, 301-308, McGraw-Hill, Inc., 1972.

(10) "Thermodynamic Properties of Steam", J.H. Keenan and F.G. Keyes, John Wiley & Sons, Inc., 1936.

(11) "Plume Rise", G.A. Briggs, U.S. Atomic Energy Commission, 1969.

(12) "The Hudson River Estuary, A Preliminary Investigation of Flow and Water-Quality Characteristics," Giese, G.L., and Barr, J.W., State of New York, Conservation Department, Water Resources Commission, Bulletin 61, P. 37, 1967.

(13) Draft Environmental Statement by the Directorate of Licensing, United States Atomic Energy Commission, related to operation of Indian Point Nuclear Generating Plant Unit No.3., Consolidated Edison Company of New York, Inc., Docket No. 50-286, Pages II-8 to II-11, October 1973.

(14) "Particulate Clouds: Dusts, Smokes and Mists" H.L. Green and W.R. Lane, Chapter 12, D. Van Nostrand Company New York, Second Ed. 1964.

(15) "Potential Environmental Modifications Produced by Large Evaporative Cooling Towers" EG&G, Inc. January, 1971.

(16) "Elements of Cloud Physics" H.R. Byers, The University of Chicago Press, 1960.

FIGURE 3·7·1

EFFECTS OF SALT DRIFT DROPLET SIZE
AND RELATIVE HUMIDITY
ON TERMINAL VELOCITY

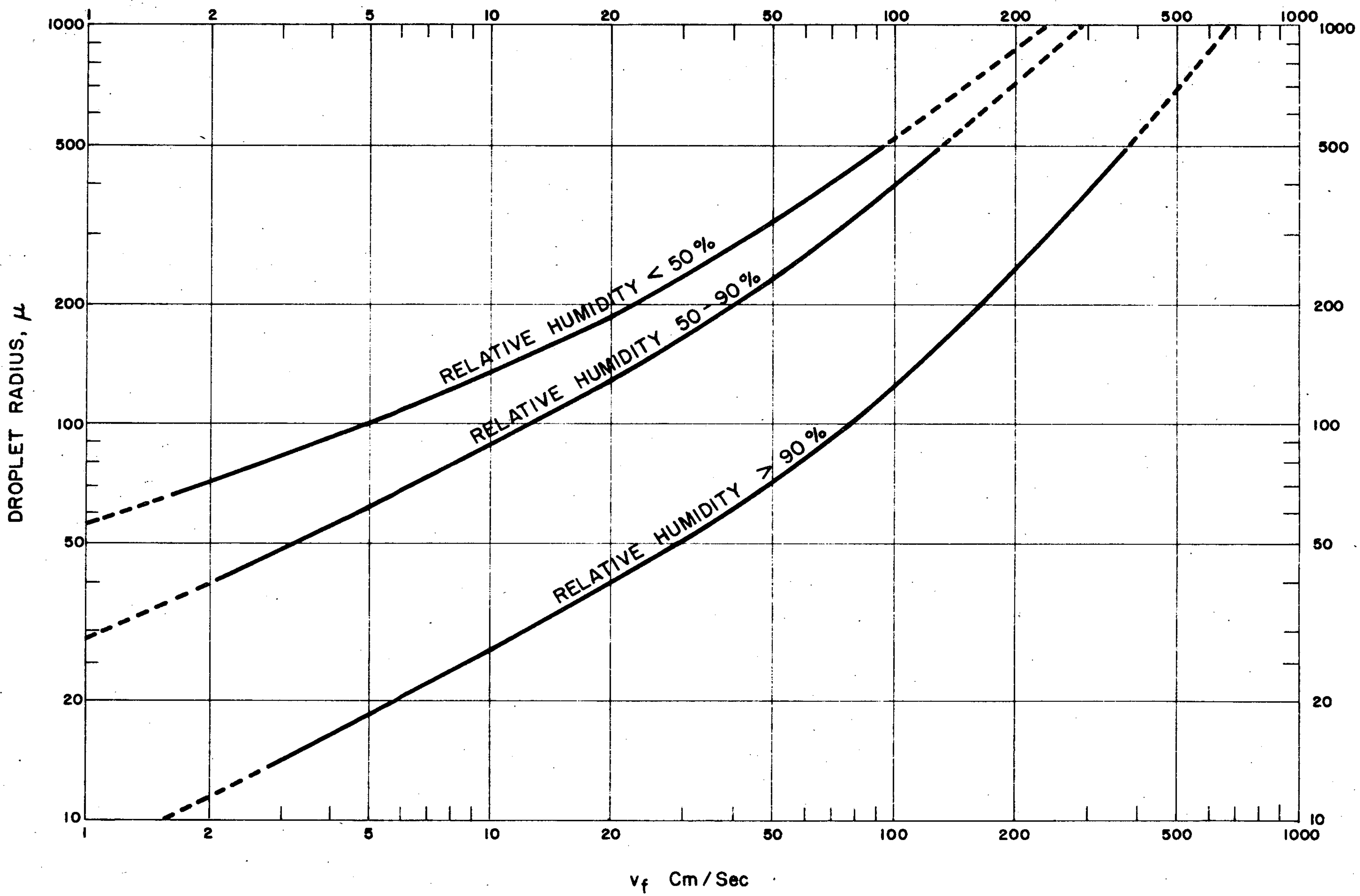

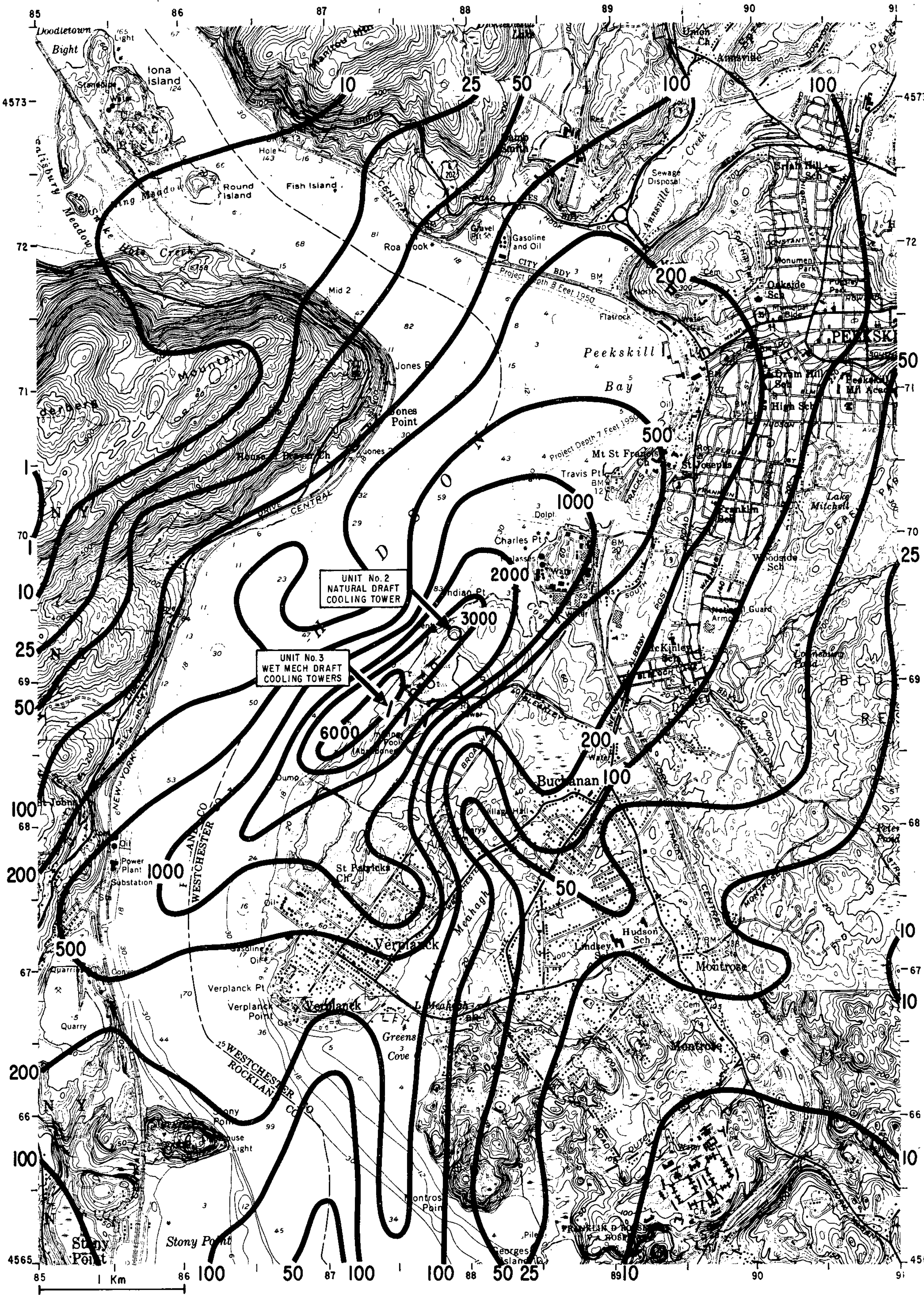

FIGURE 5.1.1
ACCUMULATED SALT DRIFT DEPOSITS
$Kg/Km^2/Mo$, AUGUST 1974
WET MECHANICAL DRAFT COOLING TOWERS

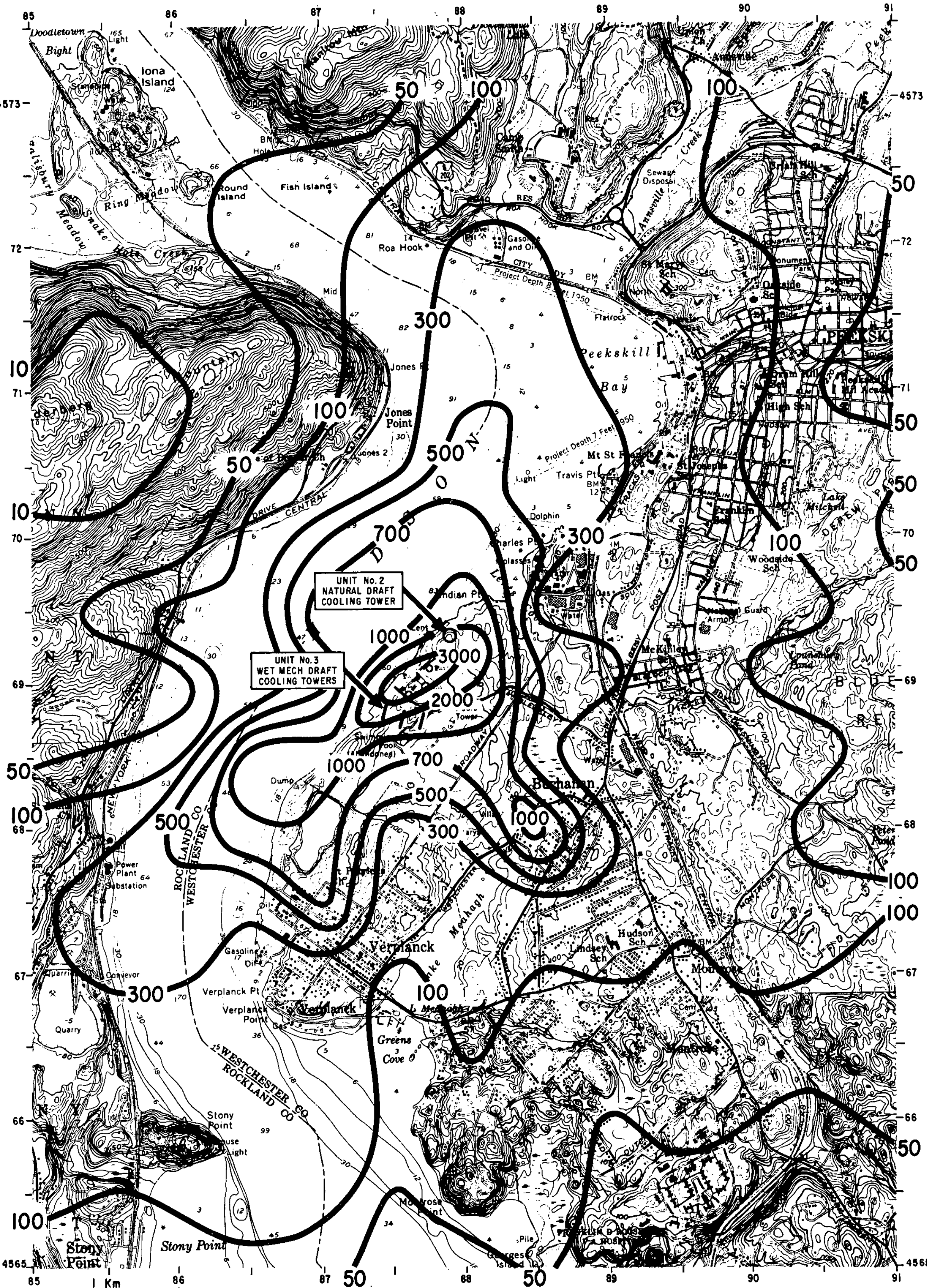

FIGURE 5.1.2

ACCUMULATED SALT DRIFT DEPOSITS
Kg / Km^2 / Mo, NOVEMBER 1973
WET MECHANICAL DRAFT COOLING TOWERS

FIGURE 5.1.3

ACCUMULATED SALT DRIFT DEPOSITS

$Kg/Km^2/Mo$, FEBRUARY 1974

WET MECHANICAL DRAFT COOLING TOWERS

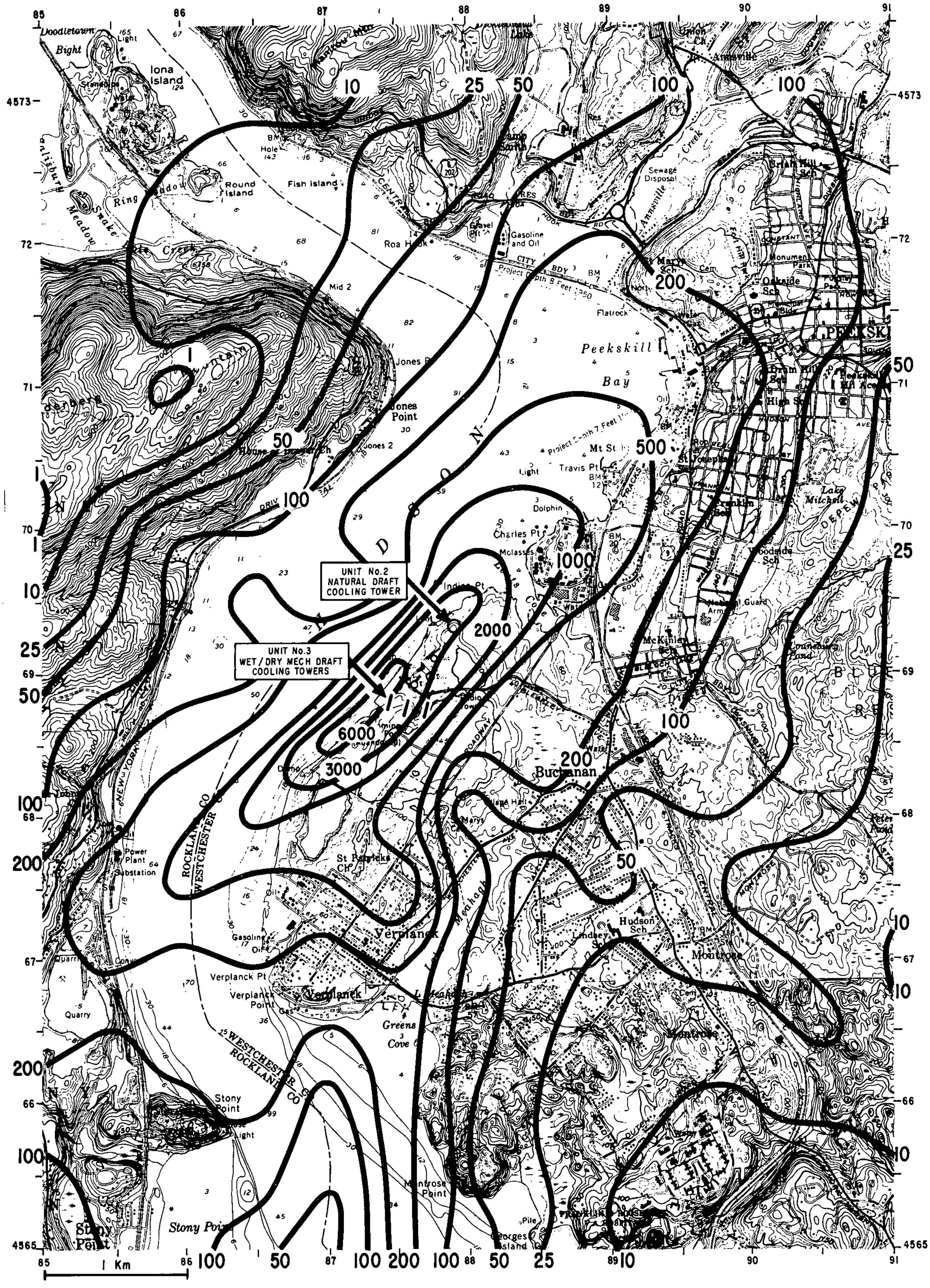

FIGURE 5.1.4

ACCUMULATED SALT DRIFT DEPOSITS

Kg / Km^2 / Mo, AUGUST 1974

WET (85%) / DRY (15%) MECHANICAL

DRAFT COOLING TOWERS

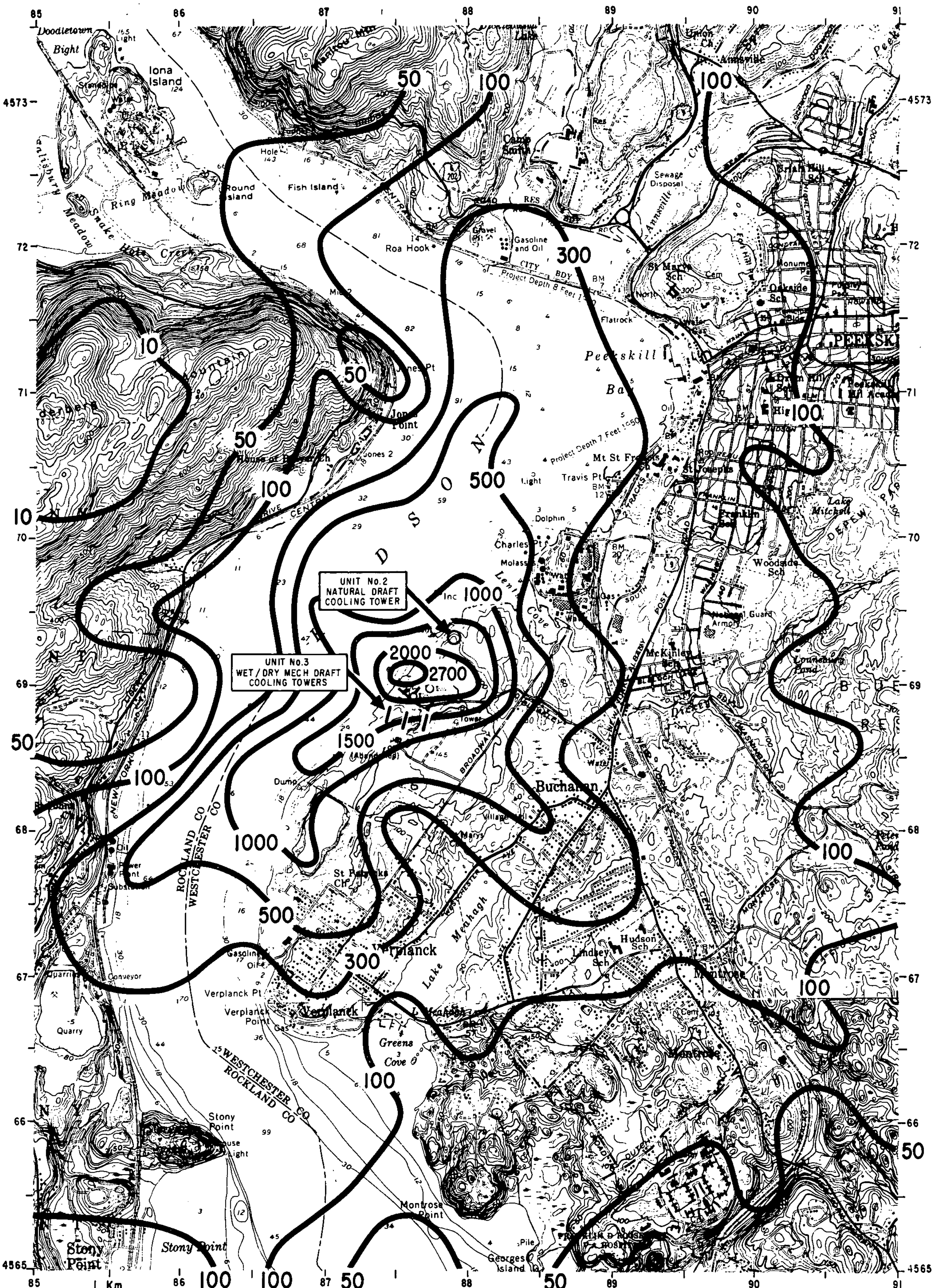

FIGURE 5.1.5

ACCUMULATED SALT DRIFT DEPOSITS
$Kg/Km^2/Mo$, NOVEMBER 1973
WET (85%) / DRY (15%) MECHANICAL
DRAFT COOLING TOWERS

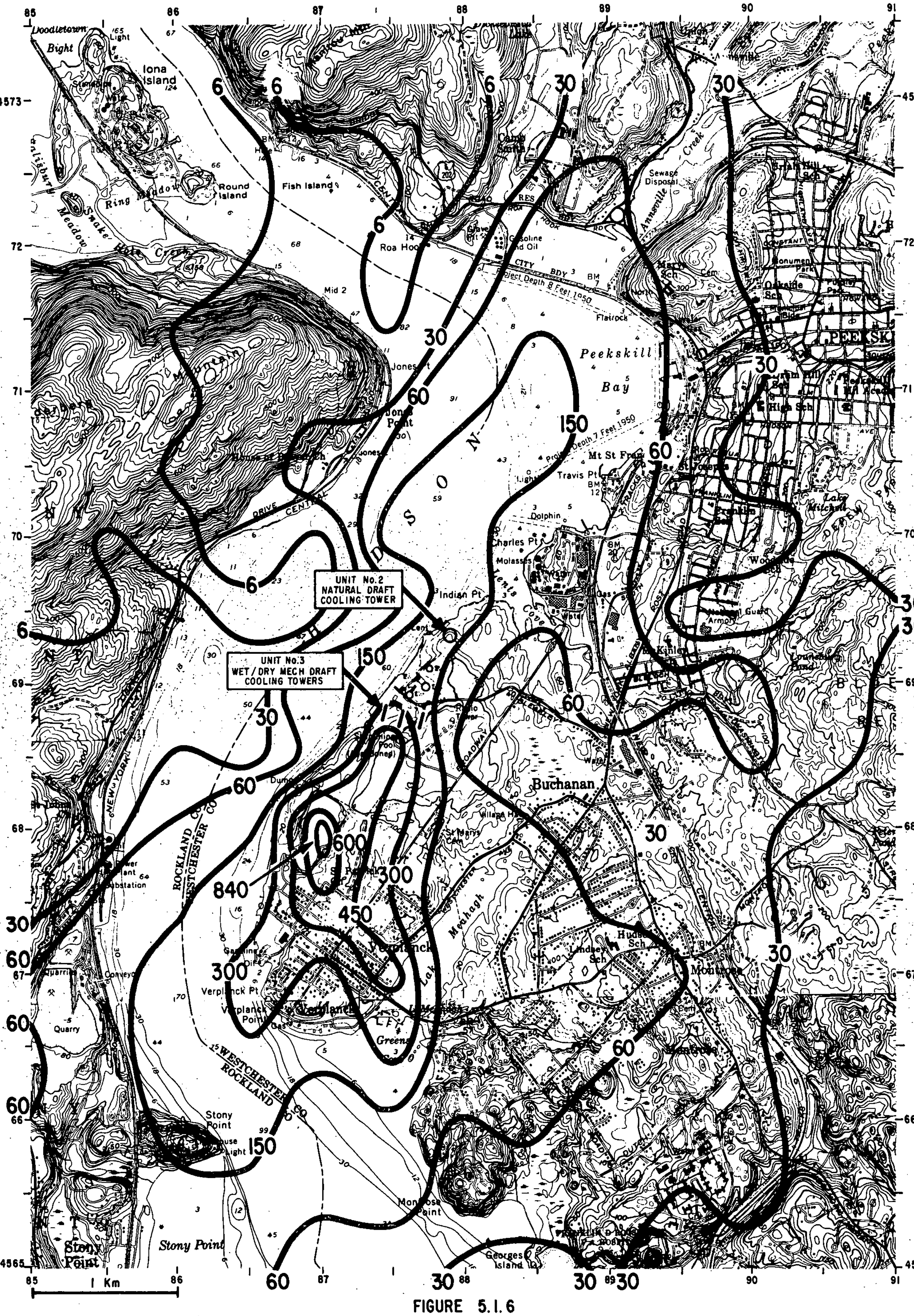

FIGURE 5.1.6

ACCUMULATED SALT DRIFT DEPOSITS
Kg / Km^2 / Mo, FEBRUARY 1974
WET (85 %) / DRY (15 %) MECHANICAL
DRAFT COOLING TOWERS

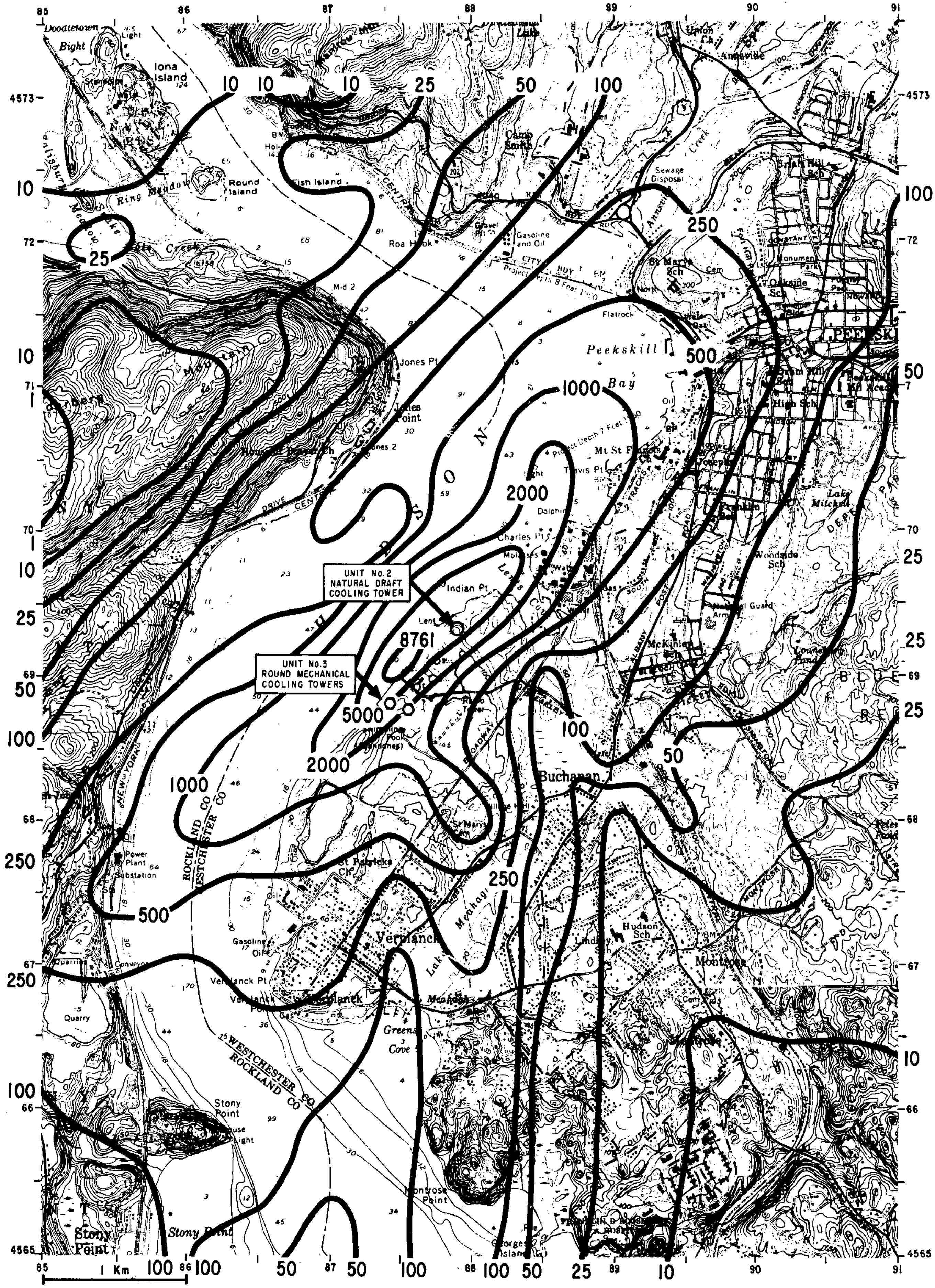

FIGURE 5.1.7
ACCUMULATED SALT DRIFT DEPOSITS
$Kg/Km^2/Mo$, AUGUST 1974
ROUND WET MECHANICAL
DRAFT COOLING TOWERS

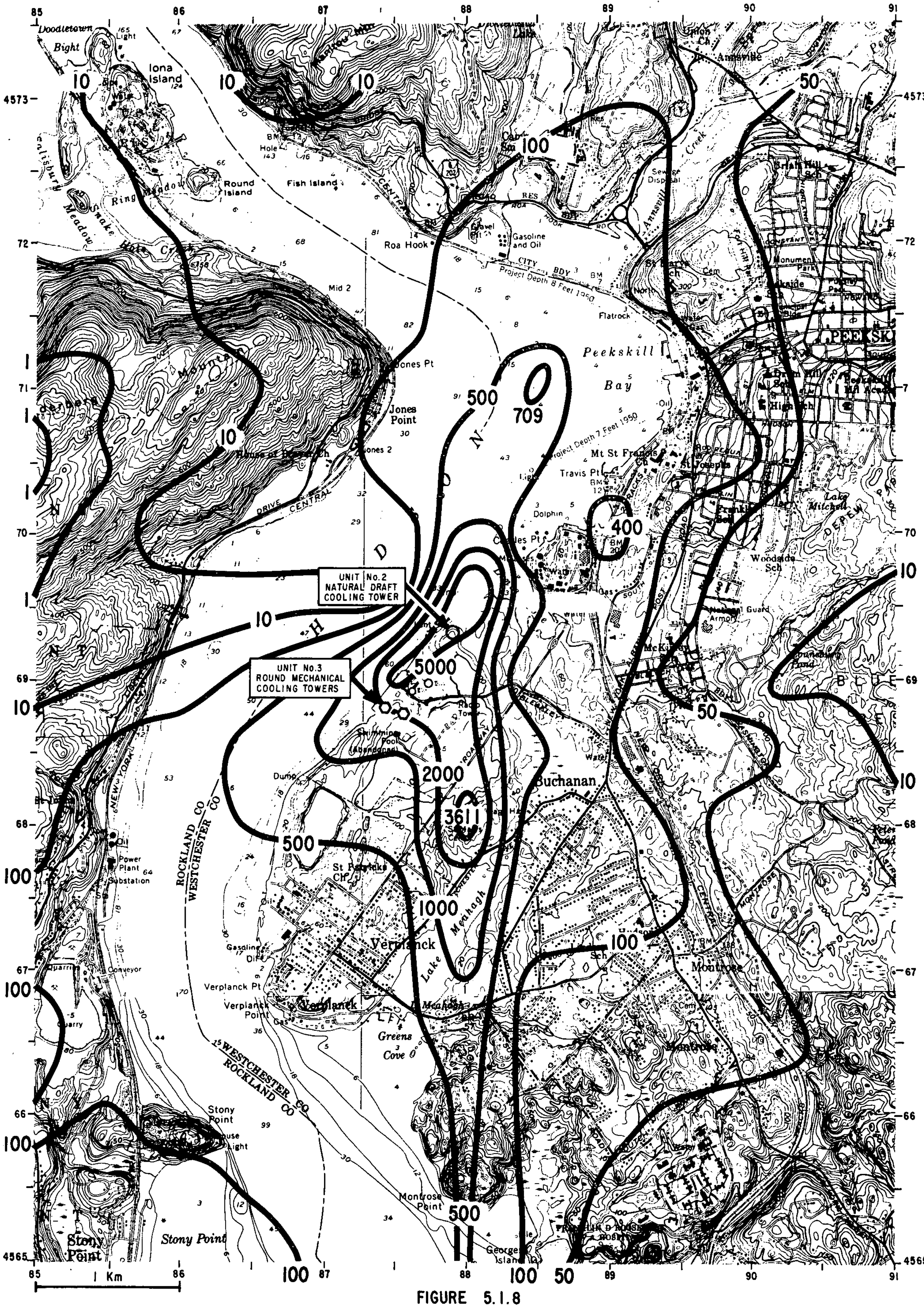

FIGURE 5.1.8
ACCUMULATED SALT DRIFT DEPOSITS
Kg / Km^2 / Mo, OCTOBER 1973
ROUND WET MECHANICAL
DRAFT COOLING TOWERS

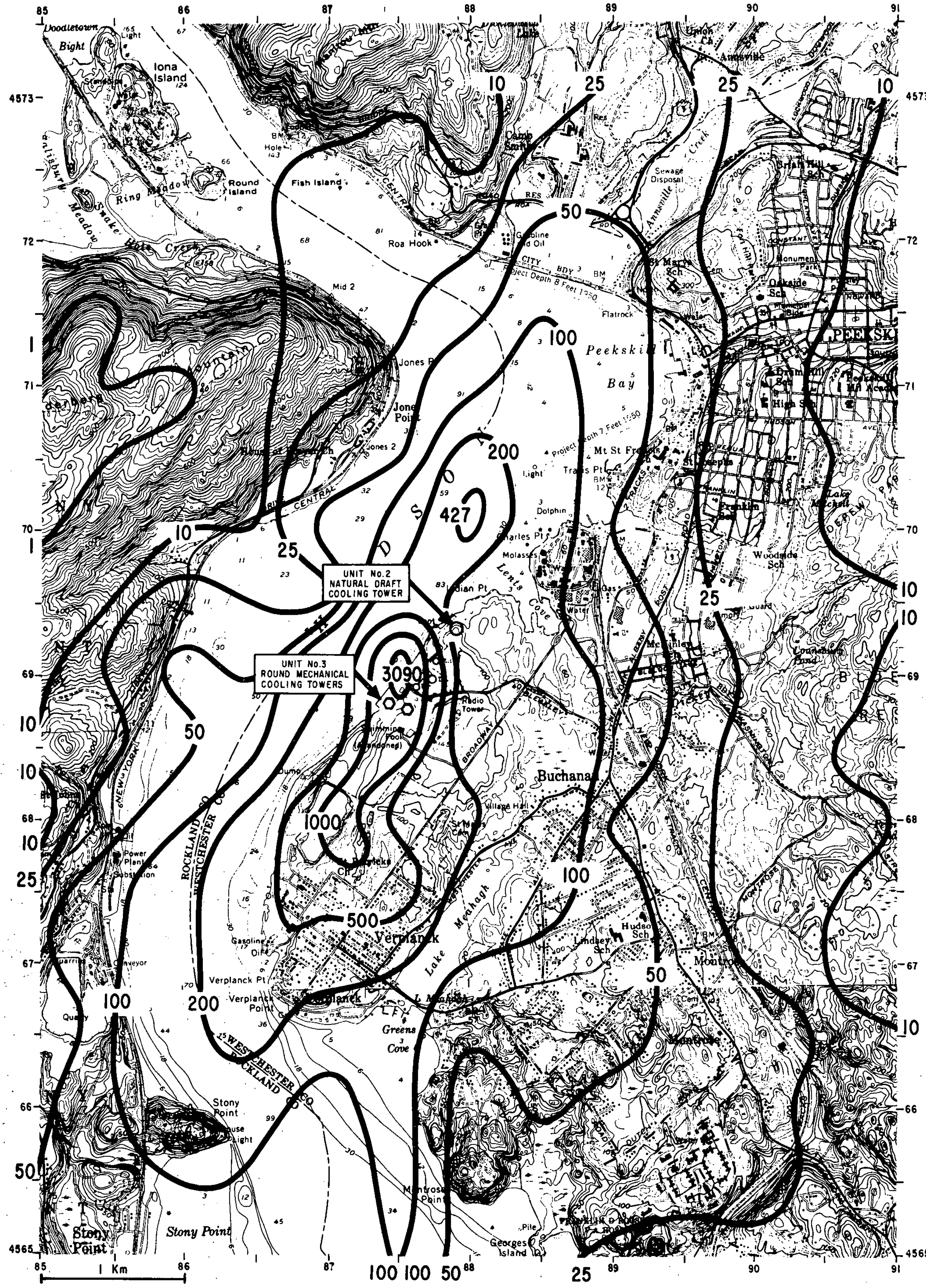

FIGURE 5.1.9

ACCUMULATED SALT DRIFT DEPOSITS

Kg/Km^2/Mo, FEBRUARY 1974

ROUND WET MECHANICAL

DRAFT COOLING TOWERS

FIGURE 5.1.10

ACCUMULATED SALT DRIFT DEPOSITS
$Kg/Km^2/Mo$, AUGUST 1974
FAN ASSISTED NATURAL
DRAFT COOLING TOWERS

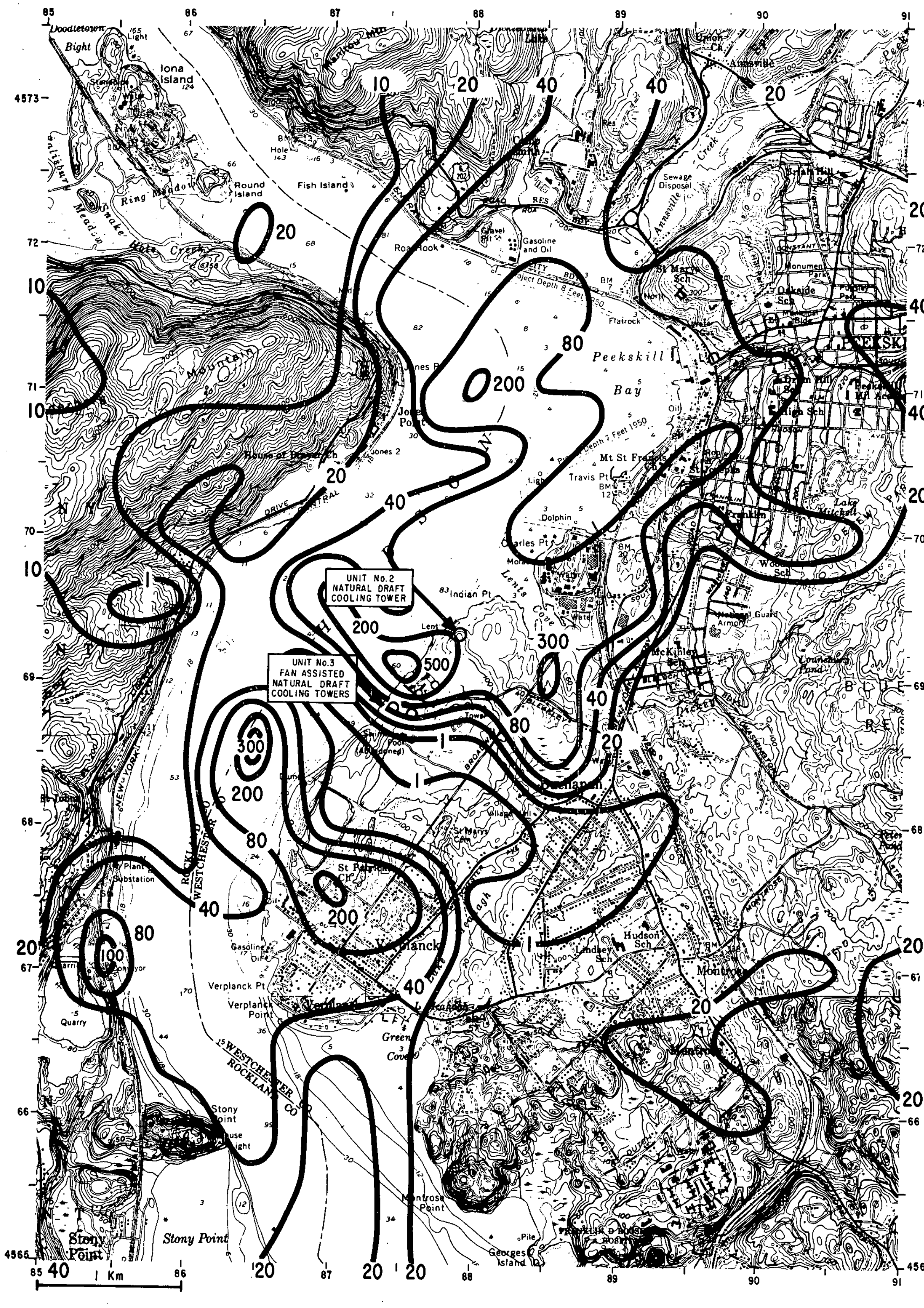

FIGURE 5.1.11

ACCUMULATED SALT DRIFT DEPOSITS
$Kg/Km^2/Mo$, OCTOBER 1973
FAN ASSISTED NATURAL
DRAFT COOLING TOWERS

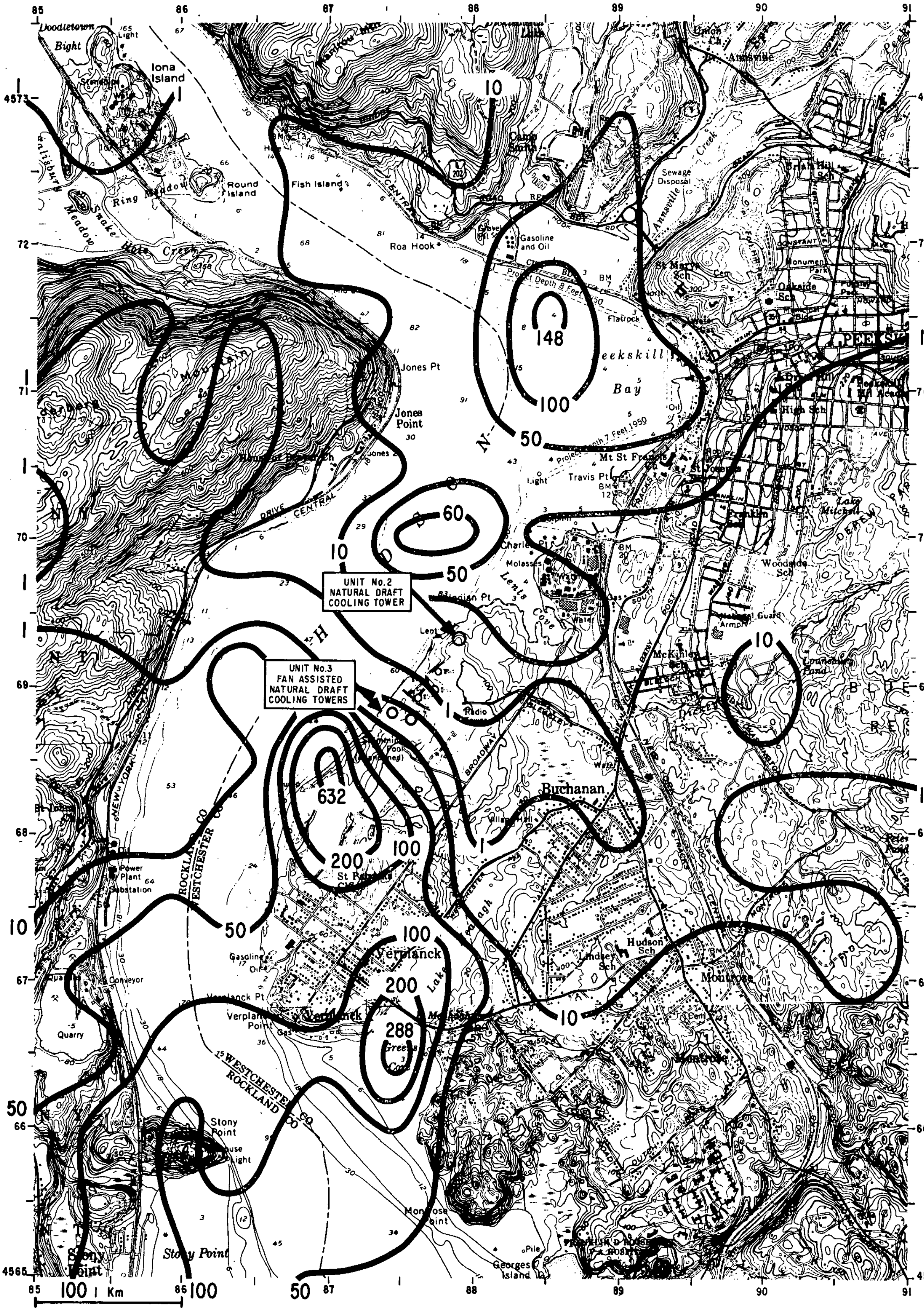

FIGURE 5.1.12
ACCUMULATED SALT DRIFT DEPOSITS
$Kg/Km^2/Mo$, FEBRUARY 1974
FAN ASSISTED NATURAL
DRAFT COOLING TOWERS

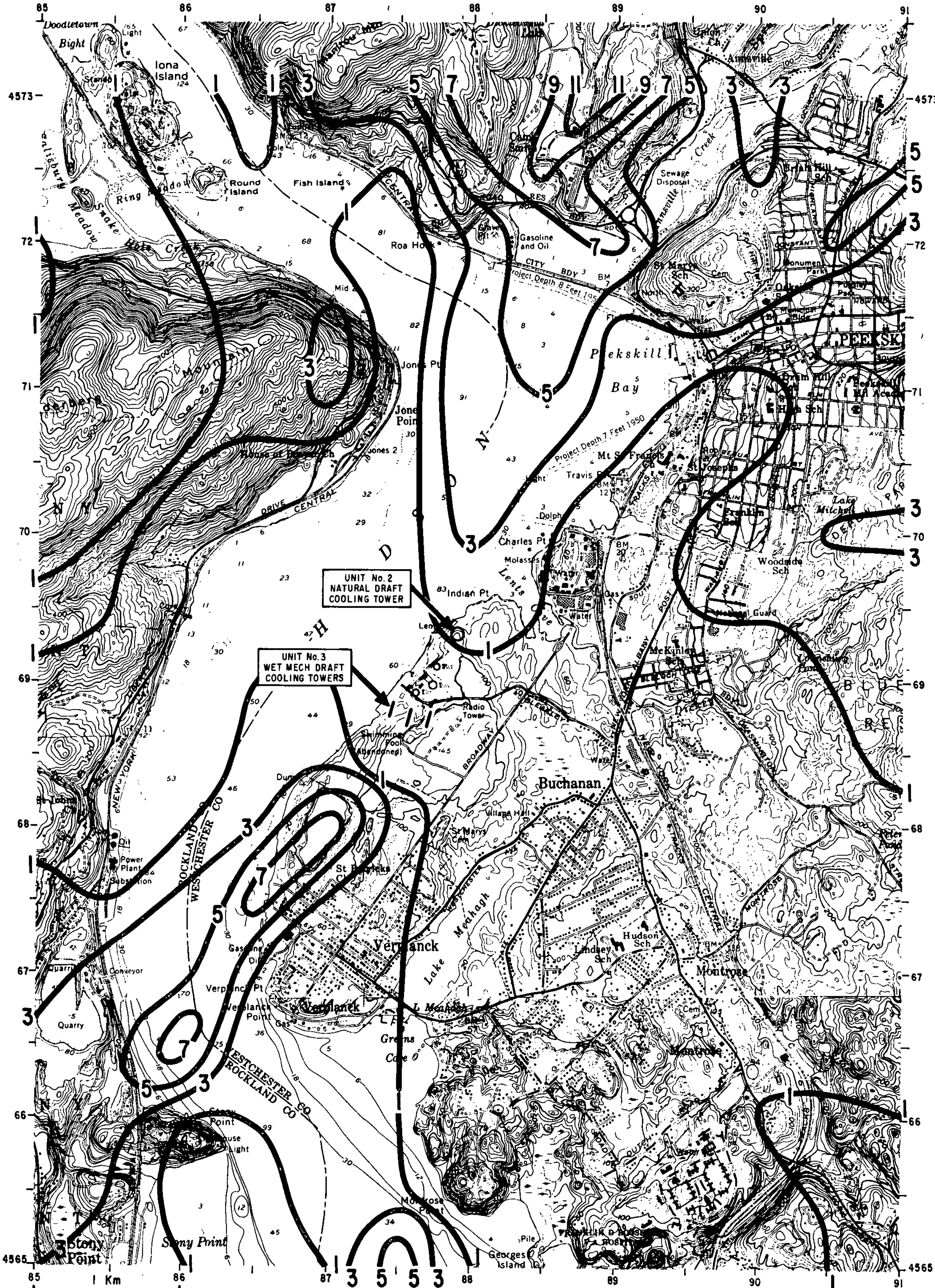

FIGURE 5.2.1

PLUME INDUCED FOG
HOURS/Mo, DECEMBER 1973
WET MECHANICAL DRAFT COOLING TOWERS

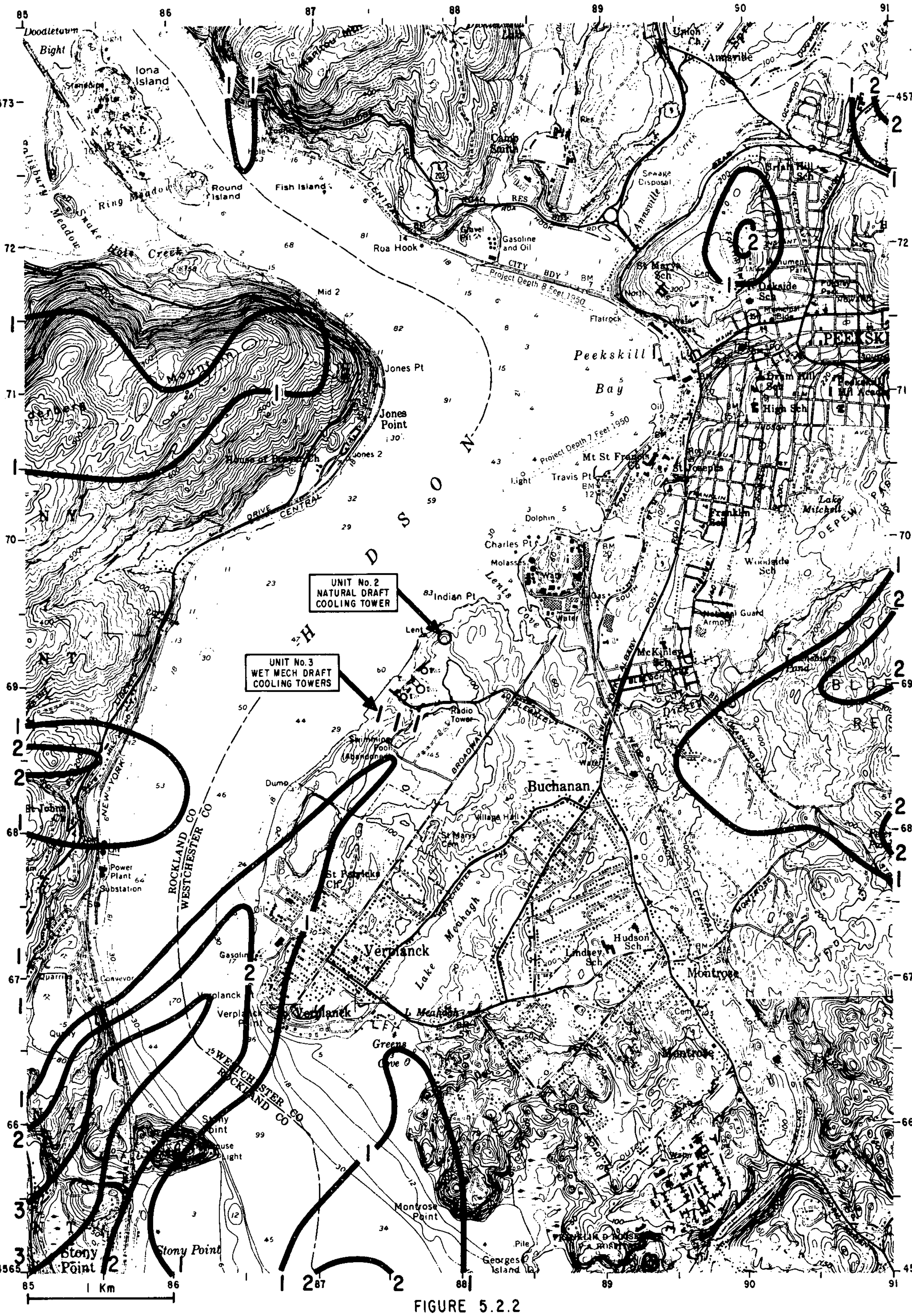

FIGURE 5.2.2

PLUME INDUCED FOG
HOURS/Mo, JANUARY 1974
WET MECHANICAL DRAFT COOLING TOWERS

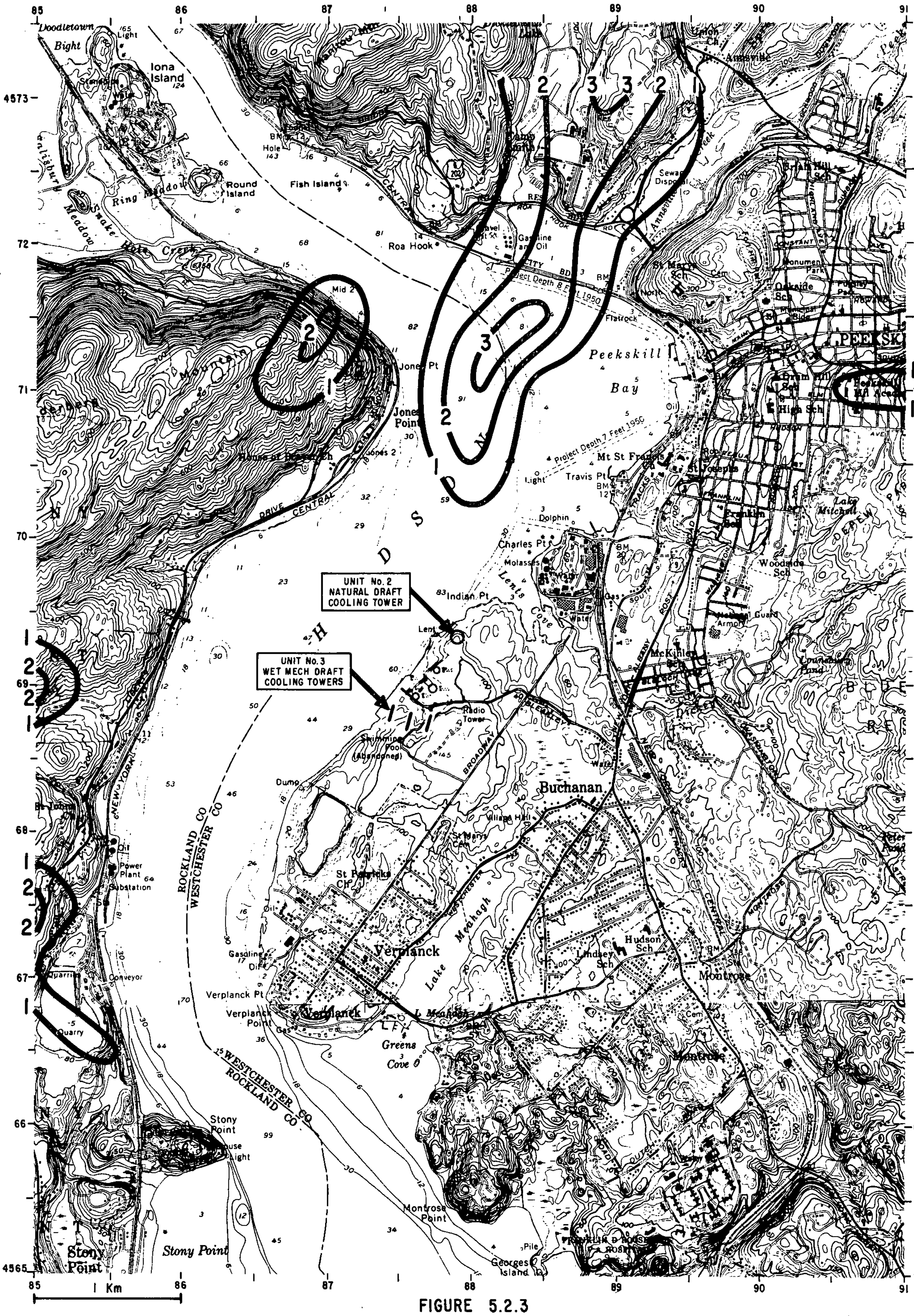

FIGURE 5.2.3

PLUME INDUCED FOG

HOURS / Mo, FEBRUAR 1974

WET MECHANICAL DRAFT COOLING TOWERS

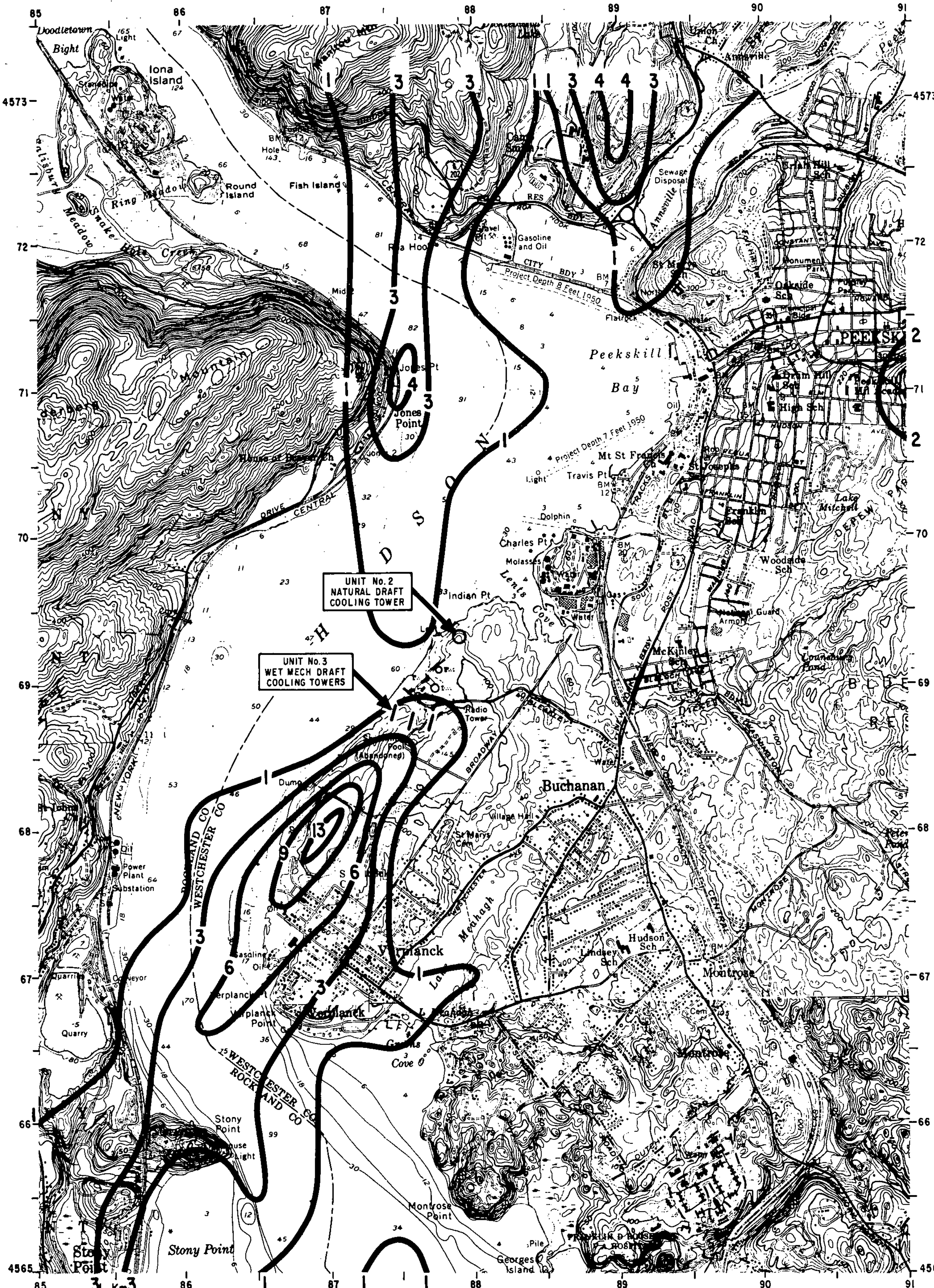

FIGURE 5.2.4

PLUME INDUCED FOG
HOURS/Mo, APRIL 1974
WET MECHANICAL DRAFT COOLING TOWERS

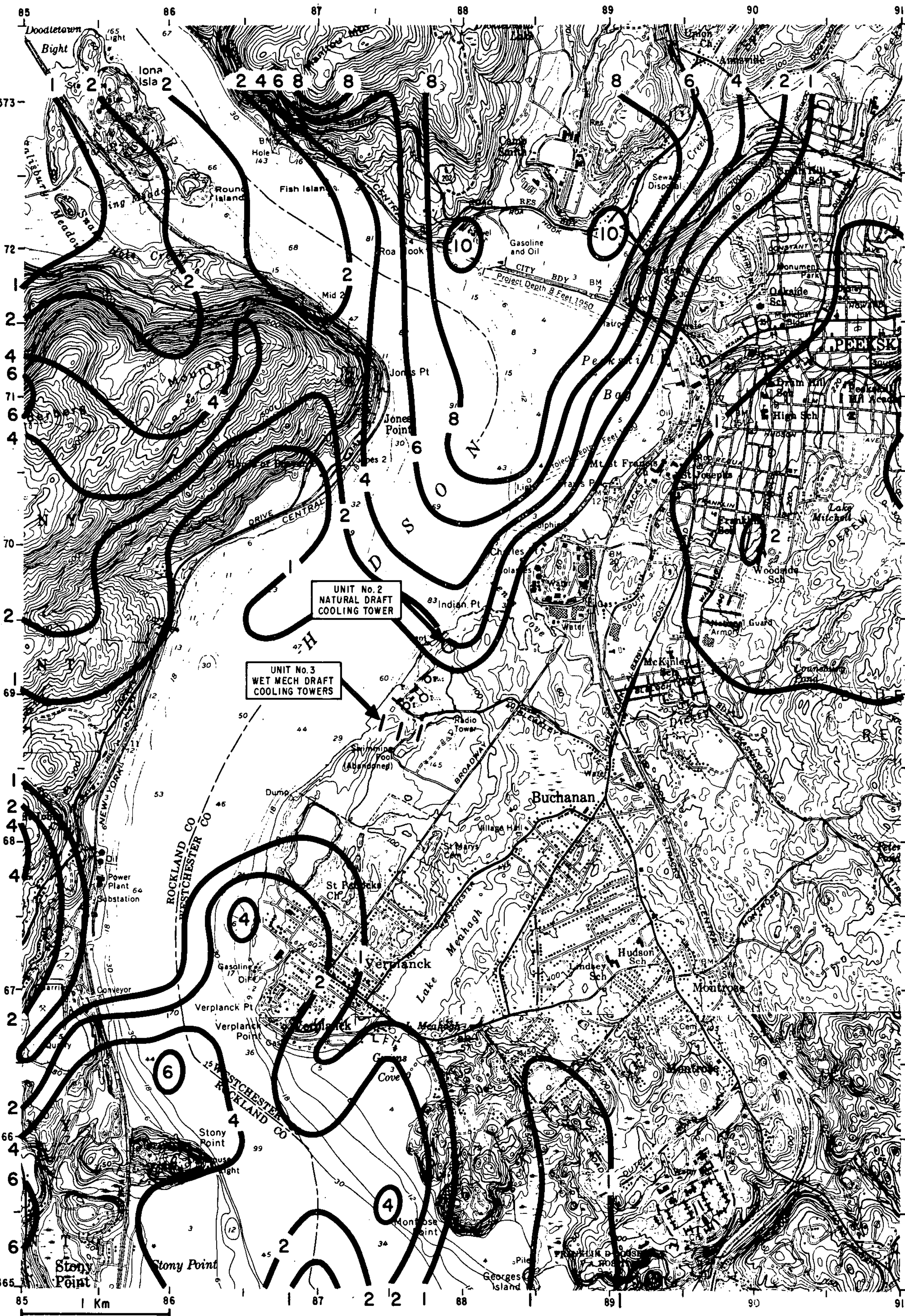

FIGURE 5.2.5

PLUME INDUCED FOG
HOURS/Mo, JUNE 1974
WET MECHANICAL DRAFT COOLING TOWERS

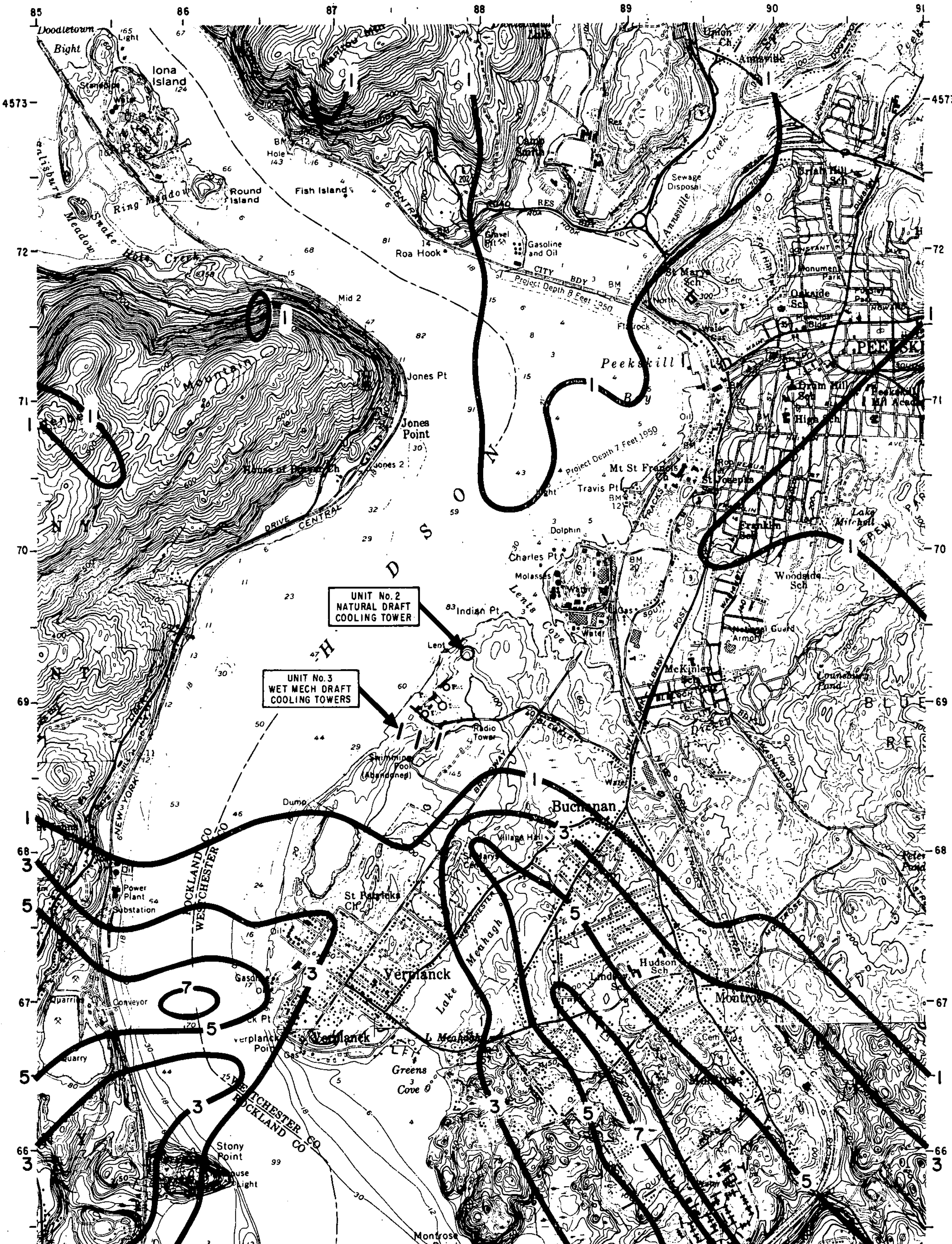

FIGURE 5.2.6

PLUME INDUCED FOG
HOURS/Mo, OCTOBER 1973
WET MECHANICAL DRAFT COOLING TOWERS

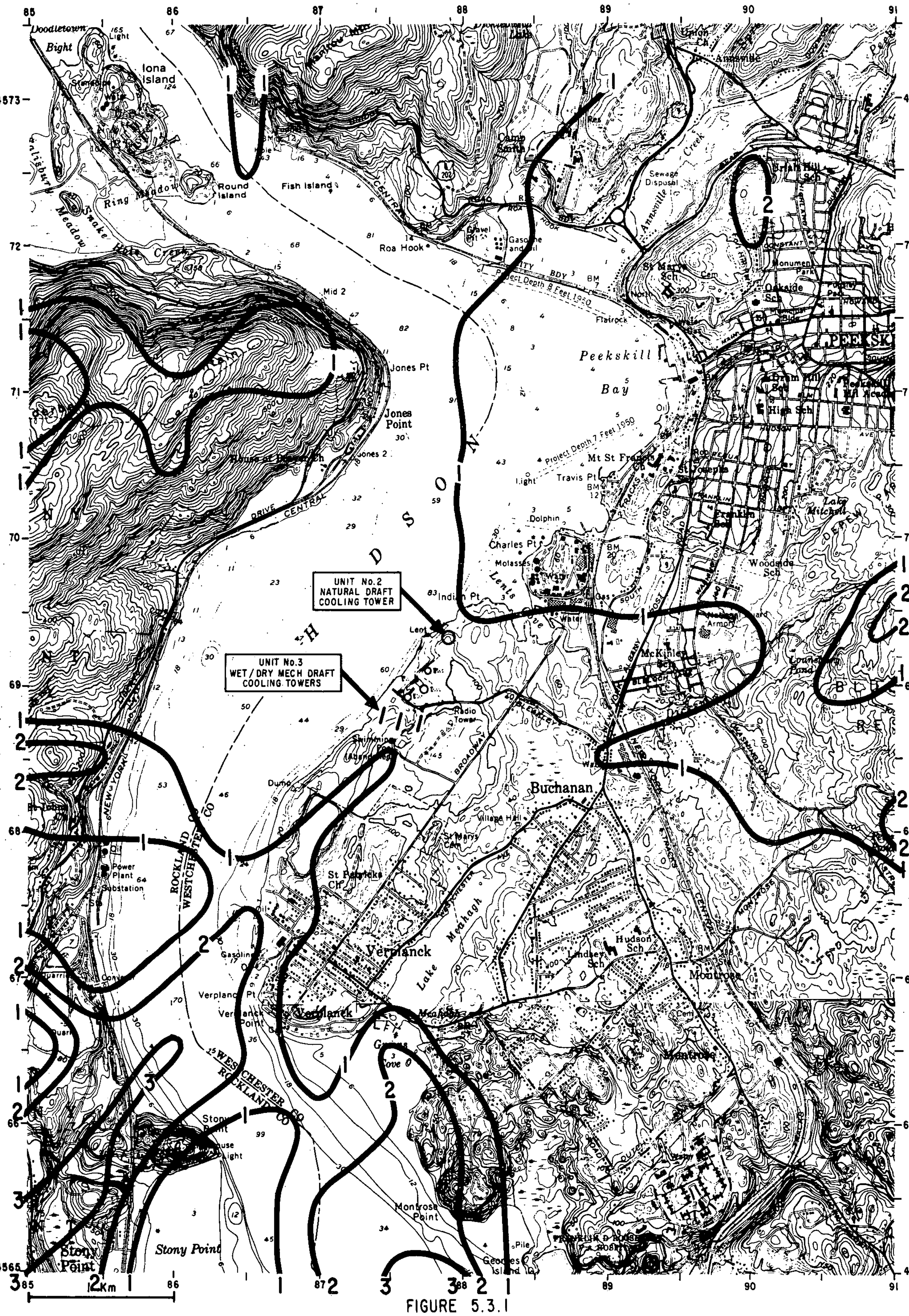

FIGURE 5.3.1

PLUME INDUCED FOG
HOURS/Mo, JANUARY 1974
WET (100%)/DRY (0%) MECHANICAL
DRAFT COOLING TOWERS

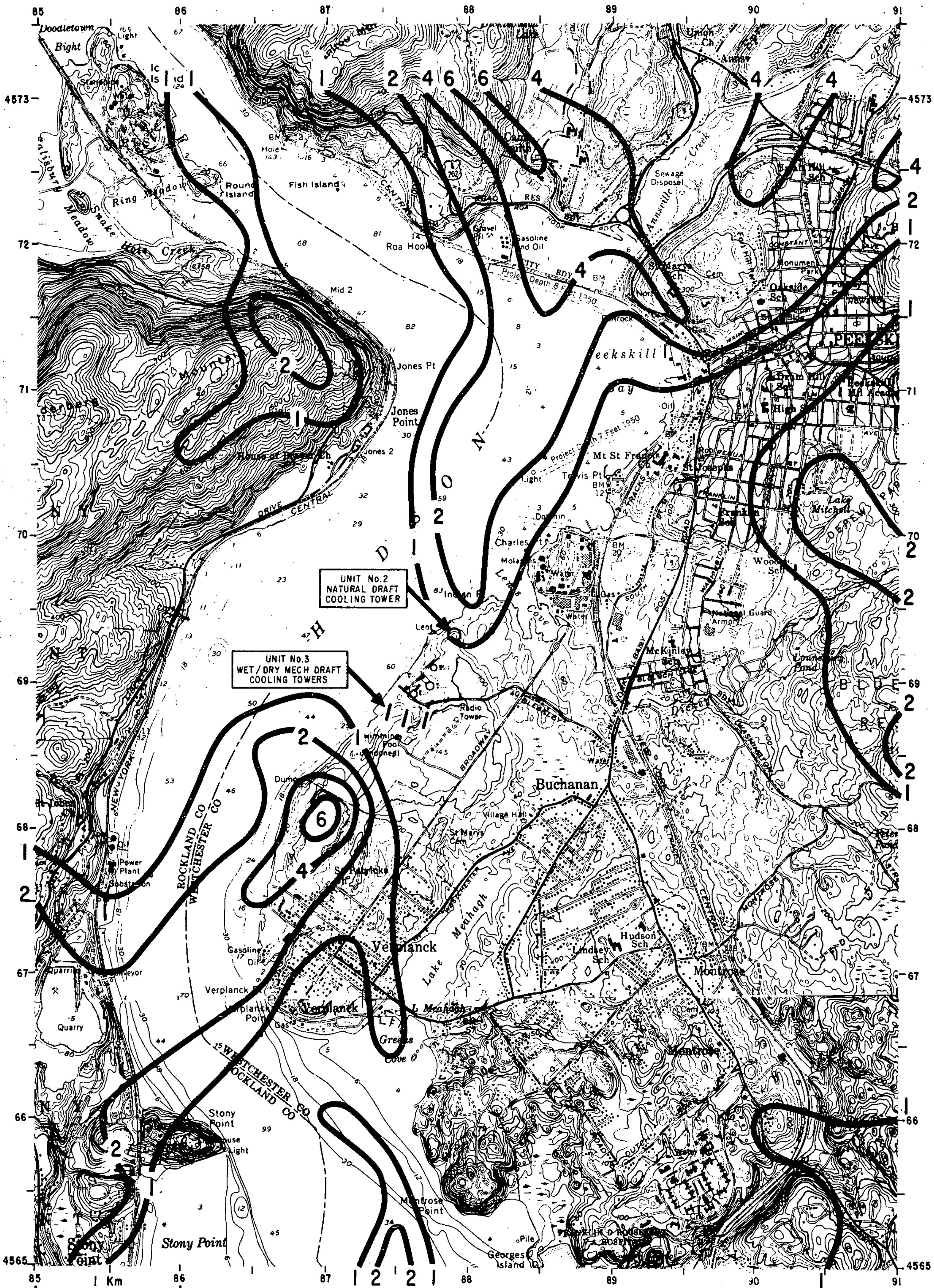

FIGURE 5.3.2

PLUME INDUCED FOG
HOURS/Mo, DECEMBER 1973
WET (92.5%) / DRY (7.5%) MECHANICAL
DRAFT COOLING TOWERS

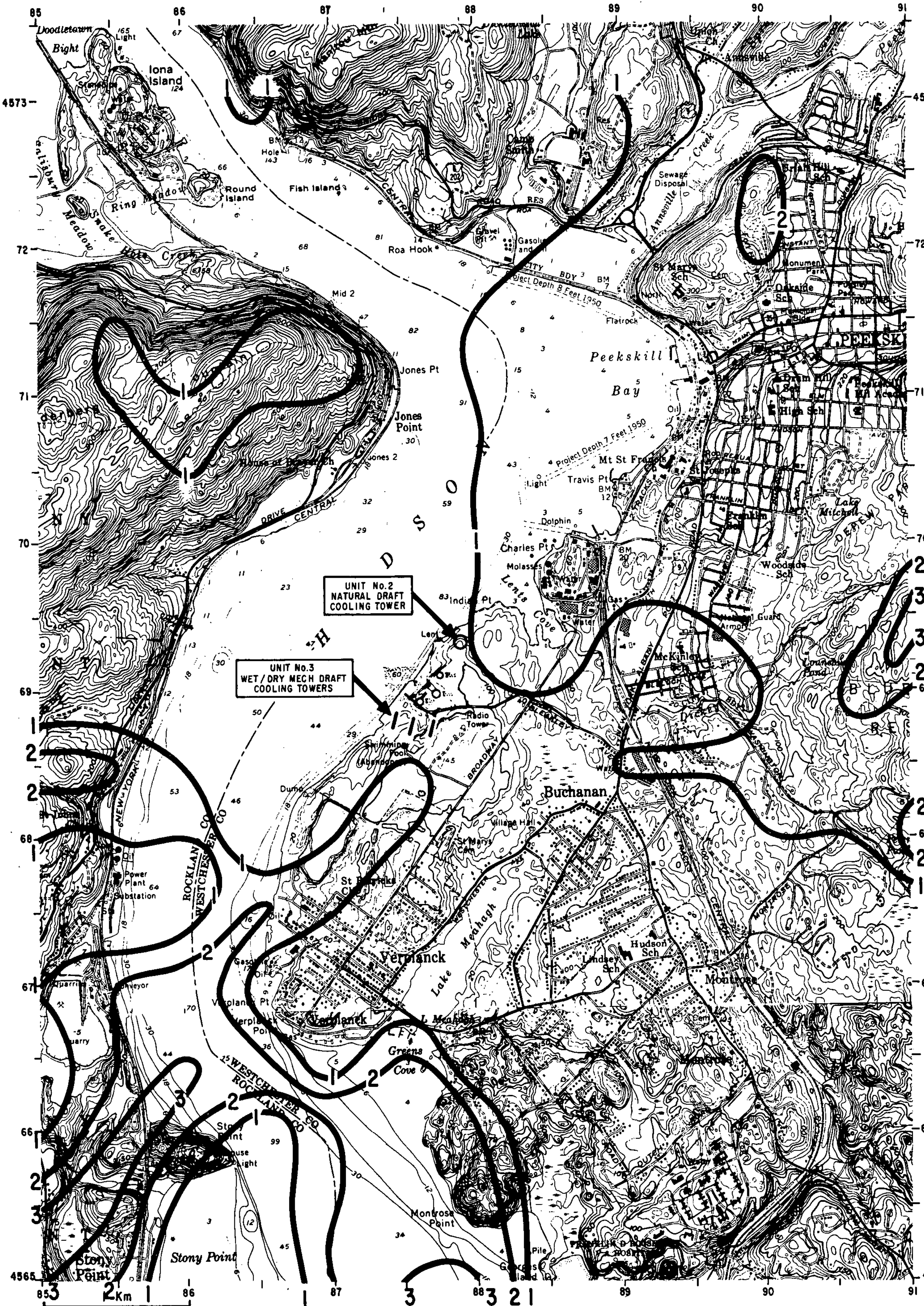

FIGURE 5.3.3
PLUME INDUCED FOG
HOURS/Mo, JANUARY 1974
WET (92.5%) / DRY (7.5%) MECHANICAL
DRAFT COOLING TOWERS

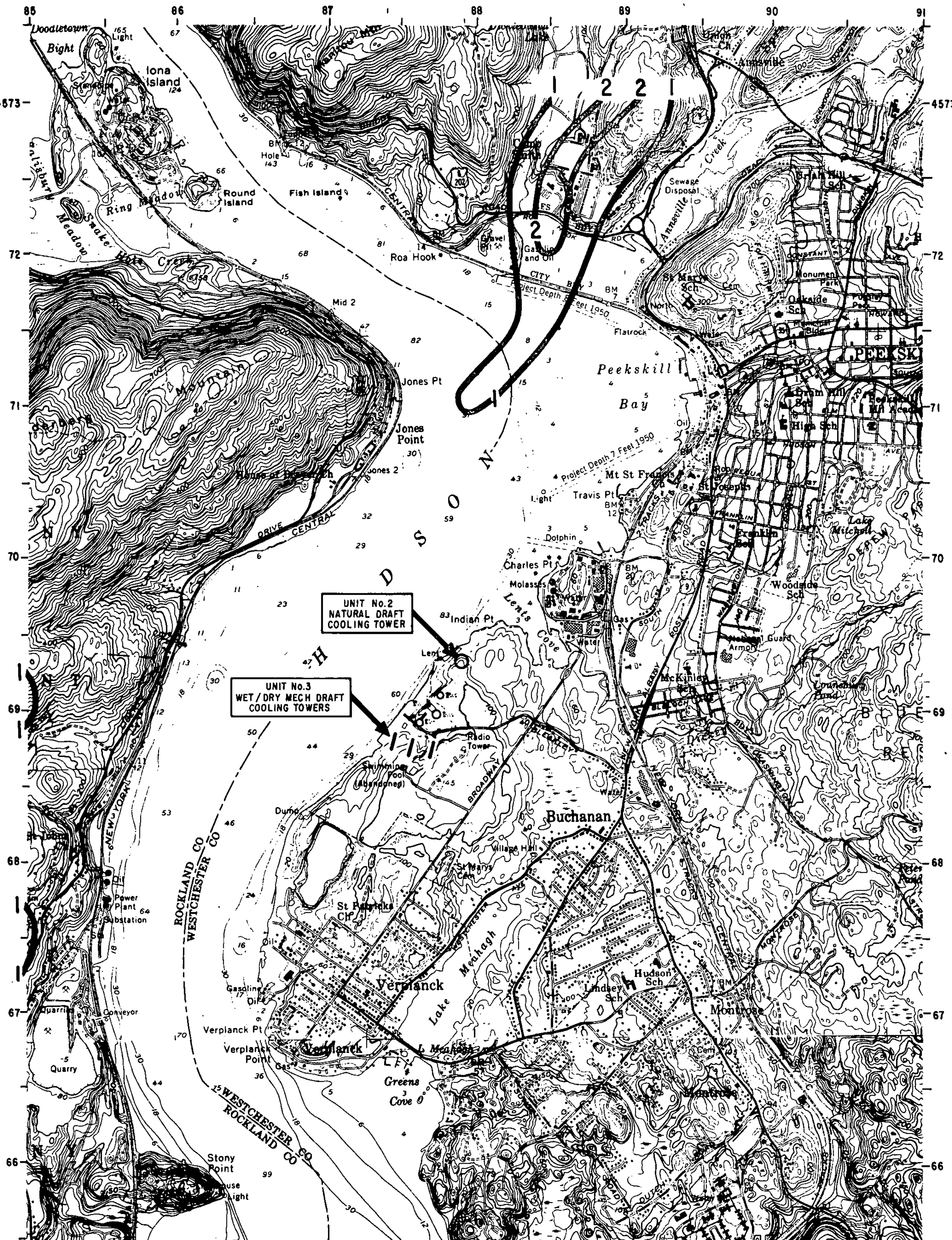

FIGURE 5.3.4

PLUME INDUCED FOG
HOURS/Mo, FEBRUARY 1974
WET (92.5%) / DRY (7.5%) MECHANICAL
DRAFT COOLING TOWERS

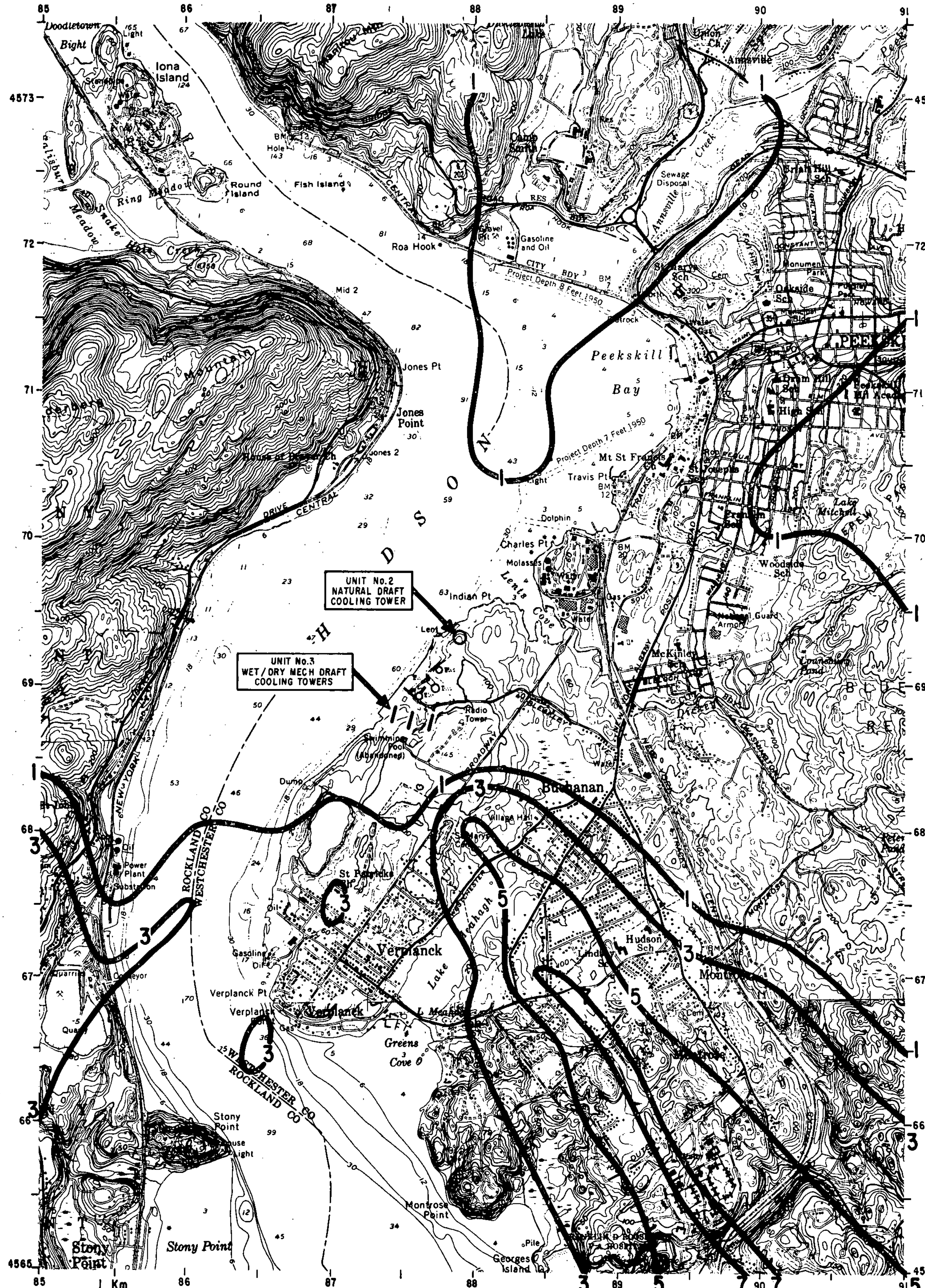

FIGURE 5.3.5

PLUME INDUCED FOG
HOURS/Mo, OCTOBER 1973
WET (92.5%) / DRY (7.5%) MECHANICAL
DRAFT COOLING TOWERS

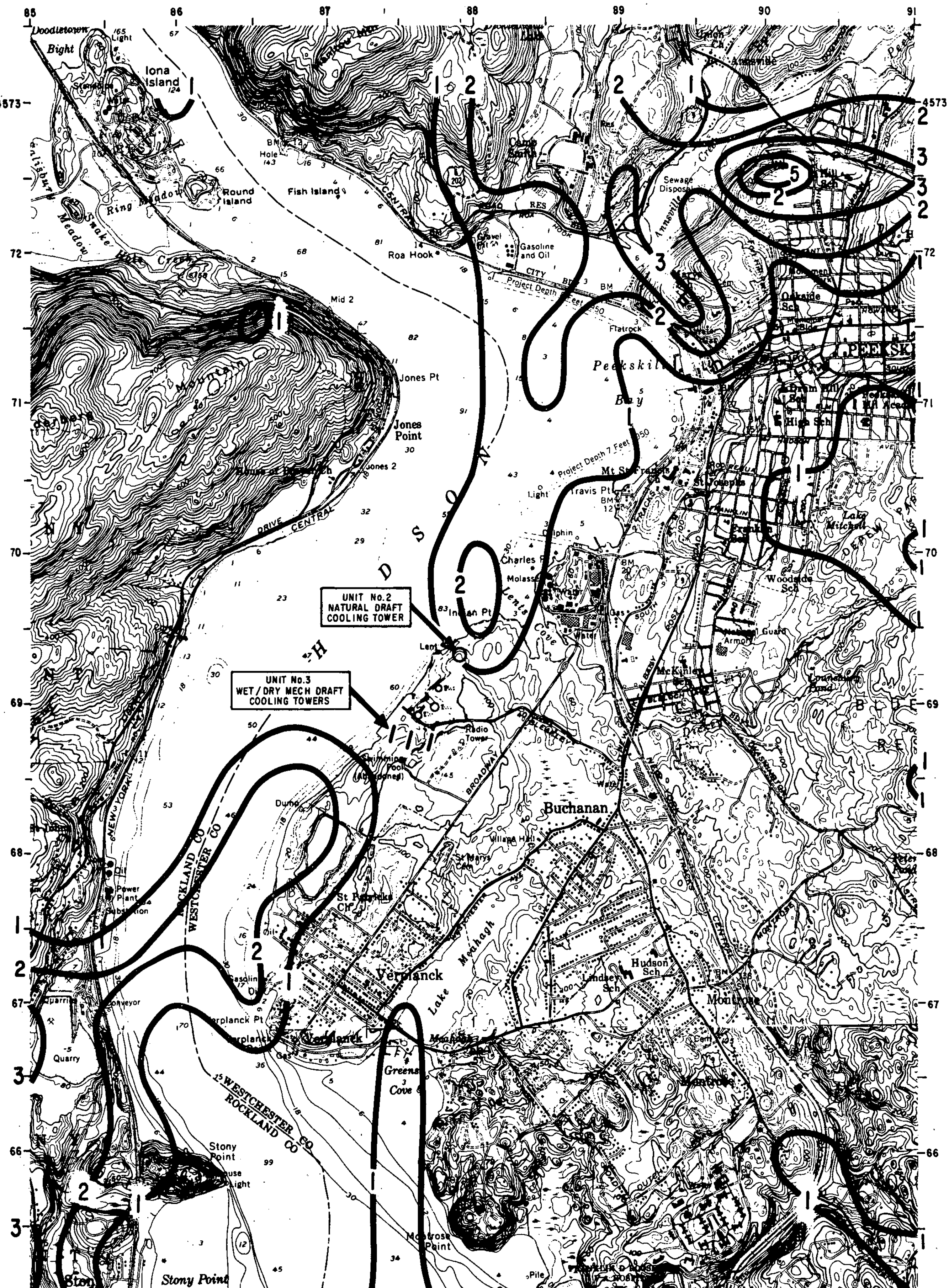

FIGURE 5.3.6

PLUME INDUCED FOG
HOURS/Mo, DECEMBER 1973
WET (85%) / DRY (15%) MECHANICAL
DRAFT COOLING TOWERS

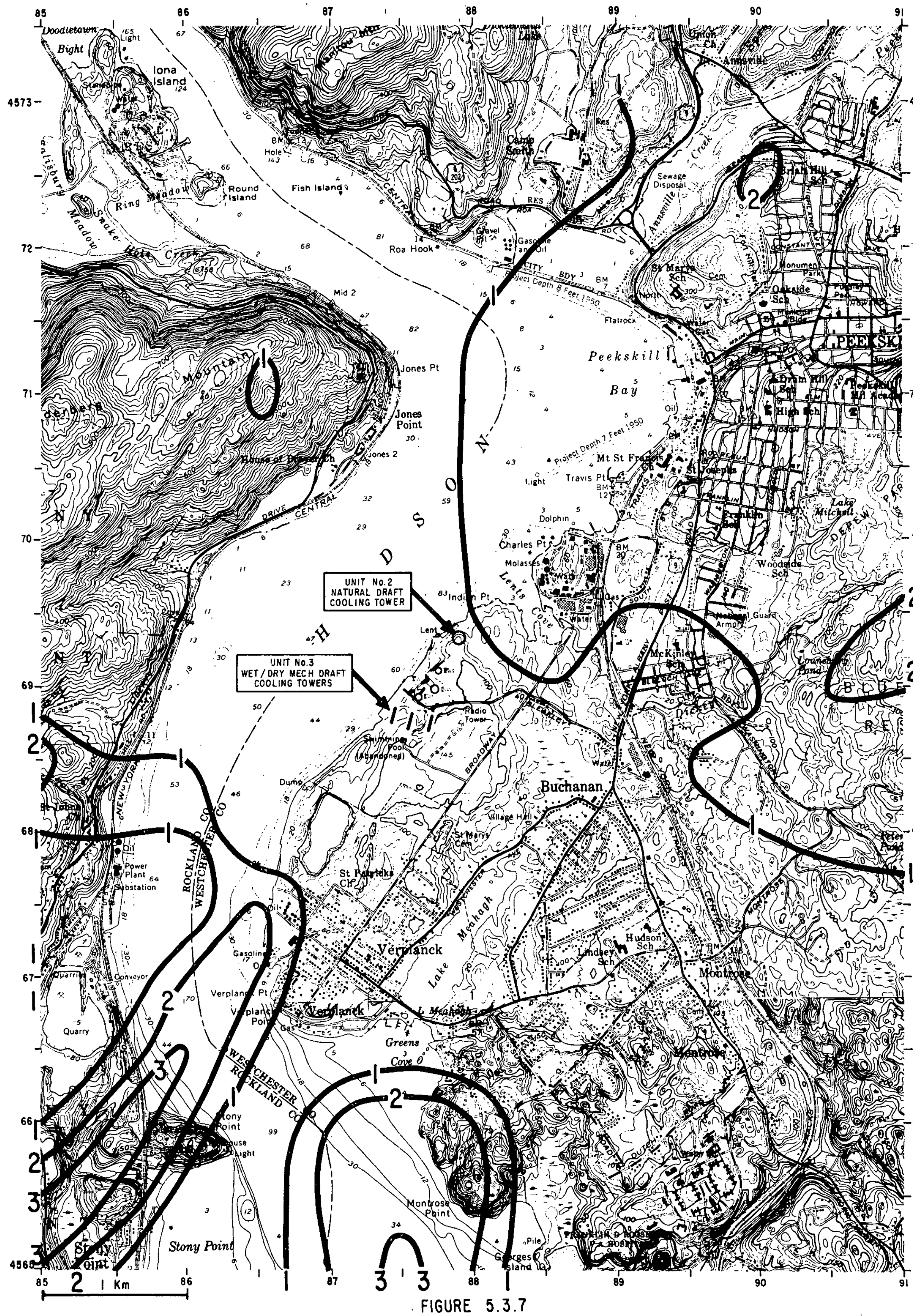

FIGURE 5.3.7

PLUME INDUCED FOG

HOURS/Mo, JANUARY 1974

WET (85%) / DRY (15%) MECHANICAL

DRAFT COOLING TOWERS

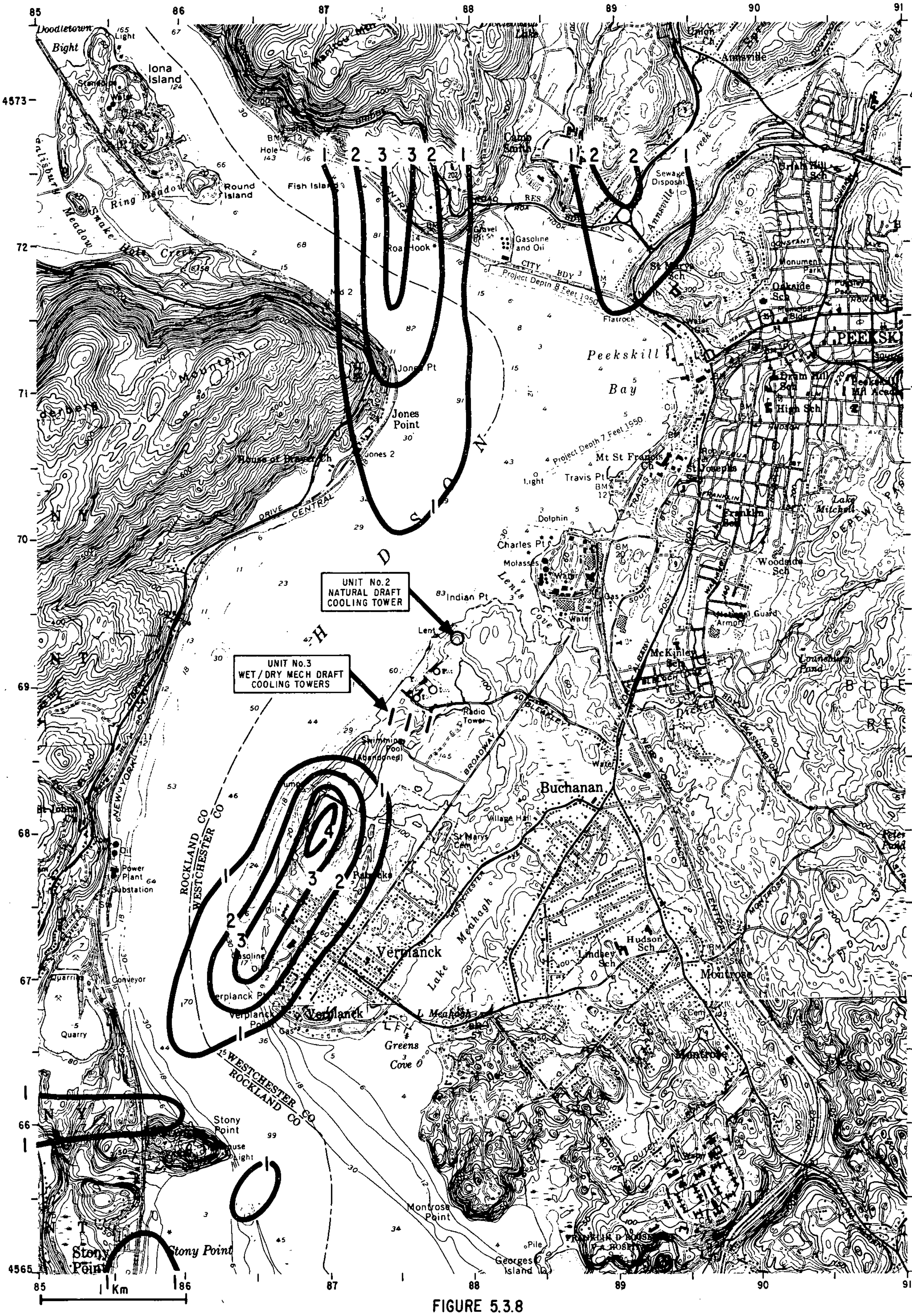

FIGURE 5.3.8

PLUME INDUCED FOG
HOURS / Mo, APRIL 1974
WET (85%) / DRY (15%) MECHANICAL
DRAFT COOLING TOWERS

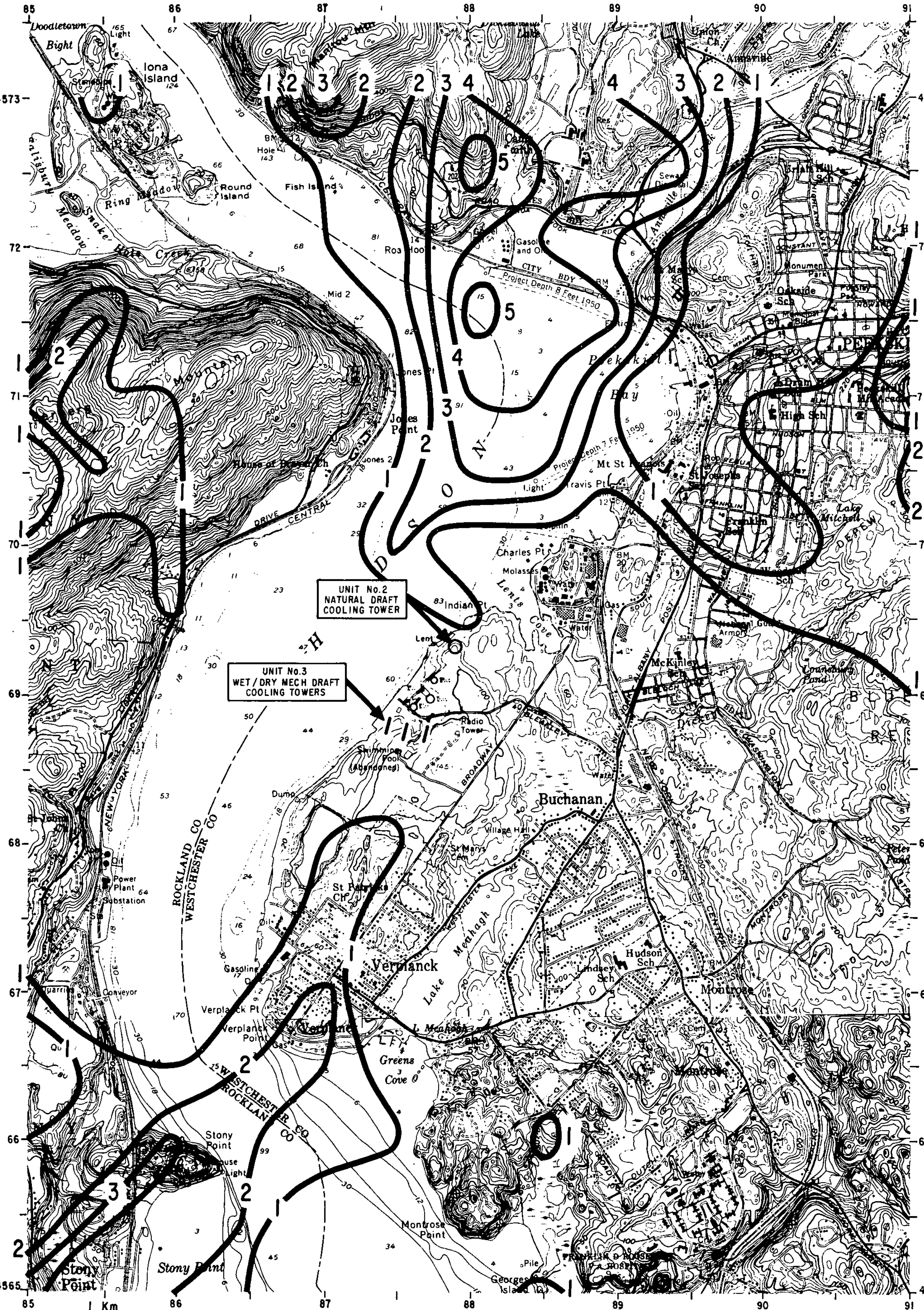

FIGURE 5.3.9
PLUME INDUCED FOG
HOURS/Mo, JUNE 1974
WET (85%) / DRY (15%) MECHANICAL
DRAFT COOLING TOWERS

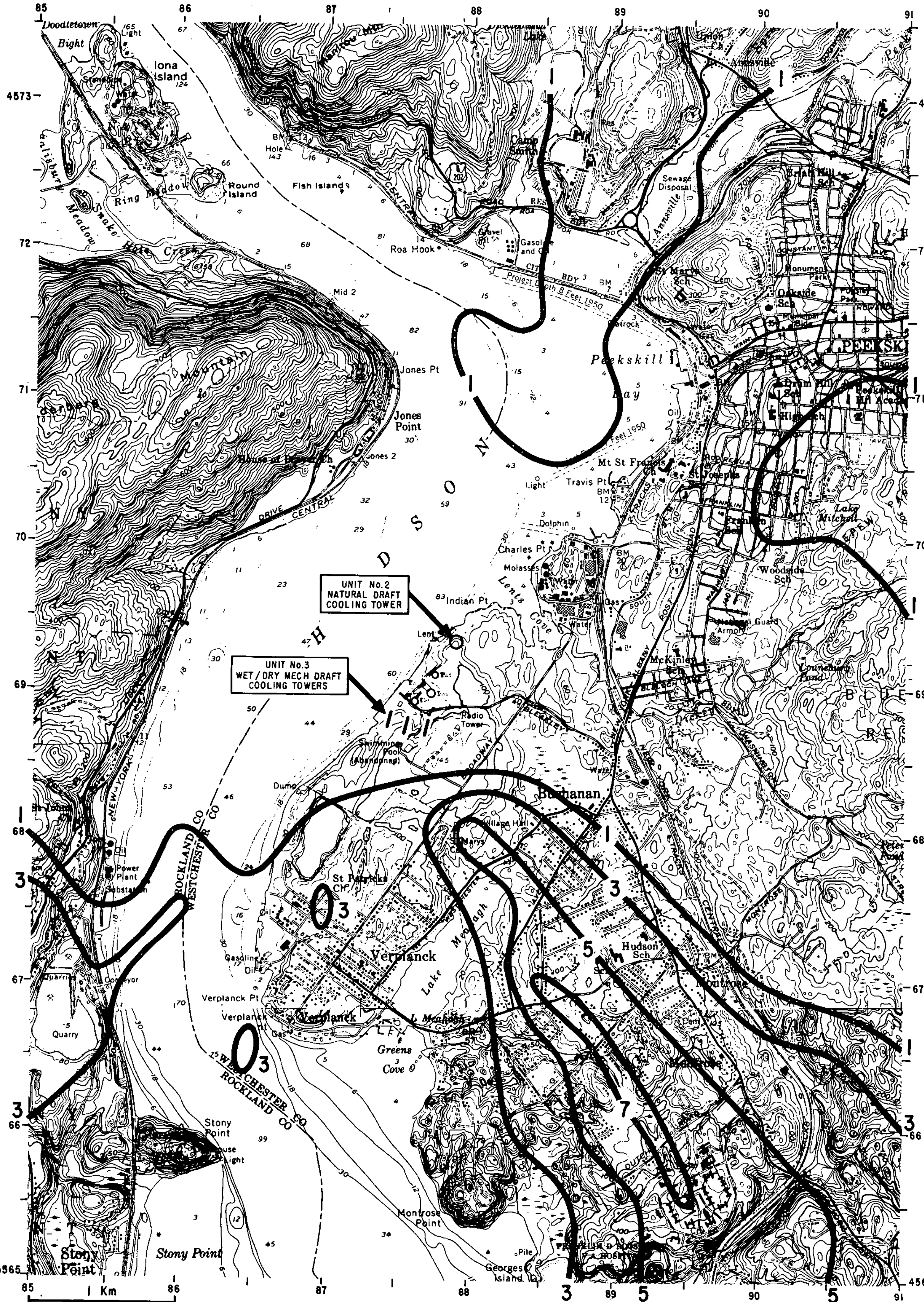

FIGURE 5.3.10

PLUME INDUCED FOG
HOURS/Mo, OCTOBER 1973
WET (85%) / DRY (15%) MECHANICAL
DRAFT COOLING TOWERS

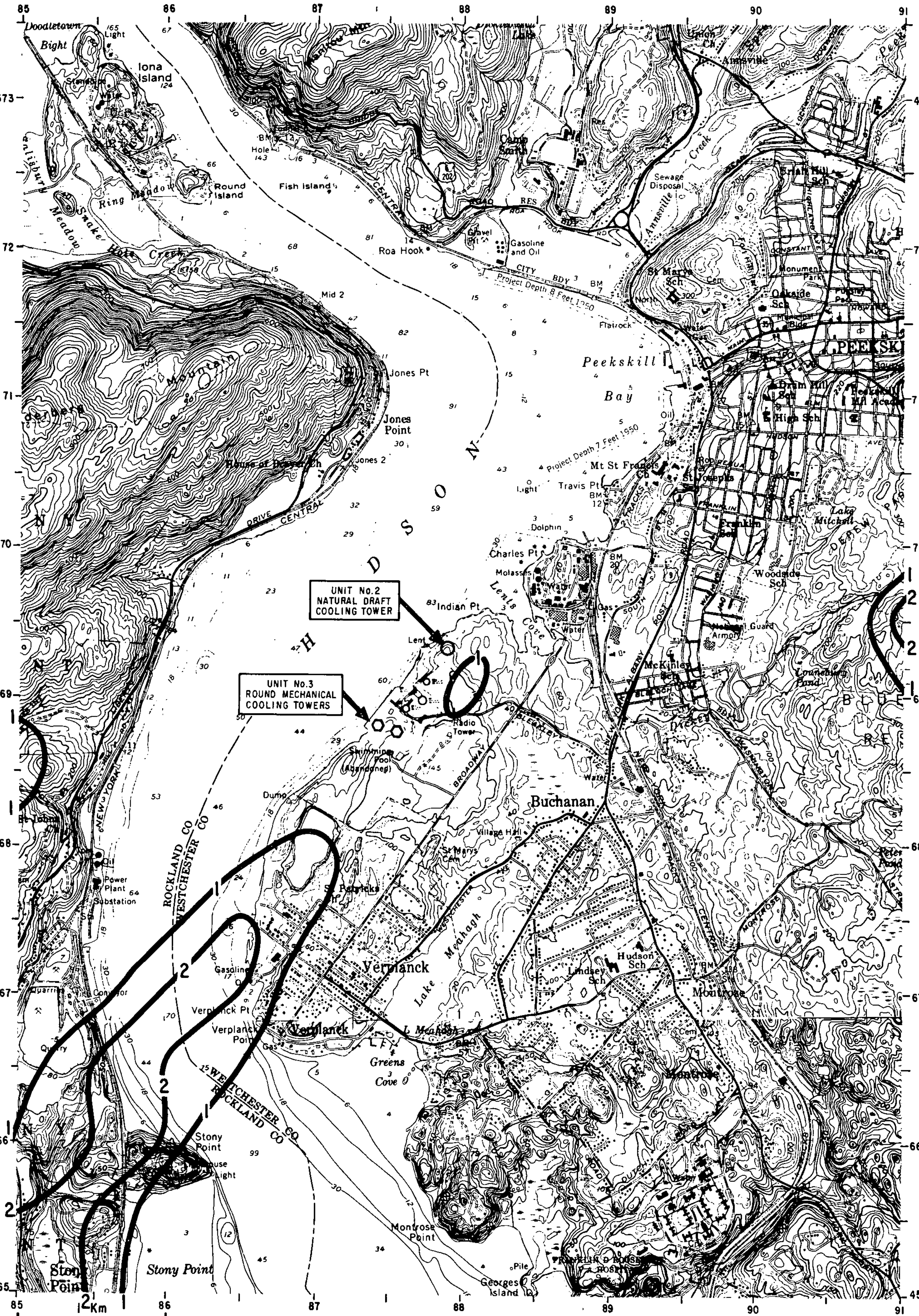

FIGURE 5.4.1

PLUME INDUCED FOG
HOURS / Mo, JANUARY 1974
ROUND WET MECHANICAL
DRAFT COOLING TOWERS

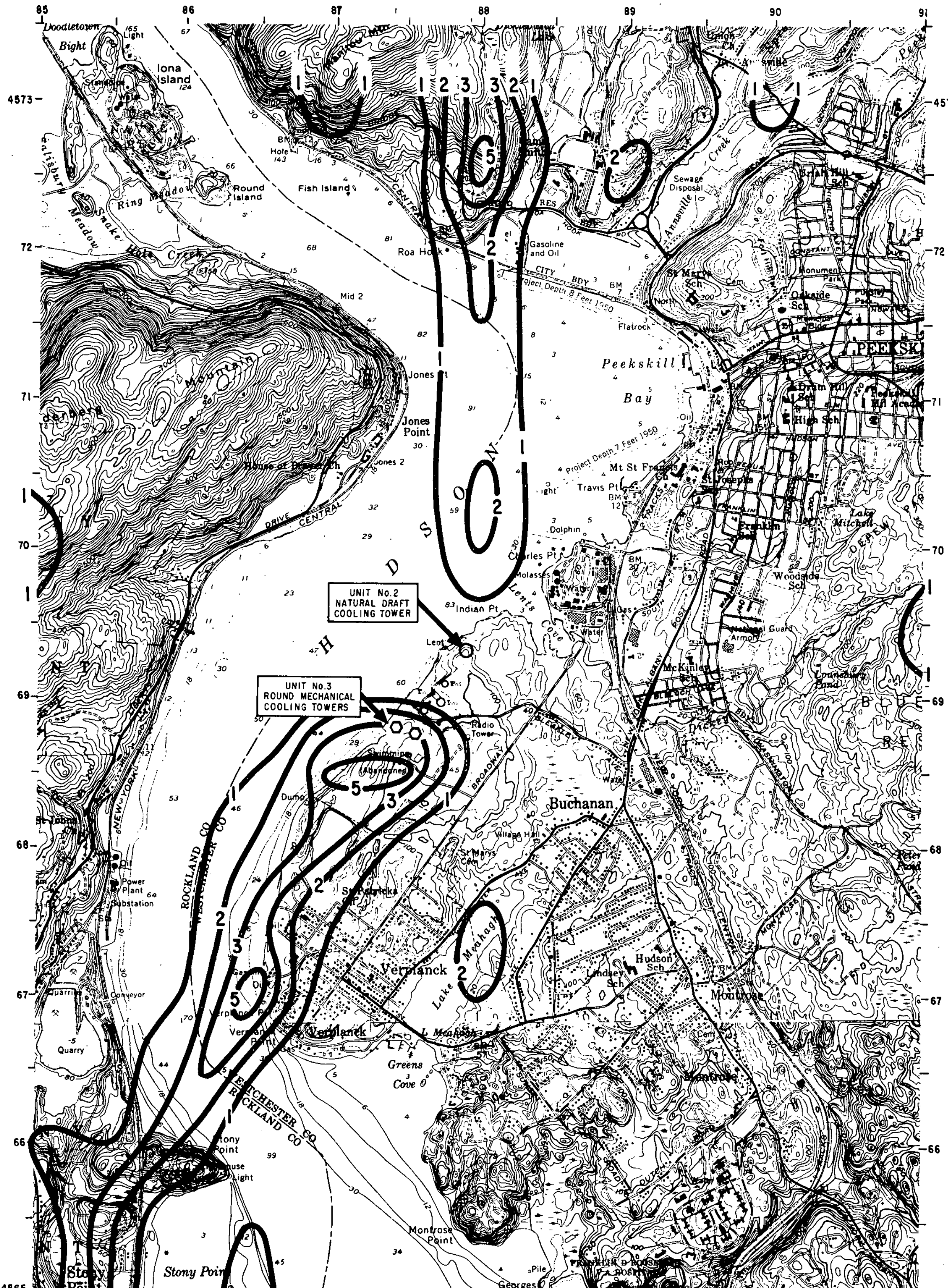

FIGURE 5.4.2

PLUME INDUCED FOG
HOURS / Mo, APRIL 1974
ROUND WET MECHANICAL
DRAFT COOLING TOWERS

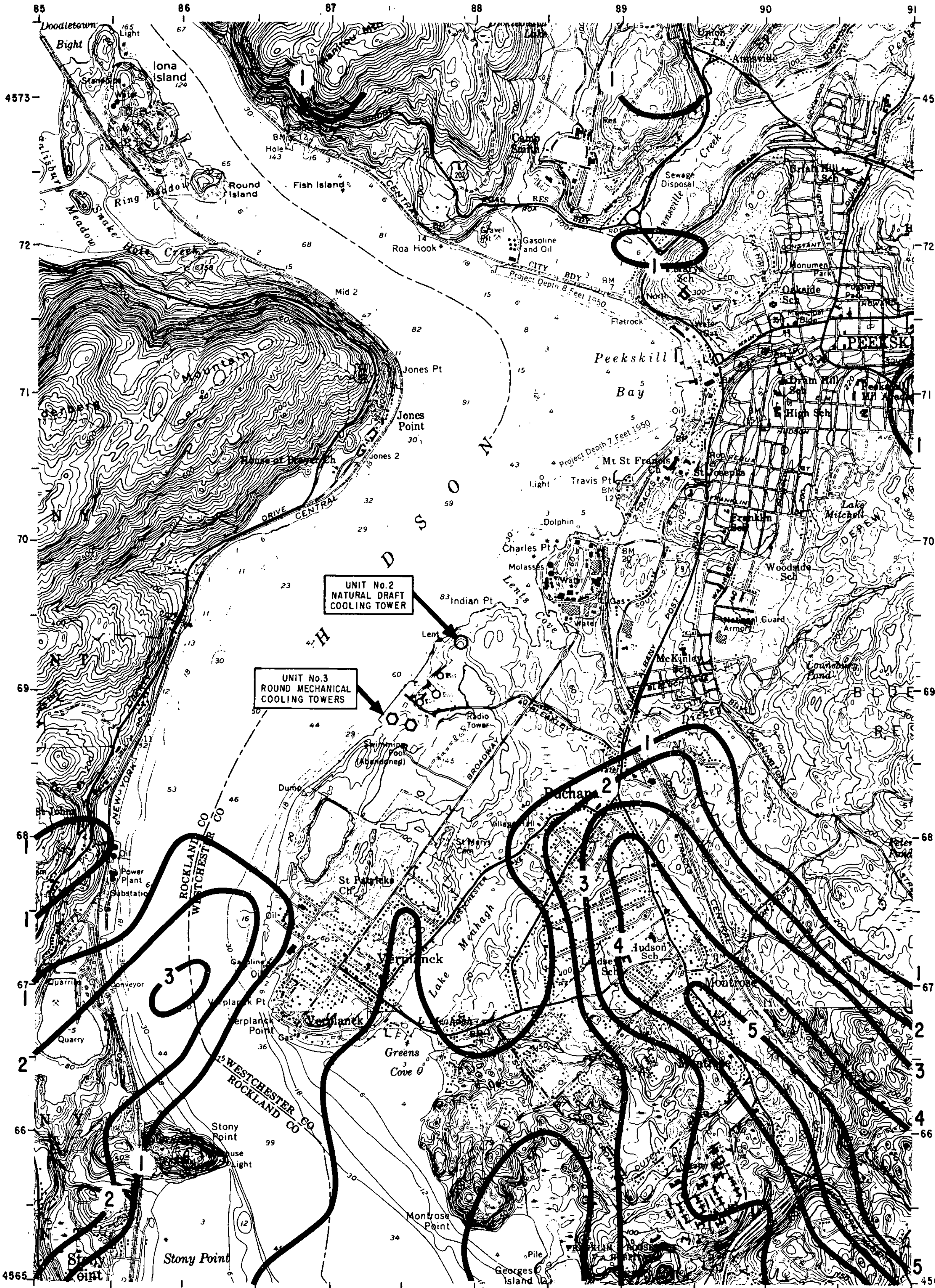

FIGURE 5.4.3

PLUME INDUCED FOG
HOURS / Mo, OCTOBER 1973
ROUND WET MECHANICAL
DRAFT COOLING TOWERS

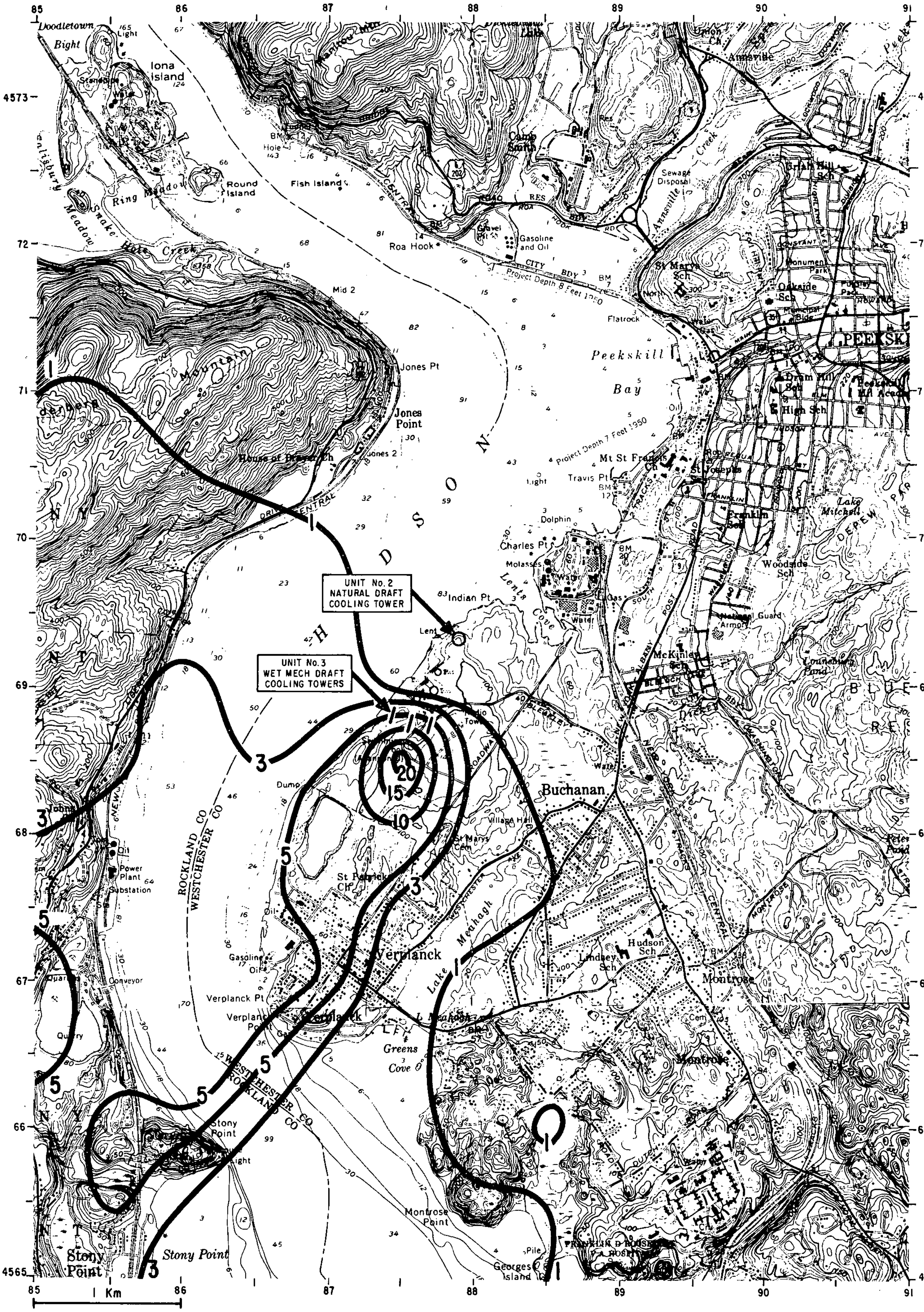

FIGURE 5.5.1

PLUME INDUCED ICING
HOURS/Mo, DECEMBER 1973
WET MECHANICAL DRAFT COOLING TOWERS

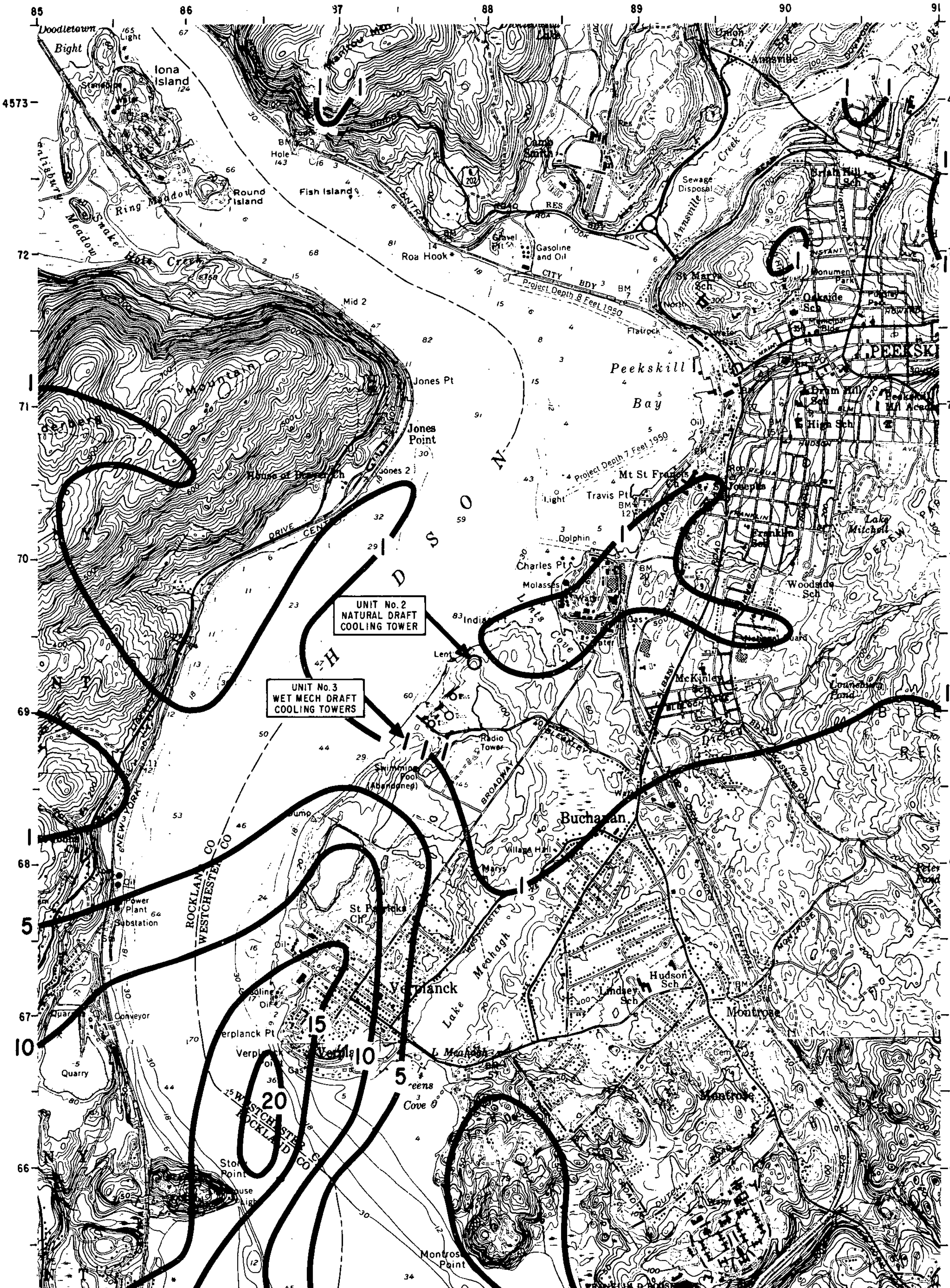

FIGURE 5.5.2

PLUME INDUCED ICING
HOURS/Mo, JANUARY 1974
WET MECHANICAL DRAFT COOLING TOWERS

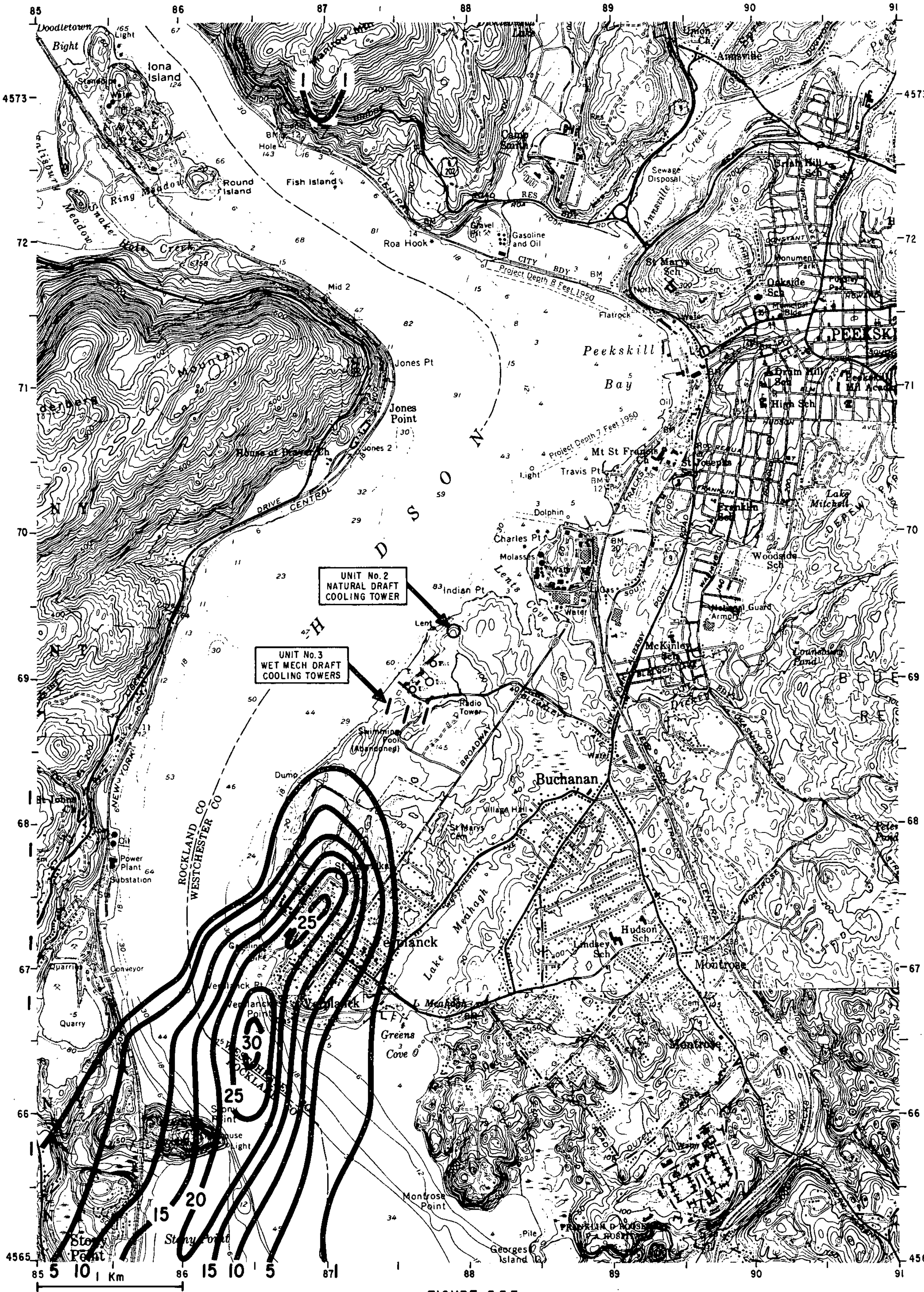

FIGURE 5.5.3

PLUME INDUCED ICING

HOURS/Mo, FEBRUARY 1974

WET MECHANICAL DRAFT COOLING TOWERS

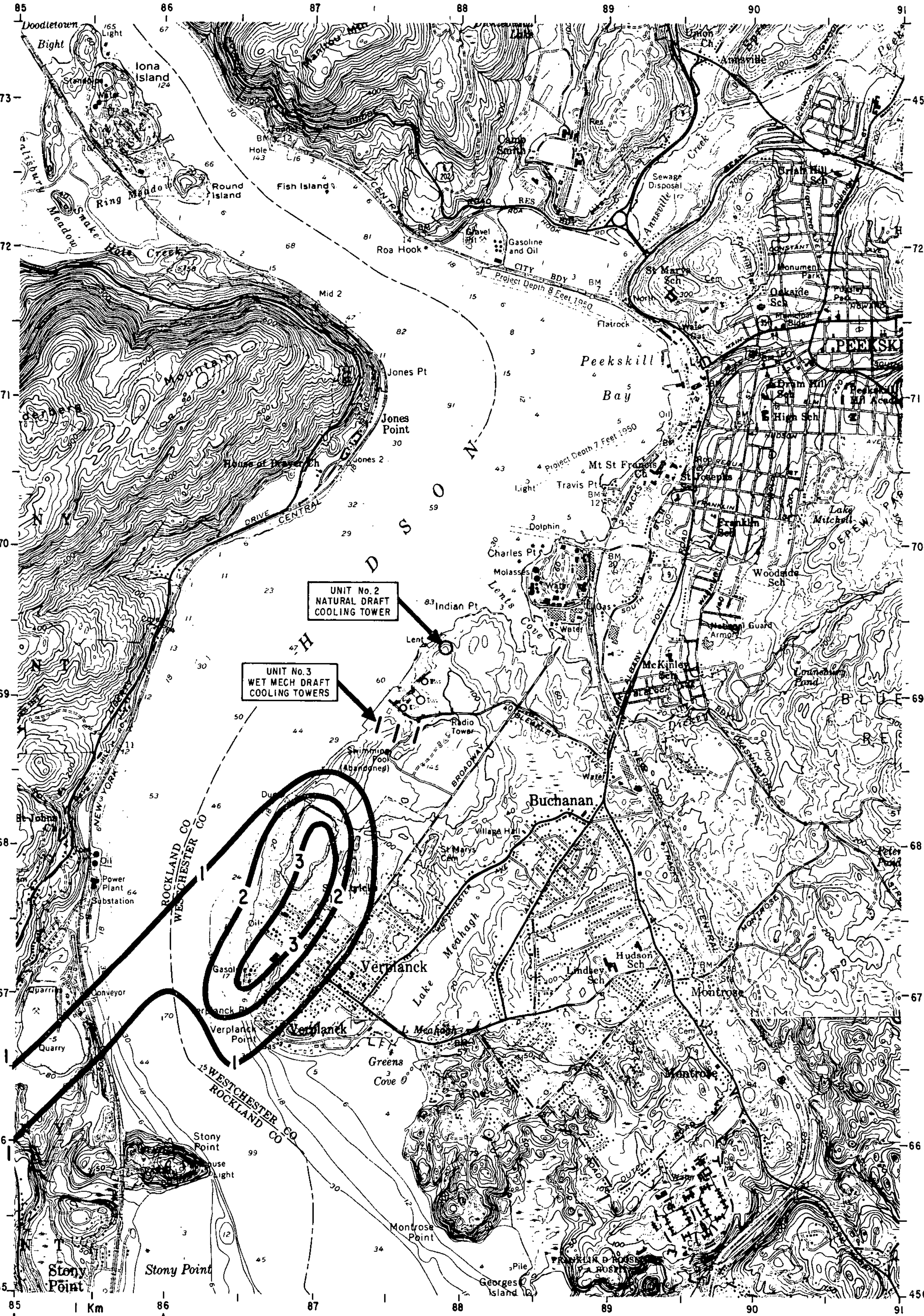

FIGURE 5.5.4

PLUME INDUCED ICING
HOURS/Mo, APRIL 1974
WET MECHANICAL DRAFT COOLING TOWERS

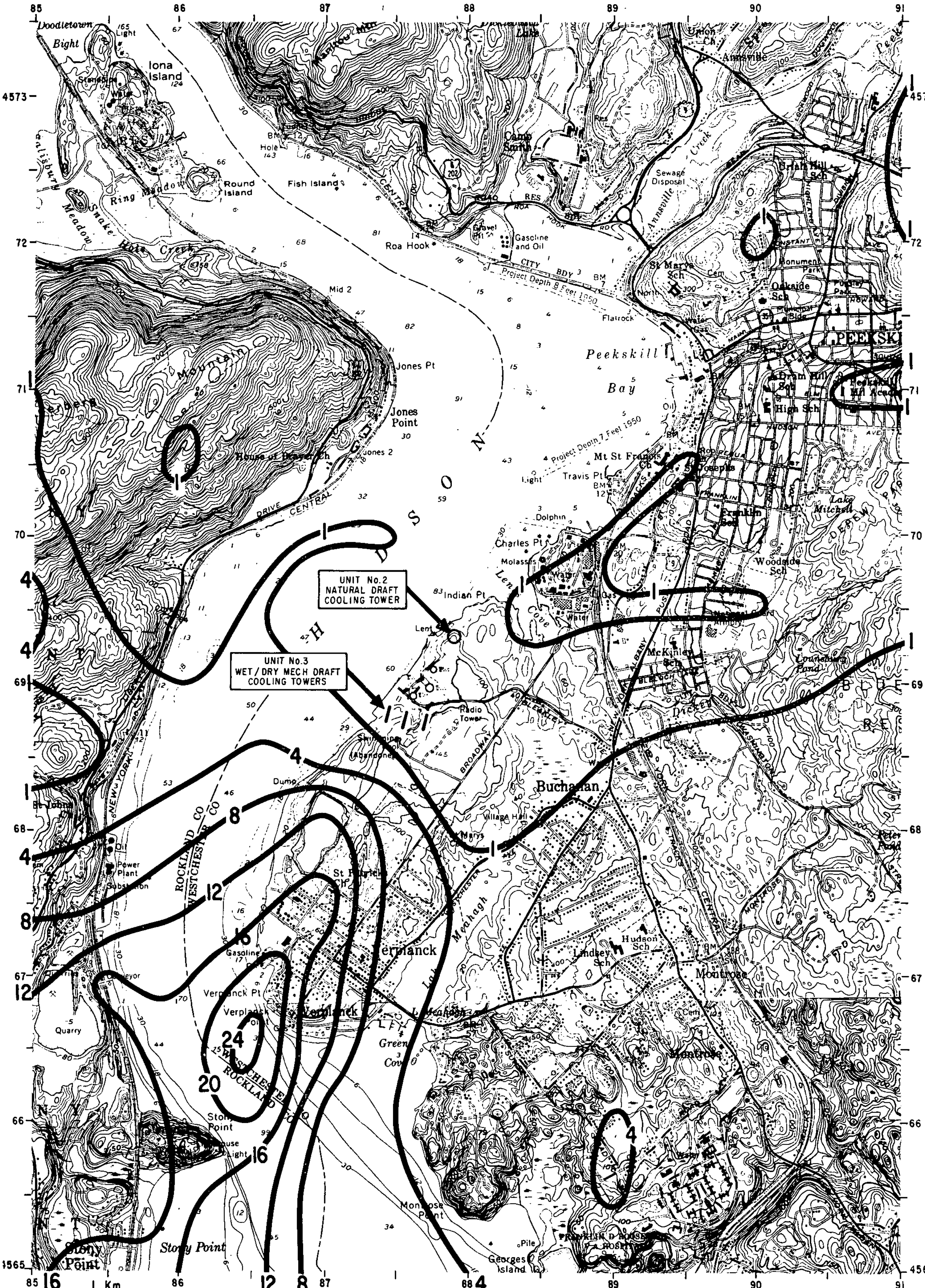

FIGURE 5.6.1
PLUME INDUCED ICING
HOURS/Mo, JANUARY 1974
WET (100%) / DRY (0%) MECHANICAL
DRAFT COOLING TOWERS

FIGURE 5.6.2
PLUME INDUCED ICING
HOURS/Mo, DECEMBER 1973
WET (92.5%) / DRY (7.5%) MECHANICAL
DRAFT COOLING TOWERS

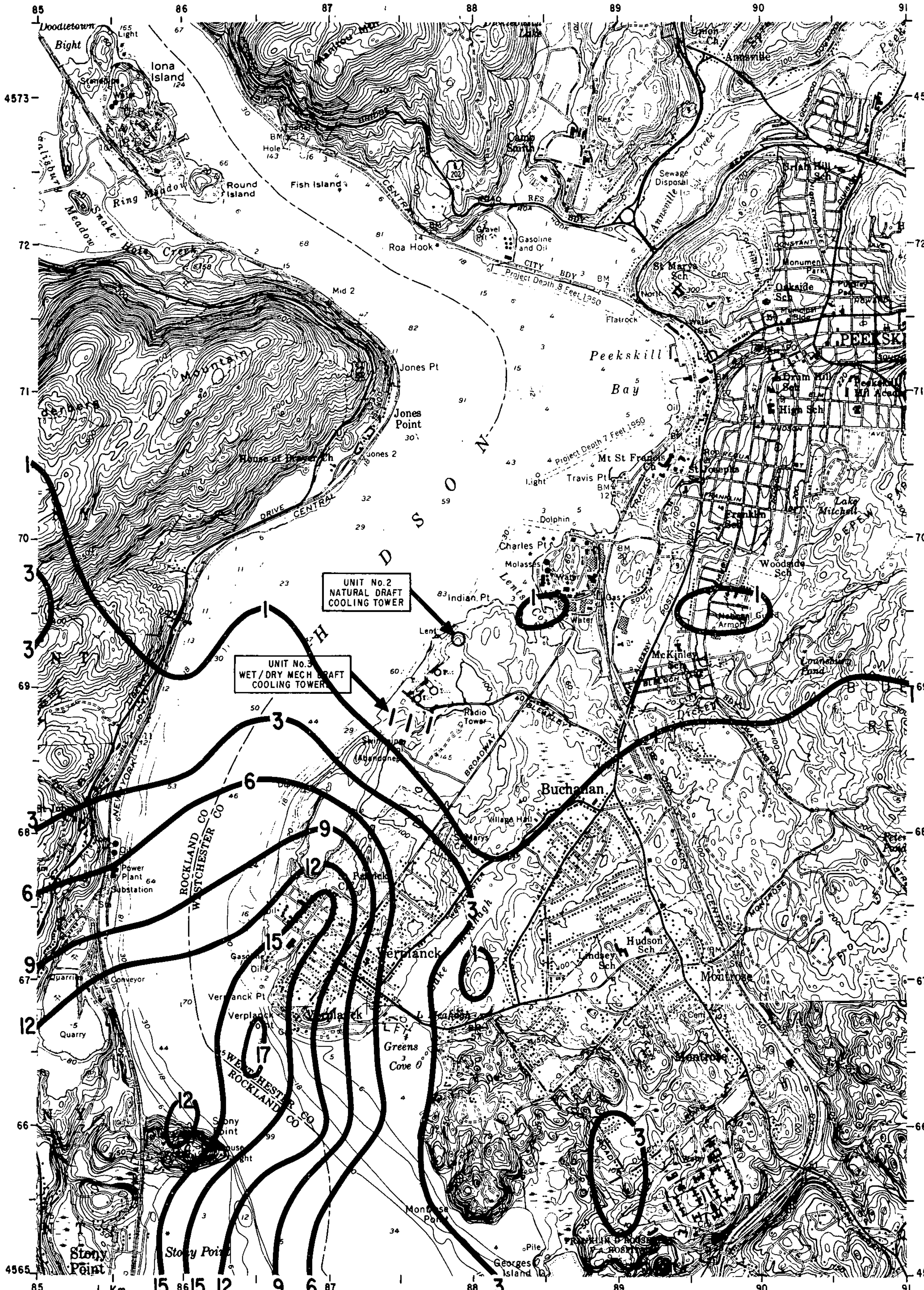

FIGURE 5.6.3
PLUME INDUCED ICING
HOURS/Mo, JANUARY 1974
WET (92.5%) / DRY (7.5%) MECHANICAL
DRAFT COOLING TOWERS

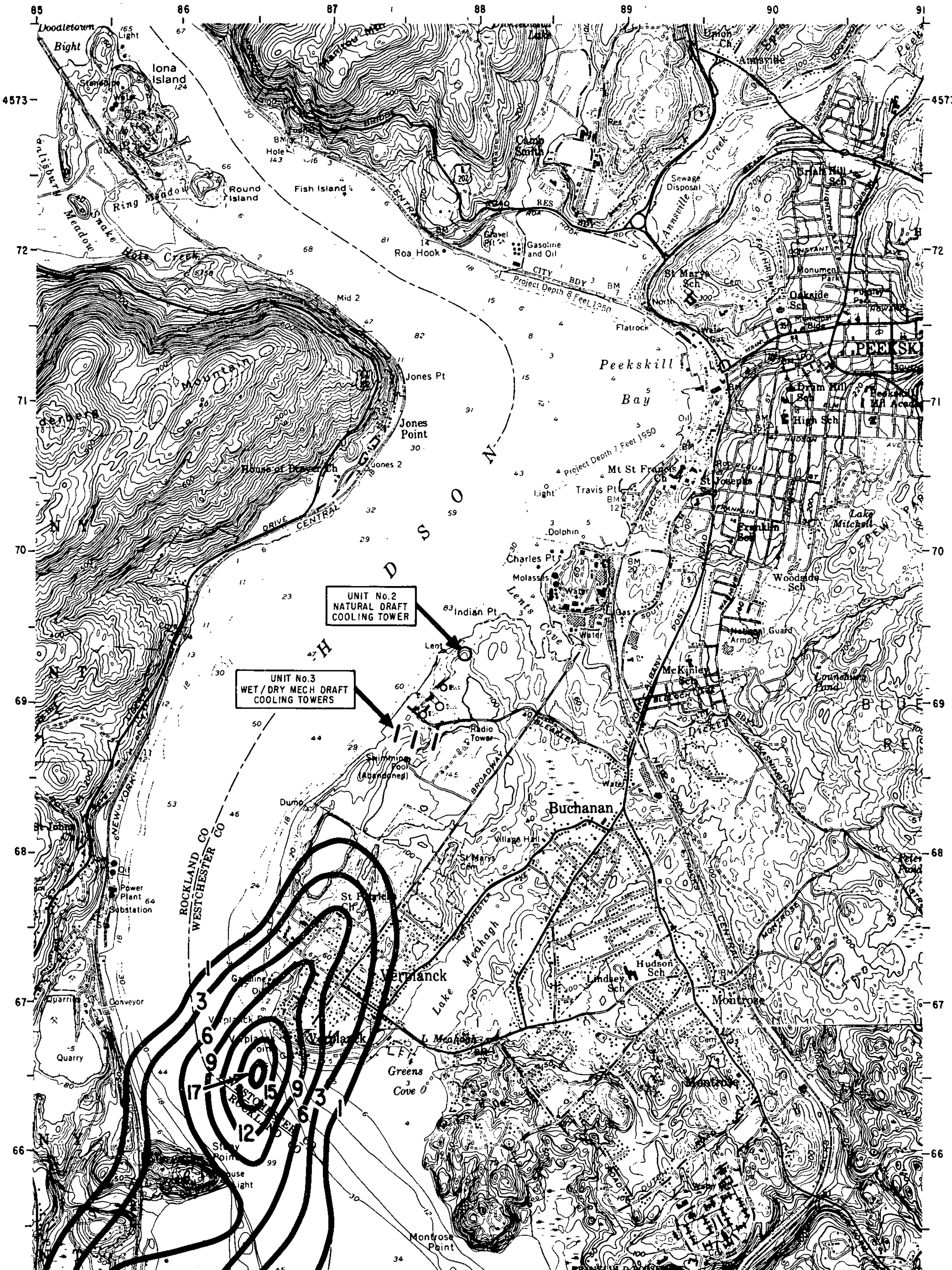

FIGURE 5.6.4

PLUME INDUCED ICING

HOURS/Mo, FEBRUARY 1974

WET (92.5%) / DRY (7.5%) MECHANICAL

DRAFT COOLING TOWERS

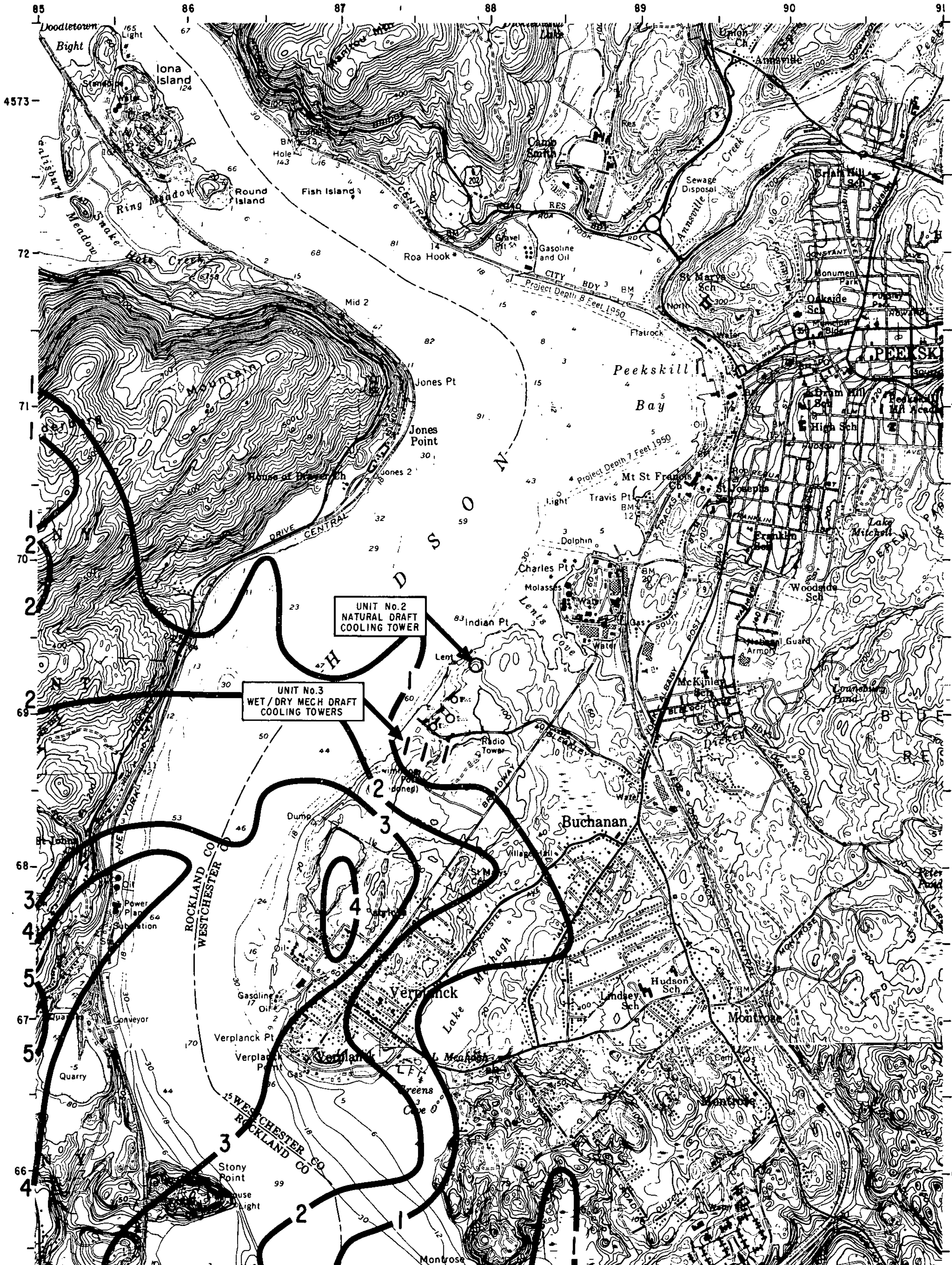

FIGURE 5.6.5
PLUME INDUCED ICING
HOURS/Mo, DECEMBER 1973
WET (85%) / DRY (15%) MECHANICAL
DRAFT COOLING TOWERS

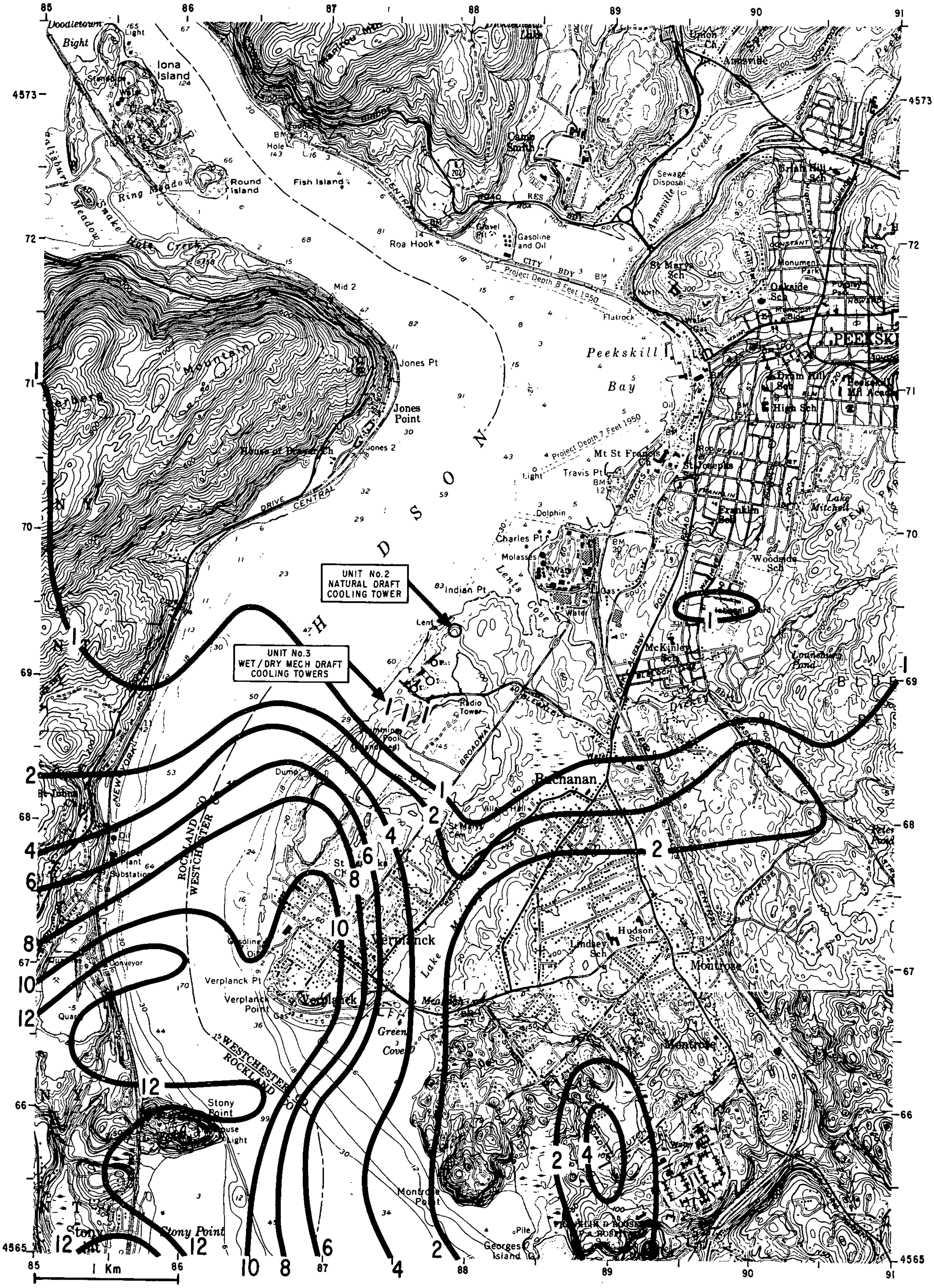

FIGURE 5.6.6

PLUME INDUCED ICING
HOURS/Mo, JANUARY 1974
WET (85%) / DRY (15%) MECHANICAL
DRAFT COOLING TOWERS

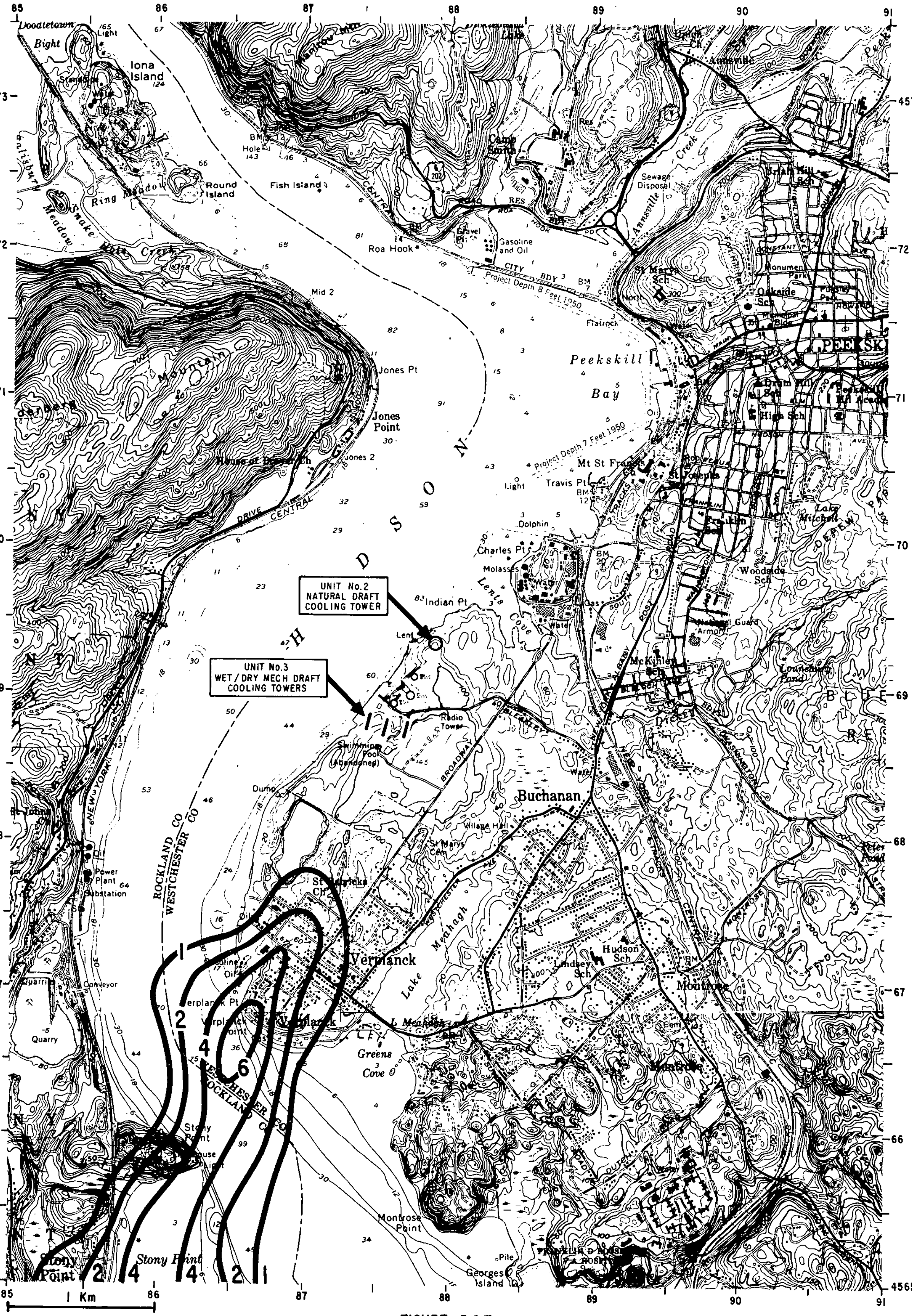

FIGURE 5.6.7

PLUME INDUCED ICING
HOURS/Mo, FEBRUARY 1974
WET (85%) / DRY (15%) MECHANICAL
DRAFT COOLING TOWERS

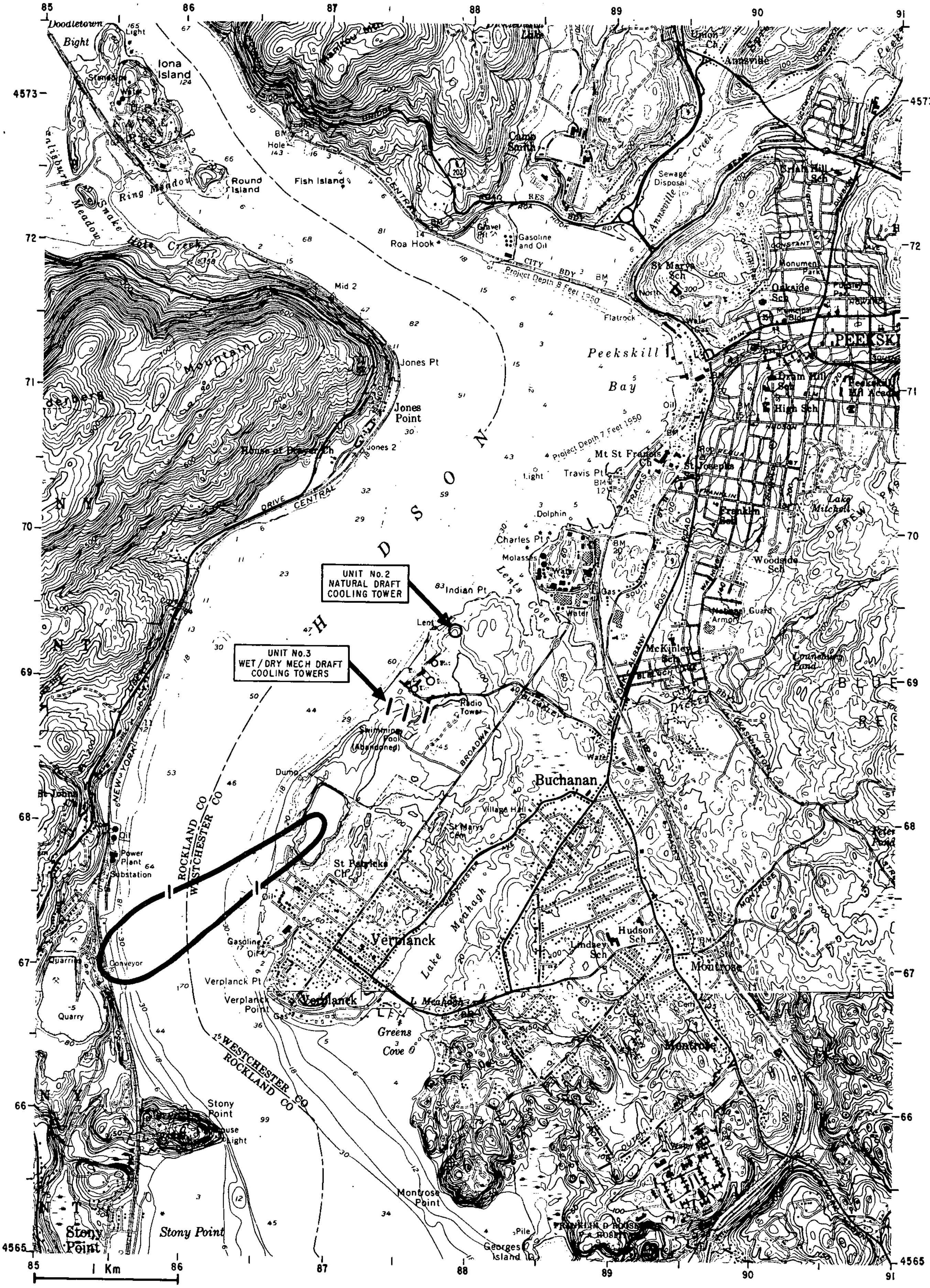

FIGURE 5.6.8

PLUME INDUCED ICING
HOURS/Mo, APRIL 1974
WET (85%) / DRY (15%) MECHANICAL
DRAFT COOLING TOWERS

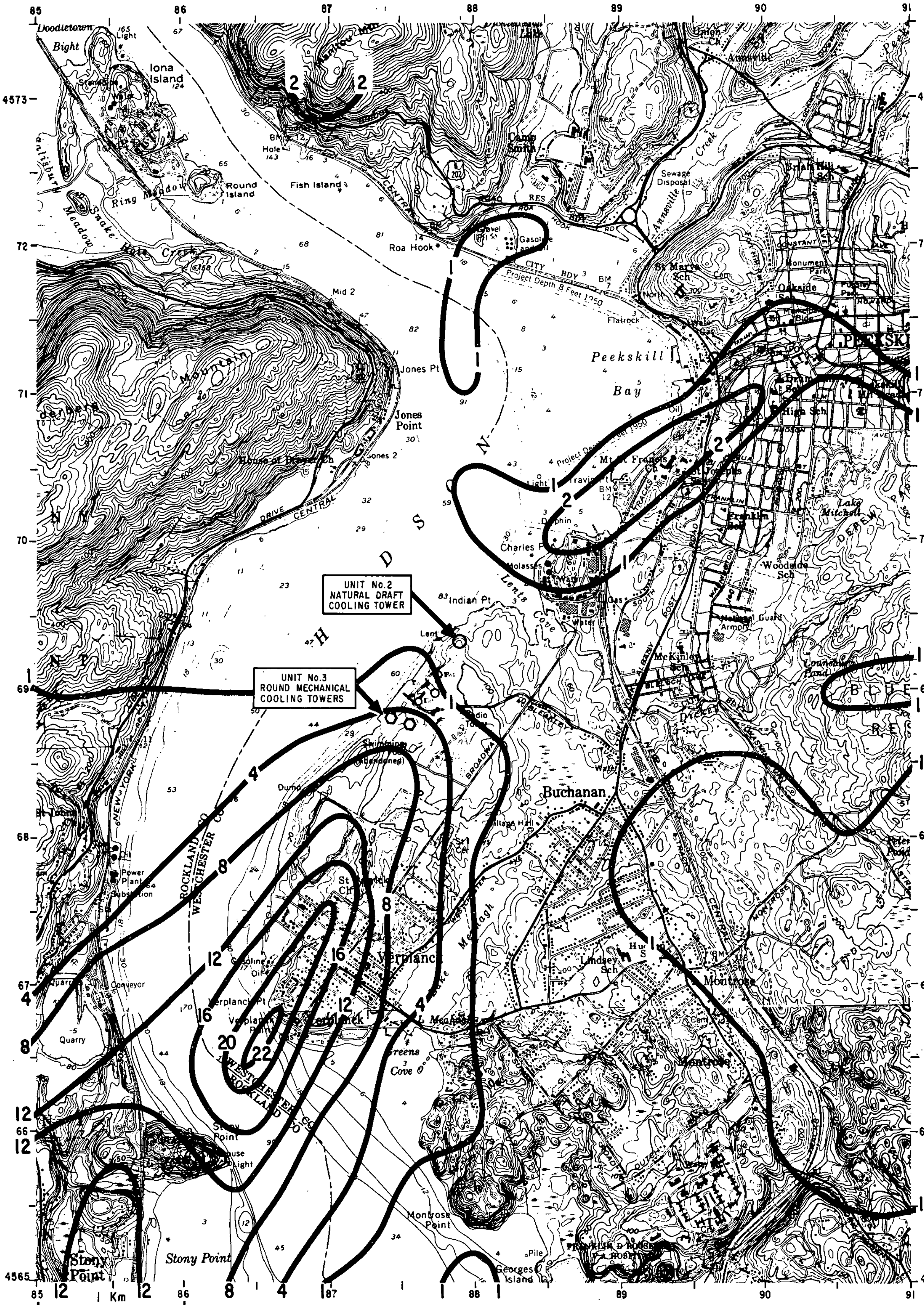

FIGURE 5.7.1

PLUME INDUCED ICING
HOURS/Mo, JANUARY 1974
ROUND WET MECHANICAL
DRAFT COOLING TOWERS

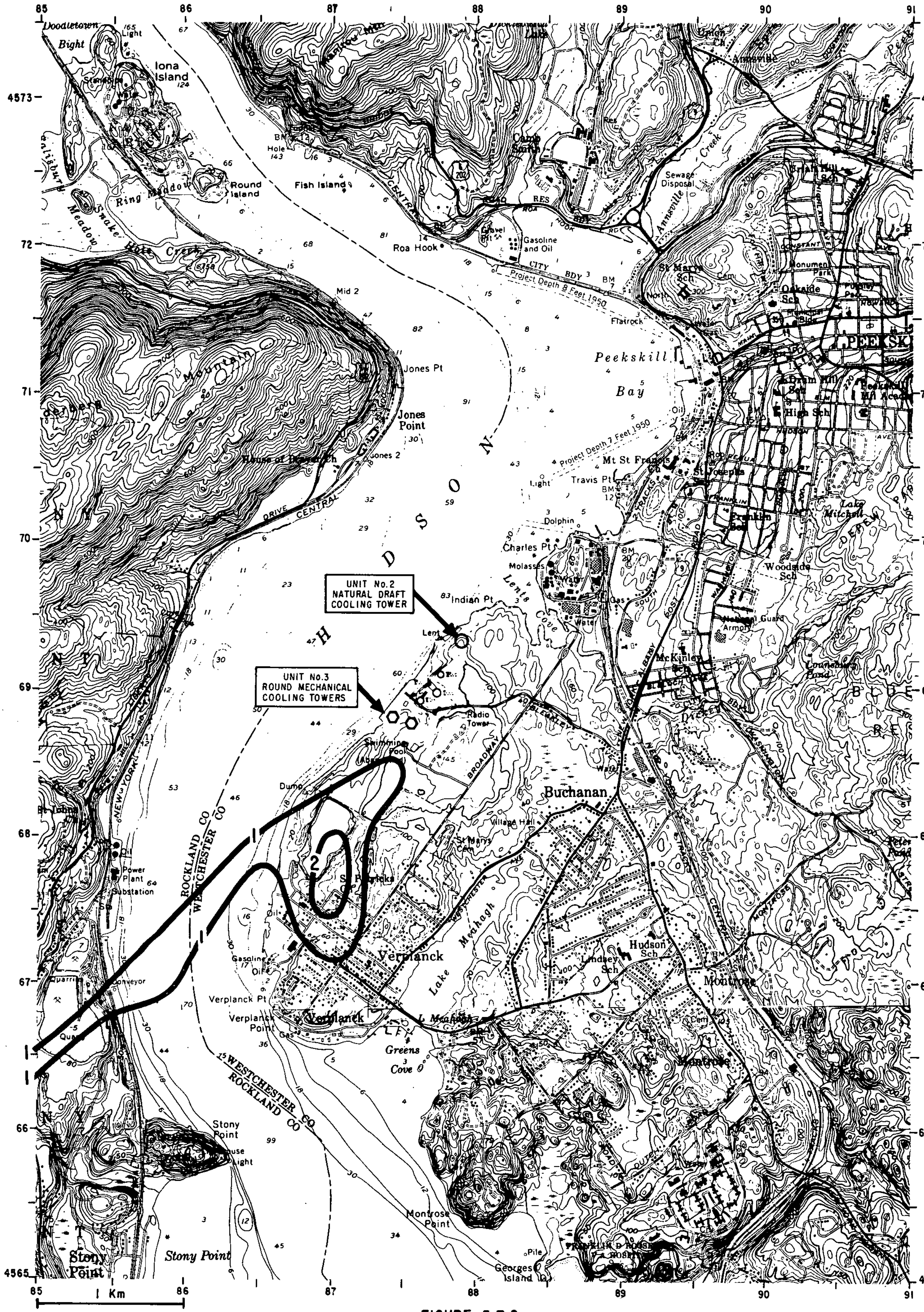

FIGURE 5.7.2

PLUME INDUCED ICING
HOURS/Mo, APRIL 1974
ROUND WET MECHANICAL
DRAFT COOLING TOWERS

APPENDIX A

Accumulated salt drift deposits for October 1973 resulting from operations of natural draft cooling towers at Units No. 2 and No. 3 as well as from operations of natural draft cooling tower at Unit No. 2 in combination with linear wet and linear wet/dry mechanical draft cooling towers at Unit No. 3 respectively, are included here.

Figure A-1	Salt Accumulation, October 1973 Unit 2 - Natural Draft Cooling Tower Unit 3 - Natural Draft Cooling Tower
Figure A-2	Salt Accumulation, October 1973 Unit 2 - Natural Draft Cooling Tower Unit 3 - Linear Wet Mechanical Draft Cooling Towers
Figure A-3	Salt Accumulation, October 1973 Unit 2 - Natural Draft Cooling Tower Unit 3 - Linear Wet/Dry Mechanical Draft Cooling Towers

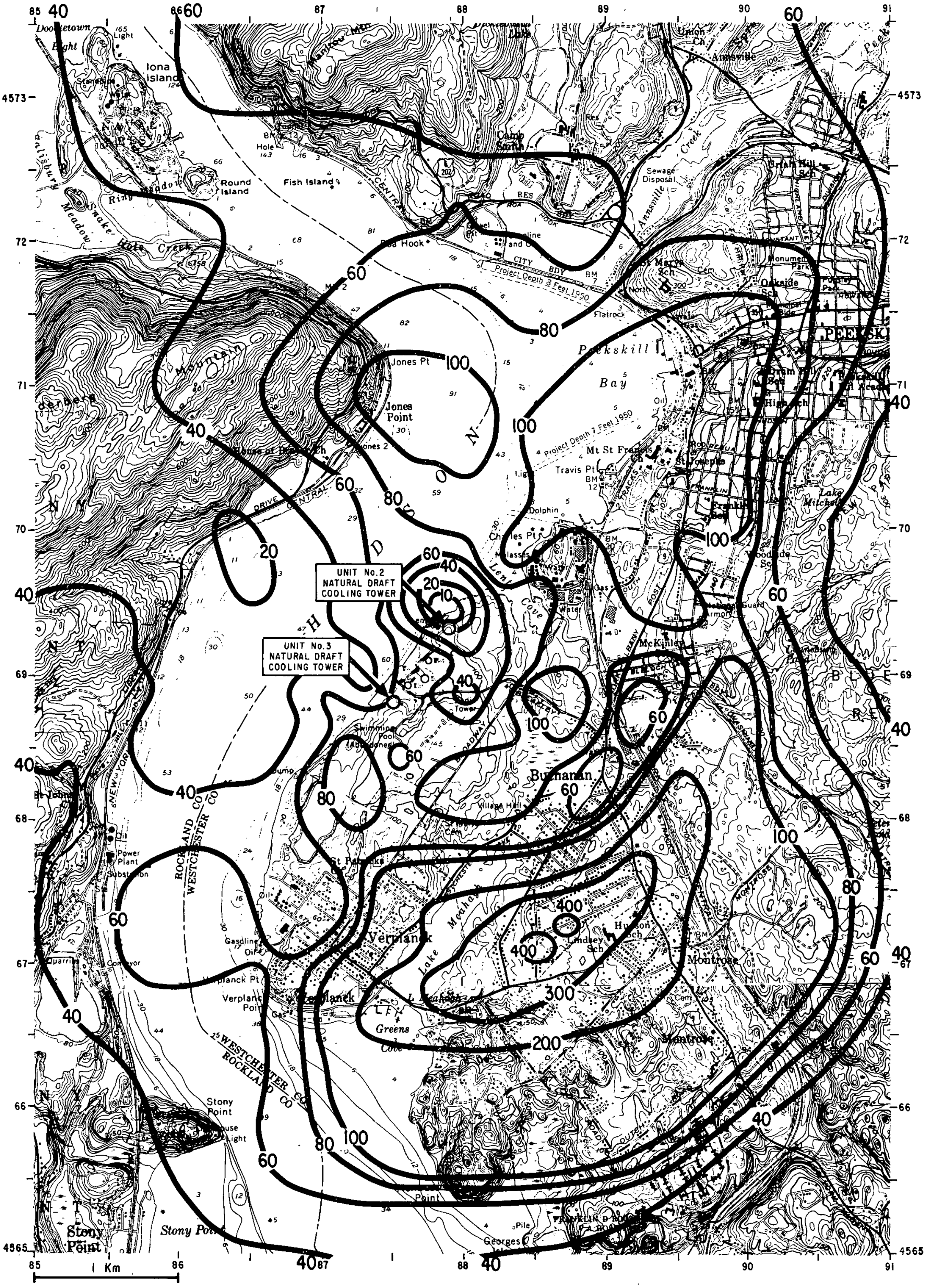

FIGURE A-1

SALT ACCUMULATION OCTOBER 1973 (Kg/Km^2)
UNIT - NATURAL DRAFT WET TOWER
UNIT - NATURAL DRAFT WET TOWER
DRIFT SALINITY 7000 ppm

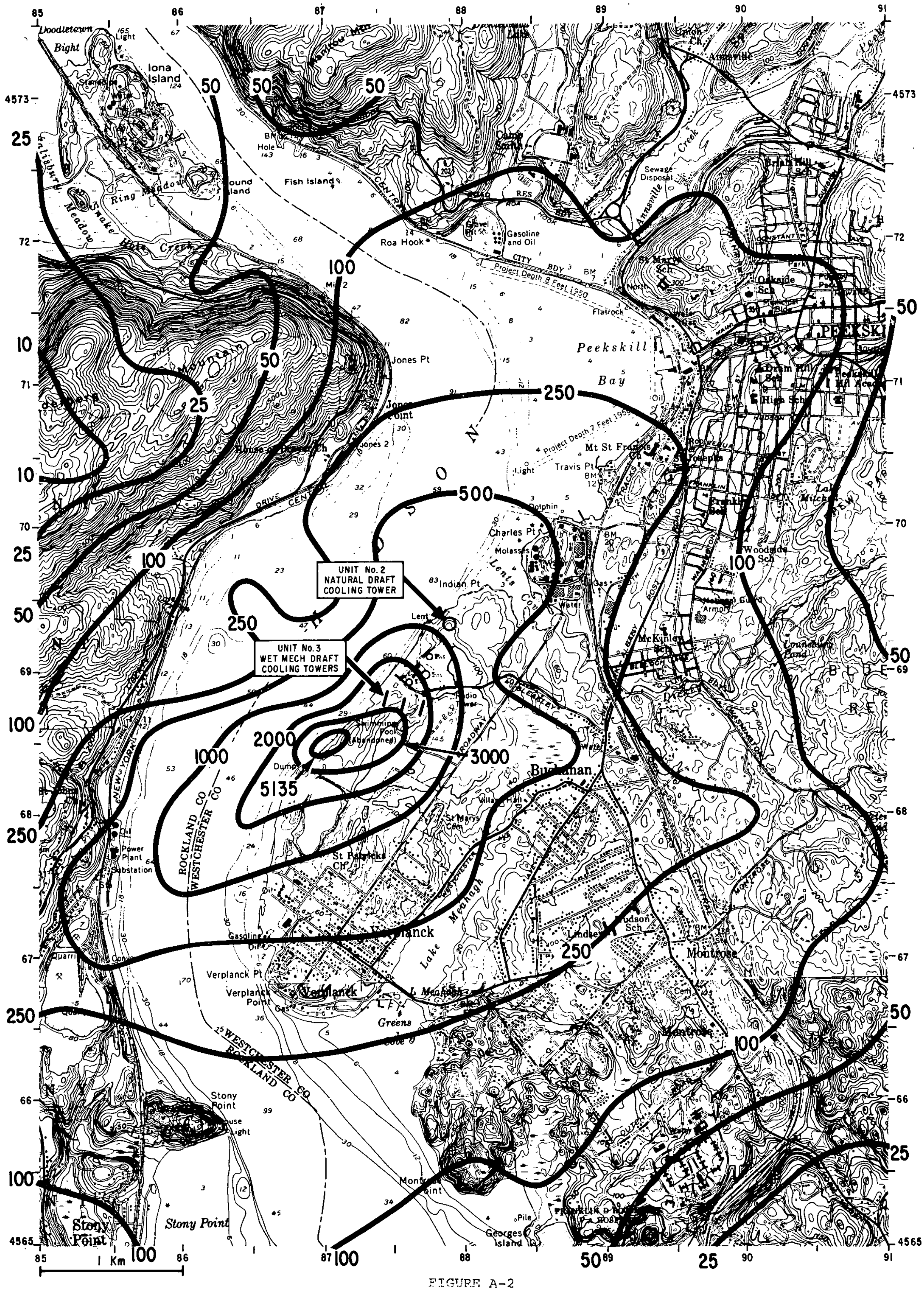

FIGURE A-2

SALT ACCUMULATION OCTOBER 1973 (Kg/Km^2)
UNIT 2- NATURAL DRAFT WET TOWER
UNIT 3- LINEAR MECHANICAL DRAFT WET TOWER
DRIFT SALINITY 7000 ppm

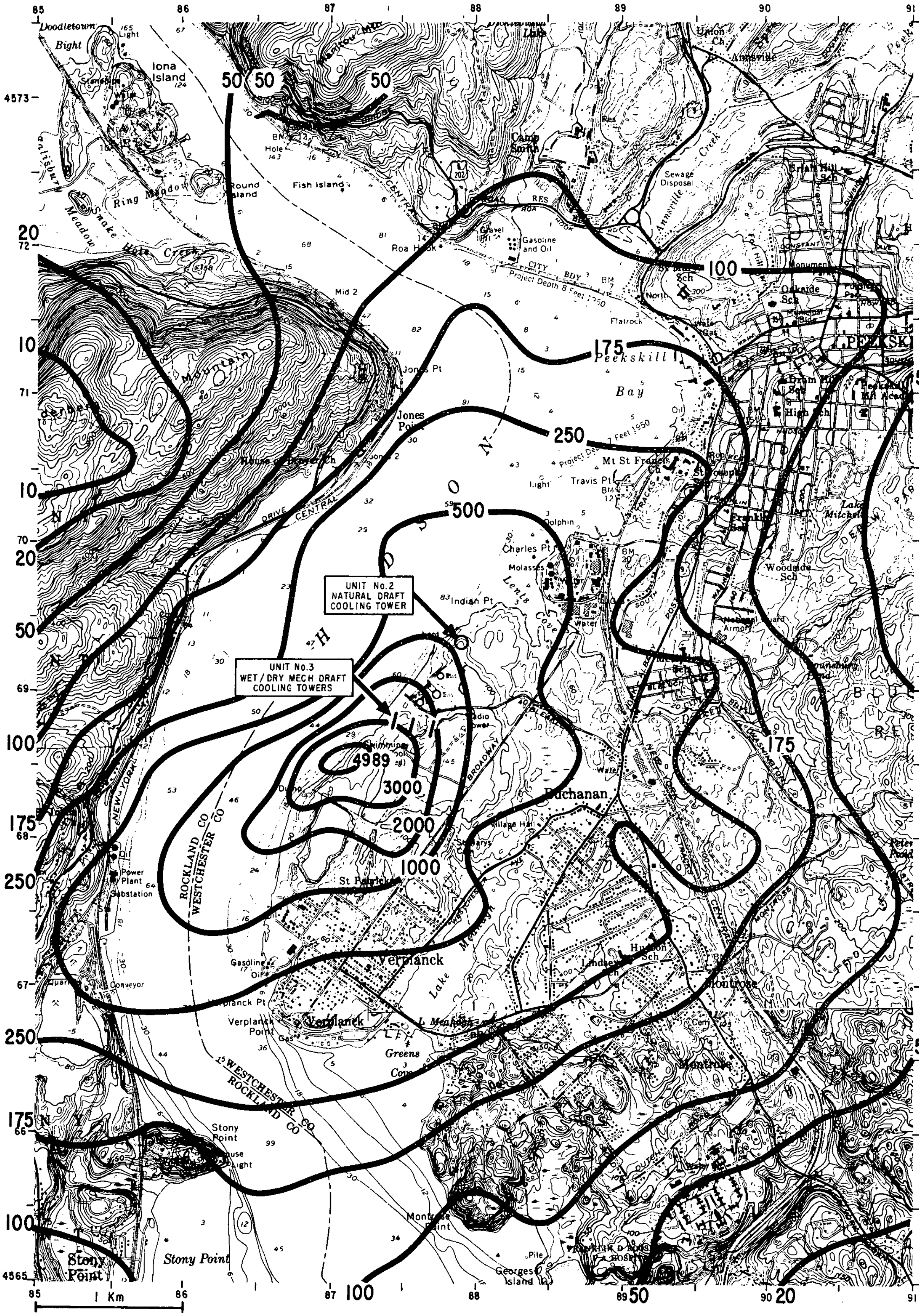

FIGURE A-3

SALT ACCUMULATION OCTOBER 1973 (Kg / Km 2)
UNIT 2 - NATURAL DRAFT WET TOWER
UNIT 3 - WET (85 %) / DRY (15%) MECHANICAL DRAFT TOWER
DRIFT SALINITY 7000 ppm

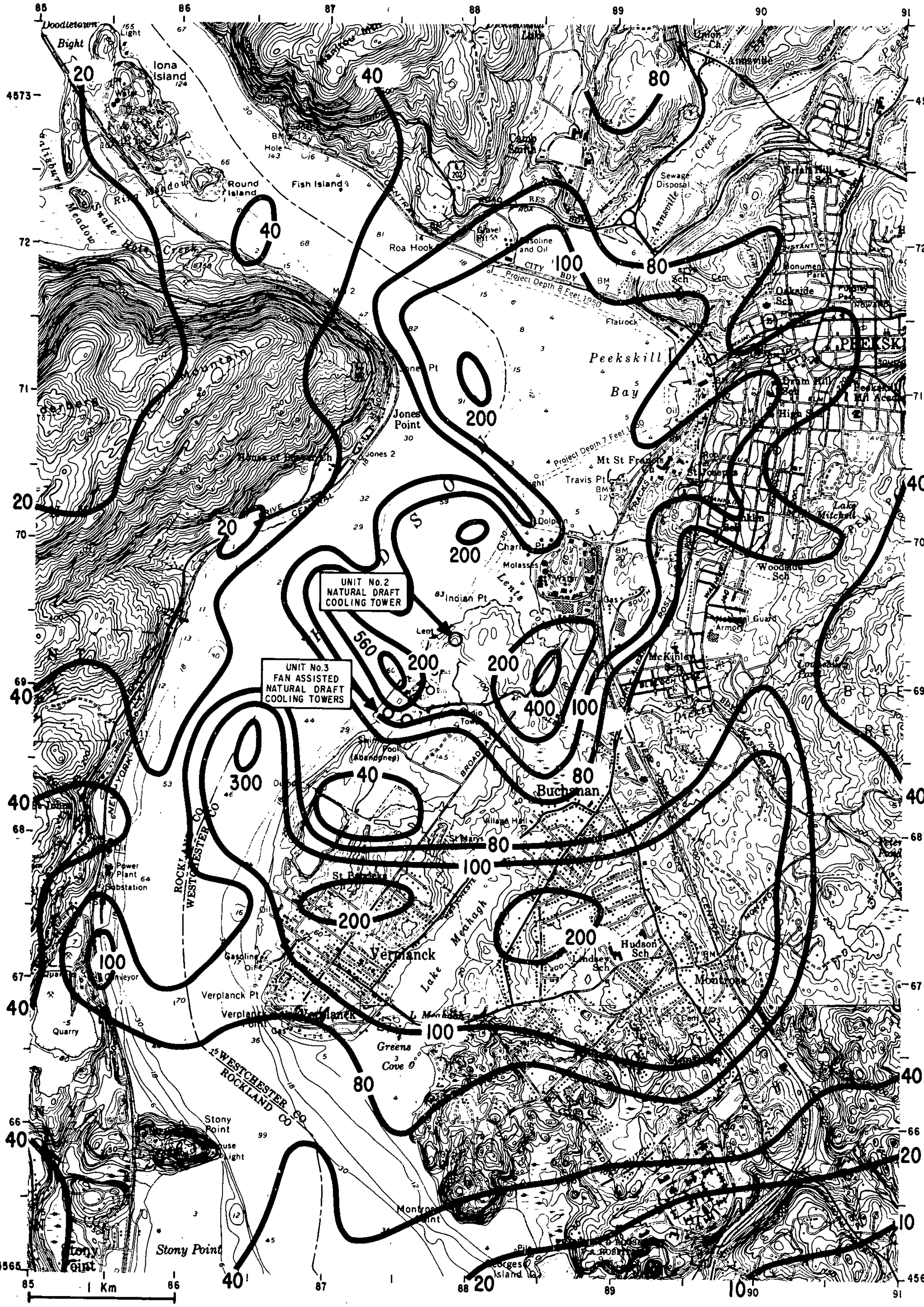

FIGURE A-4

SALT ACCUMULATION OCTOBER 1973 (Kg/Km^2)
UNIT 2 - NATURAL DRAFT WET TOWER
UNIT 3 - FAN ASSISTED NATURAL DRAFT WET TOWER
DRIFT SALINITY 7000 ppm

APPENDIX C: Ostergaard Associates, "Sound Emissions Resulting from Construction and Operation of Cooling Towers at Indian Point Unit No. 3 Nuclear Station," May 12, 1975.

OSTERGAARD ASSOCIATES

Project No. 1111H-2

SOUND EMISSIONS RESULTING FROM

CONSTRUCTION AND OPERATION

OF

COOLING TOWERS AT INDIAN POINT

UNIT NO. 3 NUCLEAR STATION

Prepared by: Paul B. Ostergaard

Norman L. Meyerson

Date: 12 May 1975

SUMMARY

A study was made to estimate the sound emissions from four types of proposed cooling towers at Indian Point Unit No. 3 assuming that a natural draft tower had been built and was in operation at Unit No. 2

The sound emissions from two types of natural draft towers and two types of mechanical towers were predicted and compared to the expected community ambient noise climate with the operation of a tower at Unit No. 2.

Along the north plant site property line, noise emissions from any type of Unit No. 3 cooling tower will not exceed noise limits of the Buchanan zoning code.

Along the east property line north of the Broadway and Bleakley Avenue intersection, either type of natural draft or mechanical draft Unit No. 3 cooling tower will not cause noise levels to exceed the Buchanan code limits. South of this intersection, either type of natural draft Unit No. 3 cooling tower will not emit noise in excess of the Buchanan code limits at the plant site property line (Broadway).

Wet mechanical Unit No. 3 towers will produce noise levels in excess of code limits over approximately 1000 feet of property line centered about a point 2000 feet south of the Broadway-Bleakley Avenue intersection. Noise emission from wet/dry mechanical draft Unit No. 3 towers will result in zoning code noise limit exceedance extending the full length of the Broadway property line south of a point 700 feet south of this intersection.

Operation of either Unit No. 3 natural draft cooling tower will not increase the residential area exposed to day-night sound levels in excess of 60 dB. For the 55 to 60 dB day-night range the exposed residential area will increase by 2 to 4 acres. A wet mechanical Unit No. 3 tower bank will increase residential area exposed to the day-night sound level of over 60 dB by three acres and over 55 dB by 10 acres. The greatest effect is realized with the operation of a wet/dry Unit No. 3 which will increase the day-night sound level of over 60 dB by four acres and over 55 dB day-night sound level by 26 acres.

Off-site construction traffic noise is expected to duplicate that of the Unit No. 2 tower, regardless of tower type since the same routes will be used for construction vehicular traffic. The

increases in day-night sound level due to Unit No. 3 off-site construction will be 54 and 89 acres for day-night levels exceeding 55 dB and 60 dB, respectively.

There will be no significant increase in community noise from on-site construction activity.

INTRODUCTION

There may be a need to install cooling towers at Indian Point Unit No. 3 in addition to those which have been proposed for Indian Point Unit No. 2. An earlier study prepared by Ostergaard Associates evaluated the sound emissions from the construction and operation of either natural draft or mechanical towers at Indian Point Unit No. 2 (see Reference 1) which presented the results of the impact in the form of curves of constant day-night sound levels[2].

Dimensions and other data concerning cooling towers for Unit No. 3, as supplied by Consolidated Edison Company of New York describe towers having a water capacity of 600 000 gpm. The proposed towers may be of natural draft or mechanical draft design.

The construction activity on and off the site would be similar to that for the towers at Indian Point Unit No. 2.

This study examines the sound emissions from tower operation, on and off-site construction activity, for Unit No. 3 tower.

The incremental changes in community noise caused by alternative types of cooling towers at Unit No. 3 were compared to community noise with a natural draft cross-flow tower operating at Unit No. 2.

The sound emissions of the towers at Units No. 2 and 3 are also compared to the municipal regulation. This regulation is described in detail in the earlier report and has not been modified as of the date of this report.

TABLE OF CONTENTS

LIST OF FIGURES

LIST OF FIGURES (Cont'd)

LIST OF TABLES

I. ANALYSIS

A. General Considerations

As a basis for determining the significance of the addition of cooling towers at Indian Point Unit No. 3, the average day-night sound level contours developed for a cross-flow type natural draft cooling tower at Indian Point Unit No. 2 combined with the average day-night ambient determined in earlier studies were used. The original study analyzed community areas within a distance of 2 000 meters from the tower location for Unit No. 2. This study included community areas within 2 000 meters from both towers. The contours developed in the earlier study had to be extrapolated based upon sound level measurements at select locations and the principal traffic routes judged to be noise sources. These extrapolations reflect day-night community noise levels controlled by vehicular traffic.

Figure 1 shows the day-night sound level contours of the ambient community noise together with the emissions from Unit No. 2 natural draft cooling tower. This is the contour map against which all other comparisons were made.

B. Cooling Towers

For construction and operation periods, sound emissions from four types of cooling towers were evaluated and their effect on adjacent community areas was predicted. Tower type 1 is a natural draft cross-flow wet design and hyperbolic in shape. The tower is rated for 600 000 gpm with a 460 feet base diameter, an overall height of 490 feet and an air intake height of 40 feet.

Tower type 2 is similar and is a counter-flow type having the same general size and operating characteristics as tower type 1.

Tower type 3 is an induced-draft mechanical cooling tower array consisting of three banks of cells. Two banks consisting of eight cells are 320 feet long and the third bank of nine cells is 360 feet long. Their width and height are 70 and 68 feet, respectively. The air intake height is approximately 40 feet.

Tower type 4 is also an induced-draft mechanical cooling tower but is a wet-dry tower. This consists of three banks of cells having nine cells in two banks and 10 cells in the third bank. The length of each of the two banks is 430 feet and the length of the third bank is 480 feet. Each bank has a height of 74 feet, a width of 70 feet and an air intake of approximately 40 feet.

The natural draft type towers are located on the east bank of the Hudson River with the tower rim approximately 500 feet or more southwesterly of Nuclear Reactor Unit No. 3

The wet type mechanical towers are in an array with the three banks lined up parallel to each other in a north-south direction. The first bank is approximately 180 feet from the river and approximately 360 feet from Turbo-generator Building No. 3. The banks are separated from each other and are perpendicular to a line running approximately east-west.

The wet-dry mechanical towers are also in an array of three parallel banks running in a north-south direction. The first bank is approximately 120 feet from the river and approximately 360 feet from Turbo-generator Building No. 3. The banks are separated from each other and are perpendicular to a line running approximately east-west.

Cross-Flow Natural Draft

The sound emissions for the cross-flow type tower were predicted using methods described in an earlier report[3]. The contours for the tower were developed with the effects of air absorption and the barriers provided by the cut and hills easterly of the tower. Details of these calculations are presented in the earlier reports.

Figure 2 shows the A-weighted sound levels contours for the Unit No. 3 cross-flow atmospheric tower with both air absorption and the effects of the barriers. Because of the high land and the cut necessary for tower installation, a complete barrier is realized over an arc of 200 degrees of the tower rim which extands from approximately a northeasterly direction to southwesterly direction. This barrier is fully effective since it shields the complete air inlet height over almost 180 degrees.

The reflection of sound off the cut in the hillside will not add materially to the sound emitted in the direction of the Hudson River. The sound which hits the cut will be generally reflected upward.

The A-weighted contours for the cross-flow tower are adjusted to give the day-night sound level, L_{dn}, assuming that the towers are operated for 24 hours a day. The L_{dn} contours shown in Figure 3 take into account the atmospheric absorption and the influence of the hillside and power plant barriers.

Counter-Flow Natural Draft

As was done for the cross-flow tower, sound level contours were developed for the counter-flow tower. This tower has much the same barrier effects as the cross-flow tower and is provided with substantial shielding by the hillside and the power plant. The A-weighted contours for the counter-flow tower are shown in Figure 4. Shown in Figure 5 are the day-night sound level contours for the same tower taking into account the barrier and atmospheric effects.

Mechanical Wet Towers

The sound emissions from the three induced-draft wet mechanical cooling tower banks were calculated using the methods presented in the earlier reports[1,3]. The directional sound level patterns for each individual tower bank were developed and the levels for each of the three tower banks combined to form a single radiation pattern by adjusting the sound pattern of each bank for barrier effects before combining into a single pattern. Figure 6 shows the A-weighted sound level patterns of the three banks of mechanical wet towers taking into account the barrier effects and atmospheric absorption.

The day-night equivalent sound levels for these towers were also developed and are shown in Figure 7.

Mechanical Wet-Dry Towers

Based upon information in Reference 4, the mechanical wet-dry towers were estimated to be three decibels higher in sound output than the wet towers. Considering tower size, radiational patterns were developed for each individual tower bank, attenuation effects applied to each individual tower for atmospheric and barrier effect, and the radiation patterns combined to produce a single A-weighted sound level contour for the towers. Figure 8 shows this radiation pattern. The day-night sound level pattern for that same tower is shown in Figure 9.

C. Off-Site Construction Traffic

Due to the sizable difference in quantities of rock and soil removal and delivery of concrete for the construction of the alternative types of towers for Unit No. 3, each is discussed independently. It is assumed that preparation of the land and construction of the Unit No. 3 tower will not be done during the concurrent 12-month period as Unit No. 2.

Natural Draft Cooling Towers

Site preparation is scheduled over a period of 12 months for excavation using 20 cubic yard trucks at the rate of six trucks per hour for eight-hour work periods. During the excavation phase, 48 full and 48 empty trucks will pass a given point on Bleakley Avenue during a daily eight-hour period. It is expected that removed rock and soil will be carted from the excavation site, across Broadway, east on Bleakley, and onto Route 9 for distribution north and south.

As in the case of the Unit No. 2 natural draft tower, construction concrete trucks will have the same impact as the excavation trucks for periods of approximately 12 hours per week during the one-year period scheduled for the pouring of foundations.

Because of the need for a monolithic basin, a 24-hour continuous pour period will require a steady stream of concrete truck traffic over a period of 92 hours.

The pouring of the shell will require the continuous daily delivery of concrete for a five-foot per day erection rate. Trucks hauling 11 cubic yards each will make 23 full load and 23 empty runs per day over three months to complete the shell.

Mechanical Draft Cooling Towers

Site preparation for this type of cooling tower involves the removal of rock and soil over the one-year site preparation period. During excavation periods of eight-hour duration, 48 full and 48 empty trucks will pass a given point on Bleakley Avenue.

D. On-Site Construction

The on-site construction noise would be similar to that described for the towers proposed for Indian Point Unit No. 2. Because of this construction similarity there will be no significant day-night sound level increase from the unit at No. 3 as was the case for Unit No. 2.

II. SOUND EMISSION OF COMBINED UNITS NO. 2 and NO. 3

A. Municipal Regulations

Buchanan

In the region of the Broadway-Bleakley Avenue intersection, the addition of cooling tower facilities at Unit No. 3 will not materially increase the dB(A) sound levels over that of only the Unit No. 2 cross-flow atmospheric cooling tower in operation, as shown in Table I. However, for all combinations, octave band sound emissions from the towers, as measured at Broadway and Bleakley Avenue, will exceed the existing Buchanan Zoning Code generally, in frequency bands 1 000 Hz through 8 000 Hz as well as for A-weight sound level.

At an intermediate location along the eastern boundary of the plant property, at a point 2 000 feet south of the intersection of Broadway and Bleakley Avenue, the noise emission for the combined operation of cross-flow tower at Unit No. 2 and a Unit No. 3 cross-flow or counter-flow tower will not exceed the maximum noise limits of the Buchanan Zoning Code. However, for each of the two types of mechanical draft towers at Unit No. 3 these code limits will be exceeded in one or more octave bands and, as well, A-weight sound limits for both types of mechanical towers.

At the intersection of Broadway and the southern property line of the plant, the noise emission from any type of tower at Unit No. 3, other than the wet/dry mechanical towers, plus the noise emission from the Unit No. 2 cross-flow tower, does not exceed the Buchanan Zoning Code octave band or A-weight maximum noise levels. In the case of a Unit No. 3 wet/dry mechanical tower, with the Unit No. 2 tower operating, the Buchanan Zoning Code limits are exceeded in four octave bands, as shown in Table I.

North of the Broadway and Bleakley Avenue intersection and at the north property line, 1 480 feet north of Unit No. 2 cross-flow tower center, the Buchanan Zoning Code noise limits are exceeded for a Unit No. 2 cross-flow tower and any type of Unit No. 3 tower. The impact at these locations is almost completely influenced by the Unit No. 2 noise emission. Octave band incremental sound pressure levels and A-weight sound levels are presented in Table I.

At the southern property line which is adjacent to a "planned industry" zone, the maximum noise levels due to Unit No. 3 cooling towers have been estimated. These maximum levels, which occur near the shoreline, are: cross-flow or counter-flow tower -- 66 dB(A); wet mechanical tower -- 72 dB(A); wet/dry mechanical tower -- 76 dB(A).

Verplanck, Peekskill and Westshore Communities

No specific numeric noise criteria or ordinance exists for these communities therefore no municipal or township noise ordinance violations are foreseen.

B. Community Noise Climate

The emission of sound into areas surrounding the Indian Point power plant has been evaluated in terms of the day-night sound level, a descriptor which is described in detail in Reference 2. This description parallels that provided in the earlier report, 1111G-1.

Cooling Towers

For each of the four types of cooling towers proposed for Indian Point Unit No. 3, the sound emission contours were superimposed on and combined with the L_{dn} contours of the present noise climate which had been combined with the sound emission contours of the cross-flow tower proposed for Unit No. 2. The result of the combination is a map with contours of constant L_{dn} of the noise climate anticipated with the cooling towers operating. The impact was studied within two areas which were set off by radii of 1 000 and 2 000 meters, respectively, from both sets of cooling towers. This creates an area which is slightly oblong in shape. Within these limits the Hudson River and the Indian Point plant property of Consolidated Edison Company of New York were excluded from the analysis.

For each pentad L_{dn} region contained within the total study area, acreage was computed for all land uses and for residential areas, and percentages were determined from these areas. The residential areas studied are shown set off by shaded boundaries in Figure 10.

Cross-Flow Tower

The cooling tower emission L_{dn} contours of Figure 3 were combined with the contours in Figure 1 to form the contour map shown in Figure 11. Table II presents a detailed distribution of the L_{dn} region in percentage of areas about the tower center having a 1 000 meter radius and for the annular area, between 1 000 and 2 000 meters. Table III presents the additional data in terms of acres involved.

Most of the noise impact from Unit No. 3 is experienced in the region south of Bleakley Avenue and extending around the southern property line of the plant site. Within 1 000 meters of the tower centers, 36.5 percent of the total area described in Table II will be in the 55 to 60 dB range of L_{dn}, an increase of 0.1 percentage points over the levels of the ambient and cross-flow tower operating at Unit No. 2. Less than one percent (0.9) of the residential area in the region will fall in the greater than 60 decibel L_{dn} range, with no increase in percentage points over the current levels with Unit No. 2 operating alone.

Counter-Flow Tower

The contours of Figure 5 were combined with the expected tower levels due to the operation of Unit No. 2 to form the map shown in Figure 12. With the counter-flow tower in operation, 37.7 percentage of the total area described in Table II, 1 000 meter radius, will be in the 55 to 60 dB range of day-night sound levels which is a 1.3 percentage point increase over the conditions without the Unit No. 3 tower in operation. For residential areas within 1 000 meters, there will be no increase in day-night sound levels having values greater than 60 decibels. Table III shows the area in acres involved.

Mechanical Wet Tower

With the contours shown in Figure 7 for the wet mechanical towers combined with the contours of the ambient and Unit No. 2 tower operation, the resulting contours are shown in Figure 13. The impact of the Unit No. 3 wet mechanical tower within 1 000 meters is such that the total area with an L_{dn} greater than 60 decibels is increased by 0.7 percentage points. For an L_{dn} of 55-60 dB the increase is 5.3 percentage points. A complete description of change in area can be seen in Table II for percentage L_{dn} and in Table III for actual areas involved.

Mechanical Wet-Dry Towers

The mechanical wet/dry tower contours of Figure 9 representing the sound emissions are combined with the emissions of Unit No. 2 tower and the ambient to form the sound contour pattern shown in Figure 14. A comparison of the total areas involved indicates that the area within 1 000 meters which is greater than 60 decibels will be increased by 1.3 percentage points and for the 55 to 60 L_{dn} range the percentage point increase will be 13.3. A complete description of area changes in terms of acres is given in Table III.

D. Off-Site Construction Traffic

Assuming that the tower for Unit No. 3 is not built at the same time as the tower for Unit No. 2, the impact from the off-site construction traffic will be the same as reported earlier in Report No. 1111G-1.

Should the two towers be constructed simultaneously, the day-night sound level will increase approximately three decibels due to the doubled truck traffic.

E. On-Site Construction

During the period of rock removal and general land preparation of Unit No. 3 cooling tower, sound level from construction equipment is expected to be approximately 57 dB(A) at the nearest residential area (Broadway and Bleakley Avenue). This is equivalent to an L_{eq} of 53 dB based upon a six-hour rock drilling period during a 15-hour construction day.

Foundation and shell construction, and other on-site mechanical activity, is expected to create a sound level at Broadway and Bleakley Avenues of 54 dB(A) when all equipment is operating. This equates to an L_{eq} of 50 dB for the daytime period.

Contours for the construction noise were not plotted because the estimated levels near the property boundary were less than L_{10} for the present noise climate and would be lower further from the plant.

F. Effect on Bordering Residential Areas

In terms of incremental increases in residential area exposed to average day-night sound levels of over 55 decibels, the effect of noise emissions from the operation of Unit No. 2 and Unit No. 3 cooling towers is shown in Table IV including off-site construction traffic effects.

REFERENCES

1. "Sound Emission Impact from Operation and Construction of Cooling Towers at Indian Point Nuclear Station", Ostergaard Associates Report No. 1111G-1, 1974.

2. Information on Levels of Environmental Noise Requisite to Protect Public Health and Welfare with an Adequate Margin of Safety (Environmental Protection Agency, Washington, 1974).

3. "Mechanisms of Sound Generation in Natural-Draft Wet Cooling Towers and the Prediction of Sound Levels at Radial Distances", Ostergaard Associates Report No. 1111A-7, 1974.

4. Hopper, B. L. and Seebold, J. G., "Sound Generation in Fans for Refinery Air Coolers", Paper No. 72-WA/FE-42 (Amer. Soc. Mech. Eng., New York, 1972).

TABLE I

A-Weight and Octave Band Sound Levels at Various Consolidated Edison Company Indian Point Property Line Locations for a Natural Draft Unit No. 2 Crossflow Cooling Tower Operating Alone and Incremental Effect with One of Four Other Types of Unit No. 3 Towers.

Octave Band Hz.	Buchanan Zoning Code	Predicted Maximum Tower Sound Emission Impacting Relevant Property Boundary Lines — Sound Pressure Level - dB re 0.00002 N/m²									
		North Property Line**					North of Broadway & Bleakley Aves.***				
		Unit #2 Only	Incremental Effect with Unit No. 3				Unit #2 Only	Incremental Effect with Unit No. 3			
		XF	XF	CF	W	W/D	XF	XF	CF	W	W/D
63	62.5	38	0	0	0	0	29	+1	+4	+13	+16
125	54	41	0	0	0	0	32	+1	+3	+ 9	+12
250	49	44	0	0	0	0	35	+1	+3	+ 5	+ 7
500	44	(45)	0	0	0	0	38	+2	+4	+ 2	+ 3
1 000	40	(47)	0	0	0	0	40	(+2)	(+2)	(+ 1)	(+ 1)
2 000	39	(48)	0	0	0	0	(41)	(+2)	(+2)	(0)	(+ 1)
4 000	35	(52)	0	0	0	0	(45)	(+1)	(+1)	(0)	(0)
8 000	35	(55)	0	0	0	0	(48)	(+1)	(+1)	(0)	(0)
A-wt.	48*	(59)	0	0	0	0	(51)	(+1)	(+1)	(0)	(0)

(Continued)

*Computed from octave band levels.

**1480 Ft. north of Unit No. 2 crossflow tower center at boundary line between park land deeded to town of Buchanan and Consolidated Edison Company.

***On Broadway 450 Ft. north of intersection with Bleakley Avenue.

XF = crossflow natural draft
CF = counterflow natural draft
W/D = wet/dry mechanical draft
W = wet mechanical draft
( ) = exceeds code

TABLE I (cont'd)

OSTERGAARD ASSOCIATES

Predicted Maximum Tower Sound Emission
Impacting Relevant Property Boundary Lines

Sound Pressure Level - dB re 0.00002 N/m^2

Octave Band Hz.	Buchanan Zoning Code	South of Broadway & Bleakley Aves.** Unit #2 Only	Incremental Effect with Unit No. 3				Broadway at South Property Line*** Unit #2 Only	Incremental Effect with Unit No. 3			
		XF	XF	CF	W	W/D	XF	XF	CF	W	W/D
63	62.5	19	+1	+3	+33	+38	15	0	+4	+29	+36
125	54	19	+3	+6	+33	(+37)	15	+2	+7	+28	+35
250	49	20	+5	+8	(+30)	(+33)	16	+4	+9	+26	+31
500	44	22	+4	+9	(+26)	(+28)	17	+4	+11	+23	(+28)
1 000	40	24	+4	+8	(+20)	(+22)	20	+3	+9	+18	(+21)
2 000	39	25	+4	+8	(+16)	(+19)	21	+3	+9	+12	(+18)
4 000	35	28	+5	+6	(+11)	(+14)	24	+4	+7	+ 7	(+12)
8 000	35	31	(+4)	0	0	+ 3	27	+4	0	0	+ 1
A-wt.	48*	34	+5	+5	(+15)	(+18)	30	+4	+6	+12	+17

*Computed from octave band levels.

**On Broadway 2000 Ft. south of intersection with Bleakley Ave.

***Intersection of Broadway and Consolidated Edison southern property line.

XF = crossflow natural draft
CF = counterflow natural draft
W = wet mechanical draft
W/D = wet/dry mechanical draft
( ) = exceeds code

18

TABLE II

Percent of Land Area within Contours of Constant Noise Levels for; a Unit No. 2 Crossflow Tower imposed on the Present Area Noise Climate, the addition of a Unit No. 3 Crossflow Tower, the addition of a Unit No. 3 Counterflow Tower, the addition of Unit No. 3 Banks of Wet Mechanical Towers, and the addition of Unit No. 3 Banks of Wet-and-Dry Mechanical Towers. The Area includes East Shore and West Shore Land exclusive of the Indian Point Plant Site of Consolidated Edison.†

L_{dn}-dB	Unit 2 / Unit 3	Crossflow None		Crossflow Crossflow		Crossflow Counterflow		Crossflow Wet Mechanical		Crossflow W/D Mechanical	
		*T	**R	T	R	T	R	T	R	T	R
		Percent of Area within 1000 Meters of Tower Centers									
>60		3.3	0.9	3.4	0.9	3.4	0.9	4.0	5.4	4.6	7.1
55-60		36.4	23.2	36.5	26.5	37.7	27.3	41.7	23.2	49.7	28.6
50-55		10.8	12.5	15.0	14.2	15.6	14.5	25.2	28.5	37.1	64.3
45-50		13.8	33.0	15.3	28.0	19.6	28.0	23.9	37.5	8.6	0
40-45		22.9	30.4	29.8	30.4	23.7	29.3	5.2	5.4	0	0
<40		12.8	0	0	0	0	0	0	0	0	0
		Percent of Area Between 1000 and 2000 Meters of Tower Centers									
>60		0	0	0	0	0	0	0	0	0	0
55-60		52.4	49.0	53.6	49.0	53.2	49.1	53.7	49.8	56.2	51.0
50-55		22.4	24.6	24.8	24.8	24.5	24.7	22.9	24.9	25.9	27.5
45-50		16.4	17.8	16.9	18.2	16.1	18.2	19.3	17.9	14.2	14.8
40-45		8.4	8.6	4.7	8.0	6.2	8.0	4.1	7.4	3.7	6.7
<40		0.4	0	0	0	0	0	0	0	0	0

* Total Area
**Residential Area
†Exclusive of the planned industry zone south of the Indian Point facility.

18

OSTERGAARD ASSOCIATES

TABLE III

Land Area in Acres within Contours of Constant Noise Levels for; a Unit No. 2 Crossflow Tower imposed on the Present Area Noise Climate, the addition of a Unit No. 3 Crossflow Tower, the addition of a Unit No. 3 Counterflow Tower, the addition of Unit No. 3 Banks of Wet Mechanical Towers, and the addition of Unit No. 3 Banks of Wet-and-Dry Mechanical Towers. The Area includes All East Shore and West Shore Land Exclusive of the Indian Point Plant Site of Consolidated Edison.

L_{dn}-dB	Unit 2 / Unit 3 →	Crossflow None		Crossflow Crossflow		Crossflow Counterflow		Crossflow Wet Mechanical		Crossflow W/D Mechanical	
		*T	**R	T	R	T	R	T	R	T	R
		Acres within 1000 Meters of Tower Centers (Total Area: 305.2 acres; total residential area: 64.2 acres)									
>60		10.3	0.6	10.3	0.6	10.3	0.6	12.2	3.4	14.0	4.6
55-60		111.0	14.9	111.4	17.0	115.2	17.5	127.3	14.9	151.7	18.3
50-55		33.0	8.0	45.9	9.1	47.7	9.3	76.8	18.3	113.3	41.3
45-50		42.0	21.2	46.8	18.0	59.9	18.0	73.0	24.2	26.2	0
40-45		69.9	19.5	90.8	19.5	72.1	18.8	15.9	3.4	0	0
<40		39.0	0	0	0	0	0	0	0	0	0
		Acres Between 1000 and 2000 Meters of Tower Centers (Total Area: 1681.7 acres; total residential area: 909.3 acres)									
>60		0	0	0	0	0	0	0	0	0	0
55-60		881.2	445.5	900.2	445.5	895.1	446.5	902.5	452.8	944.3	463.9
50-55		376.6	223.7	417.6	225.5	411.8	225.0	384.9	226.4	435.0	250.2
45-50		276.4	162.2	284.9	165.0	335.8	165.5	324.7	163.2	239.3	134.7
40-45		141.0	77.9	79.0	73.3	39.0	72.7	69.6	66.9	63.1	60.5
<40		6.5	0	0	0	0	0	0	0	0	0

* Total Area
**Residential Area

Project No. 1111H-2

18

TABLE III

Land Area in Acres within Contours of Constant Noise Levels for; a Unit No. 2 Crossflow Tower imposed on the Present Area Noise Climate, the addition of a Unit No. 3 Crossflow Tower, the addition of a Unit No. 3 Counterflow Tower, the addition of Unit No. 3 Banks of Wet Mechanical Towers, and the addition of Unit No. 3 Banks of Wet-and-Dry Mechanical Towers. The Area includes All East Shore and West Shore Land Exclusive of the Indian Point Plant Site of Consolidated Edison.†

L_{dn}-dB	Unit 2 / Unit 3: Crossflow / None		Crossflow / Crossflow		Crossflow / Counterflow		Crossflow / Wet Mechanical		Crossflow / W/D Mechanical	
	*T	**R	T	R	T	R	T	R	T	R
Acres within 1000 Meters of Tower Centers (Total Area: 305.2 acres; total residential area: 64.2 acres)										
>60	10.3	0.6	10.3	0.6	10.3	0.6	12.2	3.4	14.0	4.6
55-60	111.0	14.9	111.4	17.0	115.2	17.5	127.3	14.9	151.7	18.3
50-55	33.0	8.0	45.9	9.1	47.7	9.3	76.8	18.3	113.3	41.3
45-50	42.0	21.2	46.8	18.0	59.9	18.0	73.0	24.2	26.2	0
40-45	69.9	19.5	90.8	19.5	72.1	18.8	15.9	3.4	0	0
<40	39.0	0	0	0	0	0	0	0	0	0
Acres Between 1000 and 2000 Meters of Tower Centers (Total Area: 1681.7 acres; total residential area: 909.3 acres)										
>60	0	0	0	0	0	0	0	0	0	0
55-60	881.2	445.5	900.2	445.5	895.1	446.5	902.5	452.8	944.3	463.9
50-55	376.6	223.7	417.6	225.5	411.8	225.0	384.9	226.4	435.0	250.2
45-50	276.4	162.2	284.9	165.0	335.8	165.5	324.7	163.2	239.3	134.7
40-45	141.0	77.9	79.0	73.3	39.0	72.7	69.6	66.9	63.1	60.5
<40	6.5	0	0	0	0	0	0	0	0	0

* Total Area
**Residential Area
†Exclusive of the planned industry zone south of the Indian Point facility.

Project No. 1111H-2a

TABLE IV

Incremental Increases in Residential Areas Exposed to Average Day-Night Sound Levels in Excess of 55 dB due to the Operation of Different Unit No. 3 Cooling Towers.
(Total Acreage = 974*)

	L_{dn} 55-60	L_{dn} 60-65**	L_{dn} > 55**	L_{dn} > 60**
AMBIENT COMMUNITY AND:	AREA EXPOSED TO AVERAGE DAY-NIGHT SOUND LEVELS, ACRES		INCREASE IN AREA EXPOSED TO DAY-NIGHT SOUND LEVELS, ACRES	
Unit No. 2 Cooling Tower	460.4	0.6	0	0
Unit No. 2 and Natural Draft Cross-Flow Unit No. 3	462.5	0.6	2.1	0
Unit No. 2 and Natural Draft Counter-Flow Unit No. 3	464.0	0.6	3.6	0
Unit No. 2 and Mechanical Wet Unit No. 3	467.7	3.4	10.1	2.8
Unit No. 2 and Mechanical Wet/Dry Unit No. 3	482.2	4.6	25.8	4.0
Off-site Construction Traffic			54	89***

*Area within 2000 meters of Unit Nos. 2 and 3 Cooling Towers
**Estimated upper limit of range = 65 dB
***Within 2000 meters of Unit No. 2 Cooling Tower

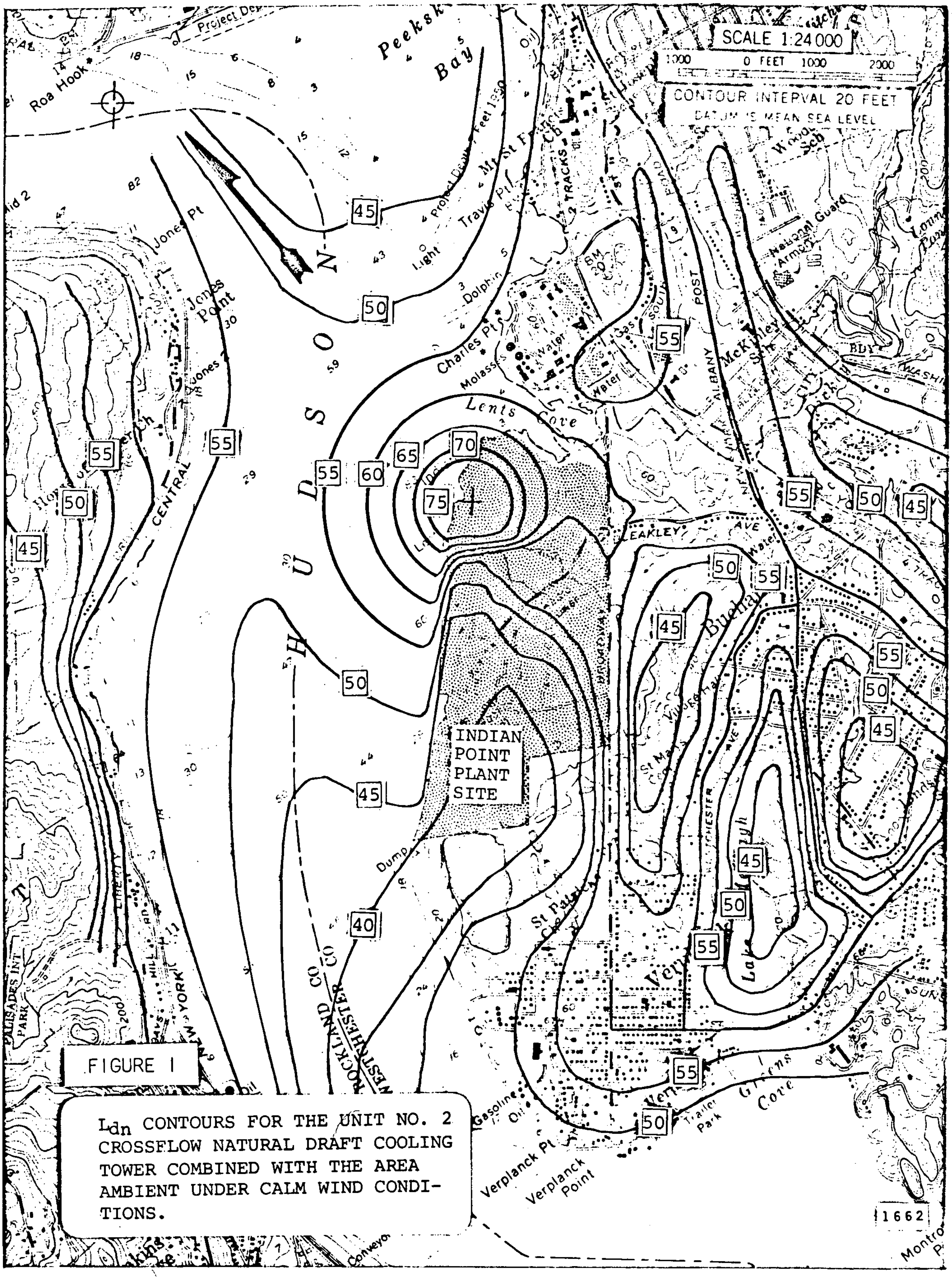

FIGURE I

L_{dn} CONTOURS FOR THE UNIT NO. 2 CROSSFLOW NATURAL DRAFT COOLING TOWER COMBINED WITH THE AREA AMBIENT UNDER CALM WIND CONDITIONS.

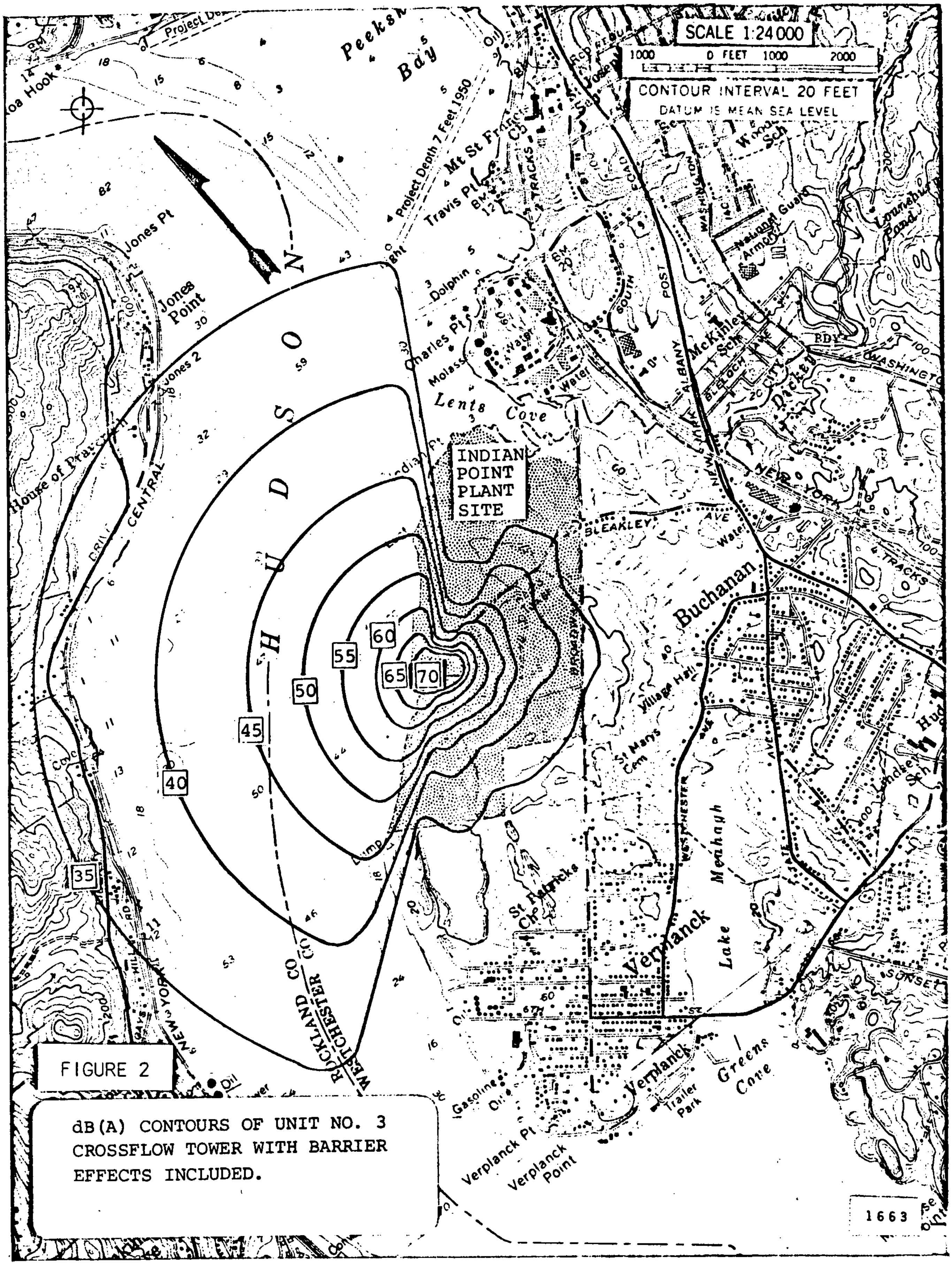

FIGURE 2

dB(A) CONTOURS OF UNIT NO. 3 CROSSFLOW TOWER WITH BARRIER EFFECTS INCLUDED.

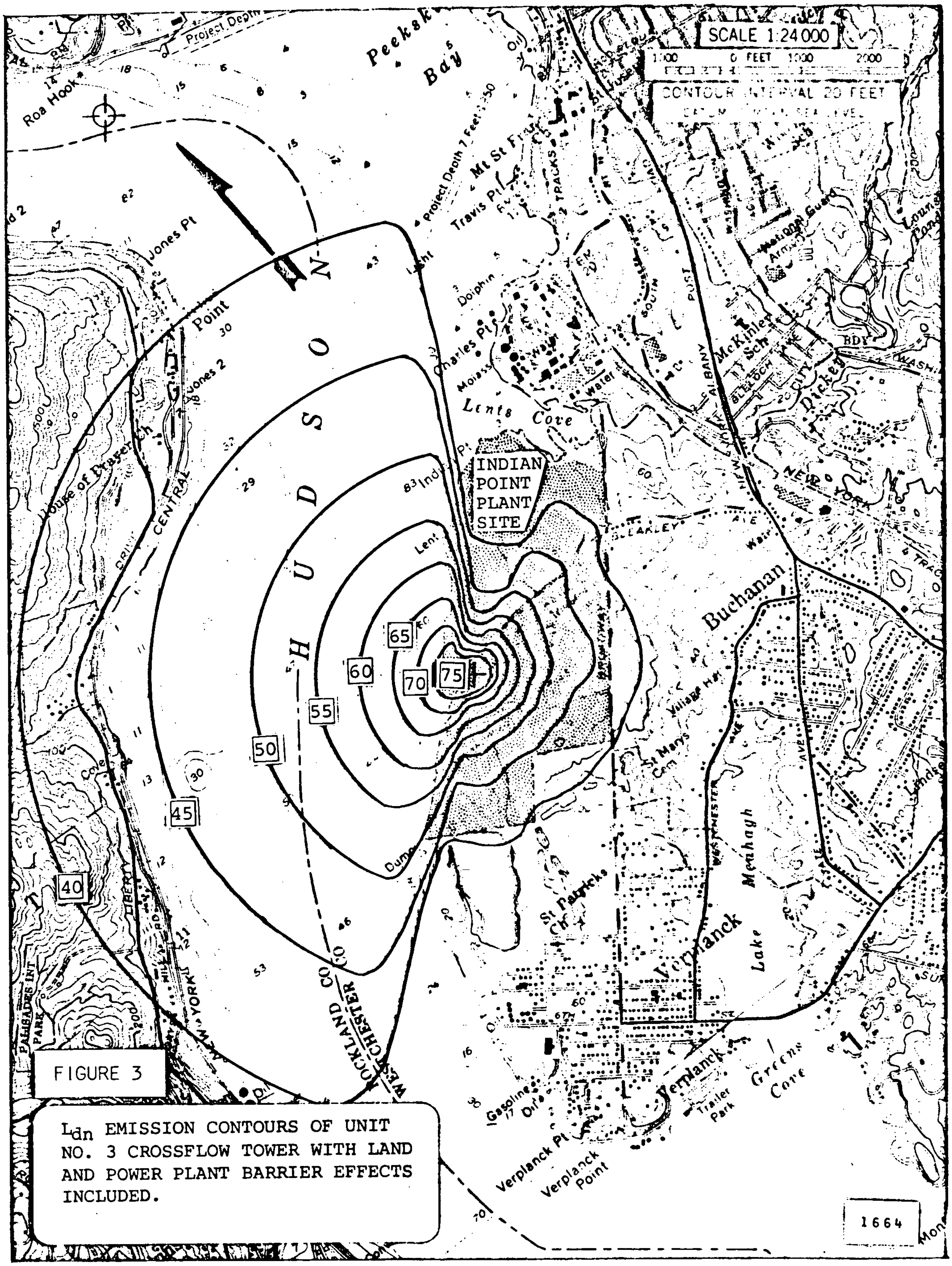

FIGURE 3

L_{dn} EMISSION CONTOURS OF UNIT NO. 3 CROSSFLOW TOWER WITH LAND AND POWER PLANT BARRIER EFFECTS INCLUDED.

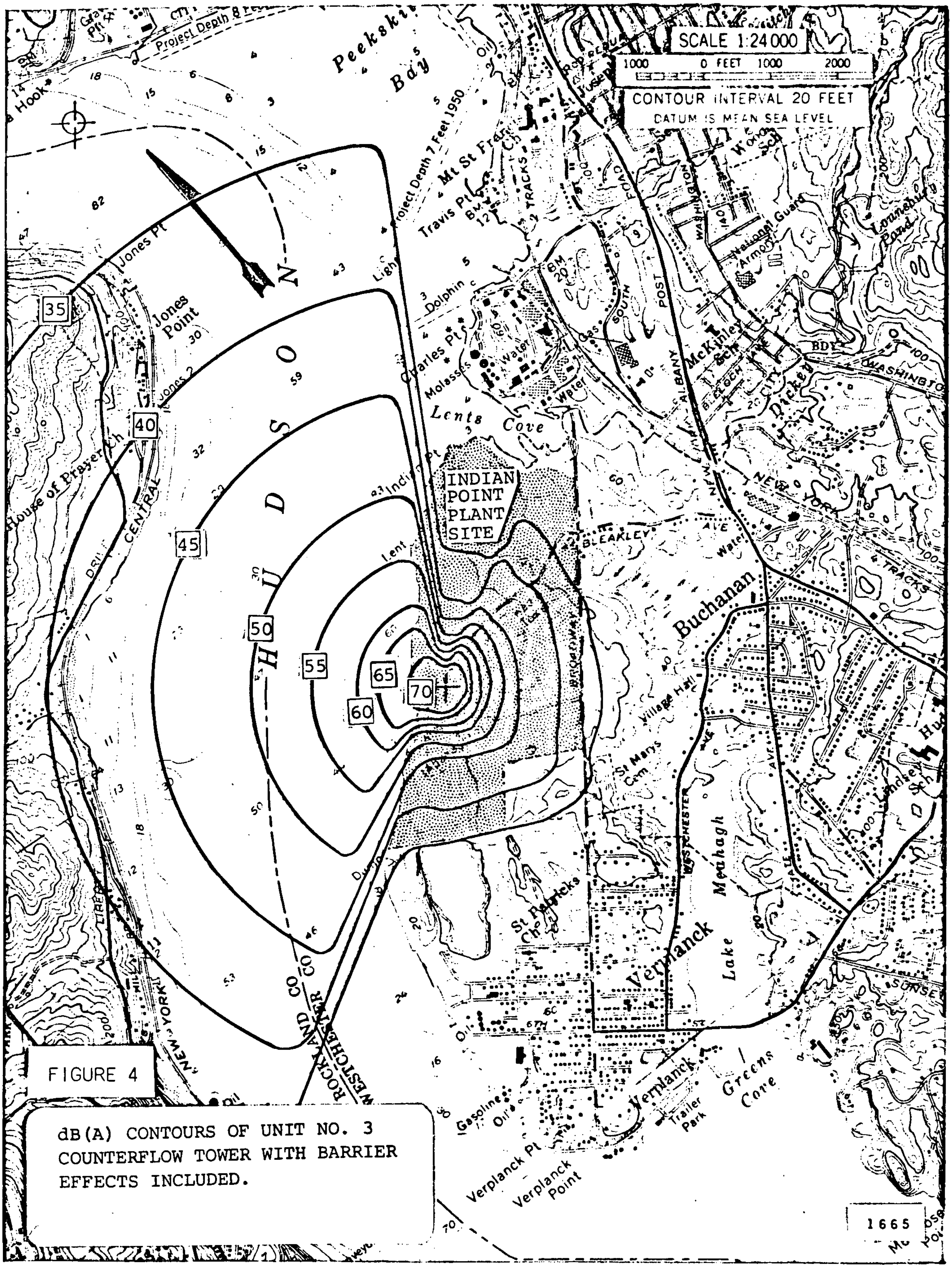

FIGURE 4

dB(A) CONTOURS OF UNIT NO. 3 COUNTERFLOW TOWER WITH BARRIER EFFECTS INCLUDED.

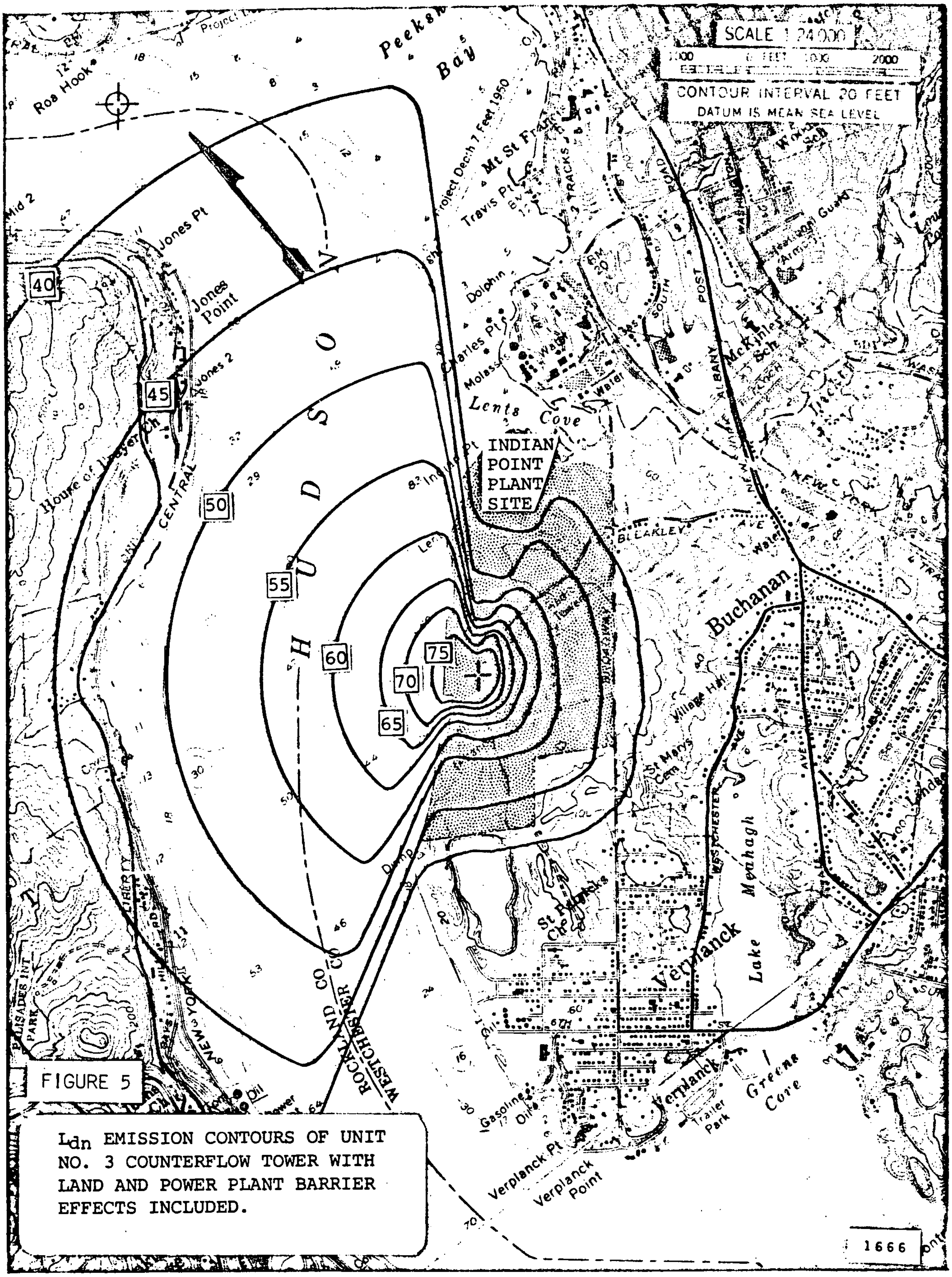

FIGURE 5

L_{dn} EMISSION CONTOURS OF UNIT NO. 3 COUNTERFLOW TOWER WITH LAND AND POWER PLANT BARRIER EFFECTS INCLUDED.

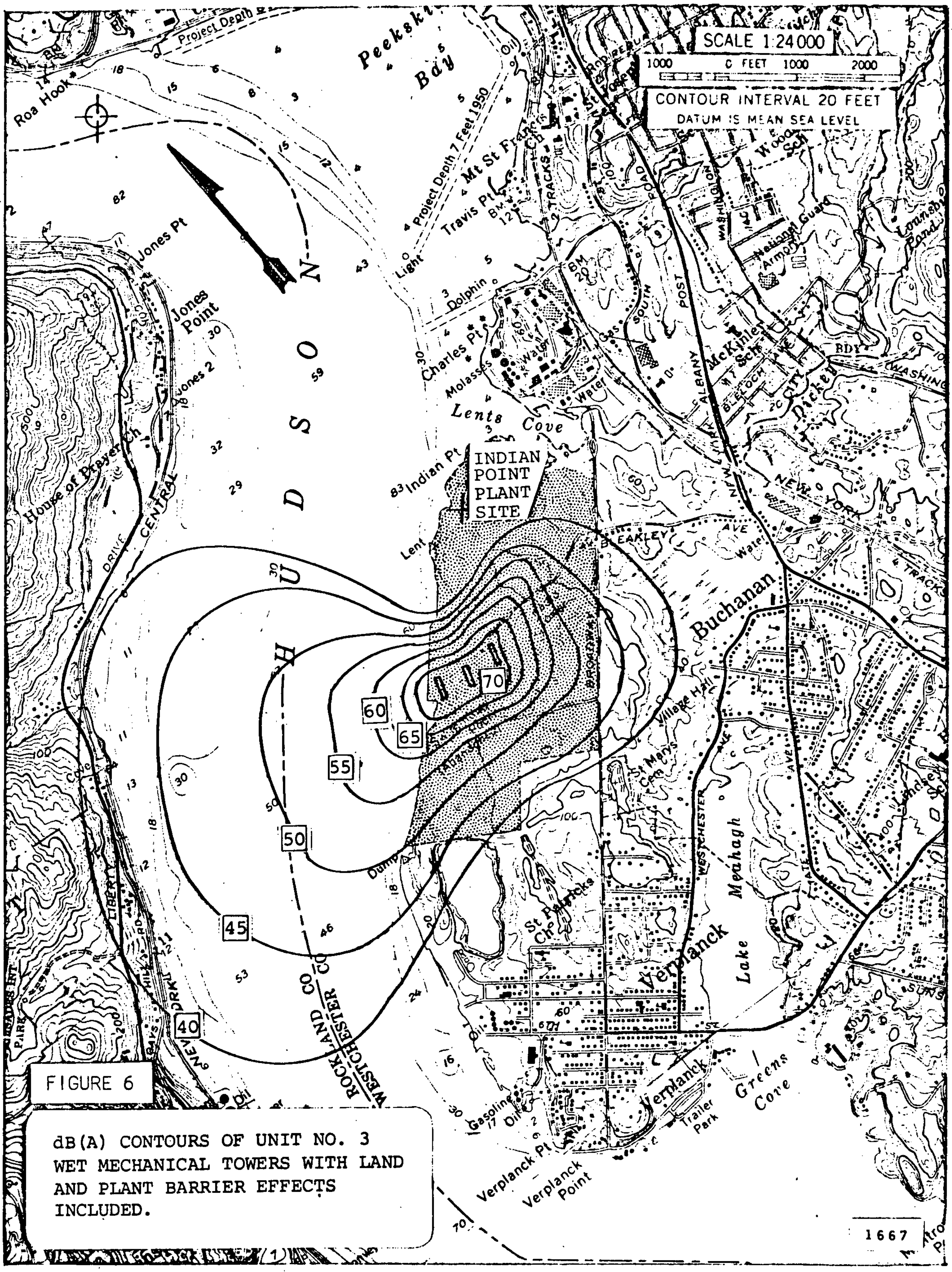

FIGURE 6

dB(A) CONTOURS OF UNIT NO. 3 WET MECHANICAL TOWERS WITH LAND AND PLANT BARRIER EFFECTS INCLUDED.

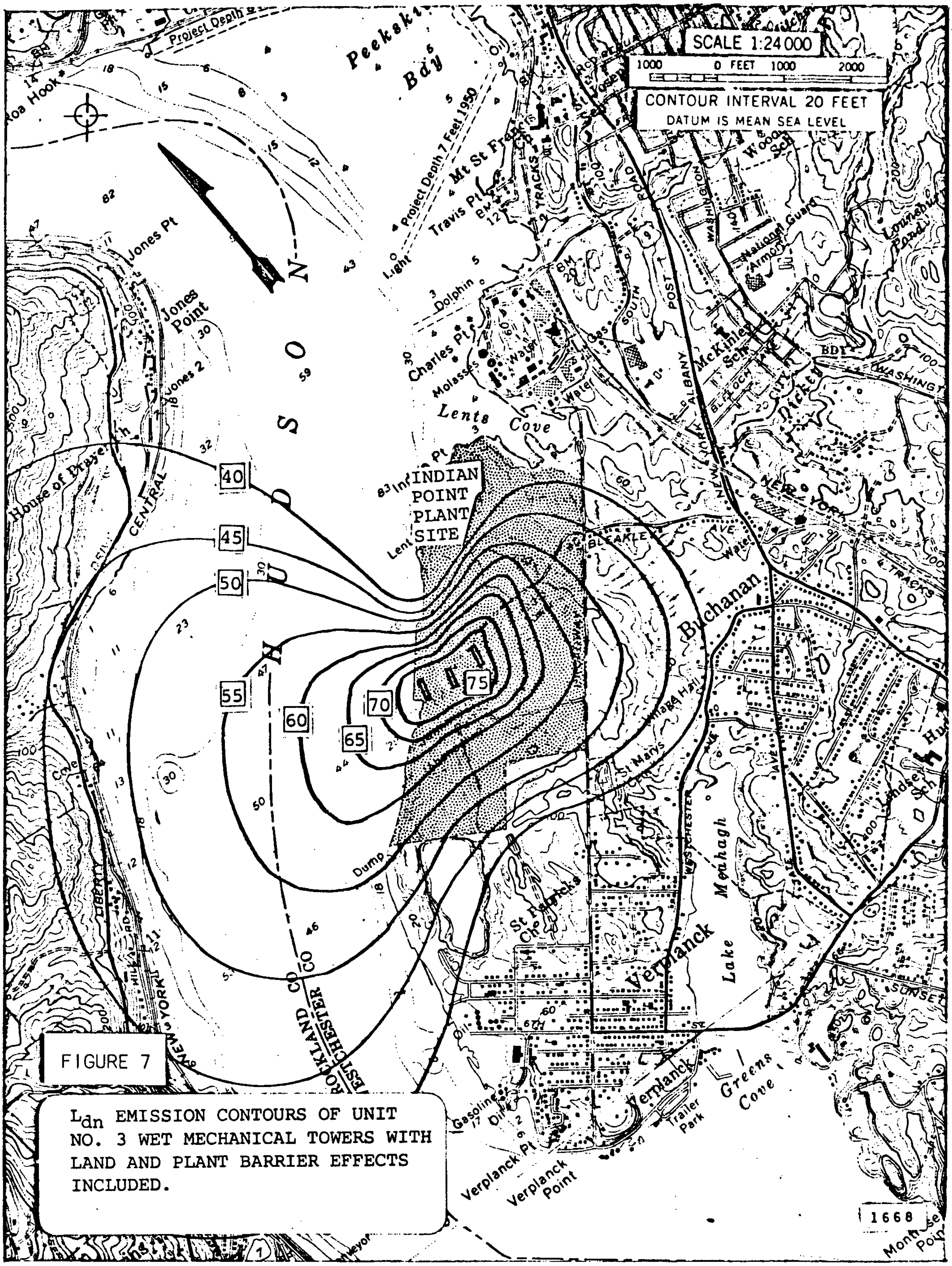

FIGURE 7

L_{dn} EMISSION CONTOURS OF UNIT NO. 3 WET MECHANICAL TOWERS WITH LAND AND PLANT BARRIER EFFECTS INCLUDED.

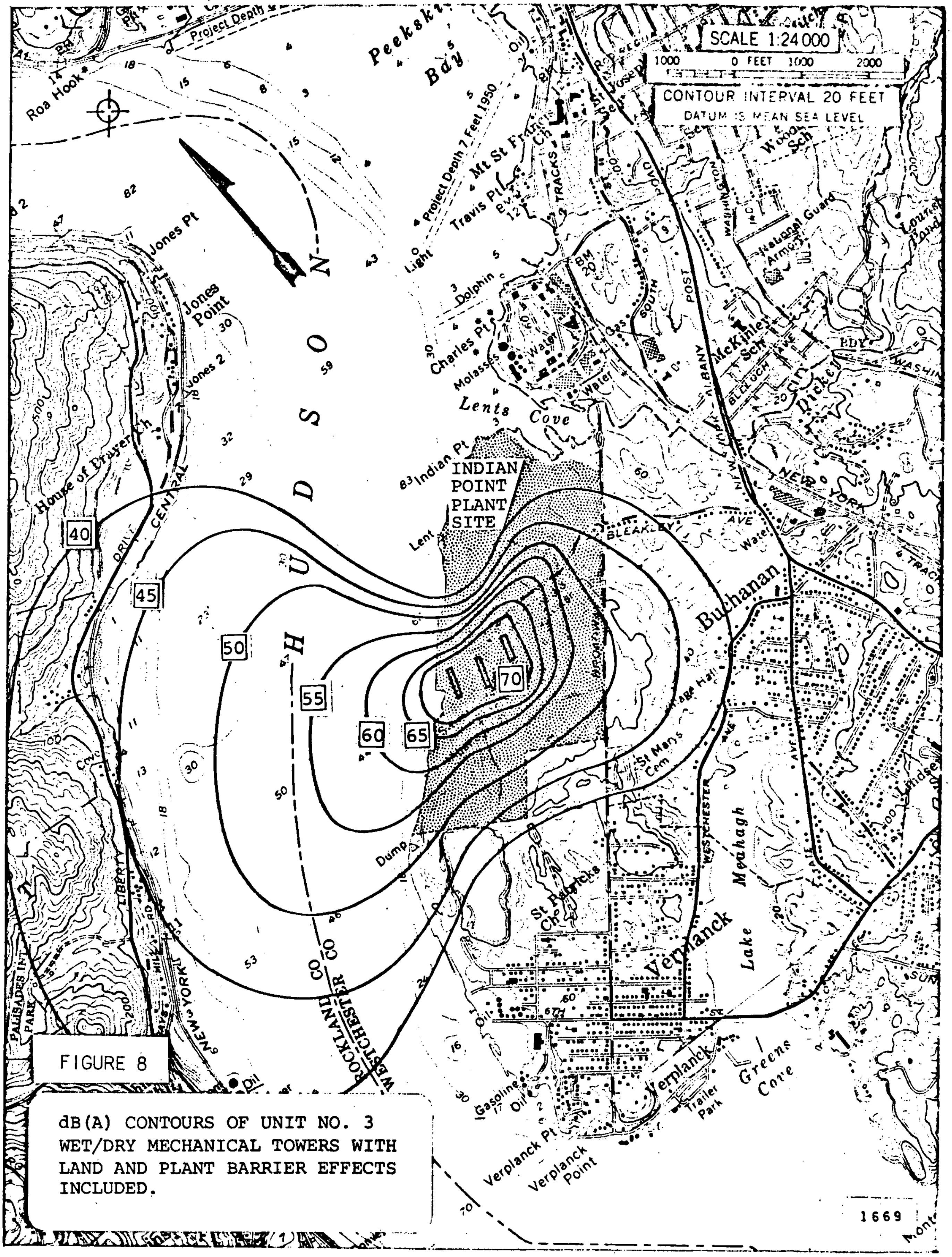

FIGURE 8

dB(A) CONTOURS OF UNIT NO. 3
WET/DRY MECHANICAL TOWERS WITH
LAND AND PLANT BARRIER EFFECTS
INCLUDED.

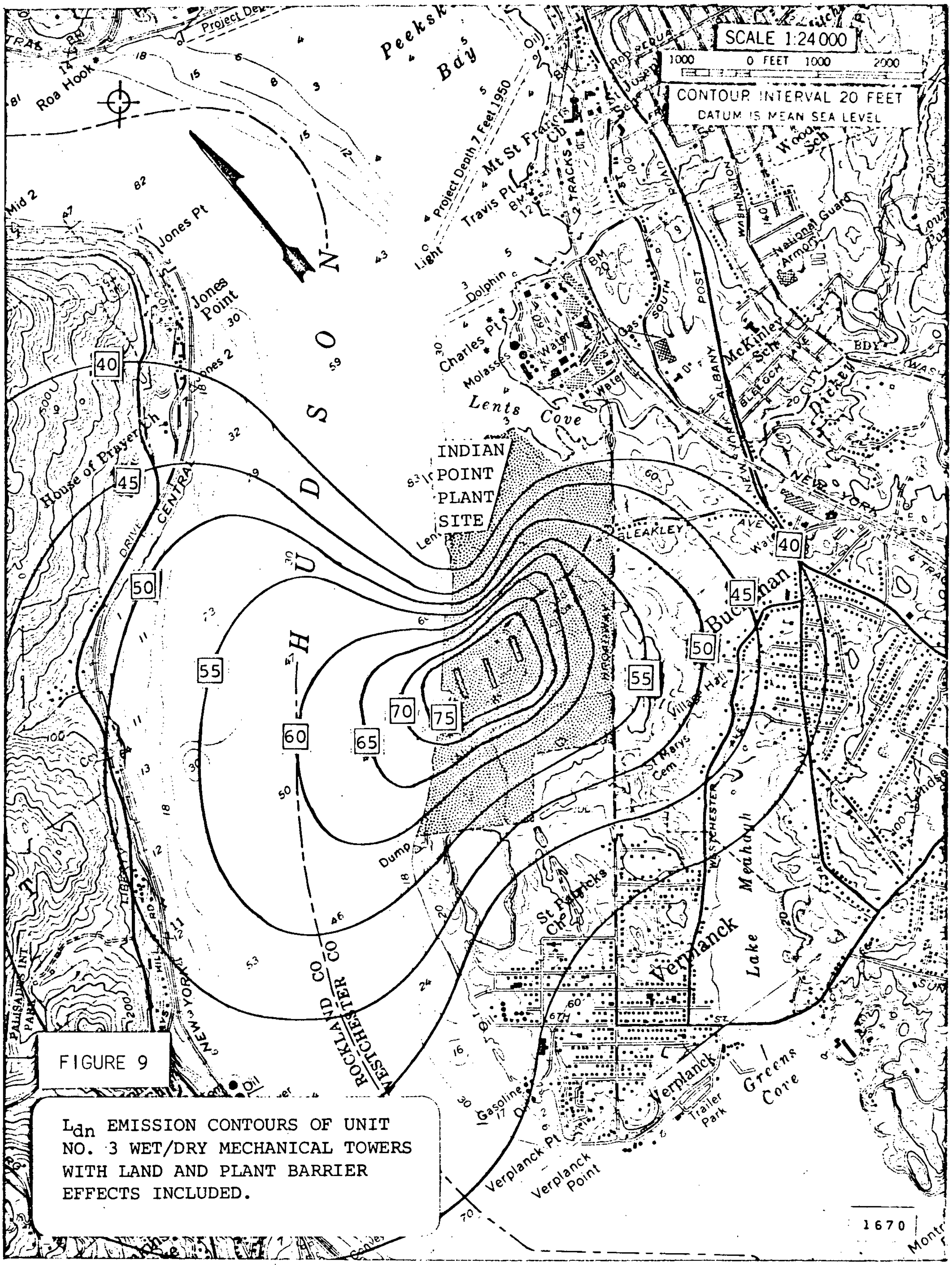

FIGURE 9

L_{dn} EMISSION CONTOURS OF UNIT NO. 3 WET/DRY MECHANICAL TOWERS WITH LAND AND PLANT BARRIER EFFECTS INCLUDED.

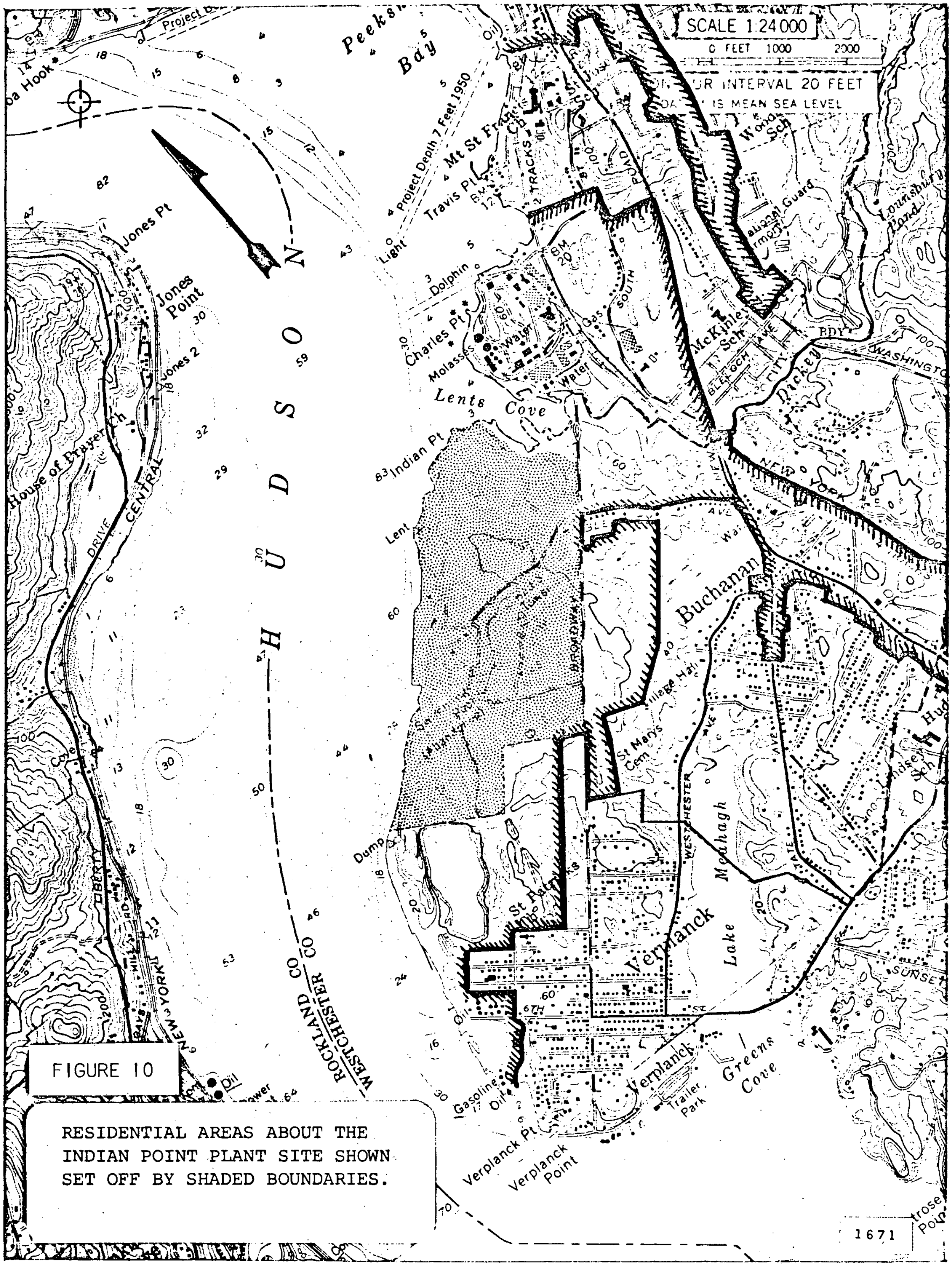

FIGURE 10

RESIDENTIAL AREAS ABOUT THE INDIAN POINT PLANT SITE SHOWN SET OFF BY SHADED BOUNDARIES.

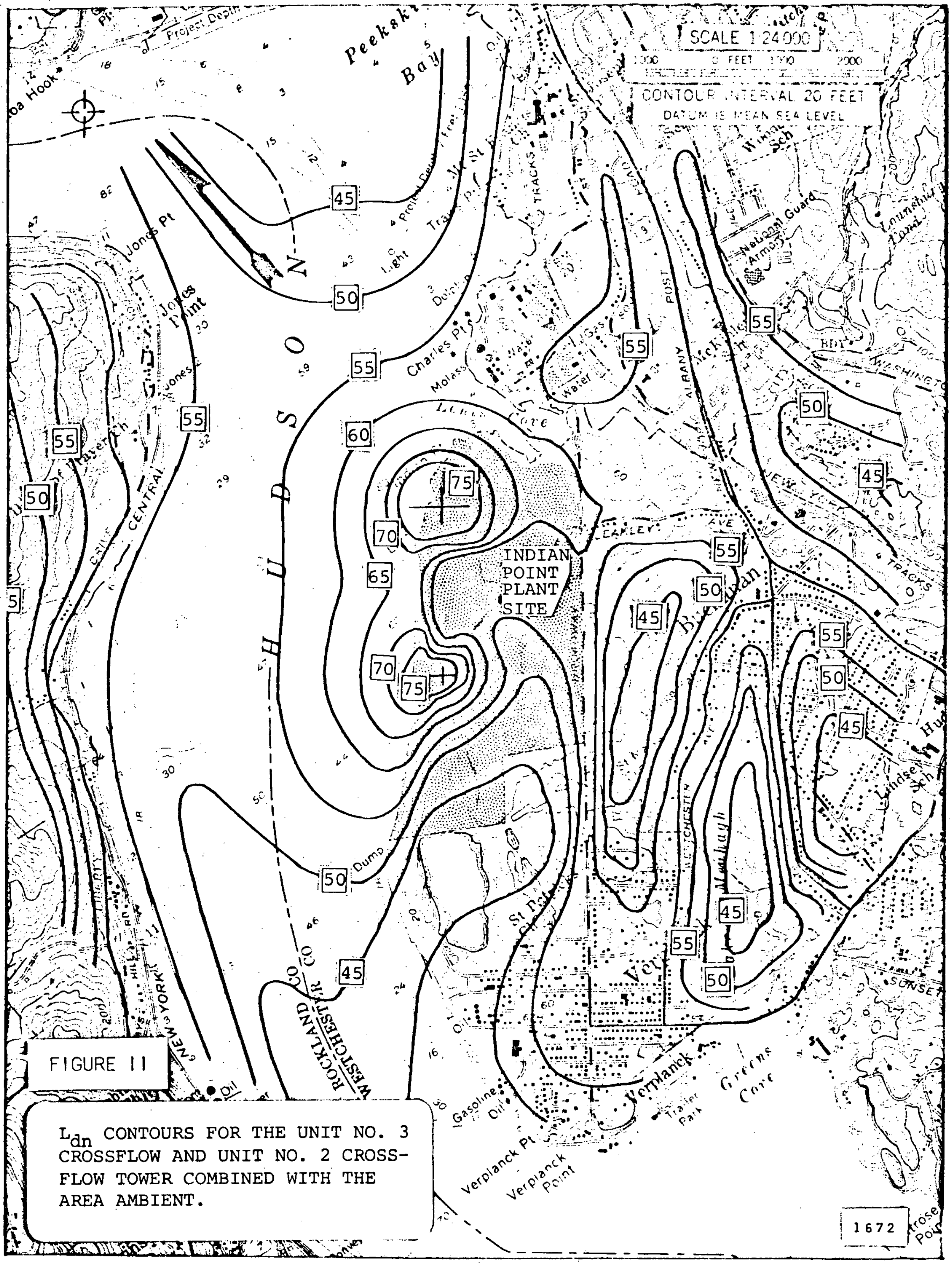

FIGURE 11

L_{dn} CONTOURS FOR THE UNIT NO. 3 CROSSFLOW AND UNIT NO. 2 CROSSFLOW TOWER COMBINED WITH THE AREA AMBIENT.

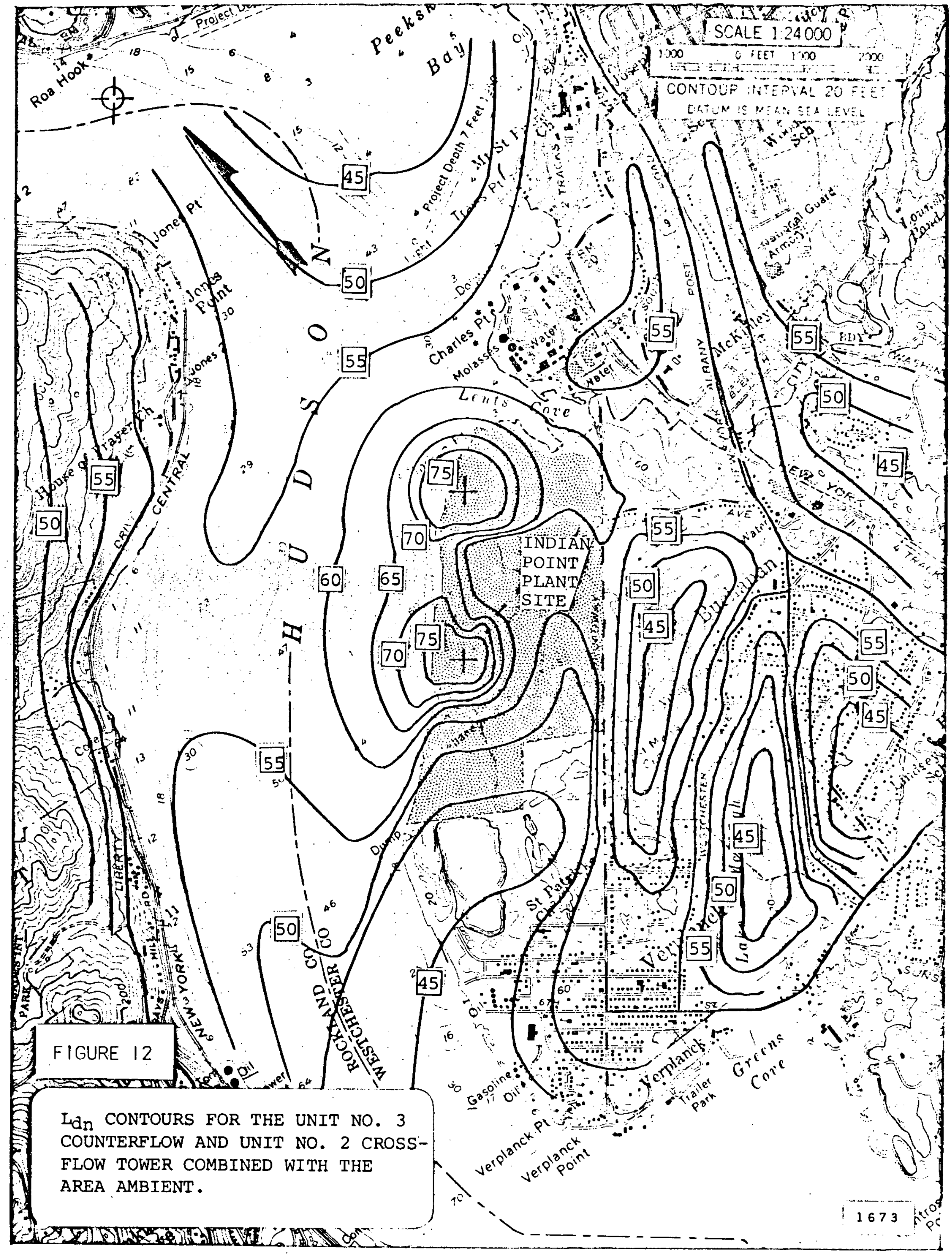

FIGURE 12

L_{dn} CONTOURS FOR THE UNIT NO. 3 COUNTERFLOW AND UNIT NO. 2 CROSS-FLOW TOWER COMBINED WITH THE AREA AMBIENT.

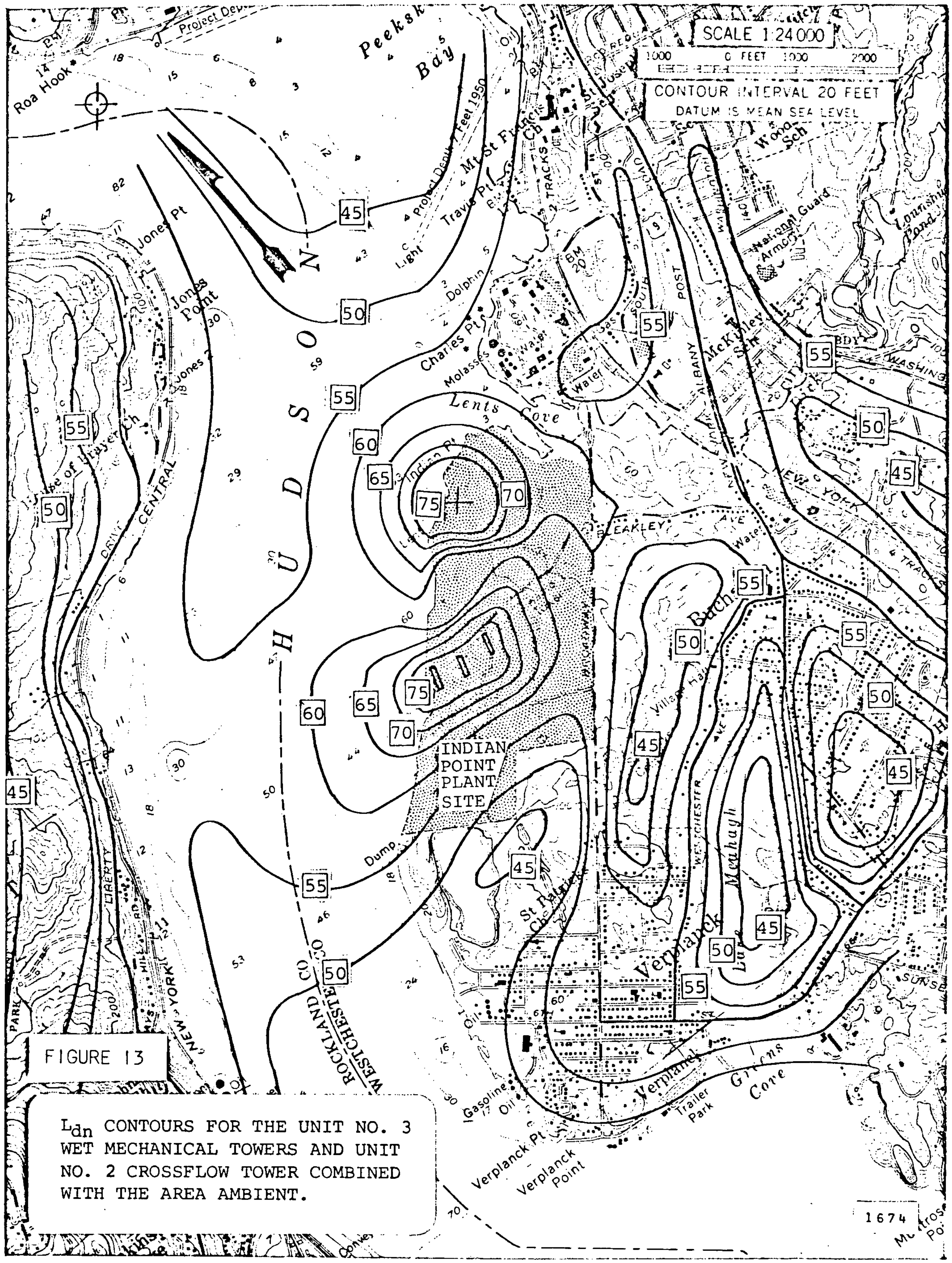

FIGURE 13

L_{dn} CONTOURS FOR THE UNIT NO. 3 WET MECHANICAL TOWERS AND UNIT NO. 2 CROSSFLOW TOWER COMBINED WITH THE AREA AMBIENT.

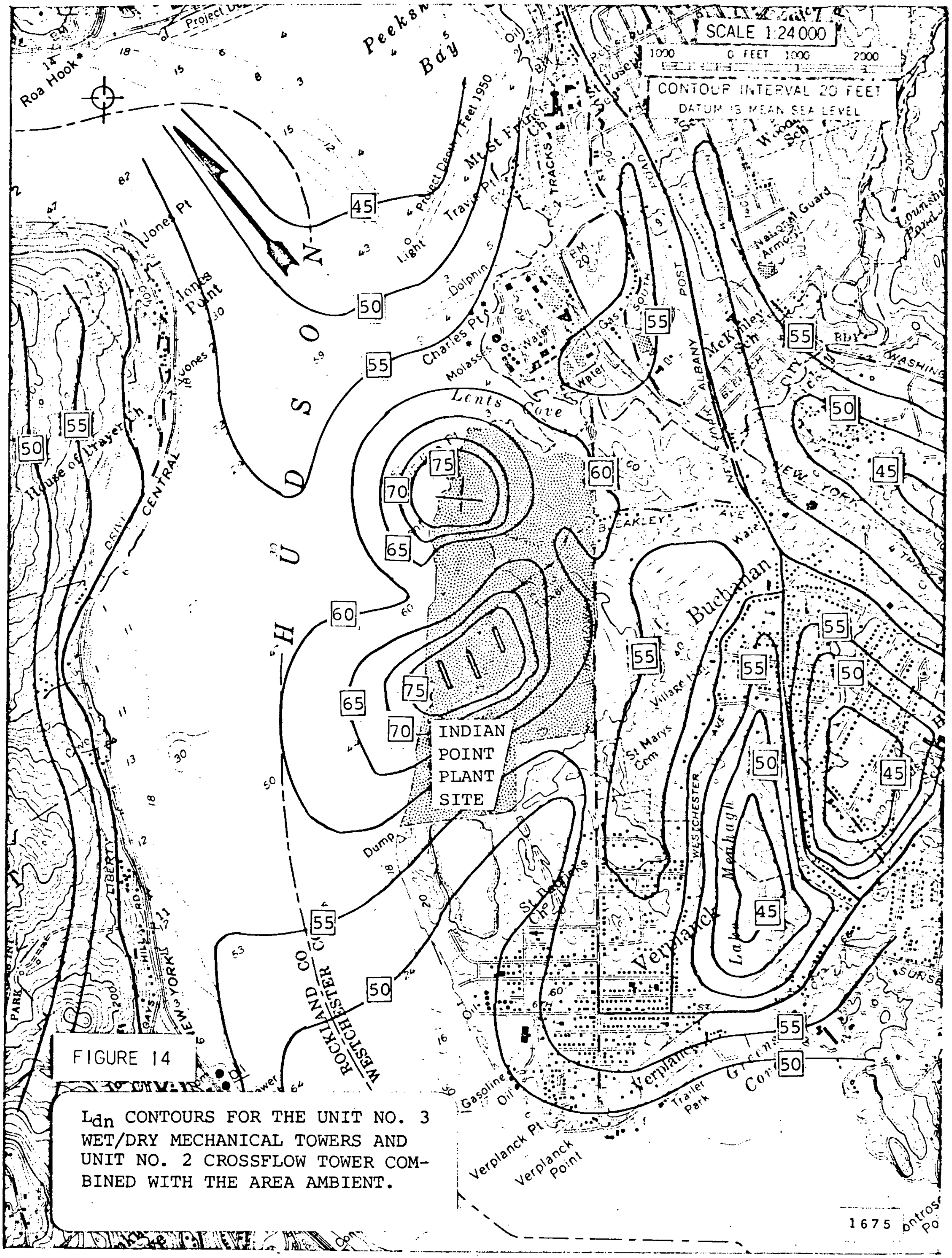

FIGURE 14

L_{dn} CONTOURS FOR THE UNIT NO. 3 WET/DRY MECHANICAL TOWERS AND UNIT NO. 2 CROSSFLOW TOWER COMBINED WITH THE AREA AMBIENT.

37-1A 6